



TECHNISCHE
UNIVERSITÄT
WIEN

DISSERTATION

USING COMPARATIVE GENOMICS TO LINK PHENOTYPES TO GENOTYPES OF THE MYCOTROPHIC FUNGUS *TRICHODERMA*

ausgeführt zum Zwecke der Erlangung des akademischen Grades eines
Doktors der technischen Wissenschaften
unter der Leitung von

Associate Prof. Dr. Irina S. Druzhinina
Institut E166

Institut für Verfahrenstechnik, Umwelttechnik und technische Biowissenschaften,
eingereicht an der Technischen Universität Wien,
Fakultät für Technische Chemie

von

Dipl. Ing. Komal Chenthamara Kariyankode

Matrikelnummer 1029670

Heiligenstädterstraße 137, 1190 Wien

Wien, am

*To my parents Rani and
Chenthamara*

Contents

Acknowledgments.....	7
Kurzfassung.....	9
Summary.....	11
Structure of the dissertation.....	13
Abbreviations.....	15
Glossary of some terms specific for this dissertation.....	17
Preface.....	19
Aims of the dissertation.....	25
Chapter 1 Ecological genomics of mycotrophic fungi.....	27
Chapter 2 Small genome of the fungus <i>Escovopsis weberi</i> , a specialized disease agent of ant agriculture.....	61
Chapter 3 Evolution of <i>Trichoderma</i> carbohydrate-active enzymes required for the degradation of plant biomass.....	73
Chapter 4 The pilot assessment of the contribution of putative xenologues genes in the development of hypocrealean genomes.....	191
Chapter 5 Ankyrin domain containing proteins are frequent in orphomes of all <i>Trichoderma</i> species.....	205
Chapter 6 Conclusive notes on the comparative analysis of the core genome of <i>Trichoderma</i> spp. and respective orphomes.....	225
Appendix I.....	CD provided with this dissertation
Appendix II.....	237
Appendix III.....	273
<i>Curriculum vitae</i> with a complete list of publications.....	279

Acknowledgments

I would like to express my sincere gratitude to my mentor **Irina Druzhinina** for giving me the opportunity to work in her group, for giving me diverse yet related research topics, for her teachings, for giving me many opportunities in teaching to bachelor and master students, for exposing me to international work and peers by supporting my trips to conferences and trainings abroad, and last but not the least for always treating me as a future colleague in training and boosting my confidence by holding me and my work with respect.

I would also acknowledge the **Austrian Research Fund FWF** for providing me with the personnel costs during my appointment as a project assistant for little more than three and a half years.

I am especially thankful to **TU Wien** for supporting two of my international visits; once through **Christiana HÖRBIGER Preis** – Preis zur Förderung der internationalen Mobilität von Nachwuchswissenschaftler-innen and another time through **TU Wien Short-term grants**.

This is also a perfect platform and time to thank **Faculty of Technical chemistry**, professors, associate professors and all other tutors for their teachings. Thank you specifically for incorporating many lectures in English language over the years, thus keeping up with the international standard. I have been affiliated since 2013 with the department, and have seen a steady change that is moving towards helping international students feel more inclusive.

I would also like to extend my thanks to **Christian P. Kubicek** and **Lea Atanasova** for their teachings during many collaborative projects.

I greatly appreciate useful discussions on hydrophobins with **Agnes Przylucka, Feng Cai,** and **Günseli Bayram Akcapinar.**

It was a great pleasure to collaborate with **Ekaterina Shelest,** who hosted me in her group in Leipzig for three weeks, during which Ankyrins project was further developed.

Thanks to **Vladimir** for being a brilliant master thesis student but more than that for being a tough negotiator, the quality that fuelled many fruitful scientific discussions on ankyrins, presented in Chapter 5 of this dissertation. Thanks to also two of my other students **Sebastian** and **Isabella** for returning the favor of my supervision and teachings by producing reliable and useful results.

The timely completion of this dissertation wouldn't be possible without the healthy work environment, credit of which goes to all core group members during the last three years. Thanks to **Carina** and **Marica,** first of all for their friendship, and for their support in administrative and lab related duties. Thanks to **Feng** for fruitful collaboration on Hydrophobins project and also for his precious friendship, both local and long-distance. Thanks to **Jian** for introducing me to the lab, while I was still a master student and for equipping me with many microbiology lab related skills. Thanks to **Youzhi** for collaboration on ankyrins and for also teaching me a few awesome data handling skills during his short time in our lab. Thanks to **Shadi** for her bright smile and coffee-break times in social room. Thanks to **Mohammad** for delicious spicy food and to **Viktorija** for brilliant cakes that the whole lab could often enjoy. Thanks to **Oya** and **Marco** for saving many of the office plants (including mine) by also thinking of watering them in midst of daily lab chaos.

Kurzfassung

Ungleich der meisten Pilze sind Schimmelpilze der Gattung *Trichoderma* (Hypocreales, Ascomycota) aggressive Parasiten anderer Pilze sowie effiziente Zersetzer pflanzlicher Biomasse. Obgleich Nahrungsveränderungen in der Gattung der hypocrealen Pilze gängig sind, gibt es keine Beispiele für diese umfassenden Substrat-Vielseitigkeit in *Trichoderma*. Viele der *Trichoderma* Spezies werden als Biodünger und Biofungizide verwendet; *T. Reesei* dient als Modellorganismus in der industriellen Produktion zellulolytischer Enzyme. Außerdem verwüsten manche opportunistische Spezies Pilzfarmen und können so als Krankheitserreger dem Menschen gefährlich werden. Aus diesem Grund ist es erforderlich die immer größere Relevanz der ubiquitären Pilzgattung *Trichoderma* sowohl in ihrer Biologie als auch Evolution zu verstehen. Eine vergleichende Analyse der drei ersten Genome hat ergeben, dass Mycoparasitismus eine angeborene Eigenschaft *Trichodermas* ist. Allerdings ist die Entwicklung anderer Eigenschaften weiterhin noch nicht entschlüsselt. Wir haben die am häufigsten vorkommenden *Trichoderma* Spezies ausgewählt und ihre genomische Entwicklung untersucht. Eine phylogenomische Untersuchung 23 hypocrealer Pilze (einschließlich neun *Trichoderma* spp. Sowie dem Verwandten *Escovopsis weberi*) hat ergeben, dass die Gattung *Trichoderma* und *E. Weberi* von einem gemeinsamen Vorfahren, welcher limitierte zellulolytische Fähigkeiten hatte und sich von anderen Pilzen oder Arthropoden ernährte, abstammen. Weiters litt das *Escovopsis weberi* Genom unter extensivem Genverlust, wodurch seine kohlehydrat-aktiven Enzyme dezimiert wurden. Die evolutionäre Analyse des *Trichoderma* Gens, welches für Pflanzenzellwand abbauende, kohlehydrataktive Enzyme sowie für Hilfsproteine (pcwdcazome, 122 Genfamilien) codiert – basierend auf einer Genbaum/Spezies Übereinstimmung - hat bewiesen, dass die Entstehung der Gattung durch bisher unbekanntes Ausmaß an lateralem Gentransfer (lateral gene transfer, LGT) einhergegangen ist. Nahezu die Hälfte der Gene im *Trichoderma* pcwdcazome (47%) wurden durch LGT pflanzennaher filamentöser Pilze, welche diversen Klassen der Ascomycota angehören, erhalten, während kein LGT von anderen potentiellen Spendern beobachtet werden konnte. Zusätzlich zu der Fähigkeit sich von nicht verwandten Pilzen (wie beispielsweise Basidiomycota) zu ernähren, können wir außerdem zeigen, dass *Trichoderma* in der Lage ist, Endoparasitismus an einer breiten Auswahl an Ascomycota, inklusive vorhandenen LGT Spendern, zu betreiben. Dieses Phänomen konnte jedoch nicht bei *E. Weberi* und nur sehr

selten bei anderen mycoparasitischen hypocrealean Pilzen beobachtet werden. Dementsprechend schlägt unsere Studie vor, dass LGT im Zusammenhang mit *Trichoderma*s Fähigkeit, von taxonomisch verwandten Pilzen (genau genommen bis hin zu Adelphoparasitismus) zu schmarotzen, steht. Das könnte dazu geführt haben, dass der primär mycotrophische Pilz *Trichoderma* sich zu einem Pflanzenbiomasseverwerter entwickelt hat. Die Beurteilung des gesamten Proteoms bezüglich lgts bestätigt, dass diese Art von starkem LGT speziell auf das pcwdcazome zutrifft und nicht auf andere Genfamilien.

Die Entwicklung *Trichoderma*s hat in der Zeit des kreidezeitlich-Paläogenen Aussterbens vor 66 (± 15) Millionen Jahren stattgefunden; die Entstehung der noch vorhandenen taxonomical sections (Longibrachiatum und *Trichoderma*) sowie Kladen (*Harzianum/Virens*) geschah im Oligozän. Die Evolution der *Harzianum* Klade und des Bereichs der *Trichoderma* wurde von signifikantem Genzuwachs begleitet; der Vorfahre der Sektion Longibrachiatum jedoch durchlief rapiden Genverlust. Ankyrine sind die Gene, welche dabei am häufigsten erlangt wurden. Die evolutionäre Analyse der Ankyrin-Domänen beinhaltenden Proteine, welche im Zuge dieser Doktorarbeit durchgeführt wurde, hat gezeigt, dass sie außerdem häufig in „Orphomes“ in allen *Trichoderma* Spezies vorkommen. Bei etwa der Hälfte der *Trichoderma* ankyrome handelt es sich um „orphan“-Proteine. Die erlangten Daten, welche in dieser Dissertation präsentiert werden, geben Einblick in die evolutionären Mechanismen des Mykoparasiten *Trichoderma* und dessen Entwicklung zu einem Generalisten.

Summary

Unlike most other fungi, molds of the genus *Trichoderma* (Hypocreales, Ascomycota) are aggressive parasites of other fungi and efficient decomposers of plant biomass. Although nutritional shifts are common among hypocrealean fungi, there are no examples of such broad substrate versatility as that observed in *Trichoderma*. Many *Trichoderma* species are used as biofertilizers and biofungicides, and *T. Reesei* is the model organism for industrial production of cellulolytic enzymes. In addition, some highly opportunistic species devastate mushroom farms and become pathogens of humans. Thus, the growing importance of the ubiquitous fungal genus *Trichoderma* requires understanding its biology and evolution. A comparative analysis of the first three genomes revealed mycoparasitism as an innate feature of *Trichoderma*. However, the evolution of other traits remained not understood. We selected most commonly occurring *Trichoderma* species and studied the evolution of their genomes. A phylogenomic analysis of 23 hypocrealean fungi (including nine *Trichoderma* spp. and the related *Escovopsis weberi*) revealed that the genus *Trichoderma* and *E. Weberi* has evolved from an ancestor with limited cellulolytic capability that fed on either fungi or arthropods. Further, the genome of *Escovopsis weberi* has undergone extensive gene loss and became depleted in carbohydrate-active enzymes. The evolutionary analysis of *Trichoderma* genes encoding plant cell wall-degrading carbohydrate-active enzymes and auxiliary proteins (pcwdcazome, 122 gene families) based on a gene tree / species tree reconciliation demonstrated that the formation of the genus was accompanied by an unprecedented extent of lateral gene transfer (LGT). Nearly one-half of the genes in *Trichoderma* pcwdcazome (47%) were obtained via LGT from plant-associated filamentous fungi belonging to different classes of Ascomycota, while no LGT was observed from other potential donors. In addition to the ability to feed on unrelated fungi (such as Basidiomycota), we also showed that *Trichoderma* is capable of endoparasitism on a broad range of Ascomycota, including extant LGT donors. This phenomenon was not observed in *E. Weberi* and rarely in other mycoparasitic hypocrealean fungi. Thus, our study suggests that LGT is linked to the ability of *Trichoderma* to parasitize taxonomically related fungi (up to adelphoparasitism in strict sense). This may have allowed primarily mycotrophic *Trichoderma* fungi to evolve into decomposers of plant biomass. The whole proteome LGT assessment confirmed this kind of massive LGT is specific for pcwdcazome and not to any other gene families.

Trichoderma evolved in the time of the Cretaceous-Palaeogene extinction event 66 (± 15) Mya, but the formation of extant sections (*Longibrachiatum* and *Trichoderma*) or clades (*Harzianum/Virens*) happened in the Oligocene. The evolution of the *Harzianum* clade and section *Trichoderma* was accompanied by significant gene gain, but the ancestor of section *Longibrachiatum* experienced rapid gene loss. Ankyrins are amongst the largest number of genes gained. The evolutionary analysis of ankyrin domain-containing proteins performed in the course of this dissertation revealed that they are also frequent in orphomes of all *Trichoderma* species. About one half of *Trichoderma* ankyrome are orphan proteins. The data presented in this dissertation offer insights into the evolutionary mechanisms of a mycoparasite *Trichoderma* towards becoming a generalist.

Structure of the dissertation

This semi-cumulative Ph.D. dissertation consists of six chapters and several supplementary sections such as a Glossary, Introduction, and Appendices. All the chapters are comprised mainly using results obtained throughout this Ph.D. Research that is based on the toolkits of Microbiology, Computational Biology, Bioinformatics and Big Data Analysis in general.

Chapter 1¹ serves as an introduction for this dissertation and summarizes the post-genomic investigations on mycotrophic fungi from different taxonomic groups with a special focus on fungal-fungal interactions of hypocrealean molds. **Chapter 2**² describes the unique features of the genome of *Escovopsis weberi*, a strictly mycotrophic fungus taxonomically close to *Trichoderma*.

The core of the Ph.D. dissertation research, however, is presented in the **Chapter 3**³ that reports an extensive study about the evolution of plant cell wall degrading carbohydrate active enzymes in *Trichoderma*. The major outcome of this study was the detection of the massive lateral transfer of genes required for the degradation of plant biomass to *Trichoderma* genomes from some fungi that this fungus can parasitize. These exciting results allowed us to propose a concept of adelphoparasitism (parasitism on closely related organisms) as an important factor contributing to the architecture of *Trichoderma* genomes and prompted the follow-up research on the lateral gene transfer in fungi. **Chapter 3**, presents the detailed evolutionary and LGT assessment of all *Trichoderma* cellulolytic enzymes that may serve as a reference for the scientists researching these genes for industrial applications.

Following up the results of the Chapter 3, **Chapter 4** presents the outcome of the pilot assessment of the contribution of putative xenologues genes in the development of hypocrealean genomes providing the list of putative LGT genes in 37 hypocrealean proteomes.

¹Chenthamara K, Druzhinina IS. Ecological Genomics of Mycotrophic Fungi. In *Mycota IV Environmental and Microbial Relationships* 2016 (pp. 215-246). Springer, Cham. Editors: Irina S. Druzhinina and Christian P. Kubicek, DOI: 10.1007/978-3-319-29532-9_12

² de Man TJ, Stajich JE, Kubicek CP, Teiling C, Chenthamara K, Atanasova L, Druzhinina IS, Levenkova N, Birnbaum SS, Barribeau SM, Bozick BA. Small genome of the fungus *Escovopsis weberi*, a specialized disease agent of ant agriculture. *Proceedings of the National Academy of Sciences*. 2016 Mar 9;201518501.

³ Druzhinina IS, Chenthamara K, Zhang J, Atanasova L, Yang D, Miao Y, Rahimi MJ, Grujic M, Cai F, Pourmehdi S, Salim KA. Massive lateral transfer of genes encoding plant cell wall-degrading enzymes to the mycoparasitic fungus *Trichoderma* from its plant-associated hosts. *PLoS Genetics*. 2018 Apr 9;14(4):e1007322.

Chapter 5 throws light on the expansion of ankyrins in the genomes of *Trichoderma* species. And in the end, **Chapter 6** provides conclusive remarks from the comparative genomics of *Trichoderma* and related fungi interconnecting the first five chapters.

Published articles included in the dissertation are supplemented by the statements on the contribution made by the Ph.D. Candidate.

Appendix I refers to a CD attached to the hard copy of the dissertation that includes all files and the Supplementary materials for Chapter 4.

Appendix II presents peer-reviewed scientific papers co-authored by the Ph.D. Candidate but not included in the dissertation; the contribution by the Ph.D. Candidate is nevertheless described.

Appendix III comprises posters presented by the Ph.D. Candidate on the international scientific conferences.

Abbreviations

ANK - Ankyrin

Ankdc - Ankyrin domain containing

BLAST - Basic Local Alignment Search Tool

BUSTED - Branch-Site Unrestricted Statistical Test for Episodic Diversification

FUBAR - Fast Unconstrained Bayesian approximation

GTR - Generalized Time Reversible (model)

Hdc-ankdc - Host-domain containing ankdc

HET - Heterokaryon Incompatibility

HGT – Horizontal gene transfer

JGI - Joint Genome Institute

LGT – Lateral gene transfer

Mbp - Million base pairs

MCL - Markov Cluster Algorithm

MEME - Mixed Effects Model of Evolution

ML - Maximum Likelihood

MSA - Multiple Sequence Analysis

MYA – Million years ago

OG – Orthogroup

Pcwdcazymes – Plant cell-wall degrading Carbohydrate-active enzymes

Glossary of some terms specific for this dissertation

Ankyrome - All genes per genome encoding proteins with the ankyrin domain

Environmental opportunist - An organism that is able to establish in a broad range of ecological niches rapidly. Such organisms are not only nutritionally versatile but are also capable of efficient dispersal, can survive biotic and abiotic stresses and win in competition with the other members of the microbial community

Generalist - Nutritional versatility on dead or live biomass

Homologous genes - Genes sharing a common evolutionary ancestor

Horizontal gene transfer - When the gene transfer occurs from species of another domain of life. For instance, from a bacteria to a fungus

Interactome - All the proteins or other molecules that are involved in molecular interactions in the cell under certain conditions

Motus - Molecular operational taxonomical units

Orphome - All the proteins in a genome/group of genomes that do not have homologs in close taxonomic relatives. Depending on the context, there might be orphomes of individuals, species, groups of species, sections or higher taxa

Orthologous genes - Homologous genes derived as a result of speciation events

Lateral gene transfer - When the gene transfer occurs from species within the same domain of life. For instance, from one fungus to another fungus

Phylome (of smth) - An exhaustive collection of the phylogenetic trees of a certain taxonomic group, gene or protein family

Proteome - All the proteins that are encoded in a genome

Paralogues - Homologous genes derived as a result of gene duplication events

Parasite - Refer to any organism that feeds on a live biomass of any type

Polyphags - Refer to any organism that feeds on a dead biomass of any type

Xenologues - Genes gained as a result of lateral gene transfer/horizontal gene transfer

Preface

Thanks to integration of technologies like Illumina (then Solexa) into DNA sequencing market in 2006 and introduction of next-generation sequencing in 2007 ([Illumina-sequencing-history](#)), the cost of genome sequencing has come down drastically since 2008 ([genome.gov/sequencing-costs](#)). This drastic reduction of sequencing costs also impacted sequencing of fungal genomes and resulted in introduction of mass fungal genomes sequencing projects such as 1000 Fungal genomes project by Joint Genome Institute (JGI) of the Department of Energy under Mycocosm (<https://genome.jgi.doe.gov/Mycocosm>), a public database maintained by JGI whereby also the genomes sequenced outside the above-mentioned project are made publicly available.

Figure 1.1A shows that Ascomycota fungi stand with most interest for genome sequencing among all fungal taxons of this level. Within Ascomycota, Eurotiomycetes, Sordariomycetes and Dothideomycetes fungi get most attention owing to their cosmopolitan occurrences and biotechnological applications. Hypocreales is the taxonomical order under class Sordariomycetes with highest number of sequenced genomes (51 as per october, 2018) investigated for varied reasons [1-15]. Hypocreales forms a monophyletic group that have originated somewhere between 170-200 mya and contains several species that follows wide variety of nutritional strategies apart from mycotrophy, such as saprotrophy, carnivory, phytotrophy [16, 17]. The diversity of nutritional strategies and ecophysologies in Hypocreales [16, 18] is reflected in the diversity of genes responsible for the production of enzymes, secondary metabolites, and other compounds what makes the fungi from this order of interest for their potential applications.

A plant pathogenic fungus (*Fusarium graminearum* PH-1) provided the first hypocrealean genome to be published [19] in 2007, closely followed by the mycotrophic fungus *Trichoderma reesei* QM 6a in 2008. This strain was sequenced because of its popularity as an industrial source of cellulases and hemicellulases and for its application in biofuel production [2]. *Trichoderma* is a cosmopolitan genus that contains species established in a diversity of habitats such as dead wood, other fungi, soil, phyllosphere including the rhizosphere, aquatic and indoor

environments [20-24]. Until now, around 300 species from this genus are described [25]. Species from this genus have **unique** ability to form variety of associations with bacteria [26], other fungi [27, 28], plants [21] and higher animals [29] ranging from saprotrophy, necrotrophy to biotrophy [30-33]. The variety of nutritional strategies of *Trichoderma* makes them interesting candidates for exploitation in many areas. For instance; To efficiently degrade lignocellulose in textile industries [2, 34], in biofuel [35], biorefinery industries [36], for biofungicides [37, 38, 39]. In addition, the ability of *Trichoderma* spp., to stimulate plant growth has lead to the use of these fungi as biofertilizers or bioeffectors [40-43]. Owing to their opportunistic property, more recently *Trichoderma* spp. Have been proposed in context of self-healing of concrete cracks [44]. In spite of having above mentioned varied applications, *Trichoderma* are best studied to exploit and understand mycotrophy [4, 31, 45-48].

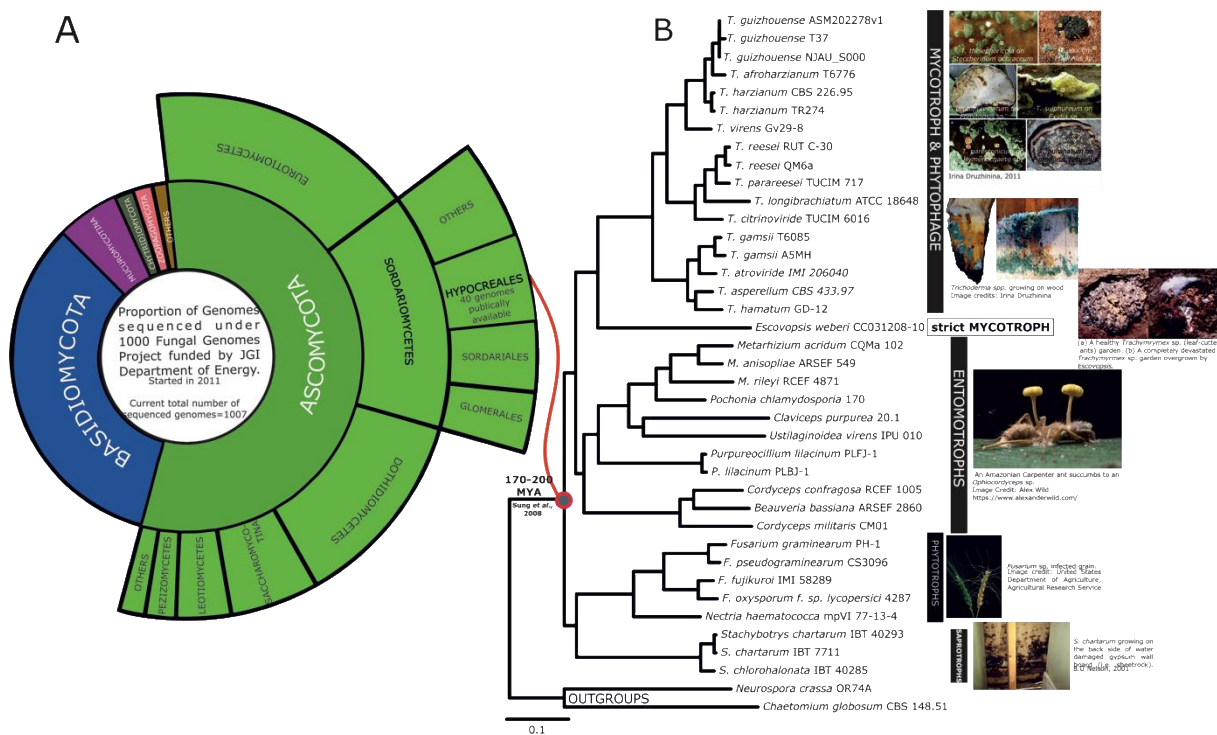


Figure 1.1 **A.** Sunburst chart depicting proportion of fungi from different groups that have been currently sequenced under 1000 genomes project in MycoCosm. **B.** A maximum likelihood phylogenetic tree including 37 hypocrealean genomes and 2 sordarilean genomes as outgroups. This phylogenetic tree is based on over 13,000 orthologous genes considering the whole proteome from considered 39 strains and, with different nutritional strategies all (or subset) of which have been considered to answer questions raised in different chapter of this dissertation. All the clades in shown ML tree are strongly supported (Details of the ML tree in Chapter 4 of this dissertation)

The availability of genomes from closely related species makes way for resolving evolutionary relationships of species of interest through the comparative genomics approach. Comparative genomics also helps to identify the genes/gene families that are essential for unique

characteristics of a particular species. Within this dissertation, genomes shown in Figure 1.1B are compared in six chapters in order to answer several questions related to ecological genomics of *Trichoderma* and evolution of these peculiar fungi.

References

1. Cuomo CA, Güldener U, Xu J-R, Trail F, Turgeon BG, Di Pietro A, et al. The *Fusarium graminearum* genome reveals a link between localized polymorphism and pathogen specialization. *Science*. 2007;317(5843):1400-2. Doi: 10.1126/science.1143708.
2. Martinez D, Berka RM, Henrissat B, Saloheimo M, Arvas M, Baker SE, et al. Genome sequencing and analysis of the biomass-degrading fungus *Trichoderma reesei* (syn. *Hypocrea jecorina*). *Nat Biotechnol*. 2008;26. Doi: 10.1038/nbt1403.
3. Coleman JJ, Rounsley SD, Rodriguez-Carres M, Kuo A, Wasmann CC, Grimwood J, et al. The Genome of *Nectria haematococca*: Contribution of Supernumerary Chromosomes to Gene Expansion. *Plos Genet*. 2009;5(8):e1000618. Doi: 10.1371/journal.pgen.1000618.
4. Kubicek CP, Herrera-Estrella A, Seidl-Seiboth V, Martinez DA, Druzhinina IS, Thon M, et al. Comparative genome sequence analysis underscores mycoparasitism as the ancestral life style of *Trichoderma*. *Genome biology*. 2011;12(4):R40.
5. Gao Q, Jin K, Ying S-H, Zhang Y, Xiao G, Shang Y, et al. Genome Sequencing and Comparative Transcriptomics of the Model Entomopathogenic Fungi *Metarhizium anisopliae* and *M. Acridum*. *Plos Genetics*. 2011;7(1):e1001264. Doi: 10.1371/journal.pgen.1001264.
6. Zheng P, Xia Y, Xiao G, Xiong C, Hu X, Zhang S, et al. Genome sequence of the insect pathogenic fungus *Cordyceps militaris*, a valued traditional Chinese medicine. *Genome Biology*. 2011;12(11):R116. Doi: 10.1186/gb-2011-12-11-r116.
7. Gao QA, Jin K, Ying SH, Zhang YJ, Xiao GH, Shang YF, et al. Genome Sequencing and Comparative Transcriptomics of the Model Entomopathogenic Fungi *Metarhizium anisopliae* and *M. Acridum*. *Plos Genetics*. 2011;7(1). Doi: ARTN e1001264
10.1371/journal.pgen.1001264. Pubmed PMID: WOS:000286653500003.
8. Zheng P, Xia YL, Xiao GH, Xiong CH, Hu X, Zhang SW, et al. Genome sequence of the insect pathogenic fungus *Cordyceps militaris*, a valued traditional Chinese medicine. *Genome Biology*. 2011;12(11). Doi: ARTN R116
10.1186/gb-2011-12-11-r116. Pubmed PMID: WOS:000301178400007.
9. Xiao G, Ying S-H, Zheng P, Wang Z-L, Zhang S, Xie X-Q, et al. Genomic perspectives on the evolution of fungal entomopathogenicity in *Beauveria bassiana*. *Sci Rep*. 2012;2:483. Doi: 10.1038/srep00483.
10. Schardl CL, Young CA, Hesse U, Amyotte SG, Andreeva K, Calie PJ, et al. Plant-Symbiotic Fungi as Chemical Engineers: Multi-Genome Analysis of the Clavicipitaceae Reveals Dynamics of Alkaloid Loci. *Plos Genetics*. 2013;9(2):e1003323. Doi: 10.1371/journal.pgen.1003323.
11. Gardiner DM, Stiller J, Kazan K. Genome Sequence of *Fusarium graminearum* Isolate CS3005. *Genome Announc*. 2014;2(2). Doi: 10.1128/genomea.00227-14.

12. Terfehr D, Dahlmann TA, Specht T, Zadra I, Kürnsteiner H, Kück U. Genome Sequence and Annotation of *Acremonium chrysogenum*, Producer of the β -Lactam Antibiotic Cephalosporin C. *Genome Announc.* 2014;2(5):e00948-14. Doi: 10.1128/genomea.00948-14. Pubmed PMID: PMC4175204.
13. Baroncelli R, Zapparata A, Piaggieschi G, Sarrocco S, Vannacci G. Draft Whole-Genome Sequence of *Trichoderma gamsii* T6085, a Promising Biocontrol Agent of Fusarium Head Blight on Wheat. *Genome Announc.* 2016;4(1):e01747-15. Doi: 10.1128/genomea.01747-15.
14. De Man TJ, Stajich JE, Kubicek CP, Teiling C, Chenthamara K, Atanasova L, et al. Small genome of the fungus *Escovopsis weberi*, a specialized disease agent of ant agriculture. *Proceedings of the National Academy of Sciences.* 2016;113(13):3567-72.
15. Druzhinina and Chenthamara JZ, Lea Atanasova, Dongqing Yang, Youzhi Miao, Mohammad J. Rahimi, Marica Grujic, Feng Cai, Shadi Pourmehdi, Kamariah Abu Salim, Alexey G. Kopchinskiy, Bernard Henrissat, Alan Kuo, Hope Hundley, Mei Wang, Andrea Aerts, Asaf Salamov, Anna Lipzen Kurt labutti, Kerrie Barry, Igor V. Grigoriev, Qirong Shen, Christian P. Kubicek. Massive lateral transfer of genes encoding plant cell wall-degrading enzymes to the mycoparasitic fungus *Trichoderma* from its plant-associated hosts. Revised manuscript resubmitted to PLOS genetics. 2018.
16. Sung GH, Poinar GO, Jr., Spatafora JW. The oldest fossil evidence of animal parasitism by fungi supports a Cretaceous diversification of fungal-arthropod symbioses. *Mol Phylogenet Evol.* 2008;49(2):495-502. Epub 2008/09/27. Doi: 10.1016/j.ympev.2008.08.028. Pubmed PMID: 18817884.
17. Zhang N, Castlebury LA, Miller AN, Huhndorf SM, Schoch CL, Seifert KA, et al. An overview of the systematics of the Sordariomycetes based on a four-gene phylogeny. *Mycologia.* 2006;98(6):1076-87. Epub 2007/05/10. Pubmed PMID: 17486982.
18. Chaverri P, Samuels GJ. Evolution of habitat preference and nutrition mode in a cosmopolitan fungal genus with evidence of interkingdom host jumps and major shifts in ecology. *Evolution.* 2013;67(10):2823-37. Doi: 10.1111/evo.12169.
19. Cuomo CA, Gueldener U, Xu JR, Trail F, Turgeon BG, Di Pietro A, et al. The *Fusarium graminearum* genome reveals a link between localized polymorphism and pathogen specialization. *Science.* 2007;317(5843):1400-2. Doi: 10.1126/science.1143708. Pubmed PMID: WOS:000249377500049.
20. Jaklitsch WM. European species of *Hypocrea* Part I. The green-spored species. *Stud Mycol.* 2009;63:1-91. Doi: 10.3114/sim.2009.63.01.
21. Druzhinina IS, Seidl-Seiboth V, Herrera-Estrella A, Horwitz BA, Kenerley CM, Monte E, et al. *Trichoderma*: the genomics of opportunistic success. *Nat Rev Microbiol.* 2011;9(10):749-59. Epub 2011/09/17. Doi: 10.1038/nrmicro2637. Pubmed PMID: 21921934.
22. Atanasova L. Chapter 2 - Ecophysiology of *Trichoderma* in Genomic Perspective. In: Gupta VK, Herrera-Estrella MS, Druzhinina RSU, Tuohy MG, editors. *Biotechnology and Biology of Trichoderma*. Amsterdam: Elsevier; 2014. P. 25-40.
23. Jaklitsch WM, Voglmayr H. Biodiversity of *Trichoderma* (Hypocreaceae) in Southern Europe and Macaronesia. *Stud Mycol.* 2015;80:1-87. Doi: 10.1016/j.simyco.2014.11.001.
25. Bissett J, Gams W, Jaklitsch W, Samuels GJ. Accepted *Trichoderma* names in the year 2015. *IMA Fungus.* 2015;6(2):263-95. Doi: 10.5598/imafungus.2015.06.02.02.
26. Hoppener-Ogawa S, Leveau JH, van Veen JA, De Boer W. Mycophagous growth of *Collimonas* bacteria in natural soils, impact on fungal biomass turnover and interactions with mycophagous *Trichoderma* fungi. *ISME J.* 2009;3(2):190-8. Epub 2008/10/17. Doi: 10.1038/ismej.2008.97. Pubmed PMID: 18923455.

27. Friedl MA, Druzhinina IS. Taxon-specific metagenomics of *Trichoderma* reveals a narrow community of opportunistic species that regulate each other's development. *Microbiology*. 2012;158(Pt 1):69-83. Epub 2011/11/15. Doi: 10.1099/mic.0.052555-0. Pubmed PMID: 22075025; pubmed Central PMCID: PMC3352360.
28. Lopez-Quintero CA, Atanasova L, Franco-Molano AE, Gams W, Komon-Zelazowska M, Theelen B, et al. DNA barcoding survey of *Trichoderma* diversity in soil and litter of the Colombian lowland Amazonian rainforest reveals *Trichoderma strigosellum* sp. Nov. And other species. *Antonie Van Leeuwenhoek*. 2013;104(5):657-74. Epub 2013/07/26. Doi: 10.1007/s10482-013-9975-4. Pubmed PMID: 23884864; pubmed Central PMCID: PMC3824238.
29. Molnár-Gábor E, Dóczy I, Hatvani L, Vágvölgyi C, Kredics L. Isolated sinusitis sphenoidalis caused by *Trichoderma longibrachiatum* in an immunocompetent patient with headache. *J Med Microbiol*. 2013;62(Pt 8):1249-52. Doi: 10.1099/jmm.0.059485-0.
30. Druzhinina IS, Seidl-Seiboth V, Herrera-Estrella A, Horwitz BA, Kenerley CM, Monte E, et al. *Trichoderma*: the genomics of opportunistic success. *Nature Reviews Microbiology*. 2011;9(10):749-59. Doi: 10.1038/nrmicro2637.
31. Atanasova, Le Crom S, Gruber S, Couplier F, Seidl-Seiboth V, Kubicek CP, et al. Comparative transcriptomics reveals different strategies of *Trichoderma* mycoparasitism. *Bmc Genomics*. 2013;14(1):121.
32. Druzhinina Irina S, Kubicek Christian P. Ecological Genomics of *Trichoderma*. The Ecological Genomics of Fungi. 2013. Doi: doi:10.1002/9781118735893.ch5.10.1002/9781118735893.ch5.
33. Xie BB, Qin QL, Shi M, Chen LL, Shu YL, Luo Y, et al. Comparative Genomics Provide Insights into Evolution of *Trichoderma* Nutrition Style. *Genome Biol Evol*. 2014;6(2):379-90. Doi: 10.1093/gbe/evu018. Pubmed PMID: WOS:000332742300011.
34. Bischof RH, Ramoni J, Seiboth B. Cellulases and beyond: the first 70 years of the enzyme producer *Trichoderma reesei*. *Microb Cell Fact*. 2016;15. Doi: 10.1186/s12934-016-0507-6.
35. Kubicek CP, Kubicek EM. Enzymatic deconstruction of plant biomass by fungal enzymes. *Curr Opin Chem Biol*. 2016;35:51-7. Epub 2016/09/11. Doi: 10.1016/j.cbpa.2016.08.028. Pubmed PMID: 27614174.
36. Bischof R, Fournis L, Limbeck A, Gamauf C, Seiboth B, Kubicek CP. Comparative analysis of the *Trichoderma reesei* transcriptome during growth on the cellulase inducing substrates wheat straw and lactose. *Biotechnol Biofuels*. 2013;6(1):127. Epub 2013/09/11. Doi: 10.1186/1754-6834-6-127. Pubmed PMID: 24016404; pubmed Central PMCID: PMC3847502.
37. Santos A, Garcia M, Cotes AM, Villamizar L. The effect of the formulation on the shelf-life of biopesticides based on two Colombian isolates of *Trichoderma koningiopsis* Th003 and *Trichoderma asperellum* Th034]. *Rev Iberoam Micol*. 2012;29(3):150-6. Epub 2011/11/26. Doi: 10.1016/j.riam.2011.11.002. Pubmed PMID: 22116019.
38. Ghosh SK, Pal S. Entomopathogenic potential of *Trichoderma longibrachiatum* and its comparative evaluation with malathion against the insect pest *Leucinodes orbonalis*. *Environ Monit Assess*. 2016;188(1):37. Epub 2015/12/18. Doi: 10.1007/s10661-015-5053-x. Pubmed PMID: 26676413.
39. Kobori NN, Mascarin GM, Jackson MA, Schisler DA. Liquid culture production of microsclerotia and submerged conidia by *Trichoderma harzianum* active against damping-off disease caused by *Rhizoctonia solani*. *Fungal Biol*. 2015;119(4):179-90. Epub 2015/03/31. Doi: 10.1016/j.funbio.2014.12.005. Pubmed PMID: 25813507.
40. Verma M, Brar SK, Tyagi RD, Surampalli RY, Valero JR. Industrial wastewaters and dewatered sludge: rich nutrient source for production and formulation of biocontrol agent, *Trichoderma viride*. *World J Microbiol Biotechnol*. 2007;23(12):1695. Epub 2007/12/01. Doi: 10.1007/s11274-007-9417-4. Pubmed PMID: 27517824.

41. Jegathambigai V, Karunaratne MD, Svinningen A, Mikunthan G. Biocontrol of root-knot nematode, *Meloidogyne incognita* damaging queen palm, *Livistona rotundifolia* using *Trichoderma* species. *Commun Agric Appl Biol Sci*. 2008;73(4):681-7. Epub 2009/02/21. Pubmed PMID: 19226812.
42. Alves-Filho ER, Maioli TU, Faria AM, Noronha FS, Silva NM, Costa MG, et al. The biocontrol fungus *Trichoderma stromaticum* downregulates respiratory burst and nitric oxide in phagocytes and IFN-gamma and IL-10. *J Toxicol Environ Health A*. 2011;74(14):943-58. Epub 2011/05/31. Doi: 10.1080/15287394.2011.573747. Pubmed PMID: 21623538.
43. Mishra N, Khan SS, Sundari SK. Native isolate of *Trichoderma*: a biocontrol agent with unique stress tolerance properties. *World J Microbiol Biotechnol*. 2016;32(8):130. Epub 2016/06/25. Doi: 10.1007/s11274-016-2086-4. Pubmed PMID: 27339311.
44. Luo J, Chen X, Crump J, Zhou H, Davies DG, Zhou G, et al. Interactions of fungi with concrete: Significant importance for bio-based self-healing concrete. *Construction and Building Materials*. 2018;164:275-85. Doi: <https://doi.org/10.1016/j.conbuildmat.2017.12.233>.
45. Baek JM, Howell CR, Kenerley CM. The role of an extracellular chitinase from *Trichoderma virens* Gv29-8 in the biocontrol of *Rhizoctonia solani*. *Curr Genet*. 1999;35(1):41-50. Epub 1999/02/18. Pubmed PMID: 10022948.
46. Brunner K, Zeilinger S, Ciliento R, Woo SL, Lorito M, Kubicek CP, et al. Improvement of the fungal biocontrol agent *Trichoderma atroviride* to enhance both antagonism and induction of plant systemic disease resistance. *Appl Environ Microbiol*. 2005;71(7):3959-65. Epub 2005/07/08. Doi: 10.1128/AEM.71.7.3959-3965.2005. Pubmed PMID: 16000810; pubmed Central PMCID: PMCPMC1168994.
47. Mukherjee AK, Sampath Kumar A, Kranthi S, Mukherjee PK. Biocontrol potential of three novel *Trichoderma* strains: isolation, evaluation, and formulation. *3 Biotech*. 2014;4(3):275-81. Epub 2014/01/01. Doi: 10.1007/s13205-013-0150-4. Pubmed PMID: 28324430; pubmed Central PMCID: PMCPMC4026447.
48. Zhang J, Bayram Akcapinar G, Atanasova L, Rahimi MJ, Przylucka A, Yang D, et al. The neutral metallopeptidase NMP1 of *Trichoderma guizhouense* is required for mycotrophy and self-defense: NMP1 of the fungicidal mold *Trichoderma guizhouense*. *Environ Microbiol*. 2015:n/a/a. Doi: 10.1111/1462-2920.12966.

Aims of the Dissertation

The precise goal of this dissertation is to link phenotypes to genotypes of fungi from the genus *Trichoderma* using comparative genomics.

To accomplish this goal, a number of self-contained analyses were done to study the following:

- Genes from hypocrealean fungi that have been studied so far in context of fungal-fungal interactions (Summarized in **Chapter 1**)
- Close genomic and ecophysiological comparison between *Trichoderma* spp. And closely related *Escovopsis weberi*, a mycoparasite found in nature in fungal gardens cultivated by leaf-cutting ants (**Chapter 2**).
- Evolution of carbohydrate-active enzymes required for the plant cell wall degradation in nine *Trichoderma* spp. By phylogenomic and molecular evolutionary analyses (**Chapter 3**).
- Inventory screening for the putative xenologues (laterally transferred genes) and duplicated genes by analyzing the proteomes from 37 hypocrealean fungi (**Chapter 4**).
- Evolution of the ankyrin domain containing gene family that represents the major genomic hallmark of *Trichoderma* (**Chapter 5**)

Chapter 1 Ecological Genomics of Mycotrophic Fungi⁴

Authors

Komal Chenthamara and Irina S Druzhinina

Affiliation

Microbiology and Applied Genomics group, Research Area Biochemical Technology, Institute of Chemical, Environmental & Bioscience Engineering ICEBE, TU Wien, Gumpendorferstrasse 1a, A1060, Vienna, Austria

Overview Interfungal interactions are common in both the ancient fungal lineages and in the most evolutionary derived “high” fungi. In this chapter, we focussed on then recent reports on genome-wide investigations of mycotrophic fungi. We described unique features that are present in intracellular mycoparasitic Cryptomycota and outlined similar and apparently convergent mechanisms employed by a diversity of fungicolous Asco- and Basidiomycota. The potential benefits and pitfalls of applications of mycoparasitic fungi for protection of agricultural crops were discussed.

Contribution by the PhD candidate

1. Literature search according to the plan for the chapter designed by candidate’s supervisor
2. Prepared draft of the chapter except the section “Conclusive Remarks on the Use of Mycotrophic Fungi in Agriculture”.
3. The list of genes of *Trichoderma* that have been studied for their role in fungal–fungal interactions (Table 12.1).
4. The list of genes of *Clonostachys rosea*, (another mycotroph) studied for their role in fungal–fungal interactions (Table 12.2).
5. Dual confrontation experiments presented in Fig 12.2, 12.3 and 12.4.
6. Revision of the drafts and preparation of the final article.

⁴ Chenthamara K, Druzhinina IS. Ecological Genomics of Mycotrophic Fungi. In *Mycota IV Environmental and Microbial Relationships 2016* (pp. 215-246). Springer, Cham.

Editors: Irina S. Druzhinina and Christian P. Kubicek, DOI: 10.1007/978-3-319-29532-9_12

12 Ecological Genomics of Mycotrophic Fungi

KOMAL CHENTHAMARA¹, IRINA S. DRUZHININA¹

CONTENTS

I. Introduction	215
II. Obligate Intracellular Mycoparasitism in Cryptomycota	216
III. Diversity of Interactions Between High Fungi	217
A. Fungi that “Stick Together”	217
B. Types of Hostile Interactions Between Fungi	218
IV. Mycotrophic Hypocrealean Fungi	220
A. <i>Escovopsis</i> : The Devastating Pest in Gardens of Leaf-Cutting Ants	220
B. Versatile Mycoparasites from the Genus <i>Trichoderma</i>	222
C. <i>Clonostachys rosea</i> Demonstrates an Alternative Toolkit for Successful Mycoparasitism	230
D. Further Candidates for Whole Genome Sequencing of Mycoparasitic Fungi	232
V. First Transcriptomic Insight into Mycoparasitism of <i>Ampelomyces quisqualis</i>	233
VI. Genomic Properties of <i>Pseudozyma flocculosa</i> , a Mycotrophic Basidiomycete That Evolved from an Advanced Plant Pathogenic Ancestor	234
VII. Conclusive Remarks on the Use of Mycotrophic Fungi in Agriculture	235
References	238

I. Introduction

A key feature of fungal communities—their interdependence with other organisms—is explained by their inability of primary production (heterotrophy). In consequence, fungi cannot form separate self-sustaining communities, and their occurrence is irrevocably linked with that of organisms on which they depend for their nutrition (Hawksworth and Mueller 2005). Contemporary interactions of fungi with plants derived from initially saprotrophic living of early fungi on dead algal material in periodic dry, limnetic ecosystems. It is conceivable that some of these fungi may have formed mutualistic associations with early terrestrial algae, which later gave rise to complex symbioses between high fungi and vascular plant modern algae. A phylogenomic study of pectinase gene expansions demonstrated that the early group of true fungi Chytridiomycota diverged from its sister clade and thus leading to the high fungi Dikarya only after pectin evolved in plant cell walls that happened not earlier than 750 million years ago (Mya) (Chang et al. 2015).

The establishment of interactions between fungi and other opisthokonts (nucleariids, other fungi and animals) is definitely more ancient than their relationships with plants and dates back to the origin of fungi as an entire monophyletic group. The divergence of the plant–animal–fungal lineages occurred likely 820–1200 Mya. Recent recalibrations of the most important fungal fossils and the construction of molecular clock phylogenetic trees allowed to put fungal evolution on a right

¹Institute of Chemical Engineering, Microbiology Group, TU Wien, Gumpendorferstrasse 1a, 1060 Vienna, Austria; e-mail: irina.druzhinina@tuwien.ac.at

track with the origin and diversification of other major lineages of multicellular eukaryotes (Lücking et al. 2009).

II. Obligate Intracellular Mycoparasitism in Cryptomycota

The availability of genomic and phylogenomic techniques shed light on the interactions between lineages of early fungi. Such studies included microsporidia (single-celled spore-forming endoparasites of animals, *Microspora*) with the ancient and relatively newly recognized group of Cryptomycota including *Rozella allomycis* (Fig. 12.1), the endoparasite of water mold (James et al. 2013; Jones et al. 2011). The latter fungus serves as the most important source of information as it is the only clade member that grows in culture. *R. allomycis* is an obligate endoparasite of the water mold fungus *Allomyces* (Blastocladiomycota) that grows as a naked mitochondriate protoplast capable of phagocytosis to devour the cytoplasm of its host. (Held 1980; James and Berbee 2012; Powell 1984) showed that *R. allomycis* has a fungal-specific chitin synthase and its resting sporangia contain chitin in cell walls. They thus conclude that Cryptomycota and *Rozella* are not evolutionary intermediates as it was previously assumed but are rather the divergent fungi that evolved from an ancestor that already had a complete suite of classical fungal characteristics.

Genome sequencing of *R. allomycis* revealed insights into the previously unfeasible nature of its interactions with its host (James et al. 2013): it is diploid and contains 6350 predicted gene models. It includes four chitin synthases, one of which (division II chitin synthase) is specific for fungi and microsporidia (Ruiz-Herrera and Ortiz-Castellanos 2010). Interestingly, among the division II chitin synthases of *R. allomycis*, one contains a myosin domain, a feature that may be required for the polarized growth during invasion of *Allomyces*, a mechanism similar to the development of the penetration tube in corn smut Ustilaginales (Basidiomycota) (Schuster et al. 2012). James et al. (2013) used Oregon Green 488 conjugate of wheat germ agglutinin fluorescent stain that binds to *N*-acetylglucosamine residues and demonstrated that the infective cyst of *R. allomycis* contains this chitin precursor and that the chitin stain



Fig. 12.1 *Rozella allomycis* parasitizing the chytrid *Allomyces*. Permission obtained from (Bruns 2006)

is most intense at those points where it penetrates the hyphae of *Allomyces*. A comparison of Cryptomycota including microsporidia with aphelids (Aphelidea, Opisthokonta) provided further insights into the interaction between the parasites and their hosts. Microsporidia and aphelids were previously considered as endoparasitic protozoans, and their placement within fungi only recently proposed (James et al. 2006; Karpov et al. 2013) and finally confirmed by phylogenomic analysis of a concatenated matrix of 200 gene sequences (James et al. 2013). Moreover, they found that *R. allomycis* genome contains orthologs of the three genes that were previously considered to be only present in microsporidian genomes and were thus interpreted as incidences of horizontal gene transfer (HGT) to serve the needs of intracellular parasitism (Cuomo et al. 2012). These are genes encoding a nucleotide phosphate transporter (NTTs; Pfam PF03219), a nucleoside H^+ symporters (PANDIT PF03825), and a chitinase class I genes (Pfam PF00182). The identification of these genes in *Rozella* represents an independent line of evidence for a close evolutionary link between Cryptomycota and microsporidia and indicates shared signatures of energy parasitism in the form of nucleotide and nucleoside transporters and genes for chitin degradation. Importantly, NTP transporters are involved in a specific theft of ATP from the host in microsporidia and the intracellular parasitic prokaryotes *Chlamydia* (*chlamydiae*) from which the genes were originally obtained by HGT (James et al. 2013; Tsaousis et al. 2008). Interestingly, the mitochondrial genome of *Rozella* showed features of degeneration that supports the hypothesis that the capacity to import ATP results in drastic genome changes for the mitochondrion. Sim-

ilar findings were also made in microsporidia, in which the capacity to retrieve ATP from their hosts by the HGT-derived bacterial NTTs is linked with a severe degeneration of their mitochondrion to a vestigial, genome-less organelle called a mitosome (Williams et al. 2002). Analysis of *Rozella*'s proteome and secretome, respectively, mainly revealed adaptations to endoparasitism that are convergent to those in other lineages of single-celled eukaryotes with a similar lifestyle. As expected for an obligate intracellular pathogen, the *Rozella* proteome is missing key components of primary metabolism. Overall, the portion of the proteome responsible for primary metabolism of *Rozella* is more similar to that of the apicomplexan parasites, *Plasmodium* and *Toxoplasma*, than that of microsporidia or other fungi. On the other hand, the amino acid metabolism of *R. allomyces* is more similar to that of Metazoa and Amoebozoa, perhaps suggestive of a phagotrophic mode of protein consumption and amino acid extraction. However, proteins involved in protein-protein interactions (e.g., signal transduction, protein folding, protein kinases, and proteins with WD40 domains) are all enriched in the *R. allomyces* proteome. James et al. (2013) hypothesized that some of the protein-protein interaction domains are actually involved in the direct manipulation of host signaling or recycling of host proteins. In support of this argument, they identified 22 genes of the Crinkler family of effector proteins. Crinkler proteins are found in many symbiotic, microbial eukaryotes but are best known in oomycete plant pathogens as secreted proteins that translocate into the host cytoplasm or nucleus to induce plant cell death. Thus, these new and most advanced genomic studies clearly demonstrate the ancient nature of intimate interactions between fungal lineages. The existence of mainly obligate and endocellular parasites in Cryptomycota sensu lato and the obvious lack of less specialized facultative associations between organisms from early fungal lineages is probably best explained by the long evolutionary history in aquatic ecosystem. Consequently, such interactions are rare among high fungi, which, however, interact in a great diversity of ways.

III. Diversity of Interactions Between High Fungi

Even before the inclusion of Cryptomycota in true fungi, this kingdom was considered as one of the most diverse members of the eukaryotic domain being probably only second after Arthropoda (Animalia). Consequently the ecology of these organisms in general and the structures of fungal communities in particular are very complex. Unfortunately fungal ecosystems and interactions are frequently described by

using the better established botanical (and rarely zoological) terminology that creates considerable confusion. The review of several inherent problems and ambiguities associated with terminologies used in general ecology to describe fungal interactions is made by Tuininga (2005). Based on the way how fungi receive nutrients, she proposed to divide inter-fungal interactions in nutritive and nonnutritive. So-called nutritive fungal interactions can then be further be differentiated into biotrophy (deriving nutrients from the cytoplasm of a living host) and necrotrophy or predation, i.e., rapid utilization of nutrients from an organism after killing it (Jeffries and Young 1994; Dighton et al. 2005; Atanasova et al. 2013). While necrotrophy is ultimately beneficial for one partner only (the host or the predator), biotrophic interactions may vary in their importance for the two fungi from mutualism (hypothetically assumed but almost not documented) to commensalism and classical parasitism.

A. Fungi that “Stick Together”

To the best of our knowledge, cases of inter-fungal mutualism are not well documented. Commensalism between fungi has been demonstrated in vitro although explanations for such observations are still insufficient. Deacon (2005), working with thermophilic fungi *Chaetomium* (Sordariales, Ascomycota) and *Thermomyces* (Eurotiales, Ascomycota), showed that the latter non-cellulolytic fungus clearly benefited from the ability of *Chaetomium* to degrade cellulose in the compost. When inoculated together, the two fungi could degrade more of the cellulose filter paper sample compared to *Chaetomium* alone. The advantages of *Chaetomium* from the presence of *Thermomyces* remain to be explained. Beneficial interactions between fungi were also shown by Friedl and Druzhinina (2012), studying infrageneric communities of *Trichoderma* (Hypocreales, Ascomycota) in vertical profiles of the two undisturbed soils in the Danube valley. They detected up to a dozen of *Trichoderma* species to coexist in a soil sample of not more than 200 mg.

Pairwise in vitro modeling of *Trichoderma* communities by cultivating one species on the culture filtrate of the other species and measuring the resulting fitness (growth rate and conidiation efficiency) revealed that many of such interactions provided a benefit, but cases of no effect or even inhibition of growth and/or conidiation were observed too. Our studies of *Trichoderma* molecular evolution and diversity in different habitats demonstrate frequent cases of sympatric speciation and cohabitation of sibling species that remains to be explained (Atanasova et al. 2010; Friedl and Druzhinina 2012; Hoyos-Carvajal et al. 2009; López-Quintero et al. 2013; Migheli et al. 2009). Besides these few examples, the absolute majority of described nutritional interactions between fungi are neither mutualistic nor based on commensalism. The aggressive behavior of fungi against each other is widely used in agriculture to suppress plant pathogenic fungi, but it may also cause adverse effects on mushroom farms and on fungal bioeffectors used for plant growth promotion such as arbuscular mycorrhizal fungi. We therefore first describe the types of such hostile interactions between fungi and then focus on several best studied cases.

B. Types of Hostile Interactions Between Fungi

“The term mycoparasitism applies strictly to those relationships in which one living *fungus* [*underlined by the authors*] acts as a nutrient source for another.” This definition by Peter Jeffries (Jeffries 1995) that limits the term to the fungal kingdom is only one of numerous similar clear statements commonly present in books and articles (Barnett 1963; Deacon 2005; Gupta et al. 2014). Ideally, the strictness of the definition should limit the use of a term to appropriate cases. Unfortunately it is not always the case in fungal ecology as numerous interactions between fungi and fungi-like protozoans (e.g., Oomycota) are also referred as mycoparasitic (Ait Barka and Clément 2008; Benhamou et al. 1999; Gaderer et al. 2015; Rey et al. 2005; Vallance et al. 2009) due to the similar impact made by these and the true mycoparasitic interactions to plant pathology. Below we describe terms related to non-mutualistic interactions between fungi:

- **Fungivory, mycophagy, or mycotrophy**—the use of fungi for food. All three terms are synonymous and may be applied (1) to

grazing on fungal hyphae (e.g., by mites or ants) or fruiting bodies (e.g., by deer or humans), (2) to various biotrophic interactions with fungi ranging from mutualism through commensalism and parasitism to predation, and (3) to saprotrophic nutrition on all types of dead fungal biomass. Fungivory nutrition is known for fungi, bacteria, plants, vertebrates (particularly for birds and mammals), invertebrates (gastropods, nematodes, and insects), and protozoans including fungi-like oomycetes and amoeba. Thus, when *Pythium* (Pythiales, Oomycota) attacks a fungus, this interaction may be referred as **mycophagy** (or fungivory or mycotrophy); in contrast, when a fungus attacks *Pythium*, another term should be used (e.g., parasitism).

- **Mycoparasitism**—the case of **mycophagy** when one fungus feeds on another fungus. It includes the true cases of parasitism when parasite does not kill its host. Such interactions are biotrophic are beneficial for a parasite (or a pathogen) and are harmful for the host.

Necrotrophic mycoparasitism—the case of **mycophagy** that is best described as predation when the feeding fungus aims to kill its prey and then feed on its dead biomass. Some authors prefer to use “prey” and “predator,” respectively, for simplicity and clarity (Atanasova et al. 2013; Barnett and Binder 1973; Druzhinina et al. 2011; Seidl et al. 2009). Necrotrophic mycoparasites tend to be more aggressive and unspecialized (Chet and Viterbo 2007). Biotrophic mycoparasites, on the other hand, are usually restricted to a certain host range and may also develop specialized structures to adsorb nutrients from their hosts. Some fungi may behave as biotrophic mycoparasites of some hosts, while in interactions with others they behave rather as predators (Zhang et al. 2015).

- **Hyperparasitism**—parasitism on a parasite. The term is not limited to fungi and may be used for any group of organisms. Different cases of mycophagy including mycoparasitism may belong to this category. For example, when the host of a mycoparasitic fungus is a plant pathogen, mycoparasite may be consid-

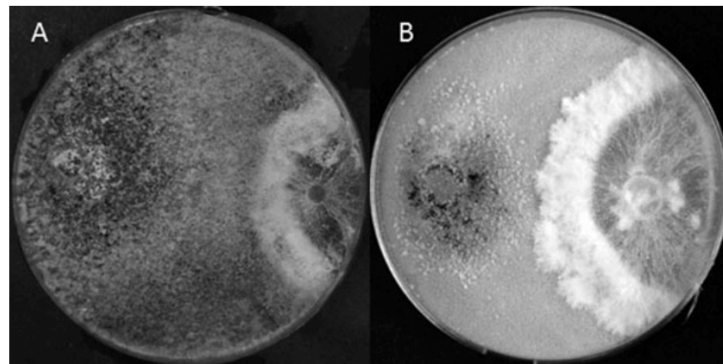


Fig. 12.2 Nutritive and nonnutritive interactions between fungi. (a) Mycoparasitism of *Trichoderma harzianum* (left) on *Athelia rolfsii*. (b) Agonism between *T. reesei* and *A. rolfsii*. *Trichoderma* (left) is overgrown by aerial hyphae of *A. rolfsii* (right) that does not parasitize on *Trichoderma*

ered as hyperparasite. It is important to note that for any hyperparasitic interactions at least two hosts and two parasites should be present. The use of this term in the absence of the primary host is not correct. For example, *Trichoderma* may be considered as a hyperparasite when it grows on sclerotia of *Athelia rolfsii* (Agaricales, Basidiomycota) that are formed on tomato plants. In this case, both *Trichoderma* and *Athelia* are parasites (and pathogens), respectively, while *Athelia* and tomato are the hosts, respectively. When the same *Trichoderma* is in vitro confronted with the same *Athelia* and it is performed in the absence of tomato, the term pathogen (or parasite) is applicable to *Trichoderma*, not to *Athelia*, and no organisms may be called as a hyperparasite.

- **Antagonism**—a type of **nonnutritive interactions** where one fungus inhibits the growth of other fungi, while continuing to grow uninhibited itself. Similar interactions include **coantagonism** with negative outcome for both fungi and **agonism** when one fungus is harmed and the other receives benefit. The latter interaction is similar to mycoparasitism, but it should not be confused with it as the benefitting fungus does not feed on the one that is harmed. An example for such interaction is *A. rolfsii* that is capable of overgrowing some strains of *Trichoderma* but does not feed on them. The benefit for *A.*

rolfsii from this behavior is the reduced competition pressure for space and resources (Fig. 12.2). Tuininga (2005) notes that the term “coantagonism” is preferable to the frequently used term “competition,” because the latter term describes only one possible mechanism of antagonistic interactions.

Other theoretically possible and nonnutritive interfungal interactions are bilaterally neutral **cohabitation**, neutral/beneficial **commensalism**, and **mutualism**, but they are very rare in fungi (vide supra) because of the usually present antagonism.

High fungi from many taxonomic groups that are able to either parasitize on plant pathogenic fungi or to antagonize them have been proposed for use in plant protection. For example, in the late 1970s, *Teratosperma sclerotivorum* (syn. *Sporidesmium sclerotivorum*, Ascomycota) that is an obligate pathogen on sclerotia of *Sclerotinia* spp. (Helotiales, Ascomycota) was suggested for use in biological control of the latter plant pathogen (see Fravel 2006 for the review). However, this technology likely did not get commercialized as the recent literature on the topic is limited: public databases contain no gene sequences for this hyperparasitic fungus (NCBI, November 22, 2015), and there is also no recent descriptions of the mechanisms of respective mycoparasitic interactions. Most of the modern antifungal biocontrol formulations use mycotrophic fungi from the order Hypocreales (Sordariomycetes, Pezizomycotina, Dikarya) that are also best studied at molecular biological, ecological, and taxonomic levels, respectively.

IV. Mycotrophic Hypocrealean Fungi

The order Hypocreales from the class Sordariomycetes contains the best studied mycoparasitic fungi such as *Trichoderma*, *Escovopsis*, and *Clonostachys*, and genome sequences have been obtained for at least one but often several of their species (Fravel 2006; Gruber et al. 2011; Karlsson et al. 2015; Kubicek et al. 2011; de Man et al. 2015; Martinez et al. 2008; Studholme et al. 2013; Xie et al. 2014). Fungi from this order show widely diverse symbiotic associations with plants, animals, and other fungi and are also capable to saprotrophic growth (Sung et al. 2008). The most common animal hosts for hypocrealean fungi are the arthropods from the orders Coleoptera, Hemiptera, and Lepidoptera (Kobayasi 1941; Mains 1958; Sung et al. 2008). Respective arthropod pathogenic hypocrealean fungi consist of several genera mainly from three families: Clavicipitaceae, Cordycipitaceae, and Ophiocordycipitaceae. Nectriaceae and Bionectriaceae mainly feed on plants (Sung et al. 2007, 2008). Although the latter authors marked the family Hypocreaceae as a mixture of fungicolous and plant-associated fungi, recent studies suggest that it is dominated by mycotrophs, of which many taxa may also grow in the rhizosphere or become endophytes (Druzhinina et al. 2011).

Sung et al. (2008) reported and described fossils of the ancient *Paleoophiocordyceps coccophagus*, a fungus belonging to the genus *Ophiocordyceps*, which represents the eldest evidence of animal parasitism by a fungus. This finding allows an estimation of the divergence times of major lineages of Hypocreales which revealed that the hypocrealean fungi were at least present since the Early Jurassic, i.e.; 193 Mya. The authors proposed that the ancestral nutritional state of hypocrealean fungi was plant based, followed by shifts first to animal and then to fungal hosts (Sung et al. 2008). According to this study, the evolution of fungal–animal symbioses of the hypocrealean fungi is characterized by the origin and diversification of three families, Clavicipitaceae, Cordycipitaceae, and Ophiocordycipitaceae, that happened 173 or 158 Mya. The family Hypocreaceae that includes such mycotrophic genera as *Trichoderma* and *Hypomyces* is inferred to have arisen at least 145 Mya (Sung et al. 2008). Their analysis also showed that shifts to fungicolous nutrition occurred several times during the evolution of hypocrealean fungi. It is

likely that mycoparasitic *Clonostachys* (Bionectriaceae) that are closely related to plant pathogenic *Fusarium* (Nectriaceae) obtained this possibility diverging from a plant-feeding host, while ancestors of *Trichoderma*, *Verticillium*, and *Escovopsis* likely evolved from animal pathogens. This is nicely illustrated by species of *Elaphocordyceps* (anamorph *Tolypocladium*, Ophiocordycipitaceae) that are mostly parasites of the ectomycorrhizal truffle genus *Elaphomyces* (Eurotiales, Ascomycota), but their next phylogenetic neighbors are all pathogens of insects.

A. *Escovopsis*: The Devastating Pest in Gardens of Leaf-Cutting Ants

The mycoparasitic hypocrealean genus *Escovopsis* is isolated from the nests of fungi-growing leaf-cutting ants, which belong to the tribe Attini (Hymenoptera, Insecta), namely, leaf-cutting ants (*Atta* and *Acromyrmex*), that share an obligate mutualism with Lepiota-ceae fungi of the genus *Leucoagaricus* such as *L. weberi* and *L. gongylophorus* (Agaricales, Basidiomycota) (Currie et al. 2006; Muchovej and Della Lucia 1990) or with pterulaceae fungi (Chapela et al. 1994; Villesen et al. 2004). These fungal cultivars have been acquired by the ants for their gardens from the environment multiple times in the course of evolution (Aylward et al. 2012; Chapela et al. 1994; Mikheyev et al. 2010). The basidiomycetes thereby form specialized hyphae called gongylidia, which serves as the main food supply for the ants (Seifert et al. 1995). In return, the ants provide the fungus with substrate for growth, means of dispersal to new locations, and protection from competitors and parasites (Muchovej and Della Lucia 1990). *Atta* colonies are one of the predominant herbivores in the Neotropics and therefore are frequently considered important agricultural pests in these areas (Hölldobler and Wilson 1990; Wallace et al. 2014). Colonies of these ants exhibit a rapid growth rate, consume hundreds of kilograms of leaves per year (Wirth et al. 2002), and cause the destruction of plantations and gardens in tropical areas of Central and South America and Costa Rica (Reynolds and Currie 2004; Wallace et al. 2014). *Escovopsis weberi* was isolated from nests of leaf-cutting ants as a natural pathogen

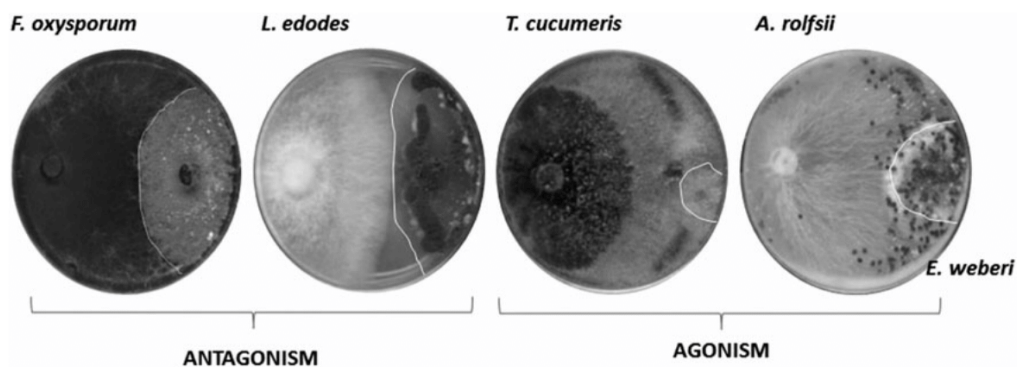


Fig. 12.3 Dual confrontations of *Escovopsis weberi* (left) with other fungi. The white line indicates the growth of *E. weberi* as detectable from the back side of the plate

of *Leucoagaricus* and was also proposed as a potential bioeffector against these ants (Reynolds and Currie 2004). According to the above explained terminology, *E. weberi* should not be assigned as a hyperparasite because *Leucoagaricus*—its host—is not a parasite but a saprotroph.

Until recently it remained unclear whether the primary nutrient source for *E. weberi* was the mushroom itself or the vegetative substrate placed on the gardens by ants, in other words whether the interaction was nutritive or rather nonnutritive. Reynolds and Currie (2004) demonstrated the true mycoparasitic nature of *E. weberi* by showing its rapid growth on pure culture of *Leucoagaricus* and negligible development on sterilized leaf fragments. Consequently, these authors described *E. weberi* as a necrotrophic mycoparasite of *Leucoagaricus* (Reynolds and Currie 2004). More recently, Marfetan et al. (2015) based on the microscopic analysis of interactions between *E. weberi* and *Leucoagaricus* spp. revealed hooklike structures and the penetration of the host hyphae and thus described *E. weberi* as a true mycoparasite. Furthermore, the most virulent *E. weberi* isolates were those which developed hooks involved in capturing *Leucoagaricus* sp. (Marfetan et al. 2015). The formation of these structures and growth rates positively correlated with virulence of individual *E. weberi* isolates, while the formation of hyphal traps did not show any correlation with virulence. Traps formed by *E. weberi* were also not able to generate pressure over their target nor degrade the *Leucoagaricus* sp. hyphae (Marfetan et al. 2015). Mycoparasitism of *E. weberi* is accompanied by secretion of enzymes and chemotropism toward *Leucoagaricus* (Marfetan et al. 2015; Reynolds and Currie 2004). Moreover water-soluble metabolites secreted by the latter fungus stimulate growth of *E. weberi* and induce its conidiation (Marfe-

tán et al. 2015). Our own results suggest that parasitism of *E. weberi* is specialized on the attack of *Leucoagaricus* spp. (K. Chenthamara and I.S. Druzhinina, unpublished data) We investigated the antifungal potential of *E. weberi* in dual confrontation assays with a standard range of plant pathogenic fungi that are used to estimate the biocontrol potential of *Trichoderma* and *Clonostachys* (Fig. 12.3). We thereby found that *E. weberi* is generally not an aggressive fungus as it is hardly able to attack *Fusarium oxysporum* (Hypocreales, Ascomycota) and is completely agonized by *Thanatephorus* sp. (*Rhizoctonia solani*, Cantharellales, Basidiomycota) and *A. rolfsii* (Agaricales, Basidiomycota). The interaction of *E. weberi* with wood-rotting fungus *Lentinula edodes* (shiitake, Agaricales, Basidiomycota) was more complex as growth of the latter one was somewhat stimulated by the presence of *E. weberi* (data not shown). Our attempts to cultivate *E. weberi* on plates that were pre-colonized by such fungi as *Trichoderma atroviride*, *Alternaria alternata* (Pleosporales, Ascomycota), *A. rolfsii*, and *L. edodes* failed, which suggested that *E. weberi* is not able to parasitize on them (data not shown).

Despite becoming a model system for the study of coevolution and host–parasite dynamics (Currie et al. 2003, 2006; Gerardo et al. 2004; Little and Currie 2008; Mendes et al. 2012; Reynolds and Currie 2004; Rodrigues et al. 2008; Seifert et al. 1995; Taerum et al. 2007, 2010), little attention has been paid to the taxonomy of *Escovopsis* until recently. In the 1990s, when the genus *Escovopsis* was proposed, only two species were known: *E. weberi* (Muchovej and Della Lucia 1990) and *E. aspergilloides* (Seifert et al. 1995). In 2013, three additional *Escovopsis* species—*E. microspora*, *E. moelleri*, and *E. lentecres-*

cens—were described, and a new genus, *Escovopsioides*, was proposed (Augustin et al. 2013). Later on, Meirelles et al. (2015) performed a survey for *Escovopsis* species in gardens of the lower attine ant *Mycetophylax morschi* in Brazil and found four strains belonging to the pink-colored *Escovopsis* clade. The examination of these strains revealed significant morphological differences when compared to previously described species of *Escovopsis* and related *Escovopsioides*. Based on sympodial type of conidiogenesis, percurrent morphology of conidiogenous cells and non-vesiculated conidiophores, Meirelles et al. (2015) described the four new strains as a new species *E. kreiselii*. Phylogenetic analyses using three nuclear markers (28S and ITS1 and 2 or the rRNA operon and the partial sequence of the translation elongation factor 1-alpha, *tef1*) from the new strains and sequences retrieved from public databases confirmed that all known fungi infecting attine ant gardens comprise a monophyletic group within the Hypocreaceae family. Specifically, *E. kreiselii* is likely associated with gardens of lower attine ants, but the mode of its pathogenicity remains uncertain. Even more interestingly, a further new species of *Escovopsis*, *E. trichodermoides*, isolated from a fungus garden of the lower attine ant *Mycocepurus goeldii*, which has highly branched, *Trichoderma*-like conidiophores lacking swollen vesicles, with reduced conidiogenous cells and distinctive conidia morphology, was described by Masiulionis et al. (2015). We compared *tef1* sequences of the two almost simultaneously described and therefore not compared *Escovopsis* species and found that they are only 90 % similar (see NCBI accession numbers KF033128 and KJ808766 for *E. trichodermoides* and *E. kreiselii*, respectively). Thus, in November 2015, there are seven species of *Escovopsis* recorded in the Index Fungorum database (<http://www.indexfungorum.org/>): *E. aspergilloides*, *E. kreiselii*, *E. lentecrescens*, *E. microspore*, *E. moelleri*, *E. trichodermoides*, and the oldest *E. weberi*. All these taxa are only known from gardens of leaf-cutting ants.

The genome of *E. weberi* was sequenced by de Man et al. (2015) and shown to have a significantly reduced size and gene content compared to closely related but less specialized mycotrophic fungi from the genus *Trichoderma*

(Kubicek et al. 2011; Martinez et al. 2008), which emphasizes the specialized nature of the interaction between *Escovopsis* and ant agriculture. While genes for primary metabolism have been retained, the *E. weberi* genome is depleted in carbohydrate-active enzymes, which may represent a reliance on a host capable to perform these functions. *E. weberi* has also lost genes necessary for sexual reproduction. Contrasting these losses, the genome encodes unique secondary metabolite biosynthesis clusters, some of which exhibit upregulated expression during host attack. The availability of the whole genome sequences of *E. weberi* and several species of *Trichoderma* makes the detailed comparison of ecophysiology of these fungi a challenging task.

B. Versatile Mycoparasites from the Genus *Trichoderma*

Of all mycoparasites and/or mycotrophs, the hypocrealean genus *Trichoderma* is probably the best studied and the most frequently applied bioeffector with the widest host/prey range (Atanasova et al. 2013; Baek et al. 1999; Brunner et al. 2005; Druzhinina et al. 2011; Elad et al. 1980; Kotasthane et al. 2015; Kubicek et al. 2011; Mukherjee et al. 2013; Studholme et al. 2013; Zhang et al. 2015). One of the many important qualities that makes *Trichoderma* outstanding as a biological control agent for plant pathogenic fungi (biocontrol; see below) is its high opportunistic potential (Jaklitsch 2011; Jaklitsch 2009) and adaptability to various ecological niches (Atanasova 2014). It has been well documented that *Trichoderma* spp. used for biocontrol can act through a diversity of mechanisms and combinations of them. Despite of the fact that these fungi are mycoparasites, necrotrophic mycoparasites, and nonspecific mycotrophs (Kubicek et al. 2011; see also Druzhinina and Kubicek 2013, for more references), they can establish themselves in the rhizosphere and stimulate plant growth and thus elicit a general plant defense reactions against pathogens (Druzhinina et al. 2011; Galletti et al. 2015; Harman 2011; Kotasthane et al. 2015). Some *Trichoderma* spp. have been also

isolated as endophytes too (Bae et al. 2009; Bongiorno et al. 2015; Chaverri et al. 2015; Gazis and Chaverri 2010; Rosmana et al. 2015). All of these characteristics make *Trichoderma* a genus of particular interest for application in agriculture as biofungicide and biofertilizer.

The genomic properties of *Trichoderma* spp. that add to their ability for biocontrol have been discussed (Martinez et al. 2008; Kubicek et al. 2011). In general these properties can be divided into such related to interactions with other fungi (Fig. 12.4) and such related to the interactions with plants and nonfungal pathogens of plants (nematodes, bacteria). As the latter topic is behind the scope of this review, the following description will only consider interfungal interactions with participation of *Trichoderma*. Druzhinina et al. (2011) and Druzhinina and Kubicek (2013) provided detailed reviews of *Trichoderma*'s ability to interact with living fungi as both mycoparasites and predators (necrotrophic mycoparasites) and also to their ability to saprotrophically feed on dead fungal biomass. The targeted biotrophic interaction of *Trichoderma* with other fungi includes such steps as sensing the presence of the host and optional coiling around their hyphae, host cell wall degradation and penetration of the host hyphae, repair of damages caused by hosts, and production of toxic secondary metabolites that may eventually kill the host and thus transforming it to a prey. In this chapter we will focus on those studies that functionally characterized genes involved in the interactions between *Trichoderma* and other fungi (Table 12.1). Most of them are involved in signal transduction during mycoparasitism, in fungal cell wall degradation, and in the production of antifungal secondary metabolites. Fewer studies focused on general and specific regulator genes such as *nox1*, *noxR*, *laeA*, *vel1*, and *xyl1* and the role of proteases.

Table 12.1 demonstrates that the absolute majority of functional genetic investigations were performed on two species of *Trichoderma* only, i.e. *T. atroviride* and *T. virens*. Atanasova et al. (2013) used DNA microarrays to compare the transcriptional response of the latter two species in comparison to *T. reesei* to the presence of *Thanatephorus cucumeris* (*Rhizoctonia solani*). They found that the three *Trichoderma* spp. exhibited a strikingly different transcriptional response already before physical contact with alien hyphae. *T. atroviride* expressed an array of genes involved in the production of secondary metabolites, GH16 β -glucanases,

various proteases, and small secreted cysteine-rich proteins. *T. virens*, on the other hand, expressed mainly the genes for biosynthesis of gliotoxin, respective precursors, and also glutathione, which is necessary for gliotoxin biosynthesis. In contrast, *T. reesei* increased the expression of genes encoding cellulases and hemicellulases and of the genes involved in solute transport. The majority of differentially regulated genes were orthologs present in all three species or both in *T. atroviride* and *T. virens*, indicating that the regulation of expression of these genes is different in the three *Trichoderma* spp. The genes expressed in all three fungi exhibited a nonrandom genomic distribution, indicating a possibility for their regulation via chromatin modification. The authors concluded that the initial *Trichoderma* mycotrophy demonstrated earlier by Kubicek et al. (2011) has differentiated into several alternative ecological strategies. In the context of their study, when *T. cucumeris* was used as an opponent for *Trichoderma*, the interactions ranged from parasitism of *T. atroviride* to predation of *T. virens* and competitive cohabitation of *T. reesei*. The neutral response of the latter species is best explained by the fact that the exclusively tropical *T. reesei* has never been isolated from soil so far and is not able to recognize temperate soil-borne *T. cucumeris* as its host or prey (Druzhinina et al. 2010). But it is important to note here that the assumption that *T. reesei* is merely a saprotrophic fungus that is not capable to mycotrophy is contradicted by numerous studies that demonstrated the ability of this fungus to attack a variety of fungi (Druzhinina et al. 2010; Atanasova et al. 2013), as also shown in Fig. 12.4.

The other conclusion that can be drawn from Table 12.1 is that the majority of the studies made were based on only a limited number of opponent fungi. In most studies either *T. cucumeris*, *A. rolfsii*, or *Botrytis cinerea* (Helotiales, Ascomycota) was used for confrontations with *Trichoderma*. As most *Trichoderma* species are capable of biotrophic and necrotrophic types of mycoparasitism and may also efficiently feed on dead fungal biomass, the conclusions of these studies therefore demonstrated only partial reduction of either one or another mycotrophic strategy employed by the respective *Trichoderma* species in given interactions. The

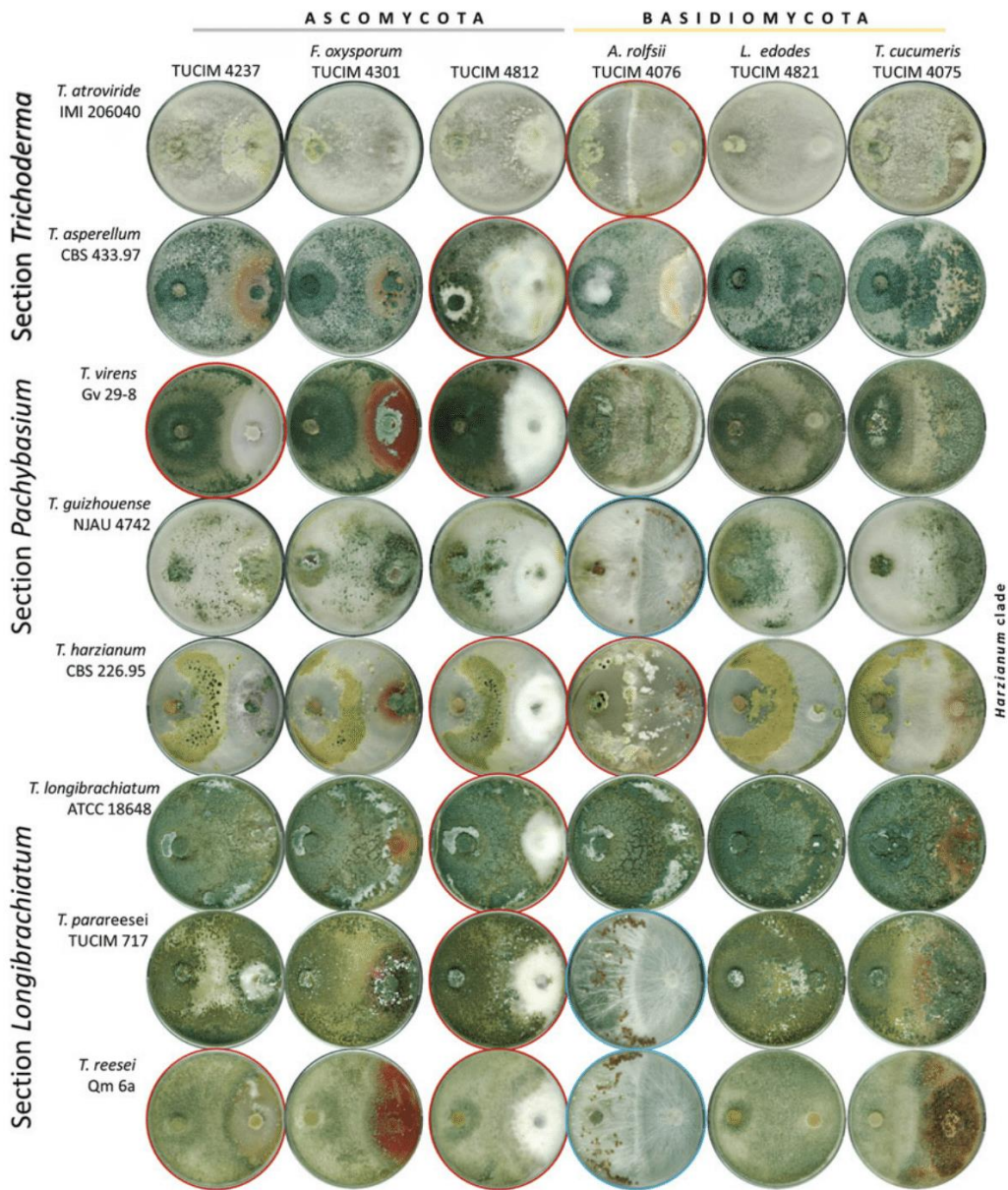


Fig. 12.4 In vitro interactions between *Trichoderma* (left) and other fungi in dual confrontation assays as observed after 10 days of incubation on PDA medium

at 25° and 12 h cyclic illumination. Cases of non-mycoparasitic interactions are marked by dark red (antagonism) and blue (agonism) background

recent study by Zhang et al. (2015) demonstrated a clear role of *nmp1* gene encoding a secreted neutral deuterolysin metallopeptidase in the predation by *T. guizhouense* [former *T. harzianum* species complex

(Chaverri et al. 2015; Li et al. 2012)] on *F. oxysporum*, *A. rolfsii*, and *A. alternata*. However, NMP1 was also found to be involved in mycoparasitism on *B. cinerea* and *S. sclerotiorum* and did not have any role in the

Ecological Genomics of Mycotrophic Fungi

225

Table 12.1 Genes of *Trichoderma* that have been studied for their role in fungal–fungal interactions

Mycoparasitism-related process	Gene	General function	Predator/parasite	Prey/host	Phenotype due to the deletion or silencing	Phenotype caused by the gene overexpression	Study	Year
Signal transduction	<i>iga1</i>	G-protein α -subunit; takes part in G-protein-mediated signaling pathway; involved in conidiation, sexual reproduction; important for sensing mating partners/preys/hosts	<i>T. atroviride</i>	<i>Thanatephorus cucumeris</i> (<i>Rhizoctonia solani</i>)	Light-independent hyper-sporulation; retarded mycoparasitic-related coiling against <i>R. solani</i> ; loss of GTPase activity, which is stimulated by the peptide toxin, Mas-7	An increase of coiling; inhibited sporulation; increased mycoparasitism on <i>R. solani</i>	Reithner et al.	2005
Signal transduction	<i>iga3</i>	G-protein α -subunit; takes part in G-protein-mediated signaling pathway; involved in conidiation, sexual reproduction; important for sensing mating partners/preys/hosts	<i>T. atroviride</i>	<i>T. cucumeris</i> (<i>R. solani</i>); <i>Borys cinerea</i>	Reduced growth; defect in chitinase secretion; loss of infection structure formation; avirulence against <i>R. solani</i> and <i>Borys cinerea</i>	n.a.	Zellinger et al.	2005
Signal transduction	<i>tac1</i>	Adenylate cyclase, a signal regulator in cAMP signaling pathway	<i>T. virens</i>	<i>Athelia rolfsii</i> (<i>Sclerotium rolfsii</i>); <i>T. cucumeris</i> (<i>R. solani</i>); <i>Pythium</i> sp. ^a	Retarded morphology; retained only 5–6% of the wild-type growth rate on agar; lowered intracellular cAMP levels below the detection limit; loss of virulence against <i>Athelia rolfsii</i> , <i>R. solani</i> , and <i>Pythium</i> sp.; negatively affected production of secondary metabolites	n.a.	Mukherjee et al.	2007
Signal transduction	<i>tmkA</i>	Mitogen-activated protein kinase (MAPK) signaling pathway gene; involved in transmitting signals for mating, filamentous growth, cell integrity, response to osmotic stress, and ascospore formation	<i>T. virens</i> , <i>T. atroviride</i>	<i>A. rolfsii</i> (<i>S. rolfsii</i>); <i>T. cucumeris</i> (<i>R. solani</i>)	Reduced ability to parasitize <i>R. solani</i> and <i>S. rolfsii</i> and the ability to induce systemic resistance in plants; improved mycoparasitism against <i>R. solani</i> in <i>T. atroviride</i> , it resulted in improved mycoparasitism	n.a.	Mukherjee et al. Viterbo et al. Mendoza-Mendoza et al. Reithner et al.	2003 2005 2003 2007
Signal transduction	<i>tmkB</i>	Mitogen-activated protein kinase (MAPK) signaling pathway gene; involved in transmitting signals for mating, filamentous growth, cell integrity, response to osmotic stress, and ascospore formation	<i>T. virens</i>	<i>A. rolfsii</i> (<i>S. rolfsii</i>); <i>T. cucumeris</i> (<i>R. solani</i>); <i>Pythium</i> sp. ^a	Reduced radial growth; constitutive conidiation in darkness; defects in cell wall integrity (autolysis of the mycelia and increased sensitivity to cell wall-degrading enzymes); attenuated ability to overgrow the plant pathogen <i>A. rolfsii</i>	n.a.	Kumar et al.	2010
Signal transduction	<i>hog1</i>	High-osmolarity glycerol response, along with other proteins is required to develop stress resistance	<i>T. harzianum</i>	<i>Phoma betae</i> (Pleosporales, Ascomycota); <i>Colletotrichum acutatum</i> (Glomerellales, Ascomycota)	Reduced osmotic and oxidative stress tolerance; reduced antagonistic activity against the tested plant pathogens	n.a.	Delgado-Jarana	2006

(continued)

226

K. Chenthamara and I.S. Druzhinina

Table 12.1 (continued)

Mycoparasitism-related process	Gene	General function	Predator/parasite	Prey/host	Phenotype due to the deletion or silencing	Phenotype caused by the gene overexpression	Study	Year
Cell wall degradation	<i>ech42</i> (<i>chl18-5</i>)	Endochitinase, secreted	<i>T. atroviride</i> , <i>T. harzianum</i> , <i>T. virens</i>	<i>A. rolfsii</i> (<i>S. rolfsii</i>); <i>T. cucumeris</i> (<i>R. solani</i>)	In <i>T. harzianum</i> : unaffected mycoparasitism of <i>A. rolfsii</i> and <i>T. cucumeris</i> . In <i>T. virens</i> : reduced mycoparasitism of <i>T. cucumeris</i>	<i>T. atroviride</i> : improved mycoparasitism	Carsolio et al. Deng et al. Baek et al.	1999 2007 1999
Cell wall degradation	<i>nag1</i>	N-acetyl- β -D-glucosaminidase, secreted	<i>T. atroviride</i> , <i>T. harzianum</i>	<i>T. cucumeris</i> (<i>R. solani</i>), <i>B. cinerea</i>	In <i>T. atroviride</i> : resulted in reduced ability to protect bean seedlings against <i>R. solani</i> . In <i>T. harzianum</i> : resulted in reduced antagonistic activity against <i>B. cinerea</i>	n.a.	Brunner et al. Dubey et al.	2003 2012
Cell wall degradation	<i>hgu3</i>	β -1,6-glucanase, secreted	<i>T. virens</i>	<i>Rhizopus oryzae</i> (Mucorales, Mucoromycotina), <i>T. cucumeris</i> (<i>R. solani</i>); <i>P. ultimum</i> ^a	No effect on growth and development; reduced ability to inhibit growth of <i>P. ultimum</i>	Improved antagonism against <i>P. altimum</i> , <i>Rhizopus oryzae</i> , and <i>T. cucumeris</i>	Djonović et al.	2006b
Cell wall degradation	<i>thpg1</i>	Endopolygalacturonase, secreted	<i>T. harzianum</i>	<i>T. cucumeris</i> (<i>R. solani</i>); <i>B. cinerea</i> ; <i>P. ultimum</i> ^a	Reduced PG activity, ability to grow on pectin medium, and ability to colonize <i>Solanum lycopersicum</i> (tomato) (Solanales, Streptophyta) roots	n.a.	Morán-Díez et al.	2009
Regulator	<i>nox1</i>	NADPH oxidase	<i>T. atroviride</i> , <i>T. harzianum</i>	<i>P. ultimum</i> ^a	Severely affected ability to form conidia in response to injury; uncompromised hyphal regeneration; loss in ability to produce reactive oxygen species (ROS) in response to injury	In <i>T. harzianum</i> : resulted in improved biocontrol potential against <i>P. ultimum</i>	Montero-Barrientos et al. Hernández-Oñate et al.	2011 2012
Regulator	<i>noxR</i>	Regulator of NADPH oxidases involved in reactive oxygen species formation	<i>T. atroviride</i>	n.a.	Affected ability to form conidia in response to injury; hyphal regeneration was not compromised	n.a.	Hernández-Oñate et al.	2012
Regulator	<i>laeA</i>	Methyltransferase. Global regulator that affects the expression of secondary metabolite gene clusters and controls sexual and asexual development	<i>T. atroviride</i>	<i>Alternaria alternata</i> ; <i>T. cucumeris</i> (<i>R. solani</i>); <i>B. cinerea</i>	Decrease in conidiation by 50% in light; no conidiation in darkness; abolishment of sporulation in response to injury; increased sensitivity to oxidative stress; affected expression of genes encoding several proteases, GH16 β -glucanases, PKases, and SSCPs; decrease in antagonism against <i>A. alternata</i> , <i>T. cucumeris</i> , and <i>B. cinerea</i> ; decrease in production of known antifungal metabolites including 6PP (6-pentyl-2H-pyran-2-one)	Increased conidiation by 30–50% in light; enhanced mycoparasitic vigor; resistance to oxidative stress (H_2O_2 , 5 mM); increased production of a known antifungal metabolite, 6PP (6-pentyl-2H-pyran-2-one)	Aghcheh et al.	2013

Ecological Genomics of Mycotrophic Fungi

227

General regulator	<i>xyr1</i>	<i>T. atroviride</i>	<i>Phytophthora capsici</i> (Peronosporales); <i>B. cinerea</i> ; <i>T. cucumeris</i> (<i>R. solani</i>)	n.a.	Reithner et al.	2014	
		Regulator protein for cellulase and hemicellulase gene expression in <i>Trichoderma</i>		Reduced transcript levels of <i>axe1</i> and <i>swc1</i> , which encode accessory cell wall-degrading enzymes; delayed response of <i>Arabidopsis thaliana</i> during <i>Trichoderma</i> - <i>Arabidopsis</i> interaction; upregulation of <i>prb1</i> expression; overall enhanced competition with studied plant pathogens probably due to overexpression of <i>prb1</i>			
Secondary metabolites	<i>tri4</i>	Cytochrome P450 monooxygenase that oxygenates trichodiene to give rise to isotrichodiol	<i>T. arundinaceum</i> , <i>T. harzianum</i>	<i>B. cinerea</i> ; <i>T. cucumeris</i> (<i>R. solani</i>)	In <i>T. arundinaceum</i> : reduced antifungal activity against <i>B. cinerea</i> and <i>T. cucumeris</i> ; reduced ability to induce the expression of <i>S. lycopersicum</i> defense-related genes belonging to the salicylic acid (SA) and jasmonate (JA) when attacked by <i>B. cinerea</i>	Malmierca et al. Cardoza et al.	2012 2015
Secondary metabolites	<i>tri5</i>	Terpene synthase	<i>T. arundinaceum</i> , <i>T. brevicompactum</i>	<i>B. cinerea</i> , <i>T. cucumeris</i> (<i>R. solani</i>)	In <i>T. arundinaceum</i> : no phytoxic activity against fungal plant pathogens and induction of plant genes involved in defense responses; altered the expression of other tri genes involved in HA biosynthesis; altered the expression of <i>hmgk</i> , <i>dppi</i> , <i>erg1</i> , and <i>erg7</i> ; all genes involved in terpene biosynthetic pathways	Malmierca et al. Tijerino et al.	2013 2011
Secondary metabolites	<i>gfp</i>	Involved in the production of gliotoxin, one of the most studied secondary metabolite in fungi that is known for its strong antimicrobial and cytotoxic activity. It is also successfully investigated as an antibiotic	<i>T. vitens</i>	<i>Sclerotinia sclerotiorum</i> ; <i>T. cucumeris</i> (<i>R. solani</i>); <i>P. ultimum</i> ^a ; <i>Galleria mellonella</i> (Lepidoptera, Arthropoda) ^b	Abolition of gliotoxin production; reduced growth; dispersed and less dense mycelium; less branched hyphae; increased sensitivity to oxidative stress (H ₂ O ₂ , 10 mM); ineffective as mycoparasites against <i>P. ultimum</i> , <i>S. sclerotiorum</i> , but retained mycoparasitic ability against <i>T. cucumeris</i> . Reduced entomopathogenic activity against <i>G. mellonella</i>	Vargas et al.	2014

(continued)

Table 12.1 (continued)

Mycoparasitism-related process	Gene	General function	Predator/parasite	Prey/host	Phenotype due to the deletion or silencing	Phenotype caused by the gene overexpression	Study	Year
Regulator	<i>vel1</i>	Velum formation protein 1; known to be one of the regulators of morphogenesis and secondary metabolism in some filamentous fungi.	<i>T. vires</i>	<i>R. solani</i> , <i>P. ulimum</i> ^a	Defective gliotoxin production; no conidiation; early chlamydospore formation under nutrient stress conditions; delayed or eliminated chlamydospore formation in nutrient-rich media; absence of mycelial and extracellular pigments; defects in the regulation of many other secondary metabolism-related genes; decrease in mycoparasitism against <i>T. cucumeris</i> and <i>P. ulimum</i>	n.a.	Mukherjee and Kenerley	2010
Secondary metabolites	<i>pkx4</i>	Polyketide synthase 4, involved in the production of the characteristic green pigment and the non-melanized structures of fruiting bodies in <i>Trichoderma</i>	<i>T. reesei</i>	<i>R. solani</i> ; <i>S. sclerotiorum</i> ; <i>A. alternata</i>	Loss of green pigmentation in their conidia; reduced resistance to UV; reduced stability of the conidial wall and the antagonistic abilities against <i>R. solani</i> , <i>S. sclerotiorum</i> , and <i>A. alternata</i> ; reduced formation of water-soluble antifungal metabolites; altered expression of other PKS-encoding genes	n.a.	Atanasova et al.	2013
Proteases	<i>prb1</i>	Alkaline serine protease, secreted	<i>T. atroviride</i> ^c	<i>T. cucumeris</i> (<i>R. solani</i>)	n.a.	Improved mycoparasitism	Flores et al.	1997
Protease	<i>sp1</i>	Serine protease, secreted	<i>T. vires</i>	<i>T. cucumeris</i> (<i>R. solani</i>)	No effect on growth rate, conidiation, extracellular protein accumulation, antibiotic profiles, or the ability to induce phytoalexins in <i>Gossypium</i> (Malvales, Streptophyta) seedlings	Increase the ability of to protect <i>Gossypium</i> seedlings	Pozo et al.	2004
Protease	<i>mmp1</i>	Neutral deuterolysin metalloprotease, secreted	<i>T. guizhouense</i>	<i>A. rolfii</i> ; <i>T. cucumeris</i> ; <i>B. cinerea</i> ; <i>S. sclerotiorum</i> ; <i>A. alternata</i> ; <i>Fusarium oxysporum</i> ; <i>F. fujikuroi</i>	Reduced mycoparasitism; no coiling around hyphae of <i>F. oxysporum</i> f. sp. <i>cubense</i> 4; reduced ability to produce antifungal secondary metabolites; reduced ability to defend against other fungi	Increased mycoparasitism; self-toxicity	Zhang et al.	2015

Accessory proteins	<i>sm1</i>	Cerato-platanin, SSCPs	<i>T. virens</i>	n.a.	Unaffected growth or development, conidial germination, production of gliotoxin, hyphal coiling, hydrophobicity, or the ability to colonize <i>Zea mays</i> roots; same levels of systemic protection as in plants that have not been treated with <i>Trichoderma</i> ; reduced level of protection in plants against diseases	Unaffected growth or development, conidial germination, production of gliotoxin, hyphal coiling, hydrophobicity, or the ability to colonize <i>Z. mays</i> roots; enhanced levels of protection against plant diseases	Dionović et al. (2006b) Salas-Marina et al. (2006) 2015
Accessory proteins	<i>sm2</i>	Cerato-platanin, SSCPs	<i>T. virens</i>	n.a.	Dramatic decrease (more in compared to <i>sm1</i>) in the ability of the fungus to induce resistance against disease caused by <i>Coellobolus heterostrophus</i> in <i>Zea mays</i> (maize) (Poales, Streptophyta)	n.a.	Gaderer et al. (2015)
Accessory proteins	<i>ep1</i>	Cerato-platanin, SSCPs	<i>T. atroviride</i> , <i>T. virens</i>	<i>Alternaria solani</i> ; <i>B. cinerea</i>	In <i>T. atroviride</i> resulted in diminished systemic protection of tomato plants (<i>S. lycopersicon</i>) against <i>A. solani</i> and <i>B. cinerea</i> , whereas in <i>T. virens</i> was less effective in protecting tomato against <i>Pseudomonas syringae</i> pv. <i>tomato</i> (Pseudomonadales, Proteobacteria) and <i>B. cinerea</i>	An increase in disease resistance against all tested pathogens	Salas-Marina et al. (2015)

^{a, b}Indicate nonfungal hosts from Oomycota and Insecta, respectively

^cThe strain IMI 206040 was initially published as *T. harzianum*

efficient attack of this fungus on *T. cucumeris* at all. Moreover, the secretion of the protein was induced when the fungus was confronted with itself on dead fungal biomass as the carbon source and was not activated when *T. guizhouense* was grown on glucose or potato dextrose agar. Besides the role of the exact protease that is definitely only one of the numerous other proteases that likely act synergistically in different *Trichoderma* species (Druzhinina et al. 2012), this study demonstrates the diversity of types of interaction that may be formed by one individual *Trichoderma* strain against a broad range of opponent fungi. It is thus impossible to assign *Trichoderma* to either exclusively biotrophic mycoparasitic fungi or describe them as necrotrophic mycoparasites or saprotrophs. Figure 12.4 illustrates the diversity of interactions between eight *Trichoderma* strains from eight species representing the three major infrageneric clades and six opponent fungi including three closely related strains of *Fusarium oxysporum* and three unrelated Basidiomycota fungi. For this reason, Druzhinina et al. (2011) proposed the more general term mycotroph as the best ecological identifier for *Trichoderma* spp. Results of Zhang et al. (2015) also demonstrate the need to study the role of individual genes in at least several possible interactions including at least parasitism and predation.

C. *Clonostachys rosea* Demonstrates an Alternative Toolkit for Successful Mycoparasitism

The mechanisms of interfungal interactions with the participation of still another hypocrealean mycotrophic fungus—*Clonostachys rosea*—have only recently attracted researchers' interest. Schroers et al. (1999) classified the mycoparasite *Gliocladium roseum* as *Clonostachys rosea* because it differed from the type species of *Gliocladium*, *G. penicillioides*, in morphology, ecology, teleomorph, and DNA sequence data. Jensen et al. (2004) used an ecological approach to present *C. rosea* as an effective mycoparasite against *Alternaria dauci* (Pleosporales, Ascomycota) and *A. radicina* on carrots (*Daucus carota* subsp. *sativus*). *C. rosea* showed a similar efficiency against these pathogens as the fungicide iprodione. A *C. rosea* strain, *C. rosea* IK726, was transformed with GFP (green fluorescent protein) and was used in biopriming of carrot seeds. Microscopy after 7 days of this biopriming showed seeds covered with a fine web of sporulating mycelium of *C. rosea*. Rodríguez et al. (2011) demonstrated the

antagonism of *C. rosea* BAF3874 against *Sclerotinia sclerotiorum* (Helotiales, Ascomycota) in pot-grown lettuce (*Lactuca sativa*) and soybean (*Glycine max*) plants and established that the strain produced antifungal compounds. They comprised a microheterogeneous mixture of peptaibols. These are short linear peptides that are rich in α -aminoisobutyric acid and bear an acetylated N-terminus and an amino alcohol at the C-terminus (Kubicek et al. 2007). They form helices that are inserted into the plasma membrane of the host causing alterations in the osmotic balance of the cell (Degenkolb et al. 2006) and inhibit membrane-bound enzymes such as cell wall polysaccharide synthases (Lorito et al. 1996). Such effects may explain some of the changes observed in the mycelium of the pathogen, including cell lysis of the hyphae and melanization (Rodríguez et al. 2011).

Recently, Karlsson et al. (2015) sequenced the whole genome of *C. rosea* IK726. A comparative phylogenetic analysis between *C. rosea*, *Trichoderma* spp., and *Fusarium* spp. suggested that *C. rosea* are sister taxa to *Fusarium* spp. (frequent plant pathogens), which belongs to family Bionectriaceae. In their study *Trichoderma* spp., which belongs to family Hypocreaceae, appeared in basal position to *C. rosea*. A comparative analysis of gene family evolution under the hypothesis that evolution of mycoparasitism in Bionectriaceae and Hypocreaceae results in selection for converging interaction mechanisms, revealed several differences between the studied mycoparasites. In comparison to *Trichoderma* spp., *C. rosea* showed expansion in several gene families such as those involved in plant cell wall degradation (polysaccharide lyase family 1 (pectin lyase), auxiliary activity family 3 (glucose-methanol-choline oxidoreductases), and auxiliary activity family 9 (lytic polysaccharide monoxygenase)); secondary metabolite synthesis (PKS, cytochrome P450 monoxygenases, PKS, and NRPS genes), likely attributing to production of antifungal components; ABC transporter and major facility superfamily membrane transporters, attributing to the fungi's high tolerance to toxins like boscalid, ZEN, and other microbial metabolites; and several ankyrin repeat proteins. In contrast, the genome of *C. rosea* contains significantly fewer carbohydrate-binding family 18 (CBM18, chitin binding) module containing genes (only two B group GH18 chitinases, only two C group GH18 chitinases, eight A group GH18 chitinases), suggesting that cell wall degradation of the fungal prey may not be a prominent strategy for interactions of *C. rosea* with other fungi.

Table 12.2 summarizes the results of functional characterization of *C. rosea* genes

Table 12.2 Genes of *Clonostachys rosea* studied for their role in fungal–fungal interactions

Mycoparasitism-related process	Genes	General function	Prey/host	Phenotype due to the deletion or silencing	Expression analysis	Study	Year
Secondary metabolites	<i>zhd101</i>	Zearalenone hydrolase	<i>F. graminearum</i>	Lowered in vitro ability to inhibit growth of the ZEA-producing <i>F. graminearum</i> . Failed to protect wheat seedlings against foot rot caused by the ZEA-producing <i>F. graminearum</i>	n.a.	Kosawang et al.	2014
Accessory proteins	<i>hyd1</i> , <i>hyd2</i> , <i>hyd3</i>	Hydrophobins	<i>F. graminearum</i> ; <i>B. cinerea</i> ; <i>T. cucumeris</i> (R. solani)	Higher growth rate of <i>Δhyd1</i> , <i>Δhyd3</i> in high salinity. Faster overgrowth of <i>Δhyd1</i> , <i>Δhyd3</i> , <i>Δhyd1</i> , and <i>Δhyd3</i> on prey/hosts. Improved protection of plants against fungal pathogens. Increased colonization ability by <i>Δhyd1</i> , <i>Δhyd3</i> on <i>Arabidopsis thaliana</i> roots	Repressed expression of <i>hyd1</i> , <i>hyd2</i> , and <i>hyd3</i> during self-interaction. High expression of <i>hyd1</i> in germinating conidia	Dubey et al.	2014
Transporter	<i>abcG29</i>	ATP-binding cassette (ABC) transporter, induced by zearalenone and the fungicides Cantus, Chipco Green, and Apron	<i>F. graminearum</i> , <i>F. oxysporum</i> f. sp. <i>radicis-lycopersici</i> ; <i>B. cinerea</i>	Delay in conidial germination and subsequent reduction in total germ tube length when subjected to H ₂ O ₂ ; increase in necrotic lesion area caused by <i>B. cinerea</i> measured on <i>A. thaliana</i> leaves pre-inoculated with <i>ΔabcG29</i> strain spores compared to the necrotic lesion area on leaves pre-inoculated with <i>C. rosea</i> WT spores; increase of <i>F. graminearum</i> foot rot disease severity in barley seedlings	n.a.	Dubey et al.	2015
Transporter	<i>abcG5</i>	ATP-binding cassette (ABC) transporter, induced by zearalenone, secondary metabolites secreted by <i>F. graminearum</i> and different classes of fungicides	<i>F. graminearum</i>	Reduced antagonism toward <i>F. graminearum</i> ; reduced biocontrol efficiency to protect barley seedlings from foot rot disease caused by <i>F. graminearum</i> ; decreased tolerance to xenobiotics secreted by <i>F. graminearum</i> and toward ZEN; iprodione- and metenoxam-based fungicides	n.a.	Dubey et al. (2014b)	2014b

required for its interaction with other fungi. The availability of the genome sequence and its comparative analysis now provides the basis for studying of those gene families that are overrepresented in the genome of this fungus (*vide supra*).

D. Further Candidates for Whole Genome Sequencing of Mycoparasitic Fungi

A number of other hypocrealean fungi are mycotrophic with different degrees of specialization. However, most of them remain poorly investigated. These are such genera as, for example, *Hypomyces* (Pöldmaa et al. 1997), *Cosmospora*, and *Verticillium*, but none of them have been investigated on the levels of genes and/or genomes. *Hypomyces*, with about 50 species recognized in recent studies (Pöldmaa 1996; Rogerson and Samuels 1985, 1989, 1993, 1994), among which more than 30 are listed in NCBI taxonomy browser (November 2015), is the largest genus of almost exclusively fungicolous fungi.

Hypomyces species occur mainly on discomycetes, boletes, agarics, or polypores. The polyporicolous *Hypomyces* are more numerous than any other group, with 19 species accepted by Rogerson and Samuels (1993). The genome of *Hypomyces chrysospermus* CBS 394.52, a bolete mold that grows on *Boletus* (Polyporales, Basidiomycota) mushrooms, turning the host a whitish, golden yellow, or tan color and making it not edible, is currently sequenced by JGI DOE in collaboration with Joe Spatafora (<https://gold.jgi.doe.gov/project?id=36363>). The same group has sequenced the whole genome sequence of *Tolypocladium inflatum* (Bushley et al. 2013), which is a pathogen of beetle larvae but is closely related to fungicolous species of *Elaphocordyceps*. The comparative analysis of *H. chrysospermus* with already sequenced fungicolous hypocrealean fungi and *T. inflatum* may give insights in convergent evolution of this lifestyle.

Sphaerodes quadrangularis (Ceratostomataceae, Hypocreales) is another example of a facultative (i.e., able to grow saprotrophically in vitro, even when the host is absent) contact biotrophic mycoparasite. It establishes an intimate relationship with its host *Fusarium avenaceum* (Nectriaceae, Hypocreales) by producing hook-shaped and clamp-like attachment structures that appeared to derive nutri-

ents and essential growth factors from living host cells (Vujanovic and Goh 2009).

Vujanovic and Goh (2009) demonstrated that *S. quadrangularis* produces hook-shaped structures within four days of subjection with *F. avenaceum*. Although *S. quadrangularis* also produces clamp-like or other contact structures, hook-shaped contact cells are more prominent. It is interesting that the diameter of hyphae parasitizing *F. avenaceum* is much smaller compared to its saprotrophic hyphae. *S. quadrangularis* also shows host specificity, as it did not form any specialized attachment structures when confronted with other *Fusarium* species. *S. mycoparasitica*, another biotrophic mycoparasite from the same genus, has however proven to be effective against a broad range of *Fusarium* species, showing positive effect on wheat (*Triticum* spp.) seed germination and seedlings growth (Vujanovic and Goh 2012). This fungus is not affected by the mycotoxins produced by *F. graminearum* such as deoxynivalenol (DON), trichothecene, and its acetyl derivatives 3-acetyldeoxynivalenol (3-ADON), 15-acetyldeoxynivalenol (ADON), and zearalenone (ZEA) (Shinha and Bhatnagar 1998), probably because of the presence of similar defense genes as found in *C. rosea* (Karlsson et al. 2015).

An interesting further target for more detailed investigations may be *Calcarisporium arbuscula* (Watson 1955) that is only putatively related to Hypocreales based on the similarity of its nucleotide sequence encoding *rpb2* gene for the RNA polymerase II large subunit 2 (NCBI accession number LN714633). Although the morphology of interaction of these fungi with their hosts that belong to Xylariales (cf. *Physalospora*) has been interpreted by Barnett (1958) as intimate balanced mycoparasitism, no advanced recent studies on this fungus have been performed. The low attention to *Calcarisporium* is demonstrated by only 18 nucleotide sequences deposited in public databases for the entire genus (NCBI, November 2015), none of which were obtained in relation to studies of interfungal interactions.

Numerous other fungicolous fungi are only investigated on the level of their taxonomy that also frequently yields unexpected results. For example, Hawksworth et al. (2010) studied *Roselliniella*, a pyrenocarpous fungi growing on lichens and forming single-celled brown ascospores and persistent interascal filaments that were previously assigned to Sordariales. The molecular phylogeny showed them to belong to Hypocreales. Jaklitsch and Voglmayr (2014) investigated and

reinstated the fungicolous genus *Thyronectria* as also belonging to Hypocreales.

V. First Transcriptomic Insight into Mycoparasitism of *Ampelomyces quisqualis*

Mycoparasitic fungi from other groups than Hypocreales are studied less intensively. One exception is the mycotrophic fungus *Ampelomyces quisqualis* (Pleosporales, Ascomycota) that is a hyperparasite of *Erysiphe*, *Podosphaera*, *Sphaerotheca*, *Uncinula*, and others that all belong to the order Erysiphales (Ascomycota) and cause powdery mildew disease of wine grapes, cucumber, carrots, mango, and other plants (Sztejnberg et al. 1989; Takamatsu 2004). In total *Ampelomyces* has been described to be associated with more than 60 species from eight different genera of the order Erysiphales and is thus the most widespread and oldest known natural enemy of powdery mildews (Kiss 2008). It is therefore frequently used for biological control of this disease (Kiss 2003, 2008; Kiss et al. 2004; Sundheim 1982).

The biology and life cycle of *A. quisqualis* has been extensively studied (Kiss et al. 2004; Kiss 2008). Conidia of *A. quisqualis* are produced in pycnidia, which develop intracellularly in the parasitized mycelia of the powdery mildew host. In the presence of water, conidia become released and form hyphae that then penetrate the nearby hyphae of powdery mildew. *A. quisqualis* can withstand cold periods in the form of pycnidia that are saprotrophically produced in the killed plant tissues, but the fungus is not an efficient saprotroph. *A. quisqualis* is able to infect and form pycnidia within powdery mildew hyphae, conidiophores, and chasmothecia that causes reduced growth and death of the parasitic mildew (Kiss 2008).

Although ecological aspects of the mycoparasitic activity in *A. quisqualis* have been widely investigated (Angeli et al. 2011, 2012; Hashioka and Nakai 1980; Kiss 2008; Kiss et al. 2004), its molecular physiology remained largely unstudied. It is known that conidia of *A. quisqualis* poorly germinate in water or in the presence of glucose but their germination is stimulated by the presence of a water-soluble substance from the host

whose chemical structure is yet unknown (Gu and Ko 1997; Sundheim 1982). Penetration of the host hyphae is made through either mechanical (Sundheim and Krekling 1982) or enzymatic processes. Rotem et al. (1999) reported the isolation of an exo- β -1,3-glucanase from *A. quisqualis*, and in vitro production of lytic enzymes has been reported for different isolates of *A. quisqualis* (Angeli et al. 2012). Siozios et al. (2015), using a high-throughput sequencing approach, established a catalog of transcripts that are formed by *A. quisqualis* during mycoparasitic interactions with *Podosphaera xanthii* (Erysiphales, Ascomycota). This catalog was then used to manufacture oligonucleotide microarrays for large-scale genome-wide analysis of transcriptional changes that occur during the early germination phase of *A. quisqualis*. They retrieved 1536 putative genes showing significant changes in transcription during the germination of *A. quisqualis*, documenting an extensive transcriptional reprogramming of *A. quisqualis* induced by the presence of the host. Genes encoding secreted proteases, virulence factors, and enzymes related to toxin biosynthesis were found to be upregulated and interpreted as putative mycoparasitism related. They also found that a rapid activation of the transcription and translation machinery in the early stages of conidial germination is crucial for the successful transition from a dormant state to vegetative growth of *A. quisqualis*. The later phase of hyphal germination is hallmarked by upregulation of the genes involved in proteasomal and vacuolar protein degradation, protein secretion, transport, and localization, and genes related to the Snf7 family of proteins, which is involved in protein sorting and transport to lysosomal compartments (Peck et al. 2004). An involvement of these proteolytic genes in mycoparasitism has also been suggested for other fungi (Grinyer et al. 2005; Monod et al. 2002; Muthumeenakshi et al. 2007; Olmedo-Monfil et al. 2002; Zhang et al. 2015). Furthermore, the authors detected homologues of secreted proteases such as dipeptidyl-peptidase 5 and the tripeptidyl-peptidase SED3 and two putative genes with homology to the M6 family of metalloprotease domain-containing proteins which all may facilitate the penetration of the host mycelium. They also identified a small secreted protein related to the ceratoplatanin family (Chen et al. 2013; Gaderer et al. 2014; Skinner et al. 2001). They are widespread among fungi and believed to be involved in fungus–host interaction phytotoxicity in different plant pathogens (Jeong et al. 2007; Pazzagli et al. 1999) or elicitors of the plant defense response in mycoparasitic *Trichoderma* spp. (Djonović et al. 2006a; Seidl et al. 2006). The actual role of this protein in the mycoparasitic action of *A. quisqualis* remains therefore to be determined.

Siozios et al. (2015) identified genes encoding proteins involved in toxin biosynthesis among the upregulated genes: a homologue of a trichodiene oxygenase, which has a key role in

the trichothecene biosynthesis pathway (Cardoza et al. 2011), and a homologue of the sterigmatocystin biosynthesis P450 monooxygenase. Finally, two of the upregulated genes encoded multidrug transporters and the major facilitator superfamily to that resembled in *C. rosea* (Karls-son et al. 2015).

Several genes reported for their role in mycoparasitism have been found in dormant conidia of *A. quisqualis*. These were cell wall-degrading enzymes, including different glycosyl hydrolases and homologues of MAPK I such as *Pmk1* of *Magnaporthe grisea* (Magnaporthales, Ascomycota) and the *Tmk1* of *T. atroviride*. In fungi, MAPK signaling pathways are involved in the transduction of a wide variety of extracellular signals and play an important role in the regulation of different developmental processes, including those related to pathogenicity (Table 12.1). The authors also noted two lectin-related proteins that are well known for carbohydrate-binding properties and are widely distributed in animals, plants, and microorganisms (Lam and Ng 2010). *A. quisqualis*-related lectins could potentially be involved in the mycoparasitic process by recognizing the powdery mildew host and facilitating penetration. This study revealed several convergent strategies deployed by mycoparasites from different taxonomic groups. Future studies, including the sequencing of the *A. quisqualis* genome, could aid our understanding of the biology and evolution of the mycoparasitic lifestyle in general.

VI. Genomic Properties of *Pseudozyma flocculosa*, a Mycotrophic Basidiomycete That Evolved from an Advanced Plant Pathogenic Ancestor

Another hyperparasitic fungus that may be used to control powdery mildews is *Pseudozyma flocculosa* (Ustilaginales, Ustilaginomycotina, Basidiomycota) that is closely related to the model plant pathogen *Ustilago maydis* yet not capable to attack plants (Kemen and Jones 2012). Lefebvre et al. (2013) presented

the comparative genomics of *P. flocculosa* and plant pathogenic smut fungi *U. maydis* (Kaemper et al. 2006), *U. hordei* (Laurie et al. 2012), and *Sporisorium reilianum* (Schirawski et al. 2010) (all from Ustilaginales). Several Ustilaginomycetes smut fungi share common features that are essential for pathogenicity. *U. maydis* interaction with maize (*Zea mays*) became the model system in phytopathology for investigation of factors essential for the establishment of the biotrophic parasitism. The genome sequence of *U. maydis* has revealed previously unknown genes that play key roles during such pathogenicity (Kaemper et al. 2006). Among these was a distinctive set of genes that coded for small secreted proteins referred to as effector proteins (or effectors), of which many had unknown functions. However, some were essential for infection and several counteracted plant defense responses, thus facilitating infection by the smut fungus (Brefort et al. 2009; Doehlemann et al. 2011).

In the case of *U. maydis*, the secreted effectors were found to be arranged in clusters and were upregulated upon recognition of the host plant, upon invasion, and in developing tumor tissue. Cluster deletion analysis proved their importance in pathogenicity (Kämper et al. 2006; Schirawski et al. 2010). The *P. flocculosa* genome comprises 6877 predicted protein coding genes and exhibited genomic features, including hallmarks of plant pathogenicity, that were very similar to the plant pathogens *U. maydis*, *Sporisorium reilianum*, and *Ustilago hordei* (Lefebvre et al. 2013). These findings and phylogenomic analysis suggested that *P. flocculosa* diverged from a plant pathogenic ancestor. Interestingly, however, Lefebvre et al. (2013) observed a loss of a specific subset of the secreted effector proteins (CSEP) reported to influence virulence in *U. maydis*. Although 345 CSEP-encoding genes were encoded by the *P. flocculosa* genome, which is a similar number as those found in the plant pathogenic Ustilaginales, orthologs for 51 out of 55 genes encoding secreted proteins that influence plant pathogenicity and virulence were absent in *P. flocculosa*. Since otherwise *P. flocculosa* has a high level of conservation of all other pathogenicity-related genes, e.g., encoding for enzymes in cell wall degradation and biosynthesis of secondary metabolites, this suggests that the loss of above described effectors represents the crucial factor which explains the not plant pathogenic lifestyle of *P. flocculosa*.

Yet the interaction between *P. flocculosa* and its fungal host might be dictated by other effector proteins. For example, the secretome of *P. flocculosa* includes two NPP1-containing proteins that are absent from plant pathogenic Ustilaginales (Kämper et al. 2006; Schirawski et al. 2010; Laurie et al. 2012) and also from other basidiomycetes and which are involved in the formation of necrosis and ethylene. They have so far only been identified in *Monilophthora perniciosa* (Agaricales), the causal agent of witches' broom disease of *Theobroma cacao* (Meinhardt et al. 2008). Interestingly, the NPP1-containing proteins exhibit structural similarities to actinoporins, which form transmembrane pores (Ottmann et al. 2009), which fits well to previous observations that the collapse of powdery mildew colonies caused by *P. flocculosa* could be due to alteration of the plasma membrane and cytoplasmic leaking (Hajlaoui and Belanger 1991; Hajlaoui et al. 1994; Mimee et al. 2009). Thus, NPP1-containing proteins could be key elements explaining the antagonism of *P. flocculosa* toward powdery mildews.

Other species-specific genes also provided further insights into how *P. flocculosa* acquired its potential to antagonize powdery mildews. For instance, two divergent GDSL lipases/esterases (Akoh et al. 2004) that contain a CE16 carbohydrate esterase motif that is exclusive to *P. flocculosa* have been identified that may be of relevance to its activity as an epiphytic competitor.

Another interesting observation differentiating *P. flocculosa* from the plant pathogens was the identification of a gene encoding a subgroup C GH18 chitinase adjacent to another gene encoding a chitin-binding LysM protein. The same genomic arrangement has also been found in mycoparasitic *Trichoderma* species (Kubicek et al. 2011). Interestingly, the LysM protein TAL6 of *T. atroviride* inhibited its own spore germination, while it had no effect on *Aspergillus niger* or *Neurospora crassa* (Ascomycota, Sordariales) (Seidl-Seiboth et al. 2013), suggesting a self-regulatory role in fungal growth and development. TAL6 could also act to protect the fungus against self-degradation by its other chitinases during mycoparasitism. Such a protective function for LysM chitinases against wheat (*Triticum aestivum*) was described during infection by for *Mycosphaerella graminicola* (Capnodiales, Ascomycota) (Marshall et al. 2011). While there is no evidence for a role of chitinases

in the biocontrol activity of *P. flocculosa* (Bélanger et al. 2012), these finding suggests that a feature is shared with the mycoparasites, which requires further investigation.

VII. Conclusive Remarks on the Use of Mycotrophic Fungi in Agriculture

The biological control of plant diseases, or biocontrol, is an agricultural technique that is based on the use of natural hyperparasites and/or antagonists of plant pathogenic organisms to prevent or combat disease; in a broad sense, biocontrol may also include the application of plant stimulating (micro)organisms that help crops sustain abiotic stresses such as drought or salinity. It is very important to note that not all organisms but only humans¹ are capable to do biocontrol. The success of biocontrol is best defined by its result—reduced disease index for crops, but not by the mechanism of action and the type of interactions involved. Thus, efficient bioeffectors (organisms used in biocontrol) may (1) stimulate plants to induce their resistance, (2) compete with plant pathogens, (3) antagonize plant pathogens by means of secondary metabolite production, or (4) directly attack such pathogens as parasites or predators. Figure 12.5 gives an overview of biocontrol relevant inter-fungal interactions. Nonnutritive antagonistic interactions are depicted in pane a, while b–d demonstrate cases of parasitism among which b and c are beneficial for the plant as the “good” fungus or bioeffector attacks either plant pathogenic nematodes (b) or plant pathogenic and therefore “bad” fungi. The nature of the interaction showed in e is disputable and may be considered as either nonnutritive mutualism (plant gets stimulated while mycoparasitic fungus may find a greater diversity of host organisms) or commensalism when only plant benefits.

¹ The cases of natural agriculture as that of leaf-cutting ants are briefly discussed above.

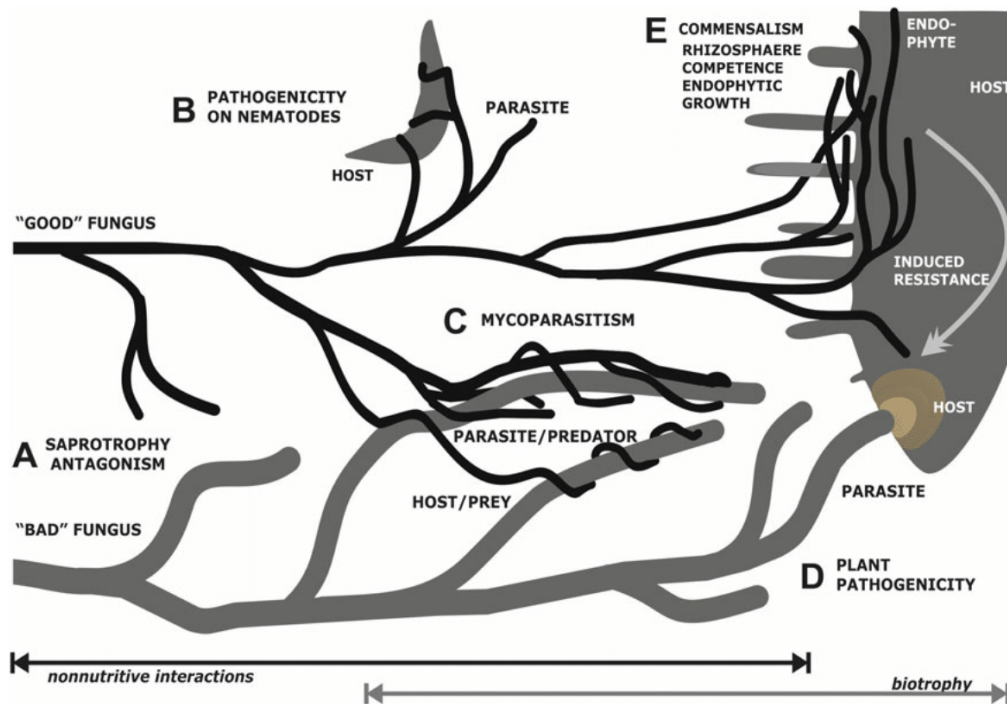


Fig. 12.5 A simplified overview of interfungal interactions that are relevant for biological control of plant pathogenic fungi and nematodes. Exclusively nonnutritive antagonistic interactions are depicted on pane (a), while (b–d) demonstrate cases of parasitism among which (b) and (c) are beneficial for the plant as the “good” fungus or bioeffector attacks either plant pathogenic nematodes (b) or plant pathogenic and therefore “bad” fungi (c). However, the cases of nutritive mycoparasitism (biotrophic and necrotrophic) may

also be accompanied by nonnutritive interactions such as antagonism or agonism. Due to the potential applications of mycoparasitic fungi for crop protection, the so-called “bad” fungi are frequently labeled as pathogens even in the absence of their host plants when solely fungal–fungal interactions are investigated. However, in such studies, these “pathogens” serve as hosts for “good” fungi that parasitize on them; therefore, the latter ones—the “good” fungi—should rather be named as pathogens

A “good” label for a bioeffector organism is conditional and may only be applied in respect of exact interactions and an exact crop plant (Fig. 12.6). The application of mycoparasitic and antagonistic fungi for biocontrol allows to reduce the use of chemical pesticides which is usually strongly supported by the general public, and therefore respective research will likely attract more attention and funding. The Directive 2009/128/EC of the European Parliament and of the Council of 21 October 2009 “establishing a framework for Community action to achieve the sustainable use of pesticides” (<http://eur-lex.europa.eu/legal-content/EN/TXT/?uri=CELEX%3A32009L0128>) contains the respective statement: “Appropriate risk management measures shall be taken and the use of low-risk plant protection products as defined in Regulation (EC) No 1107/2009 and biological control measures shall be considered in

the first place” that illustrates the future trend toward reduced use of chemical pesticides under the need to increase crop production for the growing population. However, despite the generally accepted low risk, the release of bioeffectors in the environment may also have adverse effects on both agricultural and natural ecosystems. It appears to be conceivable that introduced biocontrol fungi in case of either importation or augmentation practices will increase competition pressure for naturally present plant-beneficial microorganisms including other fungi and bacteria. For instance, the most prominent and widely accepted as “good” fungus *Trichoderma* may parasitize on arbuscular mycorrhizal fungi *Gigaspora* (Diversisporales, Glomeromycota) that are used to enhance plant nutrition and stress resistance (Lace et al. 2015) or even affect the plant as demonstrated by the colonization of

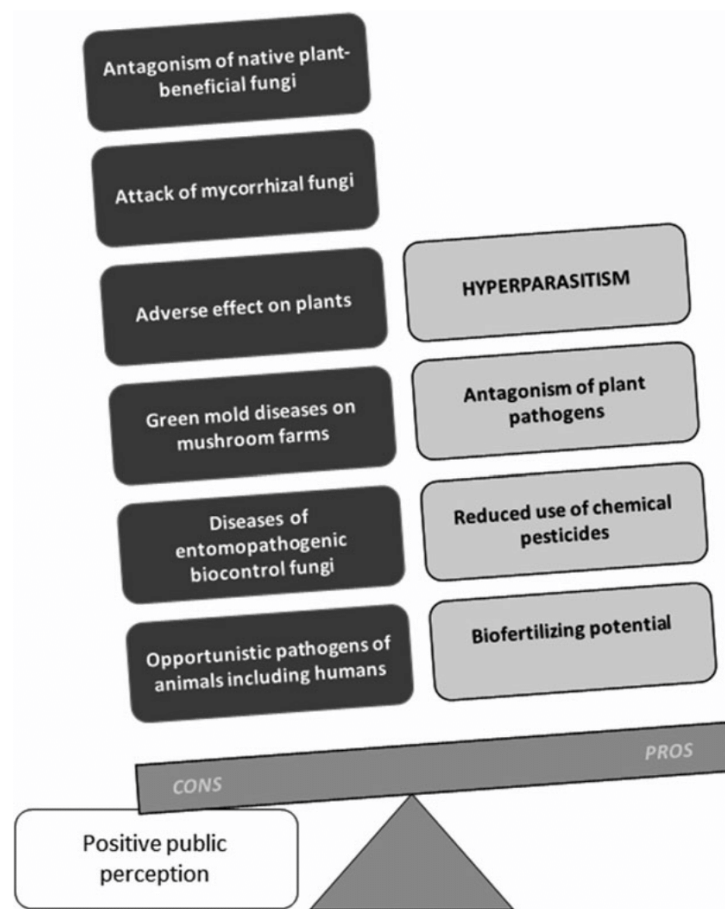


Fig. 12.6 Positive and negative arguments for the use of mycoparasitic fungi in biological control of plant pathogenic fungi

broad areas of the root epidermis of *Medicago truncatula* (Fabaceae, Angiosperms, Plantae) by *T. atroviride* leading to localized death. However, reports on direct adverse effects of biocontrol fungi on plants are rare: *T. viride* was diagnosed as a causative agent of dieback of *Pinus nigra* (Pinales, Plantae) seedling in Italy (Li Destri Nicosia et al. 2015) and different species of *Tilletiopsis* (Entylomatales, Basidiomycota) that are well-known antagonists of powdery mildews caused by Erysiphales fungi (Hijwegen 1986, 1989; Hoch and Provvidenti 1979; Klecan 1990; Knudsen and Skou 1993; Urquhart 1994). Smut fungi belonging to genus *Tilletiopsis* were demonstrated to cause “white haze” on the apple surface by Boekhout et al. (2006), in particular under conditions of ultralow oxygen storage. Clearly these fungi are able to reduce the growth of other fungi that contributes to their success as apple colonizers.

The extensive colonization of harvested apples by *T. minor* and *T. pallescens* may diminish the prospects for their commercial application as biocontrol agents, as registration as a biocontrol agent will become more complicated (Baric et al. 2010).

Several studies also document the adverse effect of fungal hyperparasites on fungi used to control insect pests. It has been shown that the mycoparasitic *Syspastospora parasitica* (Hypocreales, Ascomycota) attacks *Beauveria bassiana* (Hypocreales, Ascomycota) growing on a Colorado potato beetle (*Leptinotarsa decemlineata*) cadaver (Klinger et al. 2006). Our own data indicate that this action that may also be

performed by almost any *Trichoderma* species (Druzhinina, Atanasova, unpublished) and thus the application of *Trichoderma* may counteract the positive role of *B. bassiana* on the control of the disease. Similar to this, the chytrid fungus *Gaertneriomyces semiglobifer* (Spizellomyceales, Chytridiomycota) is capable to parasitism of entomophthoralean gypsy moth *Lymantria dispar* pathogen *Entomophaga maimaiga* (Entomophthorales, Entomophthoromycota) in soil (Hajek et al. 2013). The authors propose that mycoparasitism, whether by *G. semiglobifer* or other mycoparasitic fungi, might be partially responsible for declines in azygospore reservoirs, especially under wet conditions where the motile zoospores of chytrids would have better access to susceptible fungal host spores.

Besides the direct impact on plants and plant-interacting microorganisms, fungi used in biocontrol may also have adverse effects on mushroom production (Castle et al. 1998; Hajek et al. 2013; Hermosa et al. 1999; Kim et al. 2012; Komon-Zelazowska et al. 2007; Kredics et al. 2010; Park et al. 2006) and animals including humans as opportunistic pathogens (Komon-Zelazowska 2014). Interestingly *T. longibrachiatum* that is the most frequently detected *Trichoderma* species capable to attack even immunocompetent humans (Kredics et al. 2003; Molnár-Gábor et al. 2013; Park et al. 2006; Sandoval-Denis et al. 2014) is still referred as a “good” biocontrol fungus (Ruocco et al. 2015). Moreover, the recent broad survey of clinically relevant *Trichoderma* species that was based on the detailed DNA barcoding demonstrated that almost all most prominent plant-beneficial *Trichoderma* species such as *T. harzianum*, *T. asperellum*, *T. atroviride*, *T. gamsii*, *T. koningiopsis*, and others are capable to attack immunocompromised humans (Sandoval-Denis et al. 2014). Last but not least, the materials presented in other chapters of this book on multiple and complex interactions between fungi and bacteria allow to assume the severe impact of introduced “good” but environmentally aggressive fungi on these communities, which may cause both positive and negative consequences for soil microbiome in general and consequently on plants.

Interestingly, to the best of our knowledge, up to now there are no reports published on adverse effects of *Clonostachys rosea* on humans, cultivated mushroom, or biocontrol insects. It could be possible that the mycoparasitic ability derived from herbivorous ancestors may possess fewer number of possible adverse effects compared to mycoparasites that evolved from an entomopathogenic-like organisms. No detailed ecological risk assessment analyses on the use of mycotrophic fungi have been performed. However, the newest genome-wide mechanistic and evolutionary studies would provide sufficient background for such research.

Acknowledgments The work on this review was supported by Austrian Science Fund (FWF): project number 25613 B20 to ISD. The authors are thankful to Mohammad Rahimi (TU Wien) for the gift of his image used on Fig. 12.2b and to Christian P. Kubicek (TU Wien) for critical reading of the manuscript.

References

- Aghcheh RK, Druzhinina IS, Kubicek CP (2013) The putative protein methyltransferase LAE1 of *Trichoderma atroviride* is a key regulator of asexual development and mycoparasitism. *PLoS One* 8(6):e67144
- Ait Barka E, Clément C (2008) Plant-microbe interactions: 2008. Research Signpost, Kerala
- Akoh CC, Lee G-C, Liaw Y-C, Huang T-H, Shaw J-F (2004) GDSL family of serine esterases/lipases. *Prog Lipid Res* 43(6):534–552
- Angeli D, Maurhofer M, Gessler C, Pertot I (2011) Existence of different physiological forms within genetically diverse strains of *Ampelomyces quisqualis*. *Phytoparasitica* 40(1):37–51
- Angeli D, Puopolo G, Maurhofer M, Gessler C, Pertot I (2012) Is the mycoparasitic activity of *Ampelomyces quisqualis* biocontrol strains related to phylogeny and hydrolytic enzyme production? *Biol Control* 63(3):348–358
- Atanasova L (2014) Ecophysiology of trichoderma in genomic perspective. In: Gupta VK, Herrera-Estrella MS, Druzhinina RSU, Tuohy MG (eds) *Biotechnol. Biol. Trichoderma* [Internet]. Elsevier, Amsterdam, pp 25–40. Available from: <http://www.sciencedirect.com/science/article/pii/B9780444595768000023> (cited 2 Nov 2015)
- Atanasova L, Jaklitsch WM, Komon-Zelazowska M, Kubicek CP, Druzhinina IS (2010) Clonal species *Trichoderma parareesei* sp. nov. likely resembles the ancestor of the cellulase producer *Hypocrea*

- jecorina/T. reesei*. Appl Environ Microbiol 76 (21):7259–7267
- Atanasova L, Crom SL, Gruber S, Couplier F, Seidl-Seiboth V, Kubicek CP et al (2013) Comparative transcriptomics reveals different strategies of *Trichoderma mycoparasitism*. BMC Genomics 14 (1):121
- Augustin JO, Groenewald JZ, Nascimento RJ, Mizubuti ESG, Barreto RW, Elliot SL et al (2013) Yet more “weeds” in the garden: fungal novelties from nests of leaf-cutting ants. PLoS One 8(12):e82265
- Aylward FO, Currie CR, Suen G (2012) The evolutionary innovation of nutritional symbioses in leaf-cutter ants. Insects 3(1):41–61
- Bae H, Sicher RC, Kim MS, Kim S-H, Strem MD, Melnick RL et al (2009) The beneficial endophyte *Trichoderma hamatum* isolate DIS 219b promotes growth and delays the onset of the drought response in *Theobroma cacao*. J Exp Bot 60 (11):3279–3295
- Baek J-M, Howell CR, Kenerley CM (1999) The role of an extracellular chitinase from *Trichoderma virens* Gv29-8 in the biocontrol of *Rhizoctonia solani*. Curr Genet 35(1):41–50
- Baric S, Lindner L, Marschall K, Dalla VJ (2010) Haplotype diversity of *Tilletiopsis* spp. causing white haze in apple orchards in Northern Italy. Plant Pathol 59(3):535–541
- Barnett HL (1963) The nature of mycoparasitism by fungi. Annu Rev Microbiol 17(1):1–14
- Barnett HL (Horace L. Parasitism of *Calcarisporium parasiticum* on species of *Physalospora* and related fungi (Internet). West Virginia University. Agricultural Experiment Station; 1958 (cited 2015 Dec 1). Available from: <http://archive.org/details/parasitismofcalc420barn>
- Barnett HL, Binder FL (1973) The fungal host-parasite relationship. Annu Rev Phytopathol 11(1):273–292
- Bélanger RR, Labbé C, Lefebvre F, Teichmann B (2012) Mode of action of biocontrol agents: all that glitters is not gold. Can J Plant Pathol 34(4):469–478
- Benhamou N, Rey P, Picard K, Tirilly Y (1999) Ultrastructural and cytochemical aspects of the interaction between the mycoparasite *Pythium oligandrum* and soilborne plant pathogens. Phytopathology 89(6):506–517
- Boekhout T, Gildemacher P, Theelen B, Müller WH, Heijne B, Lutz M (2006) Extensive colonization of apples by smut anamorphs causes a new postharvest disorder. FEMS Yeast Res 6(1):63–76
- Bongiorno VA, Rhoden SA, Garcia A, Polonio JC, Azevedo JL, Pereira JO et al (2015) Genetic diversity of endophytic fungi from *Coffea arabica* cv. IAPAR-59 in organic crops. Ann Microbiol 28:1–11
- Brefort T, Doehlemann G, Mendoza-Mendoza A, Reissmann S, Djamei A, Kahmann R (2009) *Ustilago maydis* as a pathogen. Annu Rev Phytopathol 47 (1):423–445
- Brunner K, Peterbauer CK, Mach RL, Lorito M, Zeilinger S, Kubicek CP (2003) The Nag1 *N*-acetylglucosaminidase of *Trichoderma atroviride* is essential for chitinase induction by chitin and of major relevance to biocontrol. Curr Genet 43(4):289–295
- Brunner K, Zeilinger S, Ciliento R, Woo SL, Lorito M, Kubicek CP et al (2005) Improvement of the fungal biocontrol agent *Trichoderma atroviride* to enhance both antagonism and induction of plant systemic disease resistance. Appl Environ Microbiol 71(7):3959–3965
- Bruns T (2006) Evolutionary biology: a kingdom revised. Nature 443(7113):758–761
- Bushley KE, Raja R, Jaiswal P, Cumbie JS, Nonogaki M, Boyd AE et al (2013) The genome of *tolypocladium inflatum*: evolution, organization, and expression of the cyclosporin biosynthetic gene cluster. PLoS Genet 9(6):e1003496
- Cardoza RE, Malmierca MG, Hermosa MR, Alexander NJ, McCormick SP, Proctor RH et al (2011) Identification of loci and functional characterization of trichothecene biosynthesis genes in filamentous fungi of the genus *Trichoderma*. Appl Environ Microbiol 77(14):4867–4877
- Cardoza RE, McCormick SP, Malmierca MG, Olivera ER, Alexander NJ, Monte E et al (2015) Effects of trichothecene production on the plant defense response and fungal physiology: overexpression of the *Trichoderma arundinaceum* tri4 gene in *T. harzianum*. Appl Environ Microbiol 81(18):6355–6366
- Carsolio C, Benhamou N, Haran S, Cortés C, Gutiérrez A, Chet I et al (1999) Role of the *Trichoderma harzianum* endochitinase gene, ech42, in mycoparasitism. Appl Environ Microbiol 65(3):929–935
- Castle A, Speranzini D, Rghei N, Alm G, Rinker D, Bissett J (1998) Morphological and molecular identification of *trichoderma* isolates on North American mushroom farms. Appl Environ Microbiol 64(1):133–137
- Chang Y, Wang S, Sekimoto S, Aerts AL, Choi C, Clum A et al (2015) Phylogenomic analyses indicate that early fungi evolved digesting cell walls of algal ancestors of land plants. Genome Biol Evol 7 (6):1590–1601
- Chapela IH, Rehner SA, Schultz TR, Mueller UG (1994) Evolutionary history of the symbiosis between fungus-growing ants and their fungi. Science 266 (5191):1691–1694
- Chaverri P, Branco-Rocha F, Jaklitsch WM, Gaziz RO, Degenkolb T, Samuels GJ (2015) Systematics of the *Trichoderma harzianum* species complex and the re-identification of commercial biocontrol strains. Mycologia 6:14–147
- Chen H, Kovalchuk A, Keriö S, Asiegbu FO (2013) Distribution and bioinformatic analysis of the cerato-platanin protein family in Dikarya. Mycologia 105(6):1479–1488

- Chet I, Viterbo A (2007) Plant disease biocontrol and induced resistance via fungal mycoparasites, *The mycota*. Springer, Berlin, pp 127–146
- Cuomo CA, Desjardins CA, Bakowski MA, Goldberg J, Ma AT, Becnel JJ et al (2012) Microsporidian genome analysis reveals evolutionary strategies for obligate intracellular growth. *Genome Res* 22(12):2478–2488
- Currie CR, Wong B, Stuart AE, Schultz TR, Rehner SA, Mueller UG et al (2003) Ancient tripartite coevolution in the attine ant-microbe symbiosis. *Science* 299(5605):386–388
- Currie CR, Poulsen M, Mendenhall J, Boomsma JJ, Billen J (2006) Coevolved crypts and exocrine glands support mutualistic bacteria in fungus-growing ants. *Science* 311(5757):81–83
- de Man TJB, Stajich JE, Kubicek CP, Teiling C, Chenthamara K, Atanasova L et al (2015) The small genome of the fungus *Escovopsis weberi*, a specialized disease agent of ant agriculture. *Revis Deacon J* (2005) Front matter. In: *Fungal biology* (Internet). Blackwell (cited 30 Nov 2015), pp 1–7. Available from: [10.1002/9781118685068.fmatter/summary](https://doi.org/10.1002/9781118685068.fmatter/summary)
- Degenkolb T, Gräfenhan T, Nirenberg HI, Gams W, Brückner H (2006) *Trichoderma brevicompactum* complex: rich source of novel and recurrent plant-protective polypeptide antibiotics (peptaibiotics). *J Agric Food Chem* 54(19):7047–7061
- Delgado-Jarana J (2006) ThHog1 controls the hyperosmotic stress response in *Trichoderma harzianum*. *Microbiology* 152(6):1687–1700
- Deng S, Lorito M, Penttilä M, Harman GE (2007) Over-expression of an endochitinase gene (ThEn-42) in *Trichoderma atroviride* for increased production of antifungal enzymes and enhanced antagonist action against pathogenic fungi. *Appl Biochem Biotechnol* 142(1):81–94
- Dighton J, White JM, Oudemans P (2005) The fungal community. Its organization and role in the ecosystem, 3rd edn. CRC Press, Taylor & Francis, Boca Raton
- Djonović S, Pozo MJ, Dangott LJ, Howell CR, Kenerley CM (2006a) Sm1, a proteinaceous elicitor secreted by the biocontrol fungus *Trichoderma virens* induces plant defense responses and systemic resistance. *Mol Plant Microbe Interact* 19(8):838–853
- Djonović S, Pozo MJ, Kenerley CM (2006b) Tvbn3, a β -1,6-glucanase from the biocontrol fungus *Trichoderma virens*, is involved in mycoparasitism and control of *Pythium ultimum*. *Appl Environ Microbiol* 72(12):7661–7670
- Djonović S, Vargas WA, Kolomiets MV, Horndeski M, Wiest A, Kenerley CM (2007) A proteinaceous elicitor sm1 from the beneficial fungus *Trichoderma virens* is required for induced systemic resistance in maize. *Plant Physiol* 145(3):875–889
- Doehlemann G, Reissmann S, Aßmann D, Fleckenstein M, Kahmann R (2011) Two linked genes encoding a secreted effector and a membrane protein are essential for *Ustilago maydis*-induced tumour formation. *Mol Microbiol* 81(3):751–766
- Druzhinina IS, Kubicek CP (2013) Ecological genomics of trichoderma. In: Francisrtin (ed) *The ecological genomics of fungi* (Internet). Wiley, pp 89–116. doi:[10.1002/9781118735893.ch5/summary](https://doi.org/10.1002/9781118735893.ch5/summary) (cited 16 Apr 2014)
- Druzhinina IS, Komoń-Zelazowska M, Atanasova L, Seidl V, Kubicek CP (2010) Evolution and eco-physiology of the industrial producer *Hypocrea jecorina* (Anamorph *Trichoderma reesei*) and a new sympatric agamospecies related to it. *PLoS One* 5(2):e9191
- Druzhinina IS, Seidl-Seiboth V, Herrera-Estrella A, Horwitz BA, Kenerley CM, Monte E et al (2011) *Trichoderma*: the genomics of opportunistic success. *Nat Rev Microbiol* 9(10):749–759
- Druzhinina IS, Shelest E, Kubicek CP (2012) Novel traits of *Trichoderma* predicted through the analysis of its secretome. *FEMS Microbiol Lett* 337(1):1–9
- Dubey MK, Ubhayasekera W, Sandgren M, Funck Jensen D, Karlsson M (2012) Disruption of the Eng18B ENGase gene in the fungal biocontrol agent *Trichoderma atroviride* affects growth. Conidiation and antagonistic ability. *PLoS One* 7(5):e36152
- Dubey MK, Jensen DF, Karlsson M (2014) An ATP-binding cassette pleiotropic drug transporter protein is required for xenobiotic tolerance and antagonism in the fungal biocontrol agent *Clonostachys rosea*. *Mol Plant-Microbe Interact* 27(7):725–732
- Dubey M, Jensen DF, Karlsson M (2015) The ABC transporter ABCG29 is involved in H2O2 tolerance and biocontrol traits in the fungus *Clonostachys rosea*. *Mol Genet Genomics* 31:1–10
- Elad Y, Chet I, Katan J et al (1980) *Trichoderma harzianum*: a biocontrol agent effective against *Sclerotium rolfsii* and *Rhizoctonia solani*. *Phytopathology* 70(2):119–121
- Flores A, Chet I, Herrera-Estrella A (1997) Improved biocontrol activity of *Trichoderma harzianum* by over-expression of the proteinase-encoding gene prb1. *Curr Genet* 31(1):30–37
- Fravel DR (2006) Lessons learned from *Sporidesmium*, a fungal agent for control of sclerotia forming fungal pathogens. In: *Biological control: a global perspective: case studies from around the world*
- Friedl MA, Druzhinina IS (2012) Taxon-specific metagenomics of *Trichoderma* reveals a narrow community of opportunistic species that regulate each other's development. *Microbiology* 158(1):69–83
- Gaderer R, Bonazza K, Seidl-Seiboth V (2014) Ceratoplatanins: a fungal protein family with intriguing properties and application potential. *Appl Microbiol Biotechnol* 98(11):4795–4803

- Gaderer R, Lamdan NL, Frischmann A, Sulyok M, Krska R, Horwitz BA et al (2015) Sm2, a paralog of the *Trichoderma cerato-platanin* elicitor Sm1, is also highly important for plant protection conferred by the fungal-root interaction of *Trichoderma* with maize. *BMC Microbiol* 15:2
- Galletti S, Fornasier F, Cianchetta S, Lazzeri L (2015) Soil incorporation of brassica materials and seed treatment with *Trichoderma harzianum*: effects on melon growth and soil microbial activity. *Ind Crops Prod* 75:73–78
- Gazis R, Chaverri P (2010) Diversity of fungal endophytes in leaves and stems of wild rubber trees (*Hevea brasiliensis*) in Peru. *Fungal Ecol* 3(3):240–254
- Gerardo NM, Mueller UG, Price SL, Currie CR (2004) Exploiting a mutualism: parasite specialization on cultivars within the fungus-growing ant symbiosis. *Proc Biol Sci* 271(1550):1791–1798
- Grinyer J, Hunt S, McKay M, Herbert BR, Nevalainen H (2005) Proteomic response of the biological control fungus *Trichoderma atroviride* to growth on the cell walls of *Rhizoctonia solani*. *Curr Genet* 47(6):381–388
- Gruber S, Vaaje-Kolstad G, Matarese F, López-Mondéjar R, Kubicek CP, Seidl-Seiboth V (2011) Analysis of subgroup C of fungal chitinases containing chitin-binding and LysM modules in the mycoparasite *Trichoderma atroviride*. *Glycobiology* 21(1):122–133
- Gu YH, Ko WH (1997) Water agarose medium for studying factors affecting germination of conidia of *Ampelomyces quisqualis*. *Mycol Res* 101(4):422–424
- Gupta VG, Schmoll M, Herrera-Estrella A, Upadhyay RS, Druzhinina I, Tuohy M (2014) Biotechnology and biology of trichoderma. *Newnes*
- Hajek AE, Longcore JE, Rabern Simmons D, Peters K, Humber RA (2013) Chytrid mycoparasitism of entomophthorean zygospores. *J Invertebr Pathol* 114(3):333–336
- Hajlaou MR, Traquair JA, Jarvis WR, Belanger RR (1994) Antifungal activity of extracellular metabolites produced by *Sporothrix flocculosa*. *Biocontrol Sci Technol* 4(2):229–237
- Hajlaoui M, Belanger R (1991) Comparative effects of temperature and humidity on the activity of 3 potential antagonists of rose powdery mildew. *Neth J Plant Pathol* 97(4):203–208
- Harman GE (2011) Multifunctional fungal plant symbionts: new tools to enhance plant growth and productivity. *New Phytol* 189(3):647–649
- Hawksworth DL, Mueller GM (2005) Fungal communities: their diversity and distribution. *Fungal community its organ. Role Ecosyst*
- Hawksworth DL, Millanes AM, Wedin M (2010) Roselliniella revealed as an overlooked genus of hypocreales, with the description of a second species on parmelioid lichens. *Persoonia Mol Phylogeny Evol Fungi* 24:12–17
- Heijweggen T (1989) Effect of seventeen fungicolous fungi on sporulation of cucumber powdery mildew. *Neth J Plant Pathol* 94(4):185–190
- Held AA (1980) Development of zoospores in allomyces: a single zoospore produces numerous zoosporangia and resistant sporangia. *Can J Bot* 58(8):959–979
- Hermosa MR, Grondona I, Monte E (1999) Isolation of *Trichoderma harzianum* Th2 from commercial mushroom compost in Spain. *Plant Dis* 83(6):591
- Hernández-Oñate MA, Esquivel-Naranjo EU, Mendoza-Mendoza A, Stewart A, Herrera-Estrella AH (2012) An injury-response mechanism conserved across kingdoms determines entry of the fungus *Trichoderma atroviride* into development. *Proc Natl Acad Sci* 109(37):14918–14923
- Hijweggen T (1986) Biological control of cucumber powdery mildew by *Tilletiopsis minor*. *Neth J Plant Pathol* 92(2):93–95
- Hoch HC, Provvidenti R (1979) Mycoparasitic relationships: cytology of the *Sphaerotheca fuliginea*-*Tilletiopsis* spp. *Phytopathology* 69:359–362
- Hölldobler B, Wilson EO (1990) The ants. *Harvard University Press, Cambridge*
- Hoyos-Carvajal L, Orduz S, Bissett J (2009) Genetic and metabolic biodiversity of *Trichoderma* from Colombia and adjacent neotropical regions. *Fungal Genet Biol* 46(9):615–631
- Jaklitsch WM (2009) European species of *Hypocrea* Part I. The green-spored species. *Stud Mycol* 63:1–91
- Jaklitsch WM (2011) European species of *Hypocrea* part II: species with hyaline ascospores. *Fungal Divers* 48(1):1–250
- Jaklitsch WM, Voglmayr H (2014) Persistent hamathelial threads in the nectriacae, hypocreales: thyronectria revisited and re-instated. *Persoonia Mol Phylogeny Evol Fungi* 33:182–211
- James TY, Berbee ML (2012) No jacket required—new fungal lineage defies dress code: recently described zoosporic fungi lack a cell wall during trophic phase. *BioEssays* 34(2):94–102
- James TY, Kauff F, Schoch CL, Matheny PB, Hofstetter V, Cox CJ et al (2006) Reconstructing the early evolution of Fungi using a six-gene phylogeny. *Nature* 443(7113):818–822
- James TY, Pelin A, Bonen L, Ahrendt S, Sain D, Corradi N et al (2013) Shared signatures of parasitism and phylogenomics unite cryptomycota and microsporidia. *Curr Biol* 23(16):1548–1553
- Jeffries P (1995) Biology and ecology of mycoparasitism. *Can J Bot* 73(S1):1284–1290
- Jeffries P, Young TWK (1994) Interfungal parasitic relationships. *CAB International, Wallingford, Oxon*
- Jensen B, Knudsen IMB, Madsen M, Jensen DF (2004) Biopriming of infected carrot seed with an antagonist, *Clonostachys rosea*, selected for control of seedborne *alternaria* spp. *Phytopathology* 94(6):551–560
- Jeong JS, Mitchell TK, Dean RA (2007) The *Magnaporthe grisea* snodprot1 homolog, MSP1, is

- required for virulence. *FEMS Microbiol Lett* 273 (2):157–165
- Jones MDM, Forn I, Gadelha C, Egan MJ, Bass D, Massana R et al (2011) Discovery of novel intermediate forms redefines the fungal tree of life. *Nature* 474(7350):200–203
- Kaemper J, Kahmann R, Boelker M, Ma L-J, Brefort T, Saville BJ et al (2006) Insights from the genome of the biotrophic fungal plant pathogen *Ustilago maydis*. *Nature* 444(7115):97–101
- Karlsson M, Durling MB, Choi J, Kosawang C, Lackner G, Tzelepis GD et al (2015) Insights on the evolution of mycoparasitism from the genome of *Clonostachys rosea*. *Genome Biol Evol* 7(2):465–480
- Karpov SA, Mikhailov KV, Mirzaeva GS, Mirabdullaev IM, Mamkaeva KA, Titova NN et al (2013) Obligate phagotrophic aphelids turned out to branch with the earliest-diverging fungi. *Protist* 164 (2):195–205
- Kemen E, Jones JDG (2012) Obligate biotroph parasitism: can we link genomes to lifestyles? *Trends Plant Sci* 17(8):448–457
- Kim CS, Shirouzu T, Nakagiri A, Sotome K, Nagasawa E, Maekawa N (2012) *Trichoderma mienum* sp. nov., isolated from mushroom farms in Japan. *Antonie Van Leeuwenhoek* 102(4):629–641
- Kiss L (2003) A review of fungal antagonists of powdery mildews and their potential as biocontrol agents. *Pest Manag Sci* 59(4):475–483
- Kiss L (2008) Intracellular mycoparasites in action: interactions between powdery mildew fungi and ampelomyces. In: Avery SV, Stratford M, West P (eds) British mycological society symposium series (Internet). Academic, pp 37–52. Available from: <http://www.sciencedirect.com/science/article/pii/S0275028708800458> (cited 2014 Oct 23)
- Kiss L, Russell JC, Szentiványi O, Xu X, Jeffries P (2004) Biology and biocontrol potential of *Ampelomyces* mycoparasites, natural antagonists of powdery mildew fungi. *Biocontrol Sci Technol* 14 (7):635–651
- Klecan AL (1990) Reduced growth of *Erysiphe graminis* f. sp. *hordei* induced by *Tilletiopsis pallescens*. *Phytopathology* 80(4):325
- Klinger E, Groden E, Drummond F (2006) *Beauveria bassiana* horizontal infection between cadavers and adults of the colorado potato beetle, *Leptinotarsa decemlineata* (Say). *Environ Entomol* 35 (4):992–1000
- Knudsen IMB, Skou JP (1993) The effectivity of *Tilletiopsis albescens* in biocontrol of powdery mildew. *Ann Appl Biol* 123(1):173–185
- Kobayasi Y (1941) The genus *Cordyceps* and its allies. *Bull Natl Sci Mus Tokyo* 7:2–13
- Komon-Zelazowska M (2014) Molecular ecological aspects of *Trichoderma* that should be considered prior its application in agriculture and industry. Doctoral dissertation, Vienna University of Technology
- Komon-Zelazowska M, Bissett J, Zafari D, Hatvani L, Manczinger L, Woo S et al (2007) Genetically closely related but phenotypically divergent *Trichoderma* species cause green mold disease in oyster mushroom farms worldwide. *Appl Environ Microbiol* 73(22):7415–7426
- Kosawang C, Karlsson M, Véléz H, Rasmussen PH, Collinge DB, Jensen B et al (2014) Zearalenone detoxification by zearalenone hydrolase is important for the antagonistic ability of *Clonostachys rosea* against mycotoxigenic *Fusarium graminearum*. *Fungal Biol* 118(4):364–373
- Kotasthane A, Agrawal T, Kushwah R, Rahatkar OV (2015) In-vitro antagonism of *Trichoderma* spp. against *Sclerotium rolfsii* and *Rhizoctonia solani* and their response towards growth of cucumber, bottle gourd and bitter gourd. *Eur J Plant Pathol* 141(3):523–543
- Kredics L, Antal Z, Dóczy I, Manczinger L, Kevei F, Nagy E (2003) Clinical importance of the genus *Trichoderma*. *Acta Microbiol Immunol Hung* 50 (2):105–117
- Kredics L, Garcia Jimenez L, Naeimi S, Czifra D, Urbán P, Manczinger L et al (2010) A challenge to mushroom growers: the green mould disease of cultivated champignons. In: Current research, technology and education topics in applied microbiology and microbial biotechnology. FORMATEX, Badajoz, pp 295–305
- Kubicek CP, Komoń-Zelazowska M, Sándor E, Druzhinina IS (2007) Facts and challenges in the understanding of the biosynthesis of peptaibols by *Trichoderma*. *Chem Biodivers* 4(6):1068–1082
- Kubicek CP, Herrera-Estrella A, Seidl-Seiboth V, Martinez DA, Druzhinina IS, Thon M et al (2011) Comparative genome sequence analysis underscores mycoparasitism as the ancestral life style of *Trichoderma*. *Genome Biol* 12(4):R40
- Kumar A, Scher K, Mukherjee M, Pardovitz-Kedmi E, Sible GV, Singh US et al (2010) Overlapping and distinct functions of two *Trichoderma virens* MAP kinases in cell-wall integrity, antagonistic properties and repression of conidiation. *Biochem Biophys Res Commun* 398(4):765–770
- Lace B, Genre A, Woo S, Faccio A, Lorito M, Bonfante P (2015) Gate crashing arbuscular mycorrhizas: *in vivo* imaging shows the extensive colonization of both symbionts by *Trichoderma atroviride*: trichoderma mycoparasitic potential on AM partners. *Environ Microbiol Rep* 7(1):64–77
- Lam SK, Ng TB (2010) Lectins: production and practical applications. *Appl Microbiol Biotechnol* 89 (1):45–55
- Laurie JD, Ali S, Linning R, Mannhaupt G, Wong P, Güldener U et al (2012) Genome comparison of barley and maize smut fungi reveals targeted loss of RNA silencing components and species-specific presence of transposable elements. *Plant Cell* 24 (5):1733–1745

- Lefebvre F, Joly DL, Labbé C, Teichmann B, Linning R, Belzile F et al (2013) The transition from a phytopathogenic smut ancestor to an anamorphic biocontrol agent deciphered by comparative whole-genome analysis. *Plant Cell* 25(6):1946–1959
- Li Destri Nicosia MG, Mosca S, Mercurio R, Schena L (2015) Dieback of *Pinus nigra* seedlings caused by a Strain of *Trichoderma viride*. *Plant Dis* 99(1):44–49
- Li Q-R, Tan P, Jiang Y-L, Hyde KD, Mckenzie EHC, Bahkali AH et al (2012) A novel *Trichoderma* species isolated from soil in Guizhou, *T. guizhouense*. *Mycol Prog* 12(2):167–172
- Little AEF, Currie CR (2008) Black yeast symbionts compromise the efficiency of antibiotic defenses in fungus-growing ants. *Ecology* 89(5):1216–1222
- López-Quintero CA, Atanasova L, Franco-Molano AE, Gams W, Komon-Zelazowska M, Theelen B et al (2013) DNA barcoding survey of *Trichoderma* diversity in soil and litter of the Colombian lowland Amazonian rainforest reveals *Trichoderma strigosellum* sp. nov. and other species. *Antonie Van Leeuwenhoek* 104(5):657–674
- Lorito M, Farkas V, Rebuffat S, Bodo B, Kubicek CP (1996) Cell wall synthesis is a major target of mycoparasitic antagonism by *Trichoderma harzianum*. *J Bacteriol* 178(21):6382–6385
- Lücking R, Huhndorf S, Pfister DH, Plata ER, Lumbsch HT (2009) Fungi evolved right on track. *Mycologia* 101(6):810–822
- Mains EB (1958) North American entomogenous species of cordyceps. *Mycologia* 50(2):169
- Malmierca MG, Cardoza RE, Alexander NJ, McCormick SP, Hermosa R, Monte E et al (2012) Involvement of *Trichoderma* trichothecenes in the biocontrol activity and induction of plant defense-related genes. *Appl Environ Microbiol* 78(14):4856–4868
- Malmierca MG, Cardoza RE, Alexander NJ, McCormick SP, Collado IG, Hermosa R et al (2013) Relevance of trichothecenes in fungal physiology: disruption of *tri5* in *Trichoderma arundinaceum*. *Fungal Genet Biol* 53:22–33
- Marfetan JA, Romero AI, Folgarait PJ (2015) Pathogenic interaction between *Escovopsis weberi* and *Leucoagaricus* sp.: mechanisms involved and virulence levels. *Fungal Ecol* 17:52–61
- Marshall R, Kombrink A, Motteram J, Loza-Reyes E, Lucas J, Hammond-Kosack KE et al (2011) Analysis of two in planta expressed LysM effector homologs from the fungus *Mycosphaerella graminicola* reveals novel functional properties and varying contributions to virulence on wheat. *Plant Physiol* 156(2):756–769
- Martinez D, Berka RM, Henrissat B, Saloheimo M, Arvas M, Baker SE et al (2008) Genome sequencing and analysis of the biomass-degrading fungus *Trichoderma reesei* (syn. *Hypocrea jecorina*). *Nat Biotechnol* 26(5):553–560
- Masiulionis VE, Cabello MN, Seifert KA, Rodrigues A, Pagnocca FC (2015) *Escovopsis trichodermoides* sp. nov., isolated from a nest of the lower attine ant *Mycocepurus goeldii*. *Antonie Van Leeuwenhoek* 107(3):731–740
- Meinhardt LW, Rincones J, Bailey BA, Aime MC, Griffith GW, Zhang D et al (2008) *Moniliophthora perniciosa*, the causal agent of witches' broom disease of cacao: what's new from this old foe? *Mol Plant Pathol* 9(5):577–588
- Meirelles LA, Solomon SE, Bacci M, Wright AM, Mueller UG, Rodrigues A (2015) Shared escovopsis parasites between leaf-cutting and non-leaf-cutting ants in the higher attine fungus-growing ant symbiosis. *R Soc Open Sci* 2(9):150257
- Mendes TD, Rodrigues A, Dayo-Owoyemi I, Marson FAL, Pagnocca FC (2012) Generation of nutrients and detoxification: possible roles of yeasts in leaf-cutting ant nests. *Insects* 3(1):228–245
- Mendoza-Mendoza A, Pozo MJ, Grzegorski D, Martínez P, García JM, Olmedo-Monfil V et al (2003) Enhanced biocontrol activity of *Trichoderma* through inactivation of a mitogen-activated protein kinase. *Proc Natl Acad Sci* 100(26):15965–15970
- Migheli Q, Balmas V, Komoń-Zelazowska M, Scherm B, Fiori S, Kopchinskiy AG et al (2009) Soils of a Mediterranean hot spot of biodiversity and endemism (Sardinia, Tyrrhenian Islands) are inhabited by pan-European, invasive species of *Hypocrea/Trichoderma*. *Environ Microbiol* 11(1):35–46
- Mikheyev AS, Mueller UG, Abbot P (2010) Comparative dating of attine ant and lepiotaceous cultivar phylogenies reveals coevolutionary synchrony and discord. *Am Nat* 175(6):E126–E133
- Mimee B, Pelletier R, Bélanger R (2009) In vitro antibacterial activity and antifungal mode of action of flocculosin, a membrane-active cellobiose lipid. *J Appl Microbiol* 107(3):989–996
- Molnár-Gábor E, Dóczi I, Hatvani L, Vágvölgyi C, Kredics L (2013) Isolated sinusitis sphenoidalis caused by *Trichoderma longibrachiatum* in an immunocompetent patient with headache. *J Med Microbiol* 62(Pt 8):1249–1252
- Monod M, Capoccia S, Léchenne B, Zaugg C, Holdom M, Jousson O (2002) Secreted proteases from pathogenic fungi. *Int J Med Microbiol* 292(5–6):405–419
- Montero-Barrientos M, Hermosa R, Cardoza RE, Gutiérrez S, Monte E (2011) Functional analysis of the *Trichoderma harzianum* *nox1* gene, encoding an NADPH oxidase, relates production of reactive oxygen species to specific biocontrol activity against *Pythium ultimum*. *Appl Environ Microbiol* 77(9):3009–3016
- Morán-Diez E, Hermosa R, Ambrosino P, Cardoza RE, Gutiérrez S, Lorito M et al (2009) The ThPG1 endopolygalacturonase is required for the *Trichoderma harzianum* – plant beneficial interaction. *Mol Plant Microbe Interact* 22(8):1021–1031
- Muchovej JJ, Della Lucia TM (1990) *Escovopsis*, a new genus from leaf cutting ant nests to replace *Phia-*

- locladus nomem invalidum. Mycotaxon (Internet). Available from: <http://agris.fao.org/agris-search/search.do?recordID=US201302699294> (cited 1 Dec 2015)
- Mukherjee PK, Kenerley CM (2010) Regulation of morphogenesis and biocontrol properties in *Trichoderma virens* by a VELVET protein, Vell. *Appl Environ Microbiol* 76(7):2345–2352
- Mukherjee PK, Latha J, Hadar R, Horwitz BA (2003) TmkA, a mitogen-activated protein kinase of *Trichoderma virens*, is involved in biocontrol properties and repression of conidiation in the dark. *Eukaryot Cell* 2(3):446–455
- Mukherjee M, Mukherjee PK, Kale SP (2007) cAMP signalling is involved in growth, germination, mycoparasitism and secondary metabolism in *Trichoderma virens*. *Microbiology* 153(6):1734–1742
- Mukherjee PK, Horwitz BA, Singh US, Mukherjee M, Schmoll M (2013) *Trichoderma* in agriculture, industry and medicine: an overview. In: *Trichoderma: biology and applications*
- Muthumeenakshi S, Sreenivasaprasad S, Rogers CW, Challen MP, Whipps JM (2007) Analysis of cDNA transcripts from *Coniothyrium minitans* reveals a diverse array of genes involved in key processes during sclerotial mycoparasitism. *Fungal Genet Biol* 44(12):1262–1284
- Hashioka and Nakai (1980) Ultrastructure of pycnidial development and mycoparasitism of *Ampelomyces quisqualis* parasitic on *erysipales*. *Trans Mycol Soc Jpn* 21(3):329–338
- Olmedo-Monfil V, Mendoza-Mendoza A, Gómez I, Cortés C, Herrera-Estrella A (2002) Multiple environmental signals determine the transcriptional activation of the mycoparasitism related gene *prb1* in *Trichoderma atroviride*. *Mol Genet Genomics* 267(6):703–712
- Ottmann C, Luberaacki B, Küfner I, Koch W, Brunner F, Weyand M et al (2009) A common toxin fold mediates microbial attack and plant defense. *Proc Natl Acad Sci* 106(25):10359–10364
- Park MS, Bae KS, Yu SH (2006) Two new species of *Trichoderma* associated with green mold of oyster mushroom cultivation in Korea. *Mycobiology* 34(3):111
- Pazzagli L, Cappugi G, Manao G, Camici G, Santini A, Scala A (1999) Purification, characterization, and amino acid sequence of cerato-platanin, a new phytotoxic protein from *Ceratocystis fimbriata* f. sp. *platanii*. *J Biol Chem* 274(35):24959–24964
- Peck JW, Bowden ET, Burbelo PD (2004) Structure and function of human Vps20 and Snf7 proteins. *Biochem J* 377(Pt 3):693–700
- Poldmaa K (1996) A new species of hypomyces and three of cladobotryum from Estonia. Mycotaxon (Internet). Available from: <http://agris.fao.org/agris-search/search.do?recordID=US9634362> (cited 1 Dec 2015)
- Pöldmaa K, Samuels GJ, Lodge DJ (1997) Three new polyporicolous species of Hypomyces and their Cladobotryum anamorphs. *Sydowia* 49(1):80–93
- Powell MJ (1984) Fine structure of the unwalled thallus of *Rozella polyphagi* in its host *Polyphagus euglenae*. *Mycologia* 76(6):1039
- Pozo MJ, Baek J-M, García JM, Kenerley CM (2004) Functional analysis of *tvsp1*, a serine protease-encoding gene in the biocontrol agent *Trichoderma virens*. *Fungal Genet Biol* 41(3):336–348
- Reithner B, Brunner K, Schuhmacher R, Peissl I, Seidl V, Krska R et al (2005) The G protein α subunit Tgal of *Trichoderma atroviride* is involved in chitinase formation and differential production of antifungal metabolites. *Fungal Genet Biol* 42(9):749–760
- Reithner B, Schuhmacher R, Stoppacher N, Pucher M, Brunner K, Zeilinger S (2007) Signaling via the *Trichoderma atroviride* mitogen-activated protein kinase Tmk1 differentially affects mycoparasitism and plant protection. *Fungal Genet Biol* 44(11):1123–1133
- Reithner B, Mach-Aigner AR, Herrera-Estrella A, Mach RL (2014) The transcriptional regulator Xyr1 of *Trichoderma atroviride* supports the induction of systemic resistance in plants. *Appl Environ Microbiol* 00930–14
- Rey P, Le Floch G, Benhamou N, Salerno M-I, Thuillier E, Tirilly Y (2005) Interactions between the mycoparasite *Pythium oligandrum* and two types of sclerotia of plant-pathogenic fungi. *Mycol Res* 109(Pt 7):779–788
- Reynolds HT, Currie CR (2004) Pathogenicity of *Escovopsis weberi*: the parasite of the attine ant-microbe symbiosis directly consumes the ant-cultivated fungus. *Mycologia* 96(5):955–959
- Rodrigues A, Bacci M, Mueller UG, Ortiz A, Pagnocca FC (2008) Microfungal “weeds” in the leafcutter ant symbiosis. *Microb Ecol* 56(4):604–614
- Rodríguez MA, Cabrera G, Gozzo FC, Eberlin MN, Godéas A (2011) *Clonostachys rosea* BAFC3874 as a *Sclerotinia sclerotiorum* antagonist: mechanisms involved and potential as a biocontrol agent. *J Appl Microbiol* 110(5):1177–1186
- Rogerson CT, Samuels GJ (1985) Species of hypomyces and nectria occurring on discomycetes. *Mycologia* 77(5):763–783
- Rogerson CT, Samuels GJ (1989) Boleticolous species of hypomyces. *Mycologia* 81(3):413–432
- Rogerson CT, Samuels GJ (1993) Polyporicolous species of hypomyces. *Mycologia* 85(2):231–272
- Rogerson CT, Samuels GJ (1994) Agaricolous species of hypomyces. *Mycologia* 86(6):839–866
- Rosmana A, Samuels GJ, Ismaiel A, Ibrahim ES, Chaverri P, Herawati Y et al (2015) *Trichoderma asperellum*: a dominant endophyte species in cacao grown in Sulawesi with potential for controlling vascular streak dieback disease. *Trop Plant Pathol* 40(1):19–25

- Rotem Y, Yarden O, Szejnberg A (1999) The mycoparasite *Ampelomyces quisqualis* expresses exgA encoding an exo-beta-1,3-glucanase in culture and during mycoparasitism. *Phytopathology* 89(8):631–638
- Ruiz-Herrera J, Ortiz-Castellanos L (2010) Analysis of the phylogenetic relationships and evolution of the cell walls from yeasts and fungi. *FEMS Yeast Res* 10(3):225–243
- Ruocco M, Lanzuise S, Lombardi N, Woo SL, Vinale F, Marra R et al (2015) Multiple roles and effects of a novel *Trichoderma hydrophobin*. *Mol Plant-Microbe Interact* 28(2):167–179
- Salas-Marina MA, Isordia-Jasso MI, Islas-Osuna MA, Delgado-Sánchez P, Jiménez-Bremont JF, Rodríguez-Kessler M et al (2015) The Epl1 and Sm1 proteins from *Trichoderma atroviride* and *Trichoderma virens* differentially modulate systemic disease resistance against different life style pathogens in *Solanum lycopersicum*. *Front Plant Sci* 6. Available from: <http://www.ncbi.nlm.nih.gov/pmc/articles/PMC4337343/> (cited 24 Nov 2015)
- Sandoval-Denis M, Sutton DA, Cano-Lira JF, Gené J, Fothergill AW, Wiederhold NP et al (2014) Phylogeny of the clinically relevant species of the emerging fungus trichoderma and their antifungal susceptibilities. *J Clin Microbiol* 52(6):2112–2125
- Schirawski J, Mannhaupt G, Münch K, Brefort T, Schipper K, Doehlemann G et al (2010) Pathogenicity determinants in smut fungi revealed by genome comparison. *Science* 330(6010):1546–1548
- Schroers H-J, Samuels GJ, Seifert KA, Gams W (1999) Classification of the mycoparasite *Gliocladium roseum* in clonostachys as *C. rosea*, its relationship to *Bionectria ochroleuca*, and notes on other gliocladium-like fungi. *Mycologia* 91(2):365–385
- Schuster M, Treitschke S, Kilaru S, Molloy J, Harmer NJ, Steinberg G (2012) Myosin-5, kinesin-1 and myosin-17 cooperate in secretion of fungal chitin synthase. *EMBO J* 31(1):214–227
- Seidl V, Marchetti M, Schandl R, Allmaier G, Kubicek CP (2006) Epl1, the major secreted protein of *Hypocrea atroviridis* on glucose, is a member of a strongly conserved protein family comprising plant defense response elicitors. *FEBS J* 273(18):4346–4359
- Seidl V, Song L, Lindquist E, Gruber S, Koptchinskiy A, Zeilinger S et al (2009) Transcriptomic response of the mycoparasitic fungus *Trichoderma atroviride* to the presence of a fungal prey. *BMC Genomics* 10(1):567
- Seidl-Seiboth V, Zach S, Frischmann A, Spadiut O, Dietzsch C, Herwig C et al (2013) Spore germination of *Trichoderma atroviride* is inhibited by its LysM protein TAL6. *FEBS J* 280(5):1226–1236
- Seifert KA, Samson RA, Chapela IH (1995) *Escovopsis aspergilloides*, a rediscovered hyphomycete from leaf-cutting ant nests. *Mycologia* 87(3):407–413
- Shinha KK, Bhatnagar D (1998) Mycotoxins in agriculture and food safety. CRC Press, Boca Raton
- Siozios S, Tosi L, Ferrarini A, Ferrari A, Tononi P, Bellin D et al (2015) Transcriptional reprogramming of the mycoparasitic fungus *Ampelomyces quisqualis* during the powdery mildew host-induced germination. *Phytopathology* 105(2):199–209
- Skinner W, Keon J, Hargreaves J (2001) Gene information for fungal plant pathogens from expressed sequences. *Curr Opin Microbiol* 4(4):381–386
- Studholme DJ, Harris B, Le Cocq K, Winsbury R, Perera V, Ryder L et al (2013) Investigating the beneficial traits of *Trichoderma hamatum* GD12 for sustainable agriculture-insights from genomics. *Front Plant Sci* 4:258
- Sundheim L (1982) Control of cucumber powdery mildew by the hyperparasite *Ampelomyces quisqualis* and fungicides. *Plant Pathol* 31(3):209–214
- Sundheim L, Krekling T (1982) Host-parasite relationships of the hyperparasite *Ampelomyces quisqualis* and its powdery mildew host *Sphaerotheca fuliginea*. *J Phytopathol* 104(3):202–210
- Sung G-H, Hywel-Jones NL, Sung J-M, Luangsa-ard JJ, Shrestha B, Spatafora JW (2007) Phylogenetic classification of *Cordyceps* and the clavicipitaceous fungi. *Stud Mycol* 57:5–59
- Sung G-H, Poinar GO, Spatafora JW (2008) The oldest fossil evidence of animal parasitism by fungi supports a Cretaceous diversification of fungal–arthropod symbioses. *Mol Phylogenet Evol* 49(2):495–502
- Szejnberg A, Galper S, Mazar S, Lisker N (1989) *Ampelomyces quisqualis* for biological and integrated control of powdery mildews in Israel. *J Phytopathol* 124(4):285–295
- Taerum SJ, Cafaro MJ, Little AEF, Schultz TR, Currie CR (2007) Low host-pathogen specificity in the leaf-cutting ant-microbe symbiosis. *Proc Biol Sci* 274(1621):1971–1978
- Taerum SJ, Cafaro MJ, Currie CR (2010) Presence of multiparasite infections within individual colonies of leaf-cutter ants. *Environ Entomol* 39(1):105–113
- Takamatsu S (2004) Phylogeny and evolution of the powdery mildew fungi (Erysiphales, Ascomycota) inferred from nuclear ribosomal DNA sequences. *Mycoscience* 45(2):147–157
- Tijerino A, Cardoza RE, Moraga J, Malmierca MG, Vicente F, Aleu J et al (2011) Overexpression of the trichodiene synthase gene tri5 increases trichodermin production and antimicrobial activity in *Trichoderma brevicompactum*. *Fungal Genet Biol* 48(3):285–296
- Tsaousis AD, Kunji ERS, Goldberg AV, Lucocq JM, Hirt RP, Embley TM (2008) A novel route for ATP acquisition by the remnant mitochondria of *Encephalitozoon cuniculi*. *Nature* 453(7194):553–556
- Tuininga AR (2005) Interspecific interaction terminology: from mycology to general ecology. *Fungal community its organ. Role Ecosyst*. Third. CRC Press
- Urquhart EJ (1994) Growth and biological control activity of *Tilletiopsis* species against powdery mil-

- dew (*Sphaerotheca fuliginea*) on greenhouse cucumber. *Phytopathology* 84(4):341
- Vallance J, Le Floch G, Déniel F, Barbier G, Lévesque CA, Rey P (2009) Influence of *Pythium oligandrum* biocontrol on fungal and oomycete population dynamics in the rhizosphere. *Appl Environ Microbiol* 75(14):4790–4800
- Vargas WA, Mukherjee PK, Laughlin D, Wiest A, Moran-Diez ME, Kenerley CM (2014) Role of gliotoxin in the symbiotic and pathogenic interactions of *Trichoderma virens*. *Microbiology* 160 (Pt_10):2319–2330
- Villesen P, Mueller UG, Schultz TR, Adams RMM, Bouck AC (2004) Evolution of ant-cultivar specialization and cultivar switching in *Apterostigma* fungus-growing ants. *Evol Int J Org Evol* 58 (10):2252–2265
- Viterbo A, Harel M, Horwitz BA, Chet I, Mukherjee PK (2005) *Trichoderma* mitogen-activated protein kinase signaling is involved in induction of plant systemic resistance. *Appl Environ Microbiol* 71 (10):6241–6246
- Vujanovic V, Goh YK (2009) *Sphaerodes mycoparasitica* sp. nov., a new biotrophic mycoparasite on *Fusarium avenaceum*, *F. graminearum* and *F. oxysporum*. *Mycol Res* 113(Pt 10):1172–1180
- Vujanovic V, Goh YK (2012) qPCR quantification of *Sphaerodes mycoparasitica* biotrophic mycoparasite interaction with *Fusarium graminearum*: in vitro and in planta assays. *Arch Microbiol* 194 (8):707–717
- Wallace DEE, Asensio JGV, Tomas AAP (2014) Correlation between virulence and genetic structure of escovopsis strains from leaf-cutting ant colonies in Costa Rica. *Microbiology* 160(Pt_8):1727–1736
- Watson P (1955) *Calcarisporium arbuscula* living as an endophyte in apparently healthy sporophores of *Russula* and *Lactarius*. *Trans Br Mycol Soc* 38 (4):409–414
- Williams BAP, Hirt RP, Lucocq JM, Embley TM (2002) A mitochondrial remnant in the microsporidian *Trachipleistophora hominis*. *Nature* 418 (6900):865–869
- Wirth R, Herz H, Ryel RJ, Beyschlag W, Hölldobler B (2002) Herbivory of leaf-cutting ants. A case study on *atta colombica* in the tropical rainforest of Panama. Springer, Berlin
- Xie B-B, Qin Q-L, Shi M, Chen L-L, Shu Y-L, Luo Y et al (2014) Comparative genomics provide insights into evolution of *trichoderma* nutrition style. *Genome Biol Evol* 6(2):379–390
- Zeilinger S, Reithner B, Scala V, Peissl I, Lorito M, Mach RL (2005) Signal transduction by Tga3, a novel G protein α subunit of *Trichoderma atroviride*. *Appl Environ Microbiol* 71(3):1591–1597
- Zhang J, Bayram Akcapinar G, Atanasova L, Rahimi MJ, Przulucka A, Yang D et al (2015) The neutral metallopeptidase NMP1 of *Trichoderma guizhouense* is required for mycotrophy and self-defence. *Environ Microbiol* 2015 Jun 28 doi:10.1111/1462-2920.12966

Chapter 2 Small genome of the fungus *Escovopsis weberi*, a specialized disease agent of ant agriculture⁵

Authors

Tom. J. B. De Man¹, Jason E. Stajich², Christian P. Kubicek³, Clotilde Teiling⁴, **Komal Chenthamara**³, Lea Atanasova³, Irina S. Druzhinina³, Natasha Levenkova⁴, Stephanie S. L. Birnbaum¹, Seth M. Barribeau¹, Brooke A. Bozick¹, Garret Suen⁵, Cameron R. Currie⁵, and Nicole M. Gerardo¹

Affiliation

1. Department of Biology, Emory University, Atlanta, GA 30322

2. Department of Plant Pathology and Microbiology, University of California, Riverside, CA 92521

3. Microbiology and Applied Genomics group, Research Area Biochemical Technology, Institute of Chemical, Environmental & Bioscience Engineering, TU Wien, Gumpendorferstrasse 1a

Contribution by the PhD candidate

1. Manual functional annotation of the all the genes in the genome of *Escovopsis weberi* against the National Center for Biotechnology Information (NCBI) nonredundant database (Dataset S3).
2. Experiments comparing growth of *Escovopsis weberi* on alternative carbon sources to growth of *Trichoderma atroviride* using phenotype microarray plates (Figure S2).
3. Dual confrontation experiments comparing mycoparasitism between *Escovopsis weberi* and *Trichoderma* spp. which helped in designing of this research.
4. Contribution to the manuscript drafting.

⁵ de Man TJ, Stajich JE, Kubicek CP, Teiling C, **Chenthamara K**, Atanasova L, Druzhinina IS, Levenkova N, Birnbaum SS, Barribeau SM, Bozick BA. Small genome of the fungus *Escovopsis weberi*, a specialized disease agent of ant agriculture. Proceedings of the National Academy of Sciences. 2016 Mar 9:201518501.



Small genome of the fungus *Escovopsis weberi*, a specialized disease agent of ant agriculture

Tom J. B. de Man^a, Jason E. Stajich^b, Christian P. Kubicek^c, Clotilde Teiling^d, Komal Chenthamara^e, Lea Atanasova^f, Irina S. Druzhinina^g, Natasha Levenkova^d, Stephanie S. L. Birnbaum^h, Seth M. Barribeau^{a,e}, Brooke A. Bozick^g, Garret Suen^f, Cameron R. Currie^f, and Nicole M. Gerardo^{a,1}

^aDepartment of Biology, Emory University, Atlanta, GA 30322; ^bDepartment of Plant Pathology and Microbiology, University of California, Riverside, CA 92521; ^cInstitute of Chemical Engineering, Vienna University of Technology, 1060 Vienna, Austria; ^d454 Life Sciences, Roche Company, Branford, CT 06405; ^eDepartment of Biology, East Carolina University, Greenville, NC 27858; and ^fDepartment of Bacteriology, University of Wisconsin, Madison, WI 53706

Edited by Nancy A. Moran, University of Texas, Austin, TX, and approved February 9, 2016 (received for review September 23, 2015)

Many microorganisms with specialized lifestyles have reduced genomes. This is best understood in beneficial bacterial symbioses, where partner fidelity facilitates loss of genes necessary for living independently. Specialized microbial pathogens may also exhibit gene loss relative to generalists. Here, we demonstrate that *Escovopsis weberi*, a fungal parasite of the crops of fungus-growing ants, has a reduced genome in terms of both size and gene content relative to closely related but less specialized fungi. Although primary metabolism genes have been retained, the *E. weberi* genome is depleted in carbohydrate active enzymes, which is consistent with reliance on a host with these functions. *E. weberi* has also lost genes considered necessary for sexual reproduction. Contrasting these losses, the genome encodes unique secondary metabolite biosynthesis clusters, some of which include genes that exhibit up-regulated expression during host attack. Thus, the specialized nature of the interaction between *Escovopsis* and ant agriculture is reflected in the parasite's genome.

mycoparasitism | repeat-induced point mutation | *Atta cephalotes* | attine | genome reduction

The highly evolved agricultural lifestyle of leaf-cutting ants has attracted particular attention because these ants cultivate a symbiotic fungus that serves as their major food source. These ants cut leaves, preprocess them into small pieces, and feed them to the cultivated fungus (1). The capacity of the cultivated fungus to break down plant material gives ant agriculturalists access to the vast nutrient stores locked within neotropical plants (Fig. 1A) (2–5). The symbiosis between fungus-growing ants and their cultivated fungi has persisted for at least 50 million years (6).

Like human agriculture, ant agriculture is hampered by disease. The ants' fungal crops are attacked and consumed by fungal parasites of the genus *Escovopsis* (Ascomycota, Pezizomycotina: anamorphic Hypocreales) (Fig. 1A) (7), which have evolved in association with the ants and their cultivated fungi (8). *Escovopsis* infection can have detrimental impacts on garden health and, consequently, on the survival of ant colonies (9, 10). Such mycoparasitism, the phenomenon whereby one fungus is parasitic on another fungus, is rare. It is most well-known for species from the genus *Trichoderma*, some of which are used as biocontrol agents for fungal diseases and others of which attack human-cultivated fungi (11–13). In contrast to *Trichoderma* species, however, *Escovopsis* species grow poorly in their hosts' absence (SI Appendix, Figs. S1 and S2).

Escovopsis species have never been isolated outside of fungus-growing ant colonies, and different strains of *Escovopsis* are capable of attacking the fungi grown by different fungus-growing ant species (8, 14, 15). The long-term, specialized evolutionary history of the association between *Escovopsis* and their hosts provides a unique venue to explore the consequences of host specialization on pathogen genome evolution. Here, we assemble and annotate the genome of a strain of *Escovopsis weberi*. Consistent with expectations under an evolutionary transition toward using a narrow host range, and similar to many other specialized, host-associated microbes (16, 17), *E. weberi* exhibits gene loss. Contrasting other fungal pathogens, the

large genomes of which are expanded with genetic elements that influence host adaptation (18), the genome size of *Escovopsis* is small compared with those of its closest sequenced relatives.

Basic Features of the Small *Escovopsis* Genome

We sequenced the genome of *E. weberi* strain CC031208-10 isolated from a fungal garden of the leaf-cutting ant *Atta cephalotes*, a widely distributed fungus-growing ant species, the genome of which has been recently sequenced (19). This strain is closely related to *Escovopsis* strains isolated from other leaf-cutting ant colonies (SI Appendix, Fig. S3). Sequencing performed with the 454 FLX Titanium pyrosequencing platform generated ~4.4 million reads, which assembled into 29 scaffolds with a N50 of 2.58 Mbp and an overall genome assembly length of 27.20 Mbp. The G+C content of the *Escovopsis* genome is 55.74%, similar to other fungi in the Hypocreales (SI Appendix, Table S1). We identified 204 tRNA genes in association with 44 codons and all 20 amino acids (Dataset S1). Approximately 4% of the assembly consists of repetitive elements, including simple sequence repeats such as microsatellites (Dataset S1) and transposable elements (SI Appendix, Fig. S4). The genome can be viewed through the Genome Browser at gb2.fungalgenomes.org/.

Significance

Many organisms are specialists living within a narrow range of conditions. Pathogens are often adapted to efficiently exploit only a few hosts species, or sometimes, only some genotypes within a species. The genomes of such parasites are predicted to maintain genes critical for host utilization and to lose genes no longer necessary outside their constrained lifestyle. We demonstrate that the genomic content of a fungal pathogen specialized to attack and consume fungus cultivated by ants meets these predictions. Despite a reduced genome size and gene content in comparison with less specialized relatives, the genome of this agricultural pathogen retains genes necessary for production of toxins, a step critical to host attack, and for breaking down nutrients abundant in its host.

Author contributions: T.J.B.d.M., J.E.S., C.P.K., C.T., K.C., L.A., I.S.D., N.L., S.S.L.B., S.M.B., G.S., C.R.C., and N.M.G. designed research; T.J.B.d.M., J.E.S., C.P.K., K.C., L.A., I.S.D., N.L., S.S.L.B., and S.M.B. performed research; T.J.B.d.M., J.E.S., C.P.K., K.C., L.A., I.S.D., N.L., B.A.B., and N.M.G. analyzed data; and T.J.B.d.M., J.E.S., C.P.K., S.S.L.B., B.A.B., G.S., C.R.C., and N.M.G. wrote the paper.

The authors declare no conflict of interest.

This article is a PNAS Direct Submission.

Data deposition: The raw dataset has been deposited at DNA Data Bank of Japan/European Molecular Biology Laboratory/GenBank under accession PRJNA253870, and the whole-genome assembly has been deposited under accession LGSR00000000. The version described here is version LGSR01000000. RNA-seq reads have been deposited in the Sequence Read Archive under accession SRP049545.

¹To whom correspondence should be addressed. Email: nicole.gerardo@emory.edu.

This article contains supporting information online at www.pnas.org/lookup/suppl/doi:10.1073/pnas.1518501113/-DCSupplemental.

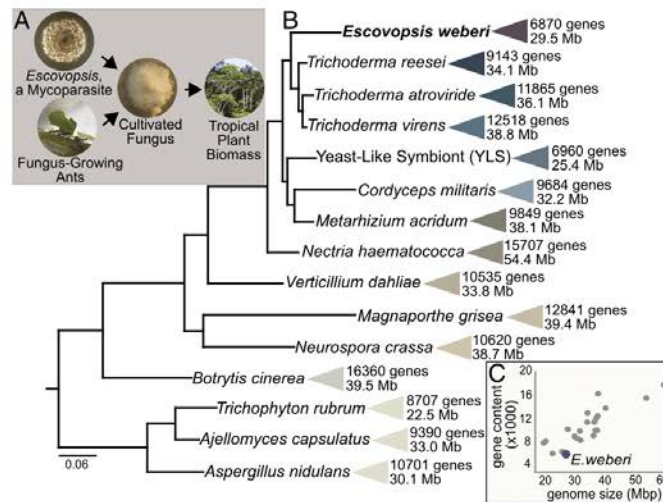


Fig. 1. *Escovopsis weberi*, a specialized mycoparasite of the fungus-growing ant symbiosis, has a small genome compared with other Pezizomycotina fungi. (A) Both fungus-growing ants and the mycoparasite *E. weberi* use the ants' cultivated fungi as their primary food source. The ability of the cultivated fungi to efficiently break down plant material gives both consumers access to the biomass of neotropical plants. (B) Size and protein-coding gene content of genomes of diverse fungi in the Pezizomycotina. Bayesian phylogeny estimated using partial amino acid alignments of three genes (*Rpb1*, *Rpb2*, *ef1-a*). All posterior probabilities are greater than 0.95. Phylogeny is rooted with *Saccharomyces cerevisiae* (not shown). (C) Relationship between genome size and gene content. A list of genomes included in this panel is in *SI Appendix, Table S1*.

Using k-mer frequency analysis as an assembly-independent estimate of genome size (Dataset S2) (20), we estimate the true genome size to be 29.45 ± 2 Mb in length, among the smallest known genomes of all Pezizomycotina (Fig. 1), the largest and most diverse group of ascomycete fungi. Indicative of a complete genome assembly, we identified 239 of 248 super-conserved Core Eukaryotic Genes (CEGs) (21, 22). *Escovopsis* has 6,870 predicted protein-coding genes (Dataset S3), substantially fewer than other Pezizomycotina (Fig. 1 and *SI Appendix, Table S1*). The average gene length (1,623 bp) and mean content of exons per gene (2.74) are similar to estimates from closely related Pezizomycotina (*SI Appendix, Table S2*). Fifty-five percent of the encoded proteins were assigned to Gene Ontology terms, and 76% contain a protein family (PFAM) domain (Dataset S4). Although the number of predicted genes is greatly reduced compared with most other Pezizomycotina, PFAM analysis as well as manual functional annotation of all genes against the National Center for Biotechnology Information (NCBI) nonredundant database (Dataset S3) indicate that the largest gene families in *Escovopsis* are also common in closely related fungi (*SI Appendix, Table S3*).

Potential Loss of Sex

An inability of *E. weberi* to undergo sexual reproduction is suggested by the striking absence of a functional Mating-Type (MAT) locus, as no complete *MAT1-2* and *MAT1-1* loci were identified (see *SI Appendix, Fig. S5*, for details). *E. weberi* also has no homologs to the small peptide pheromones necessary for sexual reproduction in *Trichoderma reesei* (23). These findings are consistent with the fact that there is no described teleomorph for *E. weberi* and suggest that this fungus—unlike most others that are predominantly found in their anamorphic form (24)—is asexual. Identification of *STE2* and *STE3* genes in the genome, homologs of *T. reesei* receptor proteins necessary for sexual reproduction (23), does suggest that *E. weberi*—or an ancestor—has a history of sexual reproduction.

Loss of sex in *E. weberi* would be surprising because *Escovopsis* presumably must adapt to an array of defenses mounted by its fungal host and associated symbionts, and sexual recombination can provide an advantage in terms of facilitating the generation of variants that are able to counter changing defenses (25, 26). In response to *Escovopsis* infection, the cultivar can use antibiotics that inhibit *Escovopsis* growth (14), the ant agriculturalists mount a number of behavioral defenses to remove the pathogen (27), and the ants support bacteria that produce *Escovopsis*-inhibiting antibiotics (28). All of these defenses could potentially change (either plastically or evolutionarily) in response to *Escovopsis* infection. There are several important considerations in the case of complex symbiotic systems such as that of the fungus-growing ant symbiosis, however. First, the cultivar, likely under the strongest selection to evolve defenses to counteract *Escovopsis* attack, reproduces mostly asexually, and somatic incompatibilities limit genetic exchange between strains (29, 30); the cultivar may be constrained to not evolve rapidly so as to maintain a mutualism with the ants [i.e., Red King hypothesis for slow evolution of mutualistic partners (31)]. Second, *Escovopsis* too can benefit from symbionts [e.g., black yeast that inhibit growth of antibiotic-producing bacteria (32)], which in turn themselves could evolve in response to changing defenses. These combined features may lessen selection to maintain sexual recombination.

Lack of Repeat-Induced Point Mutation

One important consequence of the loss of sex for the genome would be the hindrance of continued Repeat-Induced Point mutation (RIP), which requires sexual recombination (33). RIP, originally described in *Neurospora crassa* (33) and later shown to be active in *Trichoderma* (34), a genus of fungi closely related to *Escovopsis* (Fig. 1B and *SI Appendix, Fig. S6*), is a common (*SI Appendix, Table S4*), irreversible fungal-defense mechanism that preferentially alters C:G to T:A nucleotides and acts mainly on transposable elements but also on protein-coding genes (35), potentially leading to gene inactivation

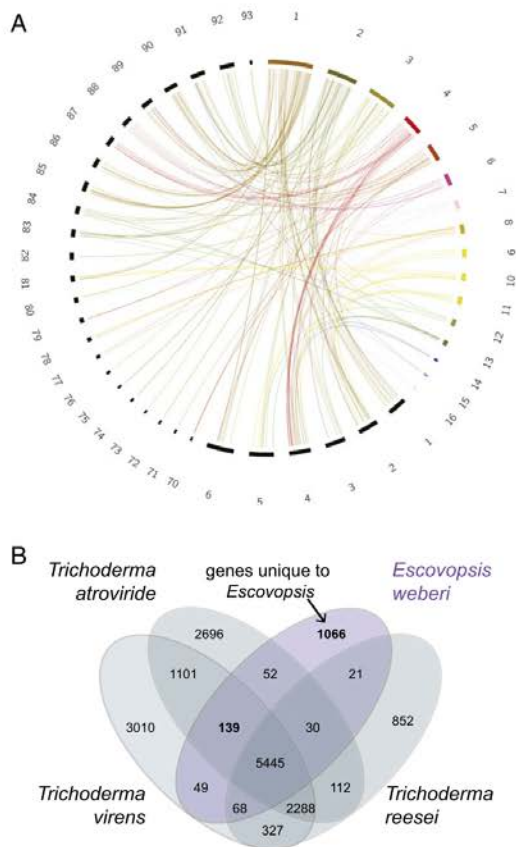


Fig. 2. Similarities between *Escovopsis* and *Trichoderma*. (A) Mesosynteny between *E. weberi* and *T. virens*. Scaffolds of *E. weberi* are multicolored. *T. virens* scaffolds are black. Only scaffolds containing syntenic regions are shown. (B) Gene content overlap between *E. weberi* and three *Trichoderma* species. Like *Escovopsis* spp., *Trichoderma* spp. are mycoparasites (fungi that attack and consume other fungi), although they are less specialized and are also able to obtain nutrients from dead organic matter. Orthologs were assigned using all-against-all BLASTP for amino acids and inparanoid/multiparanoid (sequence overlap coverage $\geq 50\%$).

and genome reduction. The *E. weberi* genome lacks four genes involved in RIP: *qip*, *qde1*, *qde3*, and *sad1* (SI Appendix, Table S5). Similar RIP deactivation in *Blumeria graminis* and other specialized plant pathogens is postulated to have led to extensive retrotransposon proliferation and genome-size expansion (16), contrasting the genomic architecture of *E. weberi*, which along with its reduced genome size, has a paucity of transposable elements (SI Appendix, Fig. S4) and gene paralogs (only four; SI Appendix, Table S6). One possibility is that RIP deactivation in *E. weberi* is a fairly recent phenomenon: the genome does contain footprints of past RIP operation (SI Appendix, Table S7), suggesting that RIP may have limited genome expansion in the past.

Genomic Similarities to Closely Related Fungi

Phylogenetic placement of *Escovopsis* within the Hypocreales (SI Appendix, Fig. S6) confirms that the most closely related fungi to *Escovopsis* with available genome sequences are within the genus

Trichoderma, which diversified from a mycoparasitic ancestor (36). *Escovopsis* diverged from *Trichoderma* ~50 million years ago (SI Appendix, Fig. S7), coincident with the evolution of ant fungiculture (6, 37). Pairwise sequence comparison of the genome sequences of *E. weberi* with both *Trichoderma atroviride* and *Trichoderma virens* (Fig. 2A) revealed a high degree of micro mesosynteny, indicating that genome segments have a similar gene content but shuffled order and orientation, likely due to intrachromosomal rearrangements (38). Compared with *T. virens*, only 6% of *E. weberi*'s genes are located outside of shared syntenic blocks; 42% of these nonsyntenic genes are species-specific to *E. weberi* and encode proteins of unknown function. Similarities to *Trichoderma* will facilitate further functional analyses of this ant agricultural pathogen.

Orthology analysis, based on bidirectional best BLAST hits, between the *E. weberi* gene set and those of three *Trichoderma* spp. (*T. atroviride*, *T. reesei*, *T. virens*), which, like *Escovopsis* spp., are mycoparasites, revealed that 80% of *E. weberi*'s genes have homologs in all three *Trichoderma* genomes, and an additional 5% are found in at least one of the *Trichoderma* genomes (Fig. 2B and Dataset S3). *E. weberi* shares more orthologs with *T. virens* and *T. atroviride* (Fig. 2B), which may be driven by their substantially higher gene content than *T. reesei* (Fig. 1B). Most of the 1,066 genes unique to *E. weberi* relative to *Trichoderma* spp. are of unknown function, and only 128 of these genes exhibit homology to proteins in other Pezizomycotina (Dataset S5), including *Metarhizium*, *Fusarium*, and *Colletotrichum* species (SI Appendix, Table S8). The latter is intriguing as *Colletotrichum* is not closely related to the genus *Escovopsis* but is a genus containing obligate pathogens (39).

Genomic Similarities to Other Specialized Fungi with Small Genomes

Although some specialized, host-associated fungi exhibit genome expansion, in part due to proliferation of retrotransposons [e.g., *B. graminis* (16)], other specialized, host-associated fungi have small genomes. For example, the Yeast Like Symbiont (YLS), an obligate, specialized fungal endosymbiont of the aphid *Cerataphis brasiliensis* (40), is predicted to have had strict association with its host insects for millions of years, replacing the role of *Buchnera aphidicola*, an obligate bacterial symbiont found in other aphid species (41). *Trichophyton rubrum*, another example, is a human skin-specific fungal pathogen and causative agent of athlete's foot (42). Like *E. weberi*, YLS and *T. rubrum* have two of the smallest estimated genome sizes among the Pezizomycotina (~25 and 22 Mb, respectively). Fifty-one percent of *E. weberi*'s 6,870 protein-coding genes have orthologs in both YLS and *T. rubrum* (SI Appendix, Fig. S8), indicative of a core gene set for these host-associated, although ecologically distinct, taxa. This overlapping core set consists mostly of housekeeping genes involved in central metabolism and in DNA, RNA, protein, and organelle biosynthesis. Genes unique to *E. weberi*, relative to those shared between the three genomes, are enriched in transcription factors (Zn2Cys6 and C2H2 type) and glycosyl hydrolases, which assist in the hydrolysis of glycosidic bonds in complex sugars (SI Appendix, Table S9). Of the 1,834 genes unique to *E. weberi* relative to YLS and *T. rubrum*, 1,064 are found in the mycoparasite *T. virens* of which 459 encode uncharacterized putative proteins. Of note, the glycosyl hydrolases present in the core set (i.e., those shared among YLS, *Trichophyton*, and *Escovopsis*) and those shared only between *T. virens* and *E. weberi* exhibit a clear bias: whereas the core set contains all of the GH13 amyolytic and GH16 β -glucanolytic hydrolases, the 1,064 genes shared with *T. virens* are strongly enriched in GH3, GH5, and GH12 endo- and exo- β -glucanases and particularly in GH18 chitinases (SI Appendix, Table S9), which may play a role in *Escovopsis* breaking down the chitin within the cell walls of host fungi.

Specialization and Gene Loss

In some respects, fungus-growing ants and *Escovopsis* occupy a similar niche, obtaining nutrients from the cultivated fungus, which has the capacity to break down diverse, abundant plant material into nutrients that the ants and parasite can use (Fig. 1A) (2, 3). Thus, there should be many degradation capacities of the cultivated fungi that *Escovopsis* spp. do not require. *E. weberi* is able to grow on several carbon sources in absence of its fungal host (SI Appendix, Fig. S2 and Dataset S6), and a specific search for presence of genes encoding enzymes of primary metabolism (i.e., carbohydrate, amino acid, lipid, and nucleic acid anabolism and catabolism) revealed that the *E. weberi* genome contains all genes required for growth on media containing an organic carbon source and salts except for genes required for the synthesis of dehydroascorbic acid, an oxidized form of ascorbic acid. When *E. weberi* growth was compared with that of *T. atroviride* using phenotype microarray plates, however, it exhibited much slower growth on most carbon sources (SI Appendix, Fig. S2 and Dataset S6). In these assays, *E. weberi* grew most rapidly on the α -glucans trehalose and maltose, which is consistent with the findings that *E. weberi* has retained genes encoding α -glucan-degrading enzymes and that the associated genes are up-regulated when *E. weberi* is growing toward and overgrowing the fungal cultivar (SI Appendix, Fig. S9 and Dataset S7). It is possible that *E. weberi* may have specialized in the utilization of these simple and unbranched α -glucans as these are the most abundant carbohydrates in its host fungus (43).

In contrast to *T. reesei* and *T. virens*, *E. weberi* is depleted in genes encoding amino acid transporters and major facilitator superfamily transporters, which transport small solutes. It also contains many fewer cytochrome P450 proteins, flavin-dependent monooxygenases, ankyrins, and PTH11 receptors, which have been implicated in host recognition by fungal pathogens (44) (SI Appendix, Table S3 and Dataset S8). Most interestingly, relative to *Trichoderma* spp., *E. weberi* exhibits strong reduction in several gene families encoding polysaccharide depolymerizing enzymes (a.k.a., carbohydrate active enzymes, CAZymes) (Fig. 3 and SI Appendix, Table S10). *E. weberi* lacks all cellobiohydrolases [Glycoside Hydrolase family 6 (GH6) and GH7], all xylanases (GH10, GH11, GH30), and also auxiliary proteins like polysaccharide monooxygenases (GH61) and the expansin-like protein swollenin. Consistent with the fact that *Escovopsis* breaks down the ants' cultivated fungus but not leaves collected by the ants to feed to their fungus (7), cellulose-binding domains, which are a hallmark of fungi that use plant material for nutrients (34), are also strongly reduced and present only in two endo- β -1,4-glucanases (GH5, GH7; orthologous to *T. reesei* endo- β -1,4-glucanases EGL and EGL1) and in two chitinases (GH18). The genome of *E. weberi* also contains only one GH family member that encodes enzymes for hydrolysis of α -galactosides and of α -arabinofuranosides (GH27, GH51); these glycoside hydrolases are expanded in *Trichoderma* (34, 36). This reduction is reminiscent to that found in some plant pathogens that also lack some GH enzymes (45). On the other hand, *E. weberi* has a similar number of chitinases (GH18, GH20) and of β -1,3/ β -1,4-glucanases (GH16) as *T. reesei*, indicating that the potential for attacking the host fungus' cell wall has been maintained. Interestingly, proteomic, transcriptomic, and draft genome sequencing have identified some of these missing enzymes to be present and highly expressed in the ant-cultivated fungus *Leucoagaricus gongylophorus* (Fig. 3 and SI Appendix, Table S10) (2, 3). Taken together, these losses are consistent with previous findings that the specialized mycoparasite *Escovopsis* breaks down fungal but not plant material (7) and suggest that *E. weberi* has lost the ability to feed on lignocellulosic plant material, an ability retained by other microbial members of fungus-growing ant gardens (46).

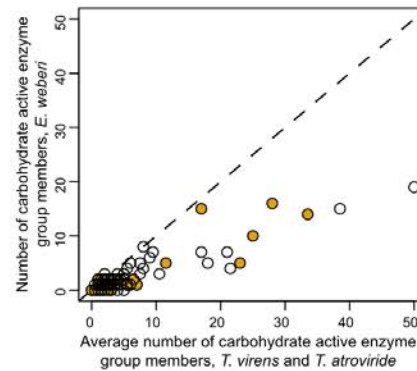


Fig. 3. The *E. weberi* genome encodes a reduced number of carbohydrate active enzymes. Carbohydrate active enzymes are divided into families. Each point represents the relation between the number of members of a given CAZyme family for *E. weberi* plotted against the average number of family members for the less specialized mycoparasites *T. virens* and *T. atroviride*. Members of some of these families, indicated in orange, are known to be highly expressed in *E. weberi*'s host fungus (2, 3). Additional details are in SI Appendix, Table S10.

Further Genomic Signatures of Exploitation of a Fungal Symbiosis

E. weberi has been shown to kill the fungi cultivated by the ants from a distance (7), a process that likely involves the secretion of toxins. Using SignalP (47), a secretion-specific signal peptide was predicted for 4.8% of *E. weberi*'s proteins (Dataset S9), about half the percentage found for *Trichoderma* (9.0, 8.6, and 8.7% in *T. reesei*, *T. atroviride*, and *T. virens*, respectively) (48). The *E. weberi* secretome is dominated by genes with no known function, particularly in comparison with *Trichoderma* (55.8% for *E. weberi* versus 25–30% for *Trichoderma* spp.).

Toward identification of low-molecular-weight toxins, we used antimash 2.0 (49) to identify 17 putative secondary metabolite biosynthesis clusters in the genome (SI Appendix, Table S11), three of which are unique to *E. weberi*. All three unique clusters are predicted to code for terpene synthases, metabolites known to be involved in the production of mycotoxins (50). Other clusters are predicted to code for polyketide synthases (PKS). Expression of some genes within these PKS clusters was significantly up-regulated when *E. weberi* was growing toward its host (Fig. 4 and Dataset S7). One such gene (ESCO_001469) encodes a protein with an amino-terminal extracellular cysteine-rich EGF-like (a.k.a. CFEM, or Common in several Fungal Extracellular Membrane proteins) domain (51). Proteins bearing this domain in the rice pathogen *Magnaporthe grisea* are involved in virulence (51), and CFEM proteins in the human pathogen *Candida albicans* influence cell-surface characteristics and biofilm formation (52). InterProScan analysis revealed seven CFEM-domain proteins in *E. weberi* (SI Appendix, Table S12), the largest domain family in those genes that are unique to *E. weberi* relative to *Trichoderma* spp. based on orthology analysis (SI Appendix, Table S13).

There is also evidence of retention of nonribosomal peptide synthases (NRPSs), enzymes known to synthesize a multitude of secondary metabolites (53). The *E. weberi* genome encodes two peptaibol synthases (ESCO_001464 and ESCO_003769), NRPSs that have been found only in *Trichoderma* and a few close relatives (54). These enzymes have been shown to inhibit cell-wall resynthesis by *Trichoderma* hosts when they are being attacked by *Trichoderma*'s cell-wall hydrolases (55). Finally, the *E. weberi*

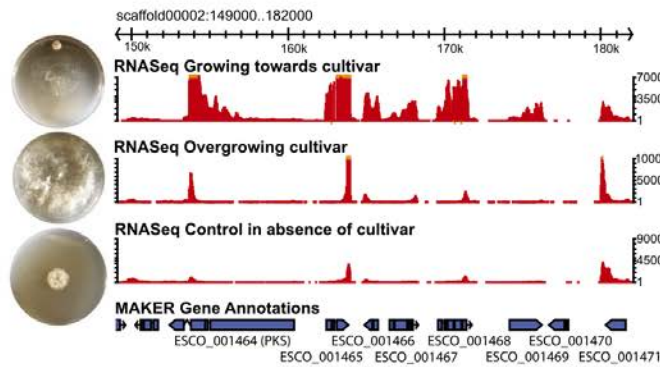


Fig. 4. Up-regulation of gene expression within a secondary metabolite cluster during interaction with cultivated host fungi. Gbrowse genome browser view of 1 of 16 secondary metabolite clusters in the *E. weberi* genome. Below the scaffold are three tracks illustrating RNA-seq-based gene expression when *E. weberi* is growing towards its host (Top), when it has overgrown its host (Middle), and in the absence of its host (Bottom); MAKER2 gene model predictions are illustrated below. Photographs next to each RNA-seq track illustrate the growth of *E. weberi* under each condition. Each Petri dish was inoculated with the cultivated fungus near the top (when present) and *E. weberi* near the center 1 wk later; photographs were taken 3–4 d after *E. weberi* inoculation. Note that *E. weberi* grows much more rapidly in the presence than in the absence of its host. See [S1 Appendix](#), [Fig. S1](#) for additional images.

genome encodes three β -lactamases (ESCO_006545, ESCO_005342, ESCO_005794) and one tetracycline resistance gene (ESCO_002770), which inactivate antibiotics. The observation that these genes have been maintained in *E. weberi* despite general genome reduction suggests a similar mycoparasitic mechanism for *Escovopsis* when attacking the ants' cultivated fungi and maintenance of mechanisms to combat antagonists within the complex microbial community of fungus-growing ant gardens.

Conclusions

Specialization over evolutionary timescales can facilitate gene loss and genome reduction. Fungus-growing ants and *Escovopsis* use the same fungus as a primary food source, and this obligate dependency is reflected in genetic modifications relative to the closest relatives of each. The genome of the ant *A. cephalotes*, for example, is depleted of genes related to nutrient acquisition, including serine proteases, genes involved in arginine biosynthesis, and a hexamerin involved in amino acid sequestration during development in other insects (19). Here we show that *E. weberi* has a small genome and reduced gene content relative to its closest sequenced relatives with broader host ranges. The *E. weberi* genome is depleted in genes associated with plant degradation yet has retained genes associated with attacking fungal hosts. Thus, dependence on the cultivated fungus shapes the genomes of the ants and *Escovopsis*, unrelated but ecologically linked organisms.

Although the reduced functional capacity of *E. weberi* is consistent with loss of genes no longer necessary given its highly specialized, mycoparasitic lifestyle, its relatively small genome, with few mobile elements and duplications, is harder to attribute to specific evolutionary processes, particularly given the inactivation of RIP, the loss of which should allow for genome expansion. Although specialized bacteria, and in particular obligate symbionts, consistently exhibit genome reduction, which is facilitated by several evolutionary processes (17), specialized fungi vary greatly in genome size. Some obligately parasitic fungi have large genomes with many transposable elements (16, 18). This is hypothesized to be in part because eukaryotes with small effective population sizes can tolerate accumulation of slightly deleterious transposable elements, multiple introns, and gene duplications (56) and in part because mobile elements can facilitate rapid adaptation in some organisms (18, 57). However, some obligately parasitic fungi, such as the microsporidium *Encephalitozoon cuniculi*, have reduced genomes with few mobile elements, which is likely due to sustained drift-influenced genome reduction (58). Interestingly, Pezizomycotina fungi with genomes less than 75 Mbp, such as *E. weberi*, exhibit a pattern of decreased genome size with increased drift (59). This may be coupled with selectively beneficial loss of genes

and other genomic content no longer essential for a host-associated, specialized lifestyle.

Specialization of *Escovopsis* spp. goes beyond just specializing on fungus-growing ant fungi in general. Different *Escovopsis* spp. have different host ranges. For example, strains isolated from colonies of *Atta* spp. ants, like the strain genomically described here, are typically able to infect fungi cultivated by *Atta* and other leaf-cutting ant species but have narrow abilities to attack fungi grown by non-leaf-cutting ant species (60). In fact, even within a symbiosis involving a single ant species and its associated fungi, there can be variation in host range, suggesting genotype-by-genotype specificity (14, 15, 60). Therefore, the annotation of this first *Escovopsis* genome provides a starting point to investigate the genomic changes underlying a dynamically evolving host-pathogen system.

Materials and Methods

Detailed descriptions of materials and methods are provided in [S1 Appendix](#). In brief, we sequenced the genome of a single strain of *E. weberi* isolated from an *A. cephalotes* colony from Gamboa, Panama, using the 454 FLX Titanium pyrosequencing platform with both fragment and paired-end approaches (2.5 whole-genome shotgun fragment run, one 8-kbp insert paired-end library run). We assembled the genome using the *De Novo* G5 Assembler v 2.6 from the Newbler software package developed by Roche. The raw dataset is deposited at DNA Data Bank of Japan/European Molecular Biology Laboratory/GenBank under PRJNA253870, and the whole-genome assembly is deposited under accession LGSR000000000. The version described here is version LGSR010000000. RNA-seq reads are deposited in the Sequence Read Archive under accession SRP049545.

We assessed genome assembly completeness using three independent methods: (i) we calculated basic statistics, including total length and fragmentation of the assembled sequences; (ii) we identified CEGs in our genome assembly using CEGMA 2.4 (22); and (iii) we took a K-mer-based genome size estimation approach. For the latter, we generated a frequency distribution of unique 31-mers in the raw sequencing reads with Jellyfish 1.1.11 (61) and included K-mers with more than 12 copies in the genome, those located to the right of the inflection point ([Dataset S2](#)), for computation of genome size.

We used MAKER 2.28 for gene discovery with exon support provided by alignment of RNA-seq transcripts from *E. weberi* grown in the presence and absence of its host and by available *Trichoderma* ESTs and proteomes, other fungal proteomes, and NCBI's NR database. Protein-coding genes were predicted with the ab initio gene predictors Augustus 2.7 (62), SNAP 0.15.4 (63), and GeneMark 2.5 (64) using exon hits from the protein and RNA-seq transcript evidence. We functionally annotated all predicted proteins using InterProScan 5–44.0 (65). The genome annotation can be visualized at [gb2.fungalgenomes.org/](#) with GBrowse (66).

We assessed evidence for RIP by computing RIP indices [TA/AT > 0.89 and CA+TG/AC+GT < 1.03 are considered evidence for RIP (67)] for the five most prevalent repeat families within the *E. weberi* genome and the unmapped reads using RIPCAL 1.0 (68). We also searched for orthologs of genes known to be involved in the RIP process in *N. crassa* (69).

ACKNOWLEDGMENTS. We thank the sequencing and production team at the 454 Sequencing Center for their help and expertise during this project, especially L. Li; the Smithsonian Tropical Research Institute in Panama for logistical support during sample collection, especially M. Paz, O. Arosemena, Y. Clemons, L. Seid, and R. Urriola; the Panamanian Autoridad Nacional del Ambiente y el Mar for collection and export permits; and F. Stewart for access to the Georgia Tech

PACE server. Genome annotation and comparisons were performed using the University of California at Riverside Institute for Integrative Biology bioinformatics high performance cluster. This research was supported by a 454 Life Sciences' 10GB sequencing grant to N.M.G., C.R.C., G.S., G. Weinstock, J. Taylor, and S. Slater. Vienna laboratory research (C.P.K., K.C., L.A., I.S.D.) was supported by the Austrian Science Foundation (Grant FWF-P 25613 to I.S.D.).

- Weber NA (1966) Fungus-growing ants. *Science* 153(3736):587–604.
- Grell MN, et al. (2013) The fungal symbiont of *Acromyrmex* leaf-cutting ants expresses the full spectrum of genes to degrade cellulose and other plant cell wall polysaccharides. *BMC Genomics* 14:928.
- Aylward FO, et al. (2013) *Leucopogon gongylophorus* produces diverse enzymes for the degradation of recalcitrant plant polymers in leaf-cutter ant fungus gardens. *Appl Environ Microbiol* 79(12):3770–3778.
- Schiott M, De Fine Licht HH, Lange L, Boomsma JJ (2008) Towards a molecular understanding of symbiont function: Identification of a fungal gene for the degradation of xylan in the fungus gardens of leaf-cutting ants. *BMC Microbiol* 8(1):40.
- Moller IE, De Fine Licht HH, Harholt J, Willits WGT, Boomsma JJ (2011) The dynamics of plant cell-wall polysaccharide decomposition in leaf-cutting ant fungus gardens. *PLoS One* 6(3):e17506–e17509.
- Schultz TR, Brady SG (2008) Major evolutionary transitions in ant agriculture. *Proc Natl Acad Sci USA* 105(14):5435–5440.
- Reynolds HT, Currie CR (2004) Pathogenicity of *Escovopsis weberi*: The parasite of the attine ant-microbe symbiosis directly consumes the ant-cultivated fungus. *Mycologia* 96(5):955–959.
- Currie CR, et al. (2003) Ancient tripartite coevolution in the attine ant-microbe symbiosis. *Science* 299(5605):386–388.
- Currie CR (2001) Prevalence and impact of a virulent parasite on a tripartite mutualism. *Oecologia* 128(1):99–106.
- Currie CR, Mueller UG, Malloch D (1999) The agricultural pathology of ant fungus gardens. *Proc Natl Acad Sci USA* 96(14):7998–8002.
- Harman GE, Howell CR, Viterbo A, Chet I, Lorito M (2004) *Trichoderma* species: Opportunistic, avirulent plant symbionts. *Nat Rev Microbiol* 2(1):43–56.
- Bailey BA, et al. (2008) Antibiosis, mycoparasitism, and colonization success for endophytic *Trichoderma* isolates with biological control potential in *Theobroma cacao*. *Biol Control* 46(1):24–35.
- Druzhinina IS, et al. (2011) *Trichoderma*: The genomics of opportunistic success. *Nat Rev Microbiol* 9(10):749–759.
- Gerardo NM, Jacobs SR, Currie CR, Mueller UG (2006) Ancient host-pathogen associations maintained by specificity of chemotaxis and antibiosis. *PLoS Biol* 4(8):e235.
- Gerardo NM, Mueller UG, Price SL, Currie CR (2004) Exploiting a mutualism: Parasite specialization on cultivars within the fungus-growing ant symbiosis. *Proc Biol Sci* 271(1550):1791–1798.
- Spanu PD, et al. (2010) Genome expansion and gene loss in powdery mildew fungi reveal tradeoffs in extreme parasitism. *Science* 330(6010):1543–1546.
- McCutcheon JP, Moran NA (2012) Extreme genome reduction in symbiotic bacteria. *Nat Rev Microbiol* 10(1):13–26.
- Raffaële S, Kamoun S (2012) Genome evolution in filamentous plant pathogens: Why bigger can be better. *Nat Rev Microbiol* 10(6):417–430.
- Suen G, et al. (2011) The genome sequence of the leaf-cutter ant *Atta cephalotes* reveals insights into its obligate symbiotic lifestyle. *PLoS Genet* 7(2):e1002007.
- Liu B, et al. (2013) Estimation of genomic characteristics by analyzing k-mer frequency in *de novo* genome projects. *arXiv.org*:1–47. Available at arxiv.org/abs/1308.2012.
- Chain PSG, et al. Genomic Standards Consortium Human Microbiome Project Jumpstart Consortium (2009) Genomics. Genome project standards in a new era of sequencing. *Science* 326(5950):236–237.
- Parra G, Bradnam K, Korfi I (2007) CEGMA: A pipeline to accurately annotate core genes in eukaryotic genomes. *Bioinformatics* 23(9):1061–1067.
- Seibel C, Tisch D, Kubicek CP, Schmoll M (2012) The role of pheromone receptors for communication and mating in *Hypocrea jecorina* (*Trichoderma reesei*). *Fungal Genet Biol* 49(10):814–824.
- Hibbett DS, Taylor JW (2013) Fungal systematics: Is a new age of enlightenment at hand? *Nat Rev Microbiol* 11(2):129–133.
- Morran LT, Parmenter MD, Phillips PC (2009) Mutation load and rapid adaptation favour outcrossing over self-fertilization. *Nature* 462(7271):350–352.
- Smith JM (1978) *The Evolution of Sex* (Cambridge Univ Press, Cambridge, UK).
- Currie CR, Stuart AE (2001) Weeding and grooming of pathogens in agriculture by ants. *Proc Biol Sci* 268(1471):1033–1039.
- Currie CR, Poulsen M, Mendenhall J, Boomsma JJ, Billen J (2006) Coevolved crypts and exocrine glands support mutualistic bacteria in fungus-growing ants. *Science* 311(5757):81–83.
- Mikheyev AS, Mueller UG, Abbot P (2006) Cryptic sex and many-to-one coevolution in the fungus-growing ant symbiosis. *Proc Natl Acad Sci USA* 103(28):10702–10706.
- Kooij PW, Poulsen M, Schiott M, Boomsma JJ (2015) Somatic incompatibility and genetic structure of fungal crops in sympatric *Atta colombica* and *Acromyrmex echinator* leaf-cutting ants. *Fungal Ecol* 18:10–17.
- Bergstrom CT, Lachmann M (2003) The Red King effect: When the slowest runner wins the coevolutionary race. *Proc Natl Acad Sci USA* 100(2):593–598.
- Little AEF, Currie CR (2008) Black yeast symbionts compromise the efficiency of antibiotic defenses in fungus-growing ants. *Ecology* 89(5):1216–1222.
- Selker EU, Cambareri EB, Jensen BC, Haack KR (1987) Rearrangement of duplicated DNA in specialized cells of *Neurospora*. *Cell* 51(5):741–752.
- Martinez D, et al. (2008) Genome sequencing and analysis of the biomass-degrading fungus *Trichoderma reesei* (syn. *Hypocrea jecorina*). *Nat Biotechnol* 26(5):553–560.
- Galagan JE, et al. (2003) The genome sequence of the filamentous fungus *Neurospora crassa*. *Nature* 422(6934):859–868.
- Kubicek CP, et al. (2011) Comparative genome sequence analysis underscores mycoparasitism as the ancestral life style of *Trichoderma*. *Genome Biol* 12(4):R40.
- Mikheyev AS, Mueller UG, Abbot P (2010) Comparative dating of attine ant and lepiotaceae cultivar phylogenies reveals coevolutionary synchrony and discord. *Am Nat* 175(6):E126–E133.
- Hane JK, et al. (2011) A novel mode of chromosomal evolution peculiar to filamentous Ascomycete fungi. *Genome Biol* 12(5):R45.
- O'Connell RJ, et al. (2012) Lifestyle transitions in plant pathogenic *Colletotrichum fungi* deciphered by genome and transcriptome analyses. *Nat Genet* 44(9):1060–1065.
- Vogel KJ, Moran NA (2013) Functional and evolutionary analysis of the genome of an obligate fungal symbiont. *Genome Biol Evol* 5(5):891–904.
- Baumann P, et al. (1995) Genetics, physiology, and evolutionary relationships of the genus *Buchnera*: Intracellular symbionts of aphids. *Annu Rev Microbiol* 49:55–94.
- Martinez DA, et al. (2012) Comparative genome analysis of *Trichophyton rubrum* and related dermatophytes reveals candidate genes involved in infection. *MBio* 3(5):e00259.
- Martin MM, Carman RM, Macconnell JG (1969) Nutrients derived from the fungus cultured by the fungus-growing ant *Atta colombica tonsipes*. *Ann Entomol Soc Am* 62(1):11–13.
- DeZwaan TM, Carroll AM, Valent B, Sweigard JA (1999) *Magnaporthe grisea* pth11p is a novel plasma membrane protein that mediates appressorium differentiation in response to inductive substrate cues. *Plant Cell* 11(10):2013–2030.
- Zhao Z, Liu H, Wang C, Xu J-R (2013) Comparative analysis of fungal genomes reveals different plant cell wall degrading capacity in fungi. *BMC Genomics* 14(1):274.
- Aylward FO, Currie CR, Suen G (2012) The evolutionary innovation of nutritional symbioses in leaf-cutter ants. *Insects* 3:41–61.
- Petersen TN, Brunak S, von Heijne G, Nielsen H (2011) SignalP 4.0: Discriminating signal peptides from transmembrane regions. *Nat Methods* 8(10):785–786.
- Druzhinina IS, Shelest E, Kubicek CP (2012) Novel traits of *Trichoderma* predicted through the analysis of its secretome. *FEMS Microbiol Lett* 337(1):1–9.
- Blin K, et al. (2013) antiSMASH 2.0: A versatile platform for genome mining of secondary metabolite producers. *Nucleic Acids Res* 41(Web Server issue):W204–W212.
- Rynkiewicz MJ, Cane DE, Christianson DW (2001) Structure of trichodiene synthase from *Fusarium sporotrichioides* provides mechanistic inferences on the terpene cyclization cascade. *Proc Natl Acad Sci USA* 98(24):13543–13548.
- Kulkarni RD, Kelkar HS, Dean RA (2003) An eight-cysteine-containing CFEM domain unique to a group of fungal membrane proteins. *Trends Biochem Sci* 28(3):118–121.
- Pérez A, et al. (2011) Some biological features of *Candida albicans* mutants for genes coding fungal proteins containing the CFEM domain. *FEMS Yeast Res* 11(3):273–284.
- Strieker M, Tanović A, Marahiel MA (2010) Nonribosomal peptide synthetases: Structures and dynamics. *Curr Opin Struct Biol* 20(2):234–240.
- Mukherjee PK, Horwitz BA, Kenerley CM (2012) Secondary metabolism in *Trichoderma*: A genomic perspective. *Microbiology* 158(Pt 1):35–45.
- Lorito M, Farkas V, Rebuffat S, Bodo B, Kubicek CP (1996) Cell wall synthesis is a major target of mycoparasitic antagonism by *Trichoderma harzianum*. *J Bacteriol* 178(21):6382–6385.
- Lynch M, Conery JS (2003) The origins of genome complexity. *Science* 302(5649):1401–1404.
- Stukenbrock EH, Croll D (2014) The evolving fungal genome. *Fungal Biol Rev* 28(1):1–12.
- Katinka MD, et al. (2001) Genome sequence and gene compaction of the eukaryote parasite *Encephalitozoon cuniculi*. *Nature* 414(6862):450–453.
- Kelkar YD, Ochman H (2012) Causes and consequences of genome expansion in fungi. *Genome Biol Evol* 4(1):13–23.
- Birnbaum SSL, Gerardo NM (2016) Patterns of specificity of the pathogen *Escovopsis* across the fungus-growing ant symbiosis. *Am Nat*, in press.
- Marçais G, Kingsford C (2011) A fast, lock-free approach for efficient parallel counting of occurrences of k-mers. *Bioinformatics* 27(6):764–770.
- Stanke M, Waack S (2003) Gene prediction with a hidden Markov model and a new intron submodel. *Bioinformatics* 19(Suppl 2):ii215–ii225.
- Korf I (2004) Gene finding in novel genomes. *BMC Bioinformatics* 5:59.
- Lomsadze A, Ter-Hovhannisyan V, Chernoff YO, Borodovsky M (2005) Gene identification in novel eukaryotic genomes by self-training algorithm. *Nucleic Acids Res* 33(20):6494–6506.
- Zdobnov EM, Apweiler R (2001) InterProScan: An integration platform for the signature-recognition methods in InterPro. *Bioinformatics* 17(9):847–848.
- Stein LD, et al. (2002) The generic genome browser: A building block for a model organism system database. *Genome Res* 12(10):1599–1610.
- Margolin BS, et al. (1998) A methylated *Neurospora* 5S rRNA pseudogene contains a transposable element inactivated by repeat-induced point mutation. *Genetics* 149(4):1787–1797.
- Hane JK, Oliver RP (2008) RIPCAL: A tool for alignment-based analysis of repeat-induced point mutations in fungal genomic sequences. *BMC Bioinformatics* 9:478.
- Borkovich KA, et al. (2004) Lessons from the genome sequence of *Neurospora crassa*: Tracing the path from genomic blueprint to multicellular organism. *Microbiol Mol Biol Rev* 68(1):1–108.

Dataset S3*

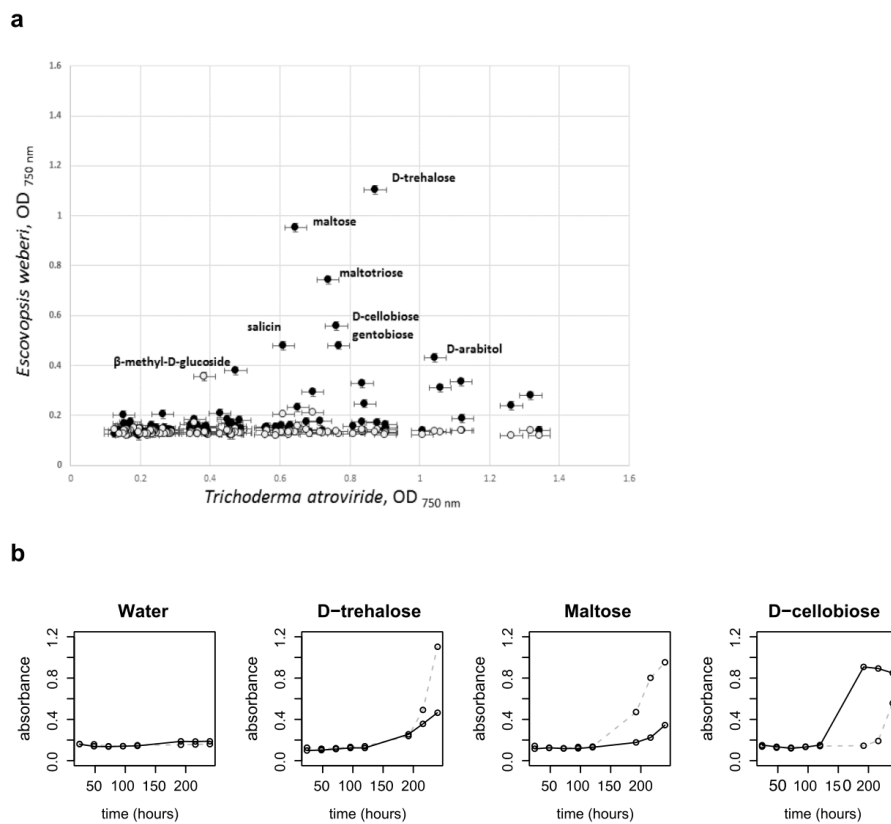
<i>Escovopsis</i> gene ID	<i>Trichoderma virens</i> based annotation	<i>Trichoderma</i> spp. Based annotation	NR database annotation
ESCO_000001	GMP synthase	GMP synthase	GMP synthase
ESCO_000002	Endo- β -1,4-glucanase CEL7B	Endo- β -1,4-glucanase CEL7B	Endo- β -1,4-glucanase CEL7B
ESCO_000003	Nmra family protein	Nmra family protein	Nmra family protein
ESCO_000004	Secondary metabolite cluster that contains PKS (tre33804)	Secondary metabolite cluster that contains PKS (tre33804) and PKS-NRPS hybrid (tre14836) genes	Secondary metabolite cluster that contains PKS (tre33804) and PKS-NRPS hybrid (tre14836) genes
ESCO_000005	PKS	PKS	PKS
ESCO_000006			
ESCO_000007	Zn2Cys6 transcriptional regulator	Zn2Cys6 transcriptional regulator	Zn2Cys6 transcriptional regulator
ESCO_000008	Late sexual development protein Isda	Late sexual development protein Isda	Late sexual development protein Isda
ESCO_000009	Zn2Cys6 transcriptional regulator	Zn2Cys6 transcriptional regulator	Zn2Cys6 transcriptional regulator
ESCO_000010	Unknown protein	Unknown protein	Unknown protein
ESCO_000011	Zn2Cys6 transcriptional regulator	Zn2Cys6 transcriptional regulator	Zn2Cys6 transcriptional regulator

ESCO_000012	Cytochrome P450 monooxygenase	Cytochrome P450 monooxygenase	Cytochrome P450 monooxygenase
ESCO_000013	GH28	GH28	GH28
ESCO_000014	GH17	GH17	GH17
ESCO_000015		Unknown protein	Unknown protein
ESCO_000016	Unknown protein	Unknown protein	Unknown protein
ESCO_000017	C2H2 transcriptional regulator	C2H2 transcriptional regulator	C2H2 transcriptional regulator
ESCO_000018	Peroxisomal membrane protein pex16	Peroxisomal membrane protein pex16	Peroxisomal membrane protein pex16
ESCO_000019	Zn2Cys6 transcriptional regulator	Zn2Cys6 transcriptional regulator	Zn2Cys6 transcriptional regulator
ESCO_000020	Fungal specific transcription factor domain-containing protein	Fungal specific transcription factor domain	Fungal specific transcription factor domain- containing protein
ESCO_000021	Transcription factor IWS1	Transcription factor IWS1	Transcription factor IWS1
ESCO_000022	RNA polymerase Rpb1	RNA polymerase Rpb1	RNA polymerase Rpb1
ESCO_000023	Flavin-containing monooxygenase	Flavin-containing monooxygenase	Flavin-containing monooxygenase
ESCO_000024		Epl1/Sm1	Epl1/Sm1

* The full dataset with annotation of 6870 genes can be accessed from [here](#)

Figure S2

Figure S2. Growth of *Escovopsis weberi* on alternative carbon sources. a) Growth of *E. weberi* on alternative carbohydrate sources at 96 hours (white circles) and 240 hours (black circles) compared to *Trichoderma atroviride* at 96 hours. Note that at the same time point (96 hours, white circles), *E. weberi* shows less growth than *T. atroviride* on most carbon sources; one notable exception is beta-methyl-D-glucoside. b) *E. weberi* growth at two temperatures over time on representative carbon sources (water as control). The best carbon sources for *Escovopsis* growth were all disaccharides: D-trehalose and maltose at 25°C (dashed lines) and D-cellobiose at 30°C (solid lines). Data are means of four biological replicates, which differed by less than 12%. Notably, trehalose is the dominant carbohydrate constituent of *Escovopsis*' host fungus(55). Additional data in Dataset S6.



Chapter 3 Evolution of *Trichoderma* carbohydrate-active enzymes required for the degradation of plant biomass



Chapter 3.1 Massive lateral transfer of genes encoding plant cell wall-degrading enzymes to the mycoparasitic fungus *Trichoderma* from its plant-associated hosts⁶

Authors

Irina S. Druzhinina¹, **Komal Chenthamara**¹, Jian Zhang², Lea Atanasova¹, Dongqing Yang², Youzhi Miao², Mohammad J. Rahimi¹, Marica Grujic¹, Feng Cai^{1, 2}, Shadi Pourmehdi¹, Kamariah Abu Salim³, Carina Pretzer¹, Alexey G. Kopchinskiy¹, Bernard Henrissat^{4,5,6}, Alan Kuo⁷, Hope Hundley⁷, Mei Wang⁷, Andrea Aerts⁷, Asaf Salamov⁷, Anna Lipzen⁷, Kurt Labutti⁷, Kerrie Barry⁷, Igor V. Grigoriev^{7,8}, Qirong Shen², Christian P. Kubicek¹

Affiliation

1. Microbiology and Applied Genomics group, Research Area Biochemical Technology, Institute of Chemical, Environmental & Bioscience Engineering, TU Wien, Gumpendorferstrasse 1a
2. Jiangsu Provincial Key Lab of Organic Solid Waste Utilization, Nanjing Agricultural University, Nanjing, China
3. Environmental and Life Sciences, Universiti Brunei Darussalam, Bandar Seri Begawan, Brunei Darussalam
4. Architecture et Fonction des Macromolécules Biologiques, CNRS, Aix-Marseille Université, Marseille, France
5. INRA, USC1408AFMB, Marseille, France
6. Department of Biological Sciences, King Abdulaziz University, Jeddah, Saudi Arabia
7. US Department of Energy Joint Genome Institute, Walnut Creek, CA, United States of America
8. Department of Plant and Microbial Biology, University of California Berkeley, Berkeley, CA, United States of America

⁶ Druzhinina IS, **Chenthamara K**, Zhang J, Atanasova L, Yang D, Miao Y, Rahimi MJ, Grujic M, Cai F, Pourmehdi S, Salim KA. Massive lateral transfer of genes encoding plant cell wall-degrading enzymes to the mycoparasitic fungus *Trichoderma* from its plant-associated hosts. *PLoS Genetics*. 2018 Apr 9;14(4):e1007322.

Contribution by the PhD candidate

Together with her advisor and Christian P. Kubicek, the PhD candidate was the major contributing scientist performing data mining, data analysis, ms writing and preparation of the figures. The detailed list of tasks for which the PhD candidate was solely responsible is listed below:

1. Comparison between properties of fungal genomes that were used in this study (S1 Table)
2. Assessment of the growth on plant and fungal biomass (S1 Figure).
3. Neutrality tests of 100 orthologous proteins that were used in phylogenomic analyses (S2 Table).
4. Evolutionary phylogenomic analysis based on 100 orthologous neutrally evolving proteins of Hypocreales and two other Sordariomycetes (Fig 1a).
5. The complete Phylome of *Trichoderma* carbohydrate-active enzymes required for the plant cell-wall degrading including accessory proteins and respective regulator proteins. Exemplary fragments of this phylome are listed in Fig 3,4,5, S2 Figure, S3 Table), and the detailed analysis is summarized in the sub-Chapter 3.
6. Carried out statistical tests like T-Rex and NOTUNG to examine Lateral Gene Transfer and Gene Duplication (S2 Figure, S4 Table).
7. Multilocus phylogeny of 128 Ascomycota fungi (Fig 6A, S7 Table).
8. Dual confrontation tests of *Trichoderma* sp. with other *Trichoderma* sp.; and other hypocrealean species (Fig 10, S3 Figure).
9. Intensive participation in visualization, writing – original draft, review and editing.

RESEARCH ARTICLE

Massive lateral transfer of genes encoding plant cell wall-degrading enzymes to the mycoparasitic fungus *Trichoderma* from its plant-associated hosts

Irina S. Druzhinina^{1*}, Komal Chenthamara¹, Jian Zhang², Lea Atanasova^{1^{aa}}, Dongqing Yang², Youzhi Miao², Mohammad J. Rahimi¹, Marica Grujic¹, Feng Cai^{1,2}, Shadi Pourmehdi¹, Kamariah Abu Salim³, Carina Pretzer¹, Alexey G. Kopchinskiy¹, Bernard Henrissat^{4,5,6}, Alan Kuo⁷, Hope Hundley⁷, Mei Wang⁷, Andrea Aerts⁷, Asaf Salamov⁷, Anna Lipzen⁷, Kurt LaButti⁷, Kerrie Barry⁷, Igor V. Grigoriev^{7,8}, Qirong Shen^{2*}, Christian P. Kubicek^{1^{ab}}


 OPEN ACCESS

Citation: Druzhinina IS, Chenthamara K, Zhang J, Atanasova L, Yang D, Miao Y, et al. (2018) Massive lateral transfer of genes encoding plant cell wall-degrading enzymes to the mycoparasitic fungus *Trichoderma* from its plant-associated hosts. *PLoS Genet* 14(4): e1007322. <https://doi.org/10.1371/journal.pgen.1007322>

Editor: Francis Martin, FRANCE

Received: November 1, 2017

Accepted: March 20, 2018

Published: April 9, 2018

Copyright: This is an open access article, free of all copyright, and may be freely reproduced, distributed, transmitted, modified, built upon, or otherwise used by anyone for any lawful purpose. The work is made available under the [Creative Commons CC0 public domain dedication](https://creativecommons.org/licenses/by/4.0/).

Data Availability Statement: The whole genome sequences used in this study have been deposited in NCBI GenBank <https://www.ncbi.nlm.nih.gov/> database, accession numbers and URLs are listed in S1 Table. The NCBI or JGI accession numbers of individual genes analyzed in this study are listed in Supporting Information S2 Table, S3 Table, S4 Table, S6 Table, and S1 Data. Single gene phylogenies produced in the phylogenomic analysis have been deposited to in iTOL database and are freely available at <http://itol.embl.de/shared/druzhininaetal>.

1 Microbiology and Applied Genomics Group, Research Area Biochemical Technology, Institute of Chemical, Environmental & Bioscience Engineering, TU Wien, Vienna, Austria, **2** Jiangsu Provincial Key Lab of Organic Solid Waste Utilization, Nanjing Agricultural University, Nanjing, China, **3** Environmental and Life Sciences, Universiti Brunei Darussalam, Bandar Seri Begawan, Brunei Darussalam, **4** Architecture et Fonction des Macromolécules Biologiques, CNRS, Aix-Marseille Université, Marseille, France, **5** INRA, USC 1408 AFMB, Marseille, France, **6** Department of Biological Sciences, King Abdulaziz University, Jeddah, Saudi Arabia, **7** US Department of Energy Joint Genome Institute, Walnut Creek, CA, United States of America, **8** Department of Plant and Microbial Biology, University of California Berkeley, Berkeley, CA, United States of America

aa Current address: University of Natural Resources and Life Sciences–BOKU, Institute of Food Technology, Vienna, Austria

ab Current address: Vienna, Austria

* irina.druzhinina@tuwien.ac.at (ISD); qirongshen@njau.edu.cn (QS)

Abstract

Unlike most other fungi, molds of the genus *Trichoderma* (Hypocreales, Ascomycota) are aggressive parasites of other fungi and efficient decomposers of plant biomass. Although nutritional shifts are common among hypocrealean fungi, there are no examples of such broad substrate versatility as that observed in *Trichoderma*. A phylogenomic analysis of 23 hypocrealean fungi (including nine *Trichoderma* spp. and the related *Escovopsis weberi*) revealed that the genus *Trichoderma* has evolved from an ancestor with limited cellulolytic capability that fed on either fungi or arthropods. The evolutionary analysis of *Trichoderma* genes encoding plant cell wall-degrading carbohydrate-active enzymes and auxiliary proteins (pcwdCAZome, 122 gene families) based on a gene tree / species tree reconciliation demonstrated that the formation of the genus was accompanied by an unprecedented extent of lateral gene transfer (LGT). Nearly one-half of the genes in *Trichoderma* pcwdCAZome (41%) were obtained via LGT from plant-associated filamentous fungi belonging to different classes of Ascomycota, while no LGT was observed from other potential donors. In addition to the ability to feed on unrelated fungi (such as Basidiomycota), we also showed that *Trichoderma* is capable of endoparasitism on a broad range of Ascomycota, including extant LGT donors. This phenomenon was not observed in *E. weberi* and rarely in other mycoparasitic hypocrealean fungi. Thus, our study suggests that LGT is linked to the ability

Funding: The work in TU Wien was supported by the Austrian Science Fund (FWF): project number P 25613 B20 to ISD and partially by WWTF-LS13-048 to ISD. The work conducted by the U.S. Department of Energy Joint Genome Institute, a DOE Office of Science User Facility, was supported by the Office of Science of the U.S. Department of Energy under Contract No. DE-AC02-05CH11231. The work performed by the Nanjing Agricultural University, China, was supported by the National Natural Science Foundation of China (31330069), and Chinese Ministry of Science and Technology (973 Program, 2015CB150500). BH gratefully acknowledges funding from IDEX Aix-Marseille (Grant Microbio-E, 2015-2017). The field work in a frame of WWTF-LS13-048 project was performed at Kuala Belalong Field Studies Centre with kind assistance of Universiti Brunei Darussalam, Brunei Darussalam. The funders had no role in study design, data collection and analysis, decision to publish, or preparation of the manuscript.

Competing interests: The authors have declared that no competing interests exist.

of *Trichoderma* to parasitize taxonomically related fungi (up to adelphoparasitism in strict sense). This may have allowed primarily mycotrophic *Trichoderma* fungi to evolve into decomposers of plant biomass.

Author summary

Individual fungi rely on particular host organisms or substrates for their nutrition. Therefore, the genomes of fungi feeding on plant biomass necessarily contain genes encoding plant cell wall-degrading enzymes, while animal parasites may depend on proteolytic activity. Molds in the genus *Trichoderma* (Ascomycota) display a unique nutritional versatility. They can feed on other fungi, attack animals, and degrade plant debris. The later property is so efficient that one species (*T. reesei*) is commercially used for the production of cellulolytic enzymes required for making biofuels and other industry. In this work, we have investigated the evolution of proteins required for plant cell wall degradation in nine *Trichoderma* genomes and found an unprecedented number of lateral gene transfer (LGT) events for genes encoding these enzymes. Interestingly, the transfers specifically occurred from Ascomycota molds that feed on plants. We detected no cases of LGT from other fungi (e.g., mushrooms or wood-rotting fungi from Basidiomycota) that are frequent hosts of *Trichoderma*. Therefore, we propose that LGT may be linked to the ability of *Trichoderma* to parasitize on related organisms. This is a characteristic ecological trait that distinguishes *Trichoderma* from other mycoparasitic fungi. In this report, we demonstrate that the lateral transfer of genes may result in a profound nutritional expansion and contribute to the emergence of a generalist capable of feeding on organic matter of any origin.

Introduction

Fungi are heterotrophs that live either inside or on the surface of their food. They feed by secreting cocktails of digestive enzymes that break down a diversity of biopolymers, such as cellulose, hemicellulose, lignin, chitin, lipids, and proteins. The resulting soluble products are subsequently absorbed into the fungal cells and metabolised. Many fungi form biotrophic interactions with other organisms (e.g. parasitism), while others decompose dead organic matter (polyphagy, see Supporting Information S1 Text for terminology) [1]. Similar to other heterotrophs, individual fungi usually rely on particular host organisms or substrates for their nutrition. This is reflected in the diverse composition of their genetically encoded digestive enzymes. Thus, fungi feeding on plant biomass (phytophags and plant parasites; Supporting Information S1 Text) use mainly lignocellulolytic enzymes [2, 3], while animal pathogens deploy proteolytic activities for this purpose [3].

Fungi of the genus *Trichoderma* (Hypocreales, Pezizomycotina, Ascomycota) display a unique nutritional versatility (Supporting Information S1 Text) as they can form biotrophic interactions with fungi (mycoparasites [4]), animals (opportunistic parasites of immunocompromised humans [5–7]), and plants (phytoparasites [8]). *Trichoderma* spp. can also feed on dead fungi (mycophagy) and efficiently degrade plant debris (phytophagy) [4]. One such species, *T. reesei*, is commercially used for the production of cellulolytic enzymes required to produce biofuels [9–11]. Other *Trichoderma* spp. are used to develop biofungicides, an attractive alternative and supplement to chemical pesticides [12]. Although the two nutritional strategies

(feeding on plant biomass and on fungi) were initially attributed to different species, ecophysiological studies have shown that all *Trichoderma* species are efficient mycoparasites, including *T. reesei* [1, 4, 13–15]. Many species possess high cellulolytic activity [16–18] and/or are symptomless parasites of plants (endophytes) [19]. A brief review of the nutritional versatility of *Trichoderma* spp. is given in Supporting Information S1 Text. Genus-wide studies of the nutritional traits of *Trichoderma* have revealed that shifts from ancestral mycoparasitism to phytophagy and back again occurred several times during *Trichoderma* evolution [16]. The best available explanation for such inter-kingdom (fungi <-> plants) nutritional jumps is the host-habitat hypothesis [20], which posits that sympatric cohabitation increases the chance of host/substrate shifts. For *Trichoderma*, a widely accepted theory proposes that ancestral species could parasitize fungal hyphae growing in decaying wood and, thus have evolved the ability to degrade plant biomass [21]. However, the mechanisms underpinning this transition are not known. Interestingly, the genome analysis of another mycoparasitic hypocrealean fungus, *Escovopsis weberi*, (which feeds on cellulolytic fungal gardens of leaf-cutting ants and therefore lives in proximity to lignocellulose) did not reveal any enrichment for genes encoding cellulases and xylanases [22]. This finding challenges the host-habitat hypothesis and shows that parasitism on a lignocellulolytic host does not necessarily result in an enhancement of lignocellulolytic machinery.

To understand the evolutionary mechanisms that lead *Trichoderma* to grow on plant biomass and, thereby expand its nutritional range, we performed a phylogenetic analysis of the plant cell wall-degrading carbohydrate-active enzymes and auxiliary proteins encoded in the genomes of nine species of *Trichoderma* that are members of three major infrageneric clades [23] plus twelve other Hypocreales fungi. Our gene tree / species tree reconciliation analysis revealed massive lateral transfer of genes (LGT) encoding plant cell wall-degrading enzymes to *Trichoderma* from plant-associated Ascomycota hosts. The results suggest that LGT from other ascomycetes was likely facilitated by expansion of *Trichoderma* mycoparasitic host range to these fungi, and this genetic phenomenon has been an important event in the evolution of this trait.

Results

All *Trichoderma* spp. can feed on plant and fungal biomass

To assess *Trichoderma* nutritional preferences with respect to plant and fungal biomass, we compared nine species belonging to the three major infrageneric groups (*T. reesei*, *T. parareesei*, *T. longibrachiatum* and *T. citrinoviride* from section *Longibrachiatum*; *T. harzianum*, *T. guizhouense*, *T. virens* from section *Pachybasium*; and *T. atroviride* and *T. asperellum* from section *Trichoderma*, Supporting Information S1 Table) with mycoparasitic *E. weberi* (Hypocreales, Ascomycota) and the cellulolytic and endophytic *Pestalotiopsis fici* (Xylariales, Ascomycota [24]). To approximate conditions in nature, we used (i) cell walls of fungus *Ganoderma lucidum* (Polyporales, Basidiomycota) and (ii) epiphyte-free dried leaves and biologically pre-degraded wood for the species *Shorea johorensis* (Dipterocarpaceae, Plantae). *G. lucidum* and *S. johorensis* were selected as sources of biomass because of the tropical occurrence of *T. reesei*, *E. weberi*, and *P. fici*, while other fungi were considered cosmopolitan. Also, we tested a diversity of plant-related substrates, such as coniferous commercial wood, microcrystalline cellulose, wheat straw, and pectin (Supporting Information S1 Fig). All fungi grew well on the cell walls of *G. lucidum*. Aside from this substrate, *E. weberi* only formed a small amount of biomass on leaves. *Trichoderma* spp. and *P. fici* grew equally well on all substrates that consisted of plant biomass. In general, the nine *Trichoderma* spp. showed remarkable

similarities in their ability to feed on plant biomass. In contrast, *E. weberi* did not exhibit this nutritional versatility.

***Trichoderma* and *Escovopsis* form a monophyletic clade and share a common ancestor with entomoparasitic fungi**

Considering the abundance of plant-associated fungi in the order Hypocreales, we hypothesized that the phytophagy of *Trichoderma* was maintained during its evolution, whereas *E. weberi* may have lost this ability over the course of its specialization that allowed it to parasitize on Agaricales mushrooms cultivated by ants [22]. To test this hypothesis, we reconstructed the evolutionary history of *Trichoderma*. We used 21 whole-genome sequences for fungi of the order Hypocreales, including *E. weberi* [22], five newly sequenced genomes of *Trichoderma* (*T. longibrachiatum*, *T. citrinoviride*, *T. harzianum*, *T. guizhouense*, and *T. asperellum*), and previously published genomes of *T. reesei* [25], *T. virens* [26], *T. atroviride* [26], and *T. parareesei* [27] (Supporting Information S1 Table). We selected 100 orthologous, neutrally evolving, unlinked genes encoding proteins required for a diversity of cellular functions (Supporting Information S2 Table). We reconstructed their individual phylogenies based on both nucleotide and amino acid sequences (Data deposited at <http://itol.embl.de/shared/druzhininaetal>). Each gene was tested for a neutral evolution using Tajima's D test (Supporting Information S2 Table) and concatenated into an alignment of 47,726 amino acids in length (Supporting Information S2 Table). The details of the phylogenetic analyses are given in Supporting Information S2 Table. This analysis revealed that the monophyletic family Hypocreaceae, represented here by the *Escovopsis* and *Trichoderma* genera, shared a last common ancestor with fungi from the families Cordycipitaceae, Ophiocordycipitaceae, and Clavicipitaceae, which are dominated by extant entomoparasitic fungi (Fig 1A). The branch leading to the plant-associated Nectriaceae family diverged earlier in the course of the evolution of the Hypocreales.

The *Trichoderma* pcwdCAZome is distinct from that of other hypocrealean fungi

The evolutionary history of *Trichoderma* explains its ability to efficiently derive nutrition from living and dead fungi ([4], see above) and its interactions with animals [4]. If the ability of *Trichoderma* to degrade plant biomass was inherited via vertical gene transfer, its phytophagy should resemble that of other Hypocreales fungi, especially those of the phytoparasitic family Nectriaceae. To test this, we identified all genes of the nine *Trichoderma* species that encode carbohydrate-active enzymes (CAZome, as defined at <http://www.cazy.org/Genomes.html>) in *Trichoderma* and selected those that are known to be involved in the plant cell wall degradation (pcwdCAZome). We retrieved proteins from all glycoside hydrolase (GH) families, which are active in hydrolysis of cellulose, the xylan backbone, other hemicelluloses and hemicellulose side chains, and pectin and its side chains. This search resulted in a total of 32 GH families. The PL1 family of pectate lyases and two accessory protein families (the AA9 lytic polysaccharide monoxygenases and the expansin-like protein swollenin) were included comprising a total of 746 proteins from the nine *Trichoderma* spp. genomes (Supporting Information S3 Table).

For this comparison, we counted genes encoding enzymes for 29 of the GH families in other Hypocreales genomes [22, 28–36] (Supporting Information S3 Table). The unrelated polyphagous fungi, *Neurospora crassa* [37] and *Chaetomium globosum* [38] (both Sordariales, Ascomycota), were used as outgroups. A comparative analysis of these fungi showed that the pcwdCAZomes of phytoparasitic *Fusarium* and *Nectria* spp. are significantly larger than those of the entomoparasitic and mycoparasitic lineages, including *Trichoderma*. However, the cluster analysis revealed similarities between the pcwdCAZome composition of the mycoparasitic

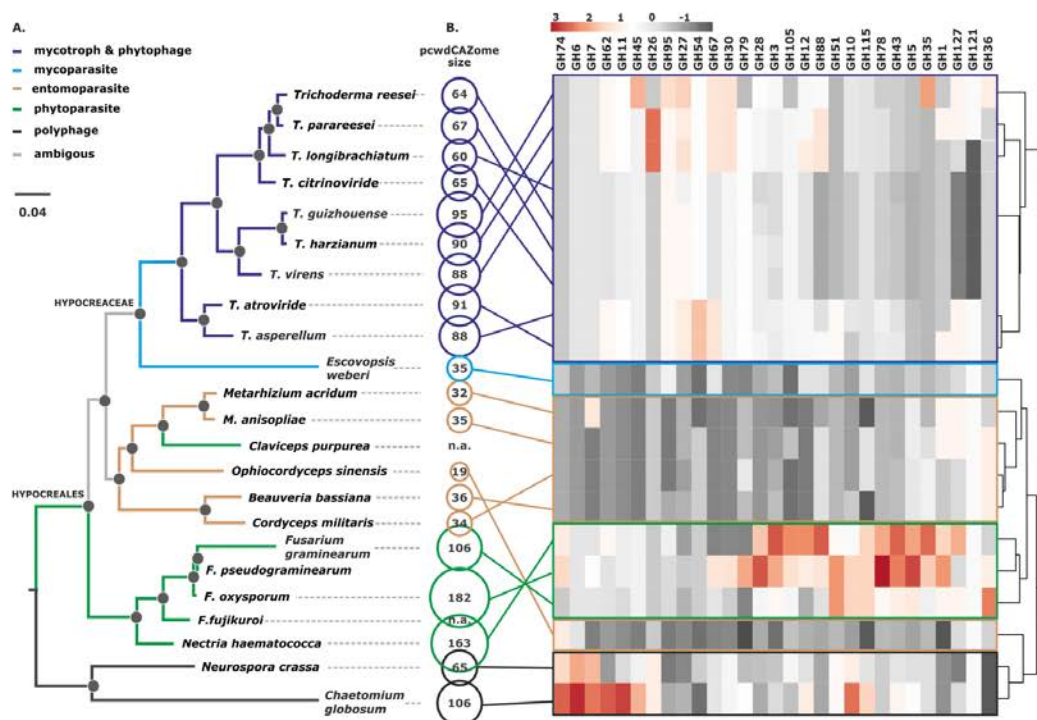


Fig 1. Phylogeny of Hypocreales and the composition of their pcwdCAZomes. A. Bayesian phylogram obtained based on the curated concatenated alignments of 100 orthologous neutrally evolving proteins of Hypocreales and two other Sordariomycetes. Black dots above nodes indicate posterior probability support > 0.95. The colors of the branches indicate the major nutritional strategy in the group (see insert) as described in Supporting Information S1 Text. B. The size of each pcwdCAZome per species is shown as a circle; n.a. means not available. The heat map shows the gene number for each GH family in the Hypocreales fungi examined; cluster analysis was performed with Euclidian distance and complete linkage for rows. The corresponding data matrix is presented in Supporting Information S3 Table. GH indicates glycosyl hydrolase family.

<https://doi.org/10.1371/journal.pgen.1007322.g001>

E. weberi and that of the entomoparasites, but not that of *Trichoderma* (Fig 1B). The latter genus possessed a pcwdCAZome that was more than twice as large as that of *E. weberi*. A principal component analysis (Fig 2) separated the pcwdCAZomes of *Trichoderma* spp. from those of *E. weberi* and the entomoparasites. Interestingly, the pcwdCAZomes were also separated from the phytoparasitic Nectriaceae. The *Trichoderma* pcwdCAZome exhibited closest similarity to the taxonomically distant fungi *N. crassa* and *C. globosum*. These data, therefore, do not support the hypothesis that the composition of *Trichoderma* pcwdCAZome is the ancestral state. Instead, it is likely the evolutionarily derived state.

Evolution of the *Trichoderma* pcwdCAZome

To trace back the evolution of the *Trichoderma* pcwdCAZome, we collected the respective protein sequences encoded in all nine genomes and individually subjected each GH family (as well as PL1, AA9, and swollenin) to phylogenetic analysis. This examination revealed a total of

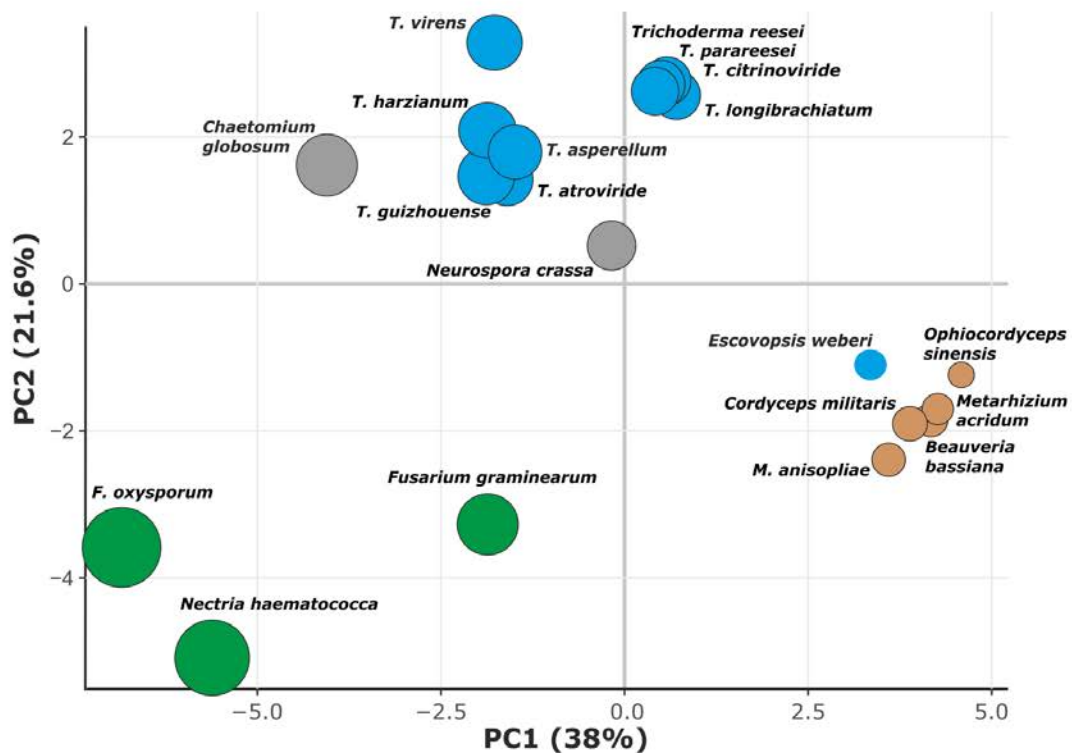


Fig 2. Principal component analysis based on the diversity of Hypocreales genes in GH families involved in plant cell wall degradation. Size of the dot corresponds to the total size of pcwdCAZome as shown in Fig 1B. Brown, blue, and green colors indicate parasitism on insects, fungi, and plants, respectively. Saprootrophic fungi are shown in grey.

<https://doi.org/10.1371/journal.pgen.1007322.g002>

122 distinct phylogenetic groups of orthologous proteins (Supporting Information S3 Table). 61 were present in all nine species, fifty only in one or two *Trichoderma* sections, and 11 occurred only in a single species: four in *T. virens*, four in *T. atroviride*, two in *T. asperellum* and one in *T. harzianum*; no orphan pcwdCAZymes were found in species from the section *Longibrachiatum*. The largest pcwdCAZomes, possessing 91–99 proteins per species, were observed in the sections *Pachybasium* and *Trichoderma*, while genomes in the section *Longibrachiatum* encoded only 66–70 such proteins. These variable sizes of the pcwdCAZome were proportional to the changes in the total number of genes in their genomes, yielding a constant value of 0.6–0.8%. Thus, none of the nine *Trichoderma* spp. are therefore specifically enriched in genes required for plant cell wall degradation, which corresponds to a similar ecophysiology for these species (see above). Three GH families (GH26 β -D-mannanases, GH51 α -L-arabinofuranosidase, and GH121 β -L-arabinobiosidase) were absent from the section *Longibrachiatum*. The highest diversity and quantity of respective proteins within *Trichoderma* were found in the GH3 (β -glycosidase), GH27 (α -D-galactosidase), GH43 (α -L-arabinofuranosidase and β -xylosidase), and GH28 (polygalacturonases) families (Supporting Information S3 Table).

Representative sequences of each of the 122 phylogenetic groups (see above) were used as queries in a sequence similarity search in the NCBI Genbank database using the Blastp algorithm (see [Materials and Methods](#) for details). The hits with high sequence similarity (see description in [Materials and Methods](#)) were combined with the corresponding *Trichoderma* sequences from the nine species and subjected to phylogenetic analysis (Supporting Information S3 Table). When the topologies of the resulting 45 trees (Supporting Information S2 Fig) were compared to the phylogeny of *Trichoderma* (see Fig 1A for Hypocreales and Fitzpatrick et al. [39] for Ascomycota), only 29 (24%) of the 122 phylogenetic groups of *Trichoderma* pcwdCAZymes occurred at positions that were concordant with it (for example, GH36 in Fig 3). Among them, 16 were also present in the mycoparasitic fungus *E. weberi*. Thirteen phylogenetic groups of the pcwdCAZome (11%) belonged to clades that contained only *Trichoderma* proteins and, therefore, their evolutionary history remains unresolved. The phylogenetic position of the major part of pcwdCAZymes— 80 phylogenetic groups (66%)—was apparently not concordant with the evolution of the genus because these proteins shared last common ancestors with proteins of diverse Ascomycota fungi, such as phytoparasitic and phytophagous Eurotiomycetes, other Sordariomycetes, Leotiomycetes, and Dothideomycetes (for examples see Figs 4 and 5).

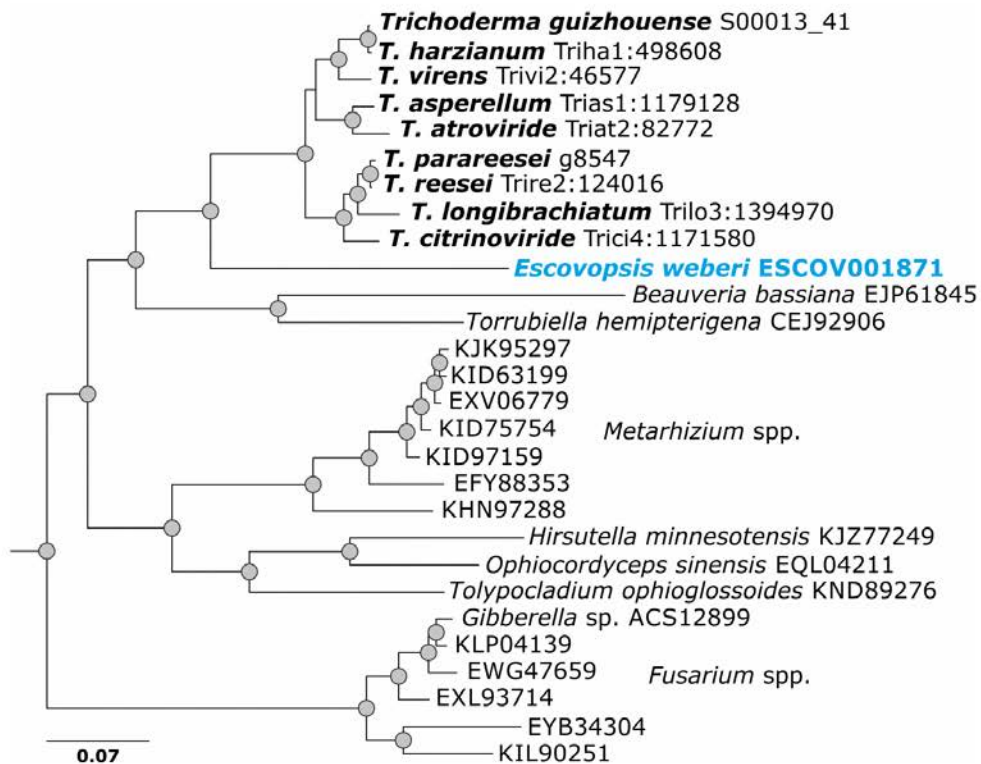


Fig 3. Evolution by vertical gene transfer of GH36 α -1,4-galactosidase Clade B (reference sequence Trire2:124016 of *T. reesei* QM 6a) in *Trichoderma*. Results for all pcwdCAZymes in *Trichoderma* are presented in Supporting Information S2 Fig.

<https://doi.org/10.1371/journal.pgen.1007322.g003>

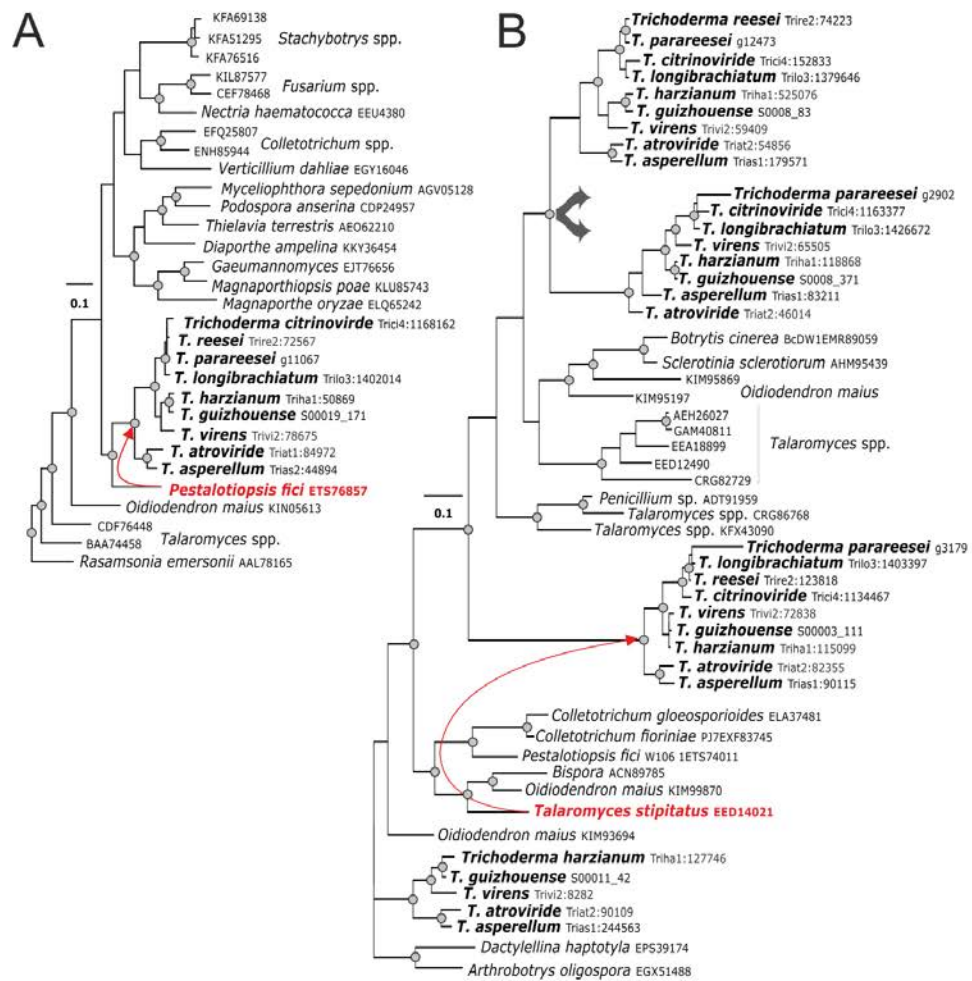


Fig 4. Evolution of selected pcdwCAZymes by putative lateral gene transfer. A. Evolution of GH6 cellobiohydrolase CEL6 (Trire2:72567) obtained by LGT from *Pestalotiopsis fici*. B. The GH11 endo- β -1,4-xylanase gene (Trire2:74223) and its duplicated copies, which have incongruent tree topologies compared to the phylogenomic tree (see Fig 1A). *Talaromyces stipitatus* (Eurotiales) was confirmed to be an LGT donor for the clade containing Trire2:123818. The phylogenetic position of the GH11 clade including *T. atroviride* Triat2:90109 is unresolved (Supporting Information S2 Fig, S4 Table).

<https://doi.org/10.1371/journal.pgen.1007322.g004>

Nearly half of the *Trichoderma* pcdwCAZome was obtained via LGT from lignocellulolytic Pezizomycotina fungi

The incongruent topologies of the phylograms of individual pcdwCAZymes (Supporting Information S2 Fig) could be the result of gene duplication (GD), gene loss, or LGT. To distinguish among these possibilities, we reconciled each protein tree for each GH/AA9/PL1 family

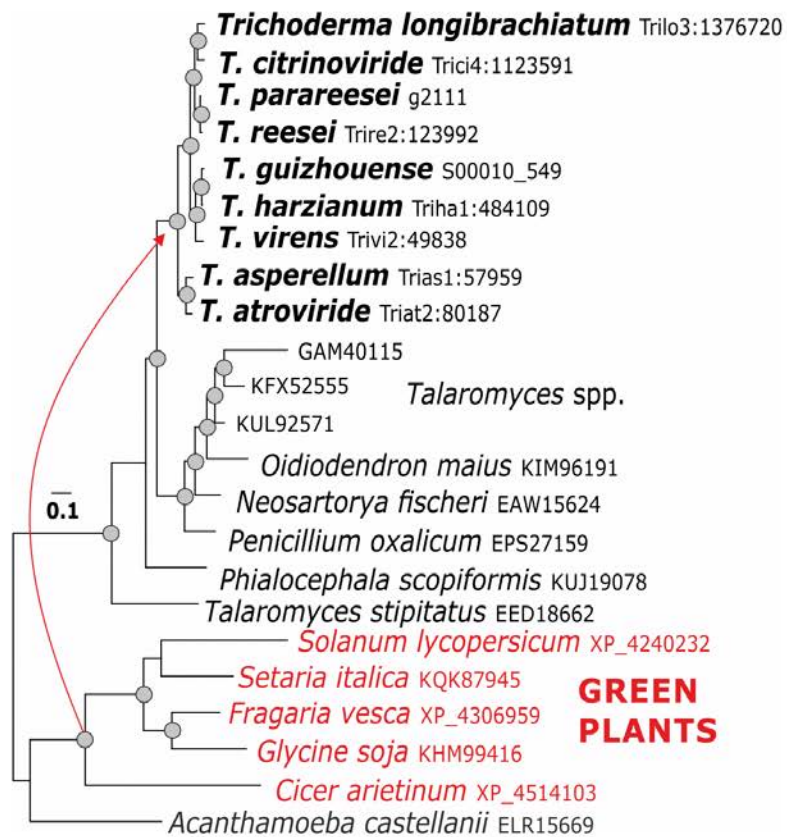


Fig 5. Evolution of swollenin in *Trichoderma*. The reference sequence Trire2:123992 of *T. reesei* QM 6a. Green plants have been identified as putative donors for LGT of this gene.

<https://doi.org/10.1371/journal.pgen.1007322.g005>

to the multilocus Ascomycota phylogeny shown in Fig 6 [40–42]. Using the approach of Wise-caver *et al.* [43], we assigned costs to GD, LGT and gene loss, and determined the most parsimonious combination of these three events to explain the individual pcwdCAZyme trees in view of the topology of the Ascomycota phylogeny (see Materials and Methods for details). Putative LGT events were only inferred when a CAZyme tree topology was contradictory to the Ascomycota phylogeny and could not be more parsimoniously reconciled by a combination of differential GD and gene loss. The respective NOTUNG results are given in Supporting Information S4 Table. This analysis suggested that at least 50 (41%) of the phylogenetic pcwdCAZyme groups were obtained through LGTs from other fungi (Fig 6, Supporting Information S2 Fig & S4 Table). Most frequent putative donors were fungi from the order Eurotiales (16 cases), followed by the ericoid mycorrhizal fungus *Oidiodendron maius* (Leotiomycetes) (7 cases) and five cases for each of the cellulolytic Xylariales (three from *Pestalotiopsis fici* two from *Eutypa lata*), and three *Diaporthe ampelina* (Diaporthales) (Fig 6, Supporting

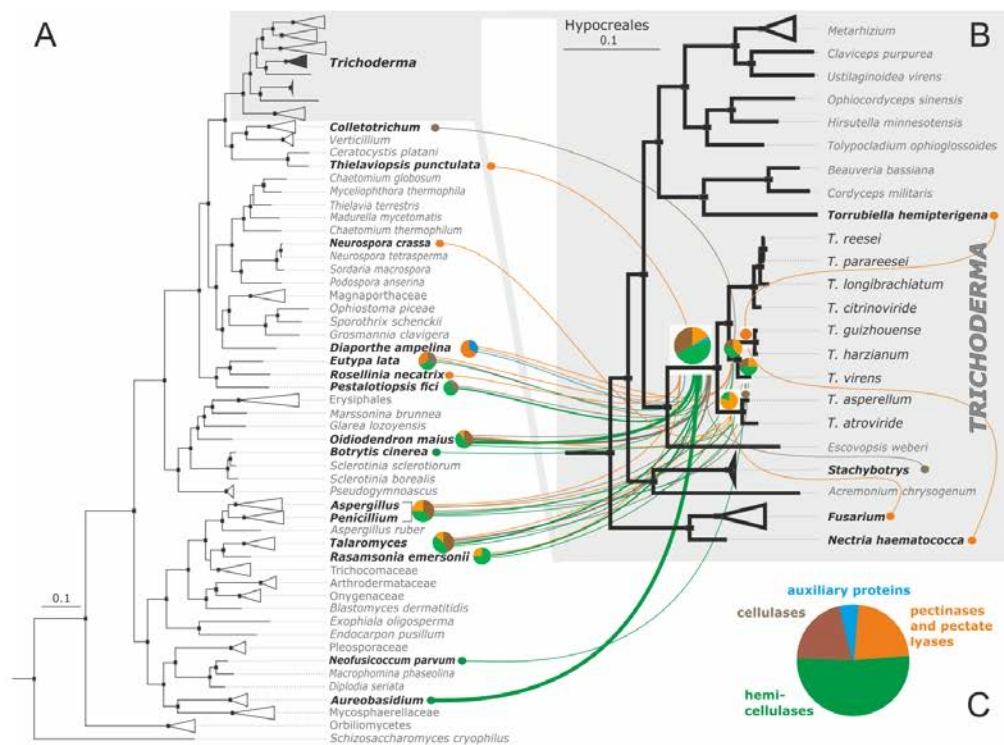


Fig 6. Evolutionary origin of *Trichoderma* pcdCAZome obtained via putative LGT from Pezizomycotina donors mapped on Bayesian multilocus phylogram. A. The multilocus Bayesian phylogram of Ascomycota. **B.** The magnified Hypocreales clade from the phylogram on A. **A & B:** Black dots above nodes indicate posterior probability > 0.99. Individual lines correspond to LGT events, and the thickness of lines is proportional to the number of genes obtained from this donor. Statistically confirmed donor fungi are shown in bold. Colors correspond to the major groups of proteins composing the pcdCAZome of *Trichoderma* (pie chart on C).

<https://doi.org/10.1371/journal.pgen.1007322.g006>

Information S2 Fig & S4 Table). At the class level, donor fungi from Eurotiomycetes (16) and Sordariomycetes (15) were dominant, but transfers from Leotiomycetes (7) and Dothidiomycetes (2) were also detected. For one putative LGT event, the phytoparasitic *Colletotrichum* from the order Glomerellales (which is closely related to Hypocreales) was recognized as a donor. Thus, at least four putative cases of LGT to *Trichoderma* from Hypocreales fungi *Torriellia*, *Stachybotrys*, *Fusarium*, and *Nectria*, respectively, have been detected (Fig 6, Supporting Information S2 Fig & S4 Table).

Surprisingly, no cases of LGT for pcdCAZymes from Basidiomycota (which are the most commonly observed hosts/substrates for *Trichoderma in vivo* [4]) were detected, although they were present in several of the gene trees. Also no cases of horizontal gene transfer from prokaryotes were found. In our analysis, green plants were identified as putative LGT donors of the auxiliary protein swollenin for *Trichoderma* (Fig 5).

We also found three cases where LGT putatively occurred before the diversification of *Trichoderma* and *Escovopsis*, i.e. the major cellulase of *Trichoderma* (GH7; cellobiohydrolase

CEL7A = CBH1), the GH 5 Endo- β -1,4-mannase and the pectate lyase PL1 (Supporting Information S2 Fig and S4 Table). The majority of genes obtained through LGT are present in all nine *Trichoderma* species and absent in *E. weberi*. Some pcwdCAZome genes are only present in sections of *Pachybasium* and *Trichoderma*, but not in the section *Longibrachiatum*.

Members of four GH families (GH6, GH26, GH51, and GH62) seem to have entirely derived from LGT events (Fig 7), which correlates with the fact that these families are absent in the entomoparasitic Hypocreales species (Fig 1B). Twelve gene families exhibited a mosaic of vertical and lateral origin (Fig 7). In these, families with the highest proportion of LGT included the GH27 α -D-galactosidases, GH78 α -L-rhamnosidase, and GH95 α -D-fucosidases. Again, these are GH families that are absent from the entomoparasitic Hypocreales (Supporting Information S3 Table).

Twelve cases of putative gene duplications resulting in 24 genes were found, which comprised some cellulase (GH5, GH12, GH45), xylanase (GH10, GH11), and hemicellulase families (GH5 β -mannanases, GH26, three in GH27 α -D-galactosidases, GH95 α -D-fucosidases, and GH28 exo-xylogalacturan hydrolases) (Supporting Information S2 Fig & S4 Table). Interestingly, many of them were present only in strains of section *Pachybasium* and *Trichoderma*, and in a few cases even only in a single species.

On a balance, considering the 29 vertically transmitted phylogenetic groups of pcwdCAZymes (including five gene duplication events that affected 10 of these genes), and the 50 phylogenetic groups that have been derived by LGT (among which 10 arose by five gene duplication events after a LGT event), we could putatively identify the evolutionary pattern of 79 phylogenetic groups (65%) of the *Trichoderma* pcwdCAZome. From the remaining 43 phylogenetic groups of pcwdCAZymes (35%) three also seem to have originated by LGT in the common ancestor of *Trichoderma* and *Escovopsis* (CEL7A, and GH5 Endo- β -1,4-mannase, and PL1 Supporting Information S2 Fig), thirteen (11%) formed isolated branches in the phylogenetic trees, and their origin cannot be determined. The remaining 28 (23%) phylogenetic groups of pcwdCAZymes exhibited tree topologies that were in conflict with the species tree, but not supported by NOTUNG analysis. Four of these genes (GH5) evolved by gene duplication (Supporting Information S2 Fig, S4 Table).

We also wondered whether any of the known regulatory proteins of *Trichoderma* pcwdCAZyme gene transcription (such as XYR1, ACE2, and ACE3) [4] would have been acquired via LGT. However, our results suggest that these genes evolved by vertical gene transfer and are present in non-lignocellulolytic entomoparasites and the mycoparasitic *E. weberi* (Supporting Information S2 Fig & S4 Table).

Because of the surprisingly large incidence of LGTs in the *Trichoderma* pcwdCAZome, we also tested whether other protein families would display such a high rate of LGT. To this end, we used a different approach: we screened the core genome of *Trichoderma* (consisting of about 7,000 orthologous genes that are shared among all *Trichoderma* spp. for which the genome sequences are available), but that are absent from genomes of *E. weberi* and other Hypocreales. This screen did not include the pcwdCAZyme encoding genes. This led to the identification of 738 genes, for which 123 genes had the nearest neighbors in blastp in Eurotiomycetes and various orders of Sordariomycetes that are taxonomically distant to *Trichoderma*. We emphasize that while these genes could have potentially been acquired by LGT—this conclusion is merely based on blastp the actual number of those genes actually derived by LGT is therefore most certainly smaller and in any case only speculative. However, it may constitute an upper limit of potential LGT events. Functional analysis showed that most of them encoded uncharacterized short-chain dehydrogenases and Zn₂/Cys₆ transcriptional regulators (Supporting Information S4 Table). Interestingly, we again could not detect basidiomycetes as putative donors of any of these genes. Cumulatively, this number of genes (123, see above) that

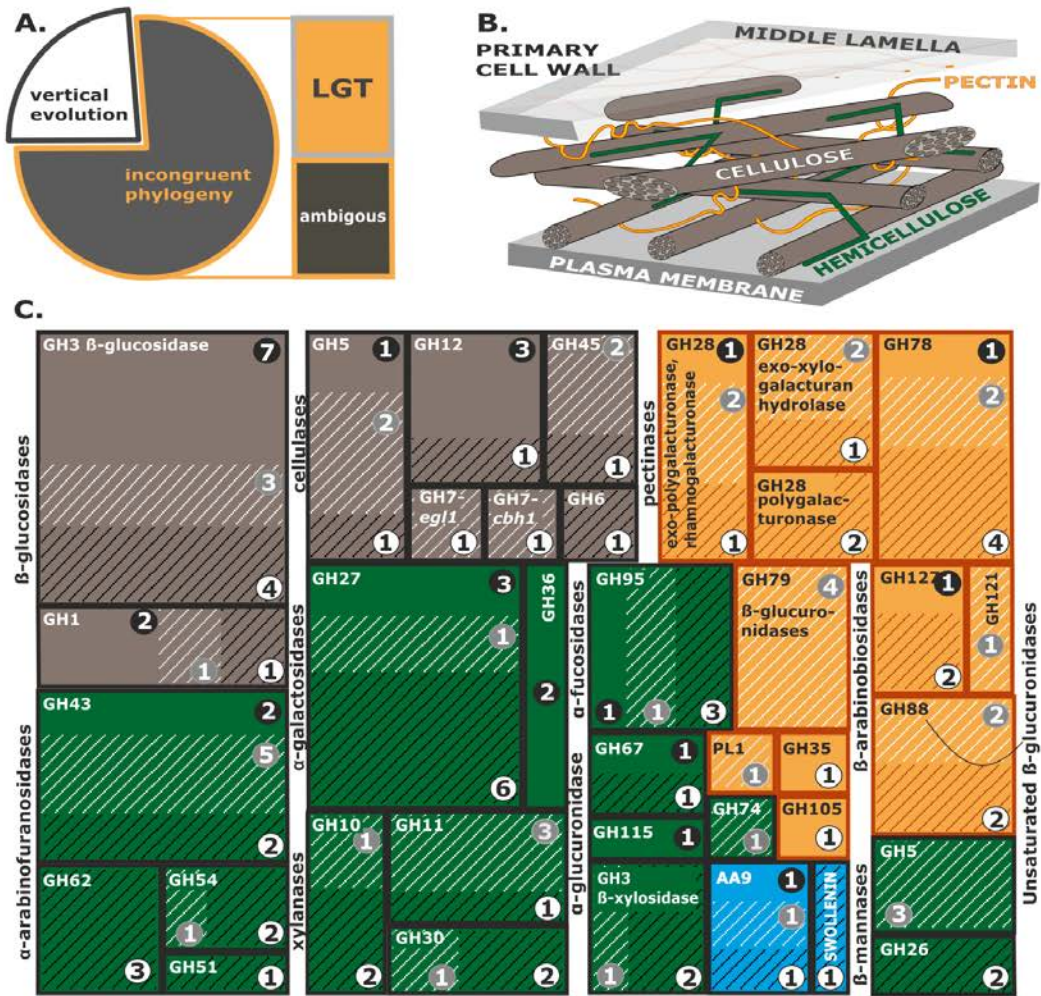


Fig 7. Composition and origin of the pcdwCAZome of *Trichoderma* based upon nine genomes. A. Summary of the evolutionary analysis and tests for LGT of individual proteins in *Trichoderma* pcdwCAZomes (N = 122) presented in Supporting Information S3 Table–S4 Table, S2 Fig. B. Schematic drawing of the primary plant cell wall. Cellulose, hemicellulose, and pectin are colored brown, green, and orange, respectively. C. The diversity and evolution of individual groups of *Trichoderma* pcdwCAZome. Brown, green, and orange rectangles correspond to enzymes involved in the degradation of cellulose, hemicellulose, and pectin, respectively. See B for the legend. Auxiliary proteins are shown in blue. Dark-shaded lines correspond to genes obtained through putative LGT, while light-shaded lines indicate additional cases of incongruent phylogeny and/or insufficient data. Numbers on white, black, or grey backgrounds correspond to the maximum total numbers of genes in each family that evolved through LGT, vertical evolution, or unknown mechanisms, respectively.

<https://doi.org/10.1371/journal.pgen.1007322.g007>

could putatively have been obtained by LGT approximates only amount 1% of an average *Trichoderma* genome. It is in agreement with published estimations of 0.1–2.8% of LGT-derived

genes for fungi [43] and significantly lower than that for pcwdCAZyme genes as reported in this paper.

LGT events are not reflected in the clustering of pcwdCAZymes in *Trichoderma* genomes

LGT has frequently been shown to involve the transfer of large genomic fragments containing several genes [43]. Since a third of the *T. reesei* pcwdCAZome occurs in 20 discrete, loose clusters [25, 44], we tested whether these clusters are the consequence of LGT. An analysis of the synteny of the chromosomal loci of the above clusters in *T. reesei* with that in the other *Trichoderma* spp. showed that the clusters were highly syntenic (>80% of all gene positions were conserved), and this pattern was independent of their chromosomal location [45]. Thirty-three of the pcwdCAZymes of *T. reesei* were organized into a total of 16 clusters (Supporting Information S5 Table), but only 13 of these pcwdCAZyme genes had been acquired by LGT. In addition, the pcwdCAZyme genes in individual clusters were obtained from different donors. Therefore, we reject the hypothesis that the LGT-derived genes may have given rise to the origin of the CAZyme clusters proposed for *Trichoderma* [25].

Alloparasitism of *Trichoderma* is complemented by parasitism on closely related Pezizomycotina, including adelphoparasitism on Hypocreales

Our analysis showed that *Trichoderma* phytophagy is indeed an apomorphic character that did not result from the convergent evolution of individual species or clades. Instead, it was obtained over the course of evolution through incidence of large-scale LGT. Putative donors include phytoparasitic fungi phylogenetically close to *Trichoderma* and possibly even neighboring groups. Interfungal interactions between *Trichoderma* and filamentous Ascomycota are rarely observed in nature [4]. However, the successful application of *Trichoderma*-based biofungicides against plant-pathogenic Ascomycota and respective studies of the roles of individual genes in mycoparasitism [46–55] support the hypothesis that such interactions take place alongside alloparasitism (parasitism on unrelated hosts) on Basidiomycota.

The possible cellular mechanisms for the uptake and incorporation of foreign DNA by fungi include conjugation, viral transduction, and conidial and hyphal fusion [56]. Although LGT between eukaryotes with cell walls has rarely been reported [57, 58], mycoparasitism has been viewed as a possible mechanism that could be linked to it [55, 59].

All fungi from the Hypocreaceae family are known to be aggressive alloparasites and they are common on sporocarps of Basidiomycota fungi *in situ* [4] (Fig 8A), *Trichoderma* spp. are effective against phytoparasites from Basidiomycota (for example [15, 26]), and the cause of the green mold disease on mushroom farms [60, 61]. In dual confrontation assays with colonies of *Lentinula edodes* (Agaricales, Basidiomycota), all *Trichoderma* spp. were able to parasitize this host, while *E. weberi* showed neither parasitism nor antagonistic reactions (Supporting Information S3 Fig). Similarly, all *Trichoderma* species were substantially more aggressive compared to *E. weberi* when confronted with its host fungus *Leucoagaricus gongylophorus* (Agaricales, Basidiomycota) (Supporting Information S3 Fig).

The evolutionary analysis of the pcwdCAZome of *Trichoderma* revealed LGT biased towards relatively close fungi (filamentous Pezizomycotina, Ascomycota). This selectivity could be explained by the ability of *Trichoderma* to parasitize Ascomycota fungi, which, in turn, is considered to be the major trait that sets *Trichoderma* apart from the other mycoparasitic Hypocreaceae fungi, such as *Escovopsis*, *Hypomyces*, and *Sphaerostilbella*, which parasitize Basidiomycota [16]. To test this hypothesis, we investigated the interactions of *Trichoderma* spp. with several model phytoparasitic Ascomycota. Scanning electron microscopy revealed

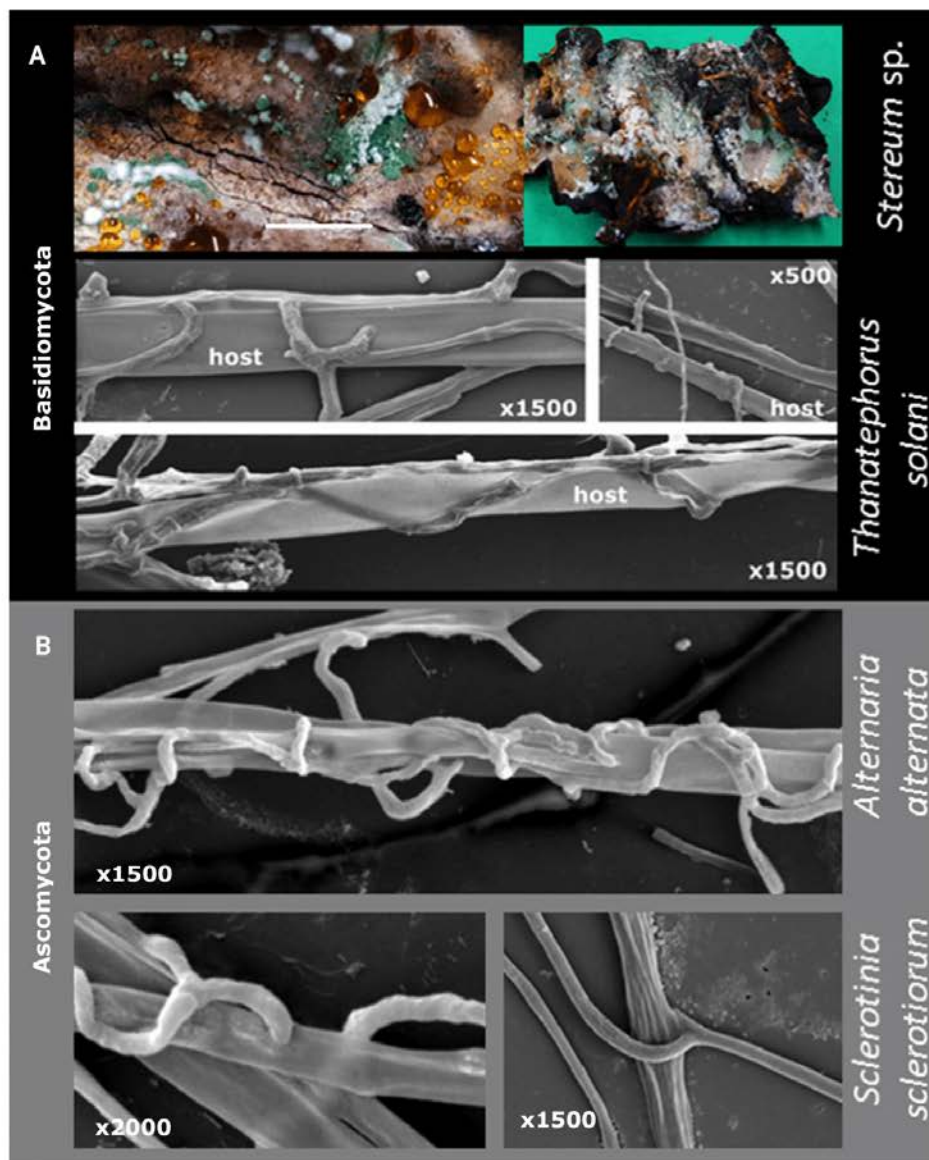


Fig 8. Mycoparasitism of *Trichoderma* on Basidiomycota (A) and Ascomycota (B). Macrophotography for A shows *T. simmonsii* TUCIM 6527 on *Stereum* sp. Bar indicates 1 cm. SEM images show hyphae of *T. guizhouense* NJAU 4742 on three hosts.

<https://doi.org/10.1371/journal.pgen.1007322.g008>

similar interactions between *Trichoderma* hyphae and Basidiomycota (*Thanatephorus solani* [syn. *Rhizoctonia solani*, Cantharellales]) and Ascomycota hosts (Fig 8B), which include chasing, coilings, and penetration of the host hyphae.

We investigated interactions between *T. reesei* and the lignocellulolytic *P. fici* [24], which was several times identified as one of the putative LGT donors (Fig 6). *P. fici* was also selected because it has been isolated from the same ecosystem where *T. reesei* is common (the phyllosphere of *Shorea* sp., Borneo) and it has comparable growth rates *in vitro* (Supporting Information S1 Fig). In dual confrontation assays on agar plates, *T. reesei* overgrew a colony of *P. fici*, but did not kill it (Fig 9A). Microscopic examination revealed a tight association between the hyphae, suggesting endoparasitism of *P. fici* by *T. reesei* (Fig 9B). Confocal microscopy revealed that cords of *P. fici* hyphae were penetrated and colonized by the thinner hyphae of *T. reesei* (Fig 9C). This experiment shows that *Trichoderma* hyphae can grow inside hyphae of at least some extant putative Ascomycota donors. Dual confrontation assays with a set of randomly selected Eurotiales fungi showed that *Trichoderma* is capable of attacking these fungi as well (Supporting Information S3 Fig). However, endoparasitism was not observed, possibly because the hyphae of the tested Eurotiales fungi were comparable in size with *Trichoderma* spp., making internal penetration difficult.

A surprising finding of this study was the detection of four cases of LGT of cellulolytic enzymes from other Hypocreales. Interestingly, *Trichoderma* is also capable of parasitizing fungi belonging to its very close phylogenetic neighbors (adelphoparasitism [62]), including *Fusarium* [55, 63]. To investigate the range of *Trichoderma* adelphoparasitism, we confronted different *Trichoderma* strains with fungi from the same genus, family, and order (Fig 10). The microscopic study revealed numerous cases of hyphal fusion that may be linked to self/non-self-recognition mechanisms in *Trichoderma* species and only in part to parasitism. Therefore, evidence for adelphoparasitism was only accepted when one colony overgrew the other. Our results showed that *T. harzianum* might attack its sister species, *T. guizhouense* (Fig 10A, see Fig 1 for phylogenomics). Any of the nine *Trichoderma* species can parasitize *E. weberi* (Fig 10B for *T. atroviride*), while the latter fungus did not attack *Trichoderma*. The majority of *Trichoderma* strains attacked and/or killed *Fusarium* spp. (Fig 10C) [55, 63], although individual strains of the latter host fungus resisted *Trichoderma* infections. A similar interaction was observed in a confrontation with *Emericellopsis alkalina*, which belongs to an *Acremonium* species complex in Hypocreales (Fig 10D). Our results show that all species of *Trichoderma* studied are capable of adelphoparasitism in the strictest sense of this term (parasitism on organisms belonging to the same genus or family [62]), and this property extends to interactions with other filamentous Ascomycota. Along with the unique ability to perform adelphoparasitism, *Trichoderma* maintains its allopasitotic properties (Supporting Information S3 Fig).

Discussion

LGT as an evolutionary shortcut to achieving nutritional versatility

In this work, we uncovered a possible evolutionary process that contributed to the development of the nutritional versatility of *Trichoderma*. Phylogenomic analysis showed that the genus shared a last common ancestor with entomoparasitic hypocrealean fungi (Cordycipitaceae, Ophiocordycipitaceae, and Clavicipitaceae). Since then, *Trichoderma* evolution has been directed towards mycotrophy. Although this path has also been taken by a number of other fungi of the family Hypocreaceae [20,55], *Trichoderma* is the most taxonomically diverse mycoparasitic fungus, harboring at least 260 molecularly defined species [64] found worldwide (NCBI Taxonomy browser, Nov. 2016). *Trichoderma* can also interact with animals [65],

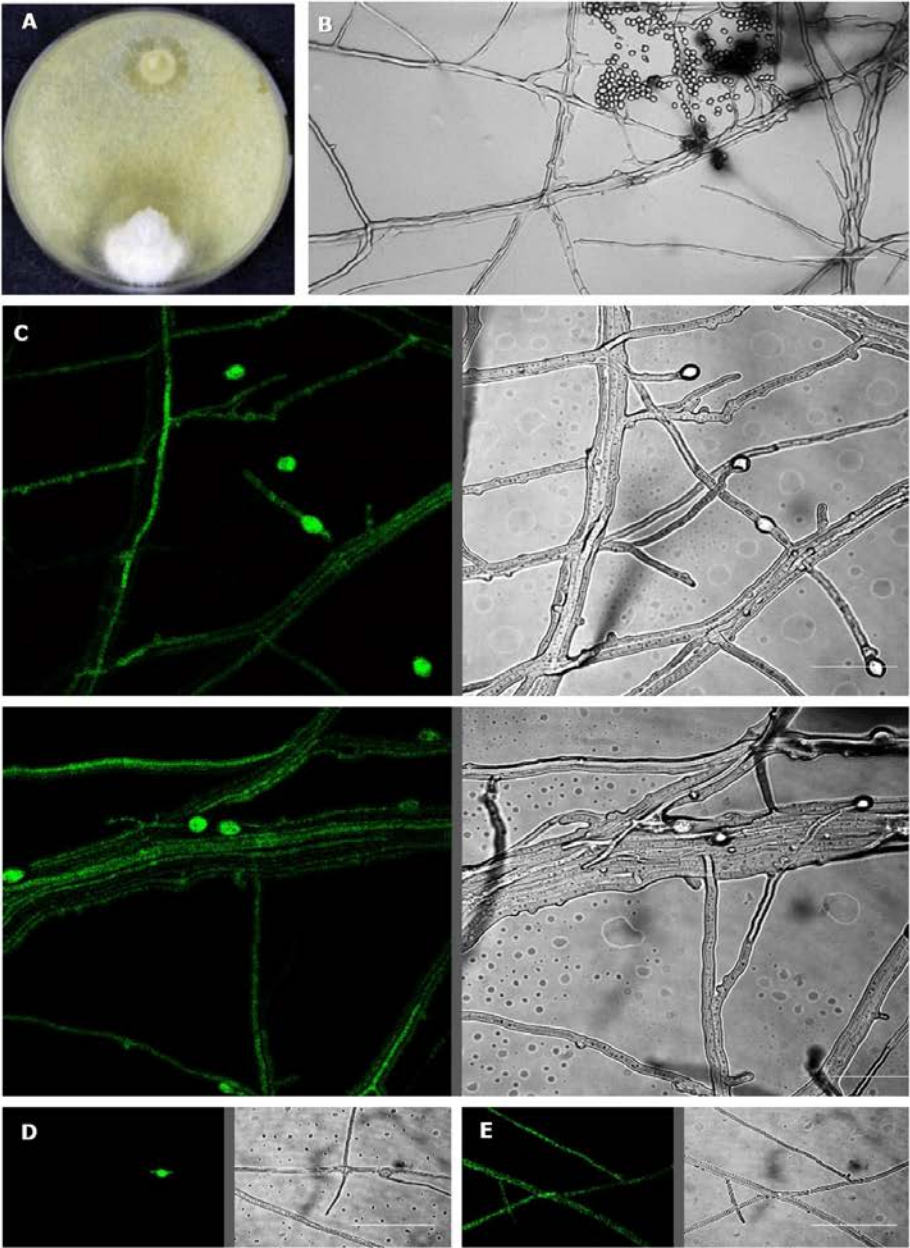


Fig 9. Mycoparasitism of GFP-labeled *T. reesei* TUCIM 4817 on *Pestalotiopsis fici* TUCIM 5788. A. Dual confrontation assay after 10 days of incubation at 28°C in darkness. B. Hyphal interactions observed using light microscopy (400x magnification). C. Confocal image showing endoparasitism of *T. reesei* on hyphae of *P. fici* on a glass slide prepared as shown in S3 Fig. D. Hyphae of *P. fici* TUCIM 5788 and a fluorescent chlamydospore of *T. reesei*. E. *T. reesei* TUCIM 4817 mycelium. Scale bar on C–E—40 μm.

<https://doi.org/10.1371/journal.pgen.1007322.g009>

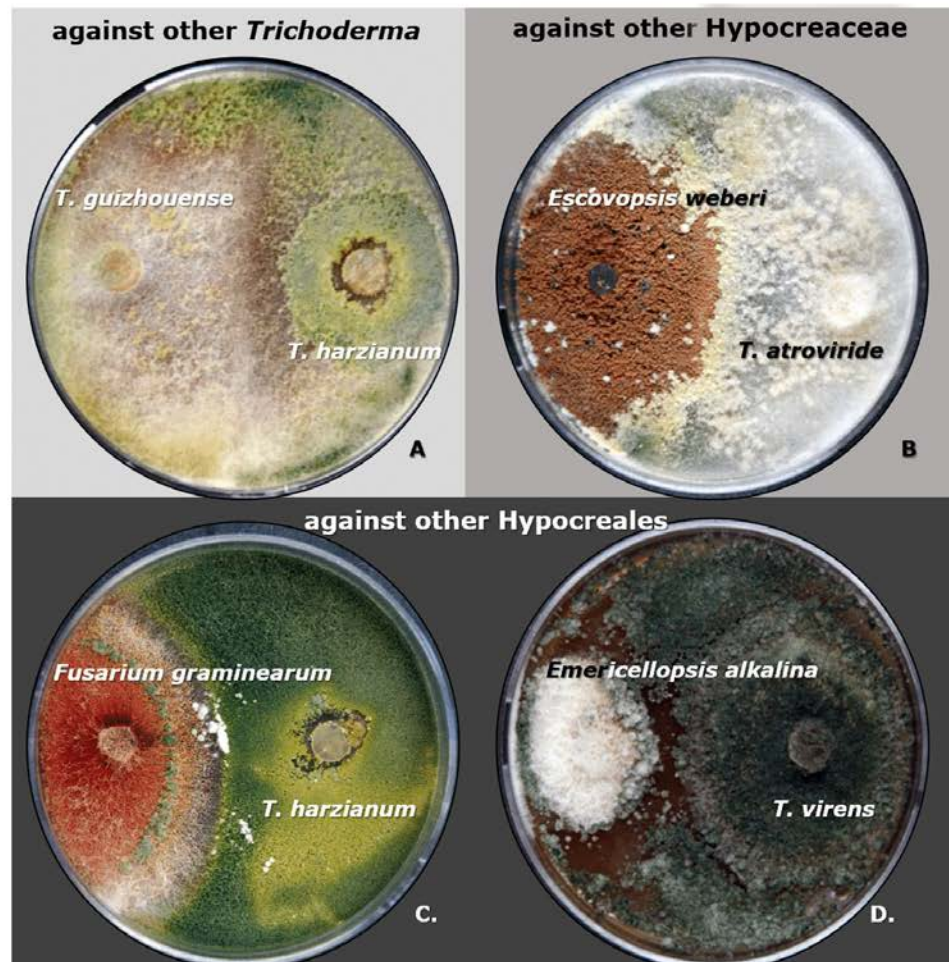


Fig 10. Adelparazitism of *Trichoderma* on members of the same genus (A), same family (B), and same order (C, D). Parasites were inoculated on the right side of each plate, and hosts are on the left side. Images were taken after 10 days of incubation at 28°C in the dark. Parasitism is assigned as a function of active overgrowth of the opponent colony. NCBI accession numbers for the DNA barcodes for fungi are given in Supporting Information S6 Table. Note to A: In this experiment, the host fungus *T. guizhouense* NJAU 4742 did not produce conidia (see other images in Supporting Information S3 Fig).

<https://doi.org/10.1371/journal.pgen.1007322.g010>

although the evolutionary state and mechanisms are not understood (see also Supporting Information S1 Text). It is known that the evolutionary history of some hypocrealean fungi involved the emergence of mycotrophy from a entomoparasitic/sarcophagic background. For example, *Elaphocordyceps* spp., deriving from the mainly entomoparasitic order Cordycipitaceae, are parasites of false truffles of the genus *Elaphomyces* (Eurotiales) [66].

Nikoh and Fukatsu [20] invoked the host-habitat hypothesis for such a “jump” from feeding on cicada nymphs to parasitism on truffles.

Due to the chemical composition of animals and fungi, the host shift from feeding on arthropods to feeding on fungi does not appear to be a difficult metabolic transition. Instead, it would only require a fine-tuning of ecological adaptations for specific hosts in one or another kingdom (i.e., mechanisms for recognition, defense, and overcoming the host). In contrast, feeding on plant biomass is an evolutionary challenge for any fungus specialized for feeding on insects or fungi. Our comparative analysis of the pcdCAZome of hypocrealean fungi revealed that members of entomoparasitic families have a relatively poor repertoire of genes required for degradation of plant biomass compared to those of the hypocrealean phytoparasites. This paucity is also present in the *Escovopsis weberi*, a parasite of Agaricales and the closest phylogenetic neighbor of *Trichoderma* for which genome information is available [22]. The reduced number of pcdCAZymes of *E. weberi* contradicts the predictions of the host-habitat hypothesis (see above) because the habitat of this fungus is directly linked to plant biomass, which is used by ants to cultivate *E. weberi*'s host fungus *Leucoagaricus* spp. The pcdCAZome of the nine *Trichoderma* spp. investigated here was found to be of intermediate size between entomoparasitic and phytoparasitic Hypocreales fungi. We demonstrate that the abilities of *Trichoderma* to feed on plant and fungal biomass are equally developed in the studied species. Consequently, nutritional extension—not shifts or “jumps”—results in nutritional versatility and provides the basis for the general environmental opportunism of this genus [4].

***Trichoderma* gained pcdCAZymes from filamentous Ascomycota hosts**

Our data suggest that nearly half of the genes encoding pcdCAZymes have been obtained by LGT from other fungi. Gene duplication, which has been described as a major source of gene innovation in fungi [67] and other organisms [68] apparently played only a minor role in the evolution of the *Trichoderma* pcdCAZome. It has been reported that 0.1–3% of the genes in a given Pezizomycotina genome were derived by LGT, usually indicating interdomain exchanges [43, 67]. When this estimation is applied to the 122 proteins of the pcdCAZome of *Trichoderma*, maximally five genes would be expected to have originated from LGT. This suggests that the frequency of LGT in pcdCAZome is an exceptional case. Surprisingly, we did not detect any transfer event from prokaryotes, and we also did not observe LGT events from Basidiomycota fungi. Marcet-Houben and Gabaldon [69] and Savory *et al.* [59] reviewed LGT events between bacteria and fungi, and listed *T. reesei* as one of the fungi comprising the highest number of bacterial-derived proteins. However, the genes transferred encoded arsenite reductases, catalases, different racemases and enzymes of peptidoglycan metabolism, but no pcdCAZymes. Because the transfer of bacterial glycoside hydrolase genes to ciliates [70] or rotifers [71] has been demonstrated to have shaped their adaptation to polysaccharide-rich environments, we expected to find such cases for *Trichoderma*. However, none of the 50 LGT events detected in this study involved a bacterial donor.

The only example of non-fungal putative LGT to *Trichoderma* was that of the gene encoding the auxiliary protein swollenin [72, 73]. The plant expansins were described to have undergone at least two LGT events to other organisms, including one event that gave rise to

amoebzoa expansins and fungal swollenins and another that gave rise to the bacterial expansins [73]. Our data are in accordance with these findings and further suggest that *Trichoderma* was among the first fungal genera to undergo LGT from plants (either directly or through other fungi).

Which features of *Trichoderma* mycoparasitism may be linked to LGT?

Historically, LGT between eukaryotes containing cell walls has been considered to be rare and linked to phagotrophy [74]. However, nearly two decades ago, Wöstemeyer *et al.* [56] hypothesized that hyphal fusion mycoparasitism might offer nearly ideal conditions for interfungal DNA exchanges. They demonstrated the transfer of genes *in vitro* from the Mucoromycotina mycoparasite *Parasitella parasitica* to its Mucoromycotina host, *Absidia glauca* [75]. Our discovery that a massive but taxonomically restricted putative LGT of pcwdCAZymes occurred in *Trichoderma* from filamentous Ascomycota hosts correlates with the expansion of *Trichoderma* mycoparasitic host range to Ascomycota. This has not occurred in other Hypocreaceae (*Escovopsis*, *Hypomyces*, *Sphaerostilbella*, etc.) that feed on Basidiomycota. Chaverri and Samuels [16] proposed that the ability to parasitize Ascomycota is likely a dominant force that has driven diversification in *Trichoderma*.

In nature, alloparasitism (parasitism of taxonomically remote hosts) is widespread, while adelphoparasitism is rare. This has mainly been described as social parasitism in Hymenoptera (Arthropoda, Animalia), while cases of cellular interactions are limited to the Rhodophyta (red algae) *Gracilariopsis andersonii* and its closely related endoparasite, *Gracilariophila oryzoides* [76]. Interestingly, a case of adelphoparasitism has also been reported recently in Hypocreales for the clavicipitoid ergot parasite *Tyrannicordyceps sclerotium*, which attacks closely related species [66]. Contrary to nutritional expansions in *Trichoderma*, *T. sclerotium* offers an additional example of the apparently common nutritional shift, at least in Hypocreales.

The mycoparasitism of *Trichoderma* on Pezizomycotina has been intensively studied *in vitro* for its use in plant protection, and, therefore, these studies are biased towards plant pathogenic fungi that are not necessarily the natural hosts. In nature, *Trichoderma* has only rarely been observed on sporophores of ascomycetes from Xylariales and Helotiales [77]. We have investigated the interactions between *Trichoderma* and extant fungi that may represent or be descendants of ancient LGT donors. A particularly convenient model donor for *Trichoderma* spp. is *Pestalotiopsis fici* (Xylariales) because both fungi are ecophysiologically compatible *in vitro*. Interestingly, Gazis and Chaverri [78] found *Pestalotiopsis* and *Trichoderma* are the most frequent endophytic fungi on the leaves and stems of rubber trees (*Hevea brasiliensis*), which confirms their sympatric occurrence in nature and, thus, the possibility for LGT. Notably, in our experiments, *P. fici* was not killed by *Trichoderma*, although intrahyphal growth was observed.

Another very interesting finding of our study is the absence of putative LGT events of pcwdCAZymes from Basidiomycota fungi, which are common *Trichoderma* hosts or substrates in nature [4, 13] and on mushroom farms [61]. Our results and numerous previous observations show that *Trichoderma* is capable of penetrating the cell wall of fungi, such as *Thanatephorus solani* and *Athelia rolfsii* (Basidiomycota). This indicates that neither fusion mycoparasitism alone nor the host-habitat hypothesis predict interfungal DNA exchanges.

The reason why LGT from Basidiomycota was not detected is not easy to explain. This finding seems to not be restricted to pcwdCAZymes because we also found no hints of LGT from basidiomycete donors in other gene families. A single case of a putative LGT from Basidiomycota to *T. reesei* has been suggested by Slot and Hibbett [77] for the nitrate-utilizing gene cluster. Their analysis suggested *Ustilago maydis* (Ustilaginales) to be a donor. Interestingly, the

Ustilaginales belong to the simple-septate Basidiomycota fungi, which do not have the complex dolipore septae found in Agaricomycotina mushrooms [79]. The dolipore may prevent the penetration of the host hyphae by *Trichoderma*. It could also be that LGT requires the growth of the parasite inside the host because during the proliferation of both hyphae, the cytoplasm and nuclei of both organisms may come in contact during mitosis. This might facilitate DNA exchange.

The likely physical difficulty to grow inside of hyphae of Basidiomycota with dolipores also suggests that mycoparasitic Hypocreaceae (*Escovopsis*, *Hypomyces*, *Sphaerostilbella*, etc.), which feed exclusively on such Basidiomycota, will not obtain genes from them. Indeed, such a case has not been reported thus far. Therefore, we hypothesize that the ability of *Trichoderma* to parasitize similar fungi (Pezizomycotina), even in extreme cases of adelphoparasitism, has been a significant ecological adaptation of this genus that subsequently enabled the observed putative LGT. We show that *Trichoderma* spp. can parasitize (overgrow and kill) some fungi belonging to the same genus, family, or order. In this study, we observed that *E. weberi* lacks this ability because it was parasitized by *Trichoderma* in all assays or did not interact.

The nutritional expansion of *Trichoderma* towards plant biomass through LGT is theoretically concordant with the “you are what you eat” concept in which the integration of a foreign DNA is a key mechanism. Yet, *Trichoderma* LGT resulted only from feeding on a limited group of hosts.

Glycoside hydrolase requirements for feeding on plant biomass

We propose that the major putative LGT events that resulted in the nutritional expansion from more ancient mycoparasitism to phytophagy took place before the diversification of *Trichoderma* into extant infrageneric groups (sections, clades and species). It is also evident that the fungus maintained both nutritional strategies. Thus, the composition of the pcwdCAZome allows us to speculate about the requirements for efficient feeding on plant biomass. The GH families, for which genes have been entirely acquired by LGT and are absent from the phylogenetic neighbors of *Trichoderma* (i.e. GH6, GH51, GH62, GH74, and swollenin), reveal that improvements in cellulose and hemicellulose degradation were a key trait for the phytophagy of this fungus. Specifically, the gain of CEL6A that proceeds from the nonreducing cellulose ends complements the presence of CEL7A that acts at the reducing end, and therefore allows a processive movement along cellulose and an increase the speed of its degradation [80]. The addition of swollenin, which disrupts the cellulose structure and generates additional free chain ends [81], provides an increased number of accessible points for the two cellobiohydrolases. Interestingly, *Trichoderma* also obtained a large number of GH27 α -D-galactosidases, GH28 pectinases, and GH10, GH11, and GH30 xylanases, suggesting their importance for the hydrolysis of both hemicelluloses and pectin.

In this regard, it is meaningful that several GH families, that are absent from the entomoparasitic hypocrealean fungi, are present in *Trichoderma* and *E. weberi* (GH7A, GH5 β -mannanases, GH12, GH67, GH74, GH95). This suggests that a part of the pcwdCAZome repertoire must have already been acquired before the split of the genera. It may also indicate that *E. weberi* likely lost the nutritional versatility of its ancestor along with a specialization for parasitizing *Leucoagaricus* spp. [22].

Conclusions

In this study, we propose that the parasitism of *Trichoderma* on phylogenetically close hosts (up to adelphoparasitism) enabled LGT to build its unique pcwdCAZome and nutritional versatility. In support of this, *Trichoderma* spp. are frequently detected as a members of

endophytic fungal communities [78] where they may either parasitize their putative cellulolytic hosts or feed on plant biomass or do both. Further studies of the evolutionary consequences of adelphoparasitism may explain other unique genomic features of *Trichoderma*. In addition, the description of the complete pcwdCAZome of nine *Trichoderma* spp. and, in the case of LGT, the identification of their putative donors may be of considerable interest to researchers studying the cellulolytic activity of this fungus for industrial applications.

Materials and methods

Organisms used in this study

Trichoderma strains used for the whole genome sequencing are given in Supporting Information S1 Table. All fungal strains and other organisms used in experiments and their respective accession numbers for DNA barcode sequences deposited in public databases and/or references are given in Supporting Information S6 Table.

Assessment of the growth on plant and fungal biomass

For inoculum preparation, fungi were cultivated on potato dextrose agar (Sigma Aldrich, Steinheim, Germany) at 28°C for 4 days. Spore suspensions (3×10^6 spores/ml) were prepared in 0.9% (w/v) NaCl with 0.025% (w/v) Tween 20 (Carl Roth, Austria). Growth tests were performed in CELLSTAR 24 Well Cell Culture plates (Greiner bio-one International). 1 ml of spore suspension of the fungus to be tested was inoculated on the following substrates: i) heat-treated (100°C for 3 hours) dried fruiting bodies of *Ganoderma lucidum* (Polyporales, Basidiomycota) (0.3% w/v), ii) epiphyte-free dried leaves of *Shorea johorensis* (Malvales, Angiosperms, Plantae) (0.3% w/v), iii) naturally degraded dead wood of *S. johorensis* (0.3% w/v), iv) commercial saw dust (local supplier, Vienna, Austria) (0.3% w/v), v) microcrystalline cellulose (0.05 mM research grade; AMS Biotechnology, Milton park, UK) in 0.5% (w/v) Agar-Agar Kobe I (Carl-Roth, Mannheim, Germany), vi) 2% (w/v) pre-treated (steam exploded) wheat straw 3% (w/v) in Agar-Agar Kobe I, vii) 0.3% pectin (w/v) in Agar-Agar Kobe I. Growth in 0.5% (w/v) Agar-Agar Kobe I was also tested as a control. All non-powdered substrates were finely ground and then sterilized at 120°C for 20 min. Experiment was carried out in quadruples. The plates were photographed after incubation at 28°C for seven days in darkness.

Interfungal interactions

Dual confrontation assays between fungi were done as described in Atanasova *et al.* [15]. For these experiments, fungi were incubated for 10 days on PDA at 25°C and 12 hours with cyclic illumination. When required, slower growing fungi (such as *Lentinula edodes* and *Leucoagaricus gongylophorus*) were inoculated 2–3 days prior to the inoculation with fast growing *Hypocreales*. The set of *Penicillium* spp. and *Pestalotiopsis fici* TUCIM 5788 strains was randomly selected from a pool of strains isolated from phylloplane of *Shorea johorensis* (Dipterocarpaceae, Plantae) from Borneo where *Trichoderma* spp. are common.

Confocal microscopy. To analyze the interfungal interaction by confocal microscopy, spores of *T. reesei* strain TUCIM 4817, carrying a *gfp* gene under the control of a histone 3A promoter, and *Pestalotiopsis fici* TUCIM 5788 were inoculated on two adjacent but separated PDA agar blocks mounted between the glass slides and the cover glass using a modified Riddell slide method [114] (Supporting information S3 Fig). The construct was incubated for 72 hours in a sterile wet chamber that hyphae of both fungi established the contacts. Live-cell imaging was performed using a Nikon C1 confocal laser scanning unit mounted on a Nikon Eclipse TE2000-E inverted microscope base (Nikon GmbH, Vienna, Austria). A Nikon Plan Apo VC

100×/1.4 with oil immersion objective lens was used. GFP was excited with an argon ion laser at 488 nm. The emitted fluorescence was separated by a Nikon MHX40500b/C100332 filter cube and detected with a photomultiplier tube within the range of 500–530 nm. Bright light images were captured simultaneously with a Nikon C1-TD transmitted light detector mounted behind the condenser turret.

Scanning electron microscopy. For scanning electron microscopy, a coverslip (1 cm²) was placed on the centre of an agar plate inoculated with partner fungi and incubated until contact between hyphae was established (in average for 72 hours). The hyphae were then fixed with 2.5% (v/v) glutaraldehyde in 0.5 M potassium phosphate buffer and used for examining by SEM (HITACHI S-3000N, Tokyo, Japan).

Genome analysis

The genomes of five *Trichoderma* species (*T. longibrachiatum* ATCC 18648, *T. citrinoviride* TUCIM 6016, *T. harzianum* CBS 226.95, *T. guizhouense* NJAU 4742 and *T. asperellum* CBS 433.97) were sequenced for this work (Supporting information S1 Table). Four of them (*T. longibrachiatum*, *T. citrinoviride*, *T. harzianum*, and *T. asperellum*) were sequenced using an Illumina platform. To this end, Illumina fragments (270 bp insert size) and 4 kbp long mate-pair (LMP) libraries were combined. The fragment libraries were produced from 1 µg of genomic DNA, sheared to 270 bp using an E210 Focused-ultrasonicator (Covaris) and size selection was carried out using SPRIselect (Beckman Coulter). The fragments were treated with end-repair, A-tailing, and ligation of Illumina adapters (Eurofins MWG Operon), using a NEBNext Ultra DNA Library Prep Kit (New England Biolabs Inc.).

Two types of LMP libraries were used, CLIP (Cre-Lox Inverse PCR) and LFPE (Ligation Free Paired-End), both of which used 15 µg of genomic DNA sheared with HydroShear (Genomic Solutions) using a selection size of 4 kb. For CLIP, the size selected DNA was ligated to adaptors containing loxP and the Illumina specific primer sequence. This adaptor ligated DNA fragments were then circularized via recombination by a Cre (NEB) excision reaction. The circularized DNA templates were then digested with a cocktail of four base cutter restriction enzymes, i.e. NlaIII, MseI, HypCH4IV (NEB), followed by self-ligation. The paired end library was then amplified via inverted PCR using an Illumina specific primer set. The size of the amplified paired end library was selected by running on a 1.8% (w/v) agarose gel followed by gel purification of the desired fragment (300–600 bp).

For LFPE library, the sheared DNA was treated with end repair adapters and ligated with biotinylated adapters. The adapter ligated DNA fragments were circularized by intra-molecular hybridization. The circularized DNA templates were digested by T7 Exonuclease and S1 Nuclease (Thermo Fisher Scientific). The digested fragments were treated with A-tailing Enzyme (NEB), followed by immobilization of mate-paired fragments on streptavidin beads (Thermo Fisher Scientific). Illumina compatible adapters (IDT, Inc) were ligated to the mate paired fragments and 12 cycles of PCR was used to enrich for the final library (KAPA Biosystems).

All prepared libraries were quantified using KAPA Biosystem's next-generation sequencing library qPCR kit and run on a Roche LightCycler 480 real-time PCR instrument. The quantified libraries were then prepared for sequencing on the Illumina HiSeq sequencing platform utilizing a TruSeq paired-end cluster kit v3 and Illumina's cBot instrument to generate a clustered flowcell for sequencing. Sequencing of the flowcell was performed on the Illumina HiSeq2000 sequencer using a TruSeq SBS sequencing kit 200 cycles v3, following a 2 x 100 bp or 2 x 150 bp run recipe.

Illumina data were QC filtered for artifact/process contamination and subsequently assembled using Rnnotator [82] for transcriptomes, and AllPathsLG [83] for genomes. The Pacific

Biosciences library was prepared from 5 µg of gDNA sheared using a Covaris LE220 focused-ultrasonicator with their Blue miniTUBES to generate sheared fragments of 3kb in length. The sheared DNA fragments were then prepared according to the Pacific Biosciences protocol and using their SMRTbell Template Preparation Kit, where the fragments were treated with DNA damage repair, had their ends repaired so that they were blunt-ended, and 5' phosphorylated. Pacific Biosciences hairpin adapters were then ligated to the fragments to create the SMRTbell template for sequencing. The SMRTbell templates were then purified using exonuclease treatments and size-selected using AMPure PB beads. Sequencing primer was then annealed to the SMRTbell templates and Version C2 sequencing polymerase was bound to them. The prepared SMRTbell template libraries were then sequenced on a Pacific Biosciences RSII sequencer using Version C2 chemistry and 2x45min sequencing movie run times.

Genomes were annotated using the JGI Annotation pipeline and made available via JGI fungal genome portal MycoCosm (jgi.doe.gov/fungi [84]). They have also been deposited at DDBJ/EMBL/GenBank as specified in Supporting Information S1 Table.

The genome of *T. guizhouense* NJAU 4742 was shotgun sequenced using a Roche 454 GS FLX system at the Chinese National Human Genome Center (Zhangjiang Hi-tech Park, Shanghai, China) with 28.4X coverage. The fragment libraries were produced from 5 µg of genomic DNA, sheared to 300–500 bp using M220 Ultrasonicator (Covaris, America) and was purified with Agencourt Ampure beads (Beckman, America). The fragment libraries were constructed with Purified DNA fragments by using DNA Library Preparation kit (Roche Applied Science, Switzerland) and fixed on magnetic beads with GS emPCR kit (Roche Applied Science). The 569 Mb raw data were achieved from 454 GS FLX system with 1,435,699 reads.

For sequence scaffolding, Solexa Mate Pair reads were used to establish the genome scaffolds. 5 µg of genomic DNA was sheared with a Hydroshear device (Gene Machine) to generate 3–5 kb DNA fragments. The library was prepared by using TruSeq DNA Sample Prep Kit-SetA (illumina, America), and amplified using TruSeq PE Cluster Kit (illumina, America), and then sequenced in Solexa sequencing machine (illumina, America). Gene calls were generated using FGENESH [85], ExonHunter [86] and AUGUSTUS version 2.7 [87].

Composition of *Trichoderma* pcwdCAZome

Annotation of the genes encoding carbohydrate active enzymes involved in plant cell wall degradation (pcwdCAZome) in the nine *Trichoderma* genomes was performed using the Carbohydrate-Active Enzyme database (CAZy) nomenclature [88, 89], by comparing each protein model from the genome by the sequence similarity search tool (blastp) to a collection of protein modules corresponding to catalytic and carbohydrate-binding modules derived from CAZy. Individual hits were then compared by HMMer to models corresponding to each CAZy family to allow an assignment of each identified protein.

Accession numbers of genes composing pcwdCAZome and respective regulatory proteins in *Trichoderma* genomes are given in Supporting Information S3 Table.

Principal component analysis and two-way cluster analysis of the Hypocreales pcwdCAZomes (Supporting Information S3 Table) were made with the use of <https://biit.cs.ut.ee/clustvis/> [90]. Cluster analysis was made with Euclidian distance and complete linkage method.

Genomic location of individual genes encoding for pcwdCAZome

To analyse whether the genomic location of the identified pcwdCAZomes would be syntenic among the nine *Trichoderma* species, we used the manually annotated chromosomes of *T. reesei* [45] as a template. Orthologs for each individual gene from the other *Trichoderma* spp.

were then located on their genomic scaffolds, and at least five genes flanking its 5' and 3' area were retrieved and identified by blastp. A synteny value of 100% was assigned between *T. reesei* and another *Trichoderma* sp. when all investigated flanking genes were orthologues and their order was conserved.

Phylogenetic analyses

Phylogenomic analysis of *Trichoderma* and other Hypocreales using 100 neutrally evolving genes. One-hundred genes were randomly selected from the genomes of the nine *Trichoderma* spp. and 12 reference Hypocreales (*Escovopsis weberi*, *Metarhizium acridium*, *M. robertsii*, *Calviceps purpurea*, *Ophiocordyceps sinensis*, *Beauveria bassiana*, *Cordyceps militaris*, *Fusarium graminearum*, *F. oxysporum* f. sp. *lycopersici*, *F. pseudograminearum*, *F. fujikuroi*, and *Nectria haematococca*; see Supporting Information S1 Table and S2 Table) based on two requirements: (a) they should display a syntenic position in all genomes, and (b) be true orthologues (no other gene encoding a protein with amino acid similarity >50% present). *Neurospora crassa* and *Chaetomium globosum* (Sordariales) were chosen as outgroups. For each gene the alignments of nucleotide sequences consisting of coding regions were prepared using ClustalW [91] and analyzed for the neutral evolution [92] using DNAsp V5.10.01 [93] based on Tajima's D test [94] as described by Rozas [95] (Supporting Information S2 Table). Multiple sequence alignments of each protein were done using ClustalW [91]. Resulting alignments were examined in Genedoc [96] and then subjected to the phylogenetic analysis online in PhyML [97] based on best amino acid substitution model acquired using "smart model selection" option (<http://www.atgc-montpellier.fr/phyml-smc/>). Maximum likelihood trees assessed using 1000 bootstrap replicates were also constructed individually for each of the 100 protein sequences and the phylome is deposited at <http://itol.embl.de/shared/druzhininaetal>. Accession numbers of all genes used in phylogenomic analysis are given in Supporting Information S2 Table.

For a combined analysis, a concatenated set of 100 proteins for each of 23 species was subjected to the alignment algorithm using the stand alone MAFFT tool [98] with G-INS-i parameters. Selection of conserved blocks was done using "relaxed" conditions in Gblocks [99]. The final concatenated alignment contained 47 726 amino acids. The selection of best amino acid substitution model was done using ProtTest 3 [100] based on BIC criterion. The Bayesian analysis was performed using MrBayes v3.2.5 [101, 102], 1 million generations and the Dayhoff I+G +F amino acid substitution model [103]. Two simultaneous, independent analyses starting from different random trees were run, each using three heated chains and one "cold" chain. Once the analyses were completed, 7500 trees were summarized after discarding the first 25% of the obtained 10,000 trees, resulting in a consensus tree. The parameters of phylogenetic analyses and accession numbers of individual genes are given in Supporting Information S2 Table.

Multilocus phylogeny of Ascomycota. To reconstruct a phylogenetic tree that included also all fungi for which putative pcwdCAZyme homologs to *Trichoderma* have been identified (see below), the amino acid sequences from four nuclear genes that have previously been shown to be suitable phylogenetic markers for Ascomycota multilocus phylogeny (histone acetyltransferase subunit of the RNA polymerase II holoenzyme, FG533; NAD-dependent glutamate dehydrogenase, FG570; translation initiation factor eIF-5, FG832; and TSR1p, a protein required for processing of 20S pre-rRNA, MS277) were retrieved from FunyBase [104] (<http://genome.jouy.inra.fr/funybase>), GenBank (<http://www.ncbi.nlm.nih.gov/genbank/>), the Joint Genome Institute (<http://genome.jgi-psf.org/programs/fungi/index.jsf?projectList>), EnsemblFungi (<http://fungi.ensembl.org/index.html>) and Broad Institute (<http://www.broadinstitute.org/>) databases. Complete sets of amino acid sequences for 128 fungi (including the nine *Trichoderma* spp.) were prepared. Concatenated alignments (provided in Supporting Information S1 Data) and an MCMC

analysis using MrBayes v3.2.5 was performed as described above. Accession numbers of individual genes from Ascomycota fungi are given in Supporting Information S7 Table.

In the case of swollenin, where the best Blastp hits included plant species, an appropriate species tree was constructed using the NCBI Taxonomy Browser.

Phylogenetic analysis of individual proteins from the *Trichoderma* pcdCAZome.

Protein sequences from the nine species that belonged to the same GH family were aligned using CLUSTALW [88] and subjected to phylogenetic analysis with PhyML embedded in TOPALI v 2.5 [105]. To retrieve the respective closest pcdCAZyme neighbors from other fungi, one or more *Trichoderma* proteins from each GH protein family (including PL1 and AA9 auxiliary proteins) were first subjected to a sequence similarity search by blastp against the NCBI database (finished by December 28, 2015). All hits with a query coverage of >90% and an E-value < 10^{-100} were collected. We initially used a less stringent E-value (< 10^{-40}), but found that the validated close neighbors were all characterized by < 10^{-100} . When this analysis failed to retrieve orthologs from closely related species, the analysis was repeated using tBlastn. Only published sequences were used. The final set of sequences was realigned using Muscle 3.8.425 [106] and integrated in the program Aliview [107]. Duplicate sequences from the same species were removed. Highly polymorphic regions were removed using the Gblocks [99] server with unconstrained parameters. The curated alignments were then subjected to evolutionary analysis using MrBayes v3.2.5 [102] as described above. The number of generations chosen for each phylogenetic tree depended on the number of sequences in the alignment. As a rule, the MCMC analysis was run for 1 million generations for all the alignments containing less than 100 sequences, and these were subsequently increased by 1 million until the standard deviation of split frequencies of the two parallel yet independent runs fell under 0.05 in the case of alignments containing more than 100 sequences. Parameters of individual phylogenetic analyses are given in Supporting Information S3 Table.

Inferring horizontal gene transfer, gene duplication and gene loss. The incongruent topologies of the phylograms of individual proteins from the pcdCAZome compared to the topology of the Hypocreales phylogenomic tree and the multilocus phylogram of Ascomycota fungi could be the result of gene duplication (GD), gene loss, or LGT. To distinguish between these possibilities, we reconciled the protein trees of each GH/AA9/PL1 family to the multilocus Ascomycota phylogeny (Fig 6A) in NOTUNG [40–42]. Using the approach of Wisecaver *et al.* [43], we assigned costs to GD, LGT, and gene loss and determined the most parsimonious combination of three events to explain the individual pcdCAZome trees in view of the topology of the Ascomycota phylogeny. An edge weight threshold of 0.9 was applied. To find the most appropriate parameters, we evaluated three different ratios of transfer to GD costs (2, 4 and 6) and compared the predicted gene transfers to those obtained by T-Rex [108]. The latter infers LGT by quantifying the proximity between two phylogenetic trees using a refinement of the Robinson and Foulds distance using midpoint rooting (see Supporting Information S4 Table). Finally, we used transfer costs twice as much as GD cost because it was the lowest ratio that identified LGT events that were in agreement with those suggested by the discordance of species and protein phylogeny. LGT events were only inferred when a CAZyme tree topology was contradictory to the Ascomycota phylogeny and could not be more parsimoniously reconciled by a combination of differential GD and gene loss. The scores are given in Supporting Information S4 Table.

Supporting information

S1 Text. Ecological terminology used in this study to describe types of nutrition found in Hypocreales fungi.
(PDF)

S1 Table. Properties of fungal genomes that were used in this study.

(XLSX)

S2 Table. Materials describing phylogenomic analysis of Hypocreales based on 100 orthologous proteins. A. Annotations of 100 orthologous proteins used in phylogenomic analysis and results of the neutrality tests. B. Protein accession numbers for 23 genomes.

(XLSX)

S3 Table. Composition and evolution of pcwdCAZome of *Trichoderma* and related fungi.A. NCBI Accession numbers of genes composing the pcwdCAZome of *Trichoderma* and regulatory proteins analyzed in this study. B. Distribution of pcwdCAZymes in GH families in Hypocreales. C. Parameters of phylogenetic analyses of individual proteins from *Trichoderma* pcwdCAZome.

(XLSX)

S4 Table. Results of statistical tests of the LGT hypothesis. A. The transfer costs for NOTUNG and comparison to LGT events predicted by T-REX. B: Results of the NOTUNG analysis of pcwdCAZome and relevant regulatory proteins. C. Summary on the evolutionary origin of pcwdCAZome of *Trichoderma* inferred in this study. D. Functional annotations of core genome *Trichoderma* genes that have no orthologous copies in other Hypocreales genomes.

(XLSX)

S5 Table. Chromosomal location of individual genes from pcwdCAZome of *T. reesei*.

(XLSX)

S6 Table. Additional organisms used in this study.

(XLSX)

S7 Table. Accession numbers of genes used for the multilocus phylogeny of Ascomycota fungi.

(XLSX)

S1 Fig. Growth of *Trichoderma* spp., *Escovopsis weberi* and *Pestalotiopsis fici* on natural substrates resembling polymers in the fungal and plant cell walls. Strains were evaluated after 10 days of incubation at 28°C in darkness. Yellow, green and white shape outlines correspond to good, weak and no growth, respectively. Data are representatives of four separate experiments.

(PDF)

S2 Fig. Phylogenetic trees of *Trichoderma* plant cell wall-degrading carbohydrate active enzymes and regulatory proteins.

(PDF)

S3 Fig. Mycoparasitism of *Trichoderma*. A. Allomycoparasitism of *Trichoderma* spp. and *E. weberi* on *Lentinula edodes*. B: Allomycoparasitism of *Trichoderma* and *E. weberi* on *Leucogarricus gongylophorus*. The dashed lines indicate growth of the host fungus as deduced from back sides of the plates. C: Set up for the microscopic investigation of *Trichoderma* (right) parasitism on *Pestalotiopsis fici* (left). 2 x 2 cm agar plugs were located between a sterile microscopy glass slide and a 5 x 2.5 cm sterile glass cover slip and aseptically inoculated with spores of two partner fungi, respectively, using a microbiological needle. Inoculated cultures were maintained at 28°C in wet chamber until hyphal contact. Microscopic investigation was done for hyphae on the cover slip surface. D. Antagonism of selected *Trichoderma* species on

Penicillium spp. Dashed line indicates growth of the opponent fungus.
(PDF)

S1 Data. Multiple sequence alignment used for the multilocus phylogeny of Ascomycota fungi.
(AA)

Acknowledgments

We thank Teresa E. Pawlowska for a critical reading of the manuscript and useful suggestions. The authors are grateful to Dr. R. Linke, TU Wien for providing *T. reesei* strain TUCIM 4817 for this study. We also acknowledge the contribution of Mr. Vineeth Subramanian and Mrs. Olga Druzhinina in sequence similarity search for the manual genomes annotation. The field work was performed at Kuala Belalong Field Studies Centre (Brunei) with kind assistance of the staff there.

Author Contributions

Conceptualization: Irina S. Druzhinina, Christian P. Kubicek.

Data curation: Irina S. Druzhinina, Komal Chenthamara, Lea Atanasova, Dongqing Yang, Youzhi Miao, Alexey G. Kopchinskiy, Bernard Henrissat, Alan Kuo, Hope Hundley, Mei Wang, Andrea Aerts, Asaf Salamov, Anna Lipzen, Kurt LaButti, Kerrie Barry, Igor V. Grigoriev, Christian P. Kubicek.

Formal analysis: Irina S. Druzhinina, Komal Chenthamara, Jian Zhang, Lea Atanasova, Youzhi Miao, Christian P. Kubicek.

Funding acquisition: Irina S. Druzhinina, Igor V. Grigoriev, Qirong Shen.

Investigation: Irina S. Druzhinina, Jian Zhang, Mohammad J. Rahimi, Marica Grujic, Feng Cai, Shadi Pourmehdi, Carina Pretzer, Christian P. Kubicek.

Methodology: Irina S. Druzhinina, Christian P. Kubicek.

Project administration: Irina S. Druzhinina.

Resources: Irina S. Druzhinina, Jian Zhang, Kamariah Abu Salim, Alexey G. Kopchinskiy, Igor V. Grigoriev, Qirong Shen.

Supervision: Irina S. Druzhinina.

Validation: Irina S. Druzhinina.

Visualization: Irina S. Druzhinina, Komal Chenthamara, Jian Zhang.

Writing – original draft: Irina S. Druzhinina, Komal Chenthamara, Christian P. Kubicek.

Writing – review & editing: Irina S. Druzhinina, Komal Chenthamara, Jian Zhang, Igor V. Grigoriev, Christian P. Kubicek.

References

1. Druzhinina IS, Kubicek CP. Ecological Genomics of *Trichoderma*. In: Martin F, editor. The Ecological Genomics of Fungi: John Wiley & Sons, Inc; 2013. p. 89–116.
2. Kubicek CP, Starr TL, Glass NL. Plant cell wall-degrading enzymes and their secretion in plant-pathogenic fungi. Annual Review of Phytopathology. 2014; 52:427–51. <https://doi.org/10.1146/annurev-phyto-102313-045831> PMID: 25001456

3. Lovett B, St Leger RJ. The Insect Pathogens. *Microbiol Spectr*. 2017; 5(2). <https://doi.org/10.1128/microbiolspec.FUNK-0001-2016> PMID: 28256192
4. Druzhinina IS, Seidl-Seiboth V, Herrera-Estrella A, Horwitz BA, Kenerley CM, Monte E, et al. *Trichoderma*: the genomics of opportunistic success. *Nature Reviews Microbiology*. 2011; 9(10):749–59. <https://doi.org/10.1038/nrmicro2637> PMID: 21921934
5. Gautheret A, Dromer F, Bourhis JH, Andremont A. *Trichoderma pseudokoningii* as a cause of fatal infection in a bone marrow transplant recipient. *Clin Infect Dis*. 1995; 20(4):1063–4. Epub 1995/04/01. PMID: 7795053.
6. Furukawa H, Kusne S, Sutton DA, Manez R, Carrau R, Nichols L, et al. Acute invasive sinusitis due to *Trichoderma longibrachiatum* in a liver and small bowel transplant recipient. *Clin Infect Dis*. 1998; 26(2):487–9. Epub 1998/03/21. PMID: 9502475.
7. Molnár-Gábor E, Döczi I, Hatvani L, Vágvolgyi C, Kredics L. Isolated sinusitis sphenoidalis caused by *Trichoderma longibrachiatum* in an immunocompetent patient with headache. *J Med Microbiol*. 2013; 62(Pt 8):1249–52. <https://doi.org/10.1099/jmm.0.059485-0> PMID: 23657526
8. Li Destri Nicosia MG, Mosca S, Mercurio R, Schena L. Dieback of *Pinus nigra* Seedlings Caused by a Strain of *Trichoderma viride*. *Plant Disease*. 2014; 99(1):44–9. <https://doi.org/10.1094/PDIS-04-14-0433-FE>
9. Bischof RH, Ramoni J, Seiboth B. Cellulases and beyond: the first 70 years of the enzyme producer *Trichoderma reesei*. *Microb Cell Fact*. 2016; 15. <https://doi.org/10.1186/s12934-016-0507-6> PMID: 27287427
10. Druzhinina IS, Kubicek CP. Familiar Stranger: Ecological Genomics of the Model Saprotroph and Industrial Enzyme Producer *Trichoderma reesei* Breaks the Stereotypes. *Adv Appl Microbiol*. 2016; 95:69–147. <https://doi.org/10.1016/bs.aambs.2016.02.001> PMID: 27261782
11. Gupta VK, Steindorff AS, Paula RGd, Silva-Rocha R, Mach-Aigner AR, Mach RL, et al. The Post-genomic Era of *Trichoderma reesei*: What's Next? *Trends in Biotechnology*. 2016;0(0). <https://doi.org/10.1016/j.tibtech.2016.06.003>
12. Mukherjee PK, Kenerley CM. Regulation of morphogenesis and biocontrol properties in *Trichoderma virens* by a VELVET protein, Vel1. *Applied and Environmental Microbiology*. 2010; 76(7):2345–52. <https://doi.org/10.1128/AEM.02391-09> PMID: 20154111
13. Jaklitsch WM. European species of *Hypocrea* Part I. The green-spored species. *Studies in Mycology*. 2009; 63:1–91. <https://doi.org/10.3114/sim.2009.63.01> PMID: 19826500
14. Druzhinina IS, Komoń-Zelazowska M, Atanasova L, Seidl V, Kubicek CP. Evolution and Ecophysiology of the Industrial Producer *Hypocrea jecorina* (Anamorph *Trichoderma reesei*) and a New Sympatric Agamospecies Related to It. *PLoS ONE*. 2010; 5(2):e9191. <https://doi.org/10.1371/journal.pone.0009191> PMID: 20169200
15. Atanasova, Le Crom S, Gruber S, Couplier F, Seidl-Seiboth V, Kubicek CP, et al. Comparative transcriptomics reveals different strategies of *Trichoderma* mycoparasitism. *BMC genomics*. 2013; 14(1):121.
16. Chaverri P, Samuels GJ. Evolution of habitat preference and nutrition mode in a cosmopolitan fungal genus with evidence of interkingdom host jumps and major shifts in ecology. *Evolution*. 2013; 67(10):2823–37. <https://doi.org/10.1111/evo.12169> PMID: 24094336
17. Delabona PdS, Farinas CS, Lima DJdS, Pradella JGdC. Experimental mixture design as a tool to enhance glycosyl hydrolases production by a new *Trichoderma harzianum* P49P11 strain cultivated under controlled bioreactor submerged fermentation. *Bioresour Technol*. 2013; 132:401–5. <https://doi.org/10.1016/j.biortech.2012.11.087> PMID: 23265822
18. Delabona PdS, Lima DJ, Robl D, Rabelo SC, Farinas CS, Pradella JGdC. Enhanced cellulase production by *Trichoderma harzianum* by cultivation on glycerol followed by induction on cellulosic substrates. *J Ind Microbiol Biotechnol*. 2016; 43(5):617–26. <https://doi.org/10.1007/s10295-016-1744-8> PMID: 26883662
19. Chaverri P, Branco-Rocha F, Jaklitsch WM, Gazis RO, Degenkolb T, Samuels GJ. Systematics of the *Trichoderma harzianum* species complex and the reidentification of commercial biocontrol strains. *Mycologia*. 2015;14–147. <https://doi.org/10.3852/14-147> PMID: 25661720
20. Nikoh N, Fukatsu T. Interkingdom host jumping underground: phylogenetic analysis of entomoparasitic fungi of the genus *cordyceps*. *Molecular Biology and Evolution*. 2000; 17(4):629–38. <https://doi.org/10.1093/oxfordjournals.molbev.a026341> PMID: 10742053
21. Rossman AY, Seifert KA, Samuels GJ, Minnis AM, Schroers H-J, Lombard L, et al. Genera in Bionectriaceae, Hypocreaceae, and Nectriaceae (Hypocreales) proposed for acceptance or rejection. *IMA Fungus*. 2013; 4(1):41–51. <https://doi.org/10.5598/imalfungus.2013.04.01.05> PMID: 23898411

22. de Man TJB, Stajich JE, Kubicek CP, Teiling C, Chenthamara K, Atanasova L, et al. Small genome of the fungus *Escovopsis weberi*, a specialized disease agent of ant agriculture. *Proc Natl Acad Sci U S A*. 2016; 113(13):3567–72. <https://doi.org/10.1073/pnas.1518501113> PMID: 26976598
23. Jaklitsch WM, Voglmayr H. Biodiversity of *Trichoderma* (Hypocreaceae) in Southern Europe and Macaronesia. *Studies in Mycology*. 2015; 80:1–87. <https://doi.org/10.1016/j.simyco.2014.11.001> PMID: 26955191
24. Wang X, Zhang X, Liu L, Xiang M, Wang W, Sun X, et al. Genomic and transcriptomic analysis of the endophytic fungus *Pestalotiopsis fici* reveals its lifestyle and high potential for synthesis of natural products. *BMC genomics*. 2015; 16:28. <https://doi.org/10.1186/s12864-014-1190-9> PMID: 25623211
25. Martinez D, Berka RM, Henrissat B, Saloheimo M, Arvas M, Baker SE, et al. Genome sequencing and analysis of the biomass-degrading fungus *Trichoderma reesei* (syn. *Hypocrea jecorina*). *Nat Biotechnol*. 2008; 26. <https://doi.org/10.1038/nbt1403> PMID: 18454138
26. Kubicek CP, Herrera-Estrella A, Seidl-Seiboth V, Martinez DA, Druzhinina IS, Thon M, et al. Comparative genome sequence analysis underscores mycoparasitism as the ancestral life style of *Trichoderma*. *Genome biology*. 2011; 12(4):R40. <https://doi.org/10.1186/gb-2011-12-4-r40> PMID: 21501500
27. Yang D, Pomraning K, Kopychinskiy A, Aghcheh RK, Atanasova L, Chenthamara K, et al. Genome Sequence and Annotation of *Trichoderma parareesei*, the Ancestor of the Cellulase Producer *Trichoderma reesei*. *Genome Announc*. 2015; 3(4):e00885–15. <https://doi.org/10.1128/genomeA.00885-15> PMID: 26272569
28. Gao Q, Jin K, Ying S-H, Zhang Y, Xiao G, Shang Y, et al. Genome Sequencing and Comparative Transcriptomics of the Model Entomopathogenic Fungi *Metarhizium anisopliae* and *M. acridum*. *PLoS Genetics*. 2011; 7(1):e1001264. <https://doi.org/10.1371/journal.pgen.1001264> PMID: 21253567
29. Schardl CL, Young CA, Hesse U, Amyotte SG, Andreeva K, Calie PJ, et al. Plant-Symbiotic Fungi as Chemical Engineers: Multi-Genome Analysis of the Clavicipitaceae Reveals Dynamics of Alkaloid Loci. *PLoS Genetics*. 2013; 9(2):e1003323. <https://doi.org/10.1371/journal.pgen.1003323> PMID: 23468653
30. Zheng P, Xia Y, Xiao G, Xiong C, Hu X, Zhang S, et al. Genome sequence of the insect pathogenic fungus *Cordyceps militaris*, a valued traditional chinese medicine. *Genome Biology*. 2011; 12(11):R116. <https://doi.org/10.1186/gb-2011-12-11-r116> PMID: 22112802
31. Cuomo CA, Guldener U, Xu J-R, Trail F, Turgeon BG, Di Pietro A, et al. The *Fusarium graminearum* genome reveals a link between localized polymorphism and pathogen specialization. *Science*. 2007; 317(5843):1400–2. <https://doi.org/10.1126/science.1143708> PMID: 17823352
32. Ma L-J, van der Does HC, Borkovich KA, Coleman JJ, Daboussi M-J, Di Pietro A, et al. Comparative genomics reveals mobile pathogenicity chromosomes in *Fusarium*. *Nature*. 2010; 464(7287):367–73. <https://doi.org/10.1038/nature08850> PMID: 20237561
33. Gardiner DM, McDonald MC, Covarelli L, Solomon PS, Rusu AG, Marshall M, et al. Comparative Pathogenomics Reveals Horizontally Acquired Novel Virulence Genes in Fungi Infecting Cereal Hosts. *PLoS Pathog*. 2012; 8(9):e1002952. <https://doi.org/10.1371/journal.ppat.1002952> PMID: 23028337
34. Coleman JJ, Rounsley SD, Rodriguez-Carres M, Kuo A, Wasmann CC, Grimwood J, et al. The Genome of *Nectria haematococca*: Contribution of Supernumerary Chromosomes to Gene Expansion. *PLoS Genet*. 2009; 5(8):e1000618. <https://doi.org/10.1371/journal.pgen.1000618> PMID: 19714214
35. Wiemann P, Sieber CMK, von Bargen KW, Studt L, Niehaus E-M, Espino JJ, et al. Deciphering the cryptic genome: genome-wide analyses of the rice pathogen *Fusarium fujikuroi* reveal complex regulation of secondary metabolism and novel metabolites. *PLoS pathogens*. 2013; 9(6):e1003475. <https://doi.org/10.1371/journal.ppat.1003475> PMID: 23825955
36. Xiao G, Ying S-H, Zheng P, Wang Z-L, Zhang S, Xie X-Q, et al. Genomic perspectives on the evolution of fungal entomopathogenicity in *Beauveria bassiana*. *Sci Rep*. 2012; 2:483. <https://doi.org/10.1038/srep00483> PMID: 22761991
37. Galagan JE, Calvo SE, Borkovich KA, Selker EU, Read ND, Jaffe D, et al. The genome sequence of the filamentous fungus *Neurospora crassa*. *Nature*. 2003; 422(6934):859–68. <https://doi.org/10.1038/nature01554> PMID: 12712197
38. Cuomo CA, Untereiner WA, Ma L-J, Grabherr M, Birren BW. Draft Genome Sequence of the Cellulolytic Fungus *Chaetomium globosum*. *Genome Announc*. 2015; 3(1). <https://doi.org/10.1128/genomeA.00021-15> PMID: 25720678
39. Fitzpatrick DA, Logue ME, Stajich JE, Butler G. A fungal phylogeny based on 42 complete genomes derived from supertree and combined gene analysis. *BMC evolutionary biology*. 2006; 6:99. <https://doi.org/10.1186/1471-2148-6-99> PMID: 17121679

40. Chen K, Durand D, Farach-Colton M. NOTUNG: a program for dating gene duplications and optimizing gene family trees. *J Comput Biol.* 2000; 7(3–4):429–47. <https://doi.org/10.1089/106652700750050871> PMID: 11108472
41. Vernot B, Stolzer M, Goldman A, Durand D. Reconciliation with non-binary species trees. *Comput Syst Bioinformatics Conf.* 2007; 6:441–52. PMID: 17951846
42. Stolzer M, Lai H, Xu M, Sathaye D, Vernot B, Durand D. Inferring duplications, losses, transfers and incomplete lineage sorting with nonbinary species trees. *Bioinformatics.* 2012; 28(18):i409–i15. <https://doi.org/10.1093/bioinformatics/bts386> PMID: 22962460
43. Wisecaver JH, Slot JC, Rokas A. The evolution of fungal metabolic pathways. *PLoS Genetics.* 2014; 10(12):e1004816. <https://doi.org/10.1371/journal.pgen.1004816> PMID: 25474404
44. Li WC, Huang CH, Chen CL, Chuang YC, Tung SY, Wang TF. *Trichoderma reesei* complete genome sequence, repeat-induced point mutation, and partitioning of CAZyme gene clusters. *Biotechnol Biofuels.* 2017; 10:170. Epub 2017/07/12. <https://doi.org/10.1186/s13068-017-0825-x> PMID: 28690679; PubMed Central PMCID: PMC5496416.
45. Druzhinina IS, Kopchinsky AG, Kubicek EM, Kubicek CP. A complete annotation of the chromosomes of the cellulase producer *Trichoderma reesei* provides insights in gene clusters, their expression and reveals genes required for fitness. *Biotechnol Biofuels.* 2016; 9:75. <https://doi.org/10.1186/s13068-016-0488-z> PMID: 27030800
46. Flores A, Chet I, Herrera-Estrella A. Improved biocontrol activity of *Trichoderma harzianum* by over-expression of the proteinase-encoding gene *prb1*. *Current Genetics.* 1997; 31(1):30–7. <https://doi.org/10.1007/s002940050173> PMID: 9000378
47. Migheli Q, González-Candelas L, Dealessi L, Camponogara A, Ramón-Vidal D. Transformants of *Trichoderma longibrachiatum* Overexpressing the beta-1,4-Endoglucanase Gene *egl1* Show Enhanced Biocontrol of *Pythium ultimum* on Cucumber. *Phytopathology.* 1998; 88(7):673–7. <https://doi.org/10.1094/PHYTO.1998.88.7.673> PMID: 18944939
48. Rocha-Ramírez V, Omero C, Chet I, Horwitz BA, Herrera-Estrella A. *Trichoderma atroviride* G-Protein α -Subunit Gene *tga1* Is Involved in Mycoparasitic Coiling and Conidiation. *Eukaryot Cell.* 2002; 1(4):594–605. <https://doi.org/10.1128/EC.1.4.594-605.2002> PMID: 12456007
49. Reithner B, Brunner K, Schuhmacher R, Peissl I, Seidl V, Krska R, et al. The G protein α subunit *Tga1* of *Trichoderma atroviride* is involved in chitinase formation and differential production of antifungal metabolites. *Fungal Genetics and Biology.* 2005; 42(9):749–60. <https://doi.org/10.1016/j.fgb.2005.04.009> PMID: 15964222
50. Zeilinger S, Reithner B, Scala V, Peissl I, Lorito M, Mach RL. Signal Transduction by *Tga3*, a Novel G Protein α Subunit of *Trichoderma atroviride*. *Applied and Environmental Microbiology.* 2005; 71(3):1591–7. <https://doi.org/10.1128/AEM.71.3.1591-1597.2005> PMID: 15746364
51. Djonović S, Pozo MJ, Kenerley CM. *Tvbgn3*, a β -1,6-Glucanase from the Biocontrol Fungus *Trichoderma virens*, Is Involved in Mycoparasitism and Control of *Pythium ultimum*. *Applied and Environmental Microbiology.* 2006; 72(12):7661–70. <https://doi.org/10.1128/AEM.01607-06> PMID: 16997978
52. Aghcheh RK, Druzhinina IS, Kubicek CP. The Putative Protein Methyltransferase LAE1 of *Trichoderma atroviride* Is a Key Regulator of Asexual Development and Mycoparasitism. *PLoS ONE.* 2013; 8(6):e67144. <https://doi.org/10.1371/journal.pone.0067144> PMID: 23826217
53. Gruber S, Zeilinger S. The transcription factor *Ste12* mediates the regulatory role of the Tmk1 MAP kinase in mycoparasitism and vegetative hyphal fusion in the filamentous fungus *Trichoderma atroviride*. *PLoS ONE.* 2014; 9(10):e111636. Epub 2014/10/31. <https://doi.org/10.1371/journal.pone.0111636> PMID: 25356841; PubMed Central PMCID: PMC4214791.
54. Gaderer R, Lamdan NL, Frischmann A, Sulyok M, Krska R, Horwitz BA, et al. *Sm2*, a paralog of the *Trichoderma cerato-platanin* elicitor *Sm1*, is also highly important for plant protection conferred by the fungal-root interaction of *Trichoderma* with maize. *BMC microbiology.* 2015; 15:2. <https://doi.org/10.1186/s12866-014-0333-0> PMID: 25591782
55. Chenthamara K, Druzhinina IS. 12 Ecological Genomics of Mycotrophic Fungi. In: Druzhinina IS, Kubicek CP, editors. *Environmental and Microbial Relationships. The Mycota: Springer International Publishing*; 2016. p. 215–46.
56. Wöstemeyer JW. Genomic Structure and Genetic Flexibility in Pathogenic Fungi. In: Carroll GC, Tudzynski P, editors. *Plant Relationships Part B. Berlin, Heidelberg: Springer Berlin Heidelberg*; 1997. p. 205–19.
57. Archibald JM, Rogers MB, Toop M, Ishida K-I, Keeling PJ. Lateral gene transfer and the evolution of plastid-targeted proteins in the secondary plastid-containing alga *Bigeloviella natans*. *Proc Natl Acad Sci U S A.* 2003; 100(13):7678–83. <https://doi.org/10.1073/pnas.1230951100> PMID: 12777624
58. Davis CC, Anderson WR, Wurdack KJ. Gene transfer from a parasitic flowering plant to a fern. *Proc Biol Sci.* 2005; 272(1578):2237–42. <https://doi.org/10.1098/rspb.2005.3226> PMID: 16191635

59. Savory F, Leonard G, Richards TA. The Role of Horizontal Gene Transfer in the Evolution of the Oomycetes. *PLoS Pathogens*. 2015; 11(5). <https://doi.org/10.1371/journal.ppat.1004805> PMID: 26020232
60. Hatvani L, Antal Z, Manczinger L, Szekeres A, Druzhinina IS, Kubicek CP, et al. Green Mold Diseases of *Agaricus* and *Pleurotus* spp. Are Caused by Related but Phylogenetically Different *Trichoderma* Species. *Phytopathology*. 2007; 97(4):532–7. <https://doi.org/10.1094/PHYTO-97-4-0532> PMID: 18943294
61. Komon-Zelazowska M, Bissett J, Zafari D, Hatvani L, Manczinger L, Woo S, et al. Genetically Closely Related but Phenotypically Divergent *Trichoderma* Species Cause Green Mold Disease in Oyster Mushroom Farms Worldwide. *Applied and Environmental Microbiology*. 2007; 73(22):7415–26. <https://doi.org/10.1128/AEM.01059-07> PMID: 17827333
62. Lincoln RJ, Boxshall GA, Clark PF. dictionary of ecology, evolution, and systematics. 1998.
63. Zhang J, Bayram Akcapinar G, Atanasova L, Rahimi MJ, Przulucka A, Yang D, et al. The neutral metalloprotease NMP1 of *Trichoderma guizhouense* is required for mycotrophy and self-defence: NMP1 of the fungicidal mould *Trichoderma guizhouense*. *Environmental Microbiology*. 2015:n/a-n/a. <https://doi.org/10.1111/1462-2920.12966> PMID: 26118314
64. Bissett J, Gams W, Jaklitsch W, Samuels GJ. Accepted *Trichoderma* names in the year 2015. *IMA Fungus*. 2015; 6(2):263–95. <https://doi.org/10.5598/ima fungus.2015.06.02.02> PMID: 26734542
65. Radwan MA, Farrag SAA, Abu-Elamayem MM, Ahmed NS. Biological control of the root-knot nematode, *Meloidogyne incognita* on tomato using bioproducts of microbial origin. *Applied Soil Ecology*. 2012; 56(Supplement C):58–62. <https://doi.org/10.1016/j.apsoil.2012.02.008>.
66. Kepler RM, Sung G-H, Harada Y, Tanaka K, Tanaka E, Hosoya T, et al. Host jumping onto close relatives and across kingdoms by *Tyrannicordyceps* (Clavicipitaceae) gen. nov. and Ustilaginoidae (Clavicipitaceae). *Am J Bot*. 2012; 99(3):552–61. <https://doi.org/10.3732/ajb.1100124> PMID: 22334447
67. Wisecaver JH, Rokas A. Fungal metabolic gene clusters-caravans traveling across genomes and environments. *Front Microbiol*. 2015; 6:161. <https://doi.org/10.3389/fmicb.2015.00161> PMID: 25784900
68. Oakley TH. Furcation and fusion: The phylogenetics of evolutionary novelty. *Dev Biol*. 2017; 431(1):69–76. Epub 2017/09/20. <https://doi.org/10.1016/j.ydbio.2017.09.015> PMID: 28923487.
69. Marcet-Houben M, Gabaldón T. Acquisition of prokaryotic genes by fungal genomes. *Trends in Genetics*. 2010; 26(1):5–8. <https://doi.org/10.1016/j.tig.2009.11.007> PMID: 19969385
70. Ricard G, McEwan NR, Dutilh BE, Jouany J-P, Macheboeuf D, Mitsumori M, et al. Horizontal gene transfer from Bacteria to rumen Ciliates indicates adaptation to their anaerobic, carbohydrates-rich environment. *BMC Genomics*. 2006; 7:22. <https://doi.org/10.1186/1471-2164-7-22> PMID: 16472398
71. Gladyshev EA, Meselson M, Arkhipova IR. Massive horizontal gene transfer in bdelloid rotifers. *Science*. 2008; 320(5880):1210–3. <https://doi.org/10.1126/science.1156407> PMID: 18511688
72. Saloheimo M, Paloheimo M, Hakola S, Pere J, Swanson B, Nyyssönen E, et al. Swollenin, a *Trichoderma reesei* protein with sequence similarity to the plant expansins, exhibits disruption activity on cellulosic materials. *Eur J Biochem*. 2002; 269(17):4202–11. PMID: 12199698
73. Nikolaidis N, Doran N, Cosgrove DJ. Plant expansins in bacteria and fungi: evolution by horizontal gene transfer and independent domain fusion. *Molecular Biology and Evolution*. 2014; 31(2):376–86. <https://doi.org/10.1093/molbev/mst206> PMID: 24150040
74. Richards TA, Soanes DM, Jones MDM, Vasieva O, Leonard G, Paszkiewicz K, et al. Horizontal gene transfer facilitated the evolution of plant parasitic mechanisms in the oomycetes. *PNAS*. 2011; 108(37):15258–63. <https://doi.org/10.1073/pnas.1105100108> PMID: 21878562
75. Wöstemeyer J, Ellenberger S, Schulz E, Siegmund L, von Burgeler A, Gerlitz N, et al. Fusion parasitism between *Parasitella parasitica* and its host *Absidia glauca*: A system between sexuality and parasitism. *Endocytobiosis and Cell Research*. 2016; 27(3):24–32.
76. Hancock L, Goff L, Lane C. Red algae lose key mitochondrial genes in response to becoming parasitic. *Genome Biol Evol*. 2010; 2:897–910. <https://doi.org/10.1093/gbe/evq075> PMID: 21081313
77. Slot JC, Hibbett DS. Horizontal transfer of a nitrate assimilation gene cluster and ecological transitions in fungi: a phylogenetic study. *PLoS ONE*. 2007; 2(10):e1097. <https://doi.org/10.1371/journal.pone.0001097> PMID: 17971860
78. Gazis R, Chaverri P. Diversity of fungal endophytes in leaves and stems of wild rubber trees (*Hevea brasiliensis*) in Peru. *Fungal Ecology*. 2010; 3(3):240–54. <https://doi.org/10.1016/j.funeco.2009.12.001>
79. Bauer R, Begerow D, Sampaio JP, Weiß M, Oberwinkler F. The simple-septate basidiomycetes: a synopsis. *Mycological Progress*. 2006; 5(1):41–66. <https://doi.org/10.1007/s11557-006-0502-0>

80. Payne CM, Knott BC, Mayes HB, Hansson H, Himmel ME, Sandgren M, et al. Fungal Cellulases. *Chem Rev*. 2015; 115(3):1308–448. <https://doi.org/10.1021/cr500351c> PMID: 25629559
81. Andberg M, Penttilä M, Saloheimo M. Swollenin from *Trichoderma reesei* exhibits hydrolytic activity against cellulosic substrates with features of both endoglucanases and cellobiohydrolases. *Bioresour Technol*. 2015; 181:105–13. <https://doi.org/10.1016/j.biortech.2015.01.024> PMID: 25643956
82. Martin J, Bruno VM, Fang Z, Meng X, Blow M, Zhang T, et al. Rnnotator: an automated de novo transcriptome assembly pipeline from stranded RNA-Seq reads. *BMC Genomics*. 2010; 11:663. <https://doi.org/10.1186/1471-2164-11-663> PMID: 21106091
83. Gnerre S, MacCallum I, Przybylski D, Ribeiro FJ, Burton JN, Walker BJ, et al. High-quality draft assemblies of mammalian genomes from massively parallel sequence data. *PNAS*. 2011; 108(4):1513–8. <https://doi.org/10.1073/pnas.1017351108> PMID: 21187386
84. Grigoriev IV, Nikitin R, Haridas S, Kuo A, Ohm R, Otillar R, et al. MycoCosm portal: gearing up for 1000 fungal genomes. *Nucleic Acids Research*. 2014; 42(Database issue):D699–704. <https://doi.org/10.1093/nar/gkt1183> PMID: 24297253
85. Solovyev V, Kosarev P, Seledsov I, Vorobyev D. Automatic annotation of eukaryotic genes, pseudogenes and promoters. *Genome Biology*. 2006; 7 Suppl 1:S10.1–2. <https://doi.org/10.1186/gb-2006-7-s1-s10> PMID: 16925832
86. Brejová B, Brown DG, Li M, Vinar T. ExonHunter: a comprehensive approach to gene finding. *Bioinformatics*. 2005; 21 Suppl 1:i57–65. <https://doi.org/10.1093/bioinformatics/bti1040> PMID: 15961499
87. Stanke M, Schöffmann O, Morgenstern B, Waack S. Gene prediction in eukaryotes with a generalized hidden Markov model that uses hints from external sources. *BMC bioinformatics*. 2006; 7:62. <https://doi.org/10.1186/1471-2105-7-62> PMID: 16469098
88. Levasseur A, Drula E, Lombard V, Coutinho PM, Henrissat B. Expansion of the enzymatic repertoire of the CAZy database to integrate auxiliary redox enzymes. *Biotechnol Biofuels*. 2013; 6(1):41. <https://doi.org/10.1186/1754-6834-6-41> PMID: 23514094
89. Lombard V, Ramulu HG, Drula E, Coutinho PM, Henrissat B. The carbohydrate-active enzymes database (CAZy) in 2013. *Nucleic Acids Res*. 2014; 42. <https://doi.org/10.1093/nar/gkt1178> PMID: 24270786
90. Metsalu T, Vilo J. ClustVis: a web tool for visualizing clustering of multivariate data using Principal Component Analysis and heatmap. *Nucleic Acids Research*. 2015; 43(W1):W566–W70. <https://doi.org/10.1093/nar/gkv468> PMID: 25969447
91. Larkin MA, Blackshields G, Brown NP, Chenna R, McGettigan PA, McWilliam H, et al. Clustal W and Clustal X version 2.0. *Bioinformatics*. 2007; 23(21):2947–8. <https://doi.org/10.1093/bioinformatics/btm404> PMID: 17846036
92. Kimura M. The neutral theory of molecular evolution and the world view of the neutralists. *Genome*. 1989; 31(1):24–31. PMID: 2687096
93. Librado P, Rozas J. DnaSP v5: a software for comprehensive analysis of DNA polymorphism data. *Bioinformatics*. 2009; 25(11):1451–2. <https://doi.org/10.1093/bioinformatics/btp187> PMID: 19346325
94. Tajima F. Statistical method for testing the neutral mutation hypothesis by DNA polymorphism. *Genetics*. 1989; 123(3):585–95. PMID: 2513255
95. Rozas J. DNA Sequence Polymorphism Analysis Using DnaSP. In: Posada D, editor. *Bioinformatics for DNA Sequence Analysis*. 537. Totowa, NJ: Humana Press; 2009. p. 337–50.
96. Nicholas KB. GeneDoc: a tool for editing and annotating multiple sequence alignments. Distributed by the author <http://www.pscedu/biomed/genedoc>. 1997.
97. Guindon S, Lethiec F, Duroux P, Gascuel O. PHYML Online—a web server for fast maximum likelihood-based phylogenetic inference. *Nucleic Acids Research*. 2005; 33(suppl 2):W557–W9. <https://doi.org/10.1093/nar/gki352> PMID: 15980534
98. Kazutaka K, Kei-ichi Kuma Ht, Miyata TA. MAFFT version 5: Improvement in accuracy of multiple sequence alignment. *Nucleic Acids Res*, Volume 33, No2. 2005.
99. Castresana J. Selection of conserved blocks from multiple alignments for their use in phylogenetic analysis. *Molecular biology and evolution*. 2000; 17(4):540–52. <https://doi.org/10.1093/oxfordjournals.molbev.a026334> PMID: 10742046
100. Darriba D, Taboada GL, Doallo R, Posada D. ProtTest 3: fast selection of best-fit models of protein evolution. *Bioinformatics*. 2011; 27(8):1164–5. <https://doi.org/10.1093/bioinformatics/btr088> PMID: 21335321
101. Huelsenbeck JP, Ronquist F. MRBAYES: Bayesian inference of phylogenetic trees. *Bioinformatics*. 2001; 17(8):754–5. <https://doi.org/10.1093/bioinformatics/17.8.754> PMID: 11524383

102. Ronquist F, Huelsenbeck JP. MrBayes 3: Bayesian phylogenetic inference under mixed models. *Bioinformatics*. 2003; 19(12):1572–4. PMID: [12912839](#)
103. Dayhoff MO, Schwartz RM, editors. Chapter 22: A model of evolutionary change in proteins 1978 1978.
104. Marthey S, Aguilera G, Rodolphe F, Gendraul A, Giraud T, Fournier E, et al. FUNYBASE: a FUNgal phYlogenomic dataBASE. *BMC bioinformatics*. 2008; 9:456. <https://doi.org/10.1186/1471-2105-9-456> PMID: [18954438](#)
105. Milne I, Lindner D, Bayer M, Husmeier D, McGuire G, Marshall DF, et al. TOPALi v2: a rich graphical interface for evolutionary analyses of multiple alignments on HPC clusters and multi-core desktops. *Bioinformatics*. 2009; 25(1):126–7. <https://doi.org/10.1093/bioinformatics/btn575> PMID: [18984599](#)
106. Edgar RC. MUSCLE: multiple sequence alignment with high accuracy and high throughput. *Nucleic Acids Research*. 2004; 32(5):1792–7. <https://doi.org/10.1093/nar/gkh340> PMID: [15034147](#)
107. Larsson A. AliView: a fast and lightweight alignment viewer and editor for large datasets. *Bioinformatics*. 2014; 30(22):3276–8. <https://doi.org/10.1093/bioinformatics/btu531> PMID: [25095880](#)
108. Boc A, Diallo AB, Makarenkov V. T-REX: a web server for inferring, validating and visualizing phylogenetic trees and networks. *Nucleic Acids Research*. 2012; 40(Web Server issue):W573–9. <https://doi.org/10.1093/nar/gks485> PMID: [22675075](#)

S1 Table

S1 Table: Properties of fungal genomes used in this study.

Order	Family	Section in the genus <i>Trichoderma</i>	Species	Strain	NCBI accession	Web link	Genome size [Mbp]	Coverage [x]	Assembly gaps [%]	No. of gene models	No. of scaffolds	Ref*
Hypocreales	Hycocreaeae	<i>Longibrachiatum</i>	<i>Trichoderma reesei</i>	Qm 6a	PRJNA225530	Web link						1
			<i>T. parareesei</i>	CBS 125925	LFMI00000000	n.a.						2
			<i>T. longibrachiatum</i>	ATCC 18648	MBDI00000000	web link	32.2	60	3.2	10938	130	this study
			<i>T. citrinoviride</i>	N/A	MBDI00000000	Web link	33.22	63	0.2	9737	533	
		<i>T. guizhouense</i>	NJAU 4742	LVVK00000000	n.a.	38.29	24	0.0922	11255	63		
		<i>T. harzianum</i>	CBS 226.95	MBGI00000000	Web link	40.98	120	0.04	14095	532		
		<i>Pachibasium</i>	<i>T. virens</i>	Gv29-8	PRJNA264113	Web link						3
			<i>T. asperellum</i>	CBS 433.97	MBGH00000000	Web link	37.5	120	0.06	12586	419	this study
		<i>Trichoderma</i>	<i>T. atroviride</i>	IMI 206040	PRJNA264112	Web link						3
			<i>Escovopsis weberi</i>	CC031208-10	PRJNA253870	Web link						4
	Clavicipitaceae	<i>Metarhizium acridium</i>	CQMa102	PRJNA38715							5	
		<i>M. robertsii</i>	ARSEF 23	PRJNA245140							6	
		<i>Calviceps purpurea</i>	20.1	PRJEA76493								
	Ophiocordycipitaceae	<i>Ophiocordyceps sinensis</i>	CO18	PRJNA59569						7		
	Cordycipitaceae	<i>Beauveria bassiana</i>	ARSEF 2860	PRJNA225503							8	
		<i>Cordyceps militaris</i>	CM01	PRJNA225510							9	
Nectriaceae	<i>Fusarium graminearum</i>	PH-1	AACM00000000							10		
	<i>F. pseudograminearum</i>	CS3096	AFNW00000000							11		
	<i>F. oxysporum</i> f. sp. <i>lycopersici</i>	4287	PRJNA342688							12		
	<i>F. fujikuroi</i>	IMI 58289	PRJEB185							13		
	<i>Nectria haematococca</i>	mpVI 77-13-4	PRJNA51499							14		
Sordariales	Sordariaceae	<i>Neurospora crassa</i>	OR74a	AABX00000000						15		
	Chaetomiaceae	<i>Chaetomium globosum</i>	CBS 148.51	PRJNA12795						16		

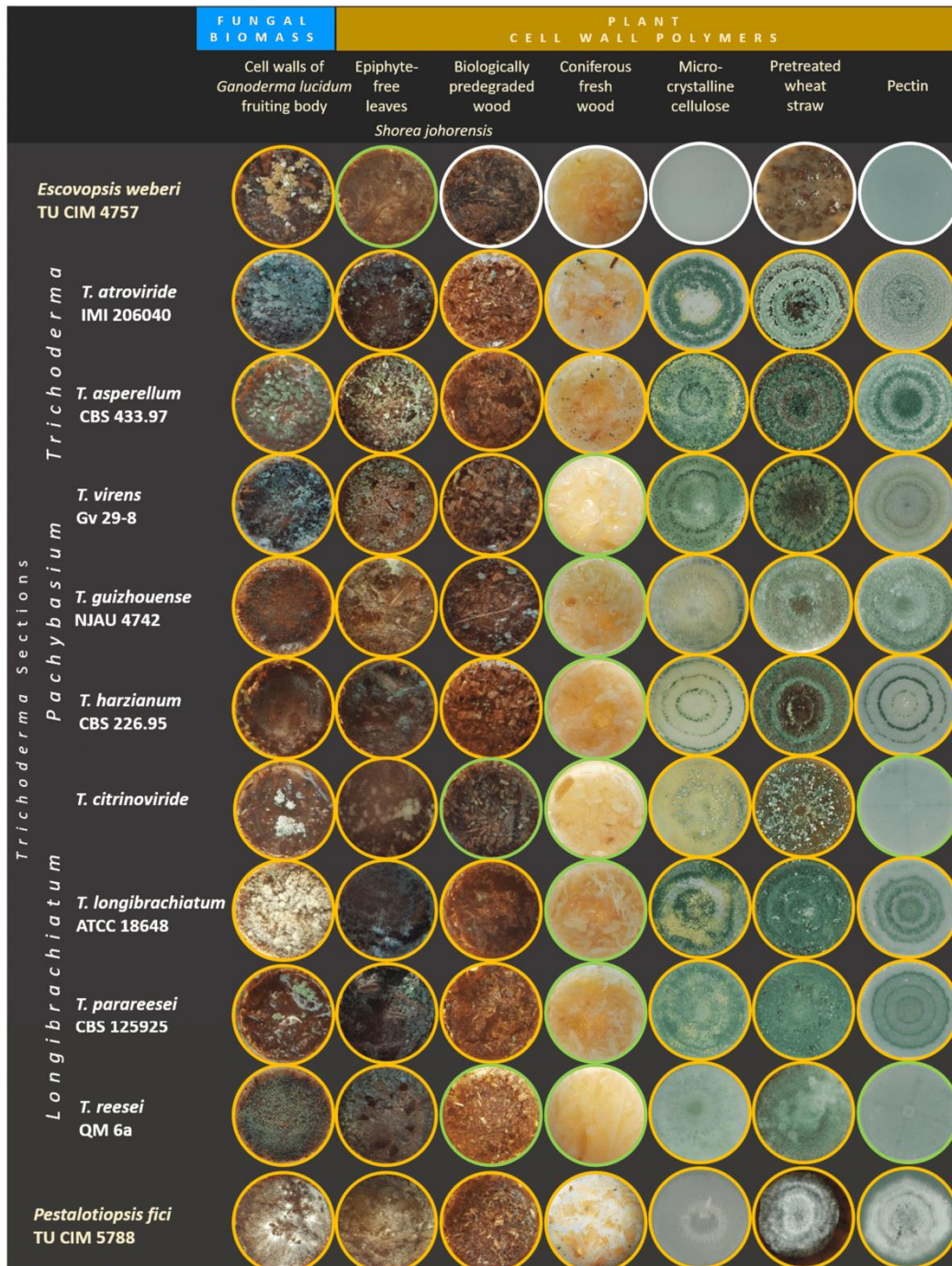
n.a. - not available

***References**

- Martinez, D. et al. Genome sequencing and analysis of the biomass-degrading fungus *Trichoderma reesei* (syn. *Hypocrea jecorina*). Nat. Biotechnol. 26, 553–560 (2008).
- Yang, D. et al. Genome Sequence and Annotation of *Trichoderma parareesei*, the Ancestor of the Cellulase Producer *Trichoderma reesei*. Genome Announc. 3, e00885-15 (2015).
- Kubicek, C. P. et al. Comparative genome sequence analysis underscores mycoparasitism as the ancestral life style of *Trichoderma*. Genome Biol. 12, R40 (2011).
- de Man, T. J. B. et al. Small genome of the fungus *Escovopsis weberi*, a specialized disease agent of ant agriculture. Proc. Natl. Acad. Sci. U. S. A. 113, 3567–3572 (2016).
- Gao, Q. et al. Genome Sequencing and Comparative Transcriptomics of the Model Entomopathogenic Fungi *Metarhizium anisopliae* and *M. acridum*. PLoS Genet. 7, e1001264
- Schardl, C. L. et al. Plant-Symbiotic Fungi as Chemical Engineers: Multi-Genome Analysis of the Clavicipitaceae Reveals Dynamics of Alkaloid Loci. PLoS Genet. 9, e1003323 (2013).
- Hu, X. et al. Genome survey uncovers the secrets of sex and lifestyle in caterpillar fungus. Chin. Sci. Bull. 58, 2846–2854 (2013).
- Xiao, G. et al. Genomic perspectives on the evolution of fungal entomopathogenicity in *Beauveria bassiana*. Sci. Rep. 2, 483 (2012).
- Zheng, P. et al. Genome sequence of the insect pathogenic fungus *Cordyceps militaris*, a valued traditional chinese medicine. Genome Biol. 12, R116 (2011).
- Cuomo, C. A. et al. The *Fusarium graminearum* genome reveals a link between localized polymorphism and pathogen specialization. Science 317, 1400–1402 (2007).
- Gardiner, D. M., Stiller, J. & Kazan, K. Genome Sequence of *Fusarium graminearum* Isolate CS3005. Genome Announc. 2, (2014).
- Ma, L.-J. et al. Comparative genomics reveals mobile pathogenicity chromosomes in *Fusarium*. Nature 464, 367–373 (2010).
- Wiemann, P. et al. Deciphering the cryptic genome: genome-wide analyses of the rice pathogen *Fusarium fujikuroi* reveal complex regulation of secondary metabolism and novel
- Coleman, J. J. et al. The Genome of *Nectria haematococca*: Contribution of Supernumerary Chromosomes to Gene Expansion. PLoS Genet 5, e1000618 (2009).
- Galagan, J. E. et al. The genome sequence of the filamentous fungus *Neurospora crassa*. Nature 422, 859–868 (2003).
- Cuomo, C. A., Untereiner, W. A., Ma, L.-J., Grabherr, M. & Birren, B. W. Draft Genome Sequence of the Cellulolytic Fungus *Chaetomium globosum*. Genome Announc. 3, (2015).

S1 Figure

S1 Figure: Growth of *Trichoderma* spp., *Escovopsis weberi* and *Pestalotiopsis fici* on natural substrates resembling polymers in the fungal and plant cell walls.



Strains were evaluated after 10 days of incubation at 28°C in darkness. Yellow, green and white shape outlines correspond to good, weak and no growth, respectively. The first four assays were done in 24-well plates. The last three columns show assays in Petri plates, 9 cm in diameter. Data are representatives of four separate experiments.

S2A Table

S2A Table: Annotations of 100 orthologous proteins used in phylogenomic analysis in phylogenomic analysis and Neutrality tests

Order in the concatenated alignment	Protein Id in <i>T. harzianum</i> CBS 226.95	Function	KOG ID	KOG CLASS	GROUP	Neutrality tests (Not significant, P > 0.10)		
						Average no. of nucleotide differences. k	Theta (per site) from Eta	Tajima's D
1	82401	Tetracycline resistance protein, TetB	KOG0254	General function prediction only	POORLY CHARACTERIZED	370.97778	0.29516	-1.06164
2	503986	Glycoside Hydrolase Family 16 protein	KOG2254	Carbohydrate transport and metabolism	METABOLISM	244.42222	0.29525	-1.03862
3	238777	Glycosyltransferase Family 32 protein	KOG1928	Carbohydrate transport and metabolism	METABOLISM	58.62222	0.2941	-1.01156
4	85356	TPR-containing nuclear phosphoprotein	KOG2002	Inorganic ion transport and metabolism	METABOLISM	467.62222	0.36846	-1.05065
5	120562	unknown protein	-	-	-	288.48889	0.34602	-0.60007
6	11235	Hemolysin III containing protein	KOG0748	Signal transduction mechanisms	CELLULAR PROCESSES AND SIGNALING	270.00	0.23338	-0.85621
7	139606	Dihydroipoamide acetyltransferase	KOG0557	Energy production and conversion	METABOLISM	162.62222	0.16159	-0.77337
8	95023	AAA+ type ATPase containing the peptidase M41 domain	KOG0734	Posttranslational modification, protein turnover, chaperones	CELLULAR PROCESSES AND SIGNALING	322.42222	0.24753	-0.79568
9	72100	Glycoside Hydrolase Family 76 protein	KOG4342	Carbohydrate transport and metabolism	METABOLISM	281.11111	0.29119	-0.87398
10		26S proteasome regulatory complex, subunit RPN10/PSMD4	KOG2884	Posttranslational modification, protein turnover, chaperones	CELLULAR PROCESSES AND SIGNALING	138.86667	0.2112	-0.84008
11	80456	unknown protein	-	-	-	659.64444	0.29444	-0.98071
12	491859	Phospholipase D1	KOG1329	Lipid transport and metabolism	METABOLISM	1031.71111	0.27733	-0.82944
13	490345	DNA replication licensing factor, MCM7 component	KOG0482	Replication, recombination and repair	INFORMATION STORAGE AND PROCESSING	322.62222	0.19584	-0.82402
14	518933	26S proteasome regulatory complex, subunit RPN12/PSMD8	KOG3151	Posttranslational modification, protein turnover, chaperones	CELLULAR PROCESSES AND SIGNALING	147.91111	0.22854	-0.93164
15	49445	Glycoside Hydrolase Family 17 protein	KOG0626	Carbohydrate transport and metabolism	METABOLISM	143.04444	0.34391	-1.249
16	481881	Flavin-containing monooxygenase	KOG1399	Secondary metabolites biosynthesis, transport and catabolism]	METABOLISM	107.31111	0.24846	-1.08928
17	10016	Tandem pore domain K+ channel	KOG1418	Inorganic ion transport and metabolism	METABOLISM	611.55556	0.38129	-1.13447
18	494174	Ferric reductase, NADH/NADPH oxidase and related proteins	KOG0039	Inorganic ion transport and metabolism, Secondary metabolites biosynthesis, transport and catabolism	METABOLISM	242.06667	0.32283	-0.88749
19	512504	Aspartate-semialdehyde dehydrogenase	KOG4777	Amino acid transport and metabolism	METABOLISM	161.71111	0.17364	-0.70201
20	478551	Na+/K+ transporter	KOG1341	Inorganic ion transport and metabolism	METABOLISM	298.73333	0.32875	-0.81919
21	79764	Copper chaperone	KOG1603	Inorganic ion transport and metabolism	METABOLISM	46.73333	0.24628	-1.10781
22	509002	Ubiquinol cytochrome c reductase, subunit RPI1	KOG1671	Energy production and conversion	METABOLISM	41.17778	0.11902	-0.61715
23	514040	UDP-N-acetylglucosamine transporter	KOG1583	Carbohydrate transport and metabolism	METABOLISM	229.11111	0.2889	-0.71549
24	503006	Predicted transporter	KOG0927	General function prediction only	POORLY CHARACTERIZED	378.22222	0.27931	-1.03525
25	76997	20S proteasome, regulatory subunit beta type PSM85/PSMB8/PRE2	KOG0175	Posttranslational modification, protein turnover, chaperones	CELLULAR PROCESSES AND SIGNALING	32.13333	0.16338	-0.8612
26	729	Helicase-like transcription factor HLTf/DNA helicase RAD5	KOG1001	Transcription, Replication, recombination and repair	INFORMATION STORAGE AND PROCESSING	158.62222	0.39308	-0.9669
27	352623	20S proteasome, regulatory subunit alpha type PSM41/PRE5	KOG0863	Posttranslational modification, protein turnover, chaperones	CELLULAR PROCESSES AND SIGNALING	115.62222	0.17339	-0.78591
28	479595	Voltage-gated shaker-like K+ channel, subunit beta/KCNAB	KOG1575	Energy production and conversion	METABOLISM	144.17778	0.24582	-1.16924
29	502882	20S proteasome, regulatory subunit alpha type PSM45/PU2	KOG0176	Posttranslational modification, protein turnover, chaperones	CELLULAR PROCESSES AND SIGNALING	81.73333	0.15522	-0.78046
30	263800	Helicase-like transcription factor HLTf/DNA helicase RAD5	KOG1001	Transcription, Replication, recombination and repair	INFORMATION STORAGE AND PROCESSING	486.42222	0.30217	-0.80022
31	478827	Arginyl-tRNA synthetase	KOG1195	Translation, ribosomal structure and biogenesis	INFORMATION STORAGE AND PROCESSING	352.91111	0.21838	-0.72517
32	97567	Carbohydrate-Binding Module Family 18 / GH Family 16 protein	KOG2806	Carbohydrate transport and metabolism	METABOLISM	129.6	0.21949	-0.9905
33	729	Golgi integral membrane protein	KOG4677	Intracellular trafficking, secretion, and vesicular transport	CELLULAR PROCESSES AND SIGNALING	695.77778	0.31667	-0.812
34	510952	Signal peptidase complex, subunit SPC25	KOG4072	Intracellular trafficking, secretion, and vesicular transport	CELLULAR PROCESSES AND SIGNALING	151.11111	0.293	-0.95396
35	89866	AAA+ type ATPase containing the peptidase M41 domain	KOG0731	Posttranslational modification, protein turnover, chaperones	CELLULAR PROCESSES AND SIGNALING	398.42222	0.22299	-0.79109
36	11153	Signal peptidase subunit	KOG4112	Intracellular trafficking, secretion, and vesicular transport	CELLULAR PROCESSES AND SIGNALING	68.37778	0.27783	-0.68123
37	281509	RNA polymerase I and III, subunit RPA40/RPC40, subunit RPA40/RPC40	KOG1521	Transcription	INFORMATION STORAGE AND PROCESSING	93.91111	0.20861	-0.90064
38	513792	Tyrosine kinase specific for activated (GTP-bound) p21cdc42Hs	KOG0192	Signal transduction mechanisms	CELLULAR PROCESSES AND SIGNALING	321.26667	0.2637	-0.77558
39	89828	Predicted membrane protein	KOG3393	Function unknown	POORLY CHARACTERIZED	180.84444	0.34539	-1.25833
40	71143	Checkpoint kinase and related serine/threonine protein kinases	KOG0590	Cell cycle control, cell division, chromosome partitioning	CELLULAR PROCESSES AND SIGNALING	337.17778	0.28231	-0.98231
41	480715	Serine/threonine protein kinase	KOG0583	Signal transduction mechanisms	CELLULAR PROCESSES AND SIGNALING	252.73333	0.23434	-0.97295
42	10328	Vacuolar assembly/sorting protein DID4	KOG3230	Intracellular trafficking, secretion, and vesicular transport	CELLULAR PROCESSES AND SIGNALING	98.27778	0.18195	-0.80594
43	493940	Uncharacterized conserved protein	KOG4690	Function unknown	POORLY CHARACTERIZED	147.86667	0.30815	-0.84363
44	3687	Ribosomal protein S6 kinase and related proteins	KOG0598	General function prediction only	POORLY CHARACTERIZED	401.64444	0.29285	-0.83202
45	484185	Serine/threonine protein kinase	KOG0690	Signal transduction mechanisms	CELLULAR PROCESSES AND SIGNALING	311.84444	0.18937	-0.57776
46	478444	Serine/threonine protein kinase Chk2 and related proteins	KOG0615	Cell cycle control, cell division, chromosome partitioning	CELLULAR PROCESSES AND SIGNALING	844.06667	0.36135	-0.87983
47	491227	Serine/threonine protein kinase	KOG0588	Cell cycle control, cell division, chromosome partitioning	CELLULAR PROCESSES AND SIGNALING	500.11111	0.25888	-0.7723
48	95880	Serine/threonine-protein kinase involved in autophagy	KOG0595	Posttranslational modification, protein turnover, chaperones, intracellular trafficking	CELLULAR PROCESSES AND SIGNALING	560.31111	0.26113	-0.86931

49	3687	Ribosomal protein S6 kinase and related proteins	KOG0598	General function prediction only	POORLY CHARACTERIZED	345.28889	0.21637	-0.73343
50	7270	Serine/threonine protein kinase	KOG0201	Signal transduction mechanisms	CELLULAR PROCESSES AND SIGNALING	432.42222	0.27716	-0.71652
51	1304	US1-interacting protein NUDE	KOG1853	Cytoskeleton	CELLULAR PROCESSES AND SIGNALING	128.62222	0.27797	-0.84769
52	126556	Nucleolar RNA-associated protein (NRAP)	KOG2054	Function unknown	POORLY CHARACTERIZED	751.00	0.3031	-0.90726
53	8065	Neurochondrin/leucine-rich protein (Neurochondrin)	KOG2611	Function unknown	POORLY CHARACTERIZED	365.44444	0.33131	-0.8455
54	4021	U4/U6-US snRNP associated protein	KOG2217	RNA processing and modification	INFORMATION STORAGE AND PROCESSING	411.84444	0.28319	-0.89529
55	490649	Vacuolar sorting protein VPS33/slp1	KOG1302	Intracellular trafficking, secretion, and vesicular transport	CELLULAR PROCESSES AND SIGNALING	363.66667	0.22756	-0.8668
56	5601	Beclin-like protein	KOG2751	Signal transduction mechanisms	CELLULAR PROCESSES AND SIGNALING	315.68889	0.28786	-0.94771
57	86453	Uncharacterized conserved protein	KOG2922	Function unknown	POORLY CHARACTERIZED	319.13333	0.25179	-0.98753
58	4377	Nuclear localization sequence binding protein	KOG4210	Transcription	AND PROCESSING	156.00	0.27912	-0.74179
59	512767	Uncharacterized conserved protein	KOG2427	Function unknown	POORLY CHARACTERIZED	243.86667	0.30228	-0.97345
60	94685	Predicted membrane protein	KOG2490	Function unknown	POORLY CHARACTERIZED	424.31111	0.26433	-1.02675
61	478447	Uncharacterized conserved protein	KOG2385	Function unknown	POORLY CHARACTERIZED	482.17778	0.35564	-0.87503
62	509997	Uncharacterized conserved protein	KOG3024	Function unknown	POORLY CHARACTERIZED	117.68889	0.2137	-0.82899
63	81478	Uncharacterized conserved protein XAP-5	KOG2894	Function unknown	POORLY CHARACTERIZED	192.73333	0.2619	-1.0635
64	125203	Uncharacterized conserved protein	KOG1228	Function unknown	POORLY CHARACTERIZED	234.17778	0.31862	-0.83608
65	80647	Uncharacterized conserved protein	KOG2861	Function unknown	POORLY CHARACTERIZED	288.28889	0.25019	-0.84617
66	477659	Predicted membrane protein	KOG3134	Function unknown	POORLY CHARACTERIZED	165.37778	0.24346	-0.75633
67	73286	Cell cycle-associated protein	KOG1852	Cell cycle control, cell division, chromosome partitioning	CELLULAR PROCESSES AND SIGNALING	232.37778	0.27322	-1.06225
68	94490	Oxysterol-binding protein	KOG2210	Signal transduction mechanisms	CELLULAR PROCESSES AND SIGNALING	141.88889	0.22258	-0.88911
69	501612	Protein kinase PCTAIRE and related kinases	KOG0594	General function prediction only	POORLY CHARACTERIZED	160.6	0.19723	-0.82607
70	493763	Ca2+/calmodulin-dependent protein kinase NIMA (never in mitosis)-related G2-specific serine/threonine protein kinase	KOG0032	Signal transduction mechanisms	CELLULAR PROCESSES AND SIGNALING	293.44444	0.21016	-0.66051
71	531645	Uncharacterized conserved protein	KOG0591	Cell cycle control, cell division, chromosome partitioning	CELLULAR PROCESSES AND SIGNALING	67.57778	0.46256	-0.82484
72	72125	Protein phosphatase 2A-associated protein	KOG2830	Signal transduction mechanisms	CELLULAR PROCESSES AND SIGNALING	274.31111	0.32197	-0.87524
73	2824	Mitochondrial ribosomal protein MRP7 (L2)	KOG4600	Translation, ribosomal structure and biogenesis	INFORMATION STORAGE AND PROCESSING	159.13333	0.25108	-0.97565
74	370513	Mitochondrial/chloroplast ribosomal protein L22	KOG1711	Translation, ribosomal structure and biogenesis	INFORMATION STORAGE AND PROCESSING	224.6	0.297	-0.89289
75	10121	unknown protein	-	-	-	282.58333	0.32011	-0.84851
76	112181	Uncharacterized conserved protein	KOG2827	Function unknown	POORLY CHARACTERIZED	194.22222	0.2934	-0.89603

77	95165	Ribosomal protein S5	KOG2646	Translation, ribosomal structure and biogenesis	INFORMATION STORAGE AND PROCESSING	171.2	0.22951	-1.1097
78	111451	Uncharacterized conserved protein	KOG2428	Function unknown	POORLY CHARACTERIZED	244.4	0.27948	-0.82248
79	480170	unknown protein	-	-	-	239.55556	0.30948	-0.95473
80	98158	Thioredoxin binding protein TBP-2/VDUP1	KOG3780	General function prediction only	POORLY CHARACTERIZED	448.86667	0.36385	-1.15674
81	499756	Uncharacterized conserved protein	KOG2734	Function unknown	POORLY CHARACTERIZED	385.4	0.28296	-0.92317
82	511717	Predicted GTP-binding protein (ODN superfamily)	KOG1491	General function prediction only	POORLY CHARACTERIZED	296.48889	0.32968	-1.12092
83	74757	Serine/threonine protein phosphatase	KOG1379	Signal transduction mechanisms	CELLULAR PROCESSES AND SIGNALING	248.55556	0.27022	-0.78698
84	502756	Predicted unusual protein kinase	KOG1235	General function prediction only	POORLY CHARACTERIZED	302.28889	0.24768	-0.87987
85	507555	Uncharacterized conserved protein	KOG3299	Function unknown	POORLY CHARACTERIZED	326.77778	0.3046	-0.92738
86	92809	Mitochondrial F1-ATPase assembly protein	KOG3281	Posttranslational modification, protein turnover, chaperones	CELLULAR PROCESSES AND SIGNALING	202.06667	0.28929	-0.93701
87	286050	unknown protein	-	-	-	346.88889	0.24156	-0.86956
88	491877	40 kDa farnesylated protein associated with peroxisomes	KOG3133	Intracellular trafficking, secretion, and vesicular transport	CELLULAR PROCESSES AND SIGNALING	185.04444	0.2698	-0.96341
89	121932	Serine/threonine protein phosphatase	KOG1379	Signal transduction mechanisms	CELLULAR PROCESSES AND SIGNALING	222.24444	0.27318	-0.87722
90	504850	Arginyl-tRNA-protein transferase	KOG1193	Posttranslational modification, protein turnover, chaperones	CELLULAR PROCESSES AND SIGNALING	292.46667	0.34457	-0.71999
91	84127	Chaperonin complex component, TCP-1 eta subunit (CCT7)	KOG0361	Posttranslational modification, protein turnover, chaperones	CELLULAR PROCESSES AND SIGNALING	152.02222	0.14221	-0.89045
92	491076	Vacuolar assembly/sorting protein VPS9	KOG2319	Intracellular trafficking, secretion, and vesicular transport	CELLULAR PROCESSES AND SIGNALING	442.44444	0.28916	-0.87259
93	500553	Serine/threonine protein phosphatase	KOG0698	Signal transduction mechanisms	CELLULAR PROCESSES AND SIGNALING	271.17778	0.25049	-0.94853
94	6904	Dual specificity phosphatase	KOG1716	Defense mechanisms	CELLULAR PROCESSES AND SIGNALING	229.22222	0.28574	-0.91421
95	495079	ER lumen protein retaining receptor	KOG3106	Intracellular trafficking, secretion, and vesicular transport	CELLULAR PROCESSES AND SIGNALING	199.48889	0.26943	-0.88923
96	106337	unknown protein	-	-	-	361.55556	0.25498	-0.97365
97	217221	Protein transporter of the TRAM (translocating chain-associating membrane) superfamily	KOG1607	Intracellular trafficking, secretion, and vesicular transport	CELLULAR PROCESSES AND SIGNALING	277.91111	0.25261	-0.77118
98	507914	Actin-related protein Arp2/3 complex, subunit Arp2	KOG0677	Cytoskeleton	CELLULAR PROCESSES AND SIGNALING	101.26667	0.14238	-0.86083
99	106405	Protein involved in mRNA turnover	KOG0816	RNA processing and modification	INFORMATION STORAGE AND PROCESSING	79.33333	0.22574	-0.65019
100	138541	Ran GTPase-activating protein	KOG1909	RNA processing and modification, Nuclear structure, Signal transduction mechanisms	INFORMATION STORAGE AND PROCESSING	135.33333	0.24054	-0.8401

S2B Table

Species	<i>Trichoderma atroviride</i>	<i>Trichoderma virens</i>	<i>Trichoderma reesei</i>	<i>Trichoderma harzianum</i>	<i>Trichoderma longibrachiatum</i>	<i>Trichoderma asperellum</i>	<i>Trichoderma citrinoviride</i>	<i>Trichoderma guihouense</i>	<i>Trichoderma parareesei</i>
Strain ID	IMI 206040	Gv29-8	Qm 6a	CBS 226.95	ATCC 18648	CBS 433.97	IMI 232088	NAU 4742	CBS 125925
Version of annotation in JGI	v2.0	v2.0	v2.0	v1.0	v1.0	v1.0	v1.0	LVVK000000000.1	LFMI000000000.1
1	201457	58016	64874	82401	361714	55122	49399	OPB36334.1	OTA05882.1
2	311401	196271	58239	503986	63437	22870	66713	OPB38985.1	OTA03246.1
3	41037	66986	65646	238777	22374	62722	7463	OPB44908.1	OTA08363.1
4	80552	114634	64175	85356	365364	68939	157453	OPB44409.1	OTA05907.1
5	292288	49798	69490	120562	362341	457853	141716	OPB45589.1	OTA01114.1
6	136196	30459	56426	11235	62616	64418	52621	OPB35980.1	OTA02815.1
7	235666	67158	3653	139606	359431	133937	51287	OPB42491.1	OTA07238.1
8	132504	29022	62986	95023	59344	47838	7120	OPB39781.1	OTA05850.1
9	247846	51932	55802	72100	64036	130802	707	OPB38186.1	OTA08616.1
10	7480	84891	65591	81451	298556	160193	66845	OPB41926.1	OTA01414.1
11	236852	61393	58282	80456	44902	66944	5697	OPB42290.1	OTA02327.1
12	243393	36325	55631	491859	50383	244178	63803	OPB37075.1	OTA03623.1
13	294914	35867	3212	490345	357610	134891	66749	OPB42986.1	OTA06815.1
14	302439	90721	48366	518933	62231	92348	164833	OPB37751.1	OTA03344.1
15	298716	111476	66792	49445	7732	62474	68345	OPB41331.1	OTA00997.1
16	302937	33294	70439	481881	103631	69394	64151	OPB43993.1	OTA06403.1
17	315909	59805	105518	10016	685	29670	165655	OPB40930.1	OTA04640.1
18	87063	125482	61116	494174	18617	55453	2594	OPB36653.1	OTA07173.1
19	300621	80881	122531	512504	346960	24207	3165	OPB35951.1	OTA07065.1
20	30674	195596	120752	478551	78813	219864	57231	OPB39333.1	-
21	300063	93024	80922	79764	62090	149963	47430	OPB43590.1	OTA06768.1
22	297251	80807	21609	509002	362645	144539	168735	OPB46999.1	OTA04013.1
23	138654	77948	29756	514040	61959	61417	17430	OPB43510.1	OTA04605.1
24	149241	29212	55814	503006	358692	54531	536	OPB38341.1	OTA00496.1
25	135900	56206	66707	76997	653	53621	169251	OPB38969.1	OTA00642.1
26	211836	44486	56682	729	362750	143849	160218	OPB38429.1	OTA02518.1
27	302192	35406	55644	352623	360608	57022	167813	OPB37308.1	OTA03063.1
28	299801	219641	68336	479595	17931	60141	46690	OPB37445.1	OTA04544.1
29	301037		55644	502882	358604	54447	167573	OPB38431.1	OTA08086.1
30	161811	112647	58631	263800	364555	57613	2741	OPB45224.1	OTA01416.1
31	188579	75497	75689	478827	15418	70823	169492	OPB39607.1	OTA02071.1
32	299218	165290	58239	97567	16155	97006	66551	OPB40888.1	OTA03715.1
33	130946	54175	63568	729	16562	43438	63160	OPB38429.1	OTA08088.1
34	129673	42016	5066	510952	68150	177565	8138	OPB41439.1	OTA03519.1
35	295500	203700	62986	89866	57130	47838	2826	OPB40163.1	OTA06457.1
36	129922	57511	121948	11153	62330	32107	163062	OPB46613.1	-
37	28889	38208	105191	281509	470	63993	5902	OPB42910.1	OTA01971.1
38	140480	49572	62181	513792	364963	148427	164016	OPB44682.1	OTA06384.1
39	297058	85866	74386	89828	21148	25832	2785	OPB40126.1	OTA01594.1
40	294017	61457	53647	71143	46051	305694	16072	OPB38655.1	OTA03125.1
41	297912	69167	67534	480715	48664	45598	50769	OPB42663.1	OTA01299.1
42	317542	209821	120940	10328	93344	248082	165409	OPB41091.1	OTA02136.1
43	36851	37118	60698	493940	353588	55653	68459	OPB36839.1	OTA00265.1
44	280585	40506	57904	3687	63035	28819	57923	OPB42169.1	OTA02064.1
45	283660	14525	111799	484185	65934	68829	169473	OPB45568.1	OTA01125.1
46	29235	65449	120806	478444	44536	63886	143294	OPB39244.1	OTA08457.1
47	226570	56894	2829	491227	63096	126050	142301	OPB39447.1	OTA07449.1
48	219318	57640	68364	95880	39959	138849	156249	OPB45144.1	OTA00160.1
49	298248	29973	57399	3687	49073	25180	158141	OPB42169.1	OTA07418.1
50	32174	159566	57016	7270	6589	136379	49623	OPB40151.1	OTA03592.1
51	2986	153171	81109	1304	5075	128196	19843	OPB42859.1	OTA03025.1
52	222293	208744	61279	126556	274874	24825	61073	OPB36907.1	OTA02257.1
53	144885	42056	80105	8065	366145	202861	-	OPB41498.1	OTA07894.1
54	289864	219900	119721	4021	48987	135639	51288	OPB42499.1	OTA07245.1
55	85337	56457	76515	490649	44207	157321	165921	OPB38982.1	OTA03250.1
56	296421	33419	22731	5601	297341	69100	154618	OPB44263.1	OTA00256.1
57	172973	114201	37067	86453	38971	434864	160085	OPB47170.1	OTA04347.1
58	152830	22717	78242	4377	23188	148442	54844	OPB37800.1	OTA03321.1
59	172730	214710	52446	512767	366678	59006	6919	OPB45747.1	OTA07006.1
60	220443	123053	68430	94685	22964	145129	29823	OPB40507.1	OTA00583.1
61	163579	29880	54208	478447	351579	45382	158799	OPB39248.1	OTA06771.1
62	52992	166273	54961	509997	67292	67583	168343	OPB40124.1	OTA01592.1
63	177404	31206	74099	81478	351313	134151	159225	OPB42549.1	OTA01636.1

64	152507	44038	4862	125203	53323	68505	66927	OPB45243.1	OTA06413.1
65	81964	31045	54202	80647	17332	56205	51569	OPB42305.1	OTA05785.1
66	290777	155005	70736	477659	59580	66525	67702	OPB37959.1	OTA00147.1
67	175575	230521	55592	73286	16583	43470	45221	OPB38408.1	OTA01978.1
68	152029	33926	68492	94490	21263	49059	66201	OPB40446.1	OTA04234.1
69	158499	36994	70266	501612	20563	153642	62163	OPB45952.1	OTA04763.1
70	42549	219049	53402	493763	367327	259993	164757	OPB37771.1	OTA08191.1
71	188833	66332	104369	531645	-	90942	19569	OPB46920.1	OTA05090.1
72	294385	179542	74861	72125	358861	54692	654	OPB38250.1	OTA01008.1
73	84263	35553	121408	2824	360745	136931	16808	OPB37185.1	OTA08129.1
74	301353	230083	22821	370513	65765	24024	140492	OPB41915.1	OTA00804.1
75	140440	181964	122067	10121	21506	147575	164325	OPB37900.1	OTA04834.1
76	297752	215604	119739	112181	359405	134403	158920	OPB42415.1	OTA00701.1
77	132473	184358	78661	95165	59389	142583	144538	OPB39818.1	OTA07029.1
78	129005	61548	21152	111451	359746	163042	168495	OPB42131.1	OTA07447.1
79	316201	31470	1735	480170	2286	135782	3241	OPB42136.1	OTA07461.1
80	240732	113039	46446	98158	344803	146583	165275	OPB41024.1	OTA01660.1
81	35792	89472	22660	499756	365487	132722	157861	OPB35933.1	OTA04367.1
82	299655	215018	81447	511717	367005	59890	54783	OPB40473.1	OTA04267.1
83	85076	214564	76083	74757	357392	53333	57688	OPB39246.1	OTA08455.1
84	300977	27740	68371	502756	358482	54348	167549	OPB38514.1	OTA02543.1
85	293410	141842	31812	507555	361557	66016	155492	OPB36518.1	OTA05036.1
86	216557	183392	22885	92809	366179	150764	-	OPB41541.1	OTA00014.1
87	250164	165435	77829	286050	19997	126789	162089	OPB43044.1	OTA08035.1
88	299866	15606	122431	491877	49443	144864	151240	OPB37094.1	OTA03633.1
89	290977	24738	66702	121932	59922	93163	147549	OPB41449.1	OTA03508.1
90	265248	50325	67205	504850	212606	150291	63976	OPB43567.1	OTA06746.1
91	137693	79907	2508	84127	361064	55680	170047	OPB36864.1	OTA06047.1
92	227596	210788	57465	491076	27121	22572	142948	OPB39334.1	-
93	128623	40568	58587	500553	45245	29572	165406	OPB41090.1	OTA05865.1
94	291210	192739	64938	6904	66631	152381	169890	OPB46429.1	OTA00770.1
95	155639	72566	81263	495079	363998	69249	168098	OPB44146.1	OTA06170.1
96	84792	82550	121774	106337	363198	127057	168912	OPB43071.1	OTA05755.1
97	241671	153138	67707	217221	53199	138723	56678	OPB45309.1	OTA00675.1
98	260186	185456	111468	507914	364279	58579	17497	OPB43834.1	OTA01579.1
99	127105	56356	107335	106405	20046	126120	4622	OPB43100.1	OTA06507.1
100	47694	30701	73570	138541	2352	135981	169955	OPB42054.1	OTA00949.1

Protein accession numbers (Protein Id) for 23 genomes used in the phylogenomic analysis.

S3 Table

Distribution of pcwdcazymes in GH families in Hypocreales

GH family	The	Tgui	Tv	Tas	Tat	Tp	Tr	Tl	Tc	Ew	Cm	Man	Mac	Bb	Os	Fg	Fo	Nc	Ncr	Cg
GH5	4	4	4	4	4	3	3	3	3	5	7	8	8	7	2	13	22	18	6	10
GH6	1	1	1	1	1	1	1	1	1	0	0	0	0	0	1	1	1	1	3	4
GH7	2	2	2	2	2	2	2	2	2	1	0	0	4	0	0	2	3	2	5	6
GH12	3	3	4	3	3	2	2	2	2	2	0	0	0	0	1	1	4	6	2	4
GH45	1	2	1	1	1	1	1	1	1	0	0	0	0	0	0	1	1	1	1	2
GH1	4	2	2	2	4	2	2	2	2	2	2	4	4	2	0	4	6	5	1	1
GH3	17	19	17	17	16	15	13	13	13	10	9	7	6	10	3	22	32	38	11	13
GH10	2	2	2	2	1	1	1	1	1	0	0	0	0	1	0	5	5	3	4	7
GH11	4	4	4	4	4	3	3	3	3	0	0	0	0	0	0	2	3	3	2	9
GH30	3	3	3	2	2	2	2	2	2	0	0	0	0	0	0	1	3	0	2	2
GH74	1	1	1	1	1	1	1	1	1	1	0	0	0	0	5	1	6	5	6	9
GH26	2	0	2	0	0	0	0	0	0	0	0	0	0	0	0	0	0	0	1	1

Species abbreviated as:	GH families										Czymes									
	The	Tgui	Tv	Tas	Tat	Tp	Tr	Tl	Tc	Ew	Cm	Man	Mac	Bb	Os	Fg	Fo	Nc	Ncr	Cg
<i>Cordyceps militaris</i>																				
<i>Metarhizium anisopliae</i>																				
<i>Metarhizium acridum</i>																				
<i>Beauveria bassiana</i>																				
<i>Ophiocordyceps sinensis</i>																				
<i>Fusarium graminearum</i>																				
<i>Fusarium oxysporum</i>																				
<i>Nectria cinnabarina</i>																				
<i>Neurospora crassa</i>																				
<i>Chaetothium globosum</i>																				

GH27	9	11	10	9	9	8	8	6	8	1	1	2	2	2	0	2	3	1	0	2
GH36	1	2	1	1	1	1	1	1	1	1	2	2	1	2	1	3	2	1	0	0
GH43	4	4	4	6	8	3	3	2	3	1	2	1	1	2	1	17	30	32	7	16
GH51	0	0	0	1	1	0	0	0	0	0	0	0	0	0	0	2	2	1	1	1
GH54	2	2	2	3	3	2	2	2	2	0	1	1	0	1	0	1	1	1	1	0
GH62	2	2	2	2	2	1	1	1	1	0	0	0	0	0	0	1	1	2	0	4
GH67	2	2	2	2	2	1	1	1	1	1	0	0	0	0	0	1	2	0	1	1
GH95	4	5	4	4	4	4	4	4	4	3	0	0	0	1	0	2	2	3	0	1
GH28	6	7	6	5	6	5	4	3	5	1	0	0	0	0	1	6	15	11	2	1
GH35	1	7	1	1	1	1	1	1	1	1	3	2	1	3	1	3	6	8	2	2
GH78	2	1	2	4	3	1	1	1	1	0	0	0	0	0	0	6	16	11	1	1
GH79	4	2	4	4	4	4	4	4	4	1	3	2	2	2	0	1	6	1	2	4
GH88	3	2	3	1	2	0	0	0	0	1	1	1	0	1	0	1	3	5	0	0
GH105	2	1	2	2	2	2	2	2	2	0	0	1	0	0	1	2	3	4	2	1
GH115	1	1	1	1	1	1	1	1	1	1	1	1	0	0	0	2	2	2	1	2

GH121	1	1	0	1	1	0	0	0	0	1	1	1	1	1	1	1	1	1	1	1
GH127	2	2	1	2	2	0	0	0	0	1	1	2	2	1	1	2	1	3	0	1
	90	95	88	88	91	67	64	60	65	35	34	35	32	36	19	106	182	169	65	106

GH - glycosyl hydrolase

Colors indicate conditional formatting from high (red) to low (green) applied to each GH family individually

S4B Table

S4B Table: Results of the NOTUNG analysis of powdCAZome and relevant regulatory proteins

GHs families	EC numbers	NOTUNG						
		Duplication and Loss			Transfer, duplication and loss			
		Event score	Duplications	Gene loss	Event score	Transfers	Duplications	Gene loss
Cellulases								
GH6 Cellobiohydrolase CEL6	EC 3.2.1.91	1090	18	82	680	16	2	17
GH7 Endo- β -1,4-glucanase CEL7B	EC 3.2.1.4	110	16	86	57	17	0	6
GH7 Cellobiohydrolase CEL7A	EC 3.2.1.91	1090	18	82	680	16	2	17
GH5 Endo- β -1,4-glucanase	EC 3.2.1.4	212	36	158	no temporary solution*			
GH5 Endo- β -1,4-glucanase clade A		28.5	5	21	16	4	0	4
GH5 Endo- β -1,4-glucanase clade B		13	4	7	11.5	3	1	1
GH5 Endo- β -1,4-glucanase clade C		29.5	2	22	20	5	0	5
GH12 Endo- β -1,4-glucanase		109	19	81	66.5	18	1	11
GH45 Endo- β -1,4-glucanase		77.5	13	58	43	9	2	13
β-glucosidases								
GH1 β -1,4-glucosidase clade A	EC 3.2.1.21	25.5	5	18	15	5	0	0
GH1 β -1,4-glucosidase clade B		55.5	9	42	33.5	10	1	2
GH1 β -1,4-glucosidase clade C		38.5	7	28	18	5	0	3
GH3 β -1,4-glucosidase		106.5	15	84	47	12	0	11
GH3 β -1,4-glucosidase clade A		50.5	9	37	40	11	0	7
GH3 β -1,4-glucosidase clade B		9	2	6	8	2	0	2
GH3 β -1,4-glucosidase clade Ca		93	16	69	65.5	15	3	16
GH3 β -1,4-glucosidase clade Cb		4.5	1	3	4	1	0	1
Xylanases								
GH10 Endo- β -1,4-xylanase	EC 3.2.1.8	68.5	13	49	36.5	9	1	8
GH11 Endo- β -1,4-xylanase		52.5	11	36	41	7	4	14
GH30 Endo- β -1,4-xylanase		175	20	145	79	19	6	13
β-xylosidases								
GH3 Xylan-1,4- β -xylosidase	EC 3.2.1.37	106.5	15	84	47	12	0	11
Xyloglucanase								
GH74 Xyloglucanase	EC 3.2.1.151		14	60	51	15	0	6
β-mannanases								
GH5 Endo- β -1,4-mannanase	EC 3.2.1.78	66.5	11	50	37.5	10	1	6
GH26 Endo- β -1,4-mannanase		14.5	3	10	9.5	2	1	2
α-galactosidase								
GH27 α -1,4-galactosidase clade A	EC 3.2.1.22	28.5	5	21	19	6	0	1
GH27 α -1,4-galactosidase clade B		28.5	5	21	19	6	0	1
GH27 α -1,4-galactosidase clade C		36.5	7	26	24	8	0	0
GH36 α -1,4-galactosidase		112	24	76	72.5	13	9	20
α-arabinofuranosidase								
xylosidase large clade	EC 3.2.1.55, EC 3.2.1.37	134.5	19	136	no temporary solution*			
GH43 clade A		115	18	88	63.5	16	1	13
GH43 clade B		14.5	3	10	12	3	0	3
GH43 small clade		45.5	9	32	27	7	2	3
xylosidase	EC 3.2.1.55	32.5	5	25	22	6	0	4
GH54 α -L-arabinofuranosidase clade A		136	24	100	66.5	18	5	5

GH54 α -L-arabinofuranosidase clade B	EC 3.2.1.33	66.5	11	50	37.5	10	1	6
GH62 α -L-arabinofuranosidase		147.5	33	98	88	18	14	13
α glucuronidase								
GH67 (xylan) α -1,2-glucuronidase	EC 3.2.1.131	94.5	13	75	49.5	14	1	6
α -fucosidase								
GH95 α -L-fucosidase	EC 3.2.1.51	232	32	175	no temporary solution*			
GH95 α -L-fucosidase clade A		133.5	19	105	no temporary solution*			
GH95 α -L-fucosidase clade Ab		14.5	3	10	12	3	0	3
GH95 α -L-fucosidase clade B		77	12	59	44	11	2	8
Pectinases								
rhamnogalacturonase	EC 3.2.1.67, EC 3.2.1.15,	236.5	35	184	no temporary solution*			
GH28 Polygalacturonase	EC 3.2.1.171,	82.5	13	63	43	12	0	7
GH28 Exo-xylogalacturan hydrolase	EC 3.2.1.-	75.5	13	56	47	12	0	11
GH78 α -L-rhamnosidase	EC 3.2.1.40	135.5	17	110	no temporary solution*			
GH78 α -L-rhamnosidase clade A		16	2	13	14.5	2	1	7
GH78 α -L-rhamnosidase clade B		12	2	9	8	2	0	2
GH78 α -L-rhamnosidase clade C		39.5	7	29	16	5	0	1
Pectate lyase								
PL1	EC 4.2.2.2	71	10	56	34	8	0	10
β -glucuronidase								
GH79 β -(4-O-methyl)glucuronidase	EC 3.2.1.31	39.5	9	26	36.5	5	4	17
Unsaturated β -glucuronidase								
hydrolase	EC 3.2.1	183	24	147	94.5	26	1	15
β -arabinobiosidase								
GH121 β -L-arabinobiosidase	EC 3.2.1.-	15.5	3	11	12	4	0	0
GH127 β -L-arabinofuranosidase	EC 3.2.1.185	241	32	193	107	31	1	13
Accessory proteins								
Swollenin		52.5	11	36	23	6	2	2
polysaccharide monooxygenase clade A		131	28	89	88.5	19	9	18
polysaccharide monooxygenase clade B		131.5	25	94	80.5	22	5	7
polysaccharide monooxygenase clade C		103	20	73	56	15	2	8
Regulators								
XYR1		75	16	51	51.5	13	2	8
ACE2		19	4	4	9	0	0	4
ACE3		23.5	5	16	12	0	0	2

S4C Table

S4C Table: Evolutionary origin of pcwdCAZome of *Trichoderma*

Enzymes	GH family	Number of genes in	Max number of	Number of vertically	Number of	Number of genes	Number of cases when	Putative donors
Cellulases	Cellobiohydrolase CEL6	6	1	0	0	1	0	<i>Pestalotiopsis</i>
	Endo- β -1,4-glucanase CEL7B	7	1	0	0	1	0	<i>Talaromyces</i> , <i>Oidiodendron</i>
	Cellobiohydrolase CEL7A	7	1	0	0	1	0	-
	Endo- β -1,4-glucanase Clade A	5	1	0	1	0	0	-
	Endo- β -1,4-glucanase Clade B	5	2	2	0	2	0	-
	Endo- β -1,4-glucanase Clade C	5	1	0	0	0	1	<i>Stachybotrys</i>
	Endo- β -1,4-glucanase Clade A	12	3	2	2	0	1	<i>Talaromyces</i>
	Endo- β -1,4-glucanase Clade B	12	1	0	1	0	0	-
	Endo- β -1,4-glucanase	45	3	2	0	2	1	<i>Colletotrichum</i>
	β -glucosidase	β -1,4-glucosidase Clade A	1	1	0	1	0	0
β -1,4-glucosidase Clade B		1	2	0	0	1	1	Donor unknown
β -1,4-glucosidase Clade C		1	1	0	1	0	0	-
β -1,4-glucosidase		3	14	0	7	3	4	<i>Talaromyces</i> , <i>Aspergillus</i> , <i>Oidiodendron</i>
Xylanases	Endo- β -1,4-xylanase	10	3	2	0	1	2	<i>Botrytis</i>
	Endo- β -1,4-xylanase	11	4	2	0	3	1	<i>Talaromyces</i>
	Endo- β -1,4-xylanase Clade A	30	1	0	0	0	1	<i>Talaromyces</i>
	Endo- β -1,4-xylanase Clade B	30	2	0	0	1	1	<i>Penicillium</i> , <i>Pestalotiopsis</i>
β -xylosidases	Xylan-1,4- β -xylosidase	3	3	0	0	1	2	<i>Talaromyces</i> , <i>Oidiodendron</i>
Xyloglucanase	Xyloglucanase	74	1	0	0	1	0	-
β -mannanases	Endo- β -1,4-mannanase	5	3	2	0	3	0	<i>Stachybotrys</i>
	Endo- β -1,4-mannanase	26	2	2	0	0	2	<i>Rasamsonia</i>
α -galactosidase	α -1,4-galactosidase	27	10	6	3	1	6	<i>Pestalotiopsis</i> , <i>Aureobasidium</i> , <i>Oidiodendron</i>
	α -1,4-galactosidase Clade A	36	1	0	1	0	0	-
	α -1,4-galactosidase Clade B	36	1	0	1	0	0	-
	α -L-arabinofuranosidase and β -xylosidase	43	9	0	2	5	2	<i>Pestalotiopsis</i> , Eurotiomycetes
	α -L-arabinofuranosidase and β -xylosidase	51	1	0	0	0	1	<i>Oidiodendron</i>
α -arabinofuranosidase	α -L-arabinofuranosidase	54	3	0	0	1	2	Eurotiomycetes
	α -L-arabinofuranosidase	62	3	0	0	0	3	<i>Neofusicoccum</i> , <i>Eutypa</i> & Donor unknown
	α -(xylan) α -1,2-glucuronidase	67	2	0	1	0	1	Donor unknown

glucuronidase	α -(4-O-methyl)-glucuronidase	115	1	0	1	0	0	0	-
α -fucosidase	α -L-fucosidase	95	5	2	1	1	3	1	<i>Rasamsonia</i>
	exo-polygalacturonase, rhamnogalacturonase	28	4	0	1	2	1	0	<i>Rasamsonia</i>
Pectinases	polygalacturonase	28	2	0	0	0	2	0	<i>Rosellinia, Diaporthe</i>
	exo-xylogalacturan hydrolase	28	3	2	0	2	1	0	<i>Nectria</i>
	α -L-rhamnosidase	78	7	0	1	2	4	0	<i>Eurotiomycetes, Oidiodendron, Thielaviopsis, Neurospora crassa</i>
Pectate lyase	PL1		1	0	0	1	0	0	-
β -galactosidases	β -galactosidase	35	1	0	1	0	0	0	-
β -glucuronidase	β -(4-O-methyl)-glucuronidase	79	4	0	0	4	0	0	-
Unsaturated β -glucuronidase	Δ -4,5-unsaturated β -glucuronyl hydrolase	88	4	0	0	2	2	0	<i>Eutypa; Torrubilella</i>
Pectin side chains	Unsaturated rhamnogalacturonyl hydrolase	105	1	0	1	0	0	0	-
β -arabinobiosidase	β -L-arabinobiosidase	121	1	0	0	1	0	0	-
	β -L-arabinofuranosidase Clade A	127	1	0	1	0	0	0	-
	β -L-arabinofuranosidase Clade B	127	2	0	0	0	2	0	<i>Diaporthe, Fusarium</i>
Accessory proteins	AA9 Copper-dependent lytic polysaccharide monoxygenase	former "GH61"	3	0	1	1	1	0	<i>Diaporthe</i>
	Swollenin	-	1	0	0	0	1	0	Green plants
Total max			122	24	29	43	50	5	

* as estimated for nine genomes in this study

** may include genes obtained through LGT to *Trichoderma* or dosely related genera (i.g. *Escovopsis*)

*** may include genes obtained by LGT to the LCA of *Trichoderma* and dosely related genera (i.g. *Escovopsis*) that are not counted as LGT to T

GD - gene duplication

LGT - lateral gene transfer

LCA - last common ancestor

GH - glycosyl hydroplase

colors indicate conditional formationg from large (red) to low (green)

S7 Table

Accession numbers of genes used for the multilocus phylogeny of Ascomycota fungi

Species	Accession numbers as available in NCBI			
	Translation initiation factor eif-5, FG832	NAD-dependent glutamate dehydrogenase, FG570	Histone acetyltransferase subunit of the RNA polymerase II holoenzyme, FG533	Tsr1p, a protein required for processing of 20S pre-rRNA, MS277
<i>Acremonium chrysogenum</i> ATCC11550	KFH40585	KFH43944	KFH45370	KFH40757
<i>Arthroderma otae</i> CBS113480	XP_002846695	XP_002846871	XP_002844936	XP_002846635
<i>Aspergillus clavatus</i> NRRL1	XP_001267824	XP_001275231	XP_001273950	XP_001275563
<i>Aspergillus flavus</i> AF70	KJJ32228	KOC07435	KOC07671	KOC10454
<i>Aspergillus nidulans</i>	XP_663671	AAP97491	XP_659898	XP_663870
<i>Aspergillus ruber</i> CBS135680	EYE91640	EYE93860	EYE93445	EYE97746
<i>Aspergillus terreus</i> NIH2624	XP_001218500	XP_001215968	XP_001218036	XP_001208611
<i>Aureobasidium melanogenum</i> CBS110374	KEQ58250	KEQ59374	KEQ66829	KEQ63129
<i>Aureobasidium namibiae</i> CBS14797	XP_013430091	XP_013425835	XP_013425056	XP_013425617
<i>Aureobasidium pullulans</i> EXF150	KEQ84828	KEQ82009	KEQ89537	KEQ83917
<i>Aureobasidium subglaciale</i> EXF2481	XP_013340846	XP_013348192	XP_013345346	XP_013346410
<i>Beauveria bassiana</i> D15	KGQ04568	KGQ04719	KGQ07699	KGQ03110
<i>Bipolaris sorokiniana</i> ND90Pr	XP_007700521	XP_007700378	XP_007697141	XP_007694048
<i>Bipolaris victoriae</i> F13	XP_014550811	EUC37283	XP_014553743	XP_014553549
<i>Blastomyces dermatitidis</i> ER3	EEQ83302	EEQ87716	EEQ87135	EEQ87580
<i>Blumeria graminis</i> f. Sp. <i>Hordei</i> strain DH14	CCU77913	CCU76728	CCU82742	CCU74971
<i>Botrytis cinerea</i> B0510	XP_001551174	XP_001546005	XP_001555701	XP_001554581

<i>Byssochlamys spectabilis</i> No5	GAD93061	GAD98634	GAD97915	GAE00117
<i>Ceratocystis platani</i>	KKF97397	KKF93380	KKF92520	KKF92488
<i>Chaetomium globosum</i>	-	XP_001229575	XP_001225084	XP_001225627
<i>Chaetomium thermophilum</i> .var. <i>Thermophilum</i> DSM1495	XP_006692916	XP_006693160	XP_006697164	XP_006690768
<i>Claviceps purpurea</i> 201	CCE32248	CCE27530	CCE31916	CCE27229
<i>Coccidioides immitis</i> RS	XP_001247026	XP_001247210	XP_001242149	XP_001245726
<i>Colletotrichum fioriniae</i> PJ-7	XP_007594157	XP_007595829	XP_007598740	XP_007589696
<i>Colletotrichum gloeosporioides</i> Naragc5	XP_007273022	XP_007280717	XP_007274706	XP_007273210
<i>Colletotrichum graminicola</i> M1001	XP_008097338	XP_008089298	XP_008089925	XP_008094082
<i>Colletotrichum higginsianum</i>	CCF33365	CCF32485	CCF41278	CCF45682
<i>Colletotrichum orbiculare</i> MAFF240422	ENH81153	ENH86491	ENH79595	ENH87819
<i>Colletotrichum sublineola</i>	KDN66453	KDN62274	KDN62435	KDN65981
<i>Cordyceps militaris</i> CM-01	XP_006672614	-	XP_006672345	XP_006666974
<i>Diaporthe ampelina</i>	KKY36125	KKY39469	KKY34351	KKY37242
<i>Diplodia seriata</i>	KKY23327	KKY20064	KKY20486	KKY13651
<i>Endocarpon pusillum</i> Z07020	XP_007785442	XP_007803903	XP_007805190	XP_007799778
<i>Erysiphe necator</i>	KHJ35773	KHJ31305	KHJ33459	KHJ32223
<i>Escovopsis weberi</i>	KOS19785	KOS21092	KOS21982	KOS19159
<i>Eutypa lata</i> UCREL1	XP_007790145	XP_007791048	XP_007797253	XP_007796337
<i>Exophiala oligosperma</i>	KIW41174	KIW41230	KIW45276	KIW39858
<i>Fusarium avenaceum</i>	KIL84745	KIL86715	KIL90440	KIL88831
<i>Fusarium fujikuroi</i> IMI58289	CCT71378	CCT73629	CCT72218	CCT74024
<i>Fusarium graminearum</i> PH-1	XP_011323961	XP_011321519	XP_011317913	XP_011321202

<i>Fusarium oxysporum</i> Fo5176	EGU75640	EGU88652	EGU85888	EGU81020
<i>Fusarium pseudograminearum</i> CS3096	XP_009254976	XP_009251531	XP_009256525	XP_009257718
<i>Fusarium verticillioides</i> 7600	EWG46746	EWG51267	EWG47370	EWG52526
<i>Gaeumannomyces graminis</i> var <i>tritici</i> R3111a1	XP_009217808	XP_009217057	XP_009222623	XP_009220373
<i>Glarea lozoyensis</i> ATCC 20868	XP_008087910	XP_008079266	XP_008087199	XP_008081765
<i>Grossmannia clavigera</i> kw1407	XP_014173332	XP_014172124	XP_014170080	XP_014175688
<i>Hirsutella minnesotensis</i> 3608	KJZ76027	KJZ76246	KJZ77117	KJZ70383
<i>Macrophomina phaseolina</i> MS6	EKG10915	EKG17612	EKG15858	EKG21725
<i>Madurella mycetomatis</i>	KOP47172	KOP40389	KOP40728	KOP46878
<i>Magnaporthe oryzae</i> 7015	XP_003713892	XP_003712804	XP_003710346	XP_003717850
<i>Magnaporthiopsis poae</i> ATCC64411	KLU87916	KLU89090	KLU85714	KLU91947
<i>Marssonina brunnea</i> f.sp. Multigermtubi mbm1	XP_007288264	XP_007295000	XP_007288845	XP_007296894
<i>Metarhizium acridum</i> cqma102	XP_007814679	XP_007807988	XP_007808318	XP_007808144
<i>Metarhizium album</i> ARSEF1941	KHO00830	KHO01177	KHN97240	KHN97747
<i>Metarhizium anisopliae</i>	KFG80865	KFG82462	KJK84401	KJK83283
<i>Metarhizium brunneum</i> ARSEF3297	XP_014542319	XP_014547521	XP_014544685	XP_014549619
<i>Metarhizium majus</i> ARSEF297	XP_014579347	XP_014580572	XP_014576767	XP_014580192
<i>Metarhizium robertsii</i> ARSEF23	XP_007819774	XP_007818669	XP_007821021	XP_007821580
<i>Microsporium gypseum</i> CBS118893	XP_003174667	XP_003170010	XP_003173533	XP_003174717
<i>Myceliophthora thermophila</i> ATCC42464	XP_003663021	XP_003663104	XP_003661902	XP_003666824
<i>Nectria haematococca</i> mpvi71134	XP_003048814	XP_003044810	XP_003047642	XP_003048538
<i>Neofusicoccum parvum</i> UCRNP2	XP_007580981	XP_007582601	XP_007585848	XP_007586119
<i>Neosartorya fischeri</i> NRRL181	XP_001260399	XP_001260222	XP_001266021	XP_001260747

<i>Neosartorya udagawae</i>	GAO86840	GAO90996	GAO82244	GAO87169
<i>Neurospora crassa</i> OR74A	XP_957252	XP_956780	XP_961595	XP_956952
<i>Neurospora tetrasperma</i> FGSC2508	XP_009851134	XP_009851230	XP_009848039	XP_009851930
<i>Oidiodendron maius</i> Zn	KIN07422	KIM94856	KIN05890	KIN02578
<i>Ophiocordyceps sinensis</i> CO18	EQK99425	EQL03134	EQL00966	EQL02306
<i>Ophiostoma piceae</i> UAMH11346	EPE03528	EPE04279	EPE08587	EPE07763
<i>Penicillium brasilianum</i>	CEJ61108	CEJ62475	CEJ60592	CEO60456
<i>Penicillium camemberti</i>	CRL25325	CRL29131	CRL26538	CRL31076
<i>Penicillium digitatum</i> Pd1	XP_014532577	XP_014535831	XP_014534415	XP_014535368
<i>Penicillium italicum</i>	KGO73776	KGO64856	KGO75861	KGO72170
<i>Penicillium oxalicum</i> 1142	EPS29411	EPS31216	EPS34317	EPS33764
<i>Penicillium roqueforti</i> FM164	CDM27092	CDM36374	CDM35772	CDM35340
<i>Penicillium rubens</i> Wisconsin 541255	XP_002558796	XP_002564843	XP_002557524	XP_002557595
<i>Pestalotiopsis fici</i> W1061	XP_007838617	XP_007832371	XP_007837762	XP_007835675
<i>Podospora anserina</i> Smat	XP_001907948	XP_001907978	XP_001911227	XP_001909286
<i>Pseudocercospora fijiensis</i> CIRAD86	XP_007924684	XP_007928020	XP_007927750	XP_007922079
<i>Pseudogymnoascus destructans</i> 2063121	XP_012740663	XP_012740546	XP_012739073	XP_012741102
<i>Pseudogymnoascus pannorum</i> VKMF4520 (FW2644)	KFZ13121	KFZ15543	KFZ09205	KFZ22821
<i>Pyrenophora teres f teres</i> 01	XP_003305639	XP_003296979	XP_003305194	XP_003301224
<i>Pyrenophora tritici repentis</i> Pt1C BFP	XP_001939654	XP_001941809	XP_001931645	XP_001942331
<i>Rasamsonia emersonii</i> CBS39364	XP_013327757	XP_013329006	XP_013328538	XP_013325377
<i>Rosellinia necatrix</i>	GAP87460	GAP87731	GAP92789	GAP83847
<i>Schizosaccharomyces cryophilus</i> OY26	XP_013021759	XP_013024449	XP_013024728	XP_013024541

<i>Sclerotinia borealis</i> F4157	ESZ92634	ESZ91548	ESZ93290	ESZ98487
<i>Sclerotinia sclerotiorum</i> 1980	XP_001585325	XP_001597916	XP_001592077	XP_001593672
<i>Sordaria macrospora</i> k-hell	XP_003344256	XP_003348872	XP_003348083	XP_003345570
<i>Sphaerulina musiva</i> SO2202	EMF13312	EMF12921	EMF11758	EMF16254
<i>Sporothrix schenckii</i> ATCC58251	ERS99084	ERS98033	ERT00617	ERS94971
<i>Stachybotrys chartarum</i> IBT 7711	KEY67454	KEY65600	KEY72911	KEY72726
<i>Stachybotrys chlorohalonata</i> IBT40285	KFA63476	KFA64546	KFA69092	KFA61210
<i>Talaromyces cellulolyticus</i>	GAM35703	GAM34038	GAM35977	GAM37634
<i>Talaromyces islandicus</i>	CRG90567	CRG84640	CRG88591	CRG88913
<i>Talaromyces marneffeii</i> ATCC18224	XP_002146590	XP_002144568	XP_002148005	XP_002148829
<i>Talaromyces stipitatus</i> ATCC10500	XP_002478899	XP_002340968	XP_002482232	XP_002485387
<i>Thielavia terrestris</i> NRRL8126	XP_003655551	XP_003655469	XP_003649459	XP_003657675
<i>Thielaviopsis punctulata</i>	KKA26865	KKA30551	KKA30016	KKA28760
<i>Tolypocladium ophioglossoides</i> CBS 100239	KND92606	KND90861	KND87416	KND92841
<i>Torrubiella hemipterigena</i>	CEJ81407	CEJ92104	CEJ94403	CEJ94139
<i>Trichoderma asperellum</i> CBS 433.97	149508	147189	62284	72524
<i>Trichoderma atroviride</i> IMI206040	298941	195239	156760	132866
<i>Trichoderma citrinoviride</i>	1129948	1121793	1126893	1136381
<i>Trichoderma guizhouense</i> NJAU 4742	OPB46086.1	OPB41095.1	OPB44921.1	OPB46249.1
<i>Trichoderma harzianum</i> CBS 226.95	322295	98433	93763	556214
<i>Trichoderma longibrachiatum</i> ATCC 18648	1423421	16127	1342124	1379254
<i>Trichoderma parareesei</i> CBS 125925	OTA08872.1	OTA02151.1	OTA00115.1	OTA04911.1
<i>Trichoderma reesei</i> QM 6a	71410	120943	4989	79817

<i>Trichoderma virens</i> Gv29-8	83678	155799	46168	77118
<i>Trichophyton tonsurans</i> CBS112818	EGD93608	EGE00928	EGD92577	EGD93652
<i>Uncinocarpus reesii</i> 1704	XP_002541248	XP_002541415	XP_002544814	XP_002583466
<i>Ustilagoidea virens</i>	GAO16418	KDB16499	KDB11495	KDB12964
<i>Verticillium alfalfae</i> vams102	XP_003003264	XP_003003088	XP_003000323	XP_003007415
<i>Verticillium dahliae</i> vds17	XP_009653581	XP_009653395	XP_009652650	XP_009656273
<i>Agaricus bisporus</i>	114395	113776	119162	119186
<i>Arthrobotrys oligospora</i>	2379	6097	11173	6523
<i>Aspergillus flavus</i>	30845	38067	36853	36445
<i>Aspergillus fumigatus</i>	2404	2222	6414	2763
<i>Auricularia subglabra</i>	1271474	1276760	1305816	1202878
<i>Gymnopus luxurians</i>	69825	67202	164030	37524
<i>Neofusicoccum parvum</i>	3316	5160	8692	9017
<i>Pleurotus ostreatus</i>	1097707	40761	1073399	1112540
<i>Plicaturopsis crispa</i>	145990	106373	41305	37427
<i>Punctularia strigosozonata</i>	94231	49580	104430	121264
<i>Sphaerobolus stellatus</i>	183735	29602	208026	225108
<i>Thermoascus aurantiacus</i>	37335	5956	2972	4101
<i>Trametes versicolor</i>	109140	156153	164836	160557
<i>Tulasnella calospora</i>	242038	213963	142430	27765

Chapter 3.2 Phylome of *Trichoderma* carbohydrate-active enzymes involved in degradation of plant cell wall (pcwdcazome) and regulatory proteins

One of the main prerequisites for the study presented in the Chapter 3⁷ was the detailed evolutionary analysis of all carbohydrate-active enzymes required for the plant cell wall degradation, assessor proteins, and their regulators. These were also necessary to carry out the subsequent statistical analyses necessary to test the hypothesis of lateral gene transfers. A reduced version of this phylome is presented in the supplement to Druzhinina *et al.* (2018).

The purpose of this subchapter to be highlighted in the dissertation is to provide a detailed overview on the evolution/acquisition of Carbohydrate-Active enzymes (cazymes) in *Trichoderma* species. The putative donors of laterally transferred pcwdcazymes might be of interest to researchers studying cellulases. For instance, the gain of CEL6A that proceeds from the nonreducing cellulose ends complements the presence of CEL7A that acts at the reducing end, and therefore allows a processive movement along cellulose and an increase the speed of its degradation, reveal that improvements in cellulose and hemicellulose degradation were a key trait for the phytophagy of this fungus. It is worthwhile to note that the version of the phylome presented in the dissertation also describes cases of the lateral gene transfers that took place before the diversification between *Trichoderma* and *Escovopsis* genera that were omitted from Druzhinina *et al.* (2018). It includes the major secreted cellobiohydrolase CEL7A (CBH1) used in industrial applications, the GH 5 Endo- β -1,4-mannanase and the pectate lyase PL1.

The sub-chapter comprises of Bayesian phylogenetic trees and uses schematic symbols to show **loss, duplication, plesiomorphic** and in total **53 gene transfer events** that enriched the ability of initially mycotrophic *Trichoderma* to feed on dead plant biomass.

Next to species name are the accession number as published in NCBI. The ids which start with Triat, Trias, Triha, Trici, Trilo, Trire, Trivi are protein ids as published in JGI (Joint Genome

⁷ Druzhinina IS, Chenthamara K, Zhang J, Atanasova L, Yang D, Miao Y, Rahimi MJ, Grujic M, Cai F, Pourmehdi S, Salim KA. Massive lateral transfer of genes encoding plant cell wall-degrading enzymes to the mycoparasitic fungus *Trichoderma* from its plant-associated hosts. PLoS Genetics. 2018 Apr 9;14(4):e1007322.

Institute) for that particular species. The protein ids for *T. Guizhouense*, *T. Parareesei*, and *Escovopsis weberi* (except those which starts with KOS) are as available in TUCIM (The TU Collections of Industrial Microorganisms) local database.

Table of Contents







PcwdCAZYmes

GH6	EC 3.2.1.91	Cellobiohydrolase CEL6	138
GH7	EC 3.2.1.4	Endo- β -1,4-glucanase CEL7B	139
GH7	EC 3.2.1.91	Cellobiohydrolase CEL7A	140
GH5	EC 3.2.1.4	Endo- β -1,4-glucanase Clade A	141
GH5	EC 3.2.1.4	Endo- β -1,4-glucanase Clade B	142
GH5	EC 3.2.1.4	Endo- β -1,4-glucanase Clade C	143
GH12	EC 3.2.1.4	Endo- β -1,4-glucanase Clade A	144
GH12	EC 3.2.1.4	Endo- β -1,4-glucanase Clade B	145
GH45	EC 3.2.1.4	Endo- β -1,4-glucanase	146
GH1	EC 3.2.1.21	β -1,4-glucosidase Clade A	147
GH1	EC 3.2.1.21	β -1,4-glucosidase Clade B	148
GH1	EC 3.2.1.21	β -1,4-glucosidase Clade C	149
GH3	EC 3.2.1.21	β -1,4-glucosidase	150

GH10	EC 3.2.1.8	Endo- β -1,4-xylanase Clade A	152
GH10	EC 3.2.1.8	Endo- β -1,4-xylanase Clade B	153
GH11	EC 3.2.1.8	Endo- β -1,4-xylanase	154
GH30	EC 3.2.1.8	Endo- β -1,4-xylanase Clade A	155
GH30	EC 3.2.1.8	Endo- β -1,4-xylanase Clade B	156
GH3	EC 3.2.1.37	Xylan-1,4- β -xylosidase	157
GH74	EC3.2.1.151	Xyloglucanase	158
GH5	EC 3.2.1.78	Endo- β -1,4-mannanase	159
GH26	EC 3.2.1.78	Endo- β -1,4-mannanase	160
GH27	EC 3.2.1.22	α -1,4-galactosidase	161
GH36	EC 3.2.1.22	α -1,4-galactosidases clade A	163
GH36	EC 3.2.1.22	α -1,4-galactosidases clade B	164
GH43	EC 3.2.1.55, EC 3.2.1.37	α -L-arabinofuranosidase and β -xylosidase	165
GH51	EC 3.2.1.55	α -L-arabinofuranosidase and β -xylosidase	166

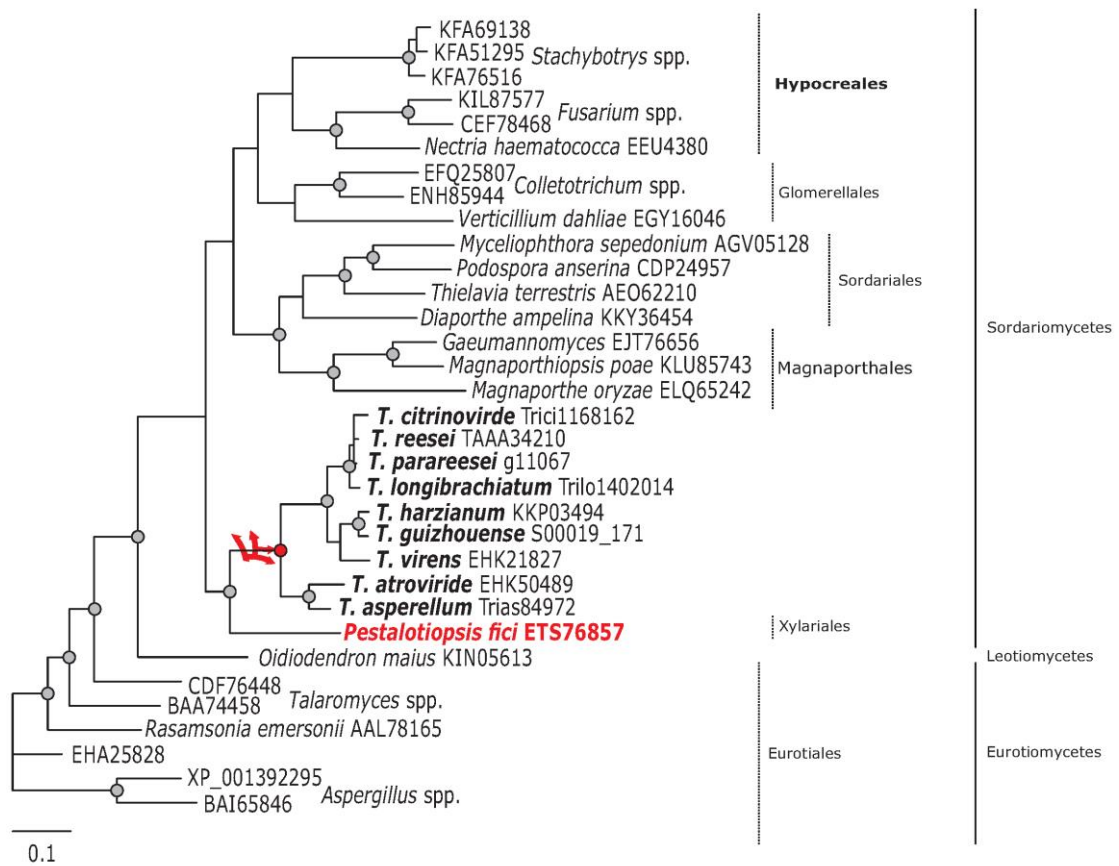
GH54	EC 3.2.1.55	α -L-arabinofuranosidase	167
GH62	EC 3.2.1.55	α -L-arabinofuranosidase	168
GH67	EC 3.2.1.131	(xylan) α -1,2-glucuronidase	169
GH115	EC 3.2.1.	A-(4-O-methyl)-glucuronidase	170
GH95	EC 3.2.1.51	α -L-fucosidase	171
GH28	EC 3.2.1.67, EC 3.2.1.171	exo-polygalacturonase and rhamnogalacturonase	172
GH28	EC 3.2.1.15	Polygalacturonase	173
GH28	EC 3.2.1.-	Exo-xylogalacturan hydrolase	174
GH78	EC 3.2.1.40	α -L-rhamnosidase	175
PL1	EC 4.2.2.2	Pectate lyase	176
GH35	EC 3.2.1.23	β -galactosidase	177
GH79	EC 3.2.1.31	β -(4-O-methyl)-glucuronidase	178
GH88	EC 3.2.1	Δ -4,5-unsaturated β -glucuronyl hydrolase	179
GH105	EC 3.2.1.172	Unsaturated rhamnogalacturonyl hydrolase	180

GH121 EC 3.2.1.-	β -L-arabinobiosidase	181
GH127 EC 3.2.1.185	β -L-arabinofuranosidase Clade A	182
GH127 EC 3.2.1.185	β -L-arabinofuranosidase Clade B	183
AA9 (formerly "GH61")	Copper-dependent lytic polysaccharide monooxygenase	184
Swollenin		186
pcwdCAZYme Regulator Proteins		
XYR1		187
ACE2		188
ACE3		189







-  LGT
-  adelphoLGT
- Donor/s
-  Incongruent topology
-  Plesiomorphy
-  Gene Duplication
-  Insufficient data

GH6
EC 3.2.1.91

Cellobiohydrolase CEL6A

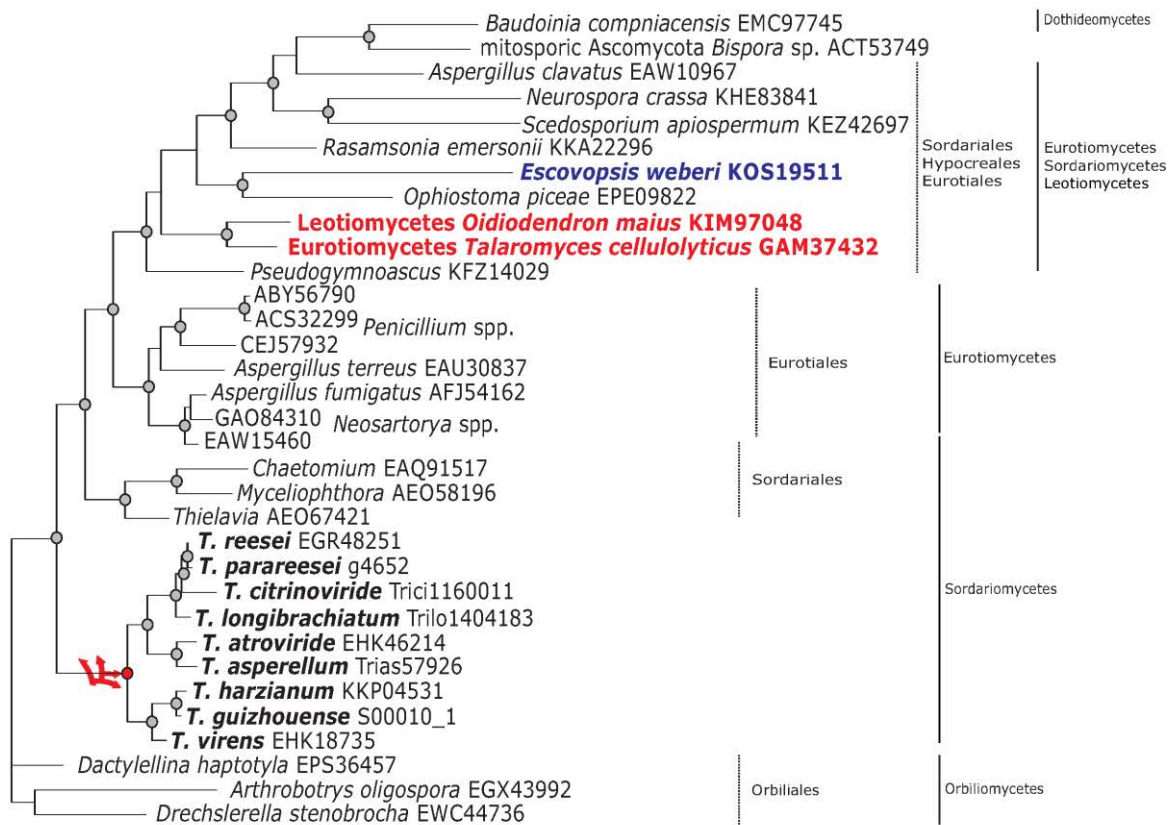


Phylogram based on Dayhoff amino acid substitution model using an alignment containing 20707 characters. Bayesian analysis was run for 1 million mcmc generations and a strict consensus tree was obtained by summarizing 7500 trees, after burning first 25% of obtained 10,000 trees. Mean tree length and variance are 7.269450E+00 and 3.9080650E-02, respectively. Posterior probabilities more than 90% are marked with circular nodes. Dashed vertical bars and non-dashed vertical bars represents the taxonomic order and taxonomic class in the phylum Ascomycota, respectively.

-  LGT
-  adelphoLGT
- Donor/s
-  Incongruent topology
-  Plesiomorphy
-  Gene Duplication
-  Insufficient data


GH7
EC 3.2.1.4

Endo-β-1,4-glucanase CEL7B



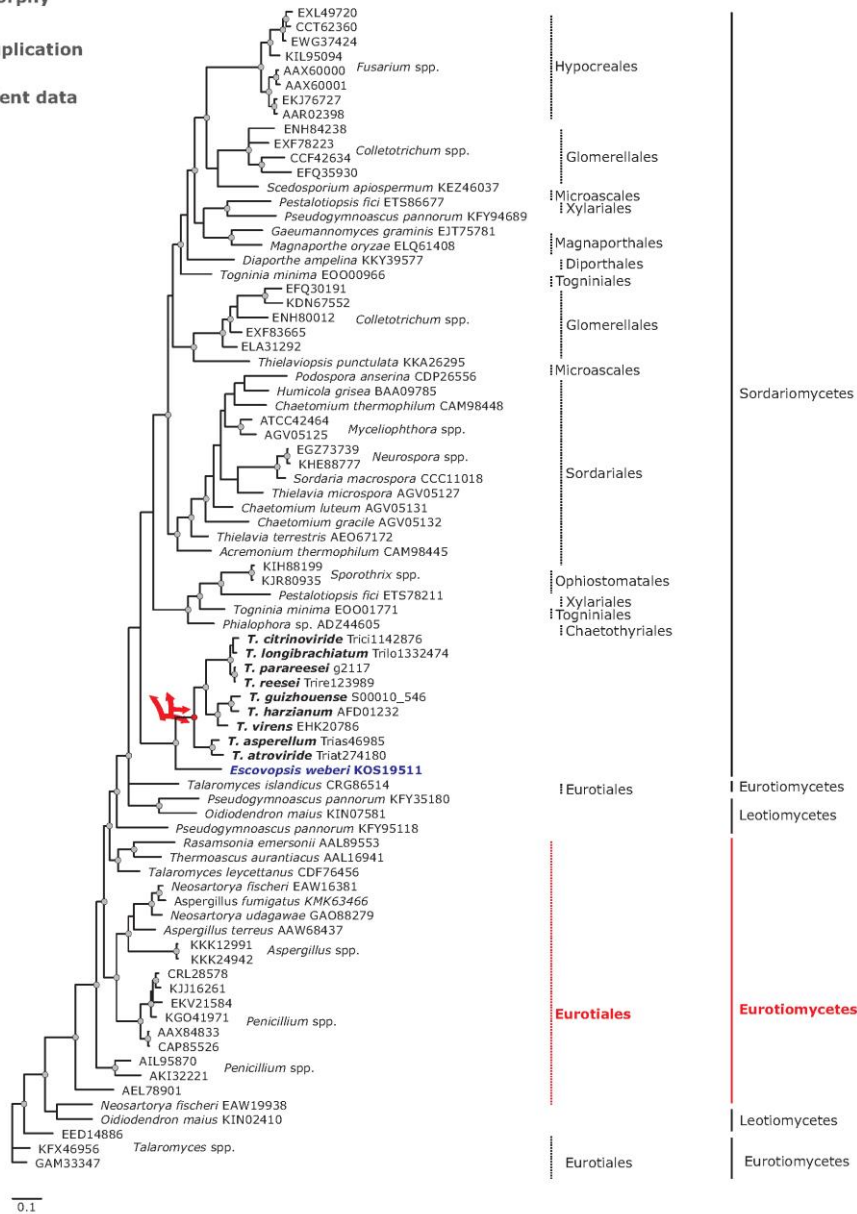
0.1

Phylogram based on Dayhoff amino acid substitution model using an alignment containing 18546 characters. Bayesian analysis was run for 1 million mcmc generations and a strict consensus tree was obtained by summarizing 7500 trees, after burning first 25% of obtained 10,000 trees. Mean tree length and variance are 7.457580E+00 and 2.1536720E-02, respectively. Posterior probabilities more than 90% are marked with circular nodes. Dashed vertical bars and non-dashed vertical bars represents the taxonomic order and taxonomic class in the phylum Ascomycota, respectively.

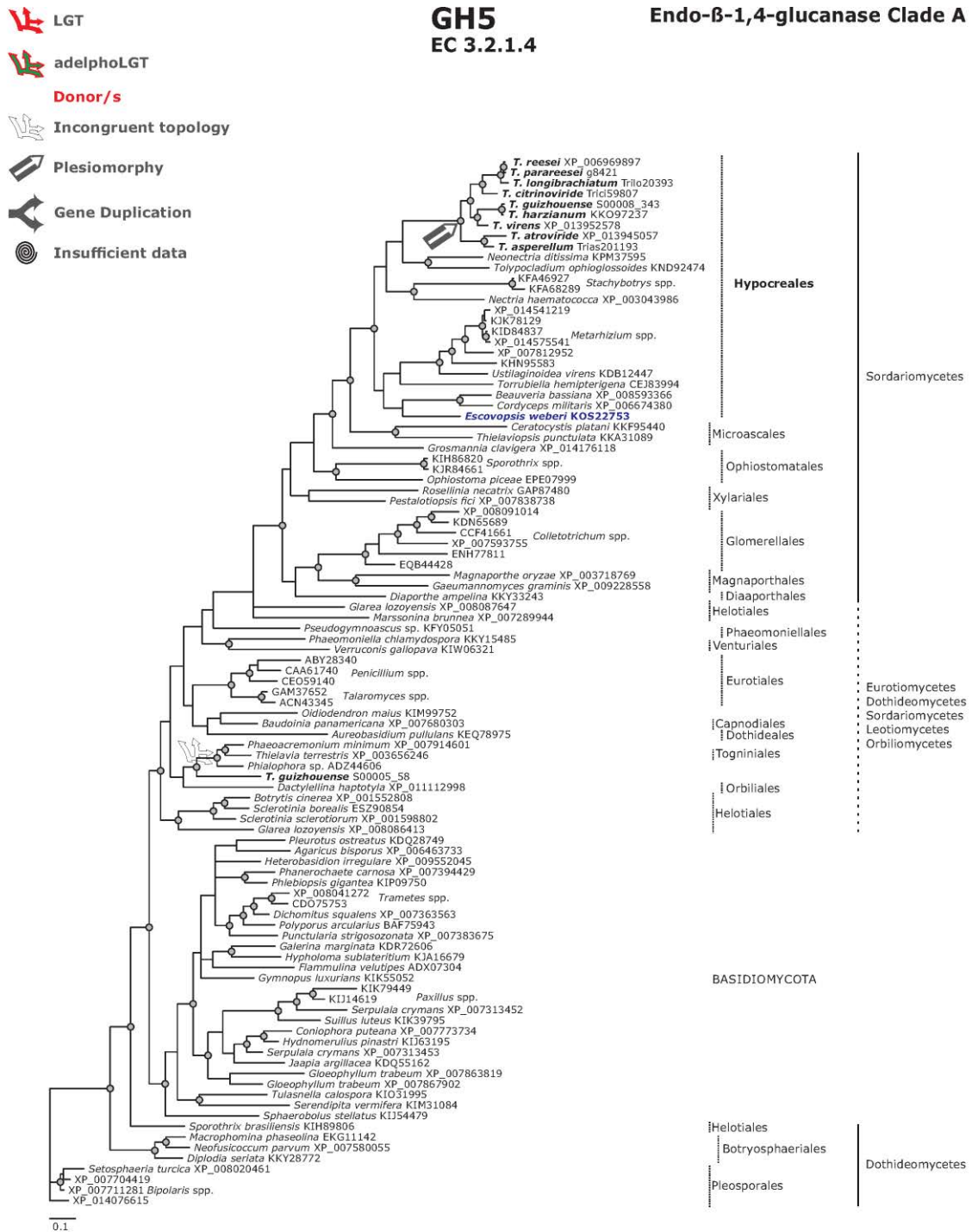
-  LGT
-  adelphoLGT
- Donor/s
-  Incongruent topology
-  Plesiomorphy
-  Gene Duplication
-  Insufficient data

**GH7
EC 3.2.1.91**

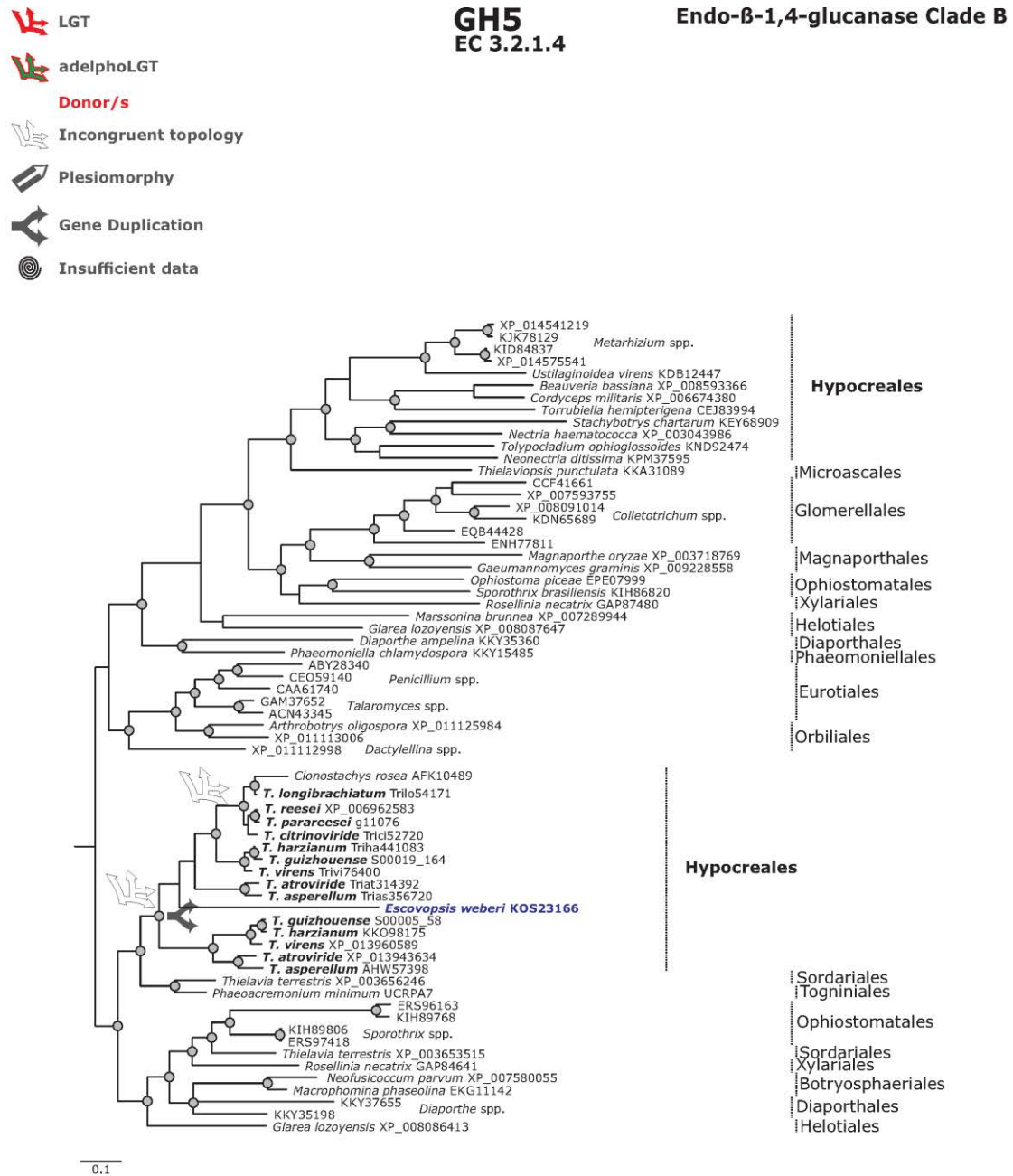
Cellobiohydrolase CEL7A









Phylogram based on Dayhoff amino acid substitution model using an alignment containing 38720 characters. Bayesian analysis was run for 1 million mcmc generations and a strict consensus tree was obtained by summarizing 7500 trees, after burning first 25% of obtained 10,000 trees. Mean tree length and variance are 9.480271E+00 and 2.2693320E-02, respectively. Posterior probabilities more than 90% are marked with circular nodes. Dashed vertical bars and non-dashed vertical bars represents the taxonomic order and taxonomic class in the phylum Ascomycota, respectively.



Phylogram based on Dayhoff amino acid substitution model using an alignment containing 70686 characters. Bayesian analysis was run for 1 million mcmc generations and a strict consensus tree was obtained by summarizing 7500 trees, after burning first 25% of obtained 10,000 trees. Mean tree length and variance are 2.425237E+01 and 7.0550690E-02, respectively. Posterior probabilities more than 90% are marked with circular nodes. Dashed vertical bars and non-dashed vertical bars represents the taxonomic order and taxonomic class in the phylum Ascomycota, respectively.

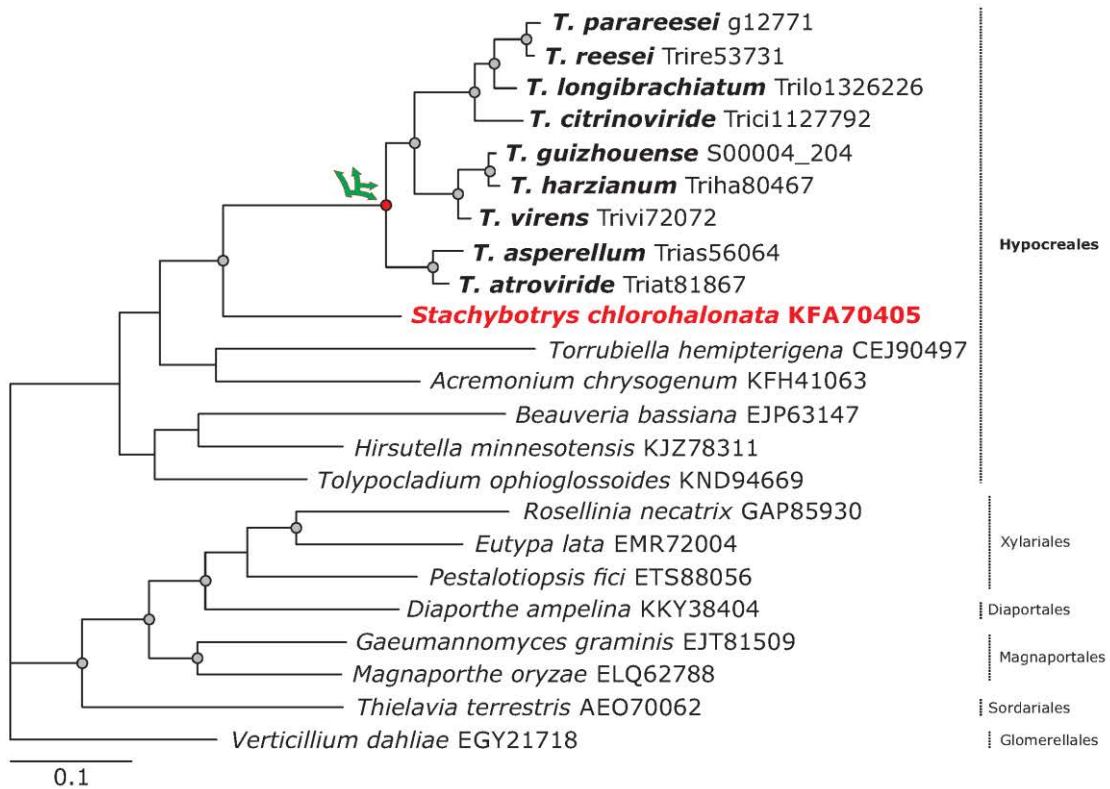


Phylogram based on Dayhoff amino acid substitution model using an alignment containing 116172 characters. Bayesian analysis was run for 10 million mcmc generations and a strict consensus tree was obtained by summarizing 75000 trees, after burning first 25% of obtained 100,000 trees. Mean tree length and variance are 3.029779E+01 and 8.9287420E-02, respectively. Posterior probabilities more than 90% are marked with circular nodes. Dashed vertical bars and non-dashed vertical bars represents the taxonomic order and taxonomic class in the phylum Ascomycota, respectively.

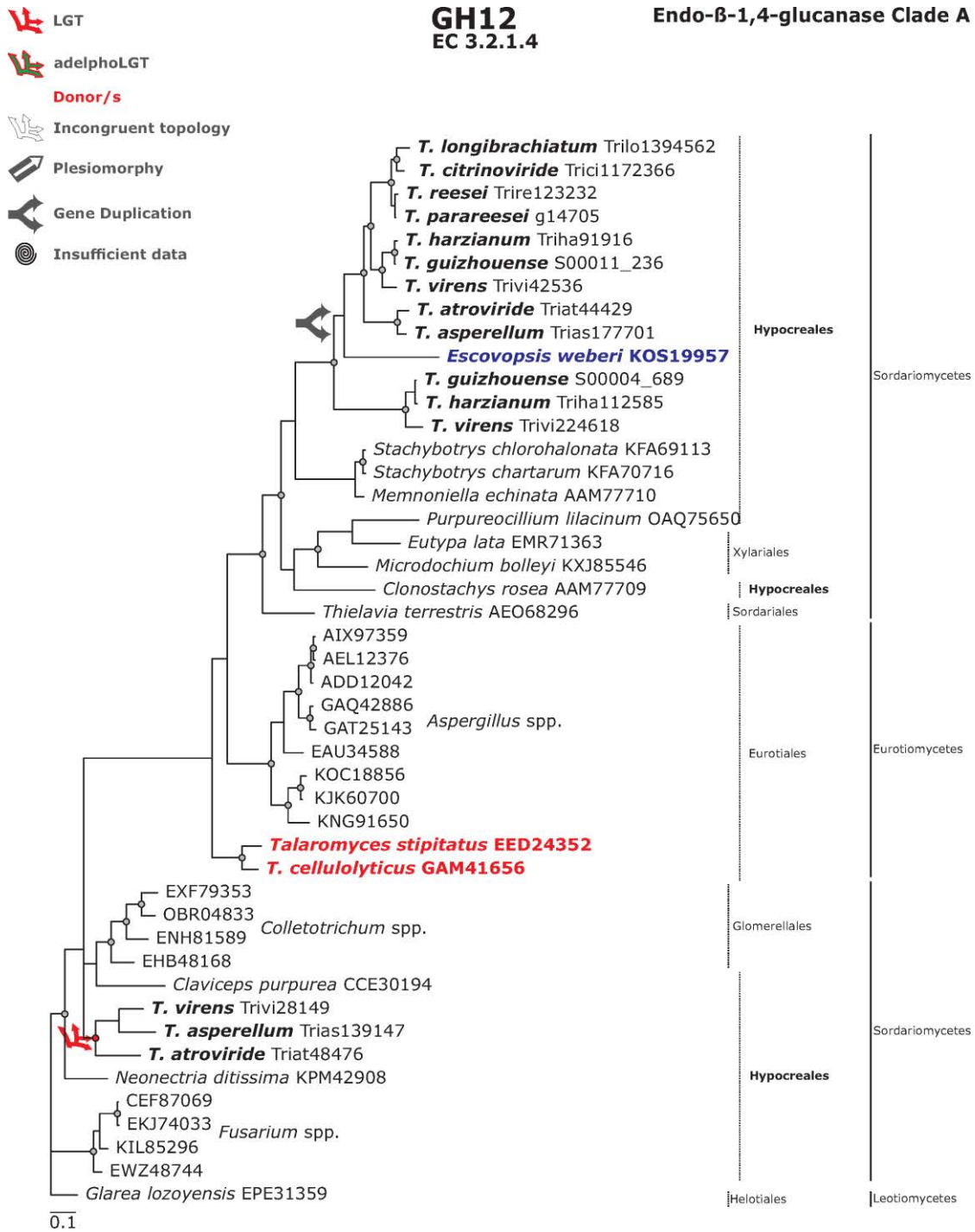
-  LGT
-  adelphoLGT
- Donor/s
-  Incongruent topology
-  Plesiomorphy
-  Gene Duplication
-  Insufficient data

GH5
EC 3.2.1.4

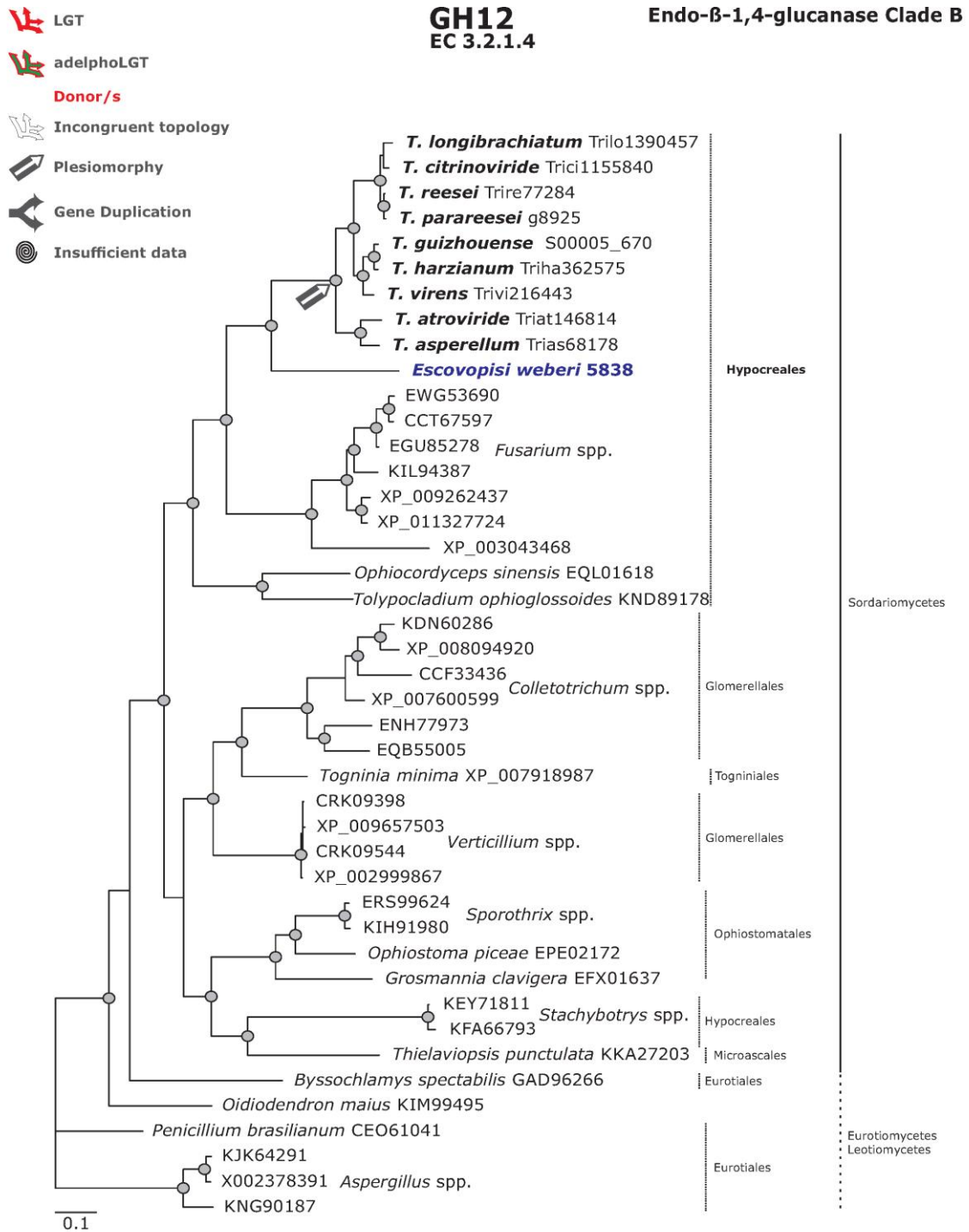
Endo-β-1,4-glucanase Clade C









Phylogram based on Dayhoff amino acid substitution model using an alignment containing 9867 characters. Bayesian analysis was run for 1 million mcmc generations and a strict consensus tree was obtained by summarizing 7500 trees, after burning first 25% of obtained 10,000 trees. Mean tree length and variance are 3.404872E+00 and 9.6194180E-03, respectively. Posterior probabilities more than 90% are marked with circular nodes. Dashed vertical bars represents the taxonomic order.



Phylogram based on Dayhoff amino acid substitution model using an alignment containing 11638 characters. Bayesian analysis was run for 1 million mcmc generations and a strict consensus tree was obtained by summarizing 7500 trees, after burning first 25% of obtained 10,000 trees. Mean tree length and variance are 7.751170E+00 and 3.915011e-002, respectively. Posterior probabilities more than 90% are marked with circular nodes. Dashed vertical bars and non-dashed vertical bars represents the taxonomic order and taxonomic class in the phylum Ascomycota, respectively.

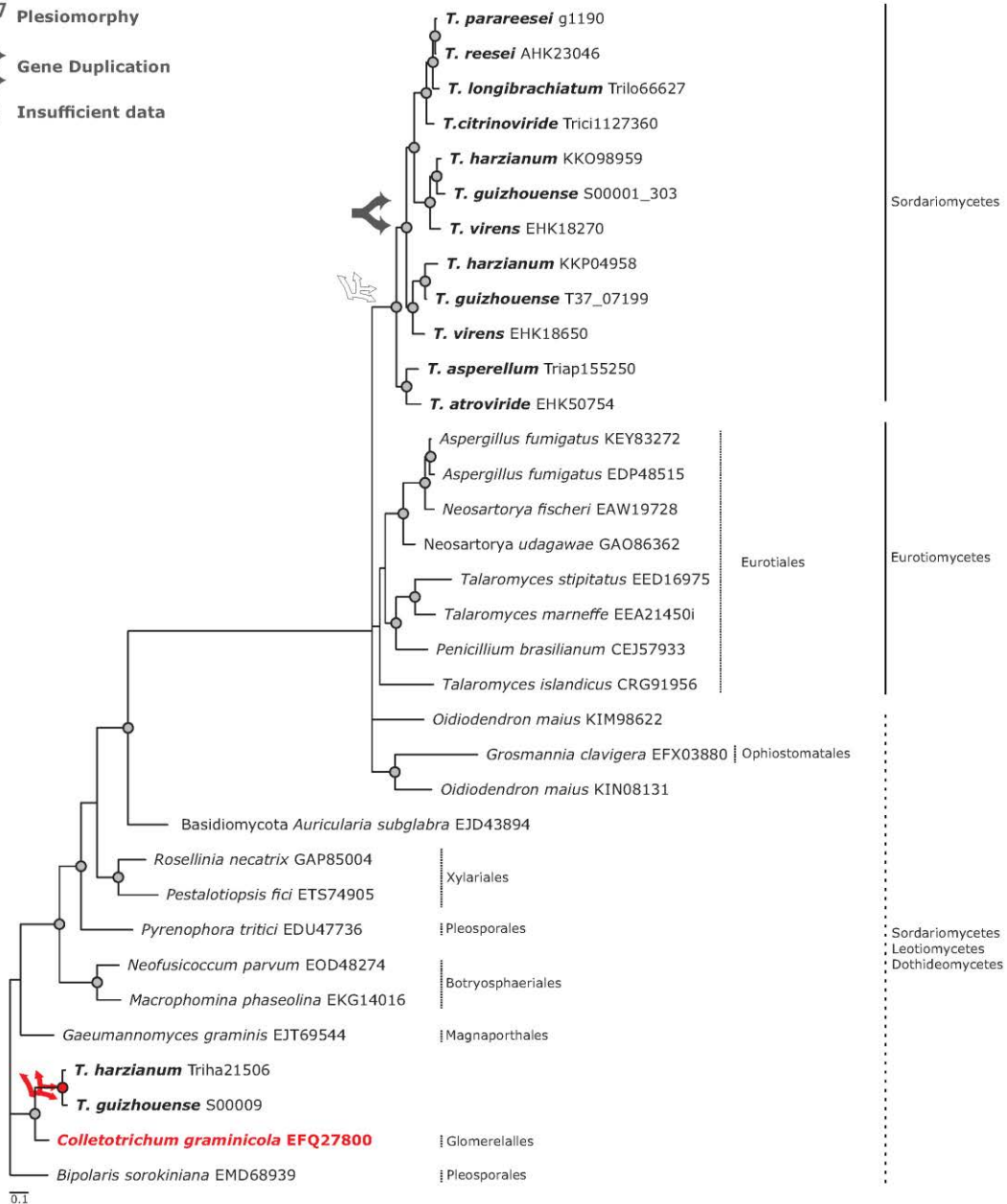


Phylogram based on Dayhoff amino acid substitution model using an alignment containing 15910 characters. Bayesian analysis was run for 1 million mcmc generations and a strict consensus tree was obtained by summarizing 7500 trees, after burning first 25% of obtained 10,000 trees. Mean tree length and variance are 7.371628E+00 and 2.7724420E-02, respectively. Posterior probabilities more than 90% are marked with circular nodes. Dashed vertical bars and non-dashed vertical bars represents the taxonomic order and taxonomic class in the phylum Ascomycota, respectively.







-  LGT
-  adelphoLGT
- Donor/s
-  Incongruent topology
-  Plesiomorphy
-  Gene Duplication
-  Insufficient data

**GH45
EC 3.2.1.4**

Endo-β-1,4-glucanase

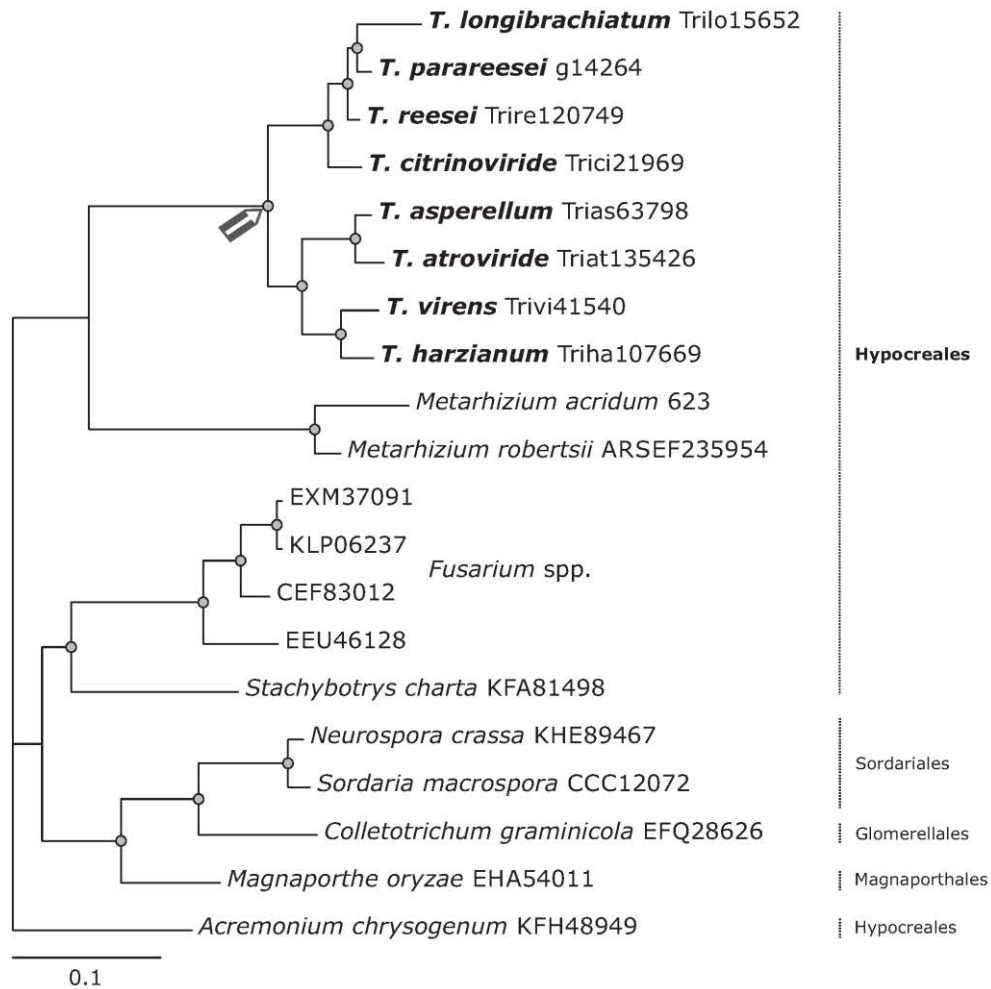


Phylogram based on Dayhoff amino acid substitution model using an alignment containing 11220 characters. Bayesian analysis was run for 1 million mcmc generations and a strict consensus tree was obtained by summarizing 7500 trees, after burning first 25% of obtained 10,000 trees. Mean tree length and variance are 8.157591E+00 and 5.7262160E-02, respectively. Posterior probabilities more than 90% are marked with circular nodes. Dashed vertical bars and non-dashed vertical bars represents the taxonomic order and taxonomic class in the phylum Ascomycota, respectively.

-  LGT
-  adelphoLGT
- Donor/s
-  Incongruent topology
-  Plesiomorphy
-  Gene Duplication
-  Insufficient data







GH1
EC 3.2.1.21

β-1,4-glucosidase Clade A



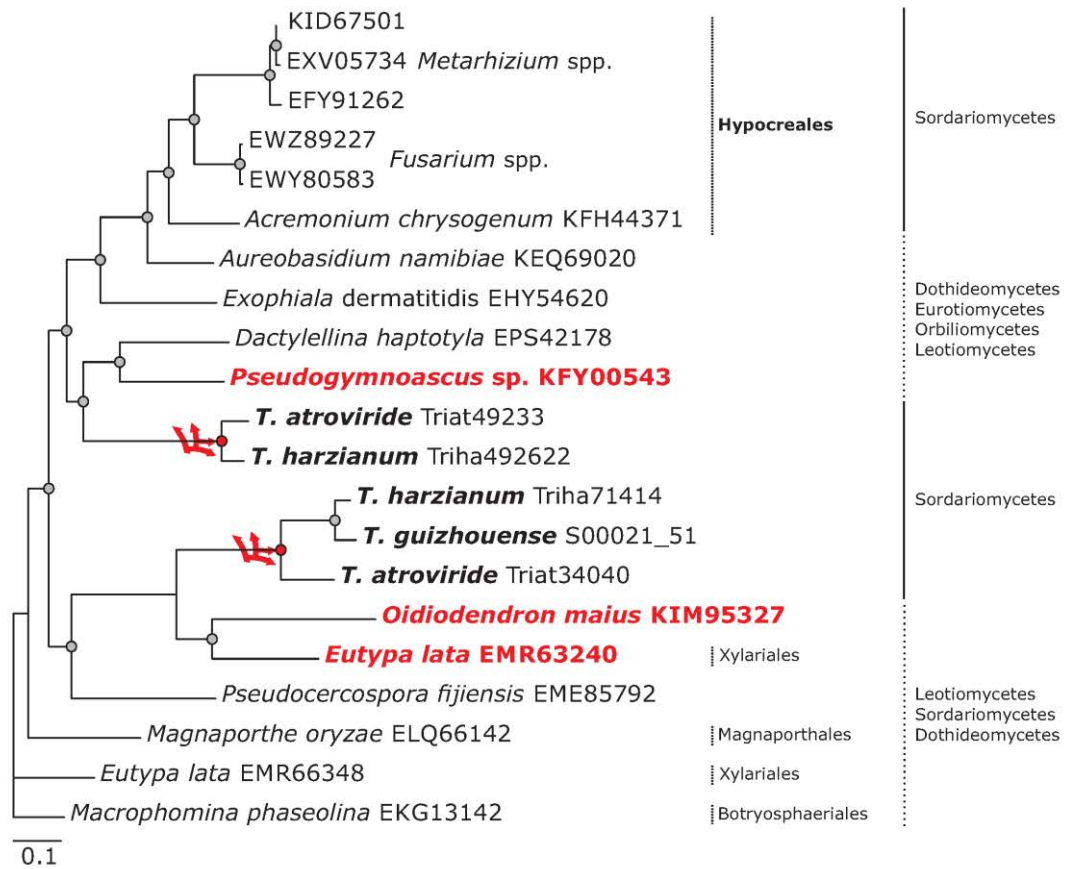
*All species fall under taxonomic class Sordariomycetes

Phylogram based on Dayhoff amino acid substitution model using an alignment containing 9620 characters. Bayesian analysis was run for 1 million mcmc generations and a strict consensus tree was obtained by summarizing 7500 trees, after burning first 25% of obtained 10,000 trees. Mean tree length and variance are 1.568965E+00 and 3.6838590E-03, respectively. Posterior probabilities more than 90% are marked with circular nodes. Dashed vertical bars represents the taxonomic order.







-  LGT
-  adelphoLGT
- Donor/s
-  Incongruent topology
-  Plesiomorphy
-  Gene Duplication
-  Insufficient data

GH1
EC 3.2.1.21

β-1,4-glucosidase Clade B

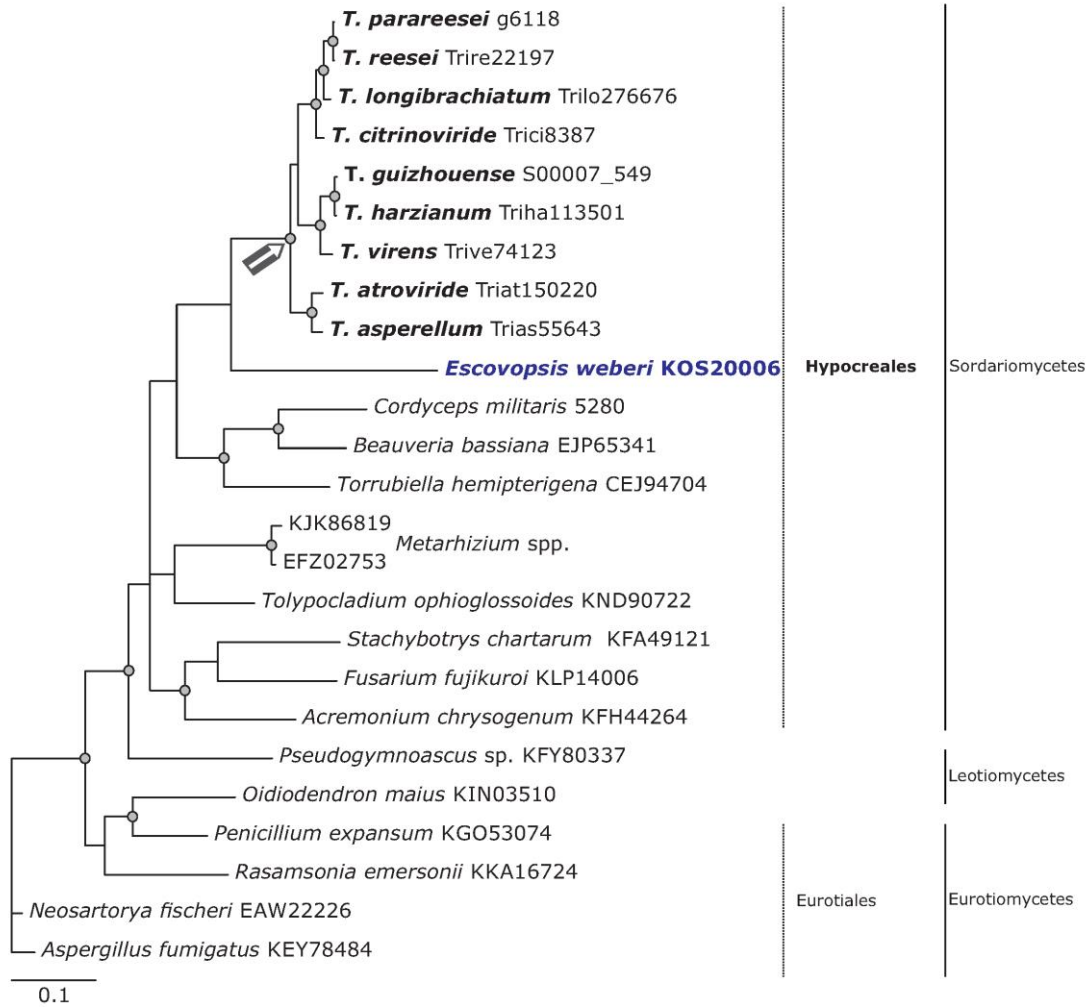


Phylogram based on Dayhoff amino acid substitution model using an alignment containing 14007 characters. Bayesian analysis was run for 1 million mcmc generations and a strict consensus tree was obtained by summarizing 7500 trees, after burning first 25% of obtained 10,000 trees. Mean tree length and variance are 4.467266E+00 and 8.8859970E-03, respectively. Posterior probabilities more than 90% are marked with circular nodes. Dashed vertical bars and non-dashed vertical bars represents the taxonomic order and taxonomic class in the phylum Ascomycota, respectively.







-  LGT
-  adelphoLGT
- Donor/s
-  Incongruent topology
-  Plesiomorphy
-  Gene Duplication
-  Insufficient data

GH1
EC 3.2.1.21

β-1,4-glucosidase Clade C

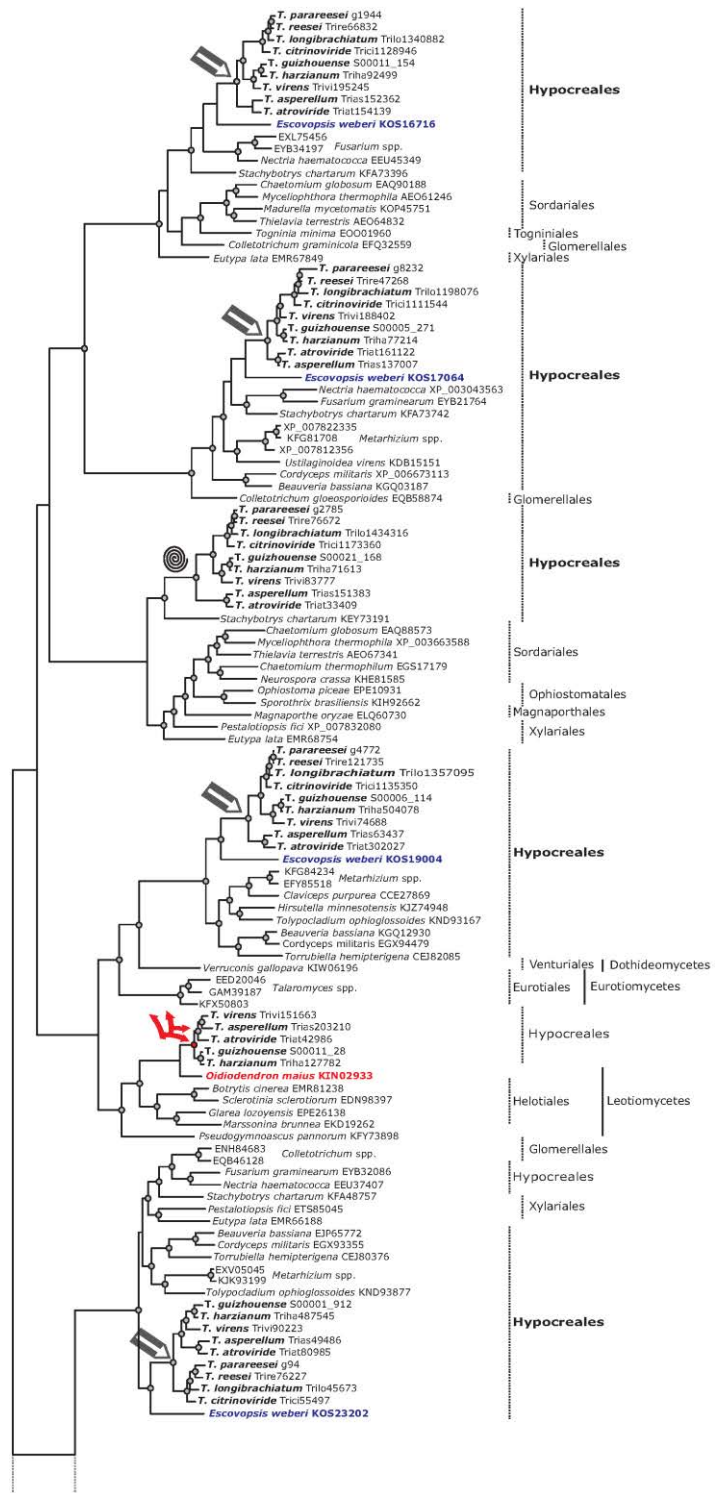


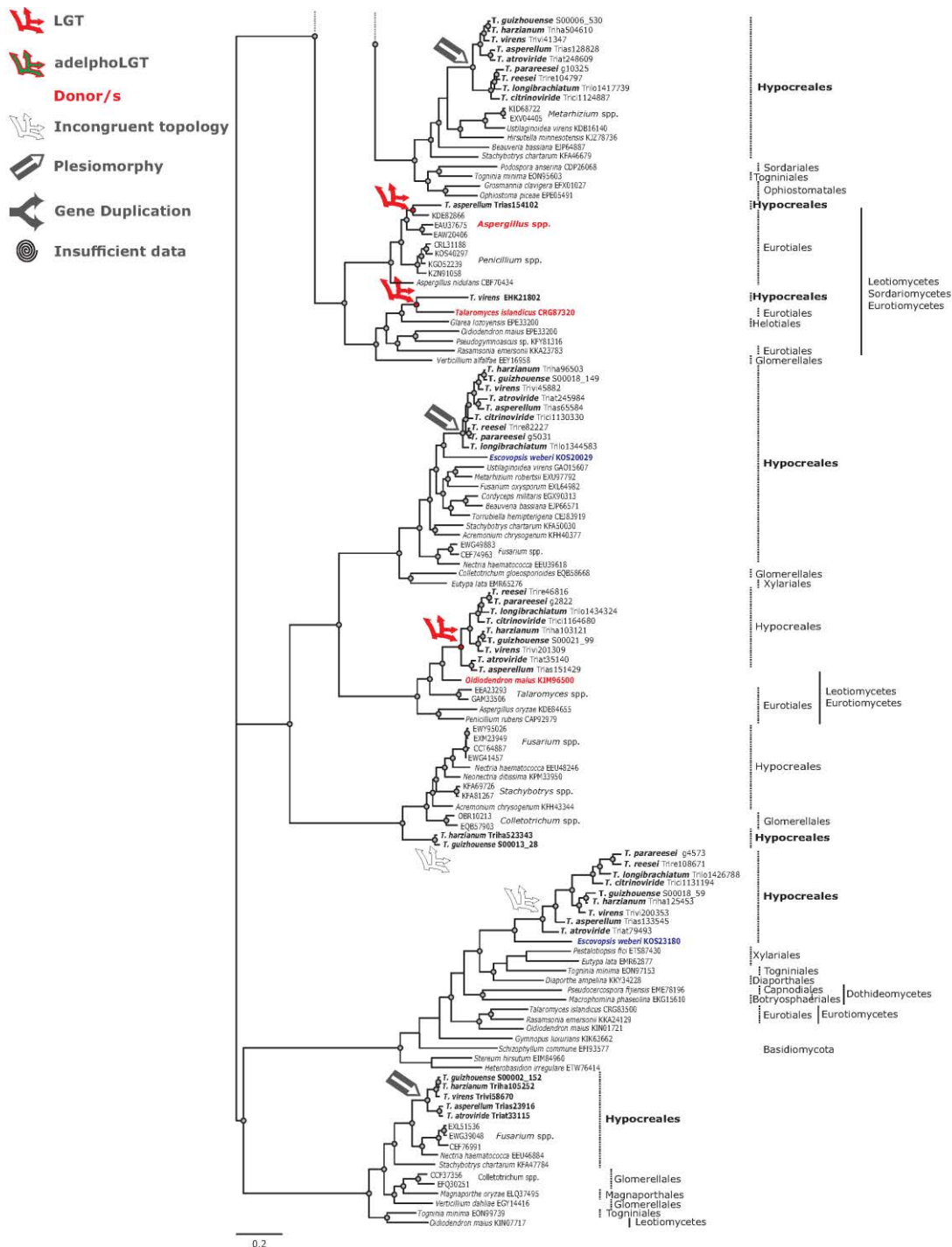
Phylogram based on Dayhoff amino acid substitution model using an alignment containing 12150 characters. Bayesian analysis was run for 1 million mcmc generations and a strict consensus tree was obtained by summarizing 7500 trees, after burning first 25% of obtained 10,000 trees. Mean tree length and variance are 2.625839E+00 and 6.1282930E-03, respectively. Posterior probabilities more than 90% are marked with circular nodes. Dashed vertical bars and non-dashed vertical bars represents the taxonomic order and taxonomic class in the phylum Ascomycota, respectively.

-  LGT
-  adelphoLGT
- Donor/s**
-  Incongruent topology
-  Plesiomorphy
-  Gene Duplication
-  Insufficient data

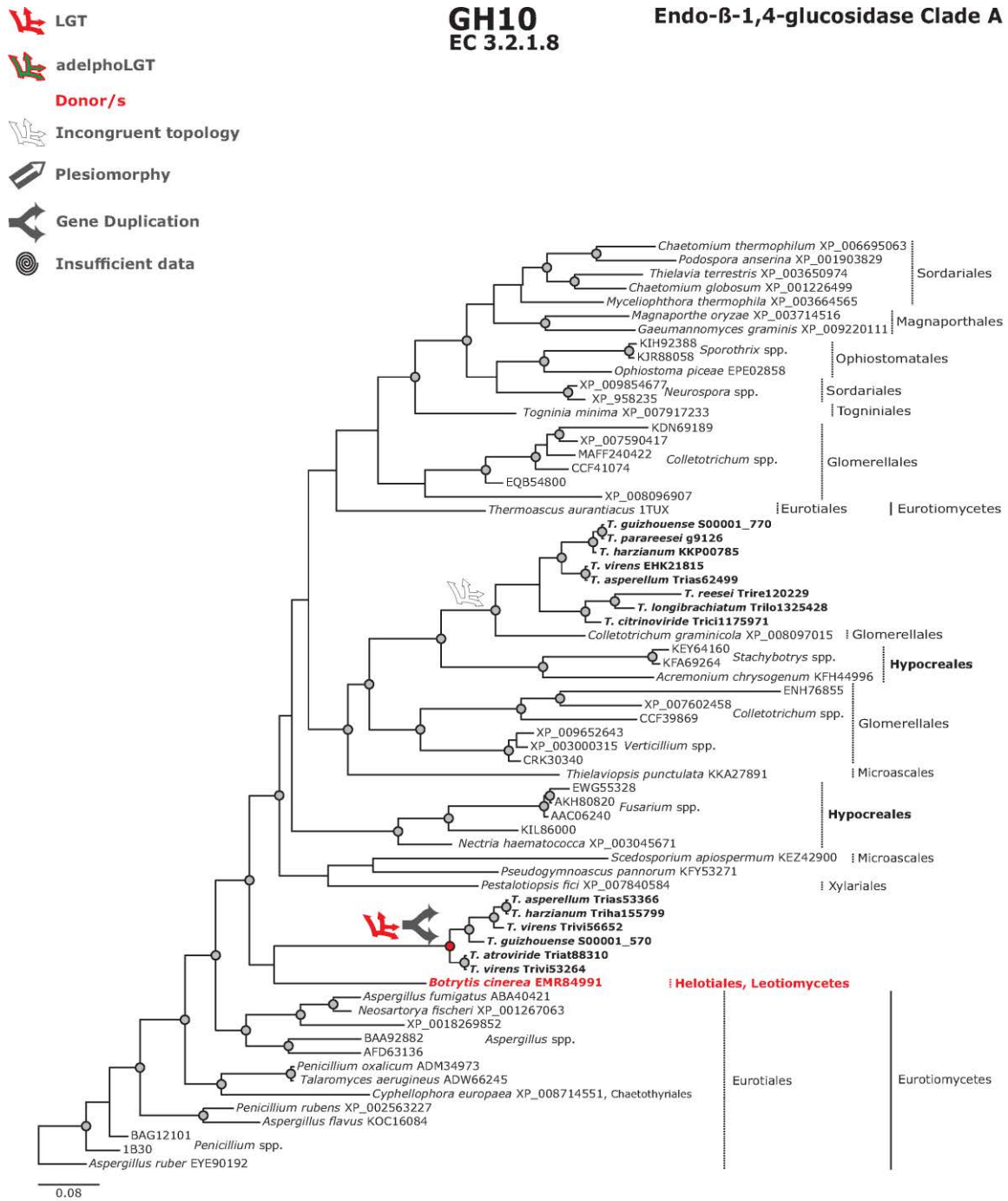
**GH3
EC 3.2.1.21**

β-1,4-glucosidase








Phylogram based on Dayhoff amino acid substitution model using an alignment containing 209655 characters. Bayesian analysis was run for 3 million mcmc generations and a strict consensus tree was obtained by summarizing 22500 trees, after burning first 25% of obtained 100,000 trees. Mean tree length and variance are 2.077053E+01 and 3.2554480E-02, respectively. Posterior probabilities more than 90% are marked with circular nodes. Dashed vertical bars and non-dashed vertical bars represents the taxonomic order and taxonomic class in the phylum Ascomycota, respectively. All non-labelled taxonomic classes are from class Sordariomycetes.

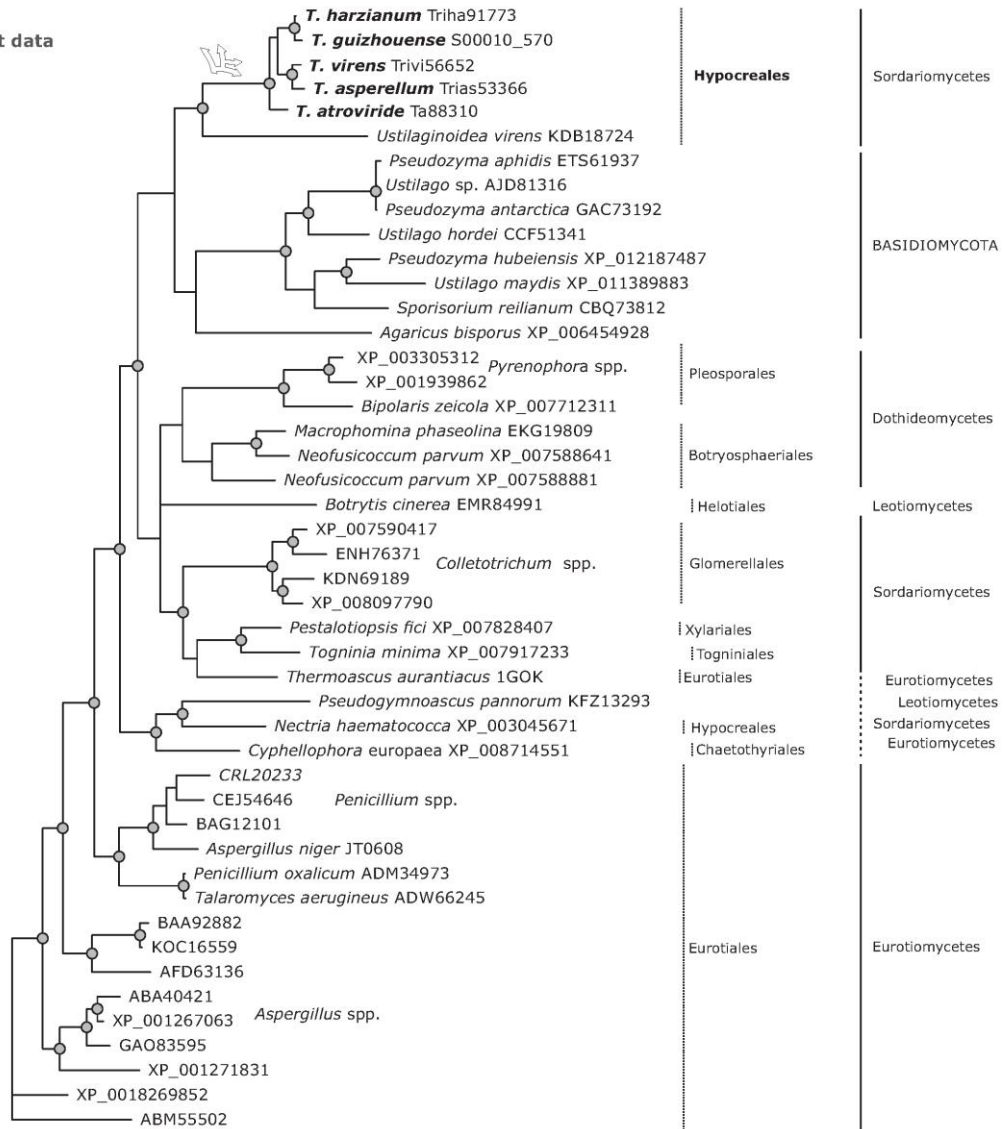


Phylogram based on Dayhoff amino acid substitution model using an alignment containing 21172 characters. Bayesian analysis was run for 1 million mcmc generations and a strict consensus tree was obtained by summarizing 7500 trees, after burning first 25% of obtained 10,000 trees. Mean tree length and variance are 8.903780E+00 and 3.1751560E-02, respectively. Posterior probabilities more than 90% are marked with circular nodes. Dashed vertical bars represents the taxonomic order. All the species belongs to the taxonomic class in the phylum Ascomycota, **Sordariomycetes** unless marked otherwise.







-  LGT
-  adelphoLGT
- Donor/s**
-  Incongruent topology
-  Plesiomorphy
-  Gene Duplication
-  Insufficient data

**GH10
EC 3.2.1.8**

Endo-β-1,4-glucosidase Clade B

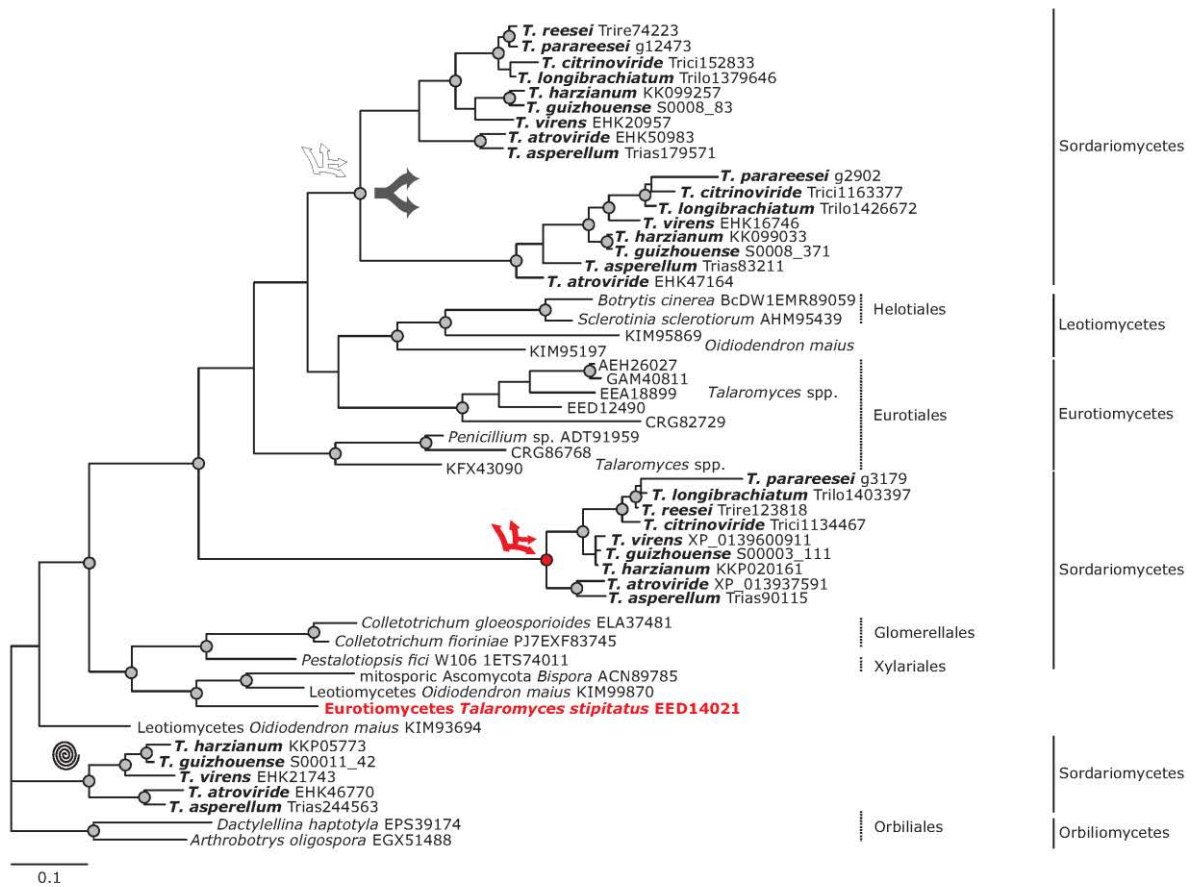


Phylogram based on Dayhoff amino acid substitution model using an alignment containing 18571 characters. Bayesian analysis was run for 1 million mcmc generations and a strict consensus tree was obtained by summarizing 7500 trees, after burning first 25% of obtained 10,000 trees. Mean tree length and variance are 7.314463E+00 and 2.5260940E-02, respectively. Posterior probabilities more than 90% are marked with circular nodes. Dashed vertical bars and non-dashed vertical bars represents the taxonomic order and taxonomic class in the phylum Ascomycota, respectively.







-  LGT
-  adelphoLGT
- Donor/s
-  Incongruent topology
-  Plesiomorphy
-  Gene Duplication
-  Insufficient data

GH11
EC 3.2.1.8

Endo-β-1,4-xylanase

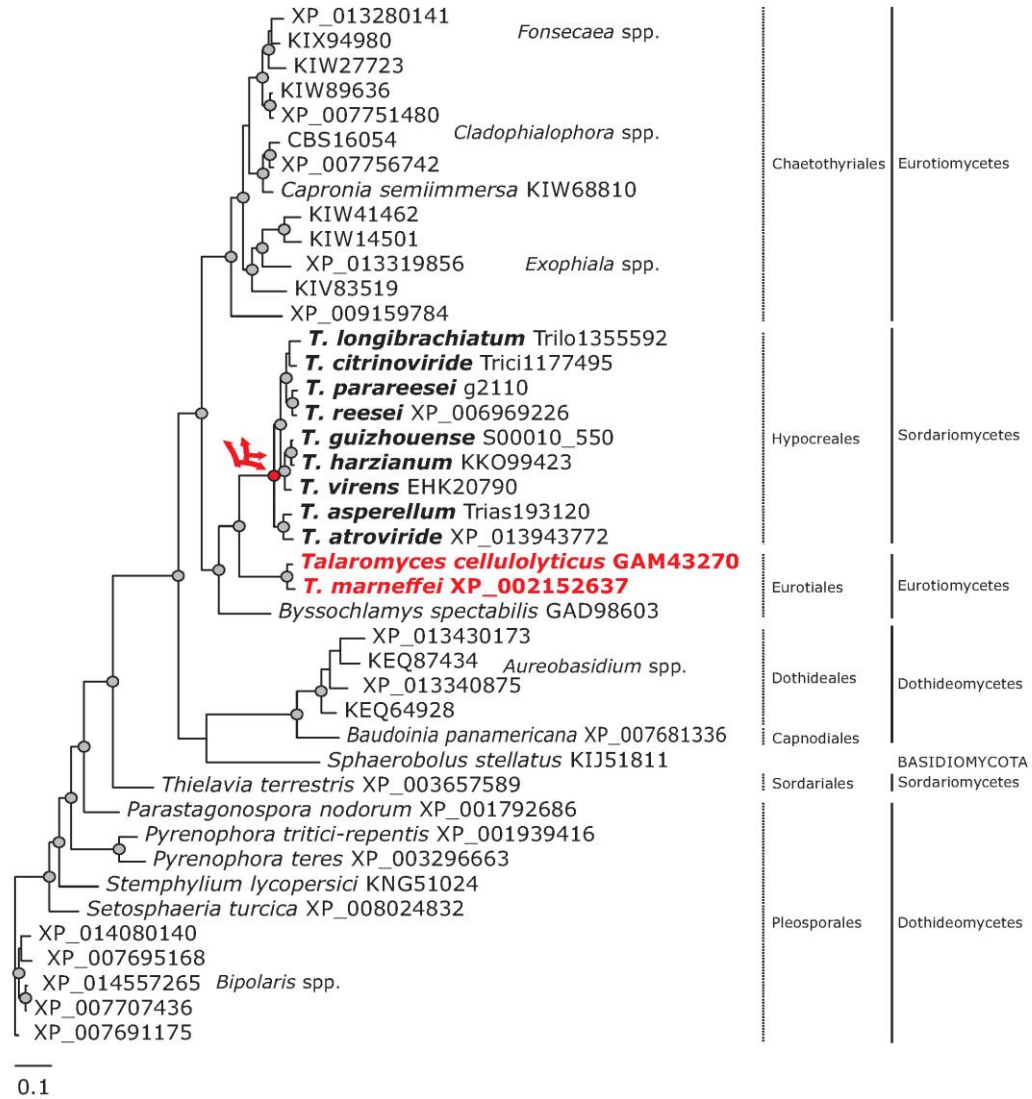


Phylogram based on Dayhoff amino acid substitution model using an alignment containing 18370 characters. Bayesian analysis was run for 0.66 million mcmc generations and a strict consensus tree was obtained by summarizing 4950 trees, after burning first 25% of obtained 6600 trees. Mean tree length and variance are 6.798910E+00 and 3.0536650E-02, respectively. Posterior probabilities more than 90% are marked with circular nodes. Dashed vertical bars and non-dashed vertical bars represents the taxonomic order and taxonomic class in the phylum Ascomycota, respectively.







-  LGT
-  adelphoLGT
- Donor/s
-  Incongruent topology
-  Plesiomorphy
-  Gene Duplication
-  Insufficient data

GH30
EC 3.2.1.8

Endo-β-1,4-xylanase Clade A

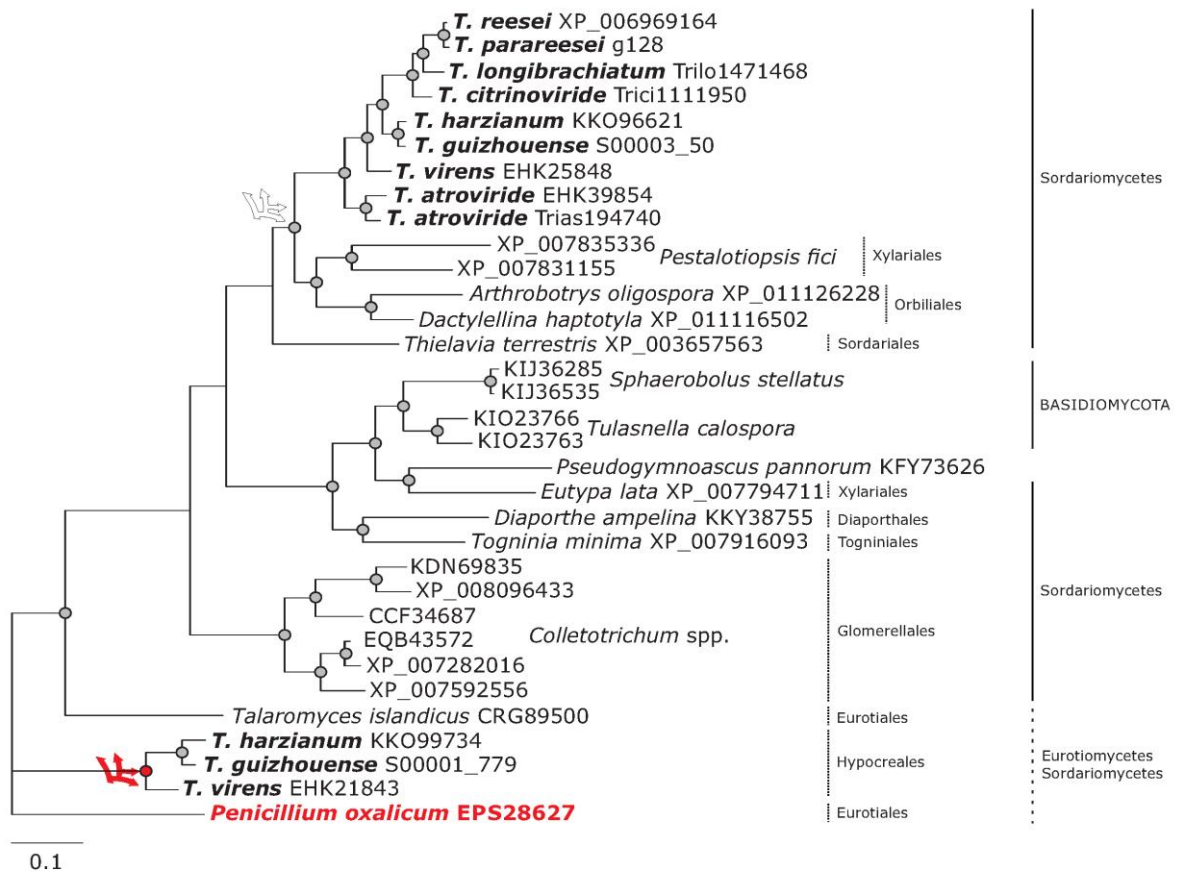


Phylogram based on Dayhoff amino acid substitution model using an alignment containing 44730 characters. Bayesian analysis was run for 1 million mcmc generations and a strict consensus tree was obtained by summarizing 7500 trees, after burning first 25% of obtained 10,000 trees. Mean tree length and variance are 4.169406E+00 and 9.7577200E-03, respectively. Posterior probabilities more than 90% are marked with circular nodes. Dashed vertical bars and non-dashed vertical bars represents the taxonomic order and taxonomic class in the phylum Ascomycota, respectively.

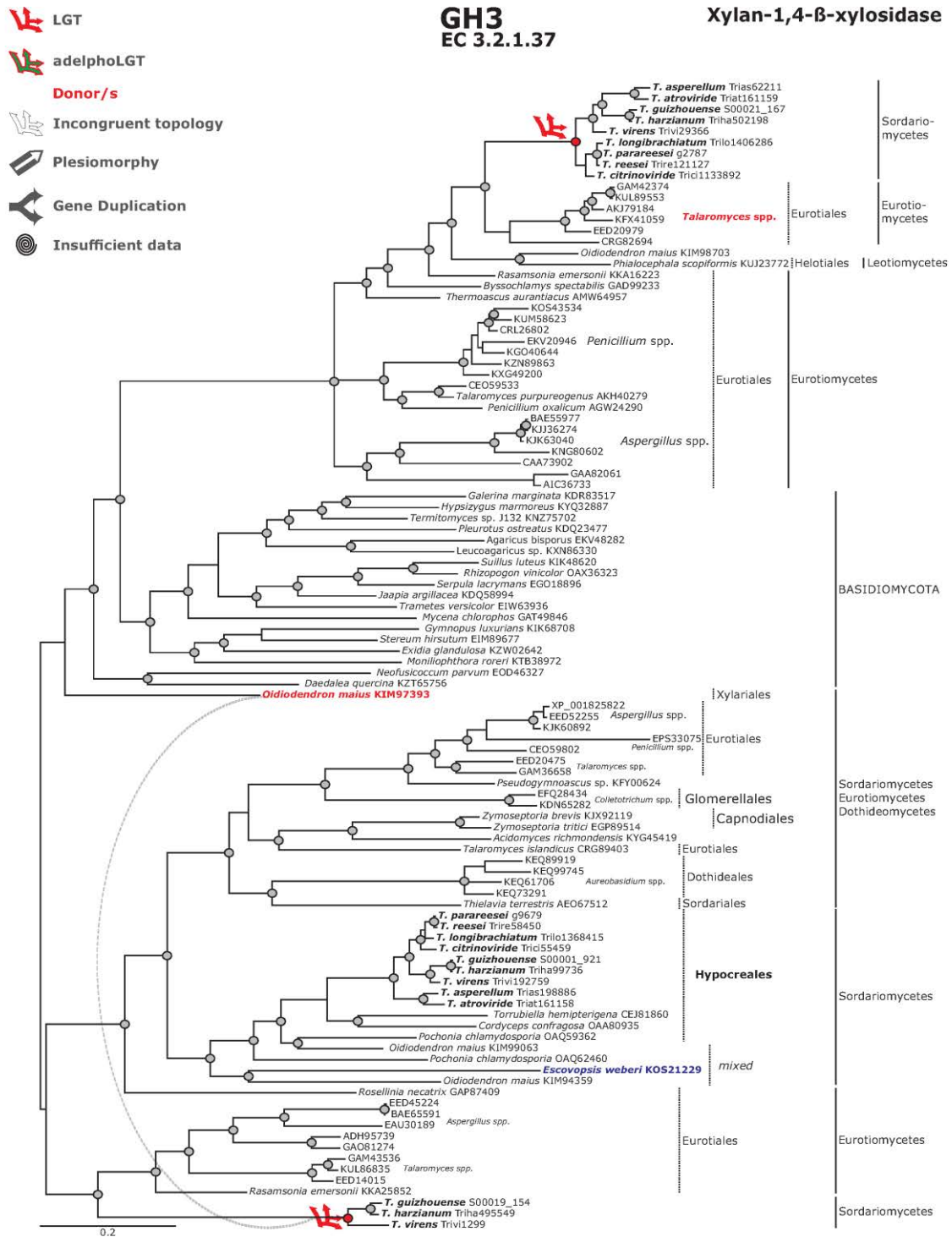
-  LGT
-  adelphoLGT
- Donor/s**
-  Incongruent topology
-  Plesiomorphy
-  Gene Duplication
-  Insufficient data

GH30
EC 3.2.1.8







Endo-β-1,4-xylanase Clade B



Phylogram based on Dayhoff amino acid substitution model using an alignment containing 15873 characters. Bayesian analysis was run for 1 million mcmc generations and a strict consensus tree was obtained by summarizing 7500 trees, after burning first 25% of obtained 10,000 trees. Mean tree length and variance are 4.491939E+00 and 1.0864500E-02, respectively. Posterior probabilities more than 90% are marked with circular nodes. Dashed vertical bars and non-dashed vertical bars represents the taxonomic order and taxonomic class in the phylum Ascomycota, respectively.

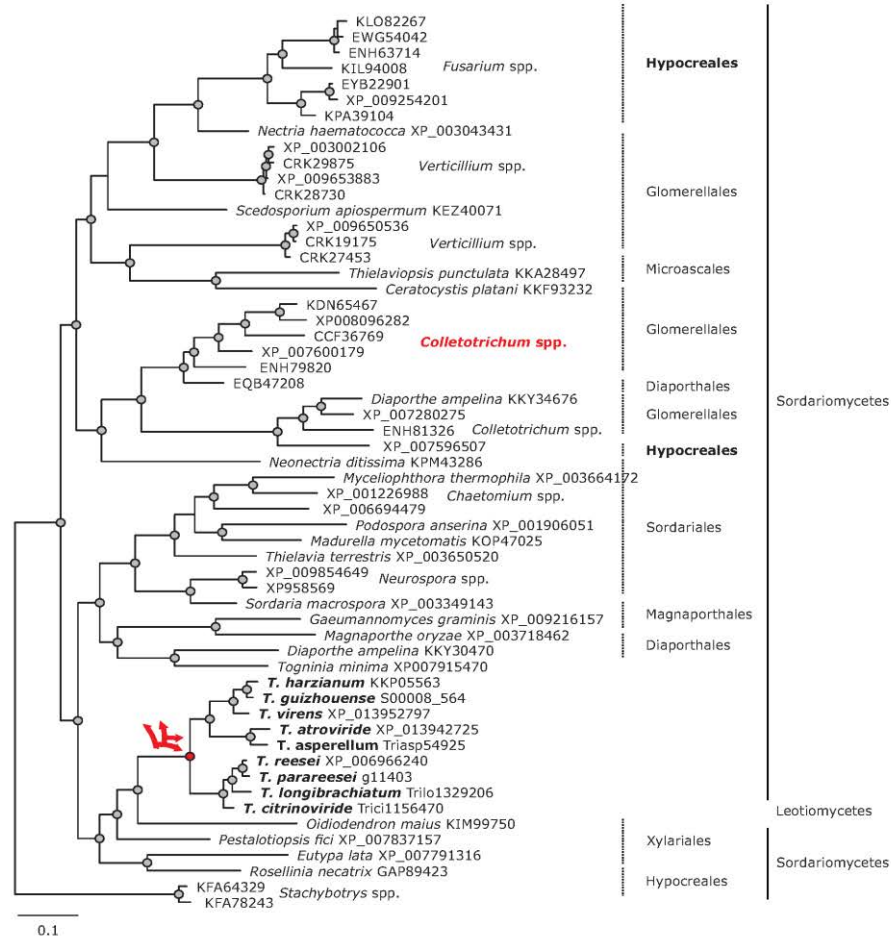


Phylogram based on Dayhoff amino acid substitution model using an alignment containing 82264 characters. Bayesian analysis was run for 2 million mcmc generations and a strict consensus tree was obtained by summarizing 15000 trees, after burning first 25% of obtained 20,000 trees. Mean tree length and variance are 1.676796E+01 and 2.6915590E-02, respectively. Posterior probabilities more than 90% are marked with circular nodes. Dashed vertical bars and non-dashed vertical bars represents the taxonomic order and taxonomic class in the phylum Ascomycota, respectively.

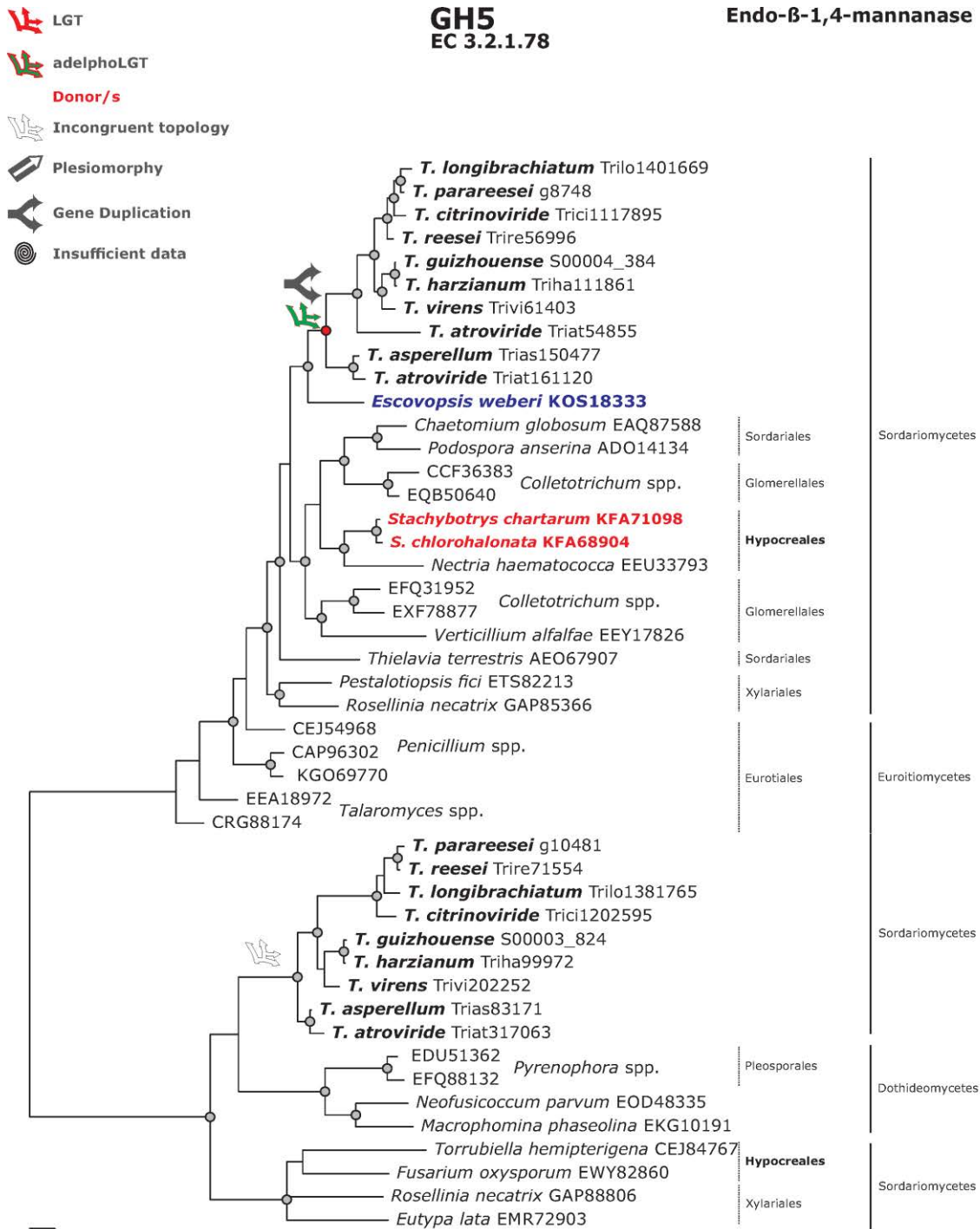
-  LGT
-  adelphoLGT
- Donor/s
-  Incongruent topology
-  Plesiomorphy
-  Gene Duplication
-  Insufficient data

**GH74
EC 3.2.1.151**

Xyloglucanase









Phylogram based on Dayhoff amino acid substitution model using an alignment containing 80880 characters. Bayesian analysis was run for 1 million mcmc generations and a strict consensus tree was obtained by summarizing 7500 trees, after burning first 25% of obtained 10,000 trees. Mean tree length and variance are 1.334523E+01 and 1.8721190E-02, respectively. Posterior probabilities more than 90% are marked with circular nodes. Dashed vertical bars and non-dashed vertical bars represents the taxonomic order and taxonomic class in the phylum Ascomycota, respectively.



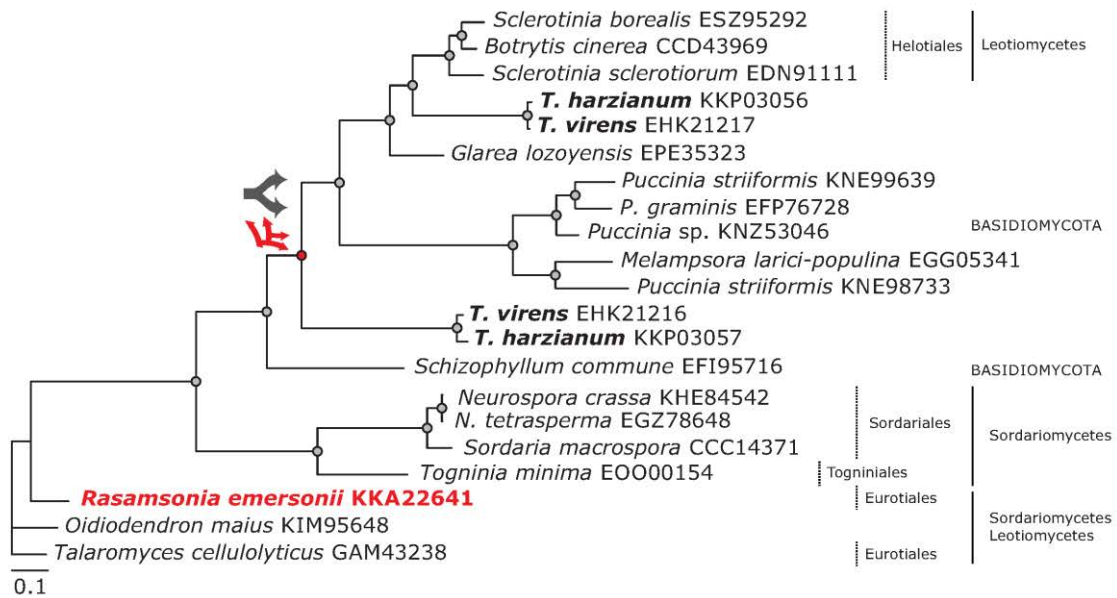
0.1

Phylogram based on Dayhoff amino acid substitution model using an alignment containing 30130 characters. Bayesian analysis was run for 1 million mcmc generations and a strict consensus tree was obtained by summarizing 7500 trees, after burning first 25% of obtained 10,000 trees. Mean tree length and variance are 1.147689E+01 and 4.8778060E-02, respectively. Posterior probabilities more than 90% are marked with circular nodes. Dashed vertical bars and non-dashed vertical bars represents the taxonomic order and taxonomic class in the phylum Ascomycota, respectively.







-  LGT
-  adelphoLGT
- Donor/s
-  Incongruent topology
-  Plesiomorphy
-  Gene Duplication
-  Insufficient data

GH26
EC 3.2.1.78

Endo-β-1,4-mannanase

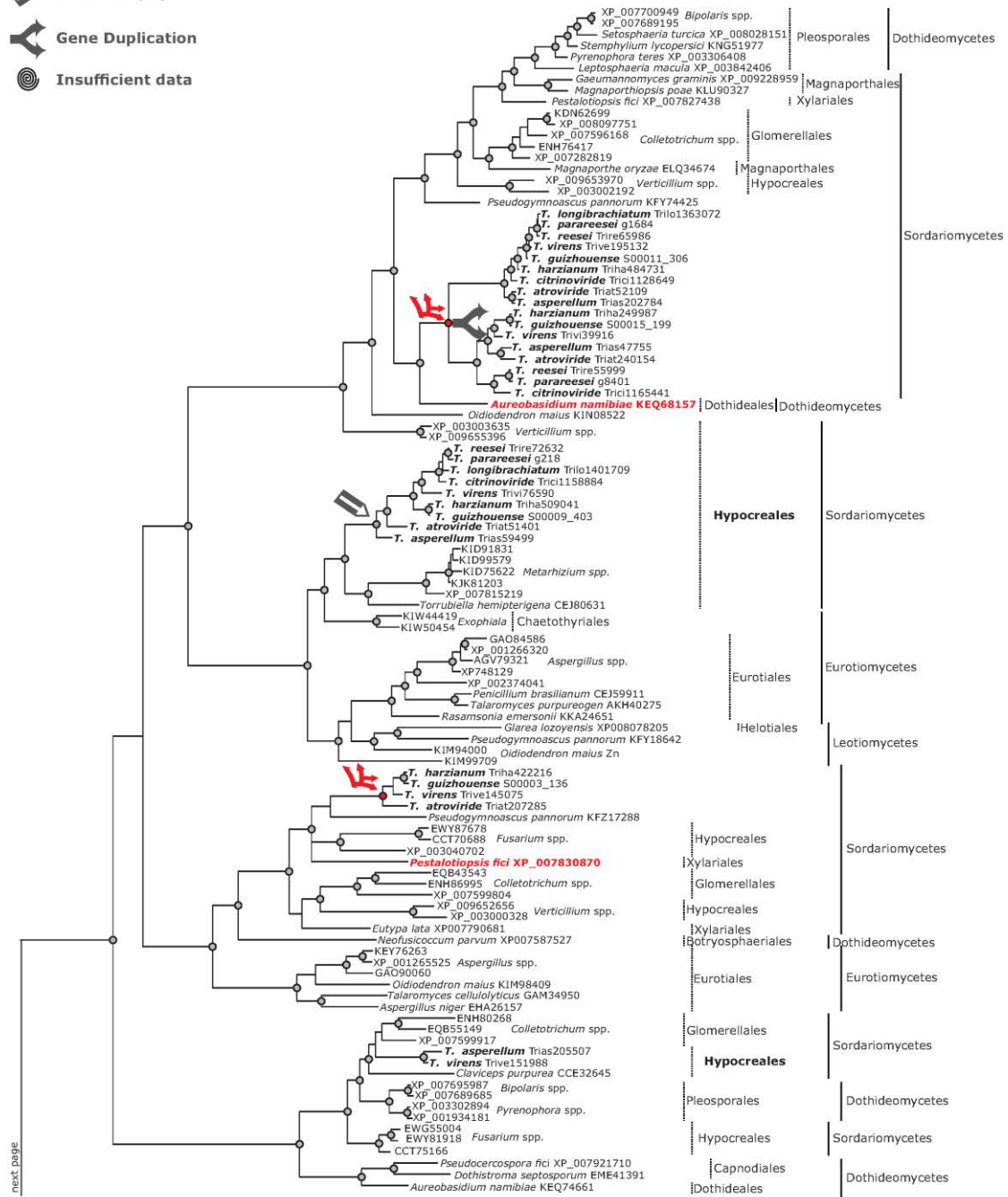


Phylogram based on Dayhoff amino acid substitution model using an alignment containing 6930 characters. Bayesian analysis was run for 1 million mcmc generations and a strict consensus tree was obtained by summarizing 7500 trees, after burning first 25% of obtained 10,000 trees. Mean tree length and variance are 5.565739E+00 and 2.7990880E-02, respectively. Posterior probabilities more than 90% are marked with circular nodes. Dashed vertical bars and non-dashed vertical bars represents the taxonomic order and taxonomic class in the phylum Ascomycota, respectively.







-  LGT
-  adelphoLGT
- Donor/s
-  Incongruent topology
-  Plesiomorphy
-  Gene Duplication
-  Insufficient data

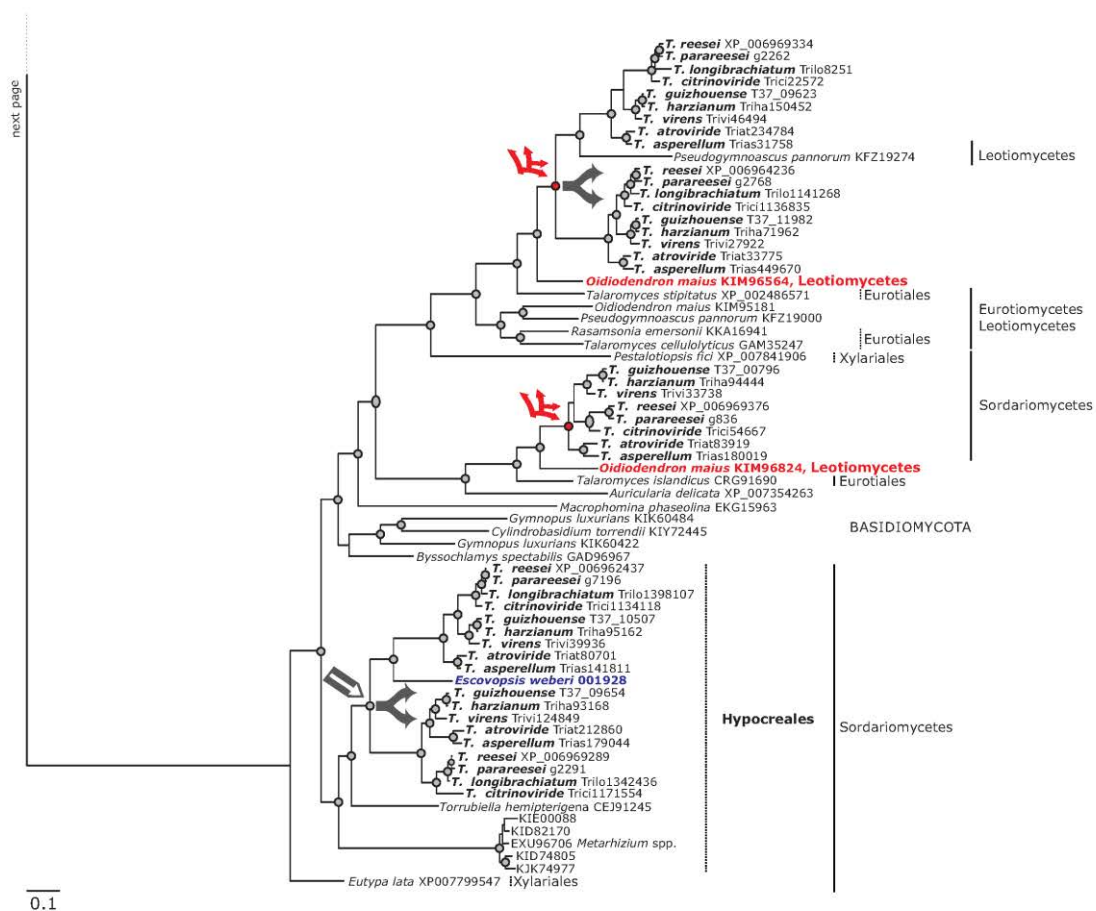
**GH27
EC 3.2.1.22**

α -1,4-galactosidase









0.1

-  LGT
-  adelphoLGT
- Donor/s**
-  Incongruent topology
-  Plesiomorphy
-  Gene Duplication
-  Insufficient data

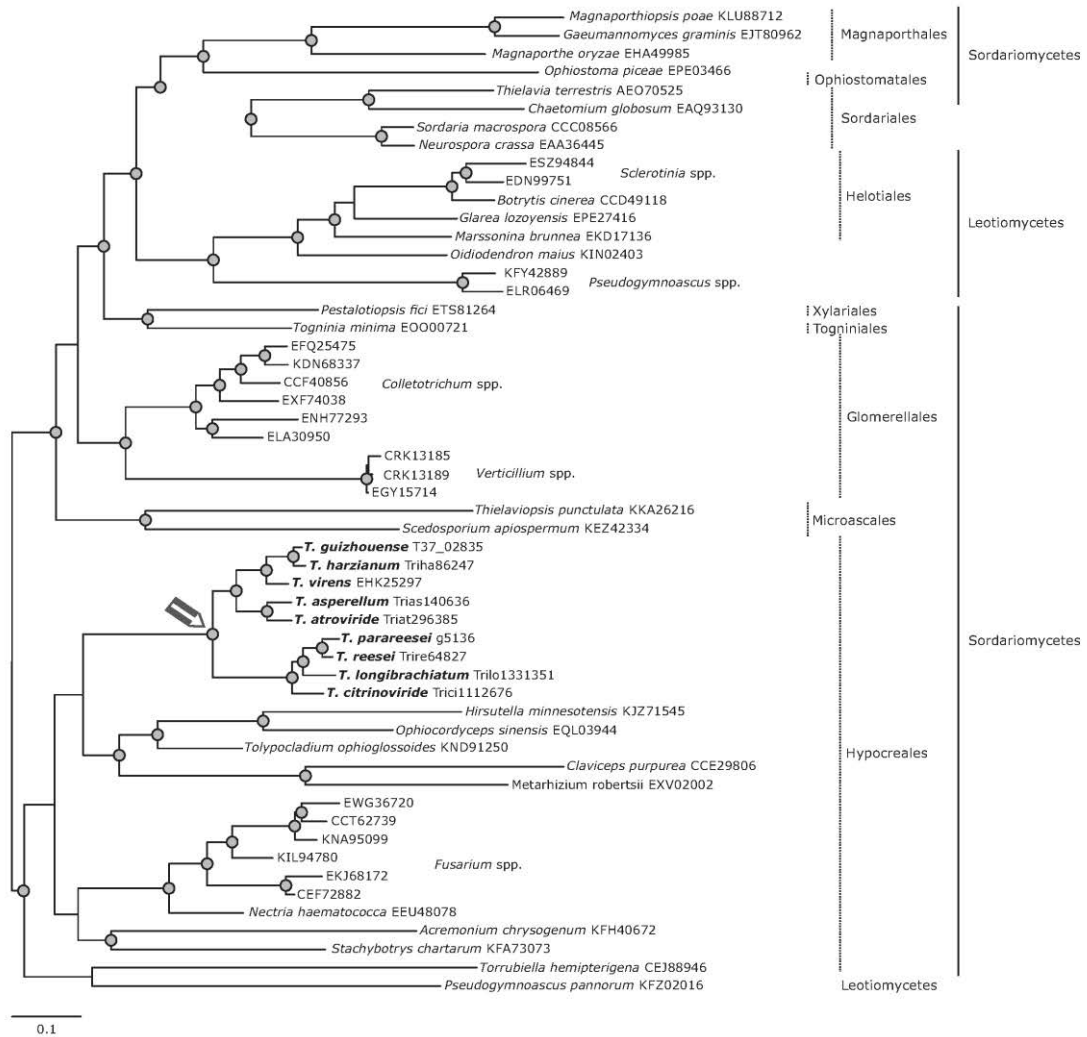


Phylogram based on Dayhoff amino acid substitution model using an alignment containing 148596 characters. Bayesian analysis was run for 5 million mcmc generations and a strict consensus tree was obtained by summarizing 37500 trees, after burning first 25% of obtained 50,000 trees. Mean tree length and variance are 3.133589E+01 and 9.2971280E-02, respectively. Posterior probabilities more than 90% are marked with circular nodes. Dashed vertical bars and non-dashed vertical bars represents the taxonomic order and taxonomic class in the phylum Ascomycota, respectively.

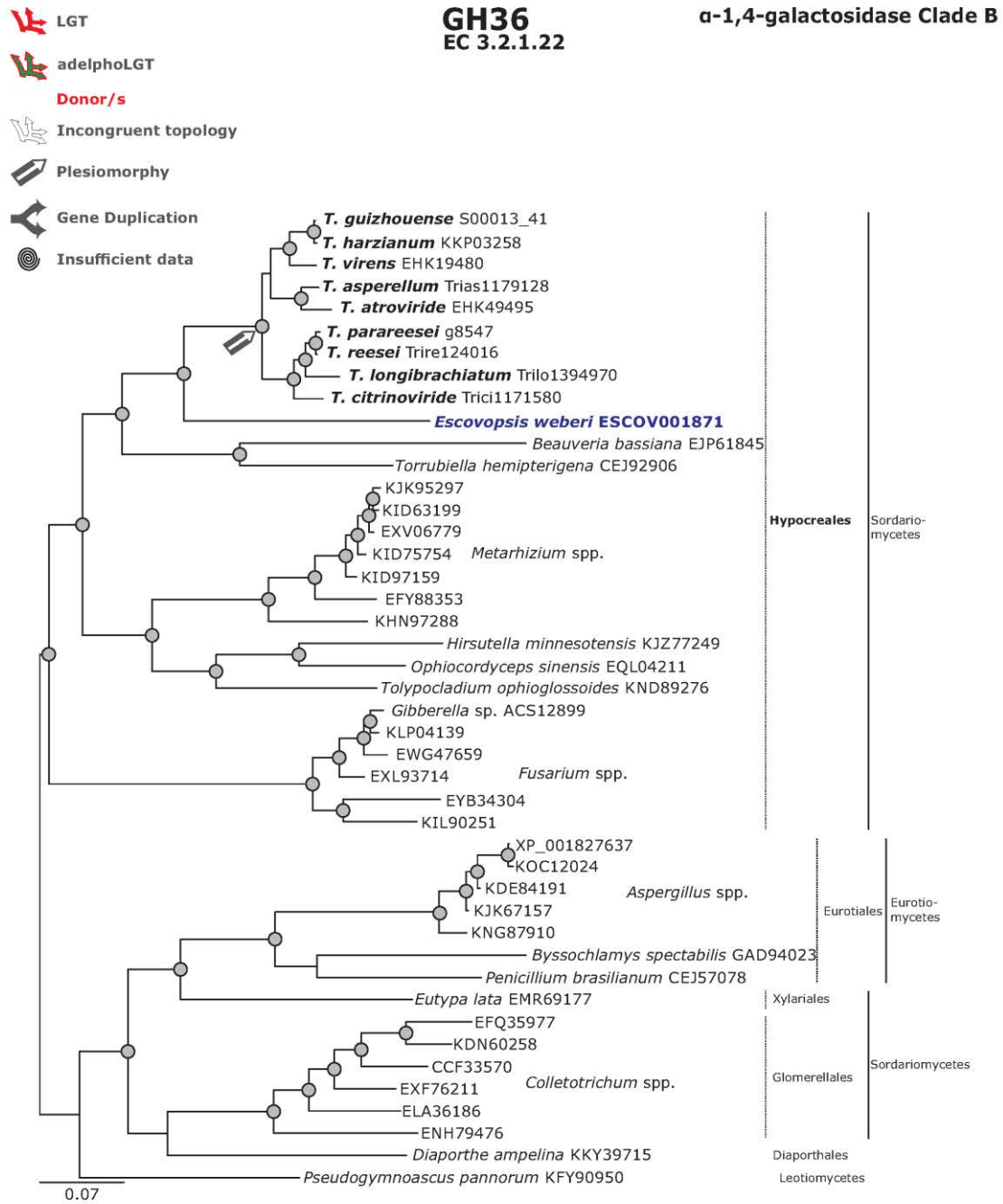
-  LGT
-  adelphoLGT
- Donor/s
-  Incongruent topology
-  Plesiomorphy
-  Gene Duplication
-  Insufficient data

**GH36
EC 3.2.1.22**

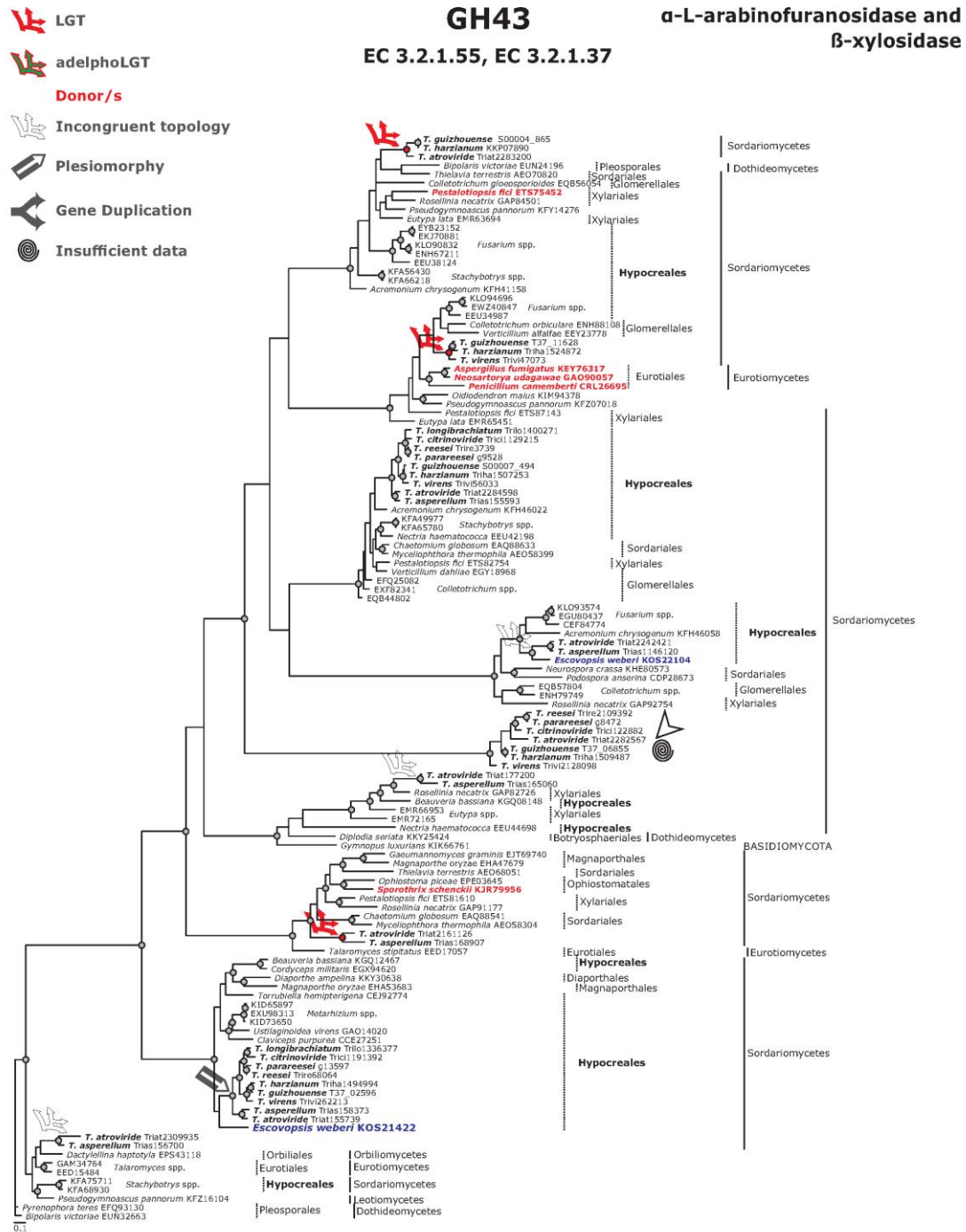
α-1,4-galactosidase Clade A









Phylogram based on Dayhoff amino acid substitution model using an alignment containing 33220 characters. Bayesian analysis was run for 1 million mcmc generations and a strict consensus tree was obtained by summarizing 7500 trees, after burning first 25% of obtained 10,000 trees. Mean tree length and variance are 4.453243e+000 and 6.667453e-003, respectively. Posterior probabilities more than 90% are marked with circular nodes. Dashed vertical bars and non-dashed vertical bars represents the taxonomic order and taxonomic class in the phylum Ascomycota, respectively.



Phylogram based on Dayhoff amino acid substitution model using an alignment containing 51030 characters. Bayesian analysis was run for 1 million mcmc generations and a strict consensus tree was obtained by summarizing 7500 trees, after burning first 25% of obtained 10,000 trees. Mean tree length and variance are 1.242005e+001 and 1.914977e-002, respectively. Posterior probabilities more than 90% are marked with circular nodes. Dashed vertical bars and non-dashed vertical bars represents the taxonomic order and taxonomic class in the phylum Ascomycota, respectively.

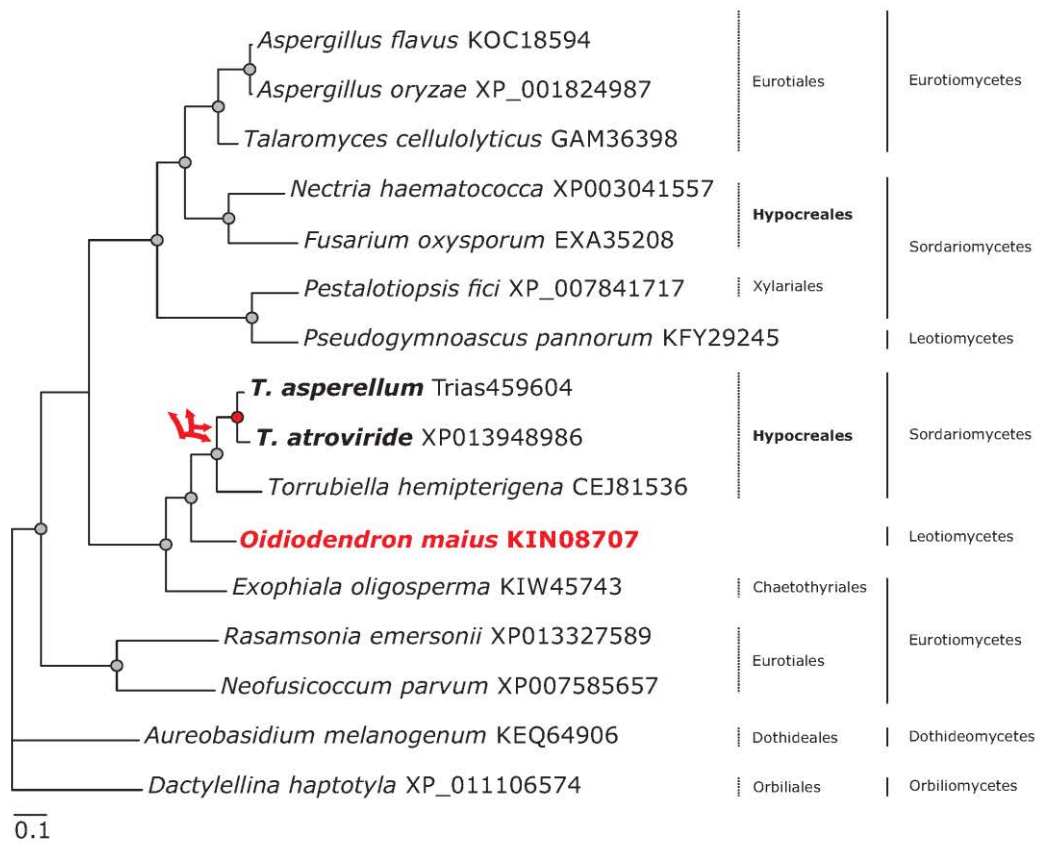


Phylogram based on Dayhoff amino acid substitution model using an alignment containing 99630 characters. Bayesian analysis was run for 3 million mcmc generations and a strict consensus tree was obtained by summarizing 22500 trees, after burning first 25% of obtained 30,000 trees. Mean tree length and variance are 3.687042E+01 and 2.1489000E-01, respectively. Posterior probabilities more than 90% are marked with circular nodes. Dashed vertical bars and non-dashed vertical bars represents the taxonomic order and taxonomic class in the phylum Ascomycota, respectively.

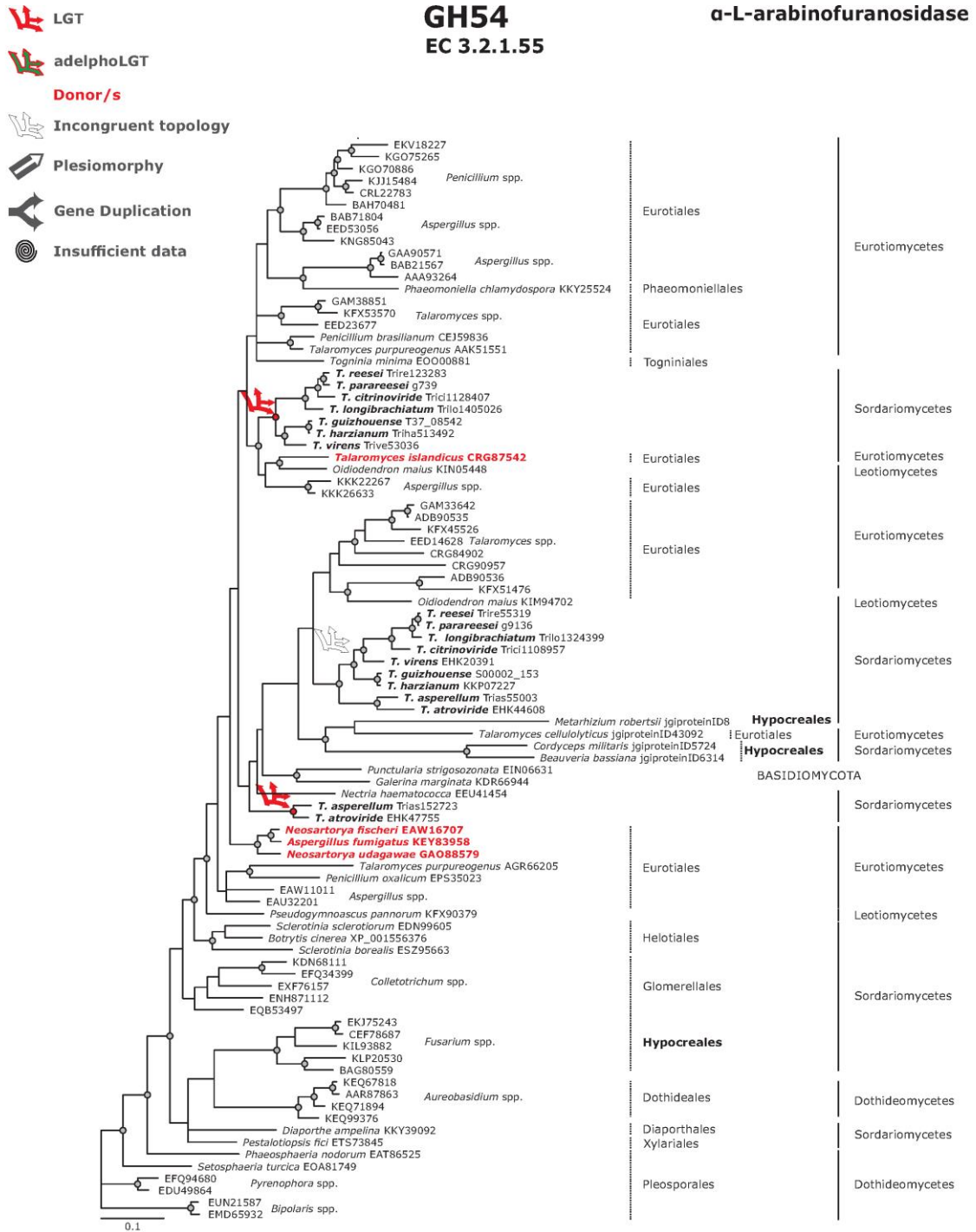
-  LGT
-  adelphoLGT
- Donor/s
-  Incongruent topology
-  Plesiomorphy
-  Gene Duplication
-  Insufficient data

GH51
EC 3.2.1.55

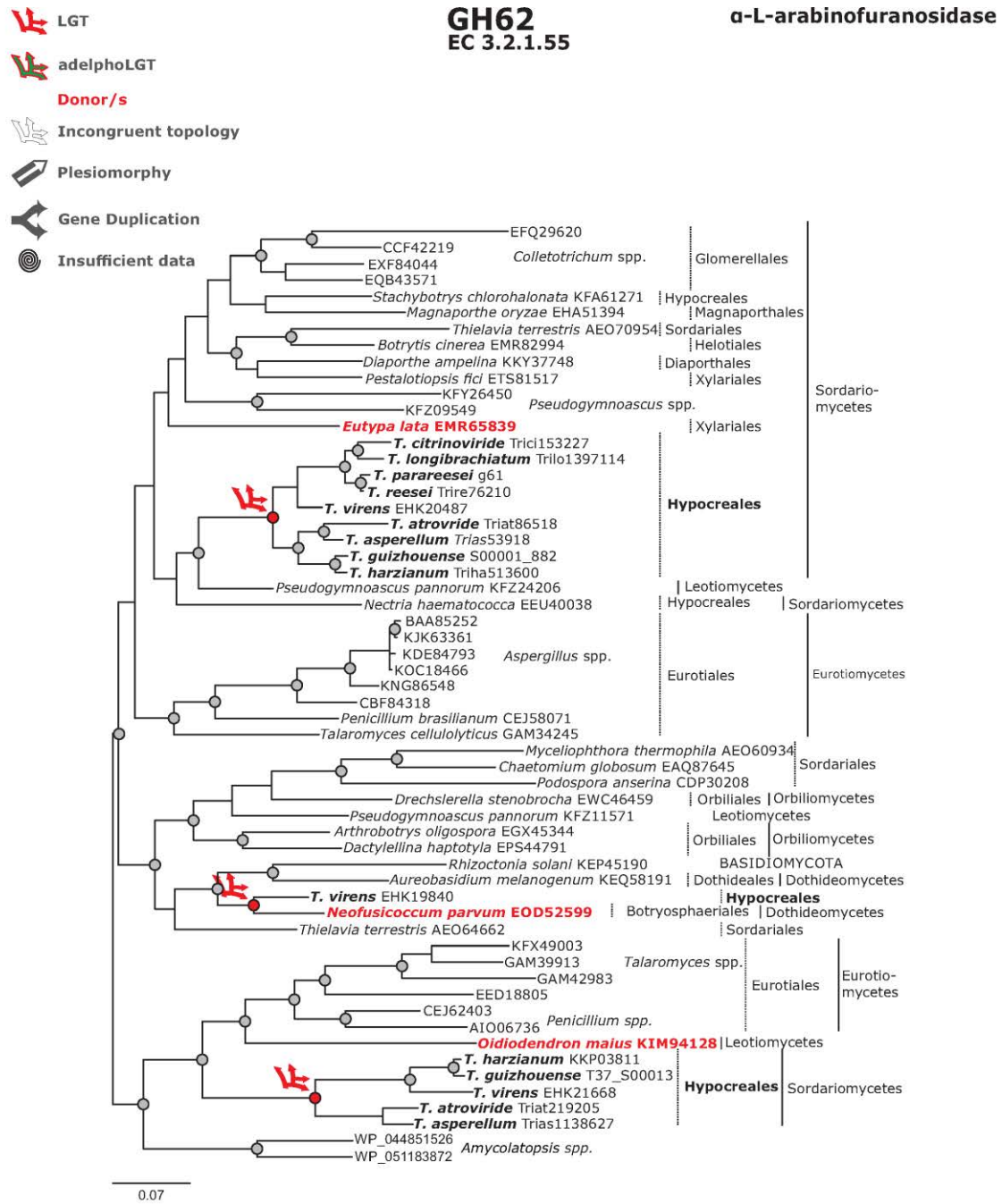
α-L-arabinofuranosidase



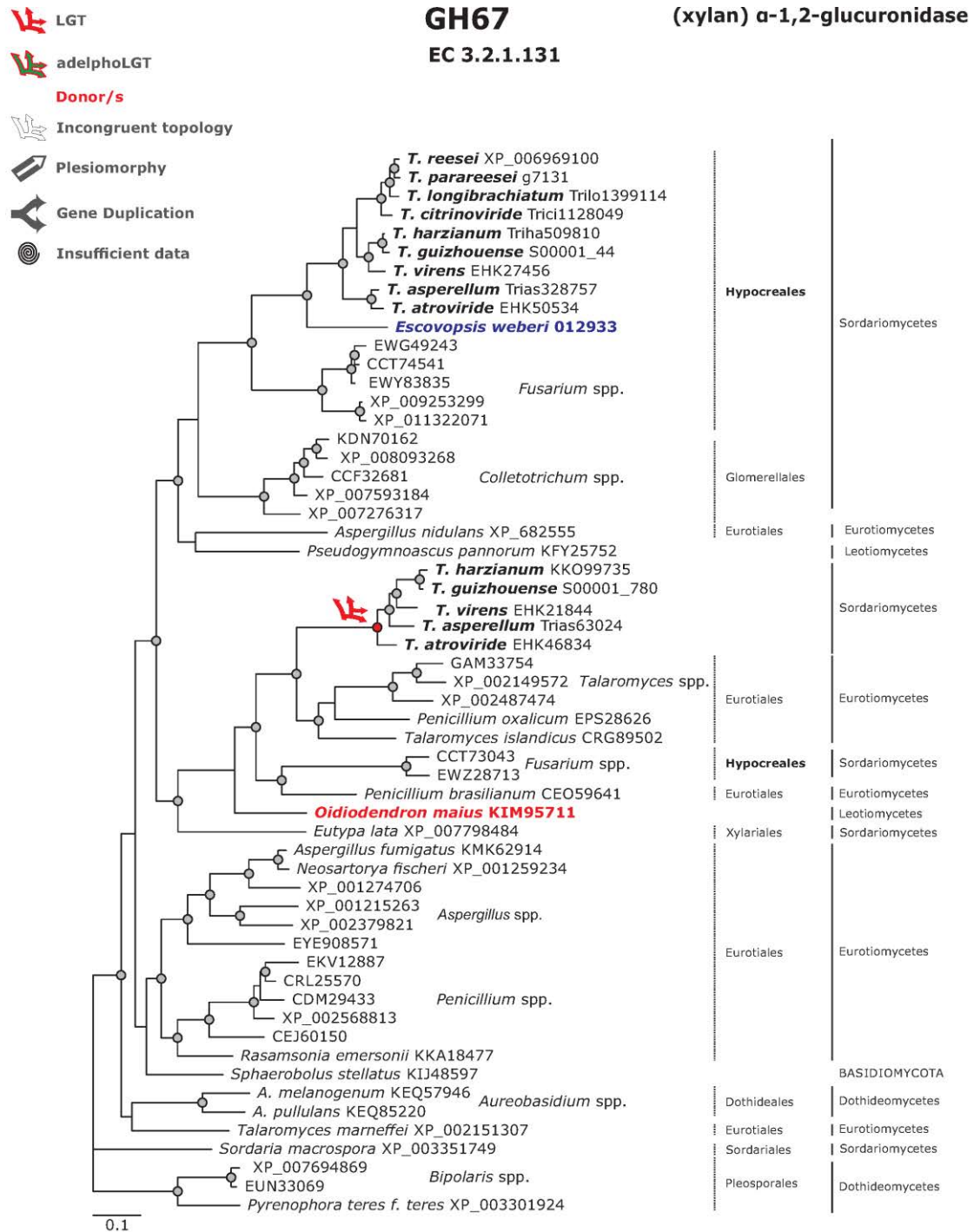
Phylogram based on Dayhoff amino acid substitution model using an alignment containing 10736 characters. Bayesian analysis was run for 1 million mcmc generations and a strict consensus tree was obtained by summarizing 7500 trees, after burning first 25% of obtained 10,000 trees. Mean tree length and variance are 1.940448E+01 and 4.3743370E-02, respectively. Posterior probabilities more than 90% are marked with circular nodes. Dashed vertical bars and non-dashed vertical bars represents the taxonomic order and taxonomic class in the phylum Ascomycota, respectively.









Phylogram based on Dayhoff amino acid substitution model using an alignment containing 47070 characters. Bayesian analysis was run for 3 million mcmc generations and a strict consensus tree was obtained by summarizing 22500 trees, after burning first 25% of obtained 30,000 trees. Mean tree length and variance are 8.226706E+00 and 1.7511440E-02, respectively. Posterior probabilities more than 90% are marked with circular nodes. Dashed vertical bars and non-dashed vertical bars represents the taxonomic order and taxonomic class in the phylum Ascomycota, respectively.



Phylogram based on Dayhoff amino acid substitution model using an alignment containing 18154 characters. Bayesian analysis was run for 1 million mcmc generations and a strict consensus tree was obtained by summarizing 7500 trees, after burning first 25% of obtained 10,000 trees. Mean tree length and variance are 6.723306e+000 and 2.384449e-002, respectively. Posterior probabilities more than 90% are marked with circular nodes. Dashed vertical bars and non-dashed vertical bars represents the taxonomic order and taxonomic class in the phylum Ascomycota, respectively.

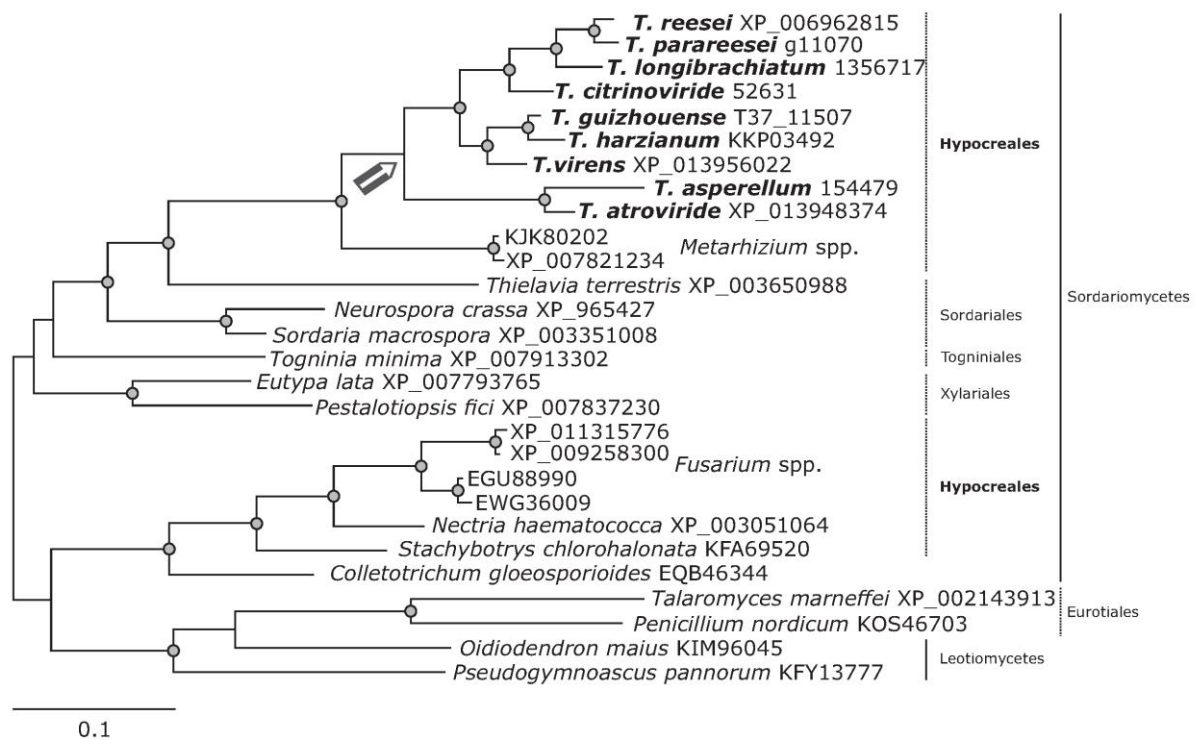


Phylogram based on Dayhoff amino acid substitution model using an alignment containing 50763 characters. Bayesian analysis was run for 1 million mcmc generations and a strict consensus tree was obtained by summarizing 7500 trees, after burning first 25% of obtained 10,000 trees. Mean tree length and variance are 1.058915E+01 and 1.4302340E-02, respectively. Posterior probabilities more than 90% are marked with circular nodes. Dashed vertical bars and non-dashed vertical bars represents the taxonomic order and taxonomic class in the phylum Ascomycota, respectively.

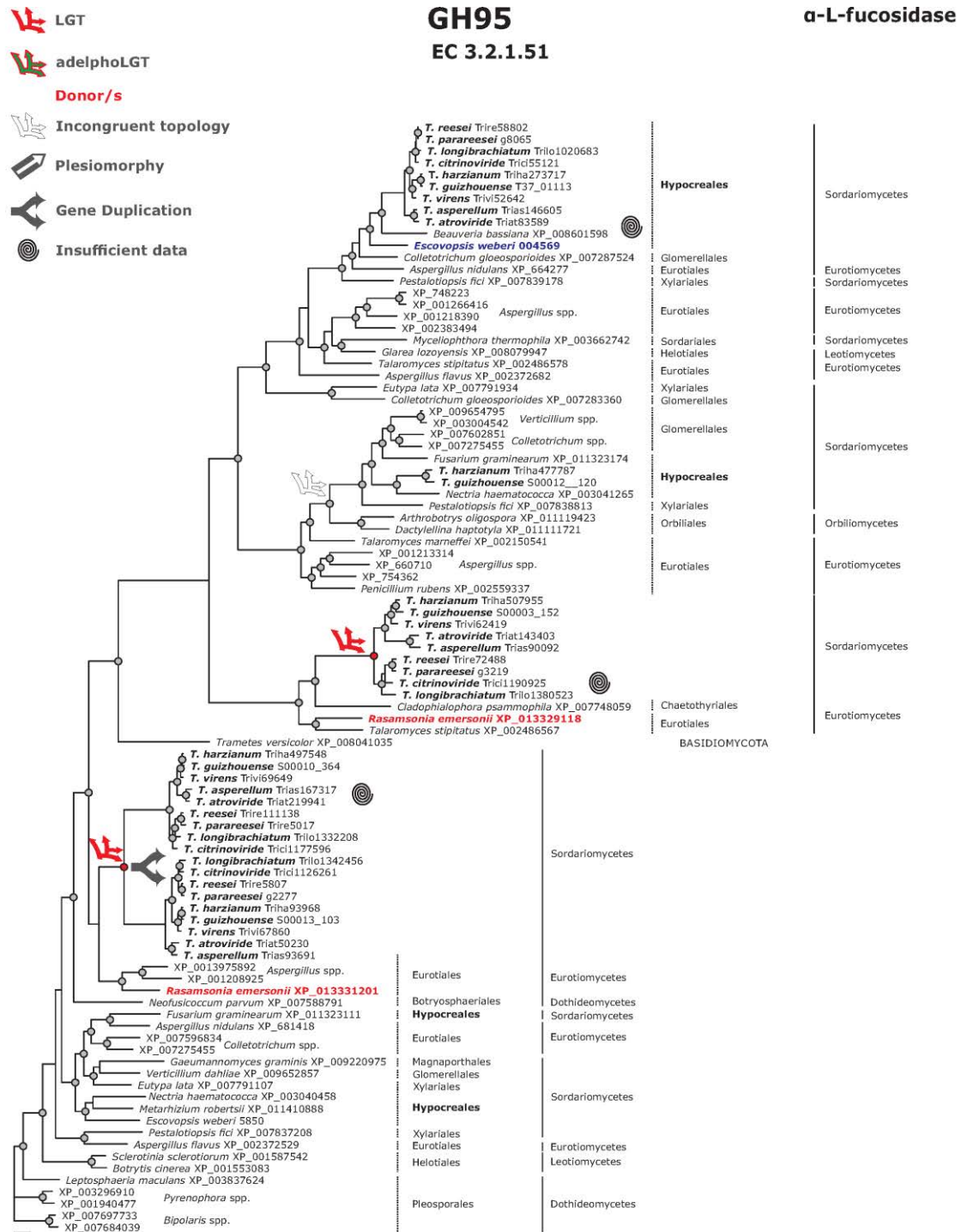
-  LGT
-  adelphoLGT
- Donor/s**
-  Incongruent topology
-  Plesiomorphy
-  Gene Duplication
-  Insufficient data

GH115
EC 3.2.1.-

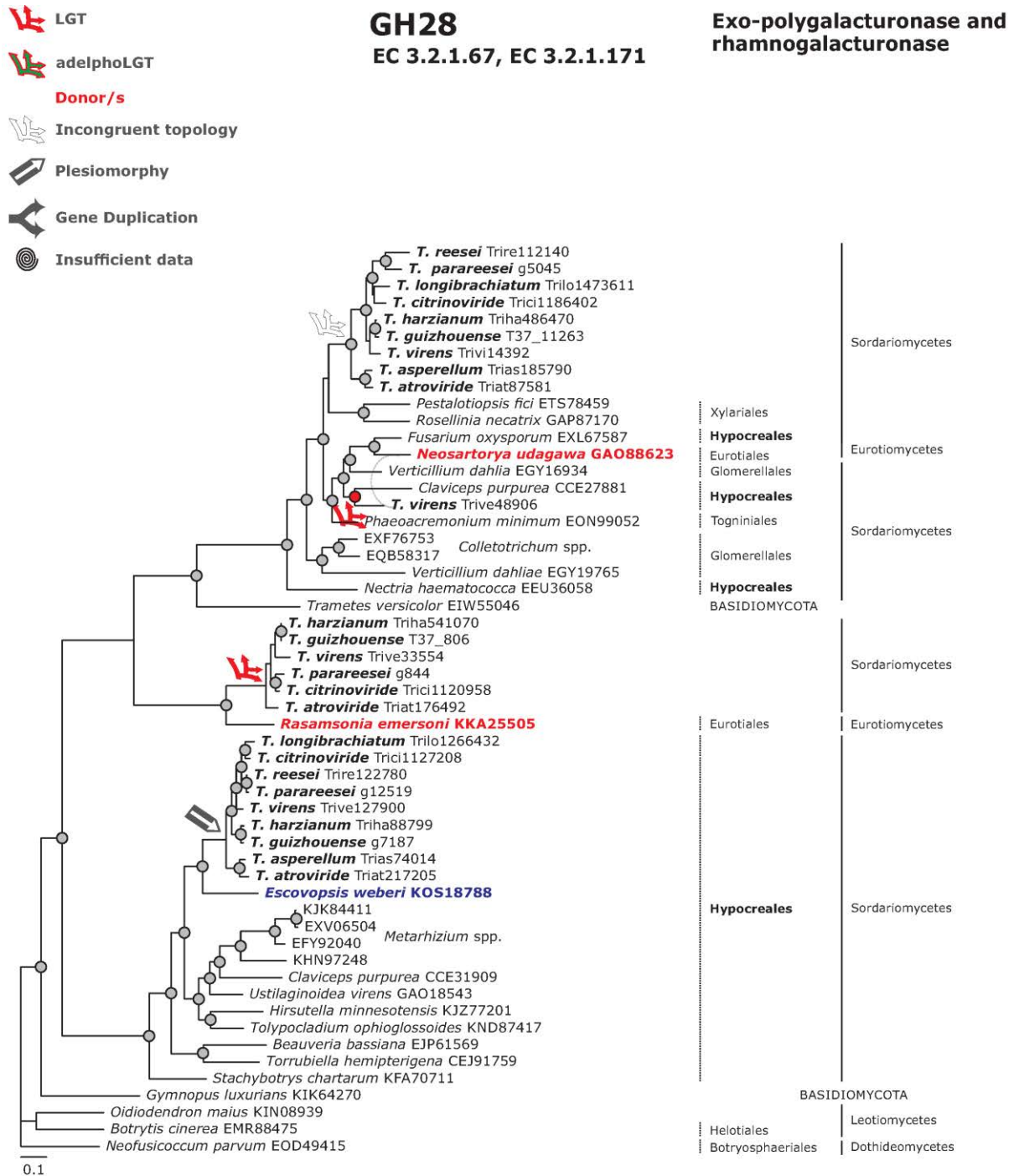
α -(4-O-methyl)-glucuronidase









Phylogram based on Dayhoff amino acid substitution model using an alignment containing 10780 characters. Bayesian analysis was run for 1 million mcmc generations and a strict consensus tree was obtained by summarizing 7500 trees, after burning first 25% of obtained 10,000 trees. Mean tree length and variance are 2.943435E+00 and 8.8934440E-03, respectively. Posterior probabilities more than 90% are marked with circular nodes. Dashed vertical bars and non-dashed vertical bars represents the taxonomic order and taxonomic class in the phylum Ascomycota, respectively.



Phylogram based on Dayhoff amino acid substitution model using an alignment containing 86762 characters. Bayesian analysis was run for 1 million mcmc generations and a strict consensus tree was obtained by summarizing 7500 trees, after burning first 25% of obtained 10,000 trees. Mean tree length and variance are 2.349982E+01 and 4.1706740E-02, respectively. Posterior probabilities more than 90% are marked with circular nodes. Dashed vertical bars and non-dashed vertical bars represents the taxonomic order and taxonomic class in the phylum Ascomycota, respectively.

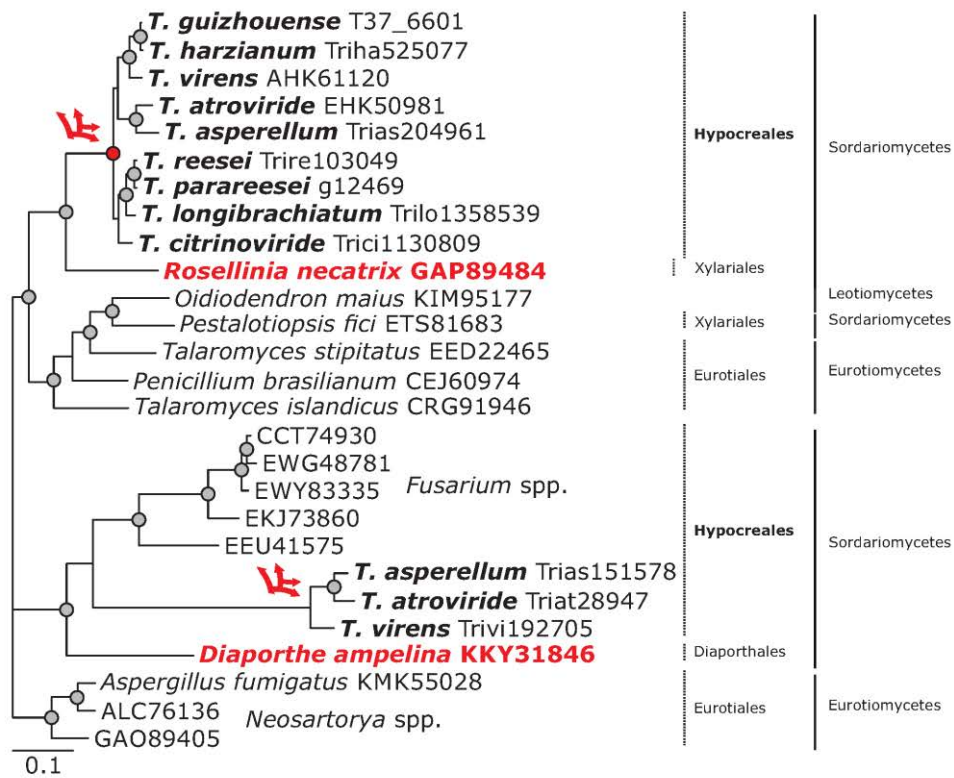


Phylogram based on Dayhoff amino acid substitution model using an alignment containing 22626 characters. Bayesian analysis was run for 1 million mcmc generations and a strict consensus tree was obtained by summarizing 7500 trees, after burning first 25% of obtained 10,000 trees. Mean tree length and variance are 1.046359E+01 and 3.3770210E-02, respectively. Posterior probabilities more than 90% are marked with circular nodes. Dashed vertical bars and non-dashed vertical bars represents the taxonomic order and taxonomic class in the phylum Ascomycota, respectively.

-  LGT
-  adelphoLGT
- Donor/s
-  Incongruent topology
-  Plesiomorphy
-  Gene Duplication
-  Insufficient data

GH28
EC 3.2.1.15

Polygalacturonase

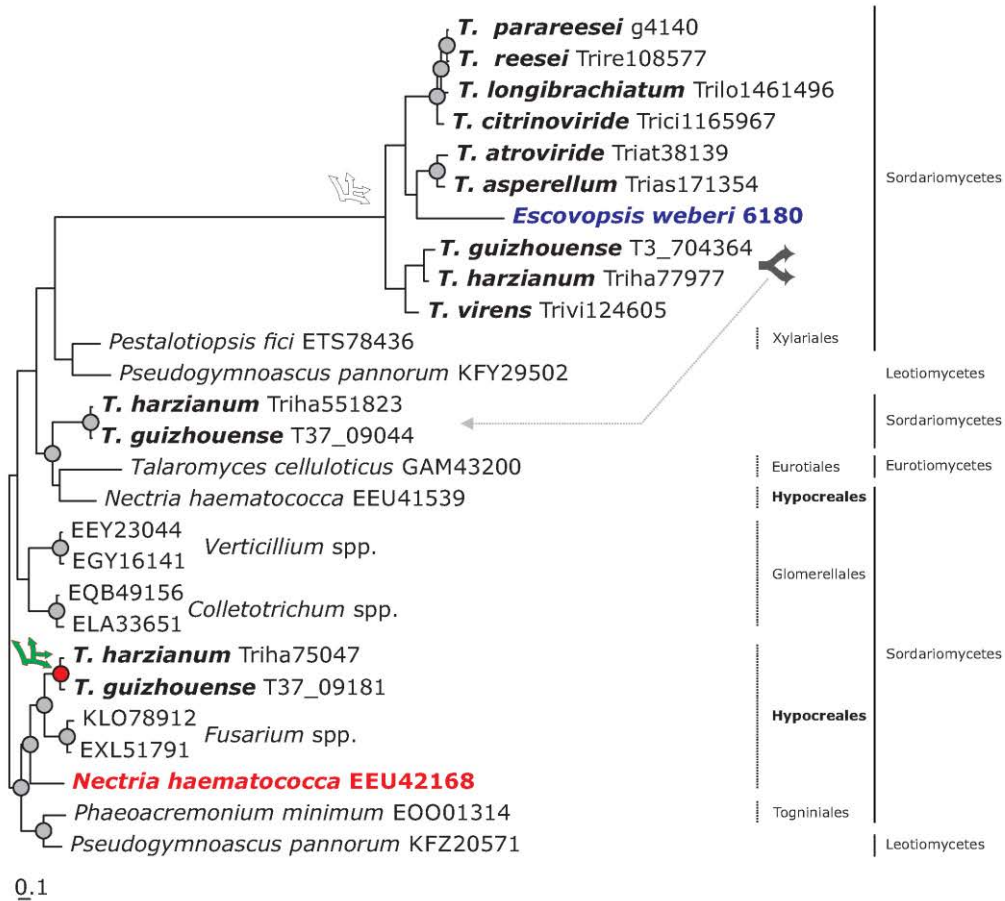


Phylogram based on Dayhoff amino acid substitution model using an alignment containing 10611 characters. Bayesian analysis was run for 1 million mcmc generations and a strict consensus tree was obtained by summarizing 7500 trees, after burning first 25% of obtained 10,000 trees. Mean tree length and variance are 2.800150E+00 and 8.0533830E-03, respectively. Posterior probabilities more than 90% are marked with circular nodes. Dashed vertical bars and non-dashed vertical bars represents the taxonomic order and taxonomic class in the phylum Ascomycota, respectively.







-  LGT
-  adelphoLGT
- Donor/s**
-  Incongruent topology
-  Plesiomorphy
-  Gene Duplication
-  Insufficient data

GH28
EC 3.2.1.-

Exo-xylogalacturan hydrolase

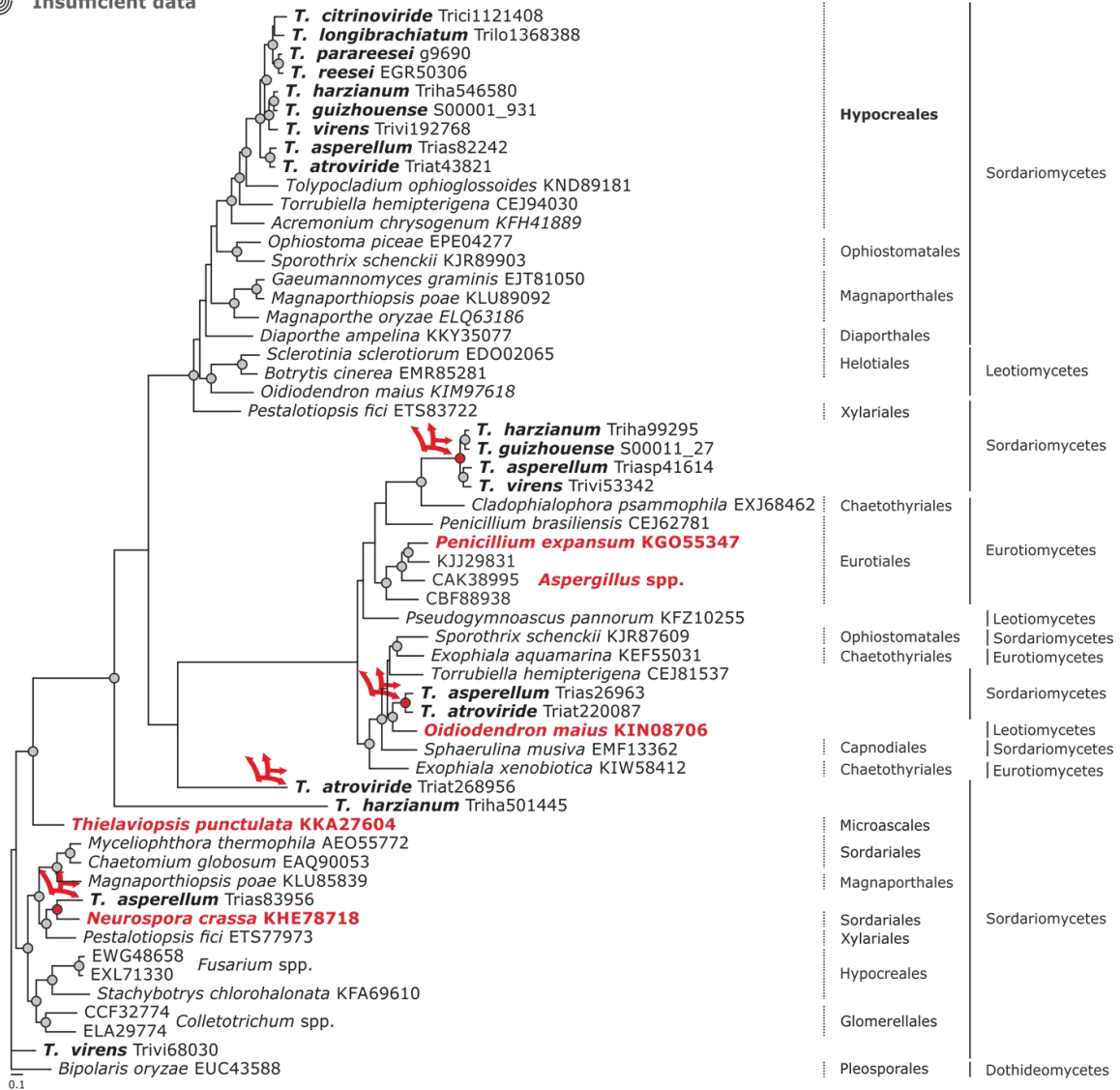


Phylogram based on Dayhoff amino acid substitution model using an alignment containing 21349 characters. Bayesian analysis was run for 1 million mcmc generations and a strict consensus tree was obtained by summarizing 7500 trees, after burning first 25% of obtained 10,000 trees. Mean tree length and variance are 1.138844E+01 and 8.8116490E-02, respectively. Posterior probabilities more than 90% are marked with circular nodes. Dashed vertical bars and non-dashed vertical bars represents the taxonomic order and taxonomic class in the phylum Ascomycota, respectively.







-  LGT
-  adelphoLGT
- Donor/s**
-  Incongruent topology
-  Plesiomorphy
-  Gene Duplication
-  Insufficient data

GH78
EC 3.2.1.40

α-L-rhamnosidase



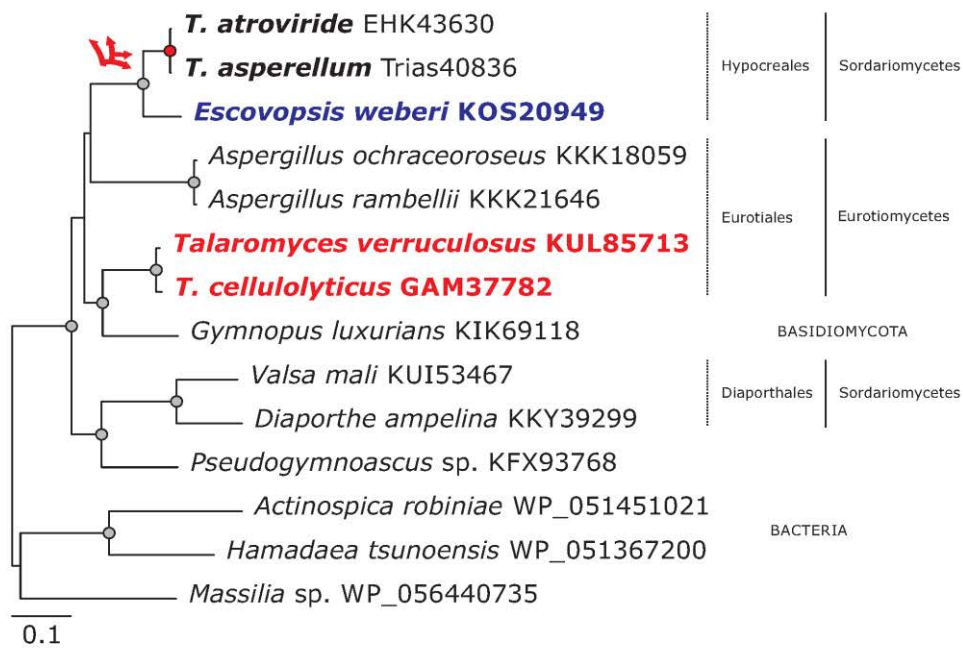
Phylogram based on Dayhoff amino acid substitution model using an alignment containing 62700 characters. Bayesian analysis was run for 1 million mcmc generations and a strict consensus tree was obtained by summarizing 7500 trees, after burning first 25% of obtained 10,000 trees. Mean tree length and variance are 1.058915E+01 and 1.4302340E-02, respectively. Posterior probabilities more than 90% are marked with circular nodes. Dashed vertical bars and non-dashed vertical bars represents the taxonomic order and taxonomic class in the phylum Ascomycota, respectively.

-  LGT
-  adelphoLGT
- Donor/s
-  Incongruent topology
-  Plesiomorphy
-  Gene Duplication
-  Insufficient data







PL1

EC 4.2.2.2

Pectate lyase



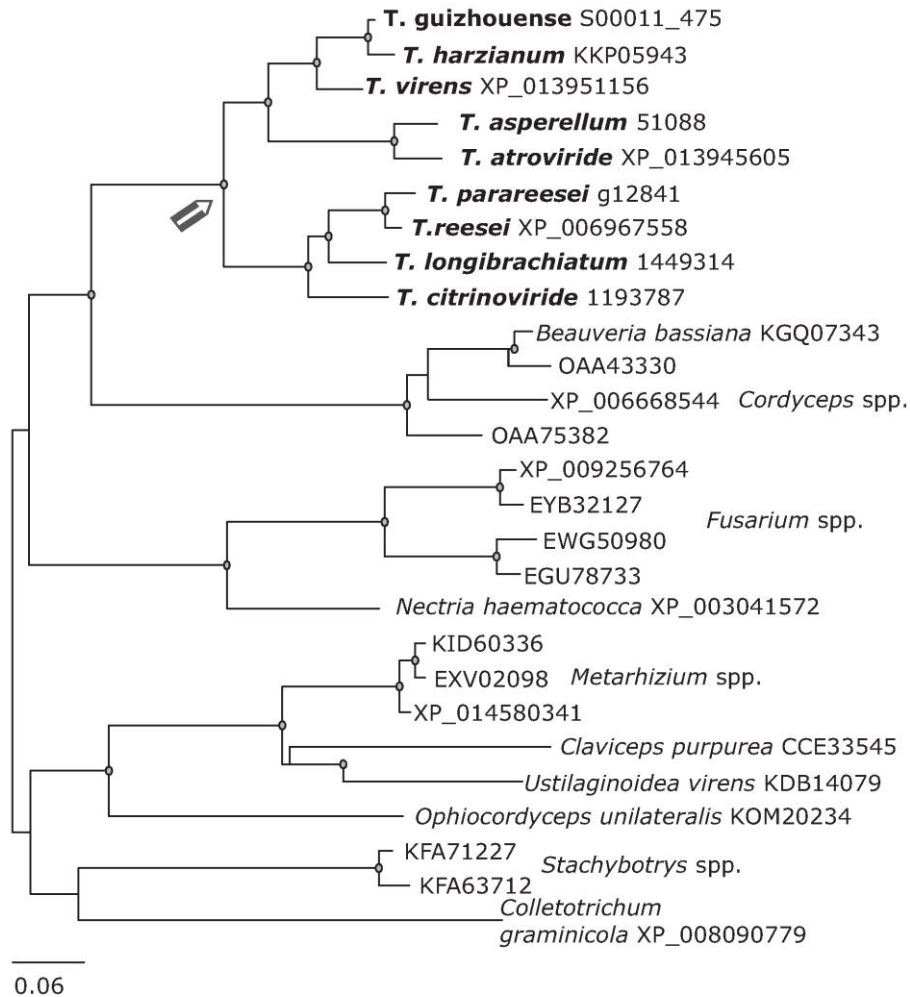
Phylogram based on Dayhoff amino acid substitution model using an alignment containing 4858 characters. Bayesian analysis was run for 1 million mcmc generations and a strict consensus tree was obtained by summarizing 7500 trees, after burning first 25% of obtained 10,000 trees. Mean tree length and variance are 2.165486E+00 and 7.1493260E-03, respectively. Posterior probabilities more than 90% are marked with circular nodes. Dashed vertical bars and non-dashed vertical bars represents the taxonomic order and taxonomic class in the phylum Ascomycota, respectively.

-  LGT
-  adelphoLGT
- Donor/s
-  Incongruent topology
-  Plesiomorphy
-  Gene Duplication
-  Insufficient data

GH35







β-galactosidase

EC 3.2.1.23



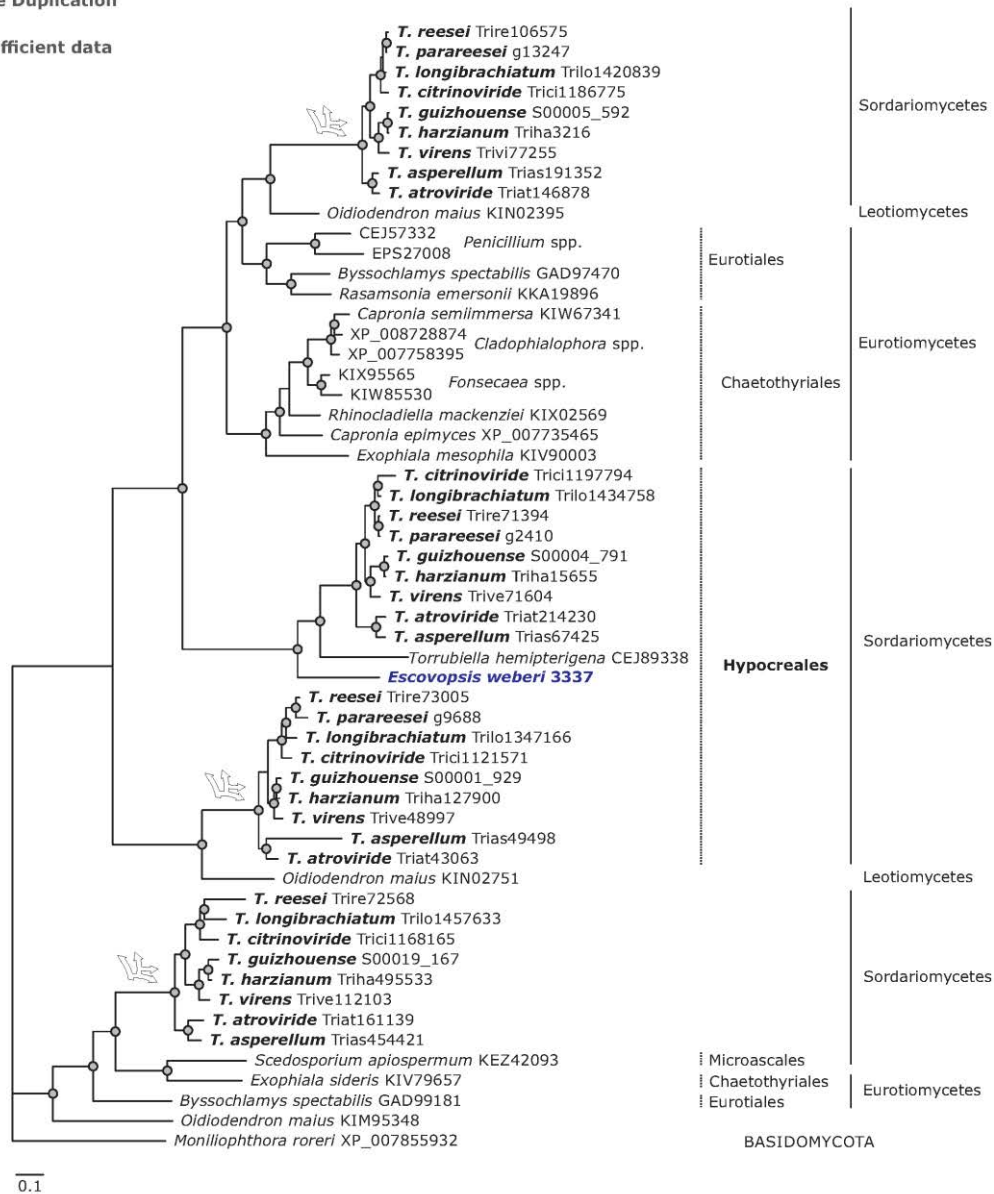
***All species fall under taxonomic class Sordariomycetes and taxonomic order Hypocreales, except *Colletotrichum graminicola* which is from order Glomerellales**

Phylogram based on Dayhoff amino acid substitution model using an alignment containing 24794 characters. Bayesian analysis was run for 1 million mcmc generations and a strict consensus tree was obtained by summarizing 7500 trees, after burning first 25% of obtained 10,000 trees. Mean tree length and variance are 3.587438E+00 and 4.1878620E-03, respectively. Posterior probabilities more than 90% are marked with circular nodes.







-  LGT
-  adelphoLGT
- Donor/s
-  Incongruent topology
-  Plesiomorphy
-  Gene Duplication
-  Insufficient data

GH79
EC 3.2.1.31

β-(4-O-methyl)-glucuronidase

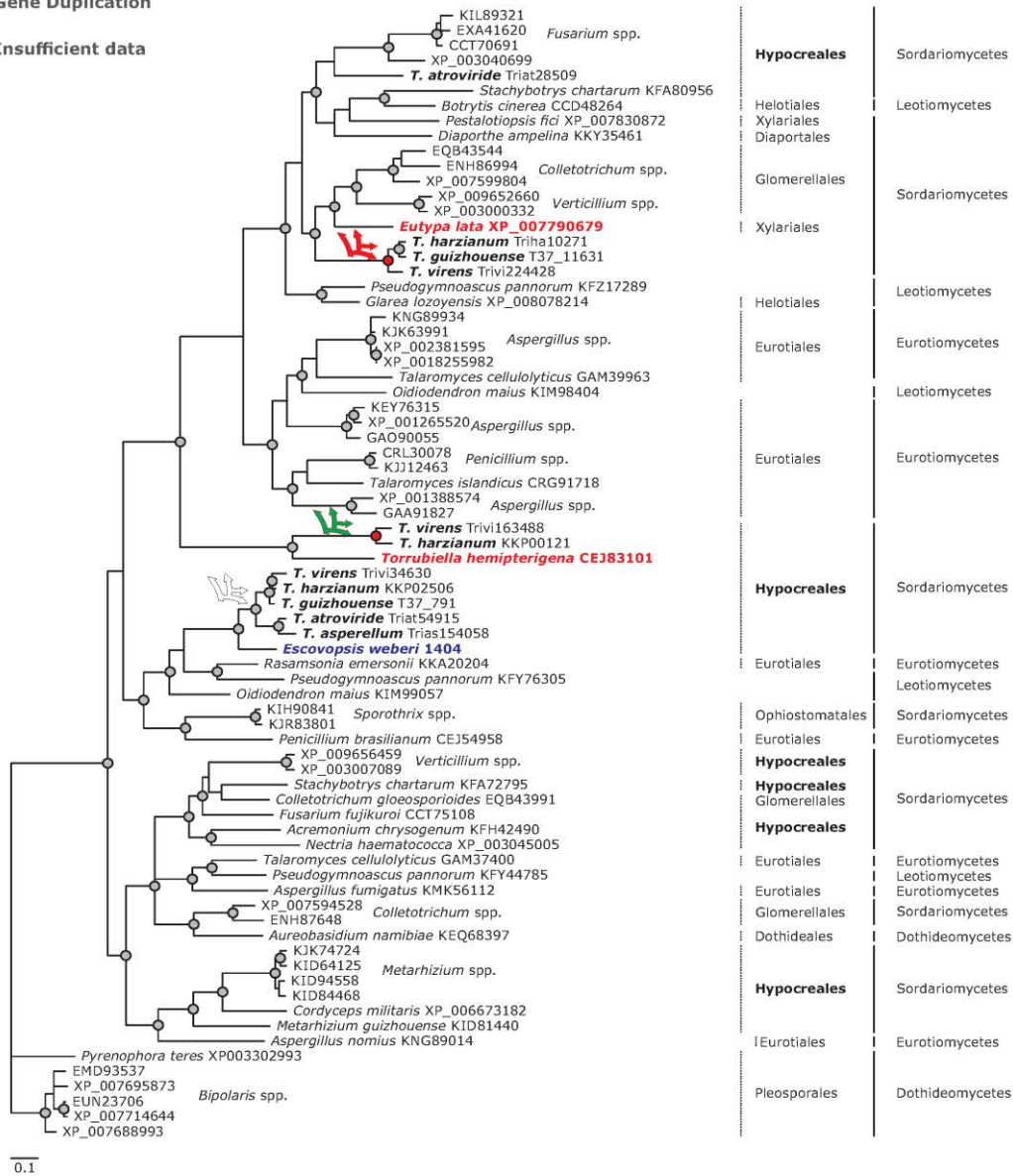


Phylogram based on Dayhoff amino acid substitution model using an alignment containing 34664 characters. Bayesian analysis was run for 1 million mcmc generations and a strict consensus tree was obtained by summarizing 7500 trees, after burning first 25% of obtained 10,000 trees. Mean tree length and variance are 1.069127E+01 and 2.7815940E-02, respectively. Posterior probabilities more than 90% are marked with circular nodes. Dashed vertical bars and non-dashed vertical bars represents the taxonomic order and taxonomic class in the phylum Ascomycota, respectively.





-  LGT
-  adelphoLGT
- Donor/s**
-  Incongruent topology
-  Plesiomorphy
-  Gene Duplication
-  Insufficient data

GH88
EC 3.2.1.-

Δ-4,5-unsaturated β-glucuronyl hydrolase

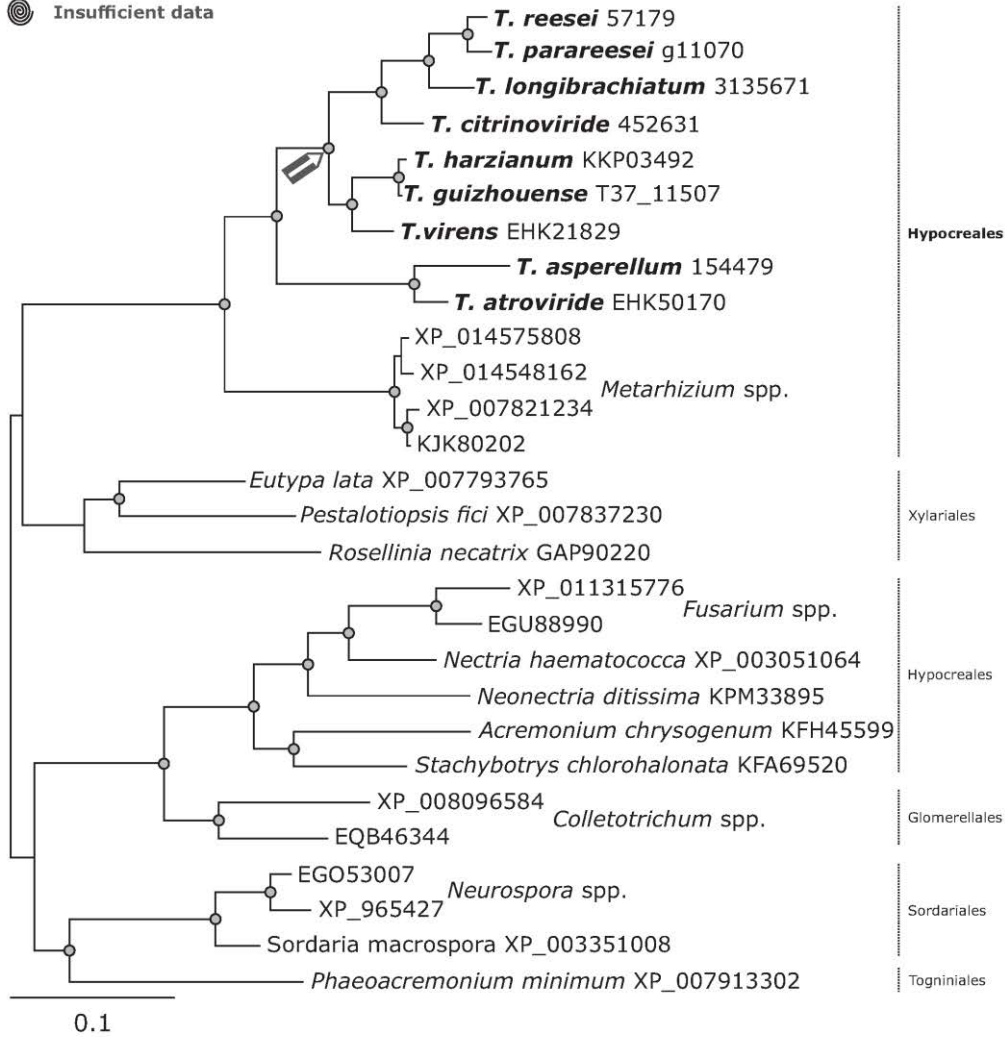


Phylogram based on Dayhoff amino acid substitution model using an alignment containing 9984 characters. Bayesian analysis was run for 1 million mcmc generations and a strict consensus tree was obtained by summarizing 7500 trees, after burning first 25% of obtained 10,000 trees. Mean tree length and variance are 2.334795E+00 and 6.8740380E-03, respectively. Posterior probabilities more than 90% are marked with circular nodes. Dashed vertical bars and non-dashed vertical bars represents the taxonomic order and taxonomic class in the phylum Ascomycota, respectively.

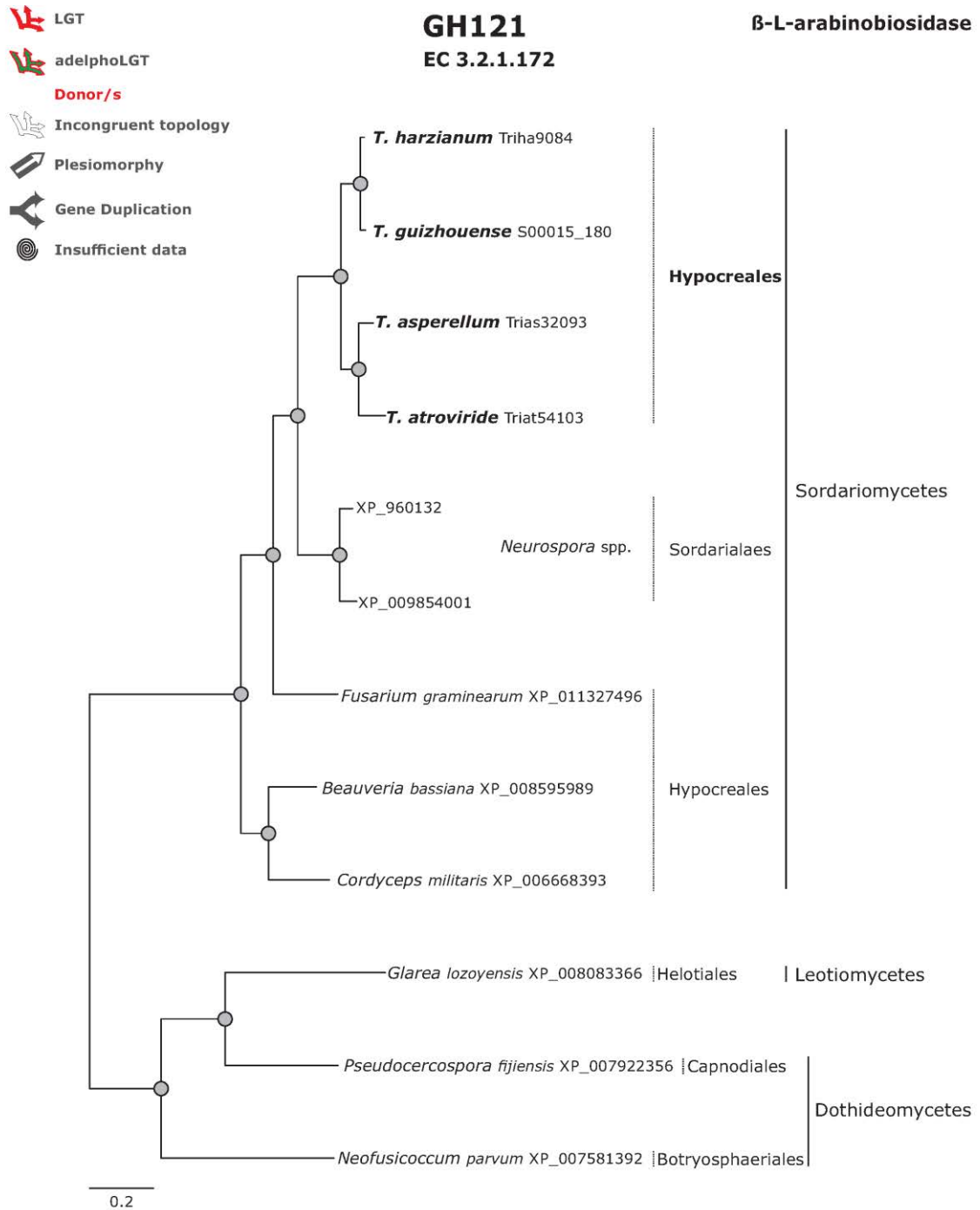
-  LGT
-  adelphoLGT
- Donor/s
-  Incongruent topology
-  Plesiomorphy
-  Gene Duplication
-  Insufficient data

GH105
EC 3.2.1.172

**Unsaturated rhamnogalacturonyl
hydrolase**









Phylogram based on Dayhoff amino acid substitution model using an alignment containing 10752 characters. Bayesian analysis was run for 1 million mcmc generations and a strict consensus tree was obtained by summarizing 7500 trees, after burning first 25% of obtained 10,000 trees. Mean tree length and variance are 2.390426E+00 and 7.1870230E-03, respectively. Posterior probabilities more than 90% are marked with circular nodes. Dashed vertical bars and non-dashed vertical bars represents the taxonomic order and taxonomic class in the phylum Ascomycota, respectively.



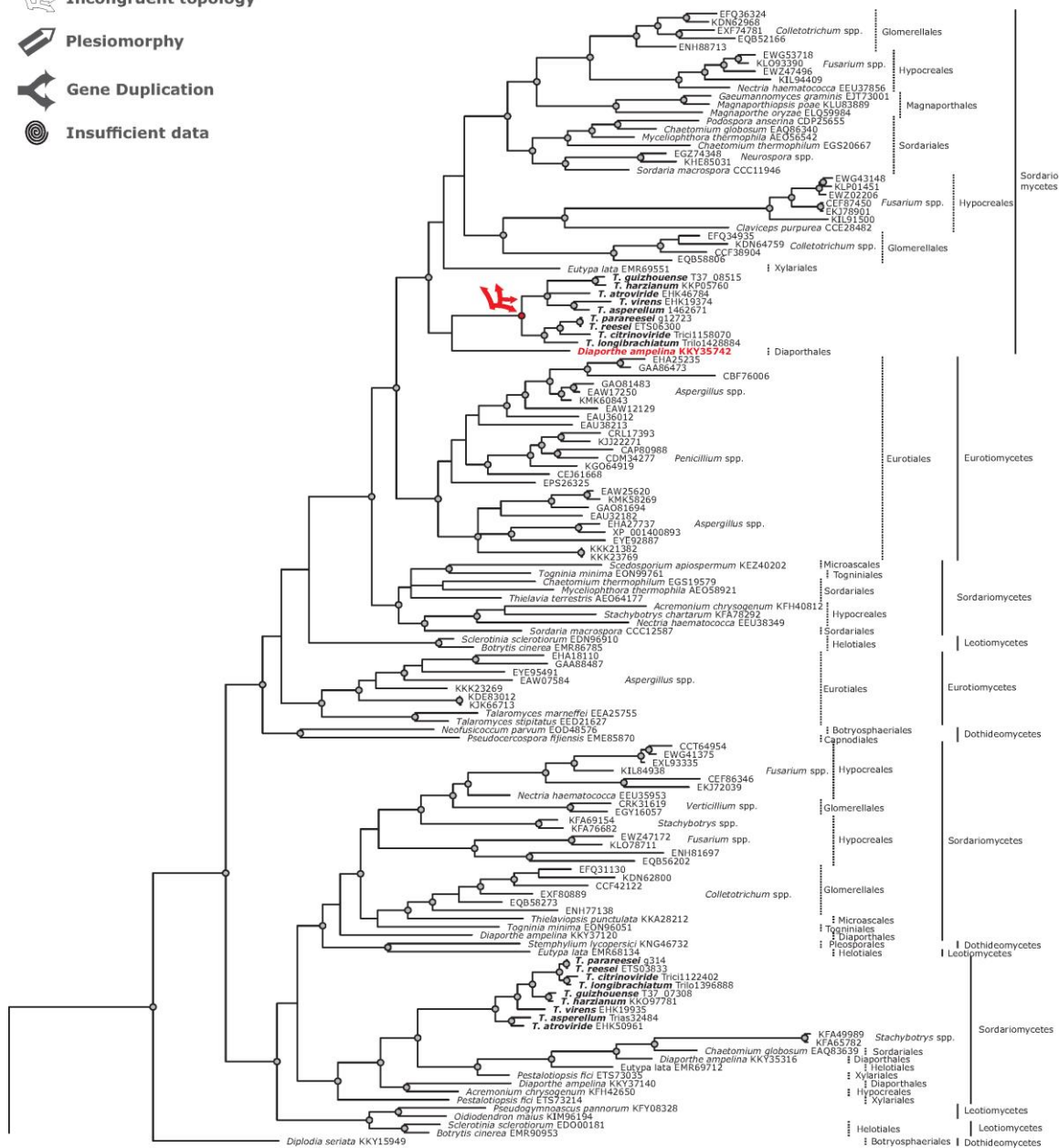
Phylogram based on Dayhoff amino acid substitution model using an alignment containing 10932 characters. Bayesian analysis was run for 1 million mcmc generations and a strict consensus tree was obtained by summarizing 7500 trees, after burning first 25% of obtained 10,000 trees. Mean tree length and variance are 3.748802e+000 and 8.399156e-003, respectively. Posterior probabilities more than 90% are marked with circular nodes. Dashed vertical bars and non-dashed vertical bars represents the taxonomic order and taxonomic class in the phylum Ascomycota, respectively.

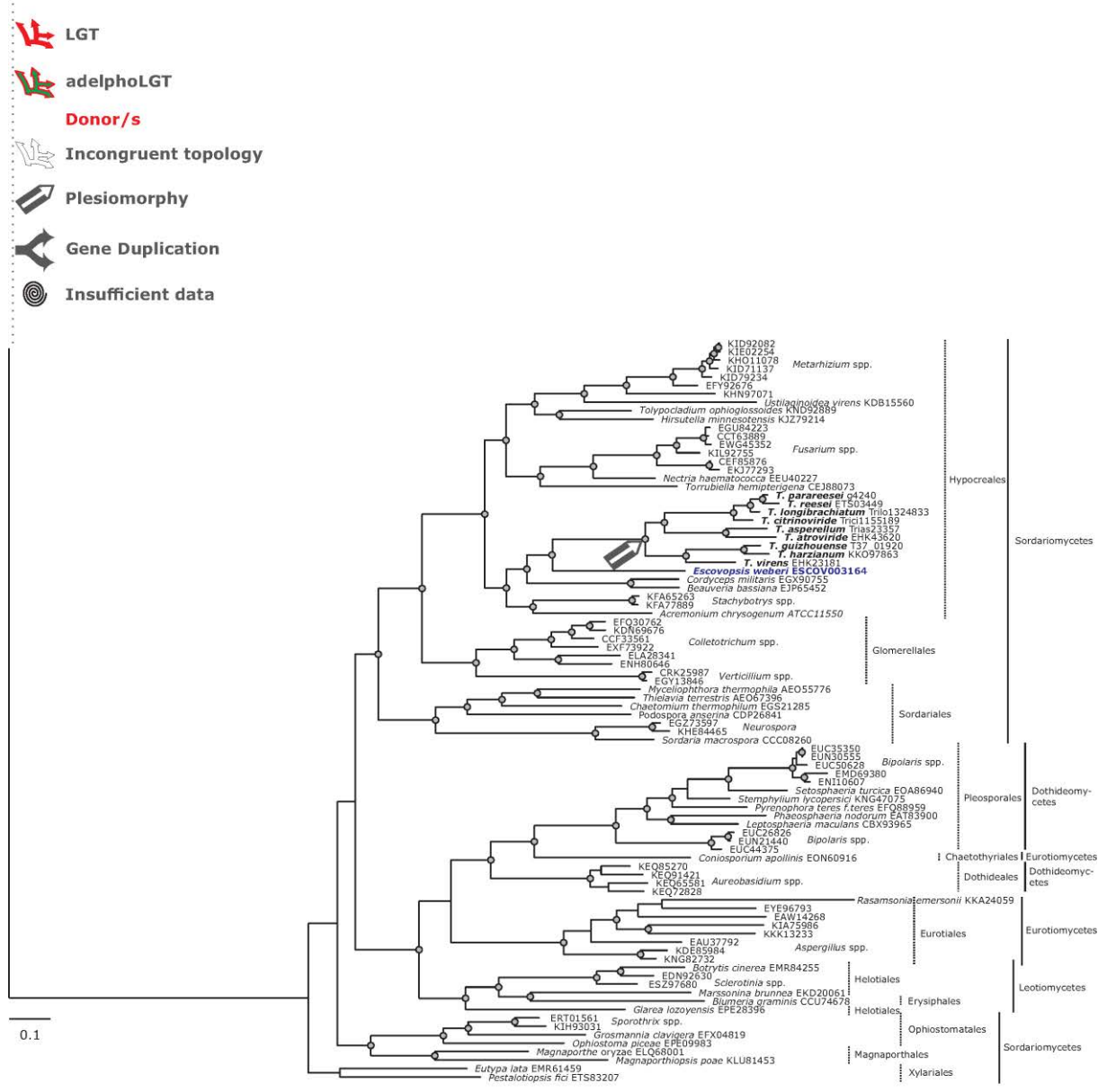


Phylogram based on Dayhoff amino acid substitution model using an alignment containing 27680 characters. Bayesian analysis was run for 1 million mcmc generations and a strict consensus tree was obtained by summarizing 7500 trees, after burning first 25% of obtained 10,000 trees. Mean tree length and variance are 8.069252e+000 and 1.439181e-002, respectively. Posterior probabilities more than 90% are marked with circular nodes. Dashed vertical bars and non-dashed vertical bars represents the taxonomic order and taxonomic class in the phylum Ascomycota, respectively.







-  LGT
-  adelphoLGT
- Donor/s**
-  Incongruent topology
-  Plesiomorphy
-  Gene Duplication
-  Insufficient data

AA9 Copper dependent lytic polysaccharide monoxygenase



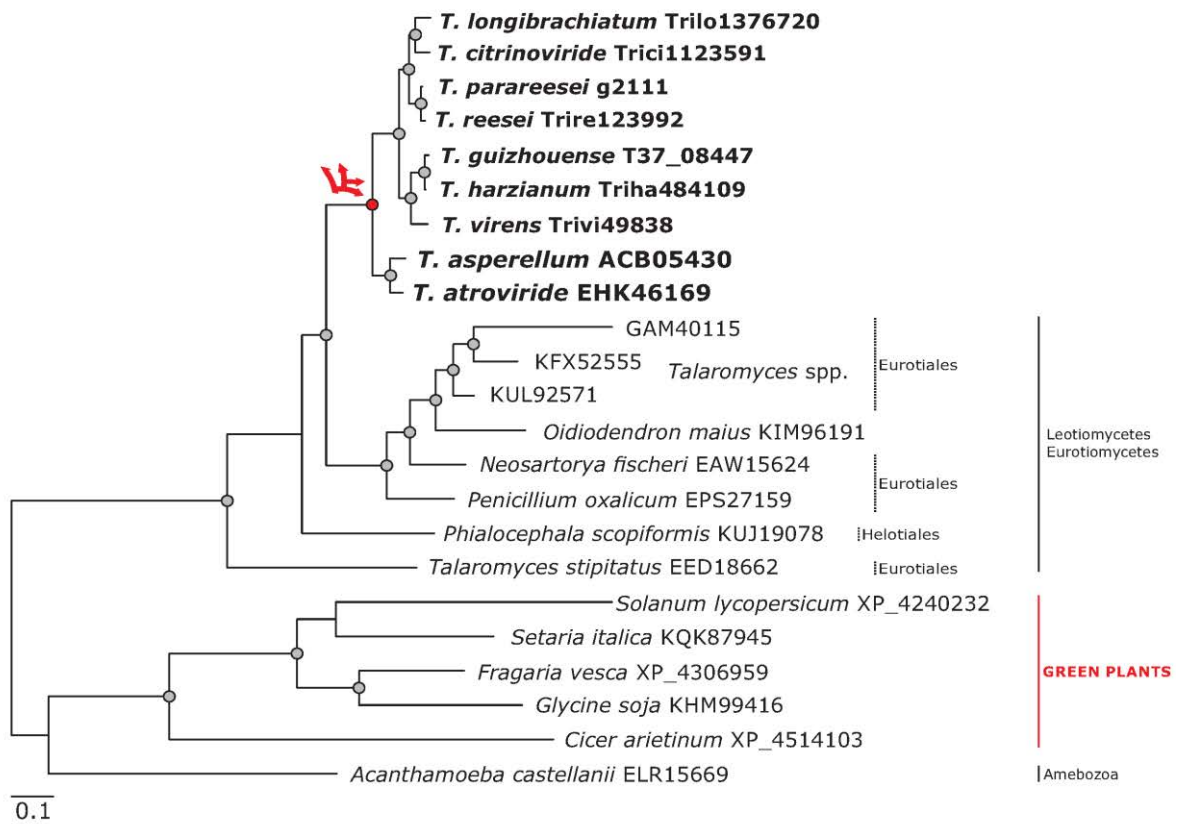


Phylogram based on Dayhoff amino acid substitution model using an alignment containing 129950 characters. Bayesian analysis was run for 1 million mcmc generations and a strict consensus tree was obtained by summarizing 7500 trees, after burning first 25% of obtained 10,000 trees. Mean tree length and variance are 5.586972E+01 and 2.1853650E-01, respectively. Posterior probabilities more than 90% are marked with circular nodes. Dashed vertical bars and non-dashed vertical bars represents the taxonomic order and taxonomic class in the phylum Ascomycota, respectively.

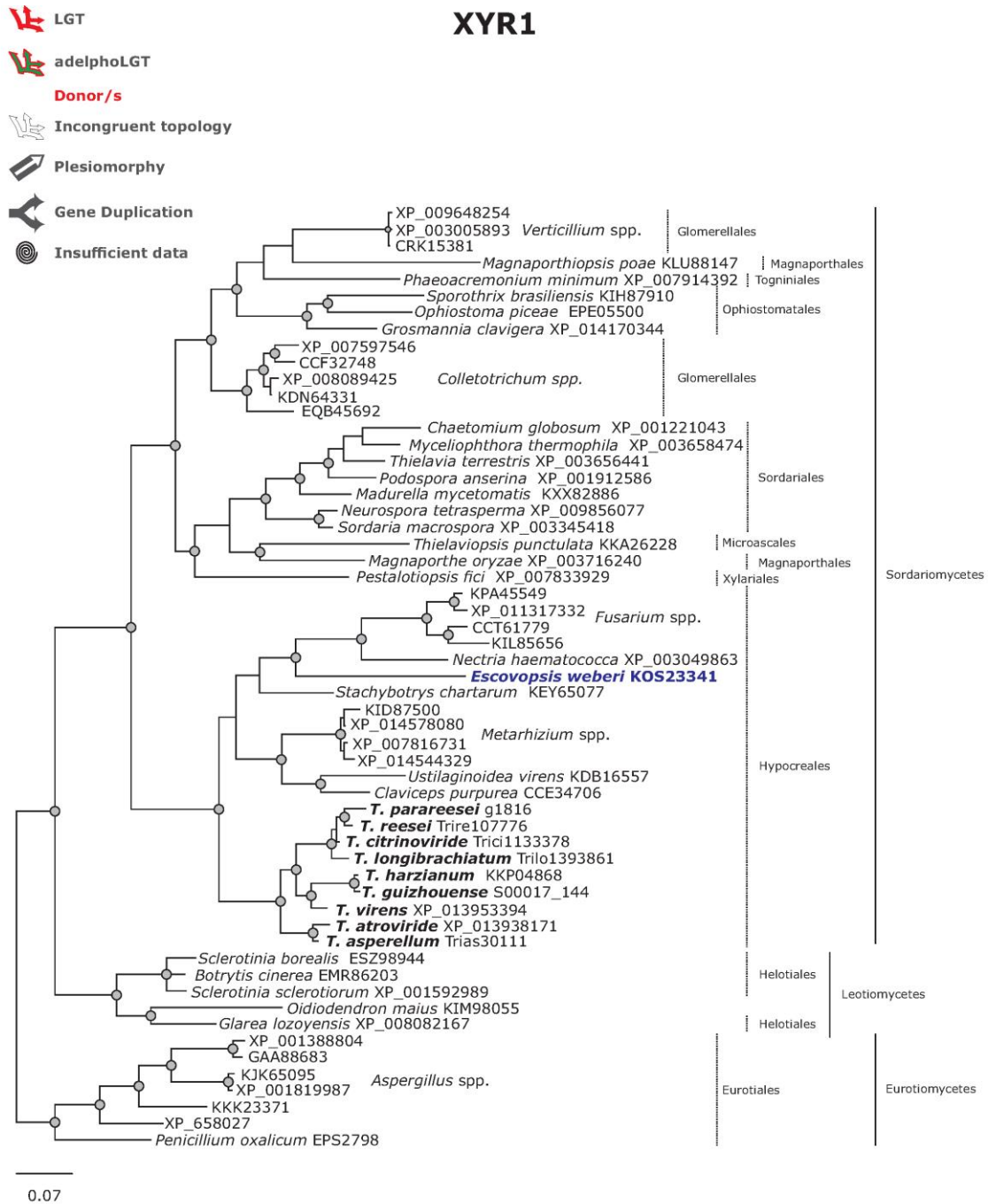
-  **LGT**
-  **adelphoLGT**
- Donor/s**
-  **Incongruent topology**
-  **Plesiomorphy**
-  **Gene Duplication**
-  **Insufficient data**

Swollenin







Auxiliary protein



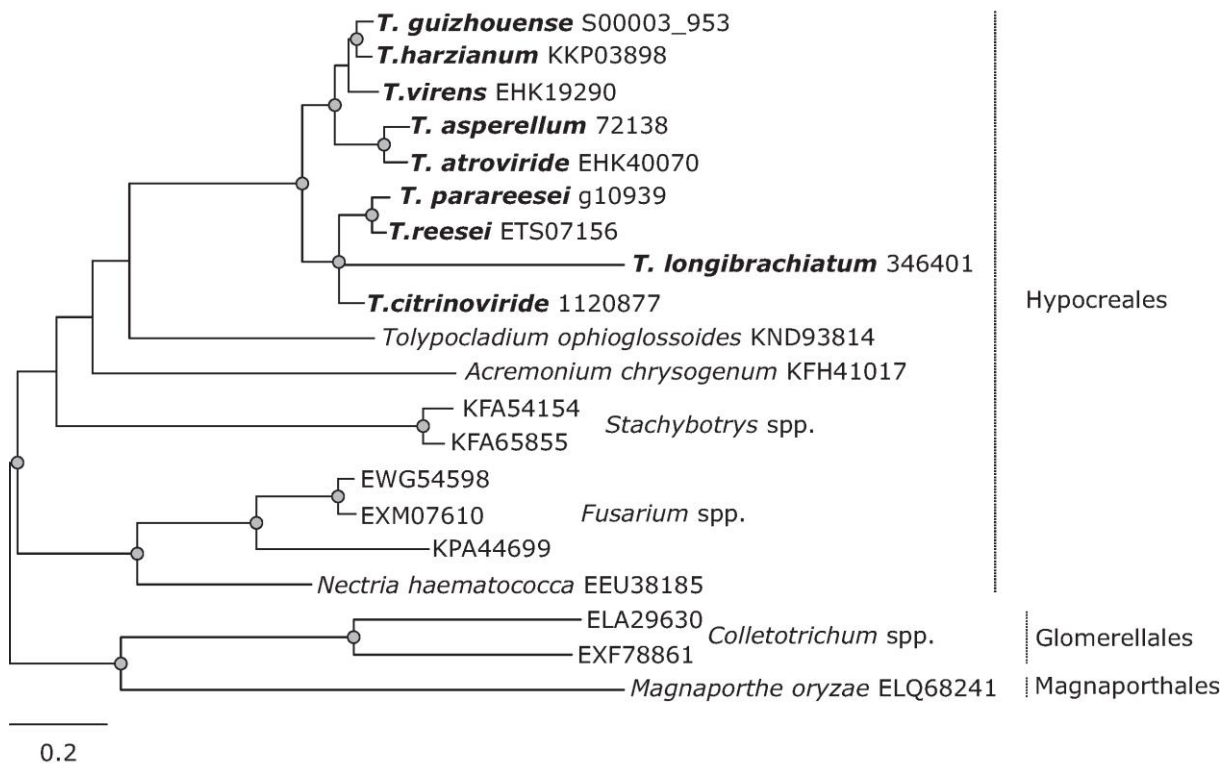
Phylogram based on Dayhoff amino acid substitution model using an alignment containing 12144 characters. Bayesian analysis was run for 1 million mcmc generations and a strict consensus tree was obtained by summarizing 7500 trees, after burning first 25% of obtained 10,000 trees. Mean tree length and variance are 7.653121E+00 and 4.9981080E-02, respectively. Posterior probabilities more than 90% are marked with circular nodes. Dashed vertical bars and non-dashed vertical bars represents the taxonomic order and taxonomic class in the phylum Ascomycota, respectively.



Phylogram based on Dayhoff amino acid substitution model using an alignment containing 18753 characters. Bayesian analysis was run for 1 million mcmc generations and a strict consensus tree was obtained by summarizing 7500 trees, after burning first 25% of obtained 10,000 trees. Mean tree length and variance are 5.781707E+00 and 2.0201740E-02, respectively. Posterior probabilities more than 90% are marked with circular nodes. Dashed vertical bars and non-dashed vertical bars represents the taxonomic order and taxonomic class in the phylum Ascomycota, respectively..







-  LGT
-  adelphoLGT
- Donor/s**
-  Incongruent topology
-  Plesiomorphy
-  Gene Duplication
-  Insufficient data

ACE2

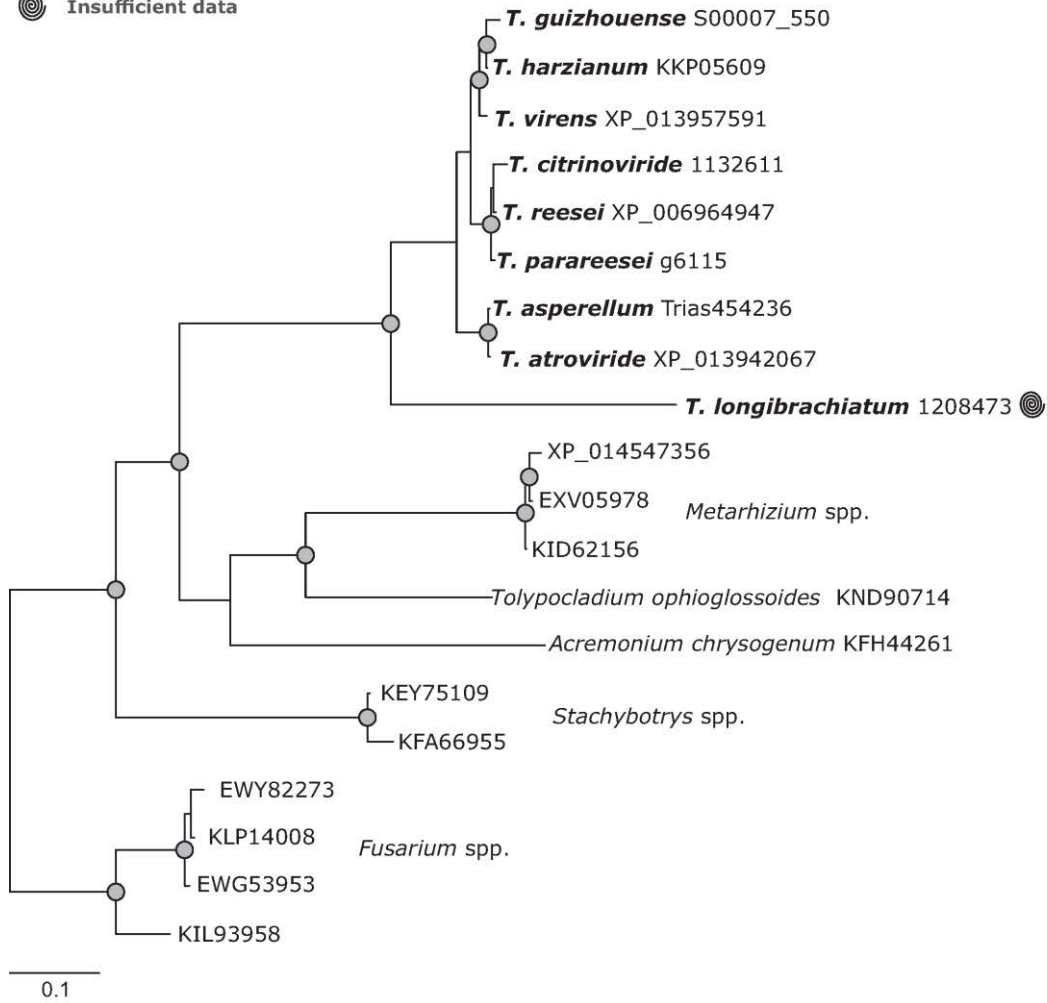


*All species fall under taxonomic class Sordariomycetes

Phylogram based on Dayhoff amino acid substitution model using an alignment containing 5910 characters. Bayesian analysis was run for 1 million mcmc generations and a strict consensus tree was obtained by summarizing 7500 trees, after burning first 25% of obtained 10,000 trees. Mean tree length and variance are 8.181301E+00 and 5.4077250E-02, respectively. Posterior probabilities more than 90% are marked with circular nodes. Dashed vertical bars represents the taxonomic order.

-  LGT
-  adelphoLGT
- Donor/s
-  Incongruent topology
-  Plesiomorphy
-  Gene Duplication
-  Insufficient data

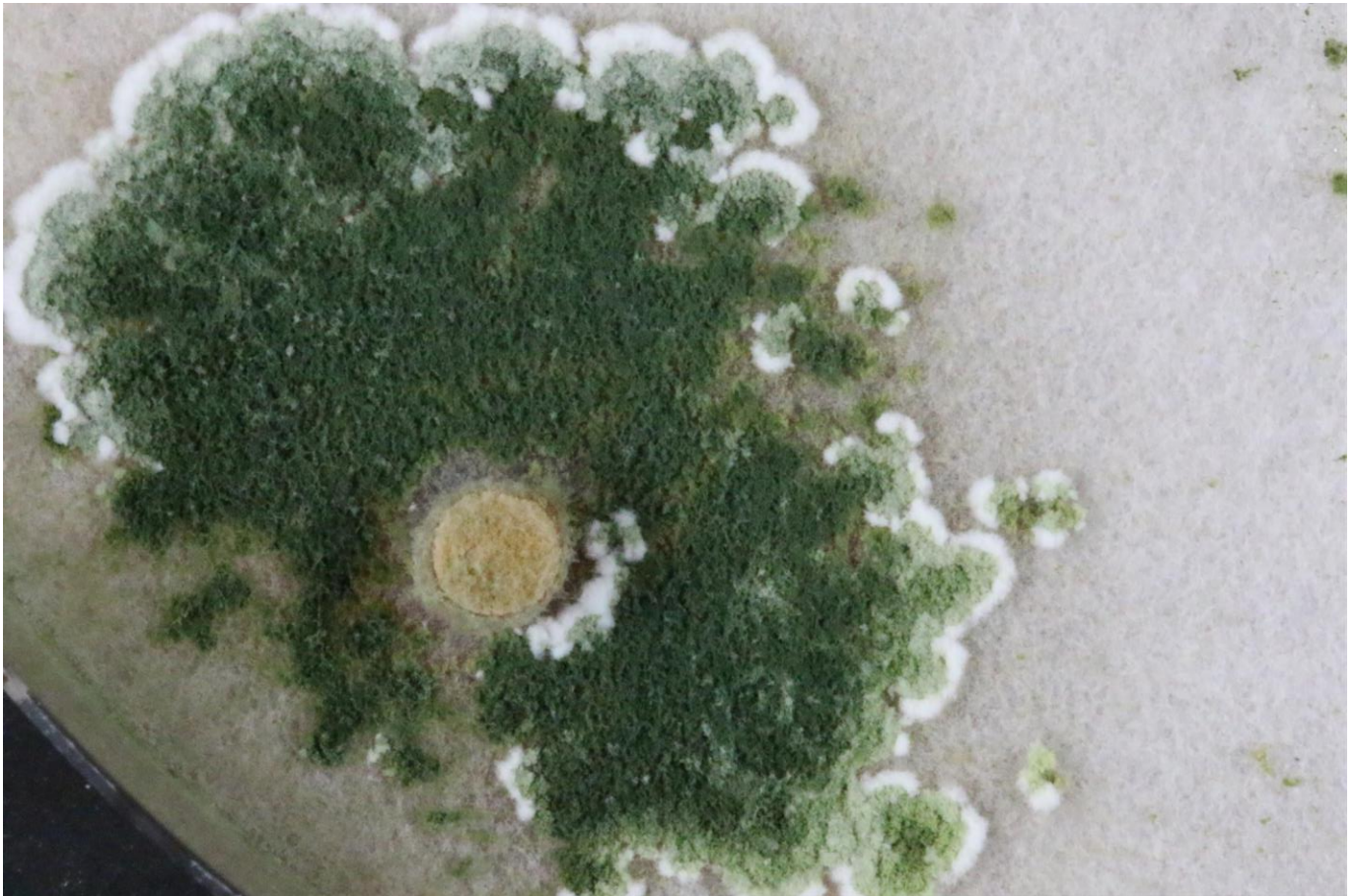
ACE3



*All species fall under taxonomic class Sordariomycetes and taxonomic order Hypocreales

Phylogram based on Dayhoff amino acid substitution model using an alignment containing 12155 characters. Bayesian analysis was run for 1 million mcmc generations and a strict consensus tree was obtained by summarizing 7500 trees, after burning first 25% of obtained 10,000 trees. Mean tree length and variance are 2.543828E+00 and 9.7324330E-03, respectively. Posterior probabilities more than 90% are marked with circular nodes.

Chapter 4 The pilot assessment of the contribution of putative xenologues genes in the development of Hypocrealean genomes



The unique property of *Trichoderma* spp. To be capable of various associations with fungi (ranging from allo- up to adelphoparasitism) and degradation of plant biomass (Described in Chapter 3), unlike other closely related fungi which are usually nutritionally specialized or they have limited versatility makes the whole proteome of *Trichoderma* spp. A promising dataset to study genes that may be facilitating such opportunism. As suggested by the discovery of Druzhinina *et al.* (2018) (Chapter 3), some of the required genes may have been acquired by *Trichoderma* by events such as Lateral Gene Transfer or Duplications. To list all the putative xenologues and paralogues in Hypocreales an orthofinder [49] analysis was carried out implementing DIAMOND [50] for faster results using whole proteomes from every genome shown in Table 4.1.

Order	Family	Species	Strain	NCBI accession	Genome size [Mbp]	Nr. Of proteins	Refs
Hypocreales	Hypocreaceae	<i>Trichoderma reesei</i>	Qm 6a	PRJNA225530	33.39	9,115	[51]
		<i>T. Reesei</i>	Rut C-30	PRJNA207855	32.68	9,849	[52]
		<i>T. Parareesei</i>	CBS 125925	LFMI00000000	32.07	9,062	[53]
		<i>T. Longibrachiatum</i>	ATCC 18648	MBDJ00000000	32.2	10,934	[15]
		<i>T. Citrinoviride</i>	TUCIM 6016	MBDI00000000	33.13	9,735	
		<i>T. Guizhouense</i>	T37	N/A		12,251	
		<i>T. Guizhouense</i>	S000		11,297		
		<i>T. Guizhouense</i>	NJAU 4742	LVVK00000000	38.33	11,255	
		<i>T. Afroharzianum</i>	T6776	PRJNA252551	39.72	11,498	[54]
		<i>T. Harzianum</i>	CBS 226.95	MBGI00000000	40.98	14,065	[15]
		<i>T. Harzianum</i>	TR274	PRJNA397414	40.87	13,925	[55]
		<i>T. Virens</i>	Gv29-8	PRJNA264113	39.02	12,406	[56]
		<i>T.hamatum</i>	GD-12	PRJNA178391	38.42	10,520	[57]
		<i>T. Asperellum</i>	CBS 433.97	MBGH00000000	37.46	12,557	[15]
		<i>T.gamsii</i>	T6085	PRJNA342687	37.90	11,171	[13]

Hypocreales	Hycocreaceae	<i>T.gamsii</i>	A5MH	PRJNA361020	38.49	10,994	NA
		<i>T. Atroviride</i>	IMI 206040	PRJNA264112	36.14	11,816	[4]
		<i>Escovopsis weberi</i>	CC031208-10	PRJNA253870	27.20	6,870	[58]
	Clavici- pitaceae	<i>Metarhizium acridium</i>	Cqma102	PRJNA38715	38.05	9,849	[5]
		<i>M.anisopliae</i>	ARSEF 549	PRJNA184754	38.49	10,891	[59]
		<i>M.rileyi</i>	RCEF 4871	PRJNA72739	32.01	8,764	[60]
		<i>Pochonia chlamyosporia</i>	170	PRJNA342685	44.21	14,204	[61]
	Cordycipitaceae	<i>Beauveria bassiana</i>	ARSEF 2860	PRJNA225503	33.69	10,364	[9]
		<i>Calviceps purpurea</i>	20.1	PRJEA76493	32.09	8,823	[10]
		<i>Cordyceps militaris</i>	CM01	PRJNA225510	32.26	9,651	[6]
		<i>C. Confragosa</i>	RCEF 1005	PRJNA72733	35.59	11,030	[60]
	Ophiocordycipitaceae	<i>Ophiocordyceps sinensis</i>	CO18	PRJNA59569	78.51	6,972	[62]
		<i>Purpureocillium lilacinum</i>	PLFJ-1	PRJNA342689	38.53	11,763	[63]
		<i>P. Lilacinum</i>	PLBJ-1	PRJNA308626	38.14	11,773	
	Nectriaceae	<i>Fusarium graminearum</i>	PH-1	AACM00000000	36.45	13,313	[19]
		<i>F. Pseudograminearum</i>	CS3096	AFNW00000000	36.97	12,397	[11]
		<i>F. Oxysporum f. Sp. Lycopersici</i>	4287	PRJNA342688	61.38	27,347	[64]
		<i>F. Fujikuroi</i>	IMI 58289	PRJEB185	43.83	14,810	[65]
		<i>Nectria haematococca</i>	Mpvi 77-13-4	PRJNA51499	51.23	15,708	[3]
	Stachybotryaceae	<i>Stachybotrys chartarum</i>	IBT 7711	PRJNA185811	36.87	11,530	[66]
		<i>Stachybotrys chartarum</i>	IBT 40293	PRJNA185808	36.48	11,453	
<i>S.chlorohalonata</i>		IBT 40285	PRJNA185807	34.39	10,706		
	<i>Ustilaginoidea virens</i>	IPU 010	PRJDB3318	33.56	6,451	[67]	
Sordariales	Sordariaceae	<i>Neurospora crassa</i>	OR74a	AABX00000000	41.1	10,812	[68]
	Chaetomiaceae	<i>Chaetomium globosum</i>	CBS 148.51	PRJNA12795	34.34	11,048	[69]

Table 4.1: Properties of fungal genomes that were used in this study.

STAG [70] was used in conjunction with the orthofinder [49]. Each orthogroup with all species present is used to infer gene trees using fastme [71, 72] and a greedy consensus tree [73] is taken of all of the individual estimates to get the final consensus tree. The support of each bipartition in the STAG consensus species tree is equal to the proportion of individual gene trees that contain this bipartition and the branch lengths in the STAG consensus species tree are the average branch lengths for each bipartition in the individual gene trees [70]. The tree produced by STAG is unrooted. The orthofinder analysis was repeated using rooted species tree (rooted against known outgroups Figure 1.1A, Node shared between *Chaetomium globosum* and *Neurospora crassa*). This introduces slight changes in orthogroups and reconcile gene trees. STRIDE [74] was then implied to decipher Gene-Duplication events by analysing each gene tree against the newly rooted species tree as described by Emms and Kelly (2018). The same comparison of each gene tree to the rooted species tree results in a list of putative xenologues too for each species.

Number of total genes from 39 genomes	4,52,007
Number of genes in orthogroups	4,24,362
Number of unassigned genes	27,645
Percentage of genes in orthogroups	93.9%
Percentage of unassigned genes	6.1%
Number of orthogroups	20,924
Number of species-specific orthogroups	102
Number of genes in species-specific orthogroups	414
Number of orthogroups with at least 4 genes (Number of individual trees)	13,754
Percentage of genes in species-specific orthogroups	0.1
Mean orthogroup size	20.3
Number of orthogroups with all species present	2,796
Number of single-copy orthogroups	1,220

Table 4.2 Overall statistics of the orthofinder analysis implementing both STAG and STRIDE

As a result of this analysis, a list of nodes where duplication has occurred was obtained by comparing of 13,754 individual gene trees with the rooted species tree (Figure 1.1). Duplication events in terminals (within the single genome) and at shared nodes (between two or more genomes) were obtained. Only nodes with 100% support that suggested a duplication event would be considered for further investigations.

This approach showed that 17,726 duplication events have occurred in 6088 orthogroups. The detailed table with these strongly supported 17,726 duplication events in 39 genomes is provided as in Appendix I provided in a CD with this dissertation along with the 13,754 reconciled gene trees (Appendix I).

Simultaneously, a list of **196** putative Horizontally⁸/Laterally⁹ transferred genes was obtained by similar comparison of individual 13,754 gene trees to the rooted species tree. Figure 4.1 shows the distribution of these laterally transferred genes among each species.

⁸ When the transfer occurs from species of another domain of life. For instance, from bacteria to fungi

⁹ When the transfer occurs from species within the same domain of life. For instance from one fungi to another fungi

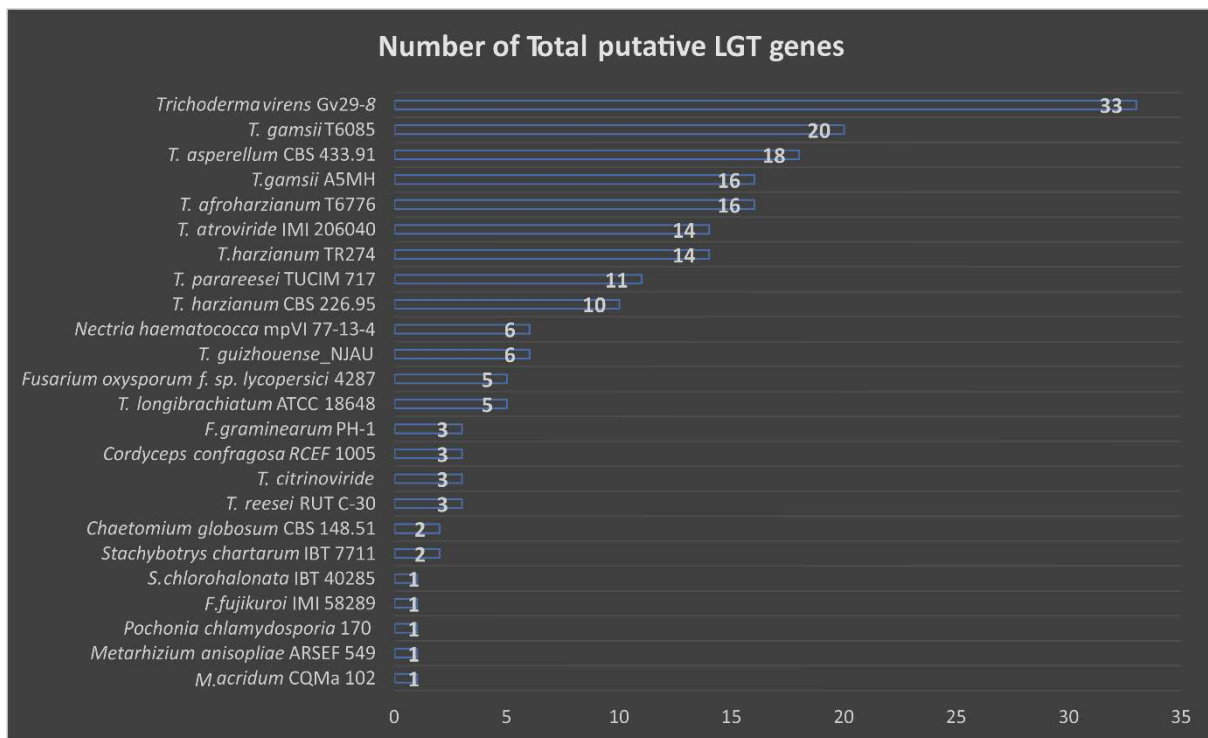


Figure 4.1: Bar chart showing laterally transferred genes in each of the species when 39 proteomes listed in Table 4.1 were analysed. Species with zero putative laterally transferred genes (Such as *E. Weberi*) are not shown.

It can be seen that the number of such genes are higher in *Trichoderma* than compared to their close carnivory phylogenetic neighbours. This may be explained by *Trichoderma*'s capability to parasitize diverse fungi [15, 75]. To support this hypothesis, there are species like *Escovopsis weberi* with a specialized genome with very specific nutritional strategy (so far isolated only from the fungal gardens of leaf cutting ants and its close neighbours [76]) where not a single gene has been putatively laterally transferred.

All of the 196 putative laterally transferred genes were searched against NCBI for their description. Most of them were hypothetical proteins, and some were of unknown functions. Those proteins with a function assigned to them are shown in Table 4.3. A detailed table with an accession number of all 196 genes is provided in Appendix I.

It is important to note that these 196 putative laterally transferred genes cannot be directly compared with lateral transferred gene events of plant cell wall degrading enzymes described in Chapter 3 and Chapter 3, because in case of latter most of the gene events have occurred to last common ancestral node for all present *Trichoderma* spp., which is not similar but complementary to the cases presented here.

S.No	Gene Accession Number	Species	Description
1	XP_003039268	<i>Nectria haematococca</i> mpvi 77-13-4	SET domain protein, partial
2	XP_018239816	<i>Fusarium oxysporum</i> f. Sp. <i>Lycopersici</i> 4287	Argininosuccinate lyase
3	XP_023437029	<i>F. Fujikuroi</i> IMI 58289	Related to protoporphyrinogen oxidase
4	XP_007816010	<i>Metarhizium acridum</i> cqma 102	ATP-binding cassette transporter, putative
5	KID60642	<i>M. Anisopliae</i> ARSEF 549	Cytochrome P450 oxidoreductase, partial
6	OAA57342	<i>Cordyceps confragosa</i> RCEF 1005	Acyl transferase/acyl hydrolase/lysophospholipase
7	OAA70101		Major facilitator superfamily domain, general substrate transporter
8	XP_018138597	<i>Pochonia chlamydosporia</i> 170	Fungal specific transcription factor
9	XP_013946518	<i>T. Atroviride</i> IMI 206040	Mpr-like GPCR protein
10	XP_013945054		Putative ankyrin repeat protein, partial
11	XP_018656148	<i>T. Gamsii</i> T6085	Acyl-coa desaturase
12	XP_018659459		Ankyrin repeat and SAM domain-containing protein
13	XP_024405772		Cytochrome P450 3A24
14	XP_018655719		Dihydroflavonol-4-reductase
15	XP_018655727		Fungal specific transcription factor domain-containing protein
16	XP_024405808		General alpha-glucoside permease
17	XP_013957351		Ankyrin domain protein
18	XP_013959919	<i>T. Virens</i> Gv29-8	Glycoside hydrolase family 18 protein
19	XP_013960079		Non-ribosomal peptide synthetase
20	KKP05589	<i>T. Afroharzianum</i> T6776	Aflatoxin B1 aldehyde reductase member 3

21	KKP06488		Pfs domain-containing protein
22	KKP06686		Polyketide synthase
23	KKP00718		Riboflavin aldehyde-forming enzyme
24	KKO99967		Scytalone dehydratase
25	XP_024744676	<i>T. Citrinoviride</i>	Actin-like atpase domain-containing protein, partial
26	XP_024744760		PBD-domain-containing protein, partial
27	PTB79931	<i>T. Longibrachiatum</i> ATCC 18648	Ankyrin
28	PTB71047		The ubiquitin-conjugating enzyme, partial

Table 4.3: Putative laterally transferred genes among 39 proteomes listed in Table 4.1 that have a described protein function

It is recognized that lateral gene transfer, especially in eukaryotes studies, should be treated with caution [77]. Therefore, further investigations should be done with these 196 genes to test the hypothesis of Lateral Gene Transfer with sophisticated statistical analyses such as NOTUNG [78], eccetera [79] and RANGER-DTL [80]. In addition, the genomic claims should be carefully supported showing the phenotypic outcomes like in case of Druzhinina *et al.*, 2018 [6].

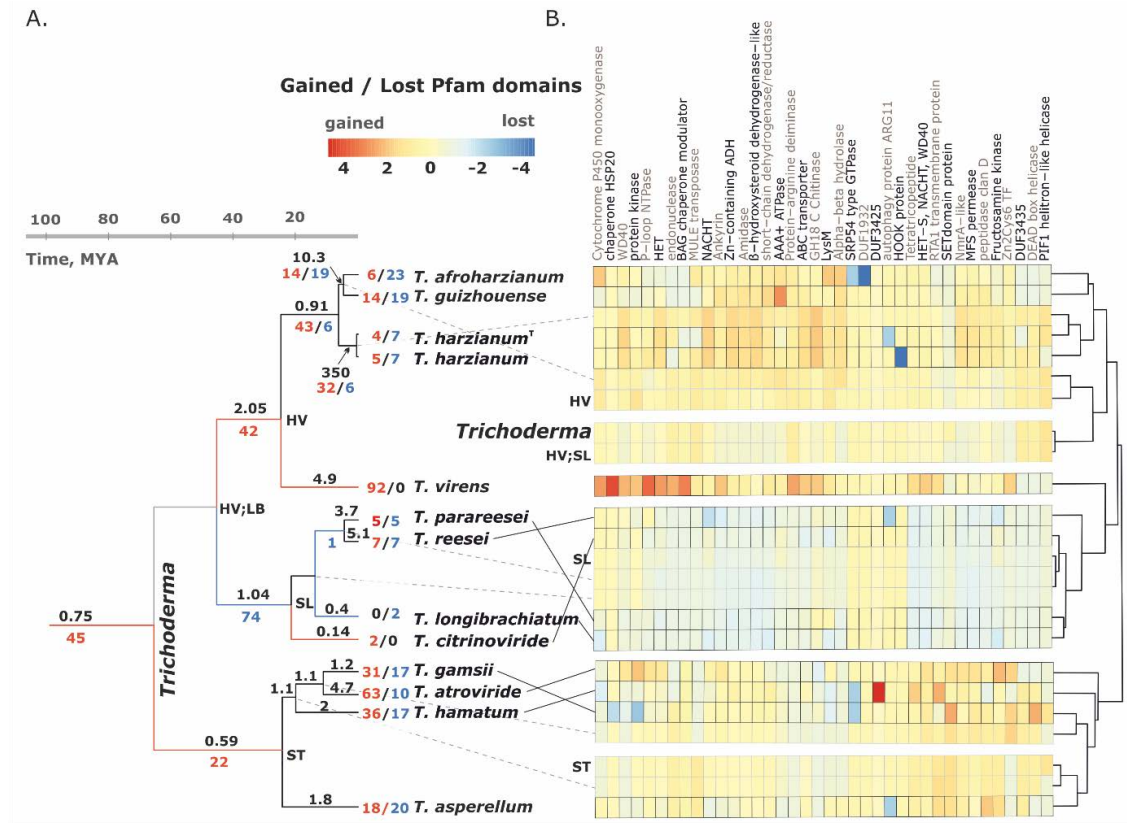


Figure 4.2 Genome evolution in *Trichoderma*.

A. The time scaled evolutionary tree: red branches indicate only gains; blue branches only losses; black branches both gains and losses. Numbers over the branches indicate the number of gene changes per Mya; numbers below the branches indicate the number of gains (red) and losses (blue). B Heat map is representing Pfam domains identified for orthomcl clusters that were gained or lost in the course of *Trichoderma* evolution.

Interestingly, in our other study, we have detected the highest number of gene gain events that putatively occurred in the course of the evolution of *T. Virens* when compared among other commonly occurring *Trichoderma* species (Figure 4.2). These findings correlate directly with the outcome of the LGT assessment of this chapter where *T. Virens* is the species with the maximum number of laterally transferred genes (Figure 4.1). It would be tempting to speculate here that the correlation between the results of these two analyses suggest that LGT is the essential, if not the major, mechanism of genome expansion in *T. Virens*. On the other hand, the gene loss in species of the Section Longibrachiatum correlates to almost no cases of LGT in these group. Symmetrically, it may suggest that these fungi were deprived of LGT and their genomes were not expanded in the way seen in such clades/sections as Harzianum/Virens or *Trichoderma*. We will refrain from such claims as more experimental or analytical evidence would be required.

This study further allows us to speculate that the abundance of transfer of genes to *Trichoderma* from a particular gene family is confined to only plant cell-wall degrading carbohydrate active enzymes and not any other gene families.

The data generated in this chapter should be helpful when the DOE JGI approved project “Genus-Wide Genomics of *Trichoderma*” will start producing new genomes (300 are expected). The new genomes can be incorporated into dataset presented here without having to repeat the similarity search using BLAST and orthofinder by integrating STAG and STRIDE, for updated phylograms, updated list of duplication events and updated list of xenologues. This will give a more accurate insight on the consequence of adelphoparasitism in context of lateral gene transfer.

References

1. Emms DM, Kelly S. Orthofinder: solving fundamental biases in whole genome comparisons dramatically improves orthogroup inference accuracy. *Genome Biology*. 2015;16(1):157. Doi: 10.1186/s13059-015-0721-2.
2. Buchfink B, Xie C, Huson DH. Fast and sensitive protein alignment using DIAMOND. *Nat Methods*. 2015;12(1):59-60. Epub 2014/11/18. Doi: 10.1038/nmeth.3176. Pubmed PMID: 25402007.
3. Martinez D, Berka RM, Henrissat B, Saloheimo M, Arvas M, Baker SE, et al. Genome sequencing and analysis of the biomass-degrading fungus *Trichoderma reesei* (syn. *Hypocrea jecorina*). *Nat Biotechnol*. 2008;26(5):553-60. Epub 2008/05/06. Doi: 10.1038/nbt1403. Pubmed PMID: 18454138.
4. Koike H, Aerts A, Labutti K, Grigoriev I, Baker S. Comparative Genomics Analysis of *Trichoderma reesei* Strains 2013. 352-67 p.
5. Yang D, Pomraning K, Kopchinskiy A, Aghcheh RK, Atanasova L, Chenthamara K, et al. Genome sequence and annotation of *Trichoderma parareesei*, the ancestor of the cellulase producer *Trichoderma reesei*. *Genome Announc*. 2015;3(4):e00885-15.
6. Druzhinina and Chenthamara JZ, Lea Atanasova, Dongqing Yang, Youzhi Miao, Mohammad J. Rahimi, Marica Grujic, Feng Cai, Shadi Pourmehdi, Kamariah Abu Salim, Alexey G. Kopchinskiy, Bernard Henrissat, Alan Kuo, Hope Hundley, Mei Wang, Andrea Aerts, Asaf Salamov, Anna Lipzen Kurt labutti, Kerrie Barry, Igor V. Grigoriev, Qirong Shen, Christian P. Kubicek. Massive lateral transfer of genes encoding plant cell wall-degrading enzymes to the mycoparasitic fungus *Trichoderma* from its plant-associated hosts. Revised manuscript resubmitted to PLOS genetics. 2018.
7. Baroncelli R, Piaggieschi G, Fiorini L, Bertolini E, Zapparata A, Pe ME, et al. Draft Whole-Genome Sequence of the Biocontrol Agent *Trichoderma harzianum* T6776. *Genome Announc*. 2015;3(3). Epub 2015/06/13. Doi: 10.1128/genomea.00647-15. Pubmed PMID: 26067977; pubmed Central PMCID: PMCPMC4463541.
8. Steindorff AS, Ramada MH, Coelho AS, Miller RN, Pappas GJ, Jr., Ulhoa CJ, et al. Identification of mycoparasitism-related genes against the phytopathogen *Sclerotinia sclerotiorum* through transcriptome and expression profile analysis in *Trichoderma harzianum*. *Bmc Genomics*. 2014;15:204. Epub 2014/03/19. Doi: 10.1186/1471-2164-15-204. Pubmed PMID: 24635846; pubmed Central PMCID: PMCPMC4004048.

9. Kubicek CP, Herrera-Estrella A, Seidl-Seiboth V, Martinez DA, Druzhinina IS, Thon M, et al. Comparative genome sequence analysis underscores mycoparasitism as the ancestral life style of *Trichoderma*. *Genome Biol.* 2011;12(4):R40. Epub 2011/04/20. Doi: 10.1186/gb-2011-12-4-r40. Pubmed PMID: 21501500; pubmed Central PMCID: PMCPMC3218866.
10. Studholme DJ, Harris B, Le Cocq K, Winsbury R, Perera V, Ryder L, et al. Investigating the beneficial traits of *Trichoderma hamatum* GD12 for sustainable agriculture-insights from genomics. *Front Plant Sci.* 2013;4:258. Epub 2013/08/03. Doi: 10.3389/fpls.2013.00258. Pubmed PMID: 23908658; pubmed Central PMCID: PMCPMC3726867.
11. Baroncelli R, Zapparata A, Piaggieschi G, Sarrocco S, Vannacci G. Draft Whole-Genome Sequence of *Trichoderma gamsii* T6085, a Promising Biocontrol Agent of Fusarium Head Blight on Wheat. *Genome Announc.* 2016;4(1):e01747-15. Doi: 10.1128/genomea.01747-15.
12. Kubicek CP, Herrera-Estrella A, Seidl-Seiboth V, Martinez DA, Druzhinina IS, Thon M, et al. Comparative genome sequence analysis underscores mycoparasitism as the ancestral life style of *Trichoderma*. *Genome biology.* 2011;12(4):R40.
13. De Man TJB, Stajich JE, Kubicek CP, Teiling C, Chenthamara K, Atanasova L, et al. The small genome of the fungus *Escovopsis weberi*, a specialized disease agent of ant agriculture. Under Revision. 2015.
14. Gao Q, Jin K, Ying S-H, Zhang Y, Xiao G, Shang Y, et al. Genome Sequencing and Comparative Transcriptomics of the Model Entomopathogenic Fungi *Metarhizium anisopliae* and *M. Acridum*. *Plos Genetics.* 2011;7(1):e1001264. Doi: 10.1371/journal.pgen.1001264.
15. Pattermore JA, Hane JK, Williams AH, Wilson BA, Stodart BJ, Ash GJ. The genome sequence of the biocontrol fungus *Metarhizium anisopliae* and comparative genomics of *Metarhizium* species. *Bmc Genomics.* 2014;15:660. Epub 2014/08/12. Doi: 10.1186/1471-2164-15-660. Pubmed PMID: 25102932; pubmed Central PMCID: PMCPMC4133081.
16. Shang Y, Xiao G, Zheng P, Cen K, Zhan S, Wang C. Divergent and Convergent Evolution of Fungal Pathogenicity. *Genome Biol Evol.* 2016;8(5):1374-87. Epub 2016/04/14. Doi: 10.1093/gbe/eww082. Pubmed PMID: 27071652; pubmed Central PMCID: PMCPMC4898799.
17. Larriba E, Jaime MD, Carbonell-Caballero J, Conesa A, Dopazo J, Nislow C, et al. Sequencing and functional analysis of the genome of a nematode egg-parasitic fungus, *Pochonia chlamydosporia*. *Fungal Genet Biol.* 2014;65:69-80. Epub 2014/02/18. Doi: 10.1016/j.fgb.2014.02.002. Pubmed PMID: 24530791.
18. Xiao G, Ying S-H, Zheng P, Wang Z-L, Zhang S, Xie X-Q, et al. Genomic perspectives on the evolution of fungal entomopathogenicity in *Beauveria bassiana*. *Sci Rep.* 2012;2:483. Doi: 10.1038/srep00483.
19. Schardl CL, Young CA, Hesse U, Amyotte SG, Andreeva K, Calie PJ, et al. Plant-Symbiotic Fungi as Chemical Engineers: Multi-Genome Analysis of the Clavicipitaceae Reveals Dynamics of Alkaloid Loci. *Plos Genetics.* 2013;9(2):e1003323. Doi: 10.1371/journal.pgen.1003323.
20. Zheng P, Xia Y, Xiao G, Xiong C, Hu X, Zhang S, et al. Genome sequence of the insect pathogenic fungus *Cordyceps militaris*, a valued traditional chinese medicine. *Genome Biology.* 2011;12(11):R116. Doi: 10.1186/gb-2011-12-11-r116.
21. Xia EH, Yang DR, Jiang JJ, Zhang QJ, Liu Y, Liu YL, et al. The caterpillar fungus, *Ophiocordyceps sinensis*, genome provides insights into the highland adaptation of fungal pathogenicity. *Sci Rep.* 2017;7. Doi: ARTN 1806 10.1038/s41598-017-01869-z. Pubmed PMID: WOS:000400959000073.

22. Wang G, Liu Z, Lin R, Li E, Mao Z, Ling J, et al. Biosynthesis of Antibiotic Leucinostatins in Bio-control Fungus *Purpureocillium lilacinum* and Their Inhibition on *Phytophthora* Revealed by Genome Mining. *Plos Pathog.* 2016;12(7):e1005685. Doi: 10.1371/journal.ppat.1005685. Pubmed PMID: PMC4946873.
23. Cuomo CA, Gueldener U, Xu JR, Trail F, Turgeon BG, Di Pietro A, et al. The *Fusarium graminearum* genome reveals a link between localized polymorphism and pathogen specialization. *Science.* 2007;317(5843):1400-2. Doi: 10.1126/science.1143708. Pubmed PMID: WOS:000249377500049.
24. Gardiner DM, Stiller J, Kazan K. Genome Sequence of *Fusarium graminearum* Isolate CS3005. *Genome Announc.* 2014;2(2). Doi: 10.1128/genomea.00227-14.
25. Ma LJ, van der Does HC, Borkovich KA, Coleman JJ, Daboussi MJ, Di Pietro A, et al. Comparative genomics reveals mobile pathogenicity chromosomes in *Fusarium*. *Nature.* 2010;464(7287):367-73. Doi: 10.1038/nature08850. Pubmed PMID: WOS:000275657100037.
26. Wiemann P, Sieber CMK, Von Bargen KW, Studt L, Niehaus EM, Espino JJ, et al. Deciphering the Cryptic Genome: Genome-wide Analyses of the Rice Pathogen *Fusarium fujikuroi* Reveal Complex Regulation of Secondary Metabolism and Novel Metabolites. *Plos Pathog.* 2013;9(6). Doi: ARTN e100347510.1371/journal.ppat.1003475. Pubmed PMID: WOS:000321206600062.
27. Coleman JJ, Rounsley SD, Rodriguez-Carres M, Kuo A, Wasmann CC, Grimwood J, et al. The Genome of *Nectria haematococca*: Contribution of Supernumerary Chromosomes to Gene Expansion. *Plos Genet.* 2009;5(8):e1000618. Doi: 10.1371/journal.pgen.1000618.
28. Semeiks J, Borek D, Otwinowski Z, Grishin NV. Comparative genome sequencing reveals chemotype-specific gene clusters in the toxigenic black mold *Stachybotrys*. *Bmc Genomics.* 2014;15:590. Epub 2014/07/13. Doi: 10.1186/1471-2164-15-590. Pubmed PMID: 25015739; pubmed Central PMCID: PMC4117958.
29. Kumagai T, Ishii T, Terai G, Umemura M, Machida M, Asai K. Genome Sequence of *Ustilagoideia virens* IPU010, a Rice Pathogenic Fungus Causing False Smut. *Genome Announc.* 2016;4(3):e00306-16. Doi: 10.1128/genomea.00306-16. Pubmed PMID: PMC4859173.
30. Galagan JE, Calvo SE, Borkovich KA, Selker EU, Read ND, Jaffe D, et al. The genome sequence of the filamentous fungus *Neurospora crassa*. *Nature.* 2003;422(6934):859-68. Doi: 10.1038/nature01554.
31. Cuomo CA, Untereiner WA, Ma L-J, Grabherr M, Birren BW. Draft Genome Sequence of the Cellulolytic Fungus *Chaetomium globosum*. *Genome Announc.* 2015;3(1). Doi: 10.1128/genomea.00021-15.
32. Emms D, Kelly S. STAG: Species Tree Inference from All Genes. *Biorxiv.* 2018.
33. Desper R, Gascuel O. Getting a tree fast: Neighbor Joining, fastme, and distance-based methods. *Curr Protoc Bioinformatics.* 2006;Chapter 6:Unit 6.3. Epub 2008/04/23. Doi: 10.1002/0471250953.bi0603s15. Pubmed PMID: 18428768.
34. Lefort V, Desper R, Gascuel O. Fastme 2.0: A Comprehensive, Accurate, and Fast Distance-Based Phylogeny Inference Program. *Mol Biol Evol.* 2015;32(10):2798-800. Epub 2015/07/02. Doi: 10.1093/molbev/msv150. Pubmed PMID: 26130081; pubmed Central PMCID: PMC4576710.
35. Felsenstein J. PHYLIP (phylogeny inference package), Version 3.62004.
36. Emms DM, Kelly S. STRIDE: Species Tree Root Inference from Gene Duplication Events. *Mol Biol Evol.* 2017;34(12):3267-78. Epub 2017/10/14. Doi: 10.1093/molbev/msx259. Pubmed PMID: 29029342; pubmed Central PMCID: PMC5850722.

37. Chenthamara K, Druzhinina IS. Ecological Genomics of Mycotrophic Fungi. In: Druzhinina IS, Kubicek CP, editors. Environmental and Microbial Relationships. Cham: Springer International Publishing; 2016. P. 215-46.
38. De Man TJB, Stajich JE, Kubicek CP, Teiling C, Chenthamara K, Atanasova L, et al. Small genome of the fungus *Escovopsis weberi*, a specialized disease agent of ant agriculture. Proc Natl Acad Sci USA. 2016;113(13):3567-72. Doi: 10.1073/pnas.1518501113.
39. Martin WF. Too Much Eukaryote LGT. Bioessays. 2017;39(12). Epub 2017/10/27. Doi: 10.1002/bies.201700115. Pubmed PMID: 29068466.
40. Chen K, Durand D, Farach-Colton M. NOTUNG: a program for dating gene duplications and optimizing gene family trees. J Comput Biol. 2000;7(3-4):429-47. Doi: 10.1089/106652700750050871.
41. Jacox E, Chauve C, Szollosi GJ, Ponty Y, Scornavacca C. Eccetera: comprehensive gene tree-species tree reconciliation using parsimony. Bioinformatics. 2016;32(13):2056-8. Epub 2016/05/07. Doi: 10.1093/bioinformatics/btw105. Pubmed PMID: 27153713.
42. Bansal MS, Kellis M, Kordi M, Kundu S. RANGER-DTL 2.0: rigorous reconstruction of gene-family evolution by duplication, transfer and loss. Bioinformatics. 2018;34(18):3214-6. Doi: 10.1093/bioinformatics/bty314

Chapter 5 Ankyrin domain containing proteins are frequent in orphomes of all *Trichoderma* species¹⁰

The first detailed comparative genomics study by Kubicek *et al.*, (2011) [1] with the first three *Trichoderma* spp. Compared with other Pezizomycotina fungi revealed the relative expansion of certain gene families in *Trichoderma* through Markov cluster algorithm (MCL) analysis. This study published and considered strongly opportunistic and cosmopolitan *T. Atroviride* and *T. Virens* and performed the first comparative genomics study with already published *T. Reesei* genome. Inspired by this study, a more extensive Markov cluster algorithm (MCL) analysis of 44 Pezizomycotina genomes in total, including the three previously mentioned *Trichoderma* spp. Was done. The MCL analysis revealed that *Trichoderma* spp. Contained an increased number of ankyrin-domain-containing (ankdc) proteins compared to the average number of these genes in considered Pezizomycotina species (Figure 5.1) [2]. Furthermore, within *Trichoderma* genus, in strongly opportunistic and cosmopolitan *T. Atroviride* and *T. Virens*, ankdc-proteins were even more expanded than in *T. Reesei*.

10 Chenthamara K, Gojic V, Druzhinina IS. Ankyrin domain containing proteins are frequent in orphomes of all *Trichoderma* species

ms in preparation

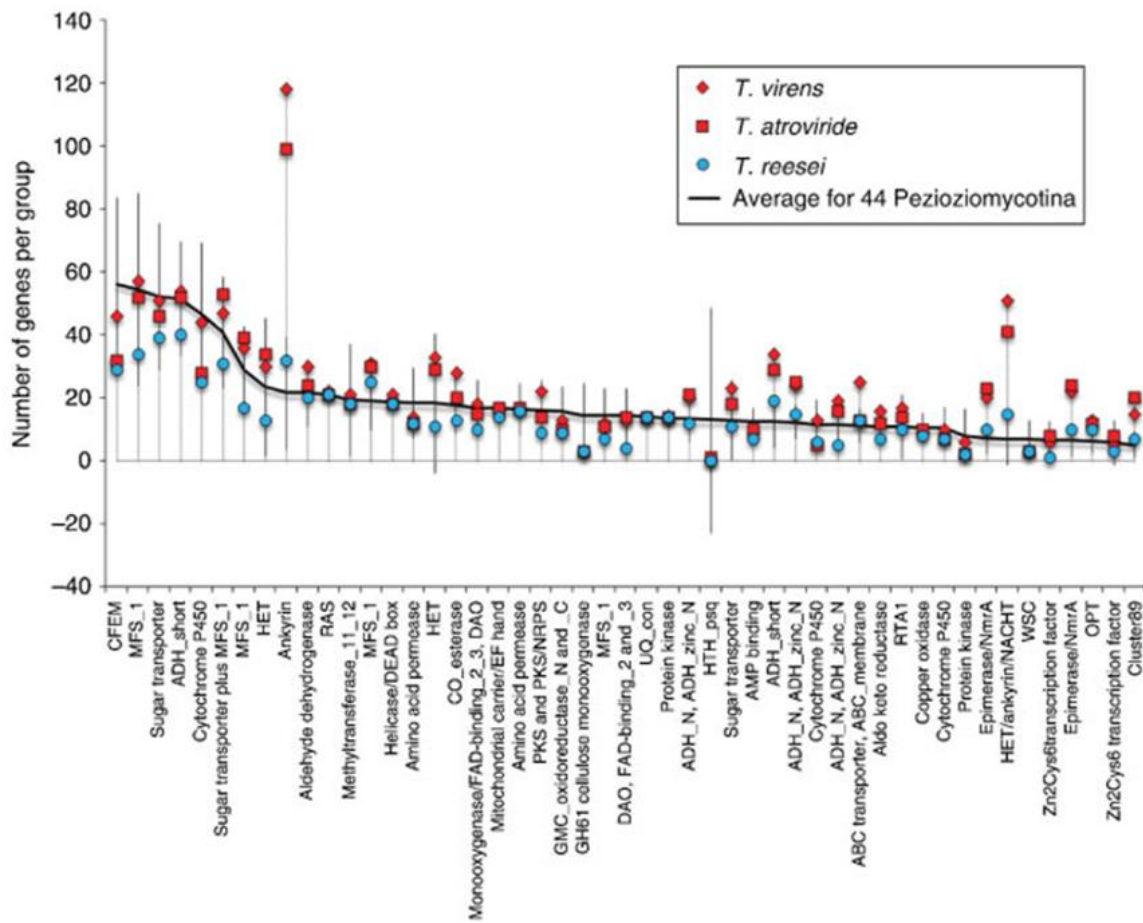


Figure 5.1 MCL analysis of gene families in 44 Pezizomycotina genomes

The ankyrin- (ANK-) repeat is a protein-protein interaction motif found in proteins in all living organisms (Figure 5.2)

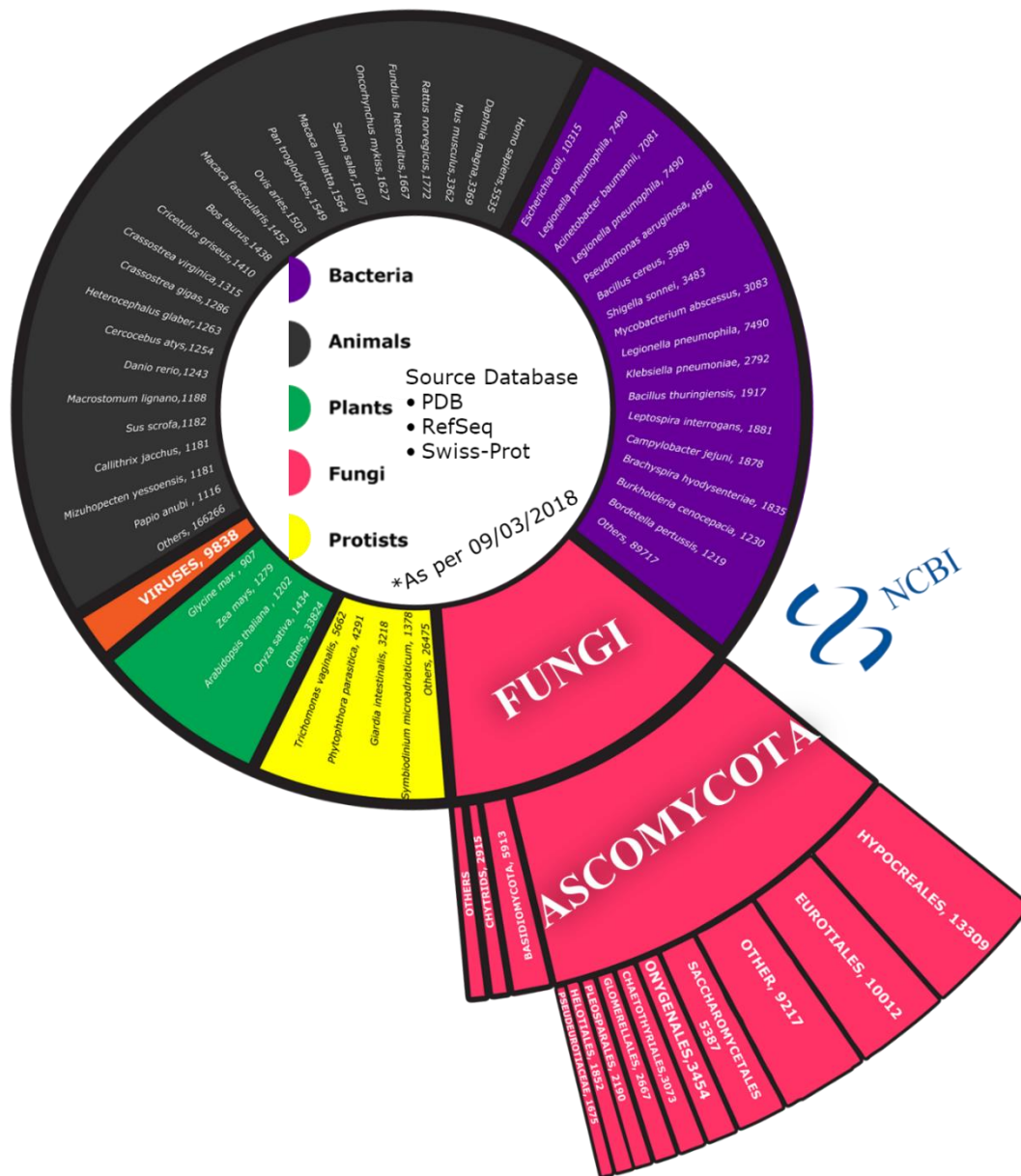


Figure 5.2 A sunburst diagram showing the distribution of ankdc-proteins across all domains of life. The number next to species name is the respective number of ankdc-proteins reported in the respective species.

Ankyrin was named after a cytoskeletal protein ankyrin which contains 22 copies of the ANK-repeat [3]. A single ANK-repeat consists of 33-amino acid residues that form a motif of a helix-turn-helix-beta-hairpin/loop fold, which is shown in Figure 5.3A. The two helices are arranged in antiparallel fashion followed by a loop region that points outward at an approximately 90° angle, resembling a structure similar to letter L [4]. Specific residues often referred to as signature residues, are relatively conserved to keep the structural integrity of the motif. The positions 4-7 are usually occupied by T-P-L-H (Threonine-Proline-Leucine-Histidine) amino

are responsible for binding of the target molecule. The residues constituting these regions of ANK-domain are generally variable to ensure functional and binding specificity (Sedgwick and Smerdon 1999). On average there are 4-7 ANK-repeats per ankdc-protein, and proteins with more ANK-repeats generally have more compact and concave structure which reflects their modular nature and enables their wide functional diversity [6].

The ankdc-proteins can be loner-proteins, containing exclusively ANK-domain(s), or they can be multidomain proteins where ANK-domain(s) are associated with a functional (host) domain. These functional domains are involved in transcription regulation, signal transduction, cell-cell signaling, cell-cycle regulation, inflammatory response, cytoskeleton integrity, toxin-encoding, transport phenomena, etc. [6, 7]. The function of ankdc-proteins in *Trichoderma* and fungi, in general, is not well understood.

This chapter is mainly aimed **to set a foundation towards explaining the expansion and roles of ankdc (ANK domain containing) genes in *Trichoderma***. For this, representative genomes of *Trichoderma* and other closely related species for a comparative genomics study of their ankdc-protein were selected.

An inventory of all ankdc-proteins from 10 *Trichoderma* spp. And eight closely related non-*Trichoderma* hypocrealean genomes (nthgs), referred to as hypocrealean ankyrome was built and were re-annotated using interproscan within the frame of a master thesis, supervised by the Ph.D. Candidate.

Objectives set within the realm of this dissertation

1. Molecular dating of selective/representative hypocrealean species used in this study
2. To verify if the expansion of ankdc proteins is exclusive to *Trichoderma* within Hypocreales, as previously thought
3. Re-annotation of ankdc genes in Hypocreales

4. To find out how many of ankdc containing proteins are pure ankyrins, and how many are associated with other pfam domains
5. To find out the percentage of Orphan ankdc containing genes in Hypocreales

One-hundred genes were randomly selected from the genomes of the nine *Trichoderma* spp. And 12 reference Hypocreales (*Escovopsis weberi*, *Metarhizium acridium*, *M. Robertsii*, *Calviceps purpurea*, *Ophiocordyceps sinensis*, *Beauveria bassiana*, *Cordyceps militaris*, *Fusarium graminearum*, *F. Oxysporum* f. Sp. *Lycopersici* strain 4287, *F. Pseudograminearum*, *F. Fujikuroi*, and *Nectria haematococca*) based on two requirements: (a) they should display a syntenic position in all genomes, and (b) be true orthologues (no other gene encoding a protein with amino acid similarity >50% present; ⁵. Statistical analysis to test the neutral theory of evolution [8] was carried out using dnasp V5.10.01 [9] based on Tajima's D test [10] as described by Rozas (2009)[11]. *Neurospora crassa* and *Chaetomium globosum* from the order Sordariales were chosen as outgroups. Accession numbers of all genes used in the phylogenomic analysis are given in Additional file Table S2B under Chapter 3. The concatenated set of 100 proteins for each species was subjected to alignment using the stand alone MAFFT tool [12] using accurate parameters. Selection of conserved blocks was made using relaxed conditions in Gblocks [13]. The final conserved concatenated alignment contained 47726 amino acids from each genome and was subjected to Bayesian analysis using mrbayes v3.2.5 [14], 1 million generations and the Dayhoff amino acid substitution model [15]. Two simultaneous, completely independent analyses starting from different random trees were run, using 3 heated chains and one "cold" chain. Once the analysis was completed, 7500 trees were summarized after discarding the first 25% of the obtained 10,000 trees, resulting in a consensus tree.

Concatenated set of corresponding 100 nucleotide sequences were also subjected to the similar analysis described as above (Data not shown). Maximum likelihood trees based on corresponding best substitution model [16] were also constructed individually for each of the 100 protein sequences to confirm the topology obtained using concatenated set.

Based on the resultant phylogenomic analysis of amino acid and nucleotide sequences, respectively, clade ages were estimated using the tool cladeage [17] as described in Matschiner *et al.*[18]. Two ancestral nodes were used for the time calibration: a common ancestral node of

the order Hypocreales was calibrated for a central 95% range of 192-194 Mya [19], and a common ancestral node between carnivore-fungivore families (Hypocreaceae, Ophiocordycipitaceae and Clavicipitaceae) was calibrated for a central 95% range of 164-166 Mya [20]. Species within these clades were forced to form a monophyletic group in order to constrain the tree topology. Two independent MCMC analyses were carried out in BEAST V2.4.0, using JTT I+G+F for amino acid and GTR for nucleotides, respectively. The best fit models were determined based on BIC criterion as implemented in phym1 [16, 21] with smart model selection (<http://www.atgc-montpellier.fr/phym1-sms/>). A strict clock rate was estimated. Two mirror analyses for each dataset were carried out in CIPRES (<http://www.phylo.org>). Their combined logs for the analyses for each dataset were diagnosed using Tracer v1.6 [17] to confirm that the effective sample size (ESS) is above 200 for the estimated parameters. Trees of respective mirror analyses were combined manually by the aid of a text editor. In each case, 25% of the first total trees were discarded using Tree annotator v2.4.0 [22] before summarizing. A maximum clade credibility tree was obtained by summarizing the trees that occurred at least 50% of times with a posterior probability of over 0.5. Node heights were estimated using mean heights. The final trees with node ages and an automatic reverse scale axis were visualized and obtained using figtree v1.4.2 (<http://tree.bio.ed.ac.uk/software/figtree/>). Approximate 95% confidence interval is obtained by selecting “Height Highest Probable Density of 95%” for node bars in figtree to show the age in the chronogram.

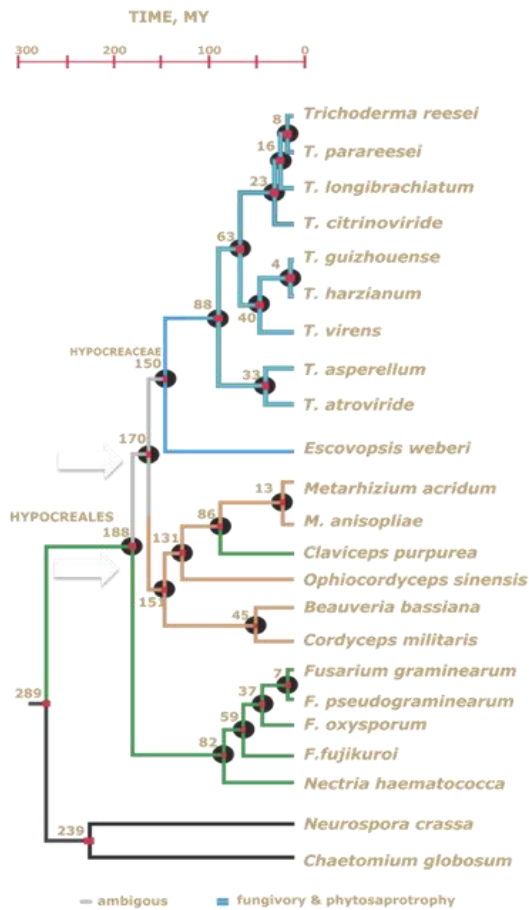


Figure 5.4 Chronogram of selective Hypocreales species.

The subsequent phylogenetic analysis revealed that the monophyletic fungivorous family Hypocreaceae represented here by *Escovopsis* and *Trichoderma* genera, shared their last common ancestor with fungi from families Cordycipitaceae, Ophiocordycipitaceae, and Clavicipitaceae that are dominated by extant entomotrophic fungi (Figure 5.4). The branch leading to plant-associated Nectriaceae family diverged earlier in the course of evolution of the Hypocreales. The results show that the common ancestor of *Trichoderma* and *E. Weberi* existed approximately 150 Mya, while the common ancestor of all modern *Trichoderma* species (the origin of the genus) can be dated back to approximately 70-90 Mya. Our phylogram is concordant with an earlier analysis which showed that *T. Atroviride* (section *Trichoderma*) most closely represents the ancestral state of the genus, while *T. Reesei* (section *Longibrachiatum*) was the evolutionary most derived species [23]. The closest and youngest *Trichoderma* species in our dataset are *T. Harzianum* and *T. Guizhouense*, respectively, that are separated by approximately 4-8 Mya while the other sibling species *T. Reesei* and *T. Parareesei* are divided by at least 7-10 Mya of independent evolution (Figure 5.4).

Statistical comparison of genomes from the taxonomical order Hypocreales (available at that time), including those that were considered in this study for detailed comparison, are presented in Table 5.1

Organism Name	Genome Size [Mbp]	N° of Gene Models	N° of ankc-proteins	Share of ankc-proteins [%]
<i>Ilyonectria robusta</i> PMI 751	59.65	20499	345	1.68
<i>I. Europaea</i> CBS 129078	62.83	20870	326	1.56
<i>Trichoderma virens</i> Gv29-8	39.02	12423	194	1.56
<i>Clonostachys rosea</i> CBS125111	52.44	18639	267	1.43
<i>T. Harzianum</i> TR274	40.87	13932	182	1.31
<i>T. Atroviride</i> IMI 206040	36.14	11828	154	1.30
<i>T. Harzianum</i> CBS 226.95	40.98	14095	179	1.27
<i>T. Gamsii</i> T6085	37.97	10944	134	1.22
<i>T. Guizhouense</i> NJAU 4742	38.29	11297	138	1.22
<i>Pochonia chlamydosporia</i> 170	44.22	14204	172	1.21
<i>Metarhizium robertsii</i> ARSEF 23	41.66	11688	135	1.16
<i>Stachybotrys elegans</i> LAHC-LSPK-M15	43.47	14925	169	1.13
<i>Fusarium fujikuroi</i> IMI 58289	43.83	14813	163	1.10
<i>F. Redolens</i> A4	52.56	17051	185	1.08
<i>Nectria haematococca</i>	51.29	15707	170	1.08
<i>T. Asperellum</i> TR356	35.39	12320	133	1.08
<i>T. Asperellum</i> CBS 433.97	37.46	12586	135	1.07
<i>T. Parareesei</i> TUCIM 717	31.13	9318	95	1.02
<i>Myrothecium inundatum</i> CBS 120646	39.21	13553	134	0.99

<i>T. Citrinoviride</i> TUCIM 6016	33.22	9737	96	0.99
<i>Neonectria ditissima</i> R09/05	45.72	12685	123	0.97
<i>F. Oxysporum</i> f. Sp. Lycopersici 4287	61.36	27347	264	0.97
<i>Beauveria bassiana</i> ARSEF 2860	33.69	10364	98	0.95
<i>M. Acridum</i> cqma 102	39.42	9849	92	0.93
<i>F. Pseudograminearum</i> CS3096	36.33	12395	115	0.93
<i>F. Verticillioides</i> 7600	41.78	20553	188	0.91
<i>T. Reesei</i> Qm6a	33.45	9143	83	0.91
<i>Mariannaea</i> sp. PMI_226	42.25	12638	113	0.89
<i>T. Longibrachiatum</i> ATCC 18648	32.24	10938	96	0.88
<i>F. Graminearum</i> v1.0	36.45	13322	114	0.86
<i>Niesslia exilis</i> CBS 358.70 v1.0	35.38	13499	99	0.73
<i>Tolypocladium inflatum</i> NRRL 8044	30.35	9998	67	0.67
<i>Purpureocillium</i> sp. Udea0106 v1.0	36.08	13642	90	0.66
<i>Acremonium strictum</i> DS1bioAY4a v1.0	35.79	13158	84	0.64
<i>Cordyceps militaris</i> CM01	32.27	9651	61	0.63
<i>A. Chrysogenum</i> ATCC 11550	28.56	8899	51	0.57
<i>Ustilaginoidea virens</i>	33.57	6451	29	0.45
<i>Valetionellopsis laxa</i> CBS 191.97 v1.0	22.13	8026	36	0.45

Table 5.1: Hypocreales genomes that were used for genome characteristics comparison

The listed *Trichoderma* spp. belong to four different taxonomical sections the Longibrachiatum, Harzianum, Trichoderma, and Virens, respectively. Within the *Trichoderma* genus, average genome size is 36.3 Mbp, while the average number of gene models is 11,618. *T. Harzianum* CBS 226.95 is the largest genome with the highest number of gene-models among all

Trichoderma spp., whereas *T. Parareesei* TUCIM 717 is the smallest genome. The Longibrachiatum section's genomes are generally smaller when compared to the rest of considered *Trichoderma* spp. And this is also the youngest section among *Trichoderma* spp.

The results of ankdc-proteins abundance comparison in Hypocreales genomes are summarized in Table 5.1. Species in the table are arranged in decreasing order of proportion of ankdc genes to the total number of genes present within them. It can be seen that *Ilyonectria* sp., which are the fungi belonging to nectriacea family and are phytotrohs share the top place with *T. Virens*, a strong mycotroph (and also phytosaprotroph) and *Clonostachys rosea* [24], another mycotroph. In *T. Virens* ankdc-proteins account for 1.56 % of all gene models which is only superseded by *Ilyonectria robusta* PMI 751 inside the Hypocreales order. Some of the highest shares of ankdc-proteins among considered Hypocreales species are found in *T. Atroviride* with 1.3 %, *T. Harzianum* with 1.27 %, *T. Gamsii* with 1.22 % and *T. Guizhouense* with 1.22 % of all genes. Below 1 % share of ankdc-proteins are found in *Trichoderma* spp. From *Longibrachiatum* section. These findings are in concordance with results from the Kubicek and Steindorff *et al.*¹¹ (also described in Chapter 6) and confirm that the expansion of ankdc-proteins in most aggressive *Trichoderma* spp. Is present. However, according to these updated results, the expansion is not exclusive to *Trichoderma* spp. Even if only the species from Hypocreales order are taken into account. Two *Ilyonectria* spp. Had the highest share of ankdc-genes and also the highest total number of ankdc-proteins. These genomes were sequenced and published in 2016 and 2017, so the data was not available at the time of preliminary investigation by Kubicek *et al.* In 2011 [23].

All the fungi listed in Figure 5.4 are categorized into four groups based on their nutritional strategy. And a tree map on ankdc gene content in each of these groups is presented in Figure 5.5. Because in this study, we focus on the expansion of ANK genes in *Trichoderma*, we compare the number of ankyrins with taxonomically close relatives (Figure 5.4, and [25]). Figure 5.5 further highlights strikingly low number of ANK repeats in *Escovopsis weberi*. Note that: *Trichoderma* and *Escovopsis* share a close common ancestor (Figure 5.4 and [25]). And so far

¹¹ Kubicek C, Steindorff A, Chenthamara K, Manganiello G, Henrissat B, Zhang J, Cai F, Kopchinskiy A, Kubicek E, Kuo A, Baroncelli R, Sarrocco S, Noronha E, Vannacci G, Shen Q, Grigoriev I, Druzhinina IS. Evolution and comparative genomics of the most common *Trichoderma* species Revised manuscript submitted for peer-review in Studies in Mycology.

Escovopsis spp. Have been isolated only from fungal garden of certain Leaf-cutting ants[26]. An indication that expansion of ankyrins is not exclusive to *Trichoderma*, but also closely related phytopathogens that are common soil fungi compels to look at the transcriptomic response of *Trichoderma* when interacting with plants or growing in soil.

Here it is important to notice, *Trichoderma*'s ankdc content is more similar to Phytotrophs than to Entomotrophs, with who *Trichoderma* shares the last common ancestor suggesting evolutionary mechanisms such as lateral gene transfer as one of the probable cause of this expansion.

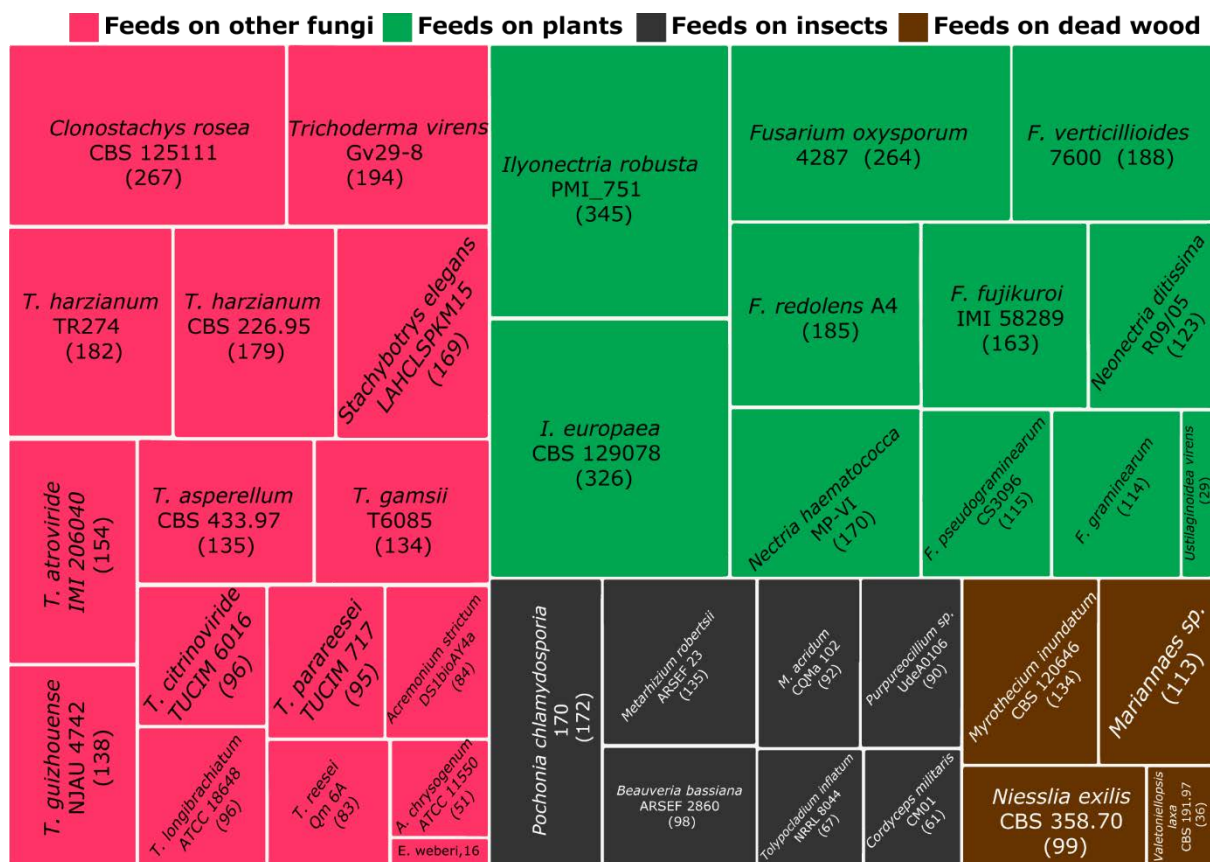


Figure 5.5 Tree map based on genome mining for ANK proteins of 38 hypocrealean species. It highlights the abundance of ANK proteins in fungi that feed on other fungi (but are also well-studied for their interactions with plants) and in those fungi that feed on other plants.

All the 2406 retrieved proteins from shown hypocreales in (Figure 5.4) were retrieved with a text-search “Ankyrin” in JGI and were re-annotated using InterProScan [27] in BLAST2GO [28]. INTERPRO considers in total 14 different protein databases. It annotates whole genes, for all the different domains that are present, and since the output is an excel table including start

and stop position for different domains within one gene, overlaps could be excluded, and all the annotated domains could be filtered.

Of 2406 proteins annotated, only 2382 proteins could be annotated with e-value less than 0.0003. So, this means out of 2406 retrieved proteins from JGI; only 2272 had an ANK domain in the genes, suggesting 134 genes that were retrieved as ankdc are false positives. Figure 5.6 shows the percentage of false positives that are annotated as ankdc containing genes in public databases in several genomes. The highest percentage of false positives of ankdc genes are in the genomes that were among first to be sequenced and annotated, like *T. Reesei* (2008) and *N. Haematococca* (2009). This naturally reflects improvement in the annotation of pfam domains in fungal genomes as the algorithms for annotation improved with years, in addition to the development of reference protein databases.

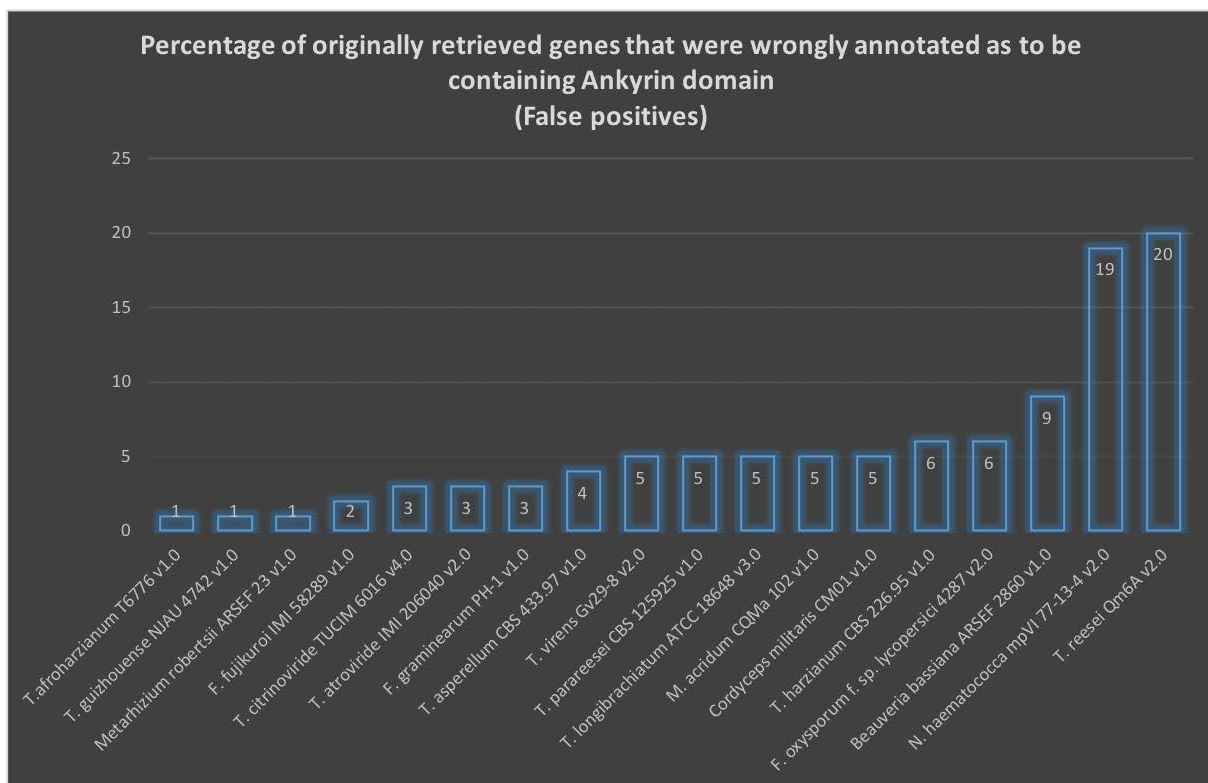


Figure 5.6 Percentage of false positives of ankdc genes in public databases

This re-annotation and correction of the base inventory of ankdc genes of all the considered hypocrealean species was done for most accurate interpretations (that is possible in the present date).

According to interproscan analysis results, Out of 2,272 ankdc-proteins in the Hypocreales, 1,215 genes (53.4%) contained ANK-domain as the only identified domain (pure ankyrins). The ankdc-proteins that contain other associated pfam domains are referred to as host-domain containing ankdc-proteins (hdc-ankdc-proteins) were 1,057 (47.6%).

Within the *Trichoderma* ankyrome, *T. Guizhouense* and *T. Afroharzianum* ankyromes contained the highest share of hdc-ankdc-proteins with 63% and 59%, respectively. *T. Virens* ankyrome has the lowest share of hdc-ankdc-proteins with 37.1%, implying that most of the ankdc proteins in *T. Virens* are pure ankyrins.

Orthofinder analysis (as described in Chapter 4) with total of 2272 ANK-dc proteins resulted in 200 putative orthogroups that had to be filtered by visual inspection based on homology between motus. After this step, 140 orthogroups containing 1053 proteins, as well as 1353 proteins as putative orphans (these proteins were not assigned to any orthogroup) were obtained. To verify their orphan status, a new orthofinder analysis was performed with only putative orphans from the previous step. After visual inspection, further 43 orthogroups, containing 119 proteins, were identified. The main reason why further orthogroups were identified is the calculation of rbnhs (Reciprocal Best Length-Normalized hit) which led to the less strict lower limit for acceptance of putative orthologs.

In conclusion, out of 2272 proteins, 1172 were assigned to 183 separate orthogroups, while the remaining 1000 proteins could be considered as orphan proteins.

A closer look into the number of orphan ankdc-protein per species is shown in Figure 5.7. The results reveal that the largest share of *Nectria haematococca* ankyromes is orphans with **71%** of all ankdc-proteins. Within the *Trichoderma* genus, **61%** of *T. Virens* ankyrome are orphans, followed by *T. Asperellum* ankyrome which has **60.7 %** orphans. In the ankyromes from *T. Parareesei* and *T afroharzianum* orphans account for **33.7 %** and **36.7 %**, respectively.

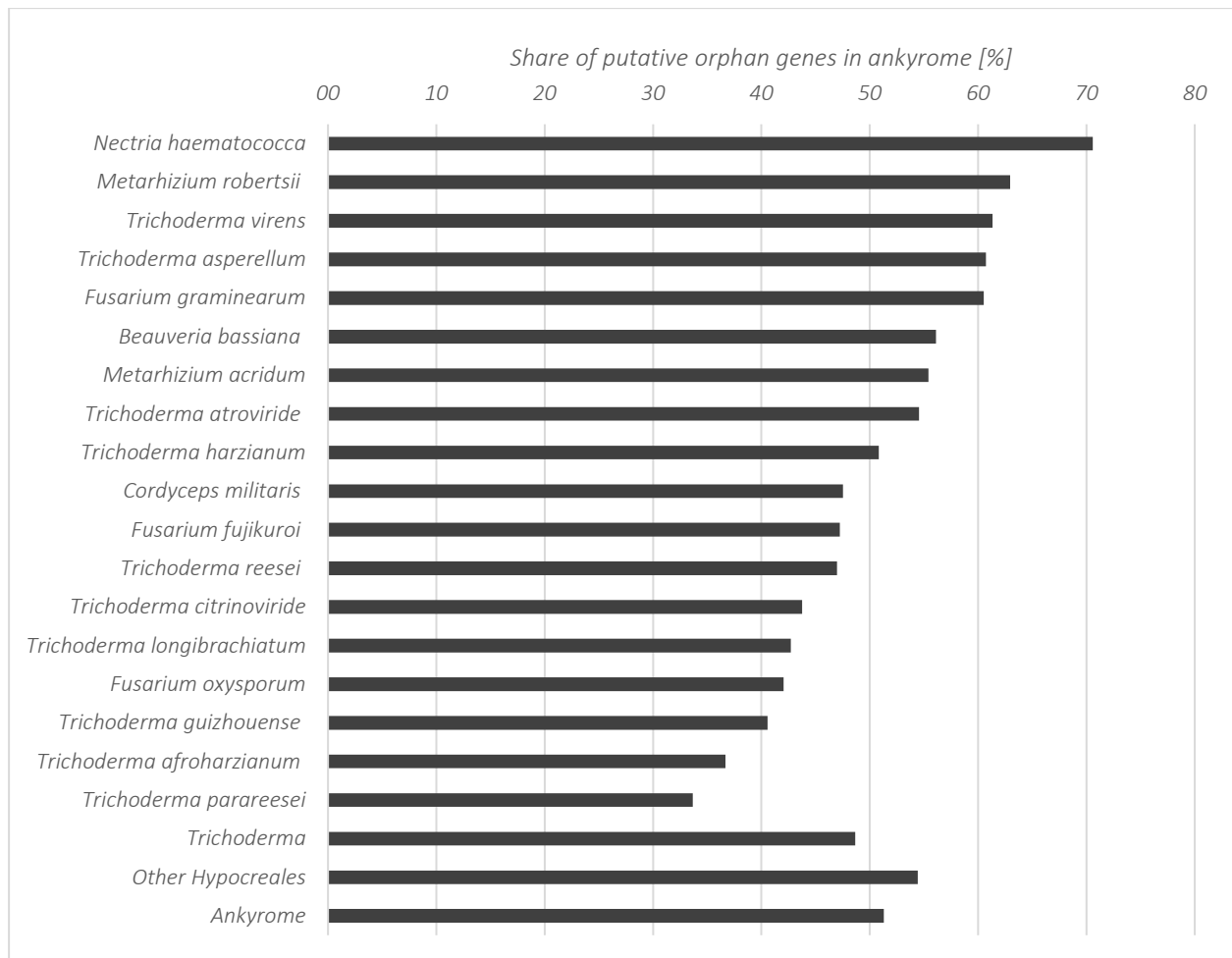


Figure 5.7 Share of orphan ankdc-proteins per species

Orthofinder orthology inference found 1172 homologous proteins distributed between 183 orthogroups of which 18 were identified as the core for *Trichoderma* spp. And 11 as core to all considered fungi from the taxonomical order Hypocreales. In most Hypocreales species the larger share of their respective ankyrome consisted of orphan ankdc-proteins. Phylogenetic analysis of 18 *Trichoderma* spp. Core ankdc-proteins resulted in tree topologies that were congruent with the multilocus chronogram (Figure 5.4) without any deviation. Selection pressure analyses of the same core ankdc-proteins using hyphy [29] methods BUSTED, MEME and FUBAR confirmed a significant ($p < 0.05$ and $P > 0.95$) purifying selection acting across all

of 18 core ankdc-proteins. **Data for this section is not shown in detail because it has been already described in a master thesis¹² supervised by the Ph.D. Candidate.**

The ankdc-gene expansion was confirmed in strongly opportunistic *Trichoderma* spp. It has been also shown that this expansion is not exclusive to *Trichoderma* spp. The high abundance of orphans in *Trichoderma ankyrome* suggests the occurrence of evolutionary mechanisms such as segmental duplications and lateral gene transfer (LGT) events by which these genes may have originated. Horizontal gene transfer between Prokaryotes and Eukaryotes as one of the gene expansion mechanisms has been suggested first by Bork (1993) [30], but later questioned by Al-Khodor *et al.* (2010) [31]., who suggested that expansion of ankdc-genes probably occurred by gene duplication and convergent evolution. Their hypothesis is based on the fact that genes containing repeats are generally more prone to such mechanisms [32], but also that ANK-repeats interact with universal proteins in nature.

As described in Druzhinina *et al.* [25], LGT of plant cell wall degradation enzymes from a wide range of phytopathogenic Ascomycota species to *Trichoderma* which *Trichoderma* could penetrate is massive, LGT could be a probable reason for this expansion. However, based on the findings alone from this study, it cannot be concluded whether the orphan ankdc-genes were obtained by means of convergent evolution or LGT. The most probable hypothesis is that these genes originated by a combination of multiple mechanisms. Further research is necessary to investigate these possibilities. Finally, the selection pressure analysis of core ankdc-proteins indicates that they have a key function in *Trichoderma* interactomes that is maintained by purifying selection.

Transcriptomic data was searched of *Trichoderma* interacting with several fungi, but a significant number of expressed ankdc genes were not found in such data¹³. However, revelation that expansion of ankyrins is not exclusive to *Trichoderma*, but also closely related phytopathogens that are common soil fungi compels to look at the transcriptomic response of *Trichoderma* when interacting with plants or growing in soil. The trends demonstrated in the

¹² Master thesis of DI Vladimir Gojic: Convergent evolution of ankyrin domains the main genomic hallmark of an industrially relevant fungus *Trichoderma*.
Supervisors: **Chenthamara K**, Druzhinina IS

Trichoderma ankyrome cannot be explained, until the purpose of these proteins is understood in more detail.

References

1. Kubicek CP, Herrera-Estrella A, Seidl-Seiboth V, Martinez DA, Druzhinina IS, Thon M, et al. Comparative genome sequence analysis underscores mycoparasitism as the ancestral life style of *Trichoderma*. *Genome biology*. 2011;12(4):R40.
2. Druzhinina IS, Kubicek CP. Ecological Genomics of *Trichoderma*. In: Martin F, editor. *The Ecological Genomics of Fungi*: John Wiley & Sons, Inc; 2013. P. 89-116.
3. Lux SE, John KM, Bennett V. Analysis of cDNA for human erythrocyte ankyrin indicates a repeated structure with homology to tissue-differentiation and cell-cycle control proteins. *Nature*. 1990;344(6261):36-42. Epub 1990/03/01. Doi: 10.1038/344036a0. Pubmed PMID: 2137557.
4. Gorina S, Pavletich NP. Structure of the p53 tumor suppressor bound to the ankyrin and SH3 domains of 53BP2. *Science*. 1996;274(5289):1001-5. Epub 1996/11/08. Pubmed PMID: 8875926.
5. Mosavi LK, Minor DL, Jr., Peng ZY. Consensus-derived structural determinants of the ankyrin repeat motif. *Proc Natl Acad Sci U S A*. 2002;99(25):16029-34. Epub 2002/12/04. Doi: 10.1073/pnas.252537899. Pubmed PMID: 12461176; pubmed Central PMCID: PMCPMC138559.
6. Mosavi LK, Cammett TJ, Desrosiers DC, Peng ZY. The ankyrin repeat as molecular architecture for protein recognition. *Protein Sci*. 2004;13(6):1435-48. Doi: 10.1110/ps.03554604. Pubmed PMID: WOS:000221630900001.
7. Bork P. Hundreds of ankyrin-like repeats in functionally diverse proteins: mobile modules that cross phyla horizontally? *Proteins*. 1993;17(4):363-74. Epub 1993/12/01. Doi: 10.1002/prot.340170405. Pubmed PMID: 8108379.
8. Kimura M. The neutral theory of molecular evolution and the world view of the neutralists. *Genome*. 1989;31(1):24-31.
9. Librado P, Rozas J. Dnasp v5: a software for comprehensive analysis of DNA polymorphism data. *Bioinformatics*. 2009;25(11):1451-2. Doi: 10.1093/bioinformatics/btp187.
10. Tajima F. Statistical method for testing the neutral mutation hypothesis by DNA polymorphism. *Genetics*. 1989;123(3):585-95.
11. Rozas J. DNA Sequence Polymorphism Analysis Using dnasp. In: Posada D, editor. *Bioinformatics for DNA Sequence Analysis*. 537. Totowa, NJ: Humana Press; 2009. P. 337-50.
12. Kazutaka K, Kei-ichi Kuma H, Miyata TA. MAFFT version 5: Improvement in accuracy of multiple sequence alignment. *Nucleic Acids Res*, Volume 33, No2. 2005.
13. Talavera G, Castresana J. Improvement of phylogenies after removing divergent and ambiguously aligned blocks from protein sequence alignments. *Systematic Biol*. 2007;56(4):564-77. Doi: 10.1080/10635150701472164. Pubmed PMID: WOS:000248359900002.

14. Ronquist F, Teslenko M, Van Der Mark P, Ayres DL, Darling A, Höhna S, et al. MrBayes 3.2: efficient Bayesian phylogenetic inference and model choice across a large model space. *Systematic Biol.* 2012;61(3):539-42.
15. Dayhoff MO, Schwartz RM, editors. Chapter 22: A model of evolutionary change in proteins 1978 1978.
16. Lefort V, Longueville JE, Gascuel O. SMS: Smart Model Selection in phylml. *Mol Biol Evol.* 2017;34(9):2422-4. Epub 2017/05/05. Doi: 10.1093/molbev/msx149. Pubmed PMID: 28472384.
17. Bouckaert R, Heled J, Kuhnert D, Vaughan T, Wu CH, Xie D, et al. BEAST 2: A Software Platform for Bayesian Evolutionary Analysis. *Plos Computational Biology.* 2014;10(4). Doi: ARTN e1003537 10.1371/journal.pcbi.1003537. Pubmed PMID: WOS:000336507500022.
18. Matschiner M, Musilova Z, Barth JMI, Starostova Z, Salzburger W, Steel M, et al. Bayesian Phylogenetic Estimation of Clade Ages Supports Trans-Atlantic Dispersal of Cichlid Fishes. *Systematic Biol.* 2017;66(1):3-22. Doi: 10.1093/sysbio/syw076. Pubmed PMID: WOS:000397124100007.
19. Sung GH, Poinar GO, Jr., Spatafora JW. The oldest fossil evidence of animal parasitism by fungi supports a Cretaceous diversification of fungal-arthropod symbioses. *Mol Phylogenet Evol.* 2008;49(2):495-502. Epub 2008/09/27. Doi: 10.1016/j.ympev.2008.08.028. Pubmed PMID: 18817884.
20. Yang EC, Xu LL, Yang Y, Zhang XY, Xiang MC, Wang CS, et al. Origin and evolution of carnivorism in the Ascomycota (fungi). *Proc Natl Acad Sci USA.* 2012;109(27):10960-5. Doi: 10.1073/pnas.1120915109. Pubmed PMID: WOS:000306641100052.
21. Guindon S, Lethiec F, Duroux P, Gascuel O. PHYML Online—a web server for fast maximum likelihood-based phylogenetic inference. *Nucleic Acids Res.* 2005;33(suppl 2):W557-W9. Doi: 10.1093/nar/gki352.
22. Bouckaert R, Heled J, Kühnert D, Vaughan T, Wu C-H, Xie D, et al. BEAST 2: A Software Platform for Bayesian Evolutionary Analysis. *PLOS Comput Biol.* 2014;10(4):e1003537. Doi: 10.1371/journal.pcbi.1003537.
23. Kubicek CP, Herrera-Estrella A, Seidl-Seiboth V, Martinez DA, Druzhinina IS, Thon M, et al. Comparative genome sequence analysis underscores mycoparasitism as the ancestral life style of *Trichoderma*. *Genome Biol.* 2011;12(4):R40. Epub 2011/04/20. Doi: 10.1186/gb-2011-12-4-r40. Pubmed PMID: 21501500; pubmed Central PMCID: PMC3218866.
24. Karlsson M, Durling MB, Choi J, Kosawang C, Lackner G, Tzelepis GD, et al. Insights on the Evolution of Mycoparasitism from the Genome of *Clonostachys rosea*. *Genome Biol Evol.* 2015;7(2):465-80. Doi: 10.1093/gbe/evu292. Pubmed PMID: PMC4350171.
25. Druzhinina and Chenthamara JZ, Lea Atanasova, Dongqing Yang, Youzhi Miao, Mohammad J. Rahimi, Marica Grujic, Feng Cai, Shadi Pourmehdi, Kamariah Abu Salim, Alexey G. Kopchinskiy, Bernard Henrissat, Alan Kuo, Hope Hundley, Mei Wang, Andrea Aerts, Asaf Salamov, Anna Lipzen Kurt labutti, Kerrie Barry, Igor V. Grigoriev, Qirong Shen, Christian P. Kubicek. Massive lateral transfer of genes encoding plant cell wall-degrading enzymes to the mycoparasitic fungus *Trichoderma* from its plant-associated hosts. Revised manuscript resubmitted to PLOS genetics. 2018.

26. De Man TJB, Stajich JE, Kubicek CP, Teiling C, Chenthamara K, Atanasova L, et al. Small genome of the fungus *Escovopsis weberi*, a specialized disease agent of ant agriculture. *Proc Natl Acad Sci USA*. 2016;113(13):3567-72. Doi: 10.1073/pnas.1518501113.
27. Finn RD, Attwood TK, Babbitt PC, Bateman A, Bork P, Bridge AJ, et al. Interpro in 2017-beyond protein family and domain annotations. *Nucleic Acids Res*. 2017;45(D1):D190-D9. Doi: 10.1093/nar/gkw1107. Pubmed PMID: WOS:000396575500029.
28. Conesa A, Götz S, García-Gómez JM, Terol J, Talón M, Robles M. Blast2GO: a universal tool for annotation, visualization and analysis in functional genomics research. *Bioinformatics*. 2005;21(18):3674-6.
29. Pond SLK, Muse SV. Hyphy: hypothesis testing using phylogenies. *Statistical methods in molecular evolution*: Springer; 2005. P. 125-81.
30. Bork P. Hundreds of ankyrin-like repeats in functionally diverse proteins: Mobile modules that cross phyla horizontally? *Proteins: Structure, Function, and Bioinformatics*. 1993;17(4):363-74.
31. Al-Khodor S, Price CT, Kalia A, Kwaik YA. Ankyrin-repeat is containing proteins of microbes: a conserved structure with functional diversity. *Trends in microbiology*. 2010;18(3):132.
32. Lynch M, Conery JS. The Evolutionary Fate and Consequences of Duplicate Genes. *Science*. 2000;290(5494):1151-5.

Chapter 6 Conclusive notes on the comparative analysis of the core genome of *Trichoderma* species and respective orphomes¹⁴

The growing importance of the ubiquitous fungal genus *Trichoderma* requires understanding its biology and evolution. The Sordariomycetes, one of the largest classes in the Division Ascomycota, display a wide range of nutritional strategies, including saprotrophy and biotrophic interactions with bacteria, plants, animals, fungi or other organisms [1]. The Sordariomycetes order with the highest number of genera is Hypocreales [2], and it comprises half of the whole-genome sequenced species of Sordariomycetes (Nov. 2017, NCBI Taxonomy Browser and MycoCosm (Figure 1.1)). Molecular data suggest that the ancestors of the Hypocreales evolved some 170 – 200 Mya as fungi associated with plants as either parasites or saprotrophs [3]. Diversification into extant taxa was accompanied by several intra- and interkingdom host shifts involving fungi, higher plants, and animals [4]. Among them, parasites of animals likely appeared first in the Jurassic period, and specialized entomoparasitic families developed during the Cretaceous period, thereby following the diversification of herbivory insects and angiosperms [3].

Mycoparasitic fungi are found in species from several fungal taxa [5], but only the *Hypocreales* contain exclusively fungicolous genera, i.e., *Hypomyces*, *Escovopsis*, and *Trichoderma*. Among these fungicolous fungal genera, *Trichoderma* is the largest taxon, with many ubiquitously distributed species. Detailed ecological and biogeographic surveys of *Trichoderma* [6-9] revealed that species of this genus are most frequently found on the fruiting bodies of other fungi and the dead wood colonized by them. While mycoparasitism in *Hypomyces* is frequently species-specific and restricted to fruiting body-forming Basidiomycota [10], the genus *Trichoderma* is unique, as many of its species can also act as parasites on Ascomycota and even phylogenetically close species [11].

¹⁴ This chapter includes materials presented in Kubicek C, Steindorff A14, **Chenthamara K**, Manganiello G, Henrissat B, Zhang J, Cai F, Kopchinskiy A, Kubicek E, Kuo A, Baroncelli R, Sarrocco S, Noronha E, Vannacci G, Shen Q, Grigoriev I, Druzhinina IS. Evolution and comparative genomics of the most common *Trichoderma* species Revised manuscript submitted for peer-review in *Studies in Mycology*.
that is not included in this dissertation

An analysis of the genomes from three species of *Trichoderma* (*T. Reesei*, *T. Virens*, and *T. Atroviride*) suggested that mycoparasitism is an innate property of *Trichoderma* [12] but that these species are also characterized by considerable nutritional versatility [13]. In addition to acting as mycoparasites, which promotes its use as a biocontrol agent against plant pathogenic fungi [12, 14], *Trichoderma* has become an opportunistic infectant of humans [15]. *Trichoderma* is rarely reported as a parasite on plants and invertebrates, but it can colonize plants as a symptomless endosymbiont [12]. Finally, many species of the genus grow efficiently on dead plant biomass, and one of its species - *T. Reesei* - is a major industrial source of cellulases and hemicellulases. Interestingly, the most opportunistic *Trichoderma* species may also grow in soil, where they can either establish in a bulk soil or colonize the rhizosphere. As plants usually positively respond to the presence of *Trichoderma*, this property attracts attention for the use of these fungi in *biofertilizers*. The fact that some *Trichoderma* species can feed on the plant, fungal and animal bodies characterizes them as generalists. (Figure 6.1).



Figure 6.1 Nutritional versatility of *Trichoderma*

It was not known how generalism evolved from the phytosaprotrophic background of the Hypocreales. Chaverri and Samuels [16] compared a phylogenetic tree of the genus *Trichoderma* with the habitats from which the individual species had been isolated and concluded that the evolution of the genus involved several interkingdom host jumps and that preference for a special habitat was gained or lost multiple times. It has been argued that the versatility of *Trichoderma* nutritional strategies is described by expansions of the spectrum of hosts and substrates due to the enrichment of its genome by the laterally transferred genes required for feeding on the plant biomass [11].

The hypothesis of the comparative genomic¹⁵ was that comparative genomic analysis of those species of *Trichoderma* that are most frequently sampled (and therefore must be the most successful generalists) and an analysis of their pattern of gene evolution would reveal the evolutionary events that shaped their nutritional diversification and environmental generalism. In addition, the elucidation of the gene inventory of the *Trichoderma* core genome (i.e., the genes that are present in all *Trichoderma* species) and its intersection with genomes of other fungi revealed the specific genomic features of these industrially relevant fungi.

Although the sequences of several *Trichoderma* genomes have already been published [11],[17-25] detailed genome-wide analyses have been published for only three *Trichoderma* species (*T. Reesei*, *T. Virens* and *T. Atroviride* [11, 17, 26-28]). To test the hypothesis raised above, the evolution and gene inventory of the genomes from 13 *Trichoderma* isolates (Figure 6.3), that together represent 12 species with a worldwide distribution and are members of three major infrageneric groups, was analyzed [8]. These 12 species were also most frequently found in our own studies of soil or rhizosphere sampled in different geographic regions such as the Canary Islands, Sardinia, Columbia, Egypt, China, Israel, South-East Asia, and Siberia [7-9, 13] and may, therefore, be called cosmopolitan. Because several of the 12 species that were selected are used as bioeffectors in biocontrol products against plant pathogenic fungi, stimulate plant growth and immunity, are opportunistic pathogens of immunocompromised humans and are causative agents of the green mould disease on mushroom farms [7, 13], they can be considered environmental opportunists in a broad sense. Although species in each of the sections and clades of *Trichoderma* have unique morphological features, their overall ecological features are similar: They are mycoparasites, can feed on cellulolytic material and can establish themselves in soil and then colonize the rhizosphere. These features suggest that these species possibly maintained the “opportunistic” features from a common ancestor, which may be reflected in the core genome.

The evolution and the changes that have arisen from this process in the gene inventory of the selected 12 species was therefore investigated. Although all the genomes were still incomplete,

¹⁵ Kubicek C, Steindorff A15, **Chenthamara K**, Manganiello G, Henrissat B, Zhang J, Cai F, Kopchinskiy A, Kubicek E, Kuo A, Baroncelli R, Sarrocco S, Noronha E, Vannacci G, Shen Q, Grigoriev I, Druzhinina IS. Evolution and comparative genomics of the most common *Trichoderma* species Revised manuscript submitted for peer-review in *Studies in Mycology*.

the small percentage of predicted missing genes (2-5 % for all species except *T. Longibrachiatum*) makes it probable that most gene families that are relevant for the interpretations and conclusions have been identified. It was particularly emphasized that the differences in gene numbers that were considered relevant were in most cases several folds higher than the number of putatively missing genes.

The results in this study¹⁶ and **Chapter 5** revealed that the mycoparasitic Hypocreales diversified between 140 and 100 Mya, the ancestor of *Trichoderma* evolved around the time of the K-Pg event and the formation of the three infrageneric groups studied (Clade *Trichoderma*, Clade *Longibrachiatum* and the *Harzianum/Virens* clade) occurred 45 - 40 Mya after the K-Pg event. The uncertainty in chronological dating makes determining whether the genus *Trichoderma* arose before or after the K-Pg event impossible.

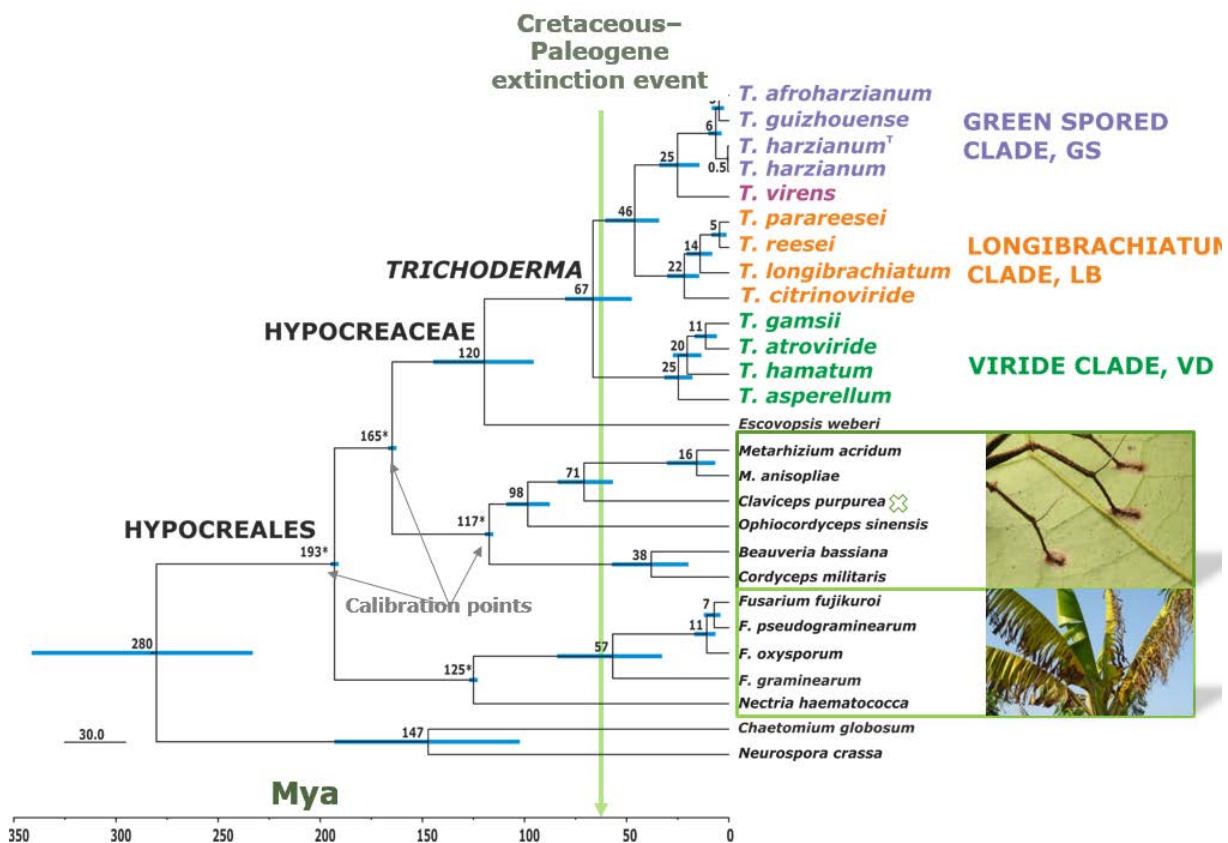


Figure 6.2 Bayesian chronogram obtained based on the concatenated alignment of 638 core orthologous proteins of Hypocreales and the two other Sordariomycetes revealing the evolution of 13 most common *Trichoderma* isolates. All nodes were supported with posterior probability=1. Chronological estimations are given on a geological time scale in Mya, and the numbers represent the corresponding node age. Numbers with asterisks at nodes indicate calibration points against the origin of Hypocreales (see Materials and Methods for details).

¹⁶ Kubicek C, Steindorff A16, **Chenthamara K**, Manganiello G, Henrissat B, Zhang J, Cai F, Kopchinskiy A, Kubicek E, Kuo A, Baroncelli R, Sarrocco S, Noronha E, Vannacci G, Shen Q, Grigoriev I, Druzhinina IS. Evolution and comparative genomics of the most common *Trichoderma* species Revised manuscript submitted for peer-review in Studies in Mycology.

Bars correspond to 95% confidence interval in time estimation based on the lognormal relaxed clock. The chronogram shown in this picture is unlinked from the one shown in Chapter 5 (Figure 5.7) in terms of their loci and the number of motus.

However, since it was shown that the genus *Trichoderma* had obtained most of the genes encoding plant cell wall-degrading enzymes required for phytosaprotrophic growth by a lateral gene transfer that likely took place before the diversification into infrageneric groups [11]. The most likely interpretation of these data is therefore that *Trichoderma* was one of the fungal genera that participated in the strong burst in fungal populations that fed on the decaying biomass of the plants killed by the K-Pg event [29]. Whether or not this increase in the number of fungi stimulated mycoparasitism can only be speculated, but successful antagonism and the ability to kill its competitor clearly may have aided *Trichoderma* in establishing a high population density on decaying plant biomass. Moreover, the ability to endoparasitise closely related species (up to adelphoparasitism) could favour host/parasite DNA exchanges and further contribute to the formation of the unique core genome of *Trichoderma* [11].

Despite the standard deviation in the dating of fungal phylogenies, our data strongly suggest that the evolution of the three *Trichoderma* sections/clades investigated occurred after the K-Pg event. The origin of extant species in the three sections/clades occurred in the early Oligocene (30 – 20 Mya), a phase characterized by cooler seasons and a significant extinction of the invertebrate marine fauna [30]. It is intriguing that this split led to an increased rate of gene gain and genome expansion in the HV clade, whereas the formation of Section *Longibrachiatum* was accompanied by significant gene loss. Kelkar and Ochman [31] reported that Pezizomycotina genomes with sizes from 25 to 75 Mb (which includes all *Trichoderma* spp. Investigated) exhibit a negative correlation between genome size and genetic drift. At first glance, this observation may be inapplicable to genome contraction in Section *Longibrachiatum* because it concerned genes from nearly all functional categories and was thus not specifically directed to support a certain trait. Alternatively, the results could be explained by the streamlining hypothesis [32], which considers selection for a more economical lifestyle the major driving force for genome reduction. According to this model, the presence or absence of multiple genes for the same function may produce only a small effect on the performance of the organism and thus have only little benefits for the cell. Sun and Blanchard [33] considered this scenario most likely to occur in relatively stable environments where competition for nutrients is severe and a smaller genome has the ecological advantage of spending less energy on growth and development. It was speculated that the *Harzianum/Virens* clade and Section

Trichoderma – but not Section *Longibrachiatum* – used this alternative to further their ecological success.

It was shown that the core genome of the genus *Trichoderma* consists of 7,000 genes and is generally similar to that of other Hypocreales. Therefore, the unique ecology and physiology of *Trichoderma* is probably explained by convergent evolution of orphomes of individual clades or species.

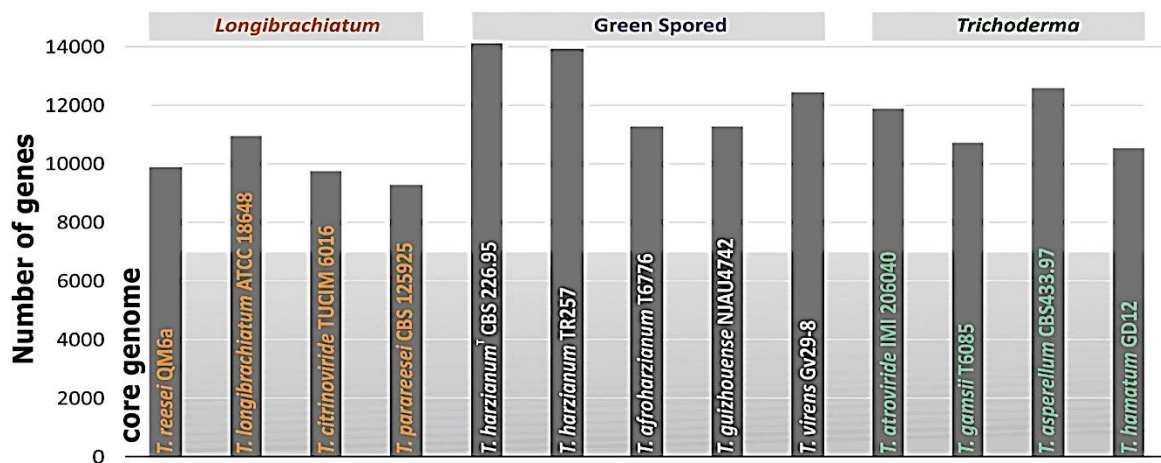


Figure 6.3 Ratio of core genome vs. The genome size in 13 isolates of 12 most frequently isolated *Trichoderma* species.

One of the hypotheses for this work¹⁷ was that gene families that were gained during *Trichoderma* evolution and are more abundant in *Trichoderma* than in other related fungi could give further insights into how this genus became an environmental opportunist. Gene families that were gained by *Trichoderma* in the highest number were those encoding proteins with an ankyrin repeats, proteins with a HET domain and MFS transporters. In addition, protein families that were present in higher numbers in *Trichoderma* than in other *Sordariomycetes* were the PNP_UDP_1 nucleotide phosphorylases and nmra-like transcriptional regulators. However, all of their analysis was beyond the scope of this dissertation. It was revealed within the realm of this dissertation that about 50% of Ankyrins in genus *Trichoderma* are Orphomes (Chapter 5).

¹⁷ Kubicek C, Steindorff A17, Chenthamara K, Manganiello G, Henrissat B, Zhang J, Cai F, Kopchinskiy A, Kubicek E, Kuo A, Baroncelli R, Sarrocco S, Noronha E, Vannacci G, Shen Q, Grigoriev I, Druzhinina IS. Evolution and comparative genomics of the most common *Trichoderma* species Revised manuscript submitted for peer-review in Studies in Mycology.

Also, complemented by the unlinked comparative genomic analysis of 12 *Trichoderma* species by Kubicek, Steindorff *et al.*⁴ revealing that when the two closely related strains of the same agamospecies were compared, proteins with ankyrin repeats accounted for the highest number of orphan genes with predicted function (Figure 6.5).

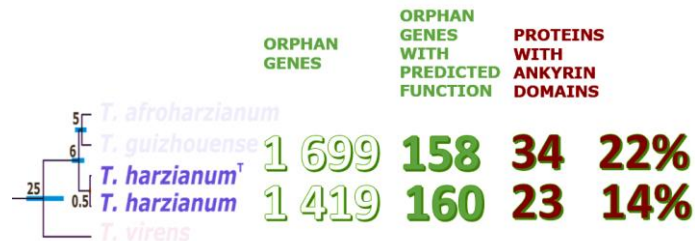


Figure 6.4 Comparison of orphan genes with predicted functions between *T. Harzianum* CBS226.95 marked with “T” and *T. Harzianum* TR274

So far, proteins with ankyrin repeats have not been systematically characterized from *Peizizomycotina*, but an expansion of proteins containing ankyrin repeats has been reported for the insect endosymbiotic bacterium *Wolbachia* [34]. Ankyrins have therefore been suggested to play an important role in the endosymbiosis of this bacterium [34]. The fact that more proteins with this protein-protein interaction module are present in *Trichoderma* than in other fungi (with *Nectria* being the only exception) suggests that signalling and metabolic processes are more tightly coordinated in *Trichoderma* than in other fungi, which could ultimately result in enhanced fitness in its habitat.

In general, a striking feature in all *Trichoderma* genomes was the high number of orphan genes, of which only a very small number is also present in the core genome. Orphan genes have been postulated to originate either as a consequence of gene duplication events, rearrangement processes, and subsequent fast divergence or from *de novo* evolution out of non-coding genomic regions [35]. Kubicek, Steindorff *et al.*¹⁸ showed that - in the case of *T. Reesei* - only a fifth of the orphan genes are in clusters that could be indicative of gene duplications and that only a very small portion of orphans (clustered and non-clustered) are near the telomeres, a

¹⁸ Kubicek C, Steindorff A18, Chenthamara K, Manganiello G, Henrissat B, Zhang J, Cai F, Kopchinskiy A, Kubicek E, Kuo A, Baroncelli R, Sarrocco S, Noronha E, Vannacci G, Shen Q, Grigoriev I, Druzhinina IS. Evolution and comparative genomics of the most common *Trichoderma* species Revised manuscript submitted for peer-review in Studies in Mycology

frequent area for gene duplication. Last but not least, these orphan genes are not preferred targets for RIP (repeat-Induced point mutation), which inactivates duplicated genes. Therefore the hypothesis of gene duplication as the major mechanism for the emergence of orphan genes is not supported. Published transcriptome data from *T. Reesei* and *T. Virens* [36, 37] show that approximately 40 % of the orphan genes are indeed expressed and therefore represent protogenes, which are exposed to natural selection [38]; the presence of this pressure was verified by showing that the orphan genes present in the core genome are under purifying selection (Chapter 5). It was therefore interesting to see the species-specific orphan genes evolve so fast that their sequences diverged beyond recognition, as discussed previously [39, and Chapter 5].

This dissertation highlights the evolution of several *Trichoderma* species that are most frequently observed in nature. The data reveal a high genomic diversity at both the section/clade level and the species level. The high polymorphism in ankyrin-containing proteins correlates with the expansions in HET genes as well as the transcription factors and enzymes for carbohydrate and secondary metabolism encoded by these genes. It possibly illustrates that *Trichoderma* constantly reshaped its genome for fast responses and successful competition in potentially novel habitats. These properties are exactly what one would expect from an environmental opportunist and a generalist.

References

1. Zhang N, Castlebury LA, Miller AN, Huhndorf SM, Schoch CL, Seifert KA, et al. An overview of the systematics of the Sordariomycetes based on a four-gene phylogeny. *Mycologia*. 2006;98(6):1076-87. Epub 2007/05/10. Pubmed PMID: 17486982.
2. Kirk P, Cannon P, Stalpers J, Minter DW. *Dictionary of the Fungi*. 10th ed 2008.
3. Sung GH, Poinar GO, Jr., Spatafora JW. The oldest fossil evidence of animal parasitism by fungi supports a Cretaceous diversification of fungal-arthropod symbioses. *Mol Phylogenet Evol*. 2008;49(2):495-502. Epub 2008/09/27. Doi: 10.1016/j.ympev.2008.08.028. Pubmed PMID: 18817884.
4. Spatafora JW, Sung GH, Sung JM, Hywel-Jones NL, White JF, Jr. Phylogenetic evidence for an animal pathogen origin of ergot and the grass endophytes. *Mol Ecol*. 2007;16(8):1701-11. Epub 2007/04/04. Doi: 10.1111/j.1365-294X.2007.03225.x. Pubmed PMID: 17402984.
5. Chenthamara K, Druzhinina IS. Ecological Genomics of Mycotrophic Fungi. In: Druzhinina IS, Kubicek CP, editors. *Environmental and Microbial Relationships*. Cham: Springer International Publishing; 2016. P. 215-46.

6. Jaklitsch WM. European species of *Hypocrea* Part I. The green-spored species. *Stud Mycol.* 2009;63:1-91. Epub 2009/10/15. Doi: 10.3114/sim.2009.63.01. Pubmed PMID: 19826500; pubmed Central PMCID: PMCPMC2757427.
7. Druzhinina Irina S, Kubicek Christian P. Ecological Genomics of *Trichoderma*. The Ecological Genomics of Fungi. 2013. Doi: doi:10.1002/9781118735893.ch5
10.1002/9781118735893.ch5.
8. Atanasova L, Druzhinina I, Jaklitsch W. Two Hundred *Trichoderma* Species Recognized on the Basis of Molecular Phylogeny 2013. 10-42 p.
9. Jaklitsch WM, Voglmayr H. Biodiversity of *Trichoderma* (Hypocreaceae) in Southern Europe and Macaronesia. *Stud Mycol.* 2015;80:1-87. Epub 2016/03/10. Doi: 10.1016/j.simyco.2014.11.001. Pubmed PMID: 26955191; pubmed Central PMCID: PMCPMC4779795.
10. Poldmaa K. Three species of *Hypomyces* growing on basidiomata of Stereaceae. *Mycologia.* 2003;95(5):921-33. Epub 2003/09/01. Pubmed PMID: 21148999.
11. Druzhinina IS, Chenthamara K, Zhang J, Atanasova L, Yang D, Miao Y, et al. Massive lateral transfer of genes encoding plant cell wall-degrading enzymes to the mycoparasitic fungus *Trichoderma* from its plant-associated hosts. *PLOS Genetics.* 2018;14(4):e1007322. Doi: 10.1371/journal.pgen.1007322.
12. Kubicek CP, Herrera-Estrella A, Seidl-Seiboth V, Martinez DA, Druzhinina IS, Thon M, et al. Comparative genome sequence analysis underscores mycoparasitism as the ancestral life style of *Trichoderma*. *Genome Biol.* 2011;12(4):R40. Epub 2011/04/20. Doi: 10.1186/gb-2011-12-4-r40. Pubmed PMID: 21501500; pubmed Central PMCID: PMCPMC3218866.
13. Druzhinina IS, Seidl-Seiboth V, Herrera-Estrella A, Horwitz BA, Kenerley CM, Monte E, et al. *Trichoderma*: the genomics of opportunistic success. *Nat Rev Microbiol.* 2011;9(10):749-59. Epub 2011/09/17. Doi: 10.1038/nrmicro2637. Pubmed PMID: 21921934.
14. Hermosa R, Rubio MB, Cardoza RE, Nicolas C, Monte E, Gutierrez S. The contribution of *Trichoderma* to balancing the costs of plant growth and defense. *Int Microbiol.* 2013;16(2):69-80. Epub 2014/01/10. Doi: 10.2436/20.1501.01.181. Pubmed PMID: 24400524.
15. Kuhls K, Lieckfeldt E, Borner T, Gueho E. Molecular reidentification of human pathogenic *Trichoderma* isolates as *Trichoderma longibrachiatum* and *Trichoderma citrinoviride*. *Med Mycol.* 1999;37(1):25-33. Epub 1999/04/14. Pubmed PMID: 10200931.
16. Chaverri P, Samuels GJ. Evolution of habitat preference and nutrition mode in a cosmopolitan fungal genus with evidence of interkingdom host jumps and major shifts in ecology. *Evolution.* 2013;67(10):2823-37. Epub 2013/10/08. Doi: 10.1111/evo.12169. Pubmed PMID: 24094336.
17. Martinez D, Berka RM, Henrissat B, Saloheimo M, Arvas M, Baker SE, et al. Genome sequencing and analysis of the biomass-degrading fungus *Trichoderma reesei* (syn. *Hypocrea jecorina*). *Nat Biotechnol.* 2008;26(5):553-60. Epub 2008/05/06. Doi: 10.1038/nbt1403. Pubmed PMID: 18454138.
18. Studholme DJ, Harris B, Le Cocq K, Winsbury R, Perera V, Ryder L, et al. Investigating the beneficial traits of *Trichoderma hamatum* GD12 for sustainable agriculture-insights from genomics. *Front Plant Sci.* 2013;4:258. Epub 2013/08/03. Doi: 10.3389/fpls.2013.00258. Pubmed PMID: 23908658; pubmed Central PMCID: PMCPMC3726867.

19. Xie BB, Qin QL, Shi M, Chen LL, Shu YL, Luo Y, et al. Comparative Genomics Provide Insights into Evolution of *Trichoderma* Nutrition Style. *Genome Biol Evol.* 2014;6(2):379-90. Doi: 10.1093/gbe/evu018. Pubmed PMID: WOS:000332742300011.
20. Yang D, Pomraning K, Kopchinskiy A, Karimi Aghcheh R, Atanasova L, Chenthamara K, et al. Genome Sequence and Annotation of *Trichoderma parareesei*, the Ancestor of the Cellulase Producer *Trichoderma reesei*. *Genome Announc.* 2015;3(4). Epub 2015/08/15. Doi: 10.1128/genomea.00885-15. Pubmed PMID: 26272569; pubmed Central PMCID: PMCPMC4536680.
21. Shi-Kunne X, Seidl MF, Faino L, Thomma BP. Draft Genome Sequence of a Strain of Cosmopolitan Fungus *Trichoderma atroviride*. *Genome Announc.* 2015;3(3). Epub 2015/05/09. Doi: 10.1128/genomea.00287-15. Pubmed PMID: 25953169; pubmed Central PMCID: PMCPMC4424285.
22. Kuo HC, Wang TY, Chen PP, Chen RS, Chen TY. Genome sequence of *Trichoderma virens* FT-333 from tropical marine climate. *FEMS Microbiol Lett.* 2015;362(7). Epub 2015/03/13. Doi: 10.1093/femsle/fnv036. Pubmed PMID: 25761749.
23. Baroncelli R, Piaggieschi G, Fiorini L, Bertolini E, Zapparata A, Pe ME, et al. Draft Whole-Genome Sequence of the Biocontrol Agent *Trichoderma harzianum* T6776. *Genome Announc.* 2015;3(3). Epub 2015/06/13. Doi: 10.1128/genomea.00647-15. Pubmed PMID: 26067977; pubmed Central PMCID: PMCPMC4463541.
24. Baroncelli R, Zapparata A, Piaggieschi G, Sarrocco S, Vannacci G. Draft Whole-Genome Sequence of *Trichoderma gamsii* T6085, a Promising Biocontrol Agent of Fusarium Head Blight on Wheat. *Genome Announc.* 2016;4(1). Epub 2016/02/20. Doi: 10.1128/genomea.01747-15. Pubmed PMID: 26893428; pubmed Central PMCID: PMCPMC4759075.
25. Compant S, Gerbore J, Antonielli L, Brutel A, Schmoll M. Draft Genome Sequence of the Root-Colonizing Fungus *Trichoderma harzianum* B97. *Genome Announc.* 2017;5(13). Epub 2017/04/01. Doi: 10.1128/genomea.00137-17. Pubmed PMID: 28360171; pubmed Central PMCID: PMCPMC5374245.
26. Schmoll M, Dattenbock C, Carreras-Villasenor N, Mendoza-Mendoza A, Tisch D, Aleman MI, et al. The Genomes of Three Uneven Siblings: Footprints of the Lifestyles of Three *Trichoderma* Species. *Microbiol Mol Biol Rev.* 2016;80(1):205-327. Epub 2016/02/13. Doi: 10.1128/MMBR.00040-15. Pubmed PMID: 26864432; pubmed Central PMCID: PMCPMC4771370.
27. Druzhinina IS, Kopchinskiy AG, Kubicek EM, Kubicek CP. A complete annotation of the chromosomes of the cellulase producer *Trichoderma reesei* provides insights in gene clusters, their expression and reveals genes required for fitness. *Biotechnol Biofuels.* 2016;9:75. Epub 2016/04/01. Doi: 10.1186/s13068-016-0488-z. Pubmed PMID: 27030800; pubmed Central PMCID: PMCPMC4812632.
28. Li WC, Huang CH, Chen CL, Chuang YC, Tung SY, Wang TF. *Trichoderma reesei* complete genome sequence, repeat-induced point mutation, and partitioning of cazyme gene clusters. *Biotechnol Biofuels.* 2017;10:170. Epub 2017/07/12. Doi: 10.1186/s13068-017-0825-x. Pubmed PMID: 28690679; pubmed Central PMCID: PMCPMC5496416.
29. Vajda V, mcloughlin S. Fungal proliferation at the Cretaceous-Tertiary boundary. *Science.* 2004;303(5663):1489-. Doi: DOI 10.1126/science.1093807. Pubmed PMID: WOS:000220000100032.
30. Ivany LC, Patterson WP, Lohmann KC. Cooler winters as a possible cause of mass extinctions at the eocene/oligocene boundary. *Nature.* 2000;407(6806):887-90. Doi: Doi 10.1038/35038044. Pubmed PMID: WOS:000089901900046.
31. Kelkar YD, Ochman H. Causes and Consequences of Genome Expansion in Fungi. *Genome Biol Evol.* 2012;4(1):13-23. Doi: 10.1093/gbe/evr124. Pubmed PMID: WOS:000301979900002.

32. Dufresne A, Garczarek L, Partensky F. Accelerated evolution associated with genome reduction in a free-living prokaryote. *Genome Biology*. 2005;6(2). Doi: ARTN R14
DOI 10.1186/gb-2005-6-2-r14. Pubmed PMID: WOS:000227026500010.
33. Sun ZY, Blanchard JL. Strong Genome-Wide Selection Early in the Evolution of *Prochlorococcus* Resulted in a Reduced Genome through the Loss of a Large Number of Small Effect Genes. *Plos ONE*. 2014;9(3). Doi: ARTN e88837 10.1371/journal.pone.0088837. Pubmed PMID: WOS:000332468900008.
34. Fenn K, Blaxter M. *Wolbachia* genomes: revealing the biology of parasitism and mutualism. *Trends Parasitol*. 2006;22(2):60-5. Doi: 10.1016/j.pt.2005.12.012. Pubmed PMID: WOS:000235575100007.
35. Tautz D, Domazet-Lošo T. The evolutionary origin of orphan genes. *Nat Rev Genet*. 2011;12(10):692-702. Epub 2011/09/01. Doi: 10.1038/nrg3053. Pubmed PMID: 21878963.
36. Bischof R, Fournis L, Limbeck A, Gamauf C, Seiboth B, Kubicek CP. Comparative analysis of the *Trichoderma reesei* transcriptome during growth on the cellulase inducing substrates wheat straw and lactose. *Biotechnol Biofuels*. 2013;6(1):127. Epub 2013/09/11. Doi: 10.1186/1754-6834-6-127. Pubmed PMID: 24016404; pubmed Central PMCID: PMC3847502.
37. Moran-Diez ME, Trushina N, Lamdan NL, Rosenfelder L, Mukherjee PK, Kenerley CM, et al. Host-specific transcriptomic pattern of *Trichoderma virens* during interaction with maize or tomato roots. *Bmc Genomics*. 2015;16:8. Epub 2015/01/23. Doi: 10.1186/s12864-014-1208-3. Pubmed PMID: 25608961; pubmed Central PMCID: PMC34326404.
38. Carvunis AR, Rolland T, Wapinski I, Calderwood MA, Yildirim MA, Simonis N, et al. Proto-genes and de novo gene birth. *Nature*. 2012;487(7407):370-4. Epub 2012/06/23. Doi: 10.1038/nature11184. Pubmed PMID: 22722833; pubmed Central PMCID: PMC3401362.
39. Wissler L, Gadau J, Simola DF, Helmkampf M, Bornberg-Bauer E. Mechanisms and dynamics of orphan gene emergence in insect genomes. *Genome Biol Evol*. 2013;5(2):439-55. Epub 2013/01/26. Doi: 10.1093/gbe/evt009. Pubmed PMID: 23348040; pubmed Central PMCID: PMC3590893.

Appendix II

HFB7 – A novel orphan hydrophobin of the Harzianum and Virens clades of *Trichoderma*, is involved in response to biotic and abiotic stresses ¹⁹

Authors

Agnes Przylucka^{1,2}, Günseli Bayram Akcapinar¹, **Komal Chenthamara**¹, Feng Cai³, Marica Grujic¹, Juriy Karpenko¹, Miriam Livoi^{1,2}, Qirong Shen¹, Christian P. Kubicek^{1*}, Irina S. Druzhinina^{1,2,†}

Affiliation

1. Microbiology and Applied Genomics group, Research Area Biochemical Technology, Institute of Chemical, Environmental & Bioscience Engineering, TU Wien, Gumpendorferstrasse 1a

2. Austrian Center of Industrial Biotechnology, Graz, Austria

3. Jiangsu Key Lab for Organic Waste Utilization and National Engineering Research Center for Organic-based Fertilizers, Nanjing Agricultural University, Nanjing, China

Contribution by the PhD candidate

1. Phylogenetic analysis showing HFB7 forms a novel clade of class II hydrophobins (Figure 1).
2. Comparison of whether the variations in the HFB7 protein sequence of 49 strains from genus *Trichoderma* would be consistent with their evolution by constructing a Bayesian phylogeny of these 49 HFB7 sequences (Figure 2 and Supplementary Figure S1)
3. Species identification by performing a phylogenetic analysis of sequences of the 4th and 5th introns of the elongation factor 1-a gene *tef1* of former *T. harzianum* species complex isolates together with those of the ex-type strains. (Supplementary Fig. S1 and species identifications in Table 1)

¹⁹ Przylucka A, Akcapinar GB, **Chenthamara K**, Cai F, Grujic M, Karpenko J, Livoi M, Shen Q, Kubicek CP, Druzhinina IS. HFB7—a novel orphan hydrophobin of the Harzianum and Virens clades of *Trichoderma*, is involved in response to biotic and abiotic stresses. *Fungal Genetics and Biology*. 2017 May 1;102:63-76.



Contents lists available at ScienceDirect

Fungal Genetics and Biology

journal homepage: www.elsevier.com/locate/yfgbi

HFB7 – A novel orphan hydrophobin of the *Harzianum* and *Virens* clades of *Trichoderma*, is involved in response to biotic and abiotic stresses



Agnes Przylucka^{a,b}, Günseli Bayram Akcapinar^a, Komal Chenthamara^a, Feng Cai^c, Marica Grujic^a, Juriy Karpenko^a, Miriam Livoi^{a,b}, Qirong Shen^c, Christian P. Kubicek^{a,1}, Irina S. Druzhinina^{a,b,*}

^aMicrobiology Group, Research Area Biochemical Technology, Institute of Chemical and Biological Engineering, TU Wien, Vienna, Austria

^bAustrian Center of Industrial Biotechnology, Graz, Austria

^cJiangsu Key Lab for Organic Waste Utilization and National Engineering Research Center for Organic-based Fertilizers, Nanjing Agricultural University, Nanjing, China

ARTICLE INFO

Article history:

Received 12 August 2016

Revised 22 December 2016

Accepted 3 January 2017

Available online 13 January 2017

Keywords:

Class II hydrophobins

Gene expression analysis

Homology modelling

Oxidative stress

Positive selection

Small secreted cysteine-rich proteins

ABSTRACT

Hydrophobins are small secreted cysteine-rich proteins exclusively found in fungi. They are able to self-assemble in single molecular layers at hydrophobic-hydrophilic interfaces and can therefore be directly involved in establishment of fungi in their habitat. The genomes of filamentous mycotrophic fungi *Trichoderma* encode a rich diversity of hydrophobins, which are divided in several groups based on their structure and evolution. Here we describe a new member of class II hydrophobins, HFB7, that has a taxonomically restricted occurrence in *Harzianum* and *Virens* clades of *Trichoderma*. Evolutionary analysis reveals that HFB7 proteins form a separate clade distinct from other *Trichoderma* class II hydrophobins and that genes encoding them evolve under positive selection pressure. Homology modelling of HFB7 structure in comparison to *T. reesei* HFB2 reveals that the two large hydrophobic patches on the surface of the protein are remarkably conserved between the two hydrophobins despite significant difference in their primary structures. Expression of *hfb7* gene in *T. virens* increases at interactions with other fungi and a plant and in response to a diversity of abiotic stress conditions, and is also upregulated during formation of aerial mycelium in a standing liquid culture. This upregulation significantly exceeds that of expression of *hfb7* under a strong constitutive promoter, and *T. virens* strains overexpressing *hfb7* thus display only changes in traits characterized by low *hfb7* expression, i.e. faster growth in submerged liquid culture. The *hfb7* gene is not expressed in conidia. Our data allow to conclude that this protein is involved in defence of *Trichoderma* against a diversity of stress factors related to the oxidative stress. Moreover, HFB7 likely helps in the establishment of the fungus in wetlands or other conditions related to high humidity. © 2017 The Authors. Published by Elsevier Inc. This is an open access article under the CC BY-NC-ND license (<http://creativecommons.org/licenses/by-nc-nd/4.0/>).

1. Introduction

Hydrophobins are small secreted cysteine-rich proteins exclusively found in fungi. Due to their amphiphilic structure they are able to self-assemble at hydrophobic-hydrophilic interfaces into ordered monolayers (Wösten and de Vocht, 2000). Thus in the fungal growth and development cycle they are able to facilitate the formation of aerial hyphae by lowering the surface tension of the liquid. Moreover, they are required for the efficient spore dispersion through air, for the attachment to hydrophobic and hydrophilic surfaces and for the stabilization of air channels in fruiting

bodies (Wösten et al., 1994; Lugones et al., 1999; Wösten, 2001). Because of their intrinsic property of self-assembly, hydrophobins are potential candidates for a diversity of applications ranging from bulk (foam stabilizers, emulsifiers) to high-value products (biosensors, fusion tags for efficient purification and immobilization, biomedical devices) (Corvis et al., 2005; Janssen et al., 2002; Khalesi et al., 2012; von Vacano et al., 2011). Several studies have also demonstrated hydrophobins as powerful implements in nanoparticle based drug delivery (Bimbo et al., 2011; Fang et al., 2014; Valo et al., 2010; Zhao et al., 2016).

Hydrophobins are conventionally grouped into two classes (class I and II) according to their interactions with solvents, hydrophobicity profiles and spacing between the conserved cysteine residues (Linder et al., 2005; Sunde et al., 2008), although this concept has recently been challenged (Jensen et al., 2010; Seidl-Seiboth et al., 2011). Nevertheless, it is assumed that class I hydrophobins are able to form highly stable monolayers known

* Corresponding author at: Microbiology Group, Research Area Biochemical Technology, Institute of Chemical and Biological Engineering, TU Wien, Gumpendorferstrasse 1a, A1060, Vienna, Austria.

E-mail address: irina.druzhinina@tuwien.ac.at (I.S. Druzhinina).

¹ Present address: Steinschöteltgasse 7, 1100 Vienna, Austria.

<http://dx.doi.org/10.1016/j.fgb.2017.01.002>

1087-1845/© 2017 The Authors. Published by Elsevier Inc.

This is an open access article under the CC BY-NC-ND license (<http://creativecommons.org/licenses/by-nc-nd/4.0/>).

as rodlets that can be only solubilized in formic or trifluoroacetic acids, while class II assemble into monolayers that can be more readily solubilized with detergents and organic solvents (Wessels et al., 1991; de Vries et al., 1993; Carpenter et al., 1992). The spacing between the eight conserved cysteine residues in class I hydrophobins shows a higher variation compared to class II.

The genus of filamentous mycotrophic fungi *Trichoderma* (Hypocreales, Ascomycota) that is enriched with environmental opportunistic species (Druzhinina et al., 2011), exhibits a high diversity of class II hydrophobins along with several proteins resembling class I. Among the diverse arsenal of *Trichoderma* class II hydrophobins, HFB1 and HFBII from *T. reesei* are the most studied. The high resolution three dimensional structures of HFB1 and HFBII are the only hydrophobin crystal structures available up to now. They have been widely tested as foam stabilizers (Basheva et al., 2011), in biosensor development (Takatsuji et al., 2013) and medical technology (Peters et al., 2016). Kubicek et al. (2008) analyzed the genome of *T. reesei* and a collection of ESTs libraries from other *Trichoderma* spp. and showed that hydrophobins in this genus are present in most infra-generic clades and evolve under purifying selection.

With the availability of the genome sequences of *T. virens* and *T. atroviride* (Kubicek et al., 2011), we have identified a novel evolutionary derived member of class II hydrophobins, HFB7, that is restricted to species related to *T. harzianum* (*Harzianum* Clade) and *T. virens* (*Virens* Clade) but is absent from Section *Longibrachiatum* (represented by *T. reesei*) and Section *Trichoderma* (represented by *T. atroviride*). Espino-Rammer et al. (2013) and Ribitsch et al. (2015) have shown that these proteins can improve the hydrolysis of polyethylene terephthalate by a microbial cutinase, thus making a further investigation of this new hydrophobin worthwhile.

Here we report the evolution of HFB7, model its structure and show the expression of the *hfb7* gene during development of *T. virens*, in interactions with fungi and plants and under abiotic stress conditions.

2. Material and methods

2.1. Strains used in this study and their identification

The isolates, newly determined species identity, origin, identifiers in international strain collections, and NCBI GenBank accession numbers of obtained gene sequences are given in Table 1. The fungal strains used in this work are available from the TU CIM – TU Wien Collection of Industrial Microorganisms (www.vt.tuwien.ac.at). For the taxonomic identification of isolates that have been previously attributed to *T. pseudoharzianum* nom. prov. sensu Druzhinina et al. (2010) or *T. cf. harzianum* according to the recently proposed taxonomy of the group by Chaverri et al. (2015), we analyzed the sequences of *tefl* gene encoding the translation elongation factor 1- α . NCBI accession numbers of *tefl* sequences are given in Table 1.

2.2. DNA extraction, PCR amplification and sequencing

For DNA extraction, isolates were cultivated on PDA plates [4% (w/v) potato dextrose agar] and the genomic DNA was extracted using the DNeasy Plant Mini Kit (Qiagen, Germany) according to manufacturer's protocol and adjusted to 10 ng/ μ l.

To investigate the occurrence of the *hfb7* in different *Trichoderma* isolates, a pair of *hfb7*-specific degenerate PCR primers was designed based on the sequences published by Kubicek et al. (2008) using *T. virens* Gv 29-8 (accession no. ABS59373) and *T. harzianum* CBS 226.95 (accession no. AJF36076.1) as templates [Table 2]. The *hfb7* amplification protocol was set up as following: initial denaturation (2 min at 95 °C) followed by 30 cycles consist-

ing of denaturation (1 min at 95 °C), annealing (1 min at 59 °C) and elongation (50 s at 72 °C). The PCR was completed with a final elongation step for 7 min at 72 °C.

Amplification of *tefl* was performed as described in Druzhinina et al. (2010). The PCR products were purified using mi-PCR purification kit (Metabion, Germany) according to the manufacturer's instructions. Sequencing was performed by Microsynth AG (Switzerland) using Sanger dideoxy sequencing.

2.3. Phylogenetic analyses and detection of selection pressure

Hydrophobin protein sequences for HFB1, HFB2, HFB7 and HFB3 were obtained from Entrez NCBI. Sequences were aligned using Muscle 3.8.425 (Edgar, 2004) program integrated in the Aliview software (Larsson, 2014). Ambiguous regions of the alignment were removed using Gblocks server [http://molevol.cmima.csic.es/castresana/Gblocks_server.html] (Castresana, 2000; Talavera and Castresana, 2007) with least stringent options. A two letter reduced amino acid alphabet, where AGTSNQDEHRKP residues were considered as hydrophilic (P) and CMFILVWY residues considered as hydrophobic (H), was used to replace all residues one by one (Murphy et al., 2000; Li et al., 2003). For this purpose, a BioPHP script (http://www.biophp.org/minitools/reduce_protein_alphabet/) was used to transform the sequences. The reduced sequences were aligned using Muscle 3.8.425. Similarly, to obtain a phylogram based on HFB7 amino acids, the sequences were aligned using integrated Muscle 3.8.425 in program Aliview. Ambiguous areas of the alignment were removed using the Gblocks server as specified above. Reduced and non-reduced alignments were subjected to phylogenetic analyses that were performed with MrBayes v3.2.5. (Huelsenbeck and Ronquist, 2001) using 1 million mcmc generations based on Dayhoff amino acid substitution model (Schwarz and Dayhoff, 1979). For each test two simultaneous, completely independent analyses starting from different random trees were run, each using three heated chains and one "cold" chain. Once the analyses were finished, 7500 trees were summarized after discarding the first 25% of obtained 10,000 trees, and a strict consensus tree was constructed. Tree was visualised and annotated using FigTree Version 1.4.2 (<http://tree.bio.ed.ac.uk/software/figtree/>).

For identification of strains by means of the analysis of *tefl* phylogenetic marker, the reference sequences for relevant *Trichoderma* species were retrieved from Chaverri et al. (2015) and Bissett et al. (2015) and were combined with the *tefl* sequences of the strains used in this study. The alignment was obtained using integrated Muscle 3.8.425. The phylogenetic analysis was performed as described above with the use of the general time reversible model of nucleotide substitutions for all sites.

Tajima's D statistic (Tajima, 1989) and K_a/K_c ratio were determined with DNAsp 5.0 (Librado and Rozas, 2009), using a sliding-window approach and alignment of cDNA sequences of *hfb7*. Codon based Fisher's test and the Codon-based Z test, implemented in MEGA 5.0 (Tamura et al., 2011) were used to test the hypotheses of selection pressure.

ConSurf server (<http://consurf.tau.ac.il>) (Ashkenazy et al., 2016) was used to estimate the degree of conservation of the amino acid residues of HFB2 and HFB7 based on the multiple sequence alignment of HFB7 orthologues. ConSurf images were rendered with Rasmol (Sayle and Milner-White, 1995).

2.4. Homology modelling of HFB7 and molecular dynamics (MD) simulations

We used SignalP (Emanuelsson et al., 2008) to identify signal peptide cleavage sequences, and ProtParam (Gasteiger et al., 2005) to predict the molecular weight and IP of HFB7.

Table 1

The strains used in this study, their TU CIM collection numbers, identifiers from other collections, origin and NCBI accession numbers for *hfb7* and *tef1* sequences.

Clade	Species	TU CIM collection number	Other collection numbers	Origin	NCBI acc no		
					<i>hfb7</i>	<i>tef1</i>	
Harzianum	<i>Trichoderma harzianum</i>	916	CBS 226.95	UK	KX373335	AY605833	
		1070	DAOM 222343	Ireland	KX373337	AY605778	
		1818		Ethiopia	KX373344	EF116562	
		206		Russia	KX373308	AY605830	
		2111		Hungary	KX373345	EF116562	
		217		Russia	KX373309	AY605829	
		261		Russia	KX373314	AY605827	
		265		Russia	KX373317	EF113554	
		3408		Papua New Guinea	KX373353	FJ577791	
		3409		Papua New Guinea	KX373354	FJ577792	
	<i>T. cf. harzianum</i>	838	CBS 115334	Costa Rica	KX373334	AY605837	
	<i>T. cf. harzianum</i>	238		Costa Rica	KX373312	AY605841	
	<i>T. afroharzianum</i>	1061	DAOM 231421	Rwanda	KX373336	AY605770	
		807		Japan	n.a.	AY605842	
		51		South Africa	KX373307	AY605845	
		2618		Ethiopia	KX373347	FJ577788	
		246		Philippines	KX373313	EF191319	
	<i>T. camerunense</i>	1722		Cameroun	KX373342	EF191327	
		1724		Cameroun	KX373343	EF191328	
		1720		Cameroun	KX373341	EF191326	
	<i>T. lentiforme</i>	646		Hawaii	KX373328	FJ577780	
		709		Brazil	KX373332	AY605851	
	<i>T. lixii</i>	2784	CBS 110080	Thailand	KX373350	FJ16622	
	<i>T. cf. lixii</i>	837	CBS 115333	Egypt	KX373333	AY605839	
	<i>T. pyrimidale</i>	272		Nepal	KX373318	AY605849	
		2673		Ethiopia	KX373349	FJ577789	
	<i>T. simmonsii</i>	4310	CBS 354.33	USA	KX373338	KX655779	
		373	DAOM 222136	Ontario, Canada	KX373323	AY605792	
		334		USA	KX373321	FJ577776	
		335		USA	KX373322	FJ577777	
		<i>T. cf. simmonsii</i>	588		Laos	KX373327	FJ577778
		<i>T. tawa</i>	1632		Thailand	KX373340	FJ463313
		<i>T. alni</i>	2657		Italy	KX373348	EF488107
		<i>T. atrobrunneum</i>	291		Nepal	KX373319	AY605848
		<i>T. atroglatinosum</i>	1627	CBS 237.63	New Zealand	KX373339	KJ871083
		<i>T. virens</i>	3530	Gv 29-8	USA	AB559373	jgi_v2_83874
	Virens		2931		Hungary	KX373351	KX655777
			2935		Hungary	KX373352	KX655778
			320		USA	KX373320	KX655770
			396		Cambodia	KX373324	KX655771
			507		Indonesia	KX373326	KX655773
		669		Hawaii, USA	KX373329	KX655774	
		681		Mexico	KX373330	KX655775	
		82		Brazil	KX373306	KX655765	
<i>T. cf. virens</i>		2558		Ivory Coast	KX373346	KX655776	
<i>T. cf. virens</i>		404		Singapore	KX373325	KX655772	
<i>T. crassum</i>		219		Russia	KX373310	KX655766	
		226		Russia	KX373311	KX655767	
		262		Russia	KX373315	KX655768	
		263		Russia	KX373316	KX655769	

Table 2

Primers used in this study for the amplification of *tef1* (*tefAPF*, *tefAPR*) and *hfb7* (*hfb7F*, *hfb7R*) for the analysis of genetic expression; primers used for the amplification of *hfb7* (*hfb7F*, *hfb7harzR*, *hfb7virR*) in genomic DNA of *T. virens* and *T. harzianum* species, respectively.

Primer name	Target locus	Sequence 5'-3'	T _m , °C	Expected amplicon length	
				cDNA	gDNA
<i>hfb7F</i>	<i>hfb7</i> including complete C ₁ - C ₈ sequence	AACCACYWCCACATTCAA	59		
<i>hfb7harzR</i>		TTCACCATCCAAGTCAACA		371	471
<i>hfb7virR</i>		TTCACCATCCAAGTACAGCTA		372	472
<i>tef1APF</i>	partial 6th exon of <i>tef1</i>	ACGCTCTGCTCGCCTACACC	59	184	184
<i>tef1APR</i>		TCACCGTTGAAACCGGAGATG			
<i>hfb7F</i>	partial <i>hfb7</i>	CTCGACTGTGGCACTCCTACTGT	59	136	281
<i>hfb7R</i>		CGACGGGCTTCTCGCAA			

Homology modelled structures of HFB7 from *T. virens* Gv 29-8 were constructed with Modeller v9.2 loop model script (Sali and Blundell, 1993). For this purpose, ultra-high resolution structure

of hydrophobin HFB2 from *T. reesei* was used as the template (pdb ID: 2B97) with 62.3% overall similarity. Twenty different models were generated and the model with the lowest discrete

optimized protein energy (DOPE) score was further selected for molecular dynamics (MD) simulations.

MD simulations were performed on HFB7 structure. NAMD/VMD software package (Phillips et al., 2005) with CHARMM27 all-atom force field (MacKerell et al., 1998) was used. Throughout the simulations water was described using the TIP3P model (Jorgensen et al., 1983). HFB7 structure was first placed in a water box with $50 \times 50 \times 48 \text{ \AA}$ dimensions (with the minimum solute-wall distance of 10 \AA). One sodium atom was added to the system for the neutralization of the protein. Simulations were performed under periodic boundary conditions at 298 K with a 2 fs time step using NVT ensemble. Data collection was done every 2 ps. The system was minimized over 50,000 steps using the conjugate gradient (CG) algorithm and the resulting structure was equilibrated for 1 ns at the same temperature. The equilibrated structure was further simulated for an additional 4 ns at 298 K. 4 ns simulation was repeated once. Root mean squared deviation (RMSD) values were calculated from trajectory files and final structures were prepared using VMD software.

The solvent accessible surface area (SASA) was determined using the homology modelled, energy minimized and equilibrated HFB7 structure and HFB2 structure available in the PDB database. SASA was determined with a 1.4 \AA solvent probe radius using a tcl script written for VMD (Phillips et al., 2005). The structures were colored based on the SASA values with VMD.

2.5. Cultivation of *T. vires*

For submerged fermentation in shake flasks *T. vires* was cultivated on PDA plates containing $100 \mu\text{g ml}^{-1}$ chloramphenicol at 28°C for seven days. Spores were collected using deionized water with 0.1% Triton X-100 (10^7 ml^{-1} spores counted via hemocytometer) and used as inoculum.

Submerged cultivation was performed in 1 L Erlenmeyer flasks at 28°C agitated at 220 rpm. Biomass was grown in 100 ml of pre-culture medium [4% carbon source (glycerol, glucose, starch), 0.4% (w/v) peptone, 37 mM KH_2PO_4 , 21 mM $(\text{NH}_4)_2\text{SO}_4$, 2 mM $\text{MgSO}_4 \cdot 7\text{H}_2\text{O}$, 3.5 mM $\text{CaCl}_2 \cdot 2\text{H}_2\text{O}$, $0.1 \mu\text{g ml}^{-1}$ hyromycin] at 28°C and 220 rpm for approx. 30 h. The medium was supplemented with 40 ml L^{-1} trace elements (0.9 mM $\text{FeSO}_4 \cdot 7\text{H}_2\text{O}$, 0.5 mM $\text{MnSO}_4 \cdot \text{H}_2\text{O}$, 0.25 mM $\text{ZnSO}_4 \cdot 7\text{H}_2\text{O}$, 0.6 mM $\text{CoCl}_2 \cdot 2\text{H}_2\text{O}$). The inoculum was then transferred to a 1 L Erlenmeyer flask containing 250 ml of the same medium. Samples were taken in intervals of 24 h. Biomass dry weight was determined by filtering 10 ml of the culture broth on Whatman 20 mm filter disks (Sigma Aldrich, Missouri, USA) and drying at 80°C to a constant weight. Total secreted protein was quantified using Bradford protein assay (Bio-Rad).

For growth of *T. vires* in liquid standing culture, 30% (w/v) Murashige Skoog basal salt mixture (Sigma-Aldrich, Missouri, USA) was supplemented with 1% (w/v) glucose (MS-G). Experiments were performed in 24-well plates, each well containing 0.7 ml medium inoculated with 0.01 ml of the spore suspension (10^6 total conidia). The plates were cultivated in standing culture at 25°C in a 12 h illumination cycle for seven days. Growth was measured as a function of turbidity at 750 nm. Mycelium was harvested after 48, 72, 96 and 120 h.

To investigate growth on the surface of solid media, 9 cm Petri plates, 1 ml of the spore suspension (10^6 total conidia) were inoculated on MS-G agar medium covered with cellophane and incubated under the same conditions as above. Mycelium was harvested every 24 h starting after the two days and before the plate was covered by the colony (seven days). All experiments were performed in triplicates.

For morphological characterization of the *T. vires* OEhfb7 strains, nine cm diameter plates containing a standardized amount

of medium (20 ml) were prepared. The media consisted of PDA medium as the rich medium, and poor medium i.e. SNA medium (1.7 % w/v synthetic nutrient deficient agar; Sifin diagnostics GmbH, Germany), and SNA plus medium which contained 1% (w/v) of glucose. The overexpression strain and control were grown at 25°C in light and darkness cycles. The radial growth was measured every 24 h.

2.6. Interactions with *Fusarium oxysporum* and *Athelia rolfsii*

Dual confrontation assays were used to study potential myco-parasitic and antagonistic actions of *T. vires*. Agar plugs (six mm diameter) of fresh culture of *Fusarium oxysporum* f. sp. *cubense* 4 TU CIM 4812 (Hypocreales, Ascomycota; see Zhang et al., 2016 for strain identity) or *Athelia rolfsii* (*Sclerotium rolfsii*, Atheliales, Basidiomycota), and 10^6 *T. vires* spores were inoculated on opposite poles of a MS-G containing agar plate (agar 2% w/v) covered with cellophane. The cultures were incubated under the same condition as used for the cultivation in liquid culture. *T. vires* mycelia were harvested before contact (48 h), when the contact between *T. vires* and its partner was established (72 h) and 24 h after the contact.

2.7. Interaction with *Solanum lycopersicum* cv. Micro-Tom seedlings

To study the interaction of *T. vires* with a plant, tomato seeds (*Solanum lycopersicum* L. cv. Micro-Tom) were surface-sterilized with 95% (v/v) ethanol for five min and 5% (v/v) sodium hypochlorite for five min. The seeds were thereafter rinsed six times with sterile deionized water. Seeds were germinated on $0.3 \times$ MS-G medium supplemented with 1% (w/v) phytigel (Sigma). For each test three 15-day-old seedlings were transplanted to a new $0.3 \times$ MS-G-phytagel plate covered with cellophane, and inoculated with 10^6 spores of *T. vires* and incubated at the same conditions (see Section 2.6).

2.8. Mechanical injury and oxidative stress

To test the response of *T. vires* to mechanical injury and oxidative stress, the fungus was incubated 48 h on MS-G agar medium covered with sterile cellophane and then (i) injured by cutting the hyphae with a sterile cold scalpel as described by Hernández-Oñate et al. (2012), or (ii) treated with 10 mM H_2O_2 , or (iii) 0.1 mM menadione (Friedl et al., 2008), or combinations of injury and later compounds were applied (vi and v). Plates were imaged 1, 3, 12, 18, 24, 36 and 48 h after impact. Biomass was harvested immediately after application of stress conditions and after 1, 3 and 24 h respectively.

2.9. Analysis of *hfb7* expression

Mycelia and/or spores were harvested and immediately frozen in liquid nitrogen. After grinding in a mortar with a pestle under liquid nitrogen, total RNA was extracted using the RNeasy Plant Mini Kit (Qiagen) according to the manufacturer's instructions. To remove DNA, the extracted RNA was incubated with DNase (DNase I, RNase free; Fermentas). The RNA quantity was measured using a NanoDrop spectrophotometer (Thermo Scientific, Massachusetts, USA). cDNAs were synthesized with the RevertAidTM First Strand cDNA Kit (Fermentas, Germany) using oligo-dT primers according to the manufacturer's protocol.

qPCR assays were performed on the real-time thermal cycler qTOWER (Jena Analytics, Germany). For the reaction $20 \mu\text{l}$ assays were prepared containing the IQ SYBR Green Supermix (Bio-Rad, Germany), a final primer concentration of $0.5 \mu\text{M}$ each and cDNA with a final concentration of $82.5 \text{ ng } \mu\text{l}^{-1}$. The amplification proto-

col was set up as following: initial denaturation (6 min at 95 °C) followed by 40 cycles consisting of denaturation (30 s at 95 °C), annealing (60 s at 60 °C) and elongation (7 min at 72 °C). For the calculation of the gene expression, samples were first normalized against the constitutively expressed transcription elongation factor 1- α (*tef1*) gene, then the fold regulation was estimated according to the $2^{-\Delta\Delta CT}$ method (Livak and Schmittgen, 2001). Primers for the amplification of target (*hfb7F*, *hfb7R*) and control gene (*tef1APF*, *tef1APR*) were designed using Primer Premier 5 software (Lalitha, 2004). The primer efficiencies of target and control gene were assessed by checking if Δct values vary with template dilution. A dilution row was prepared over a 20-fold range. The absolute value of the slope was >0.1, proving that the designed primers are sufficiently equal in efficiency.

2.10. Determination of surface hydrophobicity of hyphae

Surface hydrophobicity of hyphae was determined by measuring the water contact angle (WCA) of a droplet of deionized water on fungal mycelium grown for 72 h on solid agar medium. Water droplets of 5 μ l were set onto the surface of the material and a picture taken after ten seconds. The drop shape was analyzed using the DropSnake method (Stalder et al., 2006).

2.11. Production and characterization of a *hfb7* overexpressing strain of *T. virens*

A *T. virens* strain that overexpressed *hfb7* under the strong constitutive cDNA1 promoter (Nakari-Setälä and Penttilä, 1995) and its own signal sequences was constructed essentially as described earlier (Uzbas et al., 2012). The vector also carries the hygromycin B resistance encoding *hph* gene as dominant selection marker. The expression cassette was synthesized and subcloned by Eurofins Genomics (Bavaria, Germany). Transformation was performed as described in Penttilä et al. (1987), using the *Apal* linearized vector. Transformants were selected on PDA plates containing 100 μ g ml⁻¹ hygromycin, and mitotically stable single spores isolated. Extraction of genomic DNA and confirmation of positive mutants using gene specific primers and target gene amplification were performed as described in Section 2.2.

3. Results

3.1. HFB7 forms a novel clade of class II hydrophobins

Espino-Rammer et al. (2013) proposed HFB7 as a distinct terminal clade of *Trichoderma* hydrophobins, which is phylogenetically related to *T. reesei* HFB1 and HFB2. In order to learn whether HFB7 indeed forms its own clade and is conserved in *Trichoderma*, we used blastp and screened all available *Trichoderma* genomes (*T. reesei*, *T. parareesei*, *T. longibrachiatum*, *T. citrinoviride*, *T. harzianum*, *T. afroharzianum*, *T. virens*, *T. atroviride*, *T. asperellum*, and *T. gamsii*; Martinez et al., 2008; Kubicek et al., 2011; Yang et al., 2015; Baroncelli et al., 2015, 2016) for the presence of HFB1, HFB2 and similar class II hydrophobins. All retrieved sequences were then subjected to a phylogenetic analysis (Fig. 1). The tree based on the reduced amino acid alignment that only considers hydrophobicity of residues, rooted against the more distant *T. reesei* HFB3 (Linder et al., 2005) shows that HFB7 forms a statistically supported clade that is distinct from a monophyletic clade that comprises HFB1 and HFB2, respectively. Interestingly, the HFB7 clade only contained proteins from *T. virens* and *T. harzianum*. A blastp search of *T. virens* HFB7 against the NCBI database also revealed *T. harzianum* as the closest neighbor (75 % similarity, E-value 7e-43). The next best neighbor in NCBI was *T. reesei* HFB2, indicating

that HFB7 is an orphan protein in the closely related species *T. harzianum* and *T. virens* that is absent from all other fungi in the NCBI database, and no known orthologues are present in other fungal genera.

3.2. HFB7 has a restricted occurrence in the *Harzianum* and *Virens* Clades of *Trichoderma*

Since the above screening only involved those species for which a genome sequence is available, we developed degenerate primers specific for *hfb7* (Table 2) and used them to potentially amplify the gene from 49 isolates and species of the *Harzianum* and *Virens* Clades of *Trichoderma*, thereby making a balanced choice of geographic origin (cf. Druzhinina et al., 2010). As a negative control, these tests were also applied to *T. gamsii* and *T. reesei* (Sections *Trichoderma* and *Longibrachiatum*, respectively). However, since the taxonomy of the *Harzianum* Clade has recently been revised (Chaverri et al., 2015), we assessed the correct species identity of these isolates prior to the analysis. To this end, we performed a phylogenetic analysis of sequences of the 4th and 5th introns of the elongation factor 1- α gene *tef1* of former *T. harzianum* species complex isolates together with those of the recently established ex-type strains. The results are given in Supplementary Fig. S1 and species identifications are given in Table 1: our sample was shown to consist of (numbers in brackets specify the number of isolates) the following species that were previously termed *T. 'pseudoharzianum'* sensu Druzhinina et al. (2010, 2011) or *T. cf. harzianum* of *T. harzianum*: *T. afarasin* (1), *T. afroharzianum* (5), *T. atrobunneum* (1), *T. camerunense* (3), *T. harzianum* (8), *T. lentiforme* (2), *T. lixii* (1), *T. pyrimidale* (2), and *T. simmonsii* (4); the phylogenetically close taxa from the *Harzianum* Clade *T. atrogelatinosum* (1), *T. alni* (1), and *T. tawa* (1); and *T. virens* (9) and *T. crassum* (4) as members of the *Virens* Clade, respectively. Six isolates could not be identified with certainty by this method but formed lone lineages monophyletic with other strains (Supplementary Fig. S1), and were thus maintained in our sample. They were named *T. cf. harzianum* (2), *T. cf. virens* (2), *T. cf. simmonsii* (1) and *T. cf. lixii* (1).

As shown in Table 1, we could successfully amplify *hfb7* sequences from all 49 isolates of the *Harzianum* and *Virens* Clades of *Trichoderma* but not from the negative control, showing that the gene consistently and exclusively occurs in these two species clades.

In order to test whether the variations in the HFB7 protein sequence of these strains would be consistent with their phylogeny, we constructed a Bayesian phylogeny of the amino acid sequences of the 49 HFB7 sequences (Fig. 2) and compared them to the *tef1* species tree (Supplementary Fig. S1). The topology of the two trees appeared to be not concordant: while HFB7 from some species, like *T. harzianum*, formed a monophyletic clade, the HFB7 of others (e.g., *T. afroharzianum*) occurred in several positions. It was also interesting to note that HFB7 of *T. virens* occupied a closer position to the "*T. harzianum*" species than *T. alni* or *T. atrogelatinosum*, and that *T. lentiforme* HFB7 formed a basal cluster to both the other *Harzianum* and *Virens* HFB7s. Considering that *tef1* evolves without selection pressure and corresponds to the evolution of the *Trichoderma* (see Druzhinina et al., 2010; Chaverri et al., 2015), these data suggest either a recombination hot spot or selection pressure at *hfb7* locus.

3.3. HFB7 evolves under positive selection pressure

We have previously reported that both the class I as well as the novel cf. "class I" hydrophobin genes evolve by purifying selection without concerted evolution (Kubicek et al., 2008; Seidl-Seiboth et al., 2011). This model of "birth-and-death" evolution assumes

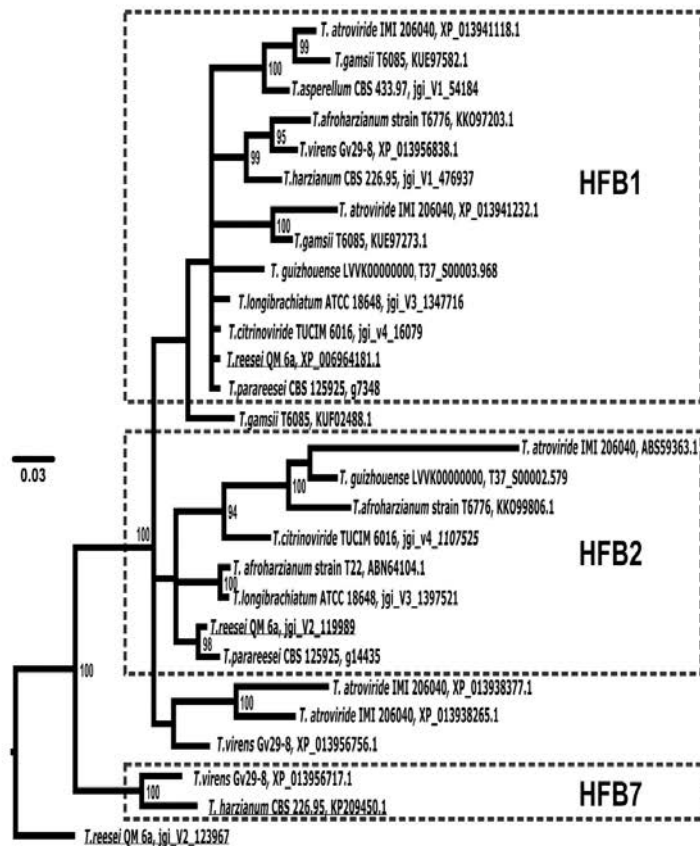


Fig. 1. Bayesian phylogram based on amino acids sequences from hydrophobins, reduced according to their hydrophobic property (Murphy et al., 2000; Li et al., 2003). Bayesian analysis was run for 1 million mcmc generations and a strict consensus tree was obtained by summarizing 7500 trees, after burning first 25% of obtained 10,000 trees. Posterior probabilities more than 90% are shown near the nodes.

that new genes are created by repeated events of gene duplication and that some of the copies are maintained in the genome for a long time whereas others are deleted or become non-functional (Nei and Rooney, 2005). Under these conditions nucleotide sequence differences between genes primarily occur at synonymous sites, thus resulting in $K_S \gg K_A$, and indeed the hydrophobins investigated so far displayed a very low K_A/K_S ratio (Kubicek et al., 2008; Seidl-Seiboth et al., 2011). When the K_A/K_S ratio was determined for HFB7, values close to one and even higher than one (*T. virens*) were obtained (Table 3). A ratio of 1 would indicate neutral evolution or absence of selection pressure, whereas a ratio above 1 would be evidence for positive selection. Since the K_A/K_S value is the mean for the whole protein, some amino acids must therefore be under positive selection. In any case, these values indicate a faster fixation rate for non-synonymous changes in HFB7 than in the other class II hydrophobins.

3.4. Protein structure of HFB7

HFB7 from *T. virens* encodes a protein of 93 aa, in which SignalP predicts the N-terminal 15 aa to form a signal peptide. The

corresponding 76 aa mature protein has a theoretical mass of 7483.7 Da and displays a theoretical IP of 6.03. It is particularly rich (>9%) in A, C, G, L, P, V, whereas R, M, W and Y are absent.

The closest hydrophobin neighbor to HFB7 is HFB2 (Fig. 1; see Section 3.1.), which exhibits overall 62.3% sequence similarity and 50.6% sequence identity with HFB7. Since structural features are highly conserved in hydrophobins (Sunde et al., 2008), we performed homology modelling towards establishing the structure of HFB7. In fact, a superimposition of HFB7 and HFB2 did not show many differences, thus increasing the quality of the homology model. Additionally, the accuracy of the model was further increased by the ultra-high resolution of the HFB2 structure in the PDB database. We also performed MD simulations of the homology modelled HFB7 structure in water to identify the structural features of HFB7 in solution. The structures obtained after 4 ns MD simulations are shown in Fig. 3A. As indicated in the figure, STAMP structural alignment has shown that both structures obtained at the end of 4 ns MD simulation 1 and simulation 2 were highly similar. Moreover, the core hydrophobin structure was stable throughout 4 ns MD simulations (Supplementary Fig. S2). Surface properties of HFB7 structure was shown in Fig. 3B by color-

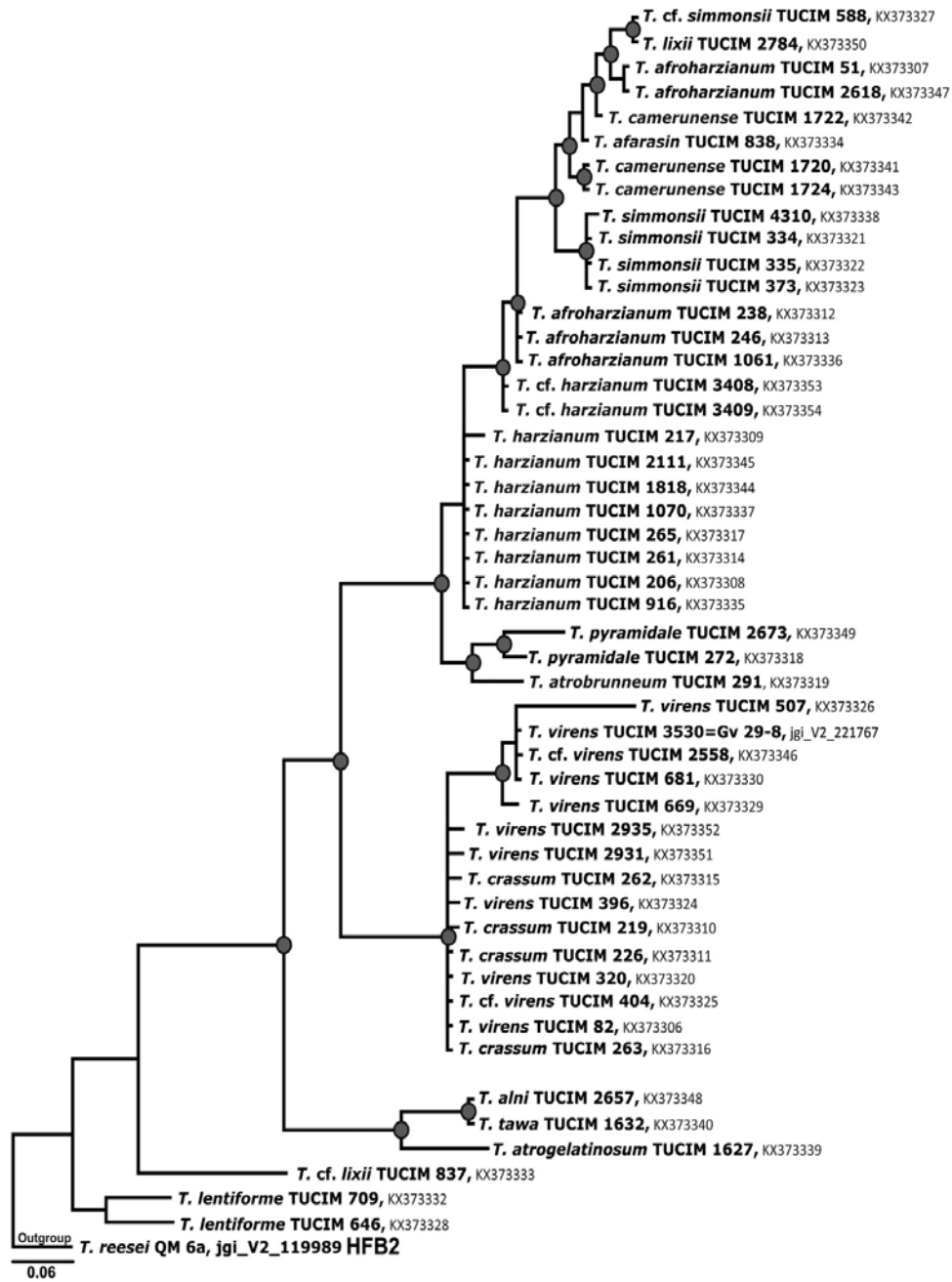


Fig. 2. Bayesian phylogram based on HFB7 aa sequences of the 49 strains that were used in this study. A HFB2 sequence from *Trichoderma reesei* QM 6a was included as an outgroup. Bayesian analysis was run for 1 million mcmc generations and a consensus tree was obtained by summarizing 7500 trees, after burning first 25 % of obtained 10,000 trees. Posterior probabilities more than 90 % are marked with circular nodes.

Table 3
Nucleotide diversity and K_a/K_s ratio of the *hfb7* exon.

	Harzianum Clade	Virens Clade	<i>hfb7</i>
Number of isolates	35	15	50
Sequence length	289		
Total number of mutations (η)	80	25	100
Nucleotide diversity (π)	0.0935	0.054	0.186
Total number of codons	96		
K_a/K_s	1.015	1.276	1.023

ing the surface of the molecule according to hydrophobicity. The hydrophobic residues forming the hydrophobic patch are found to be V24, L25, V27, A28, L30, I61, P62, A63, A64, L66, L68, L69. This patch was found to extend to the other side of the molecule forming an L-shaped large hydrophobic patch and this second patch was found to be formed with the involvement of the residues A1, P2, A3, V16, P17, L18, P35, V37, P38, V39, L40.

A ConSurf analysis of the HFB7, indicated that most of the P, C, T and F residues are highly conserved as well as the hydrophobicity is also conserved along the hydrophobic patch residues (Fig. 4). Considering that the protein evolves under positive selection pressure this finding indicates the possible role of other amino acid properties than hydrophobicity in the function of the protein.

3.5. Constitutive overexpression of *hfb7* in *T. virens* increases the growth rate in submerged culture

To study the function of *hfb7* in *T. virens*, we constructed two strains overexpressing *hfb7* under the strong and constitutive cDNAIP promoter, i.e. *OEhfb7-4871* and *OEhfb7-4872*. In these strains, the *hfb7* transcript, normalized to *tef1* as a housekeeping gene, was approximately 10–12-fold more abundant, during growth in submerged culture on glucose compared to the parental strain. During growth in submerged culture, both strains exhibited a higher growth rate and secreted more protein to the medium (Fig. 5). Cultivations on glycerol and starch showed the same trend (data not shown). Conversely, however, there was no effect on the radial growth rate or conidiation on solid media and both overexpressing strains grew equal to the parental strain in a still liquid culture (*vide infra*).

In order to test whether HFB7 would be involved in rendering the hyphae more hydrophobic, we performed WCA using water droplets. The parental strain already displayed quite high angles ($128.10 \pm 8.67^\circ$) indicating that its hyphae are hydrophobic. However, similar values ($123.70 \pm 7.20^\circ$ and $134.38 \pm 5.43^\circ$) were obtained for the *OEhfb7-4871* and *OEhfb7-4872* strains, respectively, indicating that overexpression of *hfb7* does not further increase the hydrophobicity of the hyphae.

3.6. Expression of *hfb7* parallels for the formation of aerial hyphae

To study the expression of *hfb7* during the vegetative growth of *T. virens*, the fungus was grown on MS-G medium. Under these conditions, the formation of submerged mycelium is followed by the appearance of aerial hyphae on the surface and finally by conidiation. The *hfb7* transcript showed a steady increase over the course of the different experimental stages, being lowest during submerged growth, but strongly increasing during formation of aerial mycelium. No further increase in *hfb7* expression was observed when culture matured and conidia were formed in standing liquid medium. Interestingly, *hfb7* was constitutively expressed at the equal level to *tef1* used for normalization during vegetative growth on agar plate (Fig. 6). However, as *tef1* is considered to be generally highly expressed in fungi, similar values for *hfb7* indicate a demand in this protein for the fungus.

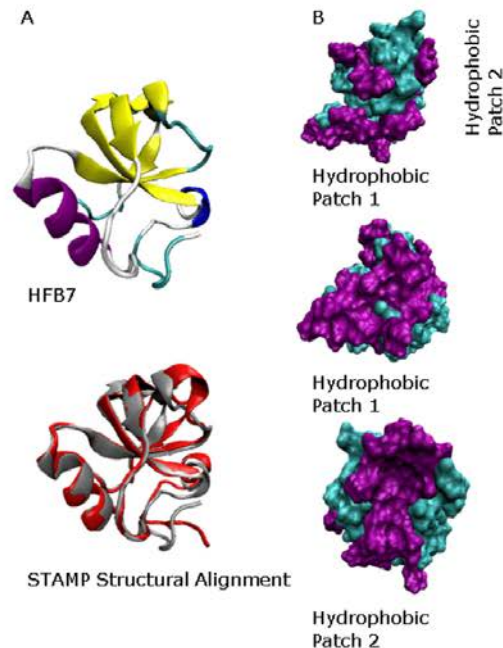


Fig. 3. Structure of HFB7 at the end of MD simulations after 4 ns runs. (A) Right: structure of HFB7 after 4 ns MD simulations colored by secondary structure; left: STAMP structural alignment was performed on the final structures of HFB7. The simulation was repeated and the resulting structure was structurally aligned with the first structure obtained from the first simulation. Gray: HFB7 after Simulation 1, Red: HFB7 after Simulation 2. (B) From left to right: surface representation of HFB7 structure colored by hydrophobicity. First hydrophobic patch of HFB7. Second hydrophobic patch of HFB7. Purple: Hydrophobic residues, Cyan: Hydrophilic residues. (For interpretation of the references to color in this figure legend, the reader is referred to the web version of this article.)

3.7. *hfb7* is downregulated in conidia

We tested if the *hfb7* transcript would be abundant in conidia. However, the amount of transcript in freshly harvested conidia was approximately 100 fold below the expression of *tef1* (0.01 ± 0.001) suggesting that this gene is not required in mature conidia.

3.8. Expression of *hfb7* parallels the interaction with tomato roots

We also investigated the expression of *hfb7* during contact with *S. lycopersicum* (tomato) roots. Incubation of *T. virens* with this plant led to the strongest expression of *hfb7* at contact with the plant, whereas it declined during prolonged interaction (Fig. 7). Yet the level of expression then was still higher than during interaction with fungi (*vide infra*).

3.9. Expression of *hfb7* is enhanced during interaction with other fungi

To learn whether *hfb7* would be expressed during the interaction of *T. virens* with other fungi, we first confronted *T. virens* with the two taxonomically unrelated fungi that are generally resistant against the attacks of this mycotrophic fungus - *Fusarium oxysporum* f. sp. *cubense* 4 (FOC4, Ascomycota) and *Athelia rolfsii* (Sclero-

72

A. Przytucka et al. / Fungal Genetics and Biology 102 (2017) 63–76

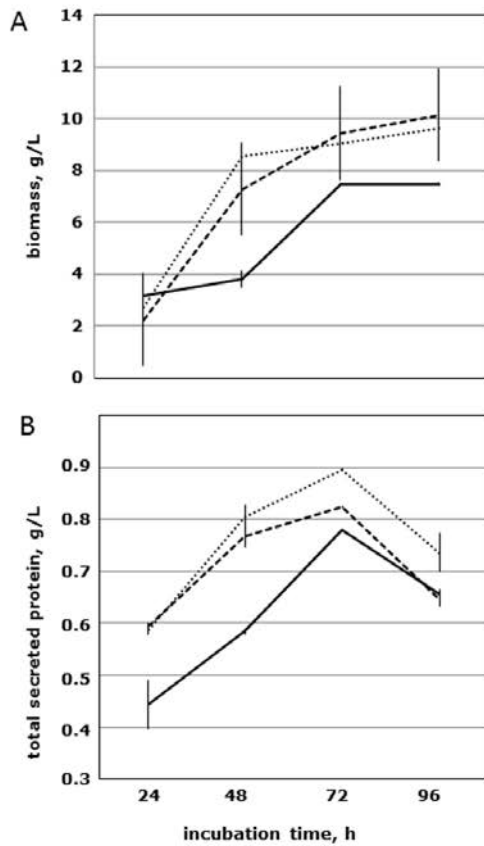


Fig. 5. Growth (A) and protein secretion (B) of *T. virens* OEhfb7-4871 (dotted line) and OEhfb7-4872 (dashed line) strains, respectively, in comparison to the wild type Cv 29-8 (solid line).

4. Discussion

Species of *Trichoderma* possess a high diversity of class II hydrophobins (Linder et al., 2005; Kubicek et al., 2008). However, despite this richness, most of the work has so far been concentrated on only a few of them, e.g. *T. reesei* HFB1 and HFB2 (Linder et al., 2005), *T. longibrachiatum* Hyt101 (Ruocco et al., 2015; an orthologue of *T. reesei* HFB2), and *T. atroviride* SRH1 (Muñoz et al., 1997). The latter occupies a phylogenetic position between the HFB1 and the HFB2 clades. Previous work interpreted them all to form a HFB1/2 clade (Kubicek et al., 2008), but our present data – based on the analysis of hydrophobins from nine *Trichoderma* genomes – clearly show that HFB1 and HFB2 form two separate phylogenetic clades. This separation is also underlined by the different roles that *hfb1* and *hfb2* play in the physiology of *T. reesei*, the former being involved in hyphal development, whereas the latter plays a role in sporulation (Nakari-Setälä et al., 1997). Likewise, *hfb1* was only expressed in vegetative cultures on glucose but not on cellulose, xylan, cellobiose or lactose, whereas *hfb2* was highly expressed in hyphae growing on media with these carbon sources, and during conidiation stimulated by N and C starvation and

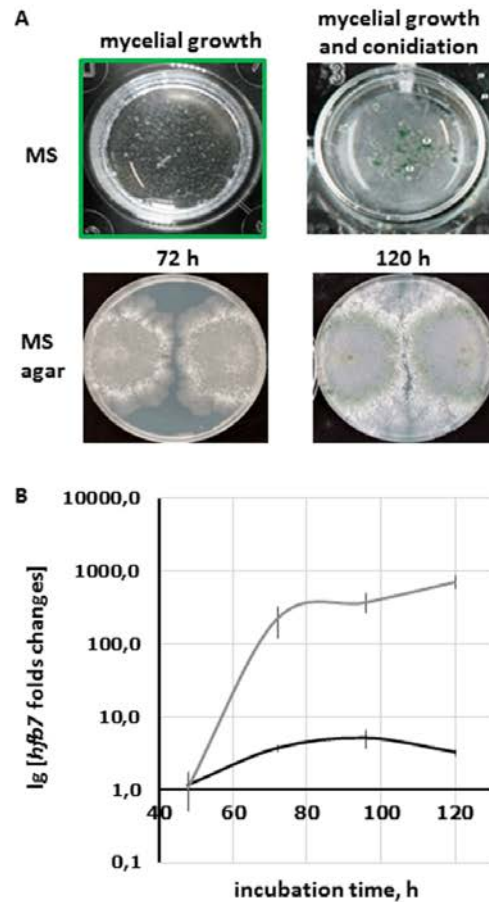


Fig. 6. Growth of *T. virens* Cv 29-8 and expression of *hfb7* gene normalized to the expression of the reference housekeeping gene *tef1*. (A) Mycelial growth in standing liquid culture MS and on MS-G agar plates. (B) Expression of the *hfb7* gene in standing liquid culture (gray line) and when confronted to itself on agar plates (black line). Vertical bars indicate standard deviations, N = 3.

illumination (Askolin et al., 2005). In addition, Hyt101 has been shown to increase the systemic resistance of plants to pathogens (Ruocco et al., 2015).

In the course of a screening for hydrophobins that may be able to stimulate the degradation of polyethylene terephthalate by cutinase, we have recently detected HFB7 that forms one of the evolutionary youngest clades in the phylogenetic tree of *Trichoderma* class II hydrophobins (Espino-Rammer et al., 2013). In the present work, we further delimited this HFB7 clade: despite of its relation to the HFB1 and HFB2, the HFB7 clade differs in two important aspects: first, it has a restricted taxonomic occurrence in *Trichoderma*, and is only present in some species of the *Harzianum* and *Virens* Clades; and second, its evolution exhibits a much faster fixation rate for non-synonymous changes than the other *Trichoderma* class II (Kubicek et al., 2008) and class I-like hydrophobins (Seidl-Seiboth et al., 2011), in which K_a/K_s was $\ll 1$. Theoretically, the K_a/K_s values obtained for the HFB7 proteins would be indicative of

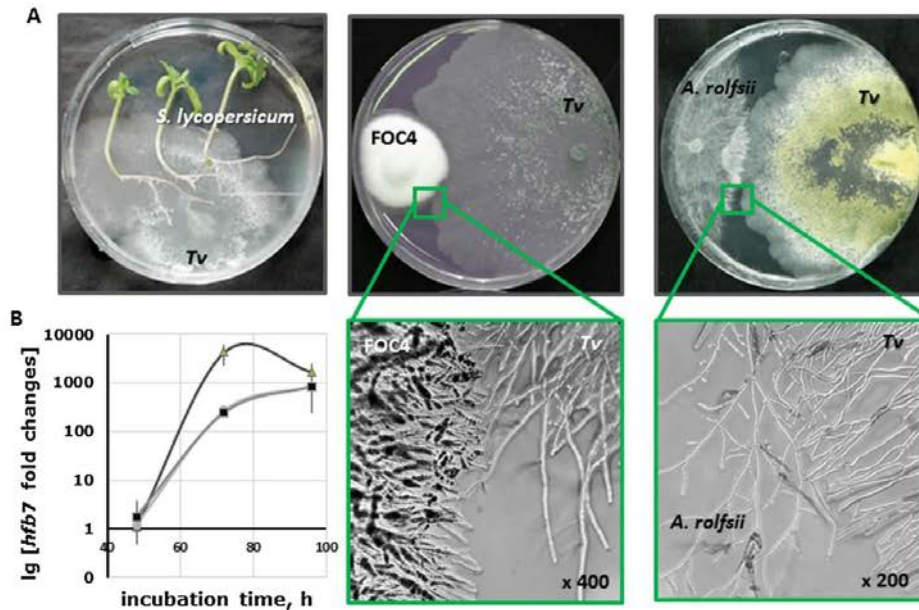


Fig. 7. (A) Biotic interactions of *T. vires* Cv 29-8 with tomato plants (*Solanum lycopersicum*) and fungi (FOC4 – *Fusarium oxysporum* f. sp. *cubense* 4, and *Athelia rolfsii*). Microscopic observations of the interacting zone are shown in framed inserts. (B) Expression of *hfb7* gene during interactions normalized to *tef1*. Triangles correspond to interactions with *S. lycopersicum*; circles and squares correspond to interactions with FOC4 and *A. rolfsii*, respectively. Vertical bars indicate standard deviation, N = 3.

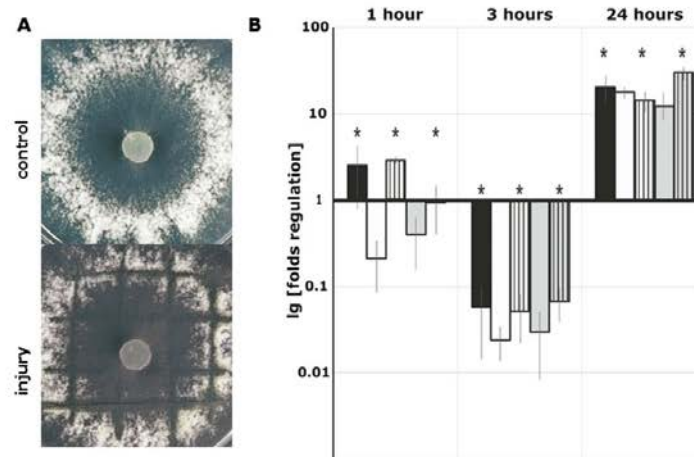


Fig. 8. Response of *T. vires* to oxidative stress. (A) Morphology of *T. vires* Cv 29-8 without any impact (control) and 24 h after mechanical injury with sterile cold scalpel. The fungus was incubated 48 h before the impact, both conditions imaged simultaneously. (B) Regulation of *hfb7* in *T. vires* Cv 29-8 after (i) mechanical injury with sterile cold scalpel (black bars), 10 mM H₂O₂ (white bars), mechanical injury and 10 mM H₂O₂ (white striped bars); 0.1 mM menadione (gray bars) and mechanical injury and 0.1 mM menadione (gray striped bars). The data are normalized to expression of *tef1* and *hfb7* values with no impact (control). Vertical lines indicate standard deviations, N = 3.

unconstrained, neutral evolution, which typically occurs in pseudogenes (Koonin and Wolf, 2010). However, since we have obtained a phenotype for the *OEhfb7* strain and have observed regulation of *hfb7* transcript formation, the possibility of *hfb7* being a pseudogene is rejected. So why do we observe these high K_a values,

which in *T. vires* and *T. crassum* even result in a slightly $K_a/K_s > 1$? We consider it is likely that some of the amino acids in HFB7 are already under positive, whereas others are still under purifying selection, and thus keep the overall K_a/K_s ratio lowered. Positive selection is a process by which new advantageous genetic variants

manifest themselves in a population. It has been shown to be a common feature of various self/non-self recognition and host defence systems in fungi (Saupe, 2000). Since HFB7 is only present in two narrow clades of *Trichoderma* (vide supra), such a role would be restricted to some species only. Since our claim of this restricted occurrence is mainly based on PCR detection, it is important to note that we confirmed the absence in other species also by carefully mining the genomes of the HFB7-negative species (i.e., *T. atroviride*, *T. asperellum*, and the species from the *Longibrachiatum* Clade). Interestingly, the *hfb7* gene is absent in *T. guizhouense* that is a member of the *Harzianum* Clade (J. Zang, F. Cai, I. Druzhinina, Q. Shen, unpublished data).

In order to learn about a role of HFB7, we constructed two *OEhfb7* strains and tested their phenotypes. Although they expressed *hfb7* about 10-fold higher than the parent strain, we only found a few phenotypic changes (i.e. faster submerged growth and formation of more biomass), no differences were observed with respect to those conditions that led to a strong increase in *hfb7* gene expression (interaction with other fungi and plants, aerial hyphae formation or response to oxidative stress). While this may be interpreted as a contradiction, one must consider that the expression under the latter conditions under the native *hfb7* promoter is in the range of 10^2 – 10^3 -fold and – although a very strong constitutive promoter was used for overexpression – thus the induced expression significantly outnumbers (10–20-fold) that of the *OEhfb7* strains. Consequently, the constitutive expression is without consequences under conditions where the native *hfb7* is anyway induced, such as contact with other fungi or plants, and thus the *OEhfb7* strains show no distinctive phenotype. This may also explain why the *OEhfb7* phenotype is restricted to the early phase (0–40 h) of submerged growth when the native *hfb7* expression is either low or not induced.

Analysis of *hfb7* expression showed that its formation parallels the development of aerial hyphae, but not of conidia, and that it is rapidly induced by mechanical injury-provoked stress. The latter has been shown in *T. atroviride* to involve an oxidative stress response (Hernández-Oñate et al., 2012). If HFB7 has indeed a function in oxidative stress response, it may serve to protect the aerial hyphae against the consequences of presence of oxygen rather than rendering the hyphal cell wall more hydrophobic. Such an interpretation is supported by our data that the hydrophobicity of the vegetative hyphae of *T. virens* wild-type and *OEhfb7* strains is similar. A protection against oxygen stress by HFB7 is also in accordance with a recent demonstration of antioxidant activities of HFB2 (Khalesi et al., 2016). While the presence of the four disulfide bonds formed by the eight cysteine residues would theoretically make any hydrophobin a potential antioxidant, subjecting *T. atroviride* – that does not have *hfb7* – to mechanical injury does not cause the upregulation of any of its hydrophobins (Hernández-Oñate et al., 2012). In our analysis *hfb7* was upregulated 24 h after application of superoxide generating compound menadione and H_2O_2 . The response to the later oxidative stress provoking compounds was equal to the mechanical injury. We conclude from this that *T. atroviride* does not use any of its hydrophobins for combating oxidative stress. The upregulation of *hfb7* expression in *T. virens* may thus be a specific and new trait in these species. Interestingly, Friedl et al. (2008) reported the use of 1 mM menadione in experiments with *T. atroviride*, while in our work *T. virens* could tolerate (by showing poor growth) only 10-fold lower concentrations. At elevated concentrations the fungus died. Thus, compared to *T. atroviride*, *T. virens* appears to be more sensitive to oxidative stress what is in line with reduced growth at illumination recorded for *T. virens* Gv 29-8 and several other strains of the species (I. Druzhinina, unpublished).

Upregulation of *hfb7* during contact with other fungi or plants may also be a direct consequence of oxidative stress: the release

of reactive oxygen species (ROS) is a common reaction of organisms when confronted with a potential pathogen or competitor, and even occurs in mutualistic interactions like mycorrhizae (Torres, 2010; Kim, 2014; Lehmann et al., 2015). It has also been directly demonstrated for *Fusarium* sp. and tomato plants (Zhang et al., 2012; Li et al., 2015), and *T. virens* is particularly rich in genes encoding FAD-linked oxidases (Kubicek et al., 2011). In our experiments, *Trichoderma* may therefore be confronted to varying degrees with both host-derived reactive oxygen species (ROS) as well as ROS produced by its own cell metabolic process. The use of thiol groups, which due to their high pKa values in protein cysteine residues (8–9), make these amino acids ideal for maintaining cellular redox homeostasis by combatting small redox perturbation by forming reactive ionized thiolate groups (Spoel and Loake, 2011). The participation of hydrophobins, which by being extracellularly located could serve as a prime protectant before ROS enter the fungal cells, therefore needs further investigations.

The reason why HFB7 emerged and has then been functionally maintained only in the *Harzianum* and the *Virens* Clades of *Trichoderma* still remains enigmatic. In this regards, it is interesting to note that these species are very frequent endophytes of epigeal parts of green plants in particular in tropics (see for example Chaverri et al., 2015). Having a habitat in direct proximity to photosynthetic machinery may have forced the evolution towards additional defence mechanisms against ROS. Alternatively, both species clades contain the most opportunistic taxa, and it is possible that their environmental success is supported by the acquisition and maintenance of genes such as *hfb7*.

5. Conclusions

In this work, we describe a new phylogenetic clade of class II hydrophobins – the HFB7 – that is only present in some species of *Trichoderma*. Both the evolution as well as the expression pattern of *hfb7* show remarkable differences to other class II hydrophobins from fungi, thus rendering it an interesting subject for future research.

Acknowledgements

This work was supported by the Austrian Science Fund (FWF) P-25613 to ISD. This research has also been partially supported by the Austrian BMWFW, BMVIT, SFG, Standortagentur Tirol, Government of Lower Austria and ZIT through the Austrian FFG-COMET-Funding Program. We are thankful to Lea Atanasova for the help in laboratory work. The authors acknowledge the permission by Igor V. Grigoriev to use sequence data from yet unpublished *T. longibrachiatum*, *T. citrinoviride*, *T. harzianum* and *T. asperellum* genomes sequenced by the Joint Genome Institute of the US Department of Energy.

Appendix A. Supplementary material

Supplementary data associated with this article can be found, in the online version, at <http://dx.doi.org/10.1016/j.fgb.2017.01.002>.

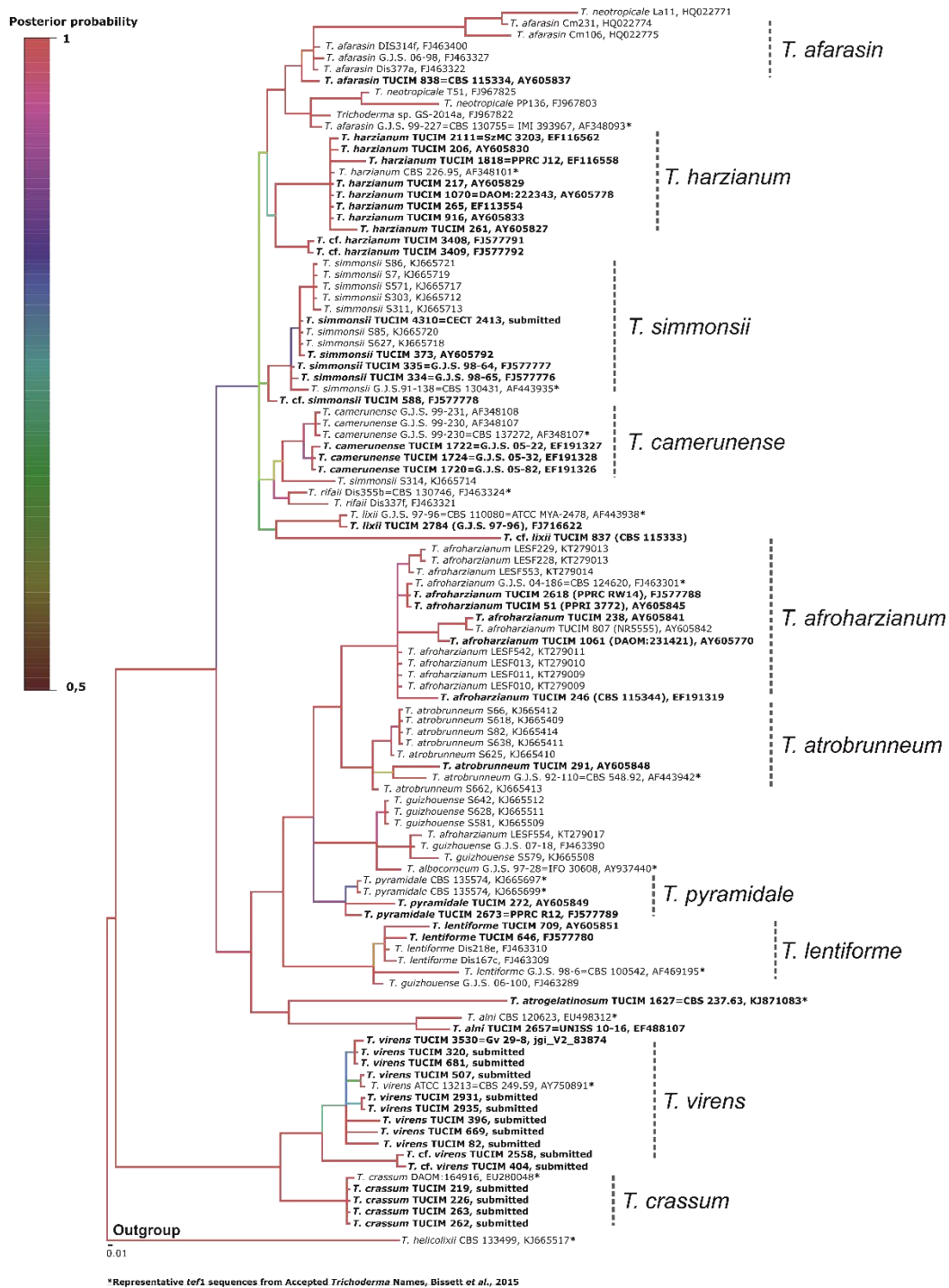
References

- Ashkenazy, H., Abadi, S., Martz, E., Chay, O., Mayrose, I., Pupko, T., Ben-Tal, N., 2016. ConSurf 2016: an improved methodology to estimate and visualize evolutionary conservation in macromolecules. *Nucl. Acids Res.* 44 (W1), W344–W350.
- Askolin, S., Penttilä, M., Wösten, H.A., Nakari-Setälä, T., 2005. The *Trichoderma reesei* hydrophobin genes *hfb1* and *hfb2* have diverse functions in fungal development. *FEMS Microbiol. Lett.* 253 (2), 281–288.

- Baroncelli, R., Piaggese, G., Fiorini, L., Bertolini, E., Zapparata, A., Pè, M.E., Sarrocco, S., Vannacci, G., 2015. Draft whole-genome sequence of the biocontrol agent *Trichoderma harzianum* T6776. *Genome Announc.* 3 (3), e00647-15.
- Baroncelli, R., Zapparata, A., Piaggese, G., Sarrocco, S., Vannacci, G., 2016. Draft whole-genome sequence of *Trichoderma gamsii* T6085, a promising biocontrol agent of fusarium head blight on wheat. *Genome Announc.* 4 (1), e01747-15.
- Basheva, E.S., Kralchevsky, P.A., Christov, N.C., Danov, K.D., Stoyanov, S.D., Blijdenstein, T.B., Kim, H.J., Pelan, E.G., Lips, A., 2011. Unique properties of bubbles and foam films stabilized by HFBII hydrophobin. *Langmuir* 27 (6), 2382–2392.
- Bimbo, L.M., Mäkilä, E., Raula, J., Laaksonen, T., Laaksonen, P., Strommer, K., Kauppinen, E.I., Salonen, J., Linder, M.B., Hirvonen, J., Santos, H.A., 2011. Functional hydrophobin-coating of thermally hydrocarbonized porous silicon microparticles. *Biomaterials* 32 (34), 9089–9099.
- Bissett, J., Gams, W., Jaklitsch, W.M., Samuels, G.J., 2015. Accepted *Trichoderma* names in the year 2015. *IMA Fungus* 6 (2), 263–295.
- Carpenter, C.E., Mueller, R.J., Kazmierczak, P., Zhang, L., Villalon, D.K., Van Alfen, N.K., 1992. Effect of a virus on accumulation of a tissue-specific cell-surface protein of the fungus *Cryphonectria (Endothia) parasitica*. *Mol. Plant-Microbe Interact.* 4, 55–61.
- Castresana, J., 2000. Selection of conserved blocks from multiple alignments for their use in phylogenetic analysis. *Mol. Biol. Evol.* 17 (4), 540–552.
- Chaverri, P., Branco-Rocha, F., Jaklitsch, W., Gazis, R., Degenkolb, T., Samuels, G.J., 2015. Systematics of the *Trichoderma harzianum* species complex and the re-identification of commercial biocontrol strains. *Mycologia* 107 (3), 558–590.
- Corvis, Y., Walcarius, A., Rink, R., Mrabet, N.T., Rogalska, E., 2005. Preparing catalytic surfaces for sensing applications by immobilizing enzymes via hydrophobin layers. *Anal. Chem.* 77 (6), 1622–1630.
- de Vries, O.M.H., Fekkes, M.P., Wosten, H.A.B., Wessels, J.G.H., 1993. Insoluble hydrophobin complexes in the walls of *Schizophyllum commune* and other filamentous fungi. *Arch. Microbiol.* 159, 330–335.
- Druzhinina, I.S., Kubicek, C.P., Komoń-Zelazowska, M., Mulaw, T.B., Bissett, J., 2010. The *Trichoderma harzianum* demon: complex speciation history resulting in coexistence of hypothetical biological species, recent agamospecies and numerous relict lineages. *BMC Evol. Biol.* 10, 94.
- Druzhinina, I.S., Seidl-Seiboth, V., Herrera-Estrella, A., Horwitz, B.A., Kenerley, C.M., Monte, E., Mukherjee, P.K., Zeilinger, S., Grigoriev, I.V., Kubicek, C.P., 2011. *Trichoderma*: the genomics of opportunistic success. *Nat. Rev. Microbiol.* 9 (10), 749–759.
- Edgar, R.C., 2004. MUSCLE: multiple sequence alignment with high accuracy and high throughput. *Nucl. Acids Res.* 32 (5), 1792–1797.
- Emanuelson, O., Brunak, S., von Heijne, G., Nielsen, H., 2008. Locating proteins in the cell using TargetP, SignalP and related tools. *Nat. Protoc.* 2 (4), 953–971.
- Espino-Rammer, L., Ribitsch, D., Przyłucka, A., Marold, A., Greimel, K.J., Herrero Acero, E., Guebitz, G.M., Kubicek, C.P., Druzhinina, I.S., 2013. Two novel class II Hydrophobins from *Trichoderma* spp. stimulate enzymatic hydrolysis of poly (ethylene terephthalate) when expressed as fusion proteins. *Appl. Environ. Microbiol.* 79 (14), 4230–4238.
- Fang, G., Tang, B., Liu, Z., Gou, J., Zhang, Y., Xu, H., Tang, X., 2014. Novel hydrophobin-coated doxorubicin nanoparticles for intravenous delivery: in vitro characteristics and in vivo performance. *Eur. J. Pharm. Sci.* 60, 1–9.
- Friedl, M.A., Schmolli, M., Kubicek, C.P., Druzhinina, I.S., 2008. Photostimulation of *Hypocrea atroviridis* growth occurs due to a cross-talk of carbon metabolism, blue light receptors and response to oxidative stress. *Microbiology* 154 (4), 1229–1241.
- Gasteiger, E., Hoogland, C., Gattiker, A., Duvaud, S., Wilkins, M.R., Appel, R.D., Bairoch, A., 2005. Protein identification and analysis tools on the ExPASy server. In: Walker, John M. (Ed.), *The Proteomics Protocols Handbook*. Humana Press, pp. 571–607.
- Hernández-Oñate, M.A., Esquivel-Naranjo, E.U., Mendoza-Mendoza, A., Stewart, A., Herrera-Estrella, A.H., 2012. An injury-response mechanism conserved across kingdoms determines entry of the fungus *Trichoderma atroviride* into development. *Proc. Natl. Acad. Sci. U.S.A.* 109 (37), 14918–14923.
- Huelsenbeck, J.P., Ronquist, F., 2001. MRBAYES: Bayesian inference of phylogenetic trees. *Bioinformatics* 17 (8), 754–755.
- Janssen, M.L., van Leeuwen, M.B., Scholtmeijer, K., van Kooten, T.G., Dijkhuizen, L., Wosten, H.A., 2002. Coating with genetic engineered hydrophobin promotes growth of fibroblasts on a hydrophobic solid. *Biomaterials* 23 (24), 4847–4854.
- Jensen, B.G., Andersen, M.R., Pedersen, M.H., Frisvad, J.C., Søndergaard, I., 2010. Hydrophobins from *Aspergillus* species cannot be clearly divided into two classes. *BMC Res. Notes* 23 (3), 344.
- Jorgensen, W.L., Chandrasekhar, J., Madura, J.D., Impey, R.W., Klein, M.L., 1983. Comparison of simple potential functions for simulating liquid water. *J. Chem. Phys.* 79, 926–935.
- Khalesi, M., Deckers, S.M., Gebruers, K., Vissers, L., Verachtert, H., Derdelinckx, G., 2012. Hydrophobins: exceptional proteins for many applications in brewery environment and other bio-industries. *Cerevisia* 37 (1), 3–9.
- Khalesi, M., Jahanbani, R., Riveros-Galan, D., Sheikh-Hassani, V., Sheikh-Zeinoddin, M., Sahibi, M., Winterburn, J., Derdelinckx, G., Moosavi-Movahedi, A.A., 2016. Antioxidant activity and ACE-inhibitory of Class II hydrophobin from wild strain *Trichoderma reesei*. *Int. J. Biol. Macromol.* 19 (91), 174–179.
- Kim, H.J., 2014. Exploitation of reactive oxygen species by fungi: roles in host-fungus interaction and fungal development. *J. Microbiol. Biotechnol.* 24 (11), 1455–1463.
- Kohlmeier, S., Smits, T.H., Ford, R.M., Keel, C., Harms, H., Wick, L.Y., 2005. Taking the fungal highway: mobilization of pollutant-degrading bacteria by fungi. *Environ. Sci. Technol.* 39 (12), 4640–4646.
- Koonin, E.V., Wolf, Y.I., 2010. Constraints and plasticity in genome and molecular-phenome evolution. *Nat. Rev. Genet.* 11, 487–498.
- Kubicek, C.P., Baker, S., Gamauf, C., Kenerley, C.M., Druzhinina, I.S., 2008. Purifying selection and birth-and-death evolution in the class II hydrophobin gene families of the ascomycete *Trichoderma/Hypocrea*. *BMC Evol. Biol.* 8, 4.
- Kubicek, C.P., Herrera-Estrella, A., Seidl-Seiboth, V., Martinez, D.A., Druzhinina, I.S., Thon, M., Zeilinger, S., Casas-Flores, S., Horwitz, B.A., Mukherjee, P.K., Mukherjee, M., Kredics, L., Alcaraz, L.D., Aerts, A., Antal, Z., Atanasova, L., Cervantes-Badillo, M.G., Challacombe, J., Chertkov, O., McCluskey, K., Culpier, F., Deshpande, N., von Döhren, H., Ebbole, D.J., Esquivel-Naranjo, E.U., Fekete, E., Flippin, M., Glaser, F., Gómez-Rodríguez, E.Y., Gruber, S., Han, C., Henrissat, B., Hermosa, R., Hernández-Oñate, M., Karaffá, L., Kosti, I., Le Crom, S., Lindquist, E., Lucas, S., Lübeck, M., Lübeck, P.S., Margeot, A., Metz, B., Misra, M., Nevalainen, H., Omann, M., Packer, N., Perrone, G., Uresti-Rivera, E.E., Salamov, A., Schmolli, M., Seiboth, B., Shapiro, H., Sukno, S., Tamayo-Ramos, J.A., Tisch, D., West, A., Wilkinson, H.H., Zhang, M., Coutinho, P.M., Kenerley, C.M., Monte, E., Baker, S.E., Grigoriev, I.V., 2011. Comparative genome sequence analysis underscores mycoparasitism as the ancestral life style of *Trichoderma*. *Genome Biol.* 12 (4), R40.
- Lalitha, S., 2004. Primer Premier 5. Biotech Software & Internet Report 1 (6), 270–272.
- Larsson, A., 2014. AliView: a fast and lightweight alignment viewer and editor for large datasets. *Bioinformatics* 30 (22), 3276–3278.
- Lehmann, S., Serrano, M., L'Haridon, F., Tjamos, S.E., Mtraux, J.P., 2015. Reactive oxygen species and plant resistance to fungal pathogens. *Phytochemistry* 112, 54–62.
- Li, T., Fan, K., Wang, J., Wang, W., 2003. Reduction of protein sequence complexity by residue grouping. *Protein Eng.* 16, 323–330.
- Li, X., Zhang, H., Tian, L., Huang, L., Liu, S., Li, D., Song, F., 2015. Tomato SlRbohB, a member of the NADPH oxidase family, is required for disease resistance against *Botrytis cinerea* and tolerance to drought stress. *Front. Plant Sci.* 23 (6), 463.
- Librado, P., Rozas, J., 2009. DnaSP v5: a software for comprehensive analysis of DNA polymorphism data. *Bioinformatics* 25 (11), 1451–1452.
- Linder, M.B., Szilvay, G.R., Nakari-Setälä, T., Penttilä, M.E., 2005. Hydrophobins: the protein-amphiphiles of filamentous fungi. *FEMS Microbiol. Rev.* 29 (5), 877–896.
- Livak, K.J., Schmittgen, T.D., 2001. Analysis of relative gene expression data using real-time quantitative PCR and the 2^{-Delta Delta C(T)} Method. *Methods* 25 (4), 402–408.
- Lugones, L.G., Wosten, H.A.B., Birkenkamp, K.U., Sjölema, K.A., Zagers, J., Wessels, J.G.H., 1999. Hydrophobins line air channels in fruiting bodies of *Schizophyllum commune* and *Agaricus bisporus*. *Mycol. Res.* 103, 635–640.
- Mackereel, A.D., Bashford, D., Bellotti, M., Dunbrack, R.L., Evansck, J.D., Field, M.J., Fischer, S., Gao, J., Guo, H., Ha, S., Joseph-McCarthy, D., Kuchnir, L., Kuczerka, K., Lau, F.T., Mattos, C., Michnick, S., Ngo, T., Nguyen, D.T., Prodhom, B., Reiher, W.E., Roux, B., Schenkrich, M., Smith, J.C., Stote, R., Straub, J., Watanabe, M., Wiórkiewicz-Kuczera, J., Yin, D., Karplus, M., 1998. All-atom empirical potential for molecular modeling and dynamics studies of proteins. *J. Phys. Chem. B* 102 (18), 3586–3616.
- Martinez, D., Berka, R.M., Henrissat, B., Saloheimo, M., Arvas, M., Baker, S.E., Chapman, J., Chertkov, O., Coutinho, P.M., Cullen, D., Danchin, E.G., Grigoriev, I.V., Harris, P., Jackson, M., Kubicek, C.P., Han, C.S., Ho, I., Larrondo, L.F., de Leon, A.L., Magnuson, J.K., Merino, S., Misra, M., Nelson, B., Putnam, N., Robbertse, B., Salamov, A.A., Schmolli, M., Terry, A., Thayer, N., Westerholm-Parvinen, A., Schoch, C.L., Yao, J., Barabote, R., Nelson, M.A., Detter, C., Bruce, D., Kuske, C.R., Xie, G., Richardson, P., Rokhsar, D.S., Lucas, S.M., Rubin, E.M., Dunn-Coleman, N., Ward, M., Brettin, T.S., 2008. Genome sequencing and analysis of the biomass-degrading fungus *Trichoderma reesei* (syn. *Hypocrea jecorina*). *Nat. Biotechnol.* 26 (5), 553–560.
- Muñoz, G., Nakari-Setälä, T., Agosin, E., Penttilä, M., 1997. Hydrophobin gene *shr1*, expressed during sporulation of the biocontrol agent *Trichoderma harzianum*. *Curr. Genet.* 32 (3), 225–230.
- Murphy, L.R., Wallqvist, A., Levy, R.M., 2000. Simplified amino acid alphabets for protein fold recognition and implications for folding. *Protein Eng.* 13, 149–152.
- Nakari-Setälä, T., Penttilä, M., 1995. Production of *Trichoderma reesei* cellulases on glucose-containing media. *Appl. Environ. Microbiol.* 61 (10), 3650–3655.
- Nakari-Setälä, T., Aro, N., Ilmén, M., Muñoz, G., Kalkkinen, N., Penttilä, M., 1997. Differential expression of the vegetative and spore-bound hydrophobins of *Trichoderma reesei*-cloning and characterization of the *hfb2* gene. *Eur. J. Biochem.* 248 (2), 415–423.
- Nei, M., Rooney, A.P., 2005. Concerted and birth-and-death evolution of multigene families. *Annu. Rev. Genet.* 39, 121–152.
- Penttilä, M., Nevalainen, H., Rättö, M., Salminen, E., Knowles, J., 1987. A versatile transformation system for the cellulolytic filamentous fungus *Trichoderma reesei*. *Gene* 61 (2), 155–164.
- Peters, R., Sandiford, L., Owen, D.M., Kemal, E., Bourke, S., Dailey, L.A., Green, M., 2016. Red-emitting protein-coated conjugated polymer nanoparticles. *Photochem. Photobiol. Sci.* 15 (11), 1448–1452.
- Phillips, J.C., Braun, R., Wang, W., Gumbart, J., Tajkhorshid, E., Villa, E., Chipot, C., Skeel, R.D., Kalé, L., Schulten, K., 2005. Scalable molecular dynamics with NAMD. *J. Comput. Chem.* 26 (16), 1781–1802.
- Pócsi, I., Miskei, M., Karányi, Z., Emri, T., Ayoubi, P., Pusztahelyi, T., Balla, G., Prade, R. A., 2005. Comparison of gene expression signatures of diamide, H2O2 and menadione exposed *Aspergillus nidulans* cultures—linking genome-wide transcriptional changes to cellular physiology. *BMC Genomics* 6, 182.

- Ribitsch, D., Herrero Acero, E., Przylucka, A., Zitzenbacher, S., Marold, A., Gamerith, C., Tscheliebnig, R., Jungbauer, A., Rennerhofer, H., Lichtenegger, H., Amenitsch, H., Bonazza, K., Kubicek, C.P., Druzhinina, I.S., Guebitz, G.M., 2015. Enhanced cutinase-catalyzed hydrolysis of polyethylene terephthalate by covalent fusion to hydrophobins. *Appl. Environ. Microbiol.* 81 (11), 3586–3592.
- Ruocco, M., Lanzuise, S., Lombardi, N., Woo, S.L., Vinale, F., Marra, R., Varlese, R., Manganiello, G., Pascale, A., Scala, V., Turrà, D., Scala, F., Lorito, M., 2015. Multiple roles and effects of a novel *Trichoderma* hydrophobin. *Mol. Plant Microbe Interact* 28 (2), 167–179.
- Sali, A., Blundell, T.L., 1993. Comparative protein modelling by satisfaction of spatial restraints. *J. Mol. Biol.* 234 (3), 779–815.
- Saupe, S.J., 2000. Molecular genetics of heterokaryon incompatibility in filamentous ascomycetes. *Microbiol. Mol. Biol. Rev.* 64 (3), 489–502.
- Sayle, R.A., Milner-White, E.J., 1995. RASMOL: biomolecular graphics for all. *Trends Biochem. Sci.* 20 (9), 374.
- Seidl-Seiboth, V., Gruber, S., Sezerman, U., Schwecke, T., Albayrak, A., Neuhof, T., von Döhren, H., Baker, S.E., Kubicek, C.P., 2011. Novel hydrophobins from *Trichoderma* define a new hydrophobin subclass: protein properties, evolution, regulation and processing. *J. Mol. Evol.* 72 (4), 339–351.
- Schwarz, R., Dayhoff, M., 1979. Matrices for detecting distant relationships. In: Dayhoff, M. (Ed.), *Atlas of Protein Sequences*. National Biomedical Research Foundation, pp. 353–358.
- Spoel, S.H., Loake, G.J., 2011. Redox-based protein modifications: the missing link in plant immune signalling. *Curr. Opin. Plant Biol.* 14, 358–364.
- Stalder, A.F., Kulik, G., Sage, D., Barbieri, L., Hoffmann, P., 2006. A snake-based approach to accurate determination of both contact points and contact angles. *Colloids Surf., A* 286 (1–3), 92–103.
- Sunde, M., Kwan, A.H., Templeton, M.D., Beever, R.E., Mackay, J.P., 2008. Structural analysis of hydrophobins. *Micron* 39 (7), 773–784.
- Takatsuki, Y., Yamasaki, R., Iwanaga, A., Lienemann, M., Linder, M.B., Haruyama, T., 2013. Solid-support immobilization of a “swing” fusion protein for enhanced glucose oxidase catalytic activity. *Colloid. Surf. ace B* 112, 186–191.
- Talavera, G., Castresana, J., 2007. Improvement of phylogenies after removing divergent and ambiguously aligned blocks from protein sequence alignments. *Syst. Biol.* 56 (4), 564–577.
- Tamura, K., Peterson, D., Peterson, N., Stecher, G., Nei, M., Kumar, S., 2011. MEGA5: molecular evolutionary genetics analysis using maximum likelihood, evolutionary distance, and maximum parsimony methods. *Mol. Biol. Evol.* 28 (10), 2731–2739.
- Tajima, F., 1989. Statistical method for testing the neutral mutation hypothesis by DNA polymorphism. *Genetics* 123 (3), 585–595.
- Torres, M.A., 2010. ROS in biotic interactions. *Physiol. Plant* 138 (4), 414–429.
- Uzbas, F., Sezerman, U., Hartl, L., Kubicek, C.P., Seiboth, B., 2012. A homologous production system for *Trichoderma reesei* secreted proteins in a cellulase-free background. *Appl. Microbiol. Biotechnol.* 93 (4), 1601–1608.
- Valo, H.K., Laaksonen, P.H., Peltonen, L.J., Linder, M.B., Hirvonen, J.T., Laaksonen, T.J., 2010. Multifunctional hydrophobin: toward functional coatings for drug nanoparticles. *ACS Nano* 4 (3), 1750–1758.
- Von Vacano, B., Xu, R., Hirth, S., Herzenstiel, I., Rückel, M., Subkowski, T., Baus, U., 2011. Hydrophobin can prevent secondary protein adsorption on hydrophobic substrates without exchange. *Anal. Bioanal. Chem.* 400 (7), 2031–2040.
- Wessels, J., De Vries, O., Asgeersdottir, S., Schuren, F., 1991. Hydrophobin genes involved in formation of aerial hyphae and fruit bodies in *Schizophyllum*. *Plant Cell* 3 (8), 793–799.
- Wösten, H.A., Schuren, F.H., Wessels, J.G., 1994. Interfacial self-assembly of a hydrophobin into an amphipathic protein membrane mediates fungal attachment to hydrophobic surfaces. *EMBO J.* 13 (24), 5848–5854.
- Wösten, H.A., de Vocht, M.L., 2000. Hydrophobins, the fungal coat unraveled. *Biochim. Biophys. Acta* 1469 (2), 79–86.
- Wösten, H.A., 2001. Hydrophobins: multipurpose proteins. *Annu. Rev. Microbiol.* 55, 625–646.
- Yang, D., Pomraning, K., Kopchinskiy, A., Karimi Aghcheh, R., Atanasova, L., Chenthamara, K., Baker, S.E., Zhang, R., Shen, Q., Freitag, M., Kubicek, C.P., Druzhinina, I.S., 2015. Genome sequence and annotation of *Trichoderma parareesei*, the ancestor of the cellulase producer *Trichoderma reesei*. *Genome Announc.* 3 (4).
- Zhang, X.W., Jia, L.J., Zhang, Y., Jiang, G., Li, X., Zhang, D., Tang, W.H., 2012. In planta stage-specific fungal gene profiling elucidates the molecular strategies of *Fusarium graminearum* growing inside wheat coleoptiles. *Plant Cell* 24, 5159–5176.
- Zhang, J., Bayram Akcapinar, G., Atanasova, L., Rahimi, M.J., Przylucka, A., Yang, D., Kubicek, C.P., Zhang, R., Shen, Q., Druzhinina, I.S., 2016. The neutral metalloproteinase NMP1 of *Trichoderma guizhouense* is required for mycotrophy and self-defence. *Environ. Microbiol.* 18 (2), 580–597.
- Zhao, L., Xu, H., Li, Y., Song, D., Wang, X., Qiao, M., Gong, M., 2016. Novel application of hydrophobin in medical science: a drug carrier for improving serum stability. *Sci. Rep.* 6, 26461.
- <http://www.vt.tuwien.ac.at>.
- http://www.biophp.org/miniTools/reduce_protein_alphabet/.
- <http://tree.bio.ed.ac.uk/software/figtree/>.
- <http://consurf.tau.ac.il>.

Supplementary Figure S1



*Representative *tef1* sequences from Accepted *Trichoderma* Names, Bissett et al., 2015

Supplementary Figure 1. Bayesian phylogram based on *tef1* sequences for taxonomic and strain specific identification. The color of branches corresponds to their respective posterior probabilities. Strains used in our study are shown in bold.

Diverse Plant-Associated Pleosporalean Fungi from Saline Areas: Ecological Tolerance and Nitrogen-Status Dependent Effects on Plant Growth²⁰

Authors

Yuan Qin¹, Xueyu Pan¹, Christian Kubicek², Irina Druzhinina², **Komal Chenthamara²**, Jessy Labbé³ and Zhilin Yuan¹

Affiliation

1. Institute of Subtropical Forestry, Chinese Academy of Forestry, Hangzhou, China
2. Microbiology and Applied Genomics group, Research Area Biochemical Technology, Institute of Chemical, Environmental & Bioscience Engineering, TU Wien, Gumpendorferstrasse 1a
3. Biosciences Division, Oak Ridge National Laboratory, Oak Ridge, TN, USA

Contribution by the PhD candidate

Identification and Molecular Phylogenetic Appraisal of Plant-Associated Pleosporalean Fungi (Figure 2 and Supplementary Figure S1).

²⁰ Qin Y, Pan X, Kubicek C, Druzhinina I, **Chenthamara K**, Labbé JL, Yuan Z. Diverse plant-associated pleosporalean fungi from saline areas: ecological tolerance and nitrogen-status dependent effects on plant growth. *Frontiers in microbiology*. 2017 Feb 6;8:158.



Diverse Plant-Associated Pleosporalean Fungi from Saline Areas: Ecological Tolerance and Nitrogen-Status Dependent Effects on Plant Growth

Yuan Qin¹, Xueyu Pan¹, Christian Kubicek², Irina Druzhinina², Komal Chenthamara², Jessy Labbé³ and Zhilin Yuan^{1*}

¹ Institute of Subtropical Forestry, Chinese Academy of Forestry, Hangzhou, China, ² Research Area Biochemical Technology, Institute of Chemical Engineering, TU Wien, Vienna, Austria, ³ Biosciences Division, Oak Ridge National Laboratory, Oak Ridge, TN, USA

OPEN ACCESS

Edited by:

Cergele Masso,
International Institute of Tropical
Agriculture, Kenya

Reviewed by:

Gwen-Aëlle Grelet,
Landcare Research, New Zealand
Jayanta Kumar Patra,
Dongguk University, South Korea

*Correspondence:

Zhilin Yuan
yuanzi@caf.ac.cn

Specialty section:

This article was submitted to
Plant-Microbe Interactions,
a section of the journal
Frontiers in Microbiology

Received: 09 November 2016

Accepted: 20 January 2017

Published: 06 February 2017

Citation:

Qin Y, Pan X, Kubicek C,
Druzhinina I, Chenthamara K,
Labbé J and Yuan Z (2017) Diverse
Plant-Associated Pleosporalean Fungi
from Saline Areas: Ecological
Tolerance and Nitrogen-Status
Dependent Effects on Plant Growth.
Front. Microbiol. 8:158.
doi: 10.3389/fmicb.2017.00158

Similar to mycorrhizal mutualists, the rhizospheric and endophytic fungi are also considered to act as active regulators of host fitness (e.g., nutrition and stress tolerance). Despite considerable work in selected model systems, it is generally poorly understood how plant-associated fungi are structured in habitats with extreme conditions and to what extent they contribute to improved plant performance. Here, we investigate the community composition of root and seed-associated fungi from six halophytes growing in saline areas of China, and found that the pleosporalean taxa (Ascomycota) were most frequently isolated across samples. A total of twenty-seven representative isolates were selected for construction of the phylogeny based on the multi-locus data (partial 18S rDNA, 28S rDNA, and transcription elongation factor 1- α), which classified them into seven families, one clade potentially representing a novel lineage. Fungal isolates were subjected to growth response assays by imposing temperature, pH, ionic and osmotic conditions. The fungi had a wide pH tolerance, while most isolates showed a variable degree of sensitivity to increasing concentration of either salt or sorbitol. Subsequent plant-fungal co-culture assays indicated that most isolates had only neutral or even adverse effects on plant growth in the presence of inorganic nitrogen. Interestingly, when provided with organic nitrogen sources the majority of the isolates enhanced plant growth especially aboveground biomass. Most of the fungi preferred organic nitrogen over its inorganic counterpart, suggesting that these fungi can readily mineralize organic nitrogen into inorganic nitrogen. Microscopy revealed that several isolates can successfully colonize roots and form melanized hyphae and/or microsclerotia-like structures within cortical cells suggesting a phylogenetic assignment as dark septate endophytes. This work provides a better understanding of the symbiotic relationship between plants and pleosporalean fungi, and initial evidence for the use of this fungal group in benefiting plant production.

Keywords: Pleosporales, dark septate endophytes, halophytes, organic nitrogen, symbiosis

INTRODUCTION

As intimate partners of plants, many groups of fungi can establish associations with roots and seeds and thereby facilitate plant growth and increase stress tolerance (Ernst et al., 2003; Rodriguez et al., 2009; de Zelicourt et al., 2013). Plant-associated microbiota comprise taxonomically diverse members, mainly including arbuscular mycorrhizal fungi (AMF), ectomycorrhizal fungi (EMF) and a number of ascomyceteous and non-mycorrhizal basidiomycetous fungi (NMF) (Gardes and Dahlberg, 1996; Khidir et al., 2010; Zuccaro et al., 2014). Mycorrhizal symbioses have been extensively described due to their important role in improving plant nutrition and stress tolerance (Evelin et al., 2009). Despite accumulating evidence that plant roots can host many more non-mycorrhizal endophytes than previous thought (Vandenkoornhuys et al., 2002; Porras-Alfaro et al., 2008; Toju et al., 2013), the ecological significance of NMF plant associations are poorly understood.

Plant fungal endophytes have been categorized into four groups on the basis of a series of criteria including host colonization pattern, transmission model (vertical transmission via host seeds and horizontal transmission via soil- or airborne spores) and fitness benefits (Rodriguez et al., 2009). Notably, class 2 fungal endophytes can establish habitat-adapted symbiosis and confer specific stress tolerance to the host plant in different extreme habitats (Rodriguez et al., 2008; Redman et al., 2011). Similarly, dark septate endophytes (DSEs) are considered to be class 4 endophytes and form melanized hyphae and microsclerotia-like structures in roots (Knapp et al., 2015; Yuan et al., 2016). DSEs are the dominant root-associated fungi and more frequent than AMFs from plants grown in extreme environments (e.g., salinity and drought) (Porras-Alfaro et al., 2008; Newsham et al., 2009). Some root opportunistic and rhizospheric fungi can also induce systemic resistance against crop diseases (Shoresh et al., 2010; Druzhinina et al., 2011; Jogaiah et al., 2013) and improve abiotic stress tolerance (McLellan et al., 2007). These findings underscore the importance of NMF in mediating plant productivity. However, it is generally poorly understood how plant-associated fungi are structured in extreme conditions, and if so, to what extent they contribute to improving plant performance.

The Pleosporales order is considered to be among the largest class within the class Dothideomycetes (Ascomycota) (Phookamsak et al., 2014; Tibpromma et al., 2015). Some genera of this order comprise ecologically important plant endophytes, including numerous DSEs (Hamayun et al., 2009; Knapp et al., 2015). Knapp et al. (2012) demonstrated that pleosporalean fungi occurred in all plant species in semi-arid grasslands of North America. Furthermore, microscopic analysis of the grass *Bouteloua gracilis* revealed that the fungal community of roots was dominated by a novel DSE belonging to Pleosporales (Porras-Alfaro et al., 2008). Large-scale culture-based surveys show that some fungal genera of the Pleosporales are common endophytes in both coastal and inland arid soils (Kageyama et al., 2008; Maciá-Vicente et al., 2008). Consequently, we surmise that pleosporalean fungi are generalist endophytes common within adverse environments. However, their basic physiological

characters and potential ecological significance has received only very limited attention.

In this work, a wide range of pleosporalean fungi were isolated from the rhizosphere, roots and seeds of halophytic plants in China. We then determined their phylogeny, sensitivity to diverse environmental stresses, and their ability to utilize various substrates of nitrogen. Further, we investigated their effects on plant growth in the presence of organic and inorganic nitrogen.

MATERIALS AND METHODS

Study Site and Sampling

A total of six halophytes were collected at three sampling sites in China. In August 2011, the healthy roots of *Phragmites australis* (family Poaceae) were collected at the inland saline and arid soil of Changji, XinJiang Province (N 44°29', E 87°93'), northwest of China. In July of 2014, roots and rhizosphere soils of *Suaeda salsa* were collected from the coastal region at the mouth of the Yellow River in DongYing, ShanDong Province (N 37°23', E 118°55'). Furthermore, the rhizosphere soil, intact roots of *S. salsa* (family Amaranthaceae), *P. australis*, *Calystegia soldanella* (family Convolvulaceae), *Carex scabrifolia* (family Cyperaceae), *Kochia scoparia* (family Amaranthaceae) and *Messerschmidia sibirica* (family Boraginaceae) were collected from a saline coastal sandy soil in QingDao, ShanDong Province (N 35°51', E 120°02') in 2015. The plant species selected are considered to be good bio-indicators of saline environments. A map of collection sites and photos of plant samples was provided in Figure 1.

Isolation of Endophytic and Rhizospheric Fungi from Six Halophytes

Fungi associated with rhizosphere soils (within a 1-mm vicinity of the roots) were isolated using the traditional serial dilution technique (Jogaiah et al., 2013). For collecting the soil samples, roots with adhering soil were mixed with 40 ml sterile phosphate buffer solution (100 mM PBS, pH = 7.2) in 50-ml tubes (BD Falcon). Tubes were vortexed at high speed for 5 min using a Vortex Genie 2 (Mo Bio Laboratories Inc., USA), allowing the release of most of the rhizosphere soils. The root samples were removed and soil suspensions were centrifuged for 15 min at 10°C at 6000 g to pellet the rhizosphere soils. Then, 1 g of each soil sample was re-suspended in 99 ml PBS and 10-fold serial dilution was made from the suspension (10^{-3} to 10^{-5}). Dilution of 10^{-4} and 10^{-5} were used to isolate fungi. 100 μ l of each diluted suspension was spread evenly onto Czapek's agar plates supplemented with 0.05 g/L streptomycin sulfate and 0.02 g/L tetracycline hydrochloride to eliminate bacterial contamination. The composition of the medium was as follows: sucrose 30 g, NaNO₃ 2.0 g, K₂HPO₄ 1.0 g, MgSO₄·7H₂O 0.5g, KCl 0.5 g, FeSO₄·H₂O 0.01g, agar 20 g and 1 liter of distilled water, pH 5.6. All plates were incubated at 25°C in darkness for at least 1 week until colonies appeared. Colonies were picked up and transferred to fresh potato dextrose agar (PDA) plates for purification.

For isolating fungal endophytes, roots and seeds (excised from the utricles) were heavily surface sterilized by immersion in ethanol (75%, v/v) for 30 s, and then soaked in 2.0% NaClO (v/v)

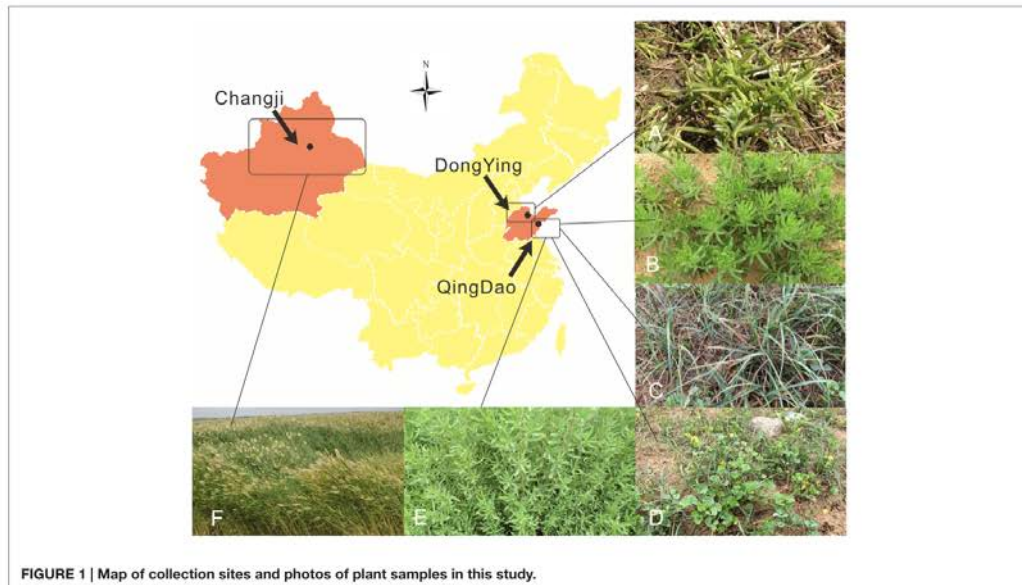


FIGURE 1 | Map of collection sites and photos of plant samples in this study.

for 5–10 min depending on the type of tissues, followed by 90% ethanol (v/v) for 30 s to remove the residual NaClO. Finally, sterilized distilled water was used to rinse the samples at least five times. The roots were dried with sterile filter paper, cut into 3–5 mm segments (for seeds cut into two halves), and placed on 2% malt extract agar (MEA, Oxoid) plates supplemented with antibiotics as mentioned above. Totally, 70 seed segments from *S. salsa* and approximately 160 root segments from each plant species were used for isolation. The plates were incubated for 2 weeks at 20°C in the dark, after which emerging hyphae developed from the tissue fragments were transferred to PDA for purification.

DNA Extraction, PCR Amplification and Sequencing

The mycelia were scraped from the PDA plates and transferred to a sterile 1.5 ml microcentrifuge tube. Fungal DNA was extracted using DNeasy Plant Mini Kit (Qiagen) according to the manufacturer's protocol. Four primer pairs, ITS1F and ITS4 (White et al., 1990), NS1 and NS4 (White et al., 1990), LR0R and LR5 (Vilgalys and Hester, 1990) as well as EF1-983F and EF1-2218R (Rehner and Buckley, 2005) were used for the amplification of internal transcribed spacer (ITS) of the rDNA cluster, partial 18S rRNA (small subunit, SSU) and 28S rRNA (large subunit, LSU), and partial transcription elongation factor 1- α (*tef1*) gene, respectively. The final volume of the PCR reaction was 50 μ l which contained 2 μ l template DNA (20–50 ng), 0.5 μ l of each forward and reverse primer (50 μ M), 25 μ l 2x Taq MasterMix (Cwbio, Beijing), and 22 μ l sterile deionized water.

The PCR reaction consisted of the following steps: a pre-denaturation at 94°C for 4 min, followed by 35 cycles of denaturation at 94°C for 40 s, annealing at 55°C for 50 s and elongation at 72°C for 1 min (2 min for LSU and SSU), and final extension at 72°C for 10 min. For *tef1* amplification, we used a touchdown PCR cycle that started with an annealing temperature of 66°C in the first cycle, reducing by 1°C in each successive cycle over the next nine cycles until it reached 56°C, which was used in the remaining 30 cycles. All purified PCR products were sent to Shanghai Sangon Biological Engineering Technology and Services Co., Ltd (Shanghai, China) and sequenced with the above primer pairs. All sequences from this study have been deposited in the GenBank database under the accession numbers presented in Table 1. ITS sequences were subjected to BLASTn searches¹ for initial identification.

Molecular Phylogeny of the Plant-Associated Pleosporealean Fungi

Preliminary ITS sequence-based identification supports the existence of a wide range of pleosporealean taxa. Thus, we aim to infer their phylogeny using three loci (SSU, LSU, and *tef1*), which have been used to give sufficient phylogenetic resolution within the Pleosporales (Tanaka et al., 2015), to provide insights into the relationships between our isolates and known pleosporealean fungi. To construct the phylogenetic tree, we retrieved the corresponding gene sequences from recently published papers focusing on the molecular phylogeny of the Pleosporales (Lumbsch and Lindemuth, 2001; de Gruyter et al., 2006, 2010;

¹<https://blast.ncbi.nlm.nih.gov/Blast.cgi>

TABLE 1 | The list of pleiosporalean isolates obtained in this study and their corresponding GenBank accession numbers of different loci (ITS, LSU, SSU, and *terf1*).

Isolate no.	Identity	Host	Isolation source	Collected site	GenBank accession no.			
					ITS	LSU	SSU	<i>terf1</i>
CYTC-R-5	Phaeosphaeriaceae sp.	Carex scabrifolia	Root	QingDao	KU991882	KU991906	KX694737	KX694764
DF-R-1	Phaeosphaeriaceae sp.	Kochia scoparia	Root	QingDao	KU991883	KU991907	KX694738	KX694765
DF-R-3	Phaeosphaeriaceae sp.	Kochia scoparia	Root	QingDao	KU991884	KU991908	KX694739	KX694766
DF-R-7	Phaeosphaeriaceae sp.	Kochia scoparia	Root	QingDao	KU991885	KU991909	KX694740	KX694767
DF-R-9	Didymosphaeriaceae sp.	Kochia scoparia	Root	QingDao	KU991886	KU991910	KX694741	KX694768
DW-R-1	Phaeosphaeriaceae sp.	Calystegia soldanella	Root	QingDao	KU991887	KU991911	KX694742	KX694769
DW-R-3	Saccaricida sp.	Calystegia soldanella	Root	QingDao	KU991888	KU991912	KX694743	KX694770
DW-R-4	Paraconiothyrium sp.	Calystegia soldanella	Root	QingDao	KU991889	KU991913	KX694744	KX694771
JP-R-2	Alternaria sp.	Suaeda salsa	Root	QingDao	KU991890	KU991914	KX694745	KX694772
JP-R-4	Phaeosphaeriaceae sp.	Suaeda salsa	Root	QingDao	KU991891	KU991915	KX694746	KX694773
JP-R-44	Didymosphaeriaceae sp.	Suaeda salsa	Root	DongYing	KJ125522	KJ125523	KX694748	KX694775
JP-R-6	Didymosphaeriaceae sp.	Suaeda salsa	Root	QingDao	KU991892	KU991916	KX694747	KX694774
LW-7	Lentitheciaceae sp.	Phragmites australis	Root	XinJiang	KU991893	KU991917	KX694749	KX694776
LW-R-2	Epicoicum sp.	Phragmites australis	Root	QingDao	KU991894	KU991918	KX694750	KX694777
LW-R-3	Paraconiothyrium sp.	Phragmites australis	Root	QingDao	KU991895	KU991919	KX694751	KX694778
R(2015)-25	Curvularia sp.	Suaeda salsa	Root	DongYing	KU991898	KU991922	KX694754	KX694780
R(2015)-29	Alternaria sp.	Suaeda salsa	Root	DongYing	KU991899	KU991923	KX694755	KX694781
R(2015)-4	Alternaria sp.	Suaeda salsa	Root	DongYing	KU991897	KU991921	KX694753	KX694782
R20	Phaeosphaeropsis sp.	Suaeda salsa	Root	DongYing	KU991896	KU991920	KX694752	KX694779
RS1-8	Alternaria sp.	Suaeda salsa	Rhizosphere	DongYing	KU991900	KU991924	KX694756	KX694783
RS-A-34	Phaeosphaeriaceae sp.	Suaeda salsa	Rhizosphere	DongYing	KU991901	KU991925	KX694757	KX694784
RS-A-88	Phaeosphaeriaceae sp.	Suaeda salsa	Rhizosphere	DongYing	KU991902	KU991926	KX694758	KX694785
RS-C-28	Phaeosphaeriaceae sp.	Suaeda salsa	Rhizosphere	DongYing	KU991903	KU991927	KX694759	KX694786
RS-JP-2	Phaeosphaeriaceae sp.	Suaeda salsa	Rhizosphere	QingDao	KU991904	KU991928	KX694760	KX694787
seed1	Preussia sp.	Suaeda salsa	Seed	DongYing	KU869522	KU991929	KX694761	KX694788
seed6	Phaeosphaeriaceae sp.	Suaeda salsa	Seed	DongYing	KU869527	KU991930	KX694762	KX694789
SYC-R-4	Didymosphaeriaceae sp.	Messerschmidia sibirica	Root	QingDao	KU991905	KU991931	KX694763	KX694790

Ariyawansa et al., 2014; Phookamsak et al., 2014; Knapp et al., 2015; Phukhamsakda et al., 2015). A concatenated set of three genes from the strains listed in **Table 1** and Supplementary Table S1, was used to create an alignment using muscle v3.8.425 (Edgar, 2004) tool integrated in AliView (Larsson, 2014). The conserved concatenated alignment based on nucleotides containing 2604 characters was subjected to Bayesian analysis using program MrBayes v3.2.5 (Huelsenbeck and Ronquist, 2001). The chain was run for 5 million generations by applying Generalized time reversible substitution model (Waddell and Steel, 1997). Two simultaneous, completely independent analyses starting from different random trees were run, using three heated chains and one “cold” chain. Once the analysis was finished, 37500 trees were summarized after discarding the first 25% of obtained 50,000 trees, and a consensus tree was obtained. Branch color corresponding to the posterior probability percentage of each clade was generated using FigTree v1.4.2². Further image improvement was performed in CorelDraw Graphics Suite X8.

Fungal Growth Responses to Environmental Stresses

To explore the adaptability of the pleosporealean fungi to adverse environmental conditions, their growth rates under various conditions (temperatures, pH, salt and osmolyte concentrations) were examined. Colony diameter was used as parameter. Mycelial plugs (5.0 mm in diameter) cut from 7-day-old PDA colonies were transferred to fresh PDA plates.

To evaluate fungal growth responses to different levels of temperatures and pH, the inoculated PDA plates were incubated at 10, 15, 20, 25, 28, and 30°C in the dark for 7 days. Similarly, fungi were cultured on PDA with a wide range of pH gradients (ranging from 6 to 11). The pH values were measured with a Mettler Toledo pH meter. All plates were incubated at 25°C. The salt stress was induced by adding different concentrations of ionic osmolytes (NaCl and KCl), and the non-ionic osmotic stress was imposed by using sorbitol. First, the PDA medium was supplemented with salt (KCl and NaCl) at concentrations of 2, 4, 6, 8, 10, and 12% (w/v), respectively. In parallel, PDA medium with non-ionic osmotic treatment was prepared using sorbitol (0.2–2.0 M) (Nikolaou et al., 2009). All plates were incubated at 25°C. Three to five replicates were performed for each treatment. This experiment was terminated after 10 days. Colony diameters of these fungi were recorded. Values were means of replications and shown in Radar charts.

Nitrogen Utilization Pattern of Pure Fungal Cultures

We used the modified Melin and Norkrans (MMN) free of nitrogen as the basal medium, to determine the ability of the fungi to utilize different inorganic and organic forms of nitrogen (Midgley et al., 2004; Bizabani and Dames, 2016). The nitrogen-free MMN medium contained (L⁻¹): 5.0 g glucose, 0.30 g KH₂PO₄, 0.14 g MgSO₄·H₂O, 50 mg CaCl₂, 25 mg NaCl, 3 mg ZnSO₄, 12.5 mg ferric EDTA and 0.13 mg thiamine-HCl, pH 4.5

²<http://tree.bio.ed.ac.uk/software/figtree/>

prior to autoclaving. For all treatments, a final N concentration was adjusted to 50 mg L⁻¹. The inorganic N source, ammonium [0.25 g L⁻¹ (NH₄)₂HPO₄] and nitrate (0.36 g L⁻¹ KNO₃), were separately added into the basal medium. A mixture of acidic, neutral, and aromatic amino acid amino acids [glutamine (Glu), glycine (Gly), valine (Val), leucine (Leu), and phenylalanine (Phe)], as well as Bovine Serum Albumin (BSA, N content 16%), were chosen as the organic N source. The two solutions were filter-sterilized with 0.45 and 0.22 μm Millipore filters and added into the autoclaved nitrogen-free basal medium separately. Three mycelial plugs of every fungus (5.0 mm in diameter) were cut with a sterile cork-borer from the edge of actively growing colonies on PDA plates, and then inoculated into 50 ml of the liquid medium in 250 ml flasks. Three replicates were prepared for each treatment. All the cultures were incubated in the dark, at 26°C and shaking at 180 r/min. After 7 days, mycelia were collected by filtration through filter paper, and the growth of fungi was measured as dried mycelial biomass (mg).

Plant-Fungal Co-culture Assay under Organic and Inorganic Nitrogen Conditions

We established the plant–fungal co-culture system to investigate the effects of fungal inoculation on plant growth. We also ask if the nitrogen status in the plant growth substrate will influence the outcome of plant–fungal interactions. In this case, both organic nitrogen in the form of amino acids and inorganic nitrogen in the form of ammonium nitrate (NH₄NO₃) and potassium nitrate (KNO₃).

The gnotobiotic rice seedlings were generated using the following steps. The rice seeds (cultivar: zhongjiazao 17) were surface sterilized as mentioned above. Seeds were sown in Petri dishes (150 mm diameter) containing 1/5 Murashige and Skoog (MS) medium and incubated at 28 ± 1°C for 96 h. Thereafter, the germinated seeds without microbial contamination were transplanted into the sterile plastic container with 1/2 MS and placed on growth chamber with a photoperiod of 12 h of light/12 h darkness and temperature of 28 ± 1°C for 5 days (Rodriguez et al., 2008). Uniform sized seedlings were selected for inoculation.

To support the growth of these diverse pleosporealean fungi as well as maintain a moderate fungal growth rate, 2 g oatmeal. L⁻¹ (Difco) as the carbon source was added into the 1/5 Murashige and Skoog (MS medium) (Mahmoud and Narisawa, 2013). Inorganic N sources (KNO₃ and NH₄NO₃) were added to the basal medium before autoclaving (Finlay et al., 1992), while a mixture of five amino acids (Glu, Gly, Val, Leu, and Phe) was filter-sterilized with 0.22 μm Millipore filters and added to the autoclaved basal medium with a final concentration of 30 mg N.L⁻¹ (Usuki and Narisawa, 2007). A total of 70 ml medium was poured into a sterile glass tube (25 mm diameter, 250 mm height). One fresh mycelial plug (5 mm in diameter) cut from colony margins was placed mycelial side down in the center of each tube, and pure PDA plugs were used as control. Prior to seedling inoculation, fungi were cultured in the medium for 3–7 days.

The 8-days-old rice seedlings were transplanted to the tubes that were pre-inoculated with fungi (five seedlings per tube). Three–five replications of each treatment were set up. Tubes were double sealed with parafilm and arranged randomly and finally kept in the growth chamber at $28 \pm 1^\circ\text{C}$ with a photoperiod of 12 h of light/12 h darkness. After incubation for 15 days, fresh biomass, plant height, root length were measured. Statistical analysis was performed using GraphPad Prism v6.0 (GraphPad, San Diego, CA, USA). Statistically significant differences between treatment and control groups were analyzed using multiple *t*-tests comparison.

Microscopic Observation of Fungal Colonization Pattern in Roots

Trypan blue staining method was used to confirm whether the pleosporealean fungi colonize the inner roots endophytically (Padamsee et al., 2016). Briefly, the roots were cleaned and fixed in 50% ethanol for 24 h. Then the samples were rinsed three times with sterilized deionized water and then soaked into 5% potassium hydroxide (KOH) for 2–3 h in a water bath at 90°C . Subsequently, the roots were acidified by 2% lactic acid for 1–2 min followed by strained with 0.05% (w/v) trypan blue (a mixture of 1:1:1 lactic acid/glycerol/distilled water) for 10 h. Finally, the roots were placed into 50% glycerin for 24 h to de-stain. The hyphal structures in roots were viewed with light microscope (Zeiss, Axio Scope A1) using differential interference contrast (DIC) illumination and an AxioCam MRc5 camera and Zen software.

RESULTS

Identification and Molecular Phylogenetic Appraisal of Plant-Associated Pleosporealean Fungi

As shown in Table 1, a preliminary BLAST analysis of ITS and LSU sequences from the 27 fungal strains isolated from halophyte roots, seeds, and rhizosphere showed that they comprised a diverse group of pleosporealean taxa.

To identify species level taxonomy and determine the relationships among our isolates and known pleosporealean species, we constructed a phylogeny using a multi-locus DNA sequence dataset (SSU, LSU, and *tef1*) from 89 taxa. *Hysterium angustatum* and *H. pulicare* (Hysteriales, Dothideomycetes) served as outgroup taxa (Figure 2). The analysis indicates that the pleosporealean fungi obtained in our work belong to seven distinct families including Phaeosphaeriaceae, Pleosporaceae, Didymellaceae, Sporormiaceae, Didymosphaeriaceae, Massarinaceae, and Lentitheciaceae, and were distributed across two suborders (Pleosporineae and Massarineae). Most isolates belong to the families Phaeosphaeriaceae, Pleosporineae, and Didymosphaeriaceae. It should be especially noted that, nine isolates isolated from three host plants and two compartments (rhizosphere and endosphere) formed a strongly supported clade sister to Phaeosphaeriaceae and Pleosporaceae, suggesting their potentially taxonomic novelty. Furthermore, LSU and/or ITS

sequences of some isolates (such as SYC-R-4, JP-R-6, DF-R-9, JP-R-44, and LW-R-2) did not match any known species, and formed several strongly supported separate clades. This suggests that they are potentially new genera and that likely many more taxa to be discovered in this order. The three individual gene trees also yielded very similar topologies (Supplementary Figure S1).

Comparison of the Utilization of Inorganic and Organic Nitrogen in Pure Cultures

All isolates investigated utilize both inorganic and organic N in liquid cultures. While final strain biomass was variable at different N sources (Figure 3F), a total of 21 isolates preferred organic N over inorganic N (Supplementary Figure S2, $P < 0.05$). Isolates of the suborder Pleosporineae produced the highest biomass on organic N. Strains LW-7 (Lentitheciaceae sp.) and LW-R-2 (*Epicoccum* sp.) accumulated the greatest biomass when NH_4^+ was the sole N-source, while the remaining four strains of R20 (*Phaeosphaeriopsis* sp.), R(2015)-25 (*Curvularia* sp.), LW-R-3 (*Paraconiothyrium* sp.), and DW-R-4 (*Paraconiothyrium* sp.) produced the greatest biomass on nitrate.

Environmental Stress Response in the Plant-Associated Pleosporealean Fungi Temperature

Effects of temperature on growth of the pleosporealean fungi were shown in Figure 3A. Although the growth rate varied among isolates, 25°C was the optimal temperature for most fungi. Of these, the isolates of JP-R-44, DW-R-1 and seed1 grew much more slowly than other isolates under the same conditions. An exception was the isolate R(2015)-25 (*Curvularia* sp.), which still grows well at 32°C .

pH

With the exception of DW-R-1 and JP-R-44, the majority of strains grow well over a wide range of pH level ranging from 6 to 11 (Figure 3B) suggesting that they are highly alkali-resistant. Isolates (LW-R-2 and CYTC-R-5) performed well at high pH suggesting adaptation to the alkali environments as is characteristic of alkalophilic fungi (Horikoshi, 1999).

Salt Stresses

All isolates were sensitive to salt. Overall, their growth rates were clearly inhibited with increasing concentrations of KCl or NaCl (Figures 3C,D), although the mycelium remained viable. Growth in the presence of increased concentrations of NaCl was considerably more inhibited than KCl at the same concentration. Only a small number of isolates were able to grow at higher NaCl concentrations. In contrast, several of them (including LW-R-2, JP-R-44, DW-R-1, and seed1) could still grow at the highest KCl concentration tested.

Non-ionic Osmotic Stress

Similar to salt sensitivity, increased sorbitol concentrations also inhibited fungal growth (Figure 3E), but the effect was much less pronounced in comparison to the ionic salt stress.

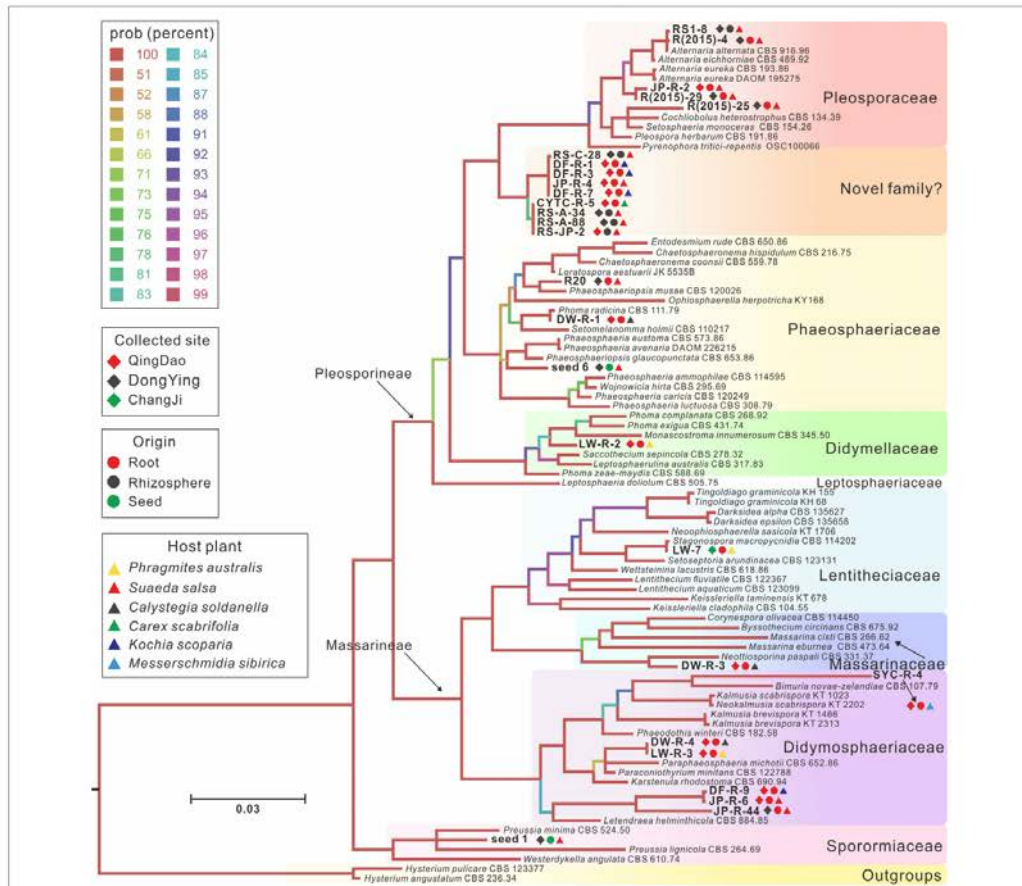


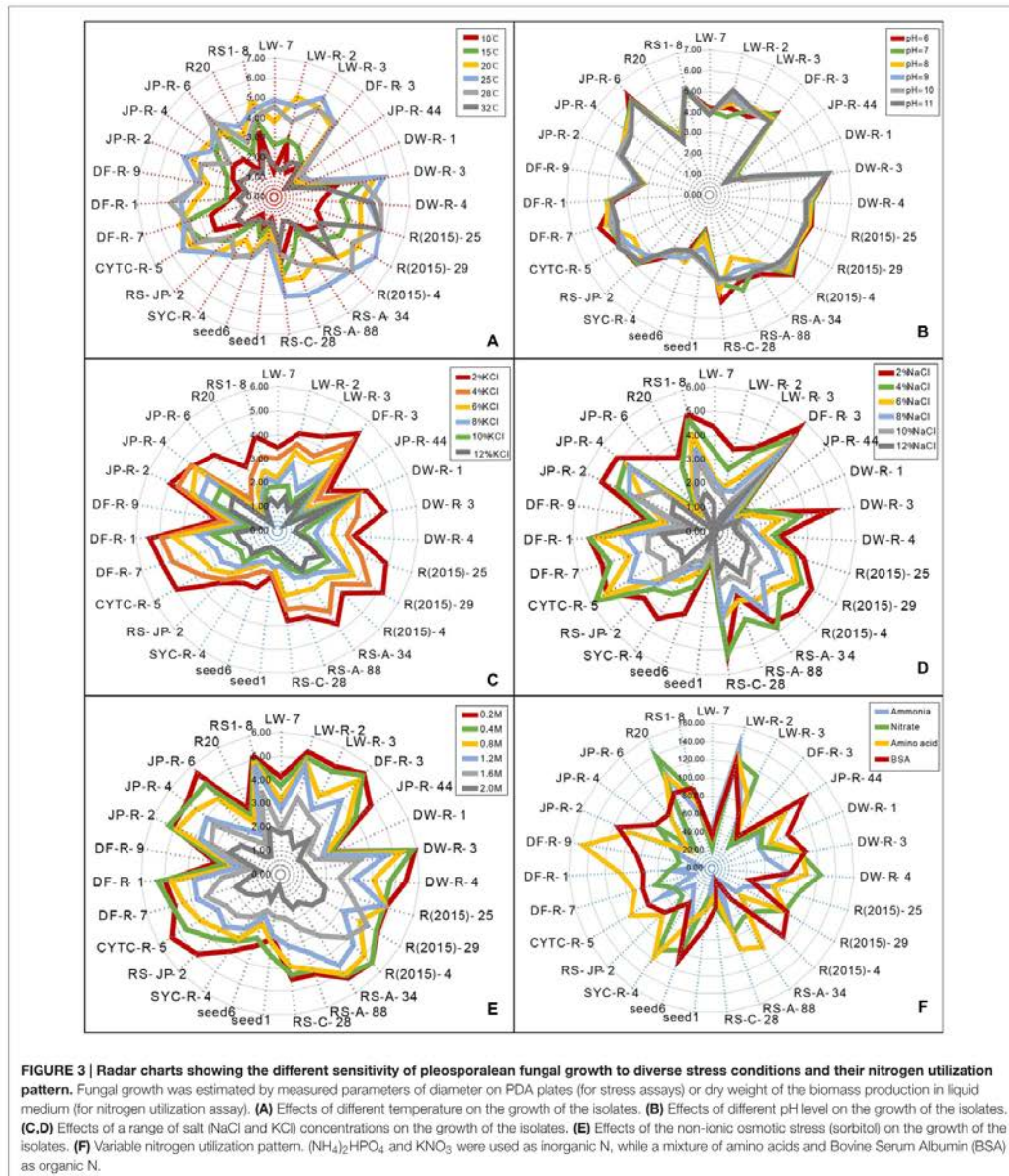
FIGURE 2 | A majority rule Bayesian phylogram showing the relationships between our isolates and currently described pleiosporalean fungi, based on the concatenated alignment of orthologous genes encoding ribosomal RNAs from two subunits, the large subunit (LSU) and small subunit (SSU), and a large fragment of the transcription elongation factor 1- α gene (*tef1*). The color of branch corresponded to the posterior probabilities percentage. Accession numbers of the three genes used for the phylogram were given in Table 1 and Supplementary Table S1. Different symbols showing collection sites, origin materials and host plants for each isolate were also indicated.

Nitrogen Status Influences the Outcome of Plant-Fungal Interactions

A plant-fungi co-cultivation system was established to explore potential beneficial effects of pleiosporalean fungi on plant growth. In view of the importance of the type of nitrogen in plant performance and productivity, we investigated whether the nitrogen source would influence the outcome of plant-fungal interactions (Upson et al., 2009; Newsham, 2011). Our preliminary data established that none of the isolates cause disease symptoms in rice seedlings (data not shown). As shown in Figure 4, plants co-cultured with fungi did not have any positive

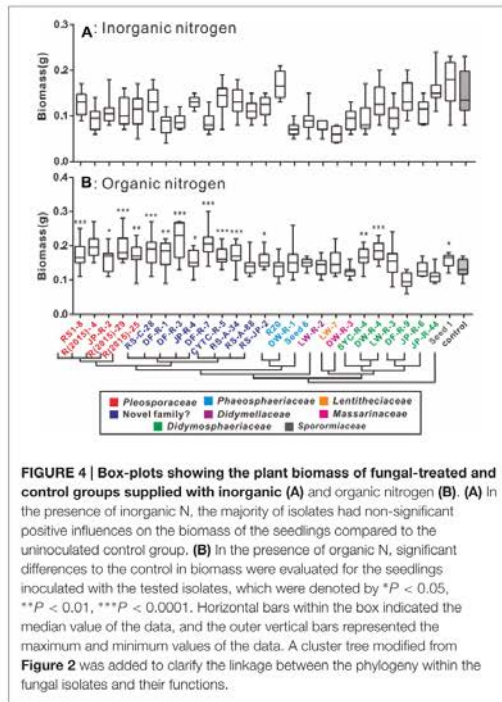
effects on plant biomass, and in some cases even negatively affected the growth when inorganic nitrogen sources (NH_4NO_3 and KNO_3) were used. While the root length of rice seedlings treated with CYTC-R-5 and plant height of JP-R-44 treated seedlings were enhanced (multiple *t*-tests comparison, $df = 26$; $P < 0.05$) (Figure 5), yet no significant differences in plant biomass were observed (Figure 4).

When organic nitrogen was provided, almost all isolates increased plant biomass production (Figure 4). Isolates DF-R-3 (*Phaeosphaeriaceae* sp.), DF-R-7 (*Phaeosphaeriaceae* sp.), DW-R-4 (*Paraconiothyrium* sp.), R(2015)-29 (*Alternaria* sp.),



and R(2015)-4 (*Alternaria* sp.) significantly promoted seedling growth (multiple *t*-tests comparison, $df = 24$; $P < 0.0001$). Also, 12 other groups clearly improved plant development (multiple *t*-tests comparison, $df = 24$; $P < 0.05$). The data also showed

that fungal induced plant biomass increases are mainly due to the accumulation of above-ground biomass as indicated by increased plant height (multiple *t*-tests comparison, $df = 24$; $P < 0.05$) and not root biomass (Figure 5).

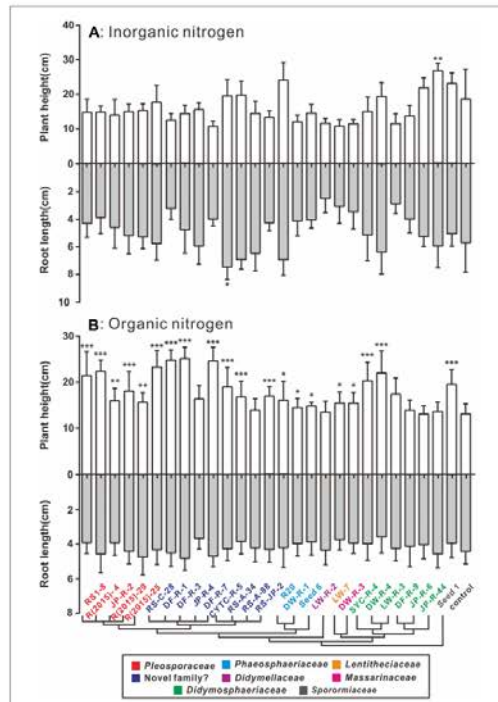


Fungal Colonization Pattern in Plant Roots

The endophytic colonization of rice roots by the pleosporelean fungi was further investigated microscopically. Six isolates [RS-A-34, RS-C-28, RS-A-88, R(2015)-25, DW-R-4 and R20] (Figures 6A–F) successfully colonized the inner root tissue as shown by the distribution of an abundant number of hyphae in the cortex and epidermis cells, both inter- and intracellularly. Melanized microsclerotia-like structures were formed upon inoculation with the isolate RS-A-34 (Figure 6A), showing the typical characters of DSEs. Root cells were filled with microsclerotia-like structures. Although inoculation of the isolates RS-C-28, RS-A-88, R(2015)-25 did not form the typical microsclerotia-like structures in roots, initiation and development of chlamyospore-like structures have likely occurred. The remaining isolates colonized rice roots only on the surface, because no fungal structures were found inside root cells. Roots inoculated with the isolates DW-R-1 and R(2015)-29 became brown to dark, but no hyphae were seen in roots.

DISCUSSION

Apart from AMF and EMF, NMF have now been recognized as an important component of the root-associated mycobiome



(Khidir et al., 2010; Andrade-Linares and Franken, 2013; Zuccaro et al., 2014). While there is accumulating evidence regarding the diversity and structure of NMF, their basic physiology and extended effects on plants are not well characterized, especially for plant-associated NMF under extreme conditions. In this work, we characterized halophyte-associated fungi from three geographic areas, six halophyte plant species and three habitats (rhizosphere, root, and seed endosphere), and found that the pleosporelean taxa can be frequently captured. This implies that they are generalist endophytes and/or epiphytes in high salinity environments, and might also mean that this group of fungi is the easiest to isolate and culture under the experimental conditions. This is consistent with other studies where pleosporelean fungi were found to be the dominant colonizers in halophytes (El-Morsy, 2000; Sun et al., 2011; Okane and Nakagiri, 2015) and plants grown in arid conditions

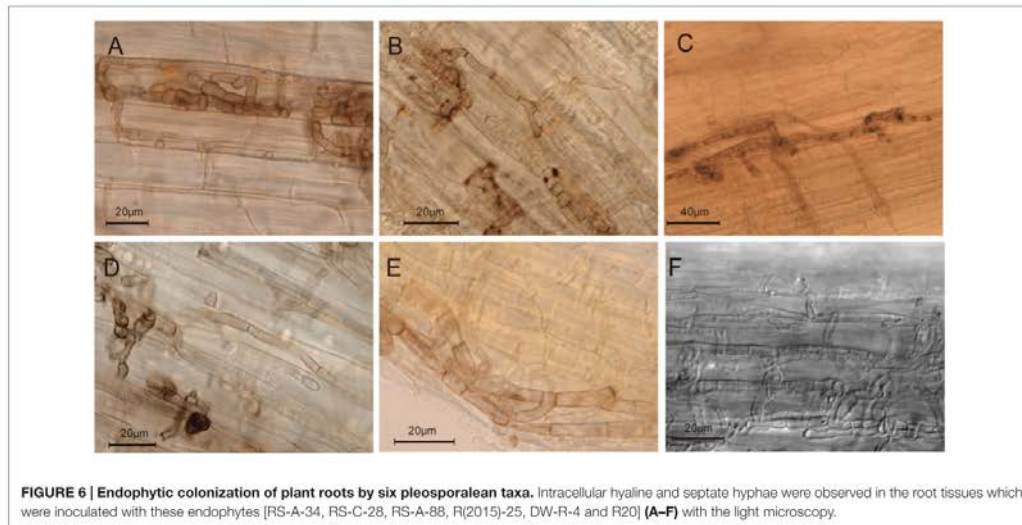


FIGURE 6 | Endophytic colonization of plant roots by six pleosporealean taxa. Intracellular hyaline and septate hyphae were observed in the root tissues which were inoculated with these endophytes [RS-A-34, RS-C-28, RS-A-88, R(2015)-25, DW-R-4 and R20] (A–F) with the light microscopy.

(Porras-Alfaro et al., 2008; Khidir et al., 2010). Especially the genera *Pleospora*, *Alternaria*, and *Phoma* were often recorded. Here we show that all pleosporealean strains isolated from our study can be categorized into seven families. Some of them are newly discovered taxa as several clades separated from known fungal taxa by long and well-supported branches (Figure 2). To the best of our knowledge, there is only a single report on a systematic morphological and phylogenetic analysis of diverse pleosporealean DSEs available (Knapp et al., 2015). Consequently, the ubiquity, diversity and novelty of plant-associated pleosporealean fungi in adverse environments will not only provide good phylogenetic resolution within the Pleosporales, but also provide the impetus to elucidate their basic physiology and roles in plant fitness.

To our knowledge, this study presents the first *in vitro* experimental evidence of the ability of pleosporealean fungi to adapt to a series of environmental stresses. Our data showed that the tested isolates are sensitive to ionic (imposed by NaCl and KCl) and non-ionic osmolytes (imposed by sorbitol) with varying degrees, which is consistent with previous observations (Larsen, 1986; Nikolaou et al., 2009; Samapundo et al., 2010). Most of our isolates were more negatively affected by NaCl stress than KCl or sorbitol stress. It is possible that Na^+ is poorly taken up by fungi, and could in fact cause alkaline stress, while K^+ can be easily absorbed and would not accumulate as KOH in the medium (Larsen, 1986). More importantly, some fungi may also utilize K^+ for surviving in unfavorable conditions (Larsen, 1986). Despite their salt sensitivity, few of them still can grow and survive in 12% NaCl (approximately 2 M NaCl). This is consistent with earlier data that the pleosporealean fungi isolated from halophytes are more likely halotolerant but not halophilic (Rodríguez et al., 2008; Lucero et al., 2011; Maciá-Vicente et al., 2012). Maciá-Vicente

et al. (2012) further speculated that rhizospheric soil fungi may be more tolerant to salt stress than endophytes, as endophytes are protected within plant roots from harsh soil conditions. Our data did not, however, support this hypothesis since there was no significant difference of growth pattern under salinity stress between endophytes and rhizospheric fungi in our conditions. All fungi tested could grow well at high pH, which may imply that both soil and host provide a well-conditioned environment with high alkali for the rhizospheric and endophytic pleosporealean fungi. Taken together, the evidence from the present study suggests that the ability of coping with multiple ecological stresses in pleosporealean fungi should be taken into consideration for their utilization in saline-alkaline soils.

It has been known that different nitrogen sources can affect ectomycorrhizal and DSEs fungal growth and biomass accumulation (Yamanaka, 1999; Rosling et al., 2004; Mandyam et al., 2010). Our results demonstrated that fungal biomass formation on different inorganic and organic substrates significantly varied among species, but most preferred amino acids over inorganic nitrogen sources presumably due to energy and carbon savings for amino acid biosynthesis. Mandyam et al. (2010) also found that several DSEs produced more biomass in the organic N (Gly) than in the inorganic N. Besides that, fungi also can use them as carbon sources for growth. The effective utilization of BSA in many isolates may reflect the occurrence of fungal-derived proteolytic enzymes for hydrolyzing proteins (Leake and Read, 1990; Bizabani and Dames, 2016). We suggest that this trait maybe related to their host plants N nutrition (Cairney and Meharg, 2003) (see further discussion below).

The influence of NMFs on growth and stress tolerance of plants are now beginning to be revealed. It has often been hypothesized that DSEs confer plant drought tolerance and

nutrient acquisition (Porrás-Alfaro et al., 2008), whereas other NMFs have been reported to have weak or even negative effects on plant growth (Jumpponen, 2001; Kageyama et al., 2008; Dovana et al., 2015). It is well-known that a number of factors determine the outcome of plant–fungal interactions, including plant genotype, the genotype and virulence of the fungi as well as the environmental conditions and nutrient status of the soil (Schulz and Boyle, 2005; Singh et al., 2011; Murphy et al., 2014). The co-cultivation assay confirmed that our isolates colonized rice seedlings asymptotically. This suggests that the inhibition of plant growth caused by pleosporealean fungi probably results from uncontrolled fungal growth, but not from the fungal virulence factors (mainly mycotoxins) (Vahabi et al., 2013).

Since plants obtain their carbon from carbon dioxide, N is the major nutrient they have to retrieve from the soil (Blair et al., 1998). For most plants, inorganic nitrogen compounds are the major source of soluble N (Roberts et al., 2009). In line with previous studies, our data strongly indicates that the nitrogen source influences plant–fungal interactions (Newsham, 2011). *In vitro* closed co-cultivation system under axenic conditions has been often used for studying plant–NMF interactions. In this case, the most frequently used substrates supporting plant and fungal growth are the MS medium (half strength or one-tenth strength) (Kageyama et al., 2008; Junker et al., 2012) and one-tenth strength of Marx-Melin-Norkrans (MMN) medium (Keim et al., 2014), which contains N in the inorganic form. Using these media, researchers found that the majority of fungal endophytes adversely affected plant growth and health, and a few of them were even pathogenic to plants (Jumpponen, 2001; Dovana et al., 2015). However, plant growth promotion can be measured in this experimental system if the fungi prove to produce auxin-like compounds *in vitro* (Sirrenberg et al., 2007; Contreras-Cornejo et al., 2009; Redman et al., 2011) despite clear evidence of *in situ* hormone production *in planta* by endophytes is yet to be elucidated. In the presence of organic N condition, most pleosporealean fungi strongly enhance plant biomass accumulation compared to the presence of inorganic N. This raises the question of why and how the N source influences the interaction with plant roots. It is known that tryptophan (Trp) is a precursor for auxin biosynthesis in fungi and plants (Redman et al., 2011). However, Trp is not present in the range of organic N sources we tested in the context of this study. Those which are present (Gly, Val, Glu, Phe, and Leu) are not known as precursors for the synthesis of plant-growth-promoters. Rather, we propose the possibility that the amino acids will become mineralized upon fungal colonization and therefore available for plant uptake. This hypothesis is supported by earlier reports showing that a wide range of DSE provide more benefits to plant in the presence of organic N than in the presence of inorganic N (Mandyam and Jumpponen, 2005; Upson et al., 2009; Alberton et al., 2010; Newsham, 2011; Mahmoud and Narisawa, 2013). DSE has been shown to synthesize proteolytic enzymes, which can mineralize the organic N compounds into the free inorganic N (Caldwell et al., 2000; Bizabani and Dames, 2016). This work further extends our view that apart from DSE, the rhizospheric and seed endophytic fungi may also possess a similar functional trait.

It has been reported that insect pathogenic fungi and EMF can transport insect-derived organic nitrogen into the plant roots (Klironomos and Hart, 2001; Behie et al., 2012, 2013). More broadly, some rhizobacterial symbionts of plants also secrete proteases and degrade denatured proteins and scavenge organic nitrogen from soil (White et al., 2015). We might say to strengthen this section that bacterial/fungal chitinase and protease activities are known to participate to the N cycle and are crucial for decomposition of soil organic nitrogen (Heinonsalo et al., 2015; Rineau et al., 2015; Knapp and Kovács, 2016). Hence, it appears likely that diverse plant-associated fungi and bacteria are important players in the soil nitrogen cycle (Behie et al., 2013). As the excessive use of inorganic nitrogen poses a great threat to natural ecosystems and crop yield (Tilman et al., 2002), our findings underscore the enormous potential for utilizing organic N mineralizing microbes in sustainable agriculture. Indeed, some of our isolates have also been shown to promote the growth of trees (e.g., American sweetgum (*Liquidambar styraciflua*) seedlings) under organic N condition (data not shown), thus suggesting the application of this system over a wider range of plants.

CONCLUSION

Our work provides new insights into the biodiversity of the widespread pleosporealean fungi associated with halophytes. Future direction will thus be focused on addressing whether these fungi are involved in plant salt tolerance. Symbiotic interactions between plant and pleosporealean fungi may serve as a new model for studying fungal-mediated plant growth and stress tolerance.

AUTHOR CONTRIBUTIONS

ZY conceived and designed the experiment. YQ performed the experiment. ZY and YQ wrote the paper. XP helped to isolate the pleosporealean fungi. ID and KC constructed the phylogenetic tree. CK and JL revised the paper.

ACKNOWLEDGMENTS

This work was financially supported by the National Natural Science Foundation of China (No. 31370704) and the Fundamental Research Funds for the Central Non-profit Research Institution of RISF-CAF (RISF2013005). JL was supported by the U.S. Department of Energy, Office of Science, Biological and Environmental Research as part of the Plant-Microbe Interfaces Scientific Focus Area (<http://pmi.ornl.gov>). Oak Ridge National Laboratory is managed by UT-Battelle, LLC, for the U.S. Department of Energy under contract DE-AC05-00OR22725. We would like to express our sincere thanks to Prof. Liyan (Xinjiang Institute of Ecology and Geography, Chinese Academy of Sciences) and Prof. Xinhua (School of Life Science, Qingdao Agricultural University) for helping us collect and identify the halophytes. We also greatly appreciate Dr. David

Weston (Biosciences Division, Oak Ridge National Laboratory) for improving the language.

SUPPLEMENTARY MATERIAL

The Supplementary Material for this article can be found online at: <http://journal.frontiersin.org/article/10.3389/fmicb.2017.00158/full#supplementary-material>

REFERENCES

- Alberton, O., Kuyper, T. W., and Summerbell, R. C. (2010). Dark septate root endophytic fungi increase growth of Scots pine seedlings under elevated CO₂ through enhanced nitrogen use efficiency. *Plant Soil* 328, 459–470. doi: 10.1007/s11104-009-0125-8
- Andrade-Linares, D. R., and Franken, P. (2013). "Fungal endophytes in plant roots: taxonomy, colonization patterns, and functions," in *Symbiotic Endophytes*, ed. R. Aroca (Berlin: Springer), 311–334.
- Ariyawansa, H. A., Tanaka, K., Thambugala, K. M., Phookamsak, R., Tian, Q., Camporesi, E., et al. (2014). A molecular phylogenetic reappraisal of the Didymosphaeriaceae (= Montagnulaceae). *Fungal Divers* 68, 69–104. doi: 10.1007/s13225-014-0305-6
- Behie, S. W., Padilla-Guerrero, I. E., and Bidochka, M. J. (2013). Nutrient transfer to plants by phylogenetically diverse fungi suggests convergent evolutionary strategies in rhizospheric symbionts. *Commun. Integr. Biol.* 6:e22321. doi: 10.4161/cib.22321
- Behie, S. W., Zelisko, P. M., and Bidochka, M. J. (2012). Endophytic insect-parasitic fungi translocate nitrogen directly from insects to plants. *Science* 336, 1576–1577. doi: 10.1126/science.1222289
- Bizabani, C., and Dames, J. F. (2016). Assimilation of organic and inorganic nutrients by *Erica* root fungi from the fynbos ecosystem. *Fungal Biol.* 120, 370–375. doi: 10.1016/j.funbio.2015.11.006
- Blair, J. M., Seastedt, T. R., Rice, C. W., and Ramundo, R. A. (1998). "Terrestrial nutrient cycling in tallgrass prairie," in *Grassland Dynamics*, eds A. K. Knapp, J. M. Briggs, D. C. Hartnett, and S. L. Collins (New York, NY: Oxford University Press), 222–243.
- Cairney, J. W. G., and Meharg, A. A. (2003). Ericoid mycorrhiza: a partnership that exploits harsh edaphic conditions. *Eur. J. Soil Sci.* 54, 735–740. doi: 10.1046/j.1365-2389.2003.00555.x
- Caldwell, B. A., Jumpponen, A., and Trappe, J. M. (2000). Utilization of major detrital substrates by dark-septate root endophytes. *Mycologia* 92, 230–232. doi: 10.2307/3761555
- Contreras-Cornejo, H. A., Macias-Rodriguez, L., Cortes-Penago, C., and López-Bucio, J. (2009). *Trichoderma virens*, a plant beneficial fungus, enhances biomass production and promotes lateral root growth through an auxin-dependent mechanism in *Arabidopsis*. *Plant Physiol.* 149, 1579–1592. doi: 10.1104/pp.108.130369
- de Gruyter, J., Aveskamp, M. M., Woudenberg, J. H. C., Verkley, G. J. M., Groenewald, J. Z., and Crous, P. W. (2006). Molecular phylogeny of *Phoma* and allied anamorph genera: towards a reclassification of the *Phoma* complex. *Mycol. Res.* 113, 508–519. doi: 10.1016/j.mycres.2009.01.002
- de Gruyter, J., Woudenberg, J. H. C., Aveskamp, M. M., Verkley, G. J. M., Groenewald, J. Z., and Crous, P. W. (2010). Systematic reappraisal of species in *Phoma* section *Paraphoma*. *Pyrenochaeta* and *Pleurophoma*. *Mycologia* 102, 1066–1081. doi: 10.3852/09-240
- de Zelicourt, A., Al-Yousif, M., and Hirt, H. (2013). Rhizosphere microbes as essential partners for plant stress tolerance. *Mol. Plant* 6, 242–245. doi: 10.1093/mp/sst028
- Dovana, F., Mucciarelli, M., Mascarello, M., and Fusconi, A. (2015). In vitro morphogenesis of *Arabidopsis* to search for novel endophytic fungi modulating plant growth. *PLoS ONE* 10:e0143353. doi: 10.1371/journal.pone.0143353
- Druzhinina, I. S., Seidl-Seiboth, V., Herrera-Estrella, A., Horwitz, B. A., Kenerley, C. M., Monte, E., et al. (2011). *Trichoderma*: the genomics of opportunistic success. *Nat. Rev. Microbiol.* 9, 749–759. doi: 10.1038/nrmicro2637
- Edgar, R. C. (2004). MUSCLE: multiple sequence alignment with high accuracy and high throughput. *Nucleic Acids Res.* 32, 1792–1797. doi: 10.1093/nar/gkh340
- El-Morsy, E. M. (2000). Fungi isolated from the endorhizosphere of halophytic plants from the Red Sea Coast of Egypt. *Fungal Divers* 5, 43–54.
- Ernst, M., Mendgen, K. W., and Wirschl, S. G. (2003). Endophytic fungal mutualists: seed-borne *Stagonospora* spp. enhance reed biomass production in axenic microcosms. *Mol. Plant Microbe Interact.* 16, 580–587. doi: 10.1094/MPMI.2003.16.7.580
- Evelin, H., Kapoor, R., and Giri, B. (2009). Arbuscular mycorrhizal fungi in alleviation of salt stress: a review. *Ann. Bot.* 104, 1263–1280. doi: 10.1093/aob/mcp251
- Finlay, R. D., Frostegård, Å., and Sonnerfeldt, A. M. (1992). Utilization of organic and inorganic nitrogen sources by ectomycorrhizal fungi in pure culture and in symbiosis with *Pinus contorta* Dougl. ex Loud. *New Phytol.* 120, 105–115. doi: 10.1111/j.1469-8137.1992.tb01063.x
- Gardes, M., and Dahlberg, A. (1996). Mycorrhizal diversity in Arctic and alpine tundra: an open question. *New Phytol.* 133, 147–157. doi: 10.1111/j.1469-8137.1996.tb04350.x
- Hamayun, M., Khan, S. A., Khan, A. L., Rehman, G., Sohn, E. Y., Shah, A. A., et al. (2009). *Phoma* herbarum as a new gibberellin-producing and plant growth-promoting fungus. *J. Microbiol. Biotechnol.* 19, 1244–1249. doi: 10.4014/jmb.0901.030
- Heinonsalo, J., Sun, H., Santalahti, M., Bäcklund, K., Hari, P., and Pumpanen, J. (2015). Evidences on the ability of mycorrhizal genus *Piloderma* to use organic nitrogen and deliver it to Scots pine. *PLoS ONE* 10:e0131561. doi: 10.1371/journal.pone.0131561
- Hirayama, K., Tanaka, K., Raja, H. A., Miller, A. N., and Shearer, C. A. (2010). A molecular phylogenetic assessment of *Massarina ingoldiana sensu lato*. *Mycologia* 102, 729–746. doi: 10.3852/09-230
- Horikoshi, K. (1999). Alkaliphiles: some applications of their products for biotechnology. *Microbiol. Mol. Biol. Rev.* 63, 735–750.
- Huelsenbeck, J. P., and Ronquist, F. (2001). MRBAYES: Bayesian inference of phylogenetic trees. *Bioinformatics* 17, 754–755. doi: 10.1093/bioinformatics/17.8.754
- Jogaiah, S., Abdelrahman, M., Tran, L. S., and Shin-ichi, I. (2013). Characterization of rhizosphere fungi that mediate resistance in tomato against bacterial wilt disease. *J. Exp. Bot.* 64, 3829–3842. doi: 10.1093/jxb/ert212
- Jumpponen, A. (2001). Dark septate endophytes – are they mycorrhizal? *Mycorrhiza* 11, 207–211. doi: 10.1007/s005720100112
- Junker, C., Draeger, S., and Schulz, B. (2012). A fine line – endophytes or pathogens in *Arabidopsis thaliana*. *Fungal Ecol.* 5, 657–662. doi: 10.1016/j.funeco.2012.05.002
- Kageyama, S. A., Mandyam, K. G., and Jumpponen, A. (2008). "Diversity, function and potential applications of the root-associated endophytes," in *Mycorrhiza*, ed. A. Varma (Berlin: Springer), 29–57.
- Keim, J., Mishra, B., Sharma, R., Ploch, S., and Thines, M. (2014). Root-associated fungi of *Arabidopsis thaliana* and *Microthlaspi perfoliatum*. *Fungal Divers* 66, 99–111. doi: 10.1007/s13225-014-0289-2
- Khidir, H. H., Eudy, D. M., Porras-Alfaro, A., Herrera, J., Natvig, D. O., and Sinsabaugh, R. L. (2010). A general suite of fungal endophytes dominate the roots of two dominant grasses in a semi-arid grassland. *J. Arid. Environ.* 74, 35–42. doi: 10.1016/j.jaridenv.2009.07.014
- Klironomos, J. N., and Hart, M. M. (2001). Food-web dynamics: animal nitrogen swap for plant carbon. *Nature* 410, 651–652. doi: 10.1038/35070643

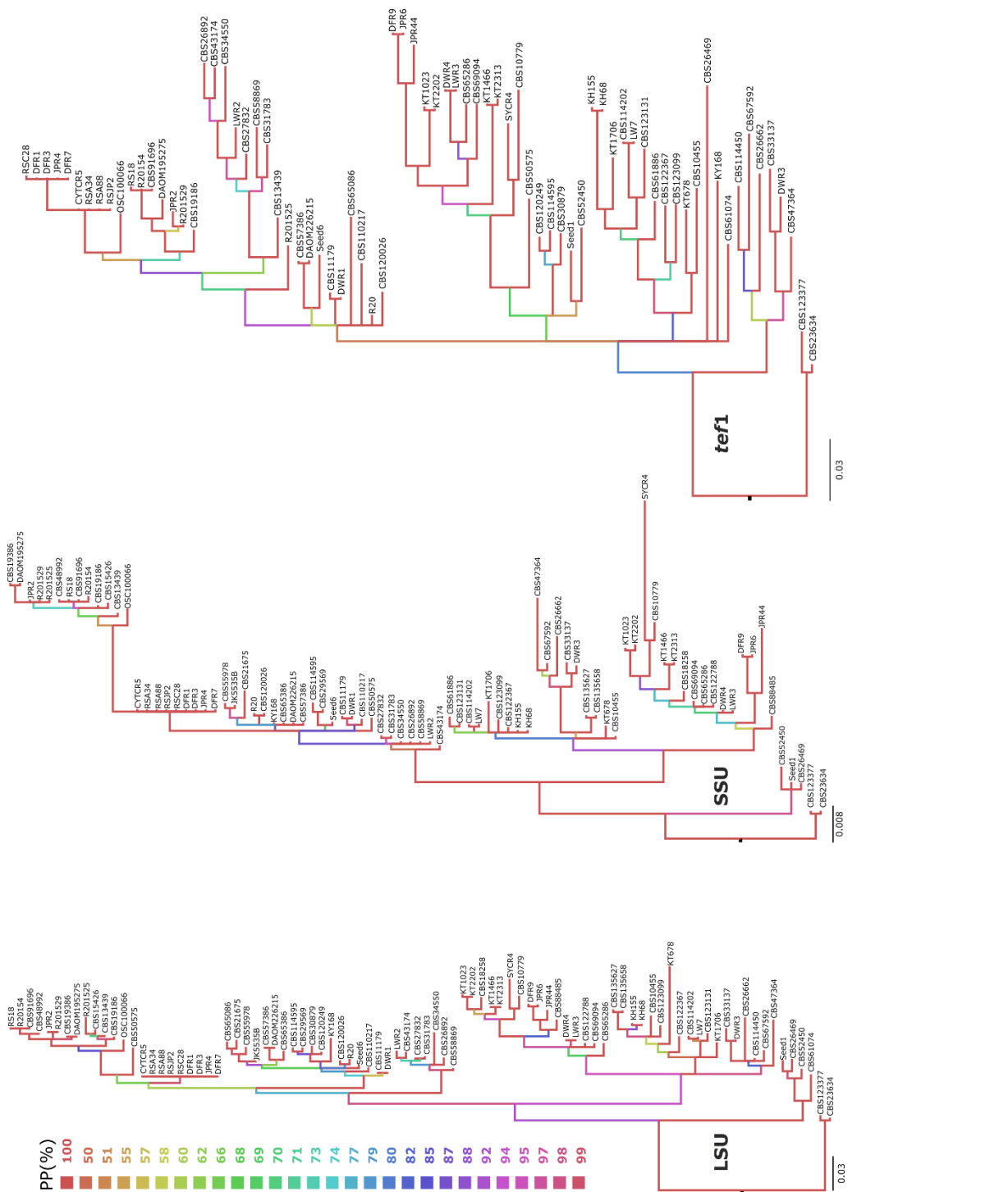
- Knapp, D. G., and Kovács, G. M. (2016). Interspecific metabolic diversity of root-colonizing endophytic fungi revealed by enzyme activity tests. *FEMS Microbiol. Ecol.* 92.fw190. doi: 10.1093/femsec/fw190
- Knapp, D. G., Kovács, G. M., Zajta, E., Groenewald, J. Z., and Crous, P. W. (2015). Dark septate endophytic pleiosporalean genera from semiarid areas. *Persoonia* 35, 87–100. doi: 10.3767/00315815X687669
- Knapp, D. G., Pintye, A., and Kovács, G. M. (2012). The dark side is not fastidious—dark septate endophytic fungi of native and invasive plants of semiarid sandy areas. *PLoS ONE* 7:e32570. doi: 10.1371/journal.pone.0032570
- Larsen, H. (1986). Halophilic and halotolerant microorganisms— an overview and historical perspective. *FEMS Microbiol. Rev.* 39, 3–7. doi: 10.1111/j.1574-6968.1986.tb01835.x
- Larsson, A. (2014). AliView: a fast and lightweight alignment viewer and editor for large datasets. *Bioinformatics* 30, 3276–3278. doi: 10.1093/bioinformatics/btu531
- Leake, J., and Read, D. (1990). Proteinase activity in mycorrhizal fungi. I. The effect of extracellular pH on the production and activity of proteinase by ericoid endophytes from soils of contrasted pH. *New Phytol.* 115, 243–250. doi: 10.1111/j.1469-8137.1990.tb00449.x
- Lucero, M. E., Adrian, U., Peter, C., Scot, D., and Shulei, S. (2011). Endophyte microbiome diversity in micropropagated *Atriplex canescens* and *Atriplex torreyi* var *griffithsii*. *PLoS ONE* 6:e17693. doi: 10.1371/journal.pone.0017693
- Lumbsch, H. T., and Lindemuth, R. (2001). Major lineages of Dothideomycetes (Ascomycota) inferred from SSU and LSU rDNA sequences. *Mycol. Res.* 105, 901–908. doi: 10.1016/S0953-7562(08)61945-0
- Lutzoni, F., Kautf, F., Cox, C. J., McLaughlin, D., Celio, G., Dentinger, B., et al. (2004). Assembling the fungal tree of life: progress, classification, and evolution of subcellular traits. *Am. J. Bot.* 91, 1446–1480. doi: 10.3732/ajb.91.10.1446
- Maciá-Vicente, J. G., Ferraro, V., Burruano, S., and Lopez-Llorca, L. V. (2012). Fungal assemblages associated with roots of halophytic and non-halophytic plant species vary differentially along a salinity gradient. *Microb. Ecol.* 64, 668–679. doi: 10.1007/s00248-012-0066-2
- Maciá-Vicente, J. G., Jansson, H. B., Abdullah, S. K., Descals, E., Salinas, J., and Lopez-Llorca, L. V. (2008). Fungal root endophytes from natural vegetation in Mediterranean environments with special reference to *Fusarium* spp. *FEMS Microbiol. Ecol.* 64, 90–105. doi: 10.1111/j.1574-6941.2007.00443.x
- Mahmoud, R. S., and Narisawa, K. (2013). A new fungal endophyte, *Scolecobasidium humicola*, promotes tomato growth under organic nitrogen conditions. *PLoS ONE* 8:e78746. doi: 10.1371/journal.pone.0078746
- Mandyam, K., and Jumpponen, A. (2005). Seeking the elusive function of the root-colonising dark septate endophytic fungi. *Stud. Mycol.* 53, 173–189. doi: 10.3114/sim.53.1.173
- Mandyam, K., Loughin, T., and Jumpponen, A. (2010). Isolation and morphological and metabolic characterization of common endophytes in annually burned tallgrass prairie. *Mycologia* 102, 813–821. doi: 10.3852/09-212
- McLellan, C. A., Turbyville, T. J., Kithsiri Wijeratne, E. M., Kerschen, A., Vierling, E., Queitsch, C., et al. (2007). A rhizosphere fungus enhances *Arabidopsis* thermotolerance through production of an HSP90 inhibitor. *Plant Physiol.* 145, 174–182. doi: 10.1104/pp.107.101808
- Midgley, D. J., Chambers, S. M., and Cairney, J. W. G. (2004). Inorganic and organic substrates as sources of nitrogen and phosphorus for multiple genotypes of two ericoid mycorrhizal fungal taxa from *Woolisia pungens* and *Leucopogon parviflorus* (Ericaceae). *Aust. J. Bot.* 52, 63–71. doi: 10.1071/BT03065
- Murphy, B. R., Hodkinson, T. R., and Doohan, F. M. (2014). Fungal endophytes of barley roots. *J. Agric. Sci.* 152, 602–615. doi: 10.1017/S0021859613000348
- Newsham, K. K. (2011). A meta-analysis of plant responses to dark septate root endophytes. *New Phytol.* 190, 783–793. doi: 10.1111/j.1469-8137.2010.03611.x
- Newsham, K. K., Upson, R., and Read, D. J. (2009). Mycorrhizas and dark septate root endophytes in polar regions. *Fungal Ecol.* 2, 10–20. doi: 10.1016/j.funeco.2008.10.005
- Nikolaou, E., Agrafioti, I., Stumpf, M., Quinn, J., Stansfield, I., and Brown, A. J. (2009). Phylogenetic diversity of stress signalling pathways in fungi. *BMC Evol. Biol.* 9:44. doi: 10.1186/1471-2148-9-44
- Okane, I., and Nakagiri, A. (2015). Assemblages of endophytic fungi on *Salicornia europaea* disjunctively distributed in Japan: towards clarification of the ubiquity of fungal endophytes on halophytes and their ecological roles. *Curr. Sci.* 109, 62–71.
- Padamsee, M., Johansen, R. B., Stuckey, S. A., Williams, S. E., Hooker, J. E., Burns, B. R., et al. (2016). The arbuscular mycorrhizal fungi colonising roots and root nodules of New Zealand kauri *Agathis australis*. *Fungal Biol.* 120, 807–817. doi: 10.1016/j.funbio.2016.01.015
- Phookamsak, R., Liu, J. K., Mckenzie, E. H. C., Manamgoda, D. S., Ariyawansa, H., Thambugala, K. M., et al. (2014). Revision of Phaeosphaeriaceae. *Fungal Divers* 10, 159–238. doi: 10.1007/s13225-014-0308-3
- Phukhamsakda, C., Ariyawansa, H. A., Phookamsak, R., Chomnunti, P., Bulgakov, T. S., Yang, J. B., et al. (2015). Muriphaeosphaeria galatellae gen. et sp. nov. in Phaeosphaeriaceae (Pleosporales). *Phytotaxa* 227, 55–65. doi: 10.11646/phytotaxa.227.1.6
- Porras-Alfaro, A., Herrera, J., Sinsabaugh, R. L., Odenbach, K. J., Lowrey, T., and Natvig, D. O. (2008). Novel root fungal consortium associated with a dominant desert grass. *Appl. Environ. Microbiol.* 74, 2805–2813. doi: 10.1128/AEM.02769-07
- Quaedvlieg, W., Verkley, G. J., Shin, H. D., Barreto, R. W., Alfenas, A. C., Swart, W. J., et al. (2013). Sizing up Septoria. *Stud. Mycol.* 75, 307–390. doi: 10.3114/sim0017
- Redman, R. S., Kim, Y. O., Woodward, C. J., Greer, C., Espino, L., Doty, S. L., et al. (2011). Increased fitness of rice plants to abiotic stress via habitat adapted symbiosis: a strategy for mitigating impacts of climate change. *PLoS ONE* 6:e14823. doi: 10.1371/journal.pone.0014823
- Rehner, S. A., and Buckley, E. (2005). A *Beauveria* phylogeny inferred from nuclear ITS and EF1- α sequences: evidence for cryptic diversification and links to *Cordyceps teleomorphs*. *Mycologia* 97, 84–98. doi: 10.3852/mycologia.97.1.84
- Rineau, F., Stas, J., Nguyen, N. H., Kuyper, T. W., Carleer, R., Vangronsveld, J., et al. (2015). Ectomycorrhizal fungal protein degradation ability predicted by soil organic nitrogen availability. *Appl. Environ. Microbiol.* 82, 1391–1400. doi: 10.1128/AEM.03191-15
- Roberts, P., Newsham, K. K., Bardgett, R. D., Farrar, J. F., and Jones, D. L. (2009). Vegetation cover regulates the quantity, quality and temporal dynamics of dissolved organic carbon and nitrogen in Antarctic soils. *Polar Biol.* 32, 999–1008. doi: 10.1007/s00300-009-0599-0
- Rodriguez, R. J., Henson, J., Van-Volkenburgh, E., Hoy, M., Wright, L., Beckwith, F., et al. (2008). Stress tolerance in plants via habitat-adapted symbiosis. *ISME J.* 2, 404–416. doi: 10.1038/ismej.2007.106
- Rodriguez, R. J., White, J. F. Jr., Arnold, A. E., and Redman, R. S. (2009). Fungal endophytes: diversity and functional roles. *New Phytol.* 182, 314–330. doi: 10.1111/j.1469-8137.2009.02773.x
- Rosling, A., Lindahl, B. D., Taylor, A. F., and Finlay, R. D. (2004). Mycelial growth and substrate acidification of ectomycorrhizal fungi in response to different minerals. *FEMS Microbiol. Ecol.* 47, 31–37. doi: 10.1016/S0168-6496(03)00222-8
- Samapundo, S., Deschuyffeleer, N., Van Laere, D., De Leyn, I., and Devlieghere, F. (2010). Effect of NaCl reduction and replacement on the growth of fungi important to the spoilage of bread. *Food Microbiol.* 27, 749–756. doi: 10.1016/j.fm.2010.03.009
- Schoch, C. L., Crous, P. W., Groenewald, J. Z., Boehm, E. W., Burgess, T. I., and de Gruyter, J. (2009). A class-wide phylogenetic assessment of Dothideomycetes. *Stud. Mycol.* 64, 1–15. doi: 10.3114/sim.2009.64.01
- Schoch, C. L., Shoemaker, R. A., Seifert, K. A., Hambleton, S., Spatafora, J. W., and Crous, P. W. (2006). A multigene phylogeny of the Dothideomycetes using four nuclear loci. *Mycologia* 98, 1041–1052. doi: 10.3852/mycologia.98.6.1041
- Schulz, B., and Boyle, C. (2005). The endophytic continuum. *Mycol. Res.* 109, 661–686. doi: 10.1017/S095375620500273X
- Shoresh, M., Harman, G. E., and Mastouri, F. (2010). Induced systemic resistance and plant responses to fungal biocontrol agents. *Annu. Rev. Phytopathol.* 48, 21–43. doi: 10.1146/annurev-phyto-073009-114450
- Singh, L. P., Gill, S. S., and Tuteja, N. (2011). Unraveling the role of fungal symbionts in plant abiotic stress tolerance. *Plant Signal. Behav.* 6, 175–191. doi: 10.4161/psb.6.2.14146
- Sirrenberg, A., Goebel, C., Grond, S., Czempinski, N., Ratzinger, A., Karlovsky, P., et al. (2007). *Piriformospora indica* affects plant growth by auxin production. *Physiol. Plant.* 131, 581–589. doi: 10.1111/j.1399-3054.2007.00983.x
- Sun, Y., Wang, Q., Lu, X. D., Okane, I., and Kakishima, M. (2011). Endophytic fungi associated with two *Suaeda* species growing in alkaline soil in China. *Mycosphere* 2, 239–248.

- Tanaka, K., Hirayama, K., Yonezawa, H., Hatakeyama, S., Harada, Y., Sano, T., et al. (2009). Molecular taxonomy of bambusicolous fungi: Tetraplosporaeraceae, a new pleosporealean family with Tetraploa-like anamorphs. *Stud. Mycol.* 64, 175–209. doi: 10.3114/sim.2009.64.10
- Tanaka, K., Hirayama, K., Yonezawa, H., Sato, G., Toriyabe, A., Kudo, H., et al. (2015). Revision of the Massariaceae (Pleosporales, Dothideomycetes). *Stud. Mycol.* 82, 75–136. doi: 10.1016/j.simyco.2015.10.002
- Tibpromma, S., Promputtha, I., Phookamsak, R., Boonmee, S., Camporesi, E. C., Yang, J. B., et al. (2015). Phylogeny and morphology of *Premilcurensis* gen. nov. (Pleosporales) from stems of *Senecio* in Italy. *Phytotaxa* 236, 40–52. doi: 10.11646/phytotaxa.236.1.3
- Tilman, D., Cassman, K. G., Matson, P. A., Naylor, R., and Polasky, S. (2002). Agricultural sustainability and intensive production practices. *Nature* 418, 671–677. doi: 10.1038/nature01014
- Toju, H., Yamamoto, S., Sato, H., Tanabe, A. S., Gilbert, G. S., and Kadowaki, K. (2013). Community composition of root-associated fungi in a *Quercus*-dominated temperate forest: "co-dominance" of mycorrhizal and root-endophytic fungi. *Ecol. Evol.* 3, 1281–1293. doi: 10.1002/ece3.546
- Upson, R., Read, D. J., and Newsham, K. K. (2009). Nitrogen form influences the response of *Deschampsia antarctica* to dark septate root endophytes. *Mycorrhiza* 20, 1–11. doi: 10.1007/s00572-009-0260-3
- Usuki, F., and Narisawa, K. (2007). A mutualistic symbiosis between a dark septate endophytic fungus, *Heteroconium chaetospora*, and a nonmycorrhizal plant. Chinese cabbage. *Mycologia* 99, 175–184. doi: 10.3852/mycologia.99.2.175
- Vahabi, K., Camehl, I., Sherameti, I., and Oelmueller, R. (2013). Growth of *Arabidopsis* seedlings on high fungal doses of *Piriformospora indica* has little effect on plant performance, stress, and defense gene expression in spite of elevated jasmonic acid and jasmonic acid-isoleucine levels in the roots. *Plant Signal. Behav.* 8:e26301. doi: 10.4161/psb.26301
- Vandenkoornhuyse, P., Baldauf, S. L., Leyval, C., Straczek, J., and Young, J. P. (2002). Extensive fungal diversity in plant roots. *Science* 295:2051. doi: 10.1126/science.295.5562.2051
- Verkley, G. J., Dukik, K., Renfurm, R., Goker, M., and Stielow, J. B. (2014). Novel genera and species of coniothyrium-like fungi in Montagnulaceae (Ascomycota). *Persoonia* 32, 25–51. doi: 10.3767/003158514X679191
- Vilgalys, R., and Hester, M. (1990). Rapid genetic identification and mapping of enzymatically amplified ribosomal DNA from several *Cryptococcus* species. *J. Bacteriol.* 172, 4238–4246. doi: 10.1128/jb.172.8.4238-4246.1990
- Waddell, P. J., and Steel, M. A. (1997). General time-reversible distances with unequal rates across sites: mixing gamma and inverse Gaussian distributions with invariant sites. *Mol. Phylogenet. Evol.* 8, 398–414. doi: 10.1006/mpev.1997.0452
- White, J. F., Chen, Q., Torres, M. S., Mattera, R., Irizarry, I., Tadych, M., et al. (2015). Collaboration between grass seedlings and rhizobacteria to scavenge organic nitrogen in soils. *AoB Plants* 7:tu093. doi: 10.1093/aobpla/plu093
- White, T. J., Bruns, T., Lee, S., and Taylor, J. W. (1990). "Amplification and direct sequencing of fungal ribosomal RNA genes for phylogenetics," in *PCR Protocols: A Guide to Methods and Applications*, eds M. A. Innis, D. H. Gelfand, J. J. Sninsky, and T. J. White (New York, NY: Academic Press, Inc), 315–322.
- Woudenberg, J. H., Groenewald, J. Z., Binder, M., and Crous, P. W. (2013). *Alternaria* redefined. *Stud. Mycol.* 75, 171–212. doi: 10.3114/sim0015
- Woudenberg, J. H. C., Seidl, M. F., Groenewald, J. Z., de Vries, M., Stielow, B., Thomma, B. P. H. J., et al. (2015). *Alternaria* section *Alternaria*: species, formae speciales or pathotypes? *Stud. Mycol.* 82, 1–21. doi: 10.1016/j.simyco.2015.07.001
- Yamanaka, T. (1999). Utilization of inorganic and organic nitrogen in pure cultures by saprotrophic and ectomycorrhizal fungi producing sporophores on urea-treated forest floor. *Mycol. Res.* 103, 811–816. doi: 10.1017/S0953756298007801
- Yuan, Z. L., Su, Z. Z., and Zhang, C. L. (2016). "Understanding the biodiversity and functions of root fungal endophytes: the ascomycete *Harpophora oryzae* as a model case," in *Environmental and Microbial Relationships*, eds I. S. Druzhinina and C. P. Kubicek (Berlin: Springer), 205–214.
- Zhang, Y., Schoch, C. L., Fournier, J., Crous, P. W., de Gruyter, J., Woudenberg, J. H., et al. (2009). Multi-locus phylogeny of Pleosporales: a taxonomic, ecological and evolutionary re-evaluation. *Stud. Mycol.* 64, 85–102. doi: 10.3114/sim.2009.64.04
- Zuccaro, A., Lahrmann, U., and Langen, G. (2014). Broad compatibility in fungal root symbioses. *Curr. Opin. Plant Biol.* 20, 135–145. doi: 10.1016/j.pbi.2014.05.013

Conflict of Interest Statement: The authors declare that the research was conducted in the absence of any commercial or financial relationships that could be construed as a potential conflict of interest.

Copyright © 2017 Qin, Pan, Kubicek, Druzhinina, Chenthamara, Labbé and Yuan. This is an open-access article distributed under the terms of the Creative Commons Attribution License (CC BY). The use, distribution or reproduction in other forums is permitted, provided the original author(s) or licensor are credited and that the original publication in this journal is cited, in accordance with accepted academic practice. No use, distribution or reproduction is permitted which does not comply with these terms.

Supplementary figure S1



Bayesian consensus phylograms for individual genetic regions (LSU, SSU, and *tef1*) showing the relationships between novel isolates and currently described pleosporalean fungi. The color of branch corresponding to the posterior probabilities percentage.

Appendix III

Komal Chenthamara-Kariyankode¹, Jian Zhang^{1,2}, Lea Atanasova¹, Alexey G. Kopchinskiy³, Kurt LaButti⁴, Alan Kuo⁴, Igor Grigoriev⁴, Christian P. Kubicek^{1, 3}, Qirong Shen² and Irina S. Druzhinina^{1, 3*}

*Irina.Druzhinina@tuwien.ac.at

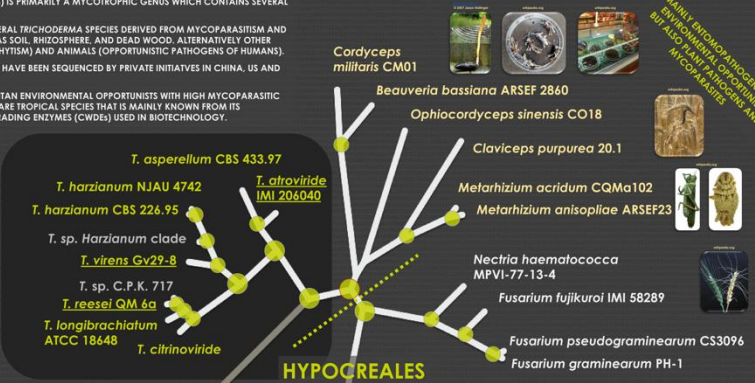


- 1) Microbiology Group, Research Area Biotechnology and Microbiology, Institute of Chemical Engineering, Vienna University of Technology, Vienna, Austria;
2) Key Laboratory of Plant Nutrition and Fertilization in Low-Middle Reaches of the Yangtze River, Ministry of Agriculture, Nanjing, China
3) Austrian Centre of Industrial Biotechnology (ACIB) GmbH c/o Institute of Chemical Engineering, University of Technology of Vienna, Vienna, Austria
4) DOE Joint Genome Institute, Walnut Creek, USA



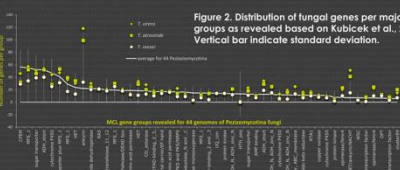
EXPLORING PHYLOGENOMICS OF TRICHODERMA: formulating a hypothesis

- ACCORDING TO THE CURRENT HYPOTHESIS, TRICHODERMA (ASCOMYCOTA, HYPOCREALES) IS PRIMARILY A MYCOTROPHIC GENUS WHICH CONTAINS SEVERAL HIGHLY OPPORTUNISTIC SPECIES WITH COSMOPOLITAN DISTRIBUTION.
DRUZHININA ET AL. 2011 PROPOSED AN OUTSTANDING OPPORTUNISTIC POTENTIAL OF SEVERAL TRICHODERMA SPECIES DERIVED FROM MYCOPARASITISM AND ALLOWED THEM TO ESTABLISH AS EFFICIENT SAPROPHITES IN SUCH ECOLOGICAL NICHE AS SOIL, RHIZOSPHERE, AND DEAD WOOD. ALTERNATIVELY OTHER SPECIES OBTAINED AN ABILITY TO FORM BIOTROPHIC ASSOCIATIONS WITH PLANTS (ENDOPHYTISM) AND ANIMALS (OPPONENTS OF PATHOGENS OF HUMANS).
GENOMES OF SEVEN SPECIES HAVE BEEN SEQUENCED BY DOE JGI. THREE OTHER GENOMES HAVE BEEN SEQUENCED BY PRIVATE INITIATIVES IN CHINA, US AND EUROPE AND ARE AVAILABLE FOR THE ANALYSIS.
ALL BUT T. REESEI GENOME SEQUENCED SPECIES ARE ECOLOGICALLY SIMILAR: COSMOPOLITAN ENVIRONMENTAL OPPORTUNISTS WITH HIGH MYCOPARASITIC POTENTIAL AND CERTAIN LEVEL OF RHIZOSPHERE COMPETENCE. T. REESEI IS A RELATIVELY RARE TROPICAL SPECIES THAT IS MAINLY KNOWN FROM ITS TELIOMORPH AND IS AN EFFICIENT PRODUCER OF CELLULASES AND OTHER CELL WALL DEGRADING ENZYMES (CWDE) USED IN BIOTECHNOLOGY.



- COMPARATIVE GENOMIC ANALYSIS (KUBICEK ET AL., 2011) SHOWED THAT THE GENOME SIZE OF TRICHODERMA FITS WELL TO PEZIZOMICOTINA (~35 MBP) WITH GENOME NUMBER VARYING BETWEEN 9 142 IN T. REESEI AND 12 423 IN T. VIRENS. A THIRD OF THE GENES ARE UNIQUE TO TRICHODERMA, SIMILARITY BETWEEN SYNTHETIC ORTHOLOGS RANGES FROM 70 TO 78%. A UNIQUE PROPERTY OF TRICHODERMA GENOME IS ITS HIGH LEVEL OF SYNTHETIC COMPARED TO OTHER FUNGAL GENOMES COMBINED WITH LOW NUMBER OF TRANSPOSONS AND LACK OF A SIGNIFICANT REPETITIVE DNA COMPONENT. THESE FEATURES CLEARLY DIFFERENTIATE TRICHODERMA FROM PLANT PATHOGENIC FUNGI SENSU RAFFAËLE & KAIMOUN, 2012 (FIGURE 1)
PREVIOUSLY IT HAS BEEN ASSUMED THAT TRICHODERMA AND SOME OTHER HYPOCREALES EVOLVED AS BIOTROPHIC ASSOCIATES OF WOOD ROTTING FUNGI (= MYCOPARASITES OF BASIDIOMYCETES) AND LATER ON FOLLOWED THEIR PREYS' HOSTS INTO THEIR HABITATS.
HERE WE PRESENT THE FIRST INDEED OF TRICHODERMA PHYLOGENOMIC ANALYSIS TOGETHER WITH 11 OTHER HYPOCREALES FUNGI OF WHICH GENOMES ARE PUBLICLY AVAILABLE (NCBI). THE MAXIMUM LIKELIHOOD PHYLOGENOM COMPOSED IN PHYML BASED ON THE ALIGNMENT OF ~50 000 aa RESIDUES FROM 100 ORTHOLOGOUS PROTEINS (TABLE 1) OF 21 HYPOCREALES AND THE TWO OUTGROUP FUNGI (NEUROSPORA CRASSA AND CHAETOMIUM GLOBOSUM) SHOWS THAT GENUS TRICHODERMA SHARES THE MOST RECENT COMMON ANCESTOR WITH CLAVICIPITACEAE AND CORDYCEPTACEAE BOTH CONTAINING ENTOMOPATHOGENIC FUNGI AND EFFICIENT ENVIRONMENTAL OPPORTUNISTS (LARGE PHYLOGRAM TO THE RIGHT; STATISTICALLY SUPPORTED NODES MARKED BY GREEN DOTS). NECTRIACEAE (FUSARIUM SPP. AND NECTRIA HAEMATOCOCCA) CLADE IS THE MOST DISTANT TO TRICHODERMA.
THE ANALYSIS OF GENE FAMILIES IN TRICHODERMA AND OTHER FUNGI INDICATED THAT PROTEINS WITH ANKYRIN (ANK) AND HET DOMAINS ARE THE MOST ENLARGED TFAMS IN THE GENUS (FIGURE 2)

Table 1: Matrix showing pectinase activity (PI 1, 3, 9) and chitinase activity (PI 4, 11) for various Trichoderma species.



PHYLOGENY AND DIVERSITY OF GENUS TRICHODERMA

Bayesian phylogram representing the most up-to-date diversity of the genus Trichoderma. The tree was inferred from the alignment of 808 nucleotides of the rpb2 gene for 194 sequences available in NCBI Genbank. Two independent MCMC runs were performed with 10 million generations and sampling frequency after each 100 generations. The first 800 trees have been removed. Nodes supported with posterior probabilities above 0.5 are marked by black circles. Vertical bars correspond to infragenetic clades recognized in the genus. Species with whole genomes sequenced are shown in green. The following ten species are not represented in the tree, because rpb2 sequences are lacking: H. albococcum, H. carneae, H. humosa, H. lacuwoodensis, T. metuliformis, T. mekongense, H. patella, H. platyura, H. virens and T. compactum.

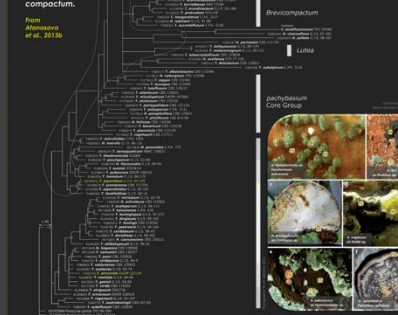


Table 1: 100 Proteins used for the concatenated multiple sequence alignment. The alignment was done in stand alone MAFFT tool with accurate parameters and then manually curated and subsequently treated with relaxed GBLOCKS. The procedure resulted in the alignment of 47673 residues for 24 taxa. Eukaryotic Orthologous Groups of proteins.

Table 1: 100 Proteins used for the concatenated multiple sequence alignment. Columns include protein ID, gene name, and species.

- REFERENCES:
ATANASOVA L, LE CROM S, GRIBBS S, COULPER J, SEDL SEIBOV V, KUBICEK CP AND S DRUZHININA (2011) COMPARATIVE TRANSCRIPTOMIC AND PROTEOMIC ANALYSIS OF BIOTROPHIC TRICHODERMA SPECIES REVEALS THE SIGNIFICANCE OF BIOTROPHIC INTERACTIONS.
ATANASOVA L, DRUZHININA IS, JANDUSIK WA, 2012. TWO TRICHODERMA SPECIES RECOGNIZED BASED ON MOLECULAR PHYLOGENY: NE NECTRIA HAEMATOCOCCA AND NECTRIA HAEMATOCOCCA.
KUBICEK CP, REESEI STRELLA A, SEDL SEIBOV V, LE CROM S, GRIBBS S, GRIGORIEV I, GRIGORIEV IV, KUBICEK CP (2011) TRICHODERMA: THE SIGNIFICANCE OF OPPORTUNISTIC SUCCESS. NATURE REV MICROBIOL 9: 11-21.
DRUZHININA IS, SEDL SEIBOV V, HERRERA-SERENA A, HERRERA KA, REESEI STRELLA A, GRIGORIEV I, REESEI S, GRIGORIEV IV, KUBICEK CP (2011) TRICHODERMA: THE SIGNIFICANCE OF OPPORTUNISTIC SUCCESS. NATURE REV MICROBIOL 9: 11-21.
KUBICEK CP, REESEI STRELLA A, SEDL SEIBOV V, LE CROM S, GRIBBS S, GRIGORIEV I, GRIGORIEV IV, KUBICEK CP (2011) TRICHODERMA: THE SIGNIFICANCE OF OPPORTUNISTIC SUCCESS. NATURE REV MICROBIOL 9: 11-21.
RAFFAËLE L AND KAIMOUN S (2012) GENOME EVOLUTION IN PLANT PATHOGENS: WHY BROWN CAN BE BETTER. NATURE REVIEWS MICROBIOLOGY 10: 417-420.

EMBO 2013 - Comparative Genomics of Eukaryotic Microorganisms, San Feliu de Guipúscua, Spain

THE ORIGIN AND ARCHITECTURE OF TRICHODERMA HYDROPHOBOME

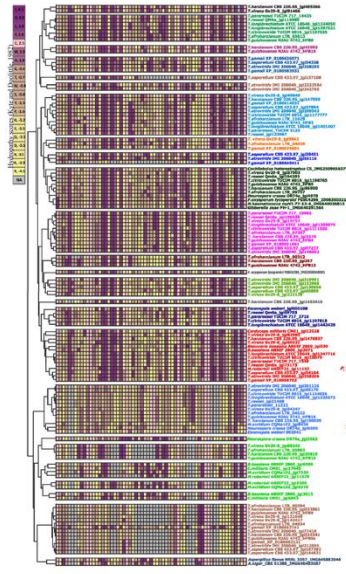


Komal Chenthamara^a, Feng Cai^{a,b}, Agnes Przylucka^a, Qirong Shen^b, Günseli Bayram Akcapinar^a, Irina Druzhinina^a
^aTU Wien; ^bNanjing Agricultural University, Nanjing, China

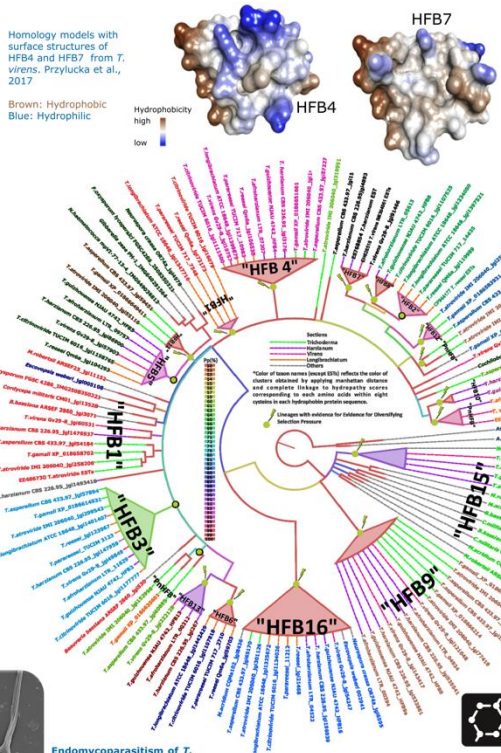
The small amphiphilic surface-active extracellular proteins that are produced exclusively by filamentous fungi may provide a mechanistic understanding of molecular adaptations that evolved along with this distinctive lifestyle. The development of many fungi includes interchanges between penetration of tissues/substrates for nutrition and growing out of them for dispersal. A hyphal organization of the body in filamentous fungi provides a high surface area-to-volume ratio that is an essential adaptation for the effective extraction of nutrients while growing on or in (semi)solid substrates or a liquid. Hyphae are specially adapted for efficient attachment to a diversity of surfaces what is also required for an exertion of penetrative mechanical forces for the invasion of substrates and tissues. The mycoparasitic genus *Trichoderma* (Hypocreales, Pezizomycotina), which also includes several cosmopolitan generalist species with high environmental opportunistic potential **have an expanded number of hydrophobins**. Previous studies have revealed that most of *Trichoderma* hydrophobins are the orphan genes that have no homologues in related organisms, while other Pezizomycotina fungi share their hydrophobins. The first genome-wide studies of *Trichoderma* provided the evidence for the operation of purifying natural selection pressure for *Trichoderma* hydrophobins that results in "birth-and-death" evolution of these proteins.



Water droplets on hyphal surface of the two Hypocrealean fungi



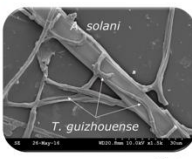
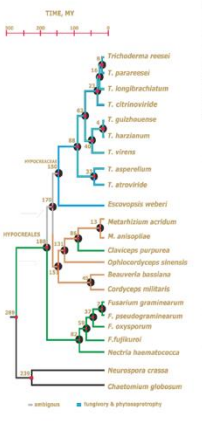
Heat map reflecting the ratios of hydrophobic residues to that of hydrophilic residues between 8 cysteines from 133 OTUs belonging to hypocreales order. OTUs, which fell into single clade are given a unique color, to discuss the concordance of this dendrogram with the main HFBome evolutionary phylogram. Purple boxes reflect most hydrophobic residues, yellow the least hydrophobic and grey boxes reflect gaps.



Here we present the evolution of hydrophobin-encoding genes in the genus *Trichoderma* and compare it to other fungi from the order Hypocreales, highlight HFB genes acquired through Lateral Gene Transfer, lineages with evidence of Episodic Diversifying Selection Pressure, and propose nomenclature for class II hydrophobins in Ascomycotic fungi.



HFBs	Statistically confirmed Donors
HFB1	<i>Metharhizium anisopliae</i>
HFB2	<i>Drechmeria coniospora</i>
HFB3	Within <i>Trichoderma</i>
HFB4	Within <i>Trichoderma</i>
HFB6	Common ancestor between <i>Bipolaris</i> spp. and <i>Pyrenophora</i> spp.
HFB7	<i>Verticillium</i> spp.
HFB5	<i>Eutypa lata</i>
HFB9	Within <i>Trichoderma</i>
HFB10	<i>Claviceps purpurea</i>
HFB11	<i>Aschersonia aleoeridis</i>
HFB12	Within <i>Trichoderma</i>
HFB13	<i>Verticillium dahliae</i>
HFB15	<i>Metharhizium album</i>
HFB16	Within <i>Trichoderma</i>
Tv222128	<i>Drechmeria coniospora</i>
Th1493416	Eurotiales spp.



Endomycoparasitism of *T. guizhouense* on *Atheria solani*. This interaction probably allows efficient DNA exchange between the fungi.

Phylogenomic analysis of *Trichoderma* spp. Bayesian chronogram obtained based on the curated concatenated alignment of 100 orthologous neutrally evolving housekeeping proteins of Hypocreales and the two other Sordariomycetes. All nodes were supported with posterior probability >0.95. Chronological estimations are given above nodes in Mya as estimated based on this chronogram. White arrows at nodes indicate calibration points against the origin of Hypocreales (Sung et al. 2008) and the origin of carnivorous in Hypocreales (Yang et al. 2012). Red bars correspond to 95% confidence in time estimation. (Druzhinina et al., ms submitted)

Data Retrieval and Phylogenetic analysis

First, the genomes of 11 *Trichoderma* spp. and 12 genomes of other Hypocreales fungi were mined for hydrophobin-encoding genes. The resulting library of amino acid sequences (133 OTUs) was subjected to the sequence alignment using MAFFT accurate algorithm. Best substitution model was found to be WAG+G+I using BIC criterion via Smart Model Selection Tool (SMS), and hence based on this model, evolutionary analysis using two independent runs of 5 million MCMC generations was carried out that resulted in reliable diagnostic parameters estimated based on potential scale reduction factor, effective sample size and average standard deviation of split frequencies.

Clustering of multivariate data based on Hydrophobicity scores of each amino acid between first and last Cysteines

Each amino acid within 8 cysteines was replaced by the hydrophobicity score proposed by Kyte and Doolittle, 1982. Gaps were considered as NA. And these missing values were computed using imputation methods by tool **ClustVis**. Manhattan distance and complete linkage were applied to each OTU. The resulting heatmap allowed us to improve our multiple sequence alignment further, and phylogram was reconstructed using the method described above.

Tests for Gene Loss, Gene duplication, Horizontal Gene Transfer and evidence of Episodic Diversifying Selection Pressure

The hypothesis of gene loss, gene duplication, and horizontal gene transfer (HGT) events were tested using NOTUNG 2.9. HGT was also verified by Trex. HFBs from 8 different *Trichoderma* species were selected and respective protein coding DNAs were aligned using MACSE tool. The strict codon alignment with consecutive Bayesian phylogram containing HFBs from all subclasses (as shown above) was subjected to BS-REL analysis in DataMonkey, to find out those branches where a proportion of sites evolves under EDS.

Material and Methods



Contact
Dr. Komal Chenthamara
 Institute of Chemical, Environmental and Biological Engineering,
 Faculty of Technical Chemistry, TU WIEN
 komal.chenthamara@tuwien.ac.at

- References**
- Lindler, M. B., Schüvy, G. R., Nakari-Setälä, T. & Penttilä, M. E. Hydrophobins: the protein-amphiphiles of filamentous fungi. *FEMS Microbiol. Rev.* **28**, 877–898 (2005).
 - Kubicek, C. P., Baker, S., Gamauf, C., Kemerley, C. M. & Druzhinina, I. S. Purifying selection and birth-and-death evolution in the class II hydrophobin gene families of the ascomycete *Trichoderma reesei*. *Gen. Evol.* **34**, 4 (2008).
 - Druzhinina, I. S. et al. *Trichoderma*: the genomics of opportunistic success. *Nat. Rev. Microbiol.* **9**, 749–759 (2011).
 - Gao, Q., Jin, K., Hong, J.H., Zhang, Y., Xiao, G., Sheng, Y., Qu, J., He, K., Xia, W., Zhou, G., Peng, G., Liu, Z., Huang, W., Wang, B., Fang, W., Wang, S., Zhang, Y., Ma, L., Li, S., Leber, K., Zhao, G.F., Ren, Y., Peng, M.C., Xia, Y., Wang, C. Genome sequencing and comparative transcriptomics of the model entomopathogenic fungus *Metharhizium anisopliae* and *M. acridum*. *PLoS Genet.* **2013**, Jan 17(11): e1002564. doi: 10.1371/journal.pgen.1002564
 - Zhang, G., Xiao, G., Xiang, C., Xu, X., Zhang, S., Zhang, H., Huang, Y., Zhou, Y., Wang, S., Zhao, G., Liu, X., Shi, L., Wang, C. Genome sequence of the insect pathogenic fungus *Coelomomyces mitis*, a valued traditional Chinese medicine. *Genome Biol.* **2011**, Nov 22(11): R118. doi: 10.1186/gb-2011-12-11-r118.
 - Druzhinina, I.S., Chenthamara, K., Zhang, J., Ananovic, L. et al., 2017. Parasitism on genetically close hosts (Lepidoptera) and lateral gene transfer powered evolution of *Trichoderma* into an opportunistic fungus (ms submitted).

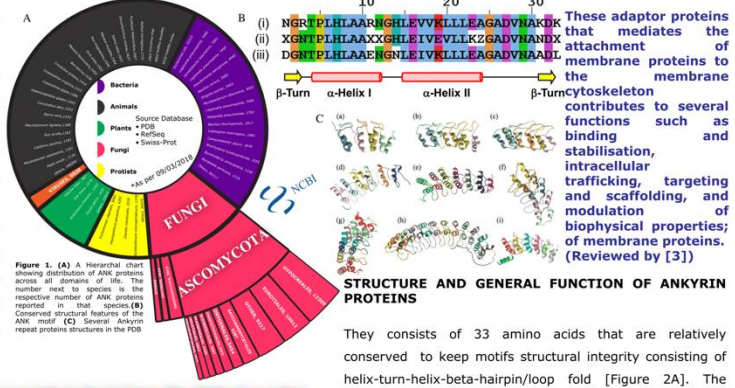
DECODING THE EXPANDED ANKYRIN-REPEAT GENE FAMILY IN TRICHODERMA



Komal Chenthamara, Vladimir Gojic, Robert Bajtela, Irina Druzhinina

BACKGROUND AND INTRODUCTION

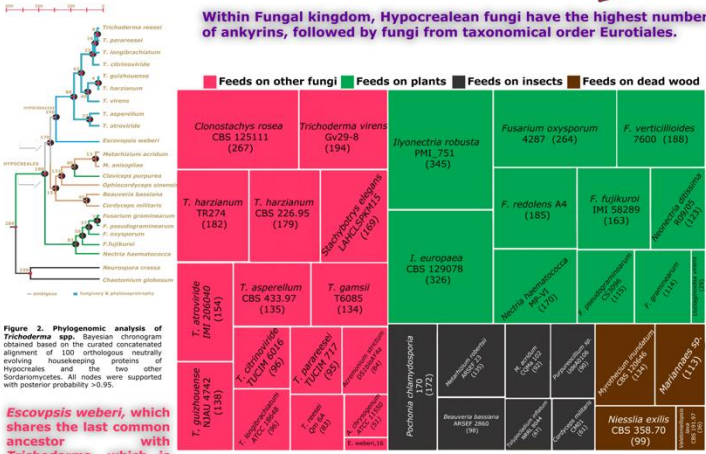
The Ankyrin (ANK) repeat is the most common protein-protein interaction motif [1]. They are found across all domains of life. However, a phylogenetic breakdown of the organisms that contain ankyrin repeats indicates that the majority are found in eukaryotes [1]. The first comparative genomic study of the mycotrophic and opportunistic genus *Trichoderma* (Hypocreales, Ascomycota) revealed a considerable expansion of ANK-repeat containing genes [2], when compared to other ecologically similar Pezizomycotina fungi. Within this study, we took a deeper look into distribution of ANK protein across all domains of life [Figure 1]. This deeper outlook highlighted the abundance of ANK within Ascomycota, and significantly lesser number of this protein among Basidiomycota.



STRUCTURE AND GENERAL FUNCTION OF ANKYRIN PROTEINS

They consists of 33 amino acids that are relatively conserved to keep motifs structural integrity consisting of helix-turn-helix-beta-hairpin/loop fold [Figure 2A]. The helices are arranged in antiparallel fashion followed by an outward pointing loop region at 90° angle. The helices of one repeat pack against the helices of the adjacent repeat while the beta hairpin/loop region, in some cases, forms A continuous beta sheet. Proteins with more Ankyrin repeats have more compact and concave structures [Figure 2B].

Within Fungal kingdom, Hypocrealean fungi have the highest number of ankyrins, followed by fungi from taxonomical order Eurotiales.



Curriculum Vitae with a complete list of publications

Personal data:

Born on 10.08.1988, New Delhi, India

Indian citizen

Lives permanently in Austria since 2011

*Current Resident Permit status: Rot-Weiß-Rot
Karte für besonders Hochqualifizierte*

Phone number: +436 9910286891

Email: komalck88@gmail.com

Current Position and Contact

Position	Project Assistant (FWF) / phd student
Address	E166-05-2 - Research Group for Microbiology and Applied Genomics, Research Area Biochemical Technology Institute of Chemical, Environmental and Bioscience Engineering Technische Universität Wien Gumpendorfer Str. 1a 1060 Vienna, Austria
Phone	+43 (1) 58801 166577
Email	Komal.chenthamara@tuwien.ac.at
Web	TU Wien Website: www.vt.tuwien.ac.at Mycocode Website: http://mycocode.tuwien.ac.at/



Join us at the JGI Genomics of Energy & Environment Meeting!
Komal Chenthamara featured during the DOE JGI User Meeting 2017, CA, USA



Qualifications

2015 – 2018	Doctoral programme, TU Wien, , Vienna, Austria
2012 – 2015	Masters in Biotechnology and Bioanalytics, TU Wien, Vienna, Austria
2011 – 2012	B2 level -German, Österreichische Orient Gesellschaft, Vienna, Austria
2006 - 2010	Bachelor of Technology (B-Tech) in Biotechnology, SRM University, Chennai, Tamil Nadu, India

Training

2018	Fungal Genomics Workshop, The DOE JGI Genomics of Energy and Environment Meeting, San Francisco, California, USA
2017	Fungal Genomics Workshop, The DOE JGI Genomics of Energy and Environment Meeting, Walnut Creek, California, USA Kbase Workshop, The DOE JGI Genomics of Energy and Environment Meeting, Walnut Creek, California, USA
2014 - 2015	Master Thesis Student in Research Group for Microbiology and Applied Genomics, TU Wien, Vienna, Austria
2013	Intern in Research Group for Microbiology and Applied Genomics, TU Wien, TU Wien, Vienna, Austria
2013	Training in Communication, BEST, Board of European Students of Technology, Vienna, Austria
2013	Training in Time Management, BEST, Board of European Students of Technology, Vienna, Austria
2012	Intern in Research Group for Bioprocess Technology, TU Wien, Vienna, Austria

2009 IELTS (International English Language Testing System), Chennai, Tamil Nadu, India

Prizes

2017 [TU Wien Christiana HÖRBIGER Preis](#) – Preis zur Förderung der internationalen Mobilität von Nachwuchswissenschaftler_innen

2016 [TU Wien Short-term grants](#) for participation in conferences for phd-students

Teaching Activities

SS2018 Lecturer for the optional course 166.648 Biology and genetics of industrial microorganisms, master Program Technical Chemistry Biotechnology and Bioanalytics, TU Wien

WS 2017/2018 Tutor for mandatory laboratory course 166.222 Biochemistry and Biotechnology, bachelor program Technical Chemistry, TU Wien

WS 2017/2018 Teaching Assistant for the mandatory course 166.231 Applied Bioinformatics Lab, master Program Technical Chemistry Biotechnology and Bioanalytics, TU Wien

WS 2016/2017 Tutor for mandatory laboratory course 166.222 Biochemistry and Biotechnology, bachelor program Technical Chemistry, TU Wien

WS 2016/2017 Teaching Assistant for the mandatory course 166.231 Applied Bioinformatics Lab, master Program Technical Chemistry Biotechnology and Bioanalytics, TU Wien

SS2017 Lecturer for the optional course 166.648 Biology and genetics of industrial microorganisms, master Program Technical Chemistry Biotechnology and Bioanalytics, TU Wien

WS2015/2016 Tutor for mandatory laboratory course 166.222 Biochemistry and Biotechnology, bachelor program Technical Chemistry, TU Wien

2014 Assistant for the mandatory laboratory course 166.193 Microbiology, master Program Technical Chemistry Biotechnology and Bioanalytics, TU Wien

List of Publications

- 2018
- 1 Research Paper: **Evolution and comparative genomics of the most common *Trichoderma* species**

Christian P. Kubicek, Andrei S. Steindorff²¹, Komal Chenthamara, Gelsomina Manganiello, Bernard Henrissat, Jian Zhang, Feng Cai, Alexey G. Kopchinskiy, Eva M. Kubicek, Alan Kuo, Riccardo Baroncelli, Sabrina Sarrocco, Eliane Ferreira Noronha, Giovanni Vannacci, Qirong Shen, Igor V. Grigoriev, Irina S. Druzhinina

Revised manuscript submitted to Studies in Mycology
 - 2 Research Paper: **"Massive lateral transfer of genes encoding plant cell wall-degrading enzymes to the mycoparasitic fungus *Trichoderma* from its plant-associated hosts."**

Irina S. Druzhinina, Komal Chenthamara, Jian Zhang, Lea Atanasova, Dongqing Yang, Youzhi Miao, Mohammad J. Rahimi, Marica Grujic, Feng Cai, Shadi Pourmehdi, Kamariah Abu Salim, Carina Pretzer, Alexey G. Kopchinskiy, Bernard Henrissat, Alan Kuo, Hope Hundley, Mei Wang, Andrea Aerts, Asaf Salamov, Anna Lipzen, Kurt labutti, Kerrie Barry, Igor V. Grigoriev, Qirong Shen, and Christian P. Kubicek

PLOS Genetics, April 9, 2018 [doi: 10.1371/journal.pgen.1007322](https://doi.org/10.1371/journal.pgen.1007322)

²¹ Shared first-authorship

2017

- 3 Short-talk and Conference paper on "**The origin and architecture of *Trichoderma hydrophobome*.**"

Komal Chenthamara, Feng Cai, Agnes Przylucka, Qirong Shen, Günseli Bayram Akcapinara, Irina Druzhinina

Vienna young Scientists Symposium, TU WIEN, June 6, 2017, Page 90-91 in [Abstract book](#)

- 4 Conference paper: "**The origin and architecture of *Trichoderma hydrophobome*.**"

Komal Chenthamara, Feng Cai, Agnes Przylucka, Qirong Shen, Günseli Bayram Akcapinara, Irina Druzhinina

Joint Genome Institute User Meeting, Walnut Creek, San Francisco, USA, March 22, 2017, Page 24 in [Abstract book](#)

- 5 Research Paper: **Diverse Plant-Associated Pleosporalean Fungi from Saline Areas: Ecological Tolerance and Nitrogen-Status Dependent Effects on Plant Growth**

Yuan Qin, Xueyu Pan, Christian Kubicek, Irina Druzhinina, Komal Chenthamara, Jessy Labbé, and Zhilin Yuan

Frontiers in Microbiology, February 6, 2017 [doi: 10.3389/fmicb.2017.00158](https://doi.org/10.3389/fmicb.2017.00158)

- 6 Research Paper: **HFB7 - A Novel Orphan Hydrophobin of the *Harzianum* and *Virens* Clades of *Trichoderma*, Is Involved in Response to Biotic and Abiotic Stresses**

Agnes Przylucka, Günseli Bayram Akcapinar, Komal Chenthamara, Feng Cai, Marica Grujic, Juriy Karpenko, Miriam Livoi, Qirong Shen, Christian P.Kubicek, Irina

S.Druzhinina Fungal Genetics and Biology, May 2017,
Pages 63-76 [doi: 10.1016/j.fgb.2017.01.002](https://doi.org/10.1016/j.fgb.2017.01.002)

2016

- 7 Research Paper: **Small genome of the fungus *Escovopsis weberi*, a specialized disease agent of ant agriculture.**

Tom J. B. De Man, Jason E. Stajich, Christian P. Kubicek, Clotilde Teiling, Komal Chenthamara, Lea Atanasova, Irina S. Druzhinina, Natasha Levenkova, Stephanie S. L. Birnbaum, Seth M. Barribeau, Brooke A. Bozick, Garret Suen, Cameron R. Currie, and Nicole M. Gerardo

PNAS, Proceedings of the National Academy of Sciences, March 2016, Pages 3567–3572
[doi:10.1073/pnas.1518501113](https://doi.org/10.1073/pnas.1518501113)

- 8 Book Chapter: **Ecological Genomics of Mycotrophic Fungi**

Komal Chenthamara and Irina S. Druzhinina

Springer - THE MYCOTA, Environmental and Microbial Relationships, Volume IV, Third edition, March 2016, [Pages 215-246](#)

2015

- 9 Research Paper: **Genome Sequence and Annotation of *Trichoderma parareesei*, the Ancestor of the Cellulose Producer *Trichoderma reesei***

Dongqing Yang, Kyle Pomraning, Alexey Kopchinskiy, Razieh Karimi Aghcheh, Lea Atanasova, Komal Chenthamara, Scott E. Baker, Ruifu Zhang, Qirong Shen, Michael Freitag, Christian P. Kubicek, and Irina S. Druzhinina

American Society for Microbiology - Genome
Announcements August 2015 doi:
[10.1128/genomeA.00885-15](https://doi.org/10.1128/genomeA.00885-15)

- 2014 10 Conference paper: "Phylogenomics of *Trichoderma*."

Komal Chenthamara, Lea Atanasova, Dongqin Yang, Jian Zhang, Alexey G. Kopchinskiy, Igor Grigoriev, Christian P. Kubicek, Qirong Shen, Irina S. Druzhinina

12th European Conference on Fungal Genetics, March 23rd-27th, Spain, 2014, Page 184 in [Abstract book](#)
- 2013 11 Conference paper: "A unique genomic architecture of *Trichoderma* species from Section Longibrachiatum- with emphasis on carbohydrate-active enzymes."

EMBO 2013, Comparative Genomics of Eukaryotic Microorganisms, Sant Feliu de Guixols, Spain, Abstract not available online

Manuscripts in preparation for 2019

1. Chenthamara K, Cai F, Von Rotz S, Cervenka I, Druzhinina IS. Genome-wide pattern search reveals a plethora of previously unknown Hydrophobins in *Trichoderma*
2. Chenthamara K, Gojic V, Druzhinina IS. Ankyrin domain containing proteins are frequent in orphomes of all *Trichoderma* species